

Continuum Damage Mechanics

SOLID MECHANICS AND ITS APPLICATIONS

Volume 185

Series Editor: G.M.L. GLADWELL

Department of Civil Engineering

University of Waterloo

Waterloo, Ontario, Canada N2L 3G1

Aims and Scope of the Series

The fundamental questions arising in mechanics are: Why?, How?, and How much? The aim of this series is to provide lucid accounts written by authoritative researchers giving vision and insight in answering these questions on the subject of mechanics as it relates to solids.

The scope of the series covers the entire spectrum of solid mechanics. Thus it includes the foundation of mechanics; variational formulations; computational mechanics; statics, kinematics and dynamics of rigid and elastic bodies; vibrations of solids and structures; dynamical systems and chaos; the theories of elasticity, plasticity and viscoelasticity; composite materials; rods, beams, shells and membranes; structural control and stability; soils, rocks and geomechanics; fracture; tribology; experimental mechanics; biomechanics and machine design.

The median level of presentation is the first year graduate student. Some texts are monographs defining the current state of the field; others are accessible to final year undergraduates; but essentially the emphasis is on readability and clarity.

For further volumes:

<http://www.springer.com/series/6557>

Sumio Murakami

Continuum Damage Mechanics

A Continuum Mechanics Approach
to the Analysis of Damage and Fracture



Sumio Murakami
Nagoya University
Professor Emeritus
3-63-3 Hinata-cho, Mizuho-ku
467-0047 Nagoya
Japan
sy-murakami@wb3.so-net.ne.jp

This book is based on an enlarged and revised version of the Japanese book of the same title
printed by Morikita Publishing Co. Ltd., Tokyo.

ISSN 0925-0042

ISBN 978-94-007-2665-9

e-ISBN 978-94-007-2666-6

DOI 10.1007/978-94-007-2666-6

Springer Dordrecht Heidelberg London New York

Library of Congress Control Number: 20111942517

© Springer Science+Business Media B.V. 2012

No part of this work may be reproduced, stored in a retrieval system, or transmitted in any form or by
any means, electronic, mechanical, photocopying, microfilming, recording or otherwise, without written
permission from the Publisher, with the exception of any material supplied specifically for the purpose
of being entered and executed on a computer system, for exclusive use by the purchaser of the work.

Printed on acid-free paper

Springer is part of Springer Science+Business Media (www.springer.com)

Preface

A half century has passed since Professor L. M. Kachanov, a Russian authority of nonlinear solid mechanics, proposed a quantitative notion of *Damage* in order to predict the brittle creep rupture time of metals for the first time. Then, together with Professor Y. N. Rabotnov, another authority in Russia in this field, he laid the basis of a new branch of *Damage Mechanics* or *Continuum Damage Mechanics*.

Starting with metallic materials, the objective of damage mechanics research has been extended thereafter to concrete, geological materials, polymers, composites and other materials. The extent of problems discussed by damage mechanics has been enlarged to a wide variety of damage phenomena including elastic-plastic damage, elastic-brittle damage, fatigue damage, dynamic and spall damage, etc.

Damage mechanics which originally started as a phenomenological theory of damage and fracture has been reinforced logically by the help of well established theoretical frameworks of material science, nonlinear continuum mechanics, irreversible thermodynamics, micromechanics, computational mechanics, etc., and now has been established as a precise and systematic discipline for damage and fracture analysis. The results of the development of this field of mechanics have been published in several excellent books and treatises. However, some of them may be readable only for readers with specially trained scientific background.

Recent developments in engineering and technology have brought about serious and enlarged demands for the reliability, safety and economy in wide field of science, ranging from aeronautics, civil and structural engineering to automotive and production engineering. This, in turn, has caused more interest in continuum damage mechanics and its engineering applications.

This book aims to give a concise overview of the current state of damage mechanics, and then to show the fascinating possibility of this promising branch of mechanics. The author, therefore, intended to provide researchers, engineers and graduate students of various mechanical grounding with an intelligible and self-contained textbook to study this rational and fruitful mechanics.

The book consists of two Parts and an Appendix. Part I is concerned with the foundation of continuum damage mechanics. Basic concept of material damage and the mechanical representation of damage state of various kinds are described in [Chapters 1 and 2](#). In [Chapters 3 through 5](#), irreversible thermodynamics, thermodynamic constitutive theory and its application to the modeling of the

constitutive and the evolution equations of damaged materials are described as a systematic basis for the subsequent development throughout the book.

Part II describes the application of the fundamental theories developed in Part I to typical damage and fracture problems encountered in various fields of current engineering. Important engineering aspects of elastic-plastic or ductile damage, their damage mechanics modeling and their further refinement are first discussed in [Chapter 6](#). [Chapters 7](#) and [8](#) are concerned with the modeling of fatigue, creep, creep-fatigue and their engineering application. Damage mechanics modeling of complicated crack closure behavior in elastic-brittle and composite materials are discussed in [Chapters 9](#) and [10](#). In [Chapter 11](#), applicability of the local approach to fracture by means of damage mechanics and finite element method, and the ensuing mathematical and numerical problems are briefly discussed.

A proper understanding of the subject matter requires the knowledge of tensor algebra and tensor calculus. At the end of this book, therefore, foundations of tensor analysis are presented in the Appendix, especially for readers with insufficient mathematical background, but with keen interest in this exciting field of mechanics.

For the publication of this book, the author has been greatly indebted to many people for their enlightening, guidance and support. The author is grateful particularly to Professor J. Lemaitre at LMT (Laboratoire de Mécanique et Technologie), ENS (Ecole Normal Supérieure) de Cachan, France, for his lifelong friendship and stimulation to the academic activity of the author. In 1970s, Professor Lemaitre started his damage mechanics research together with Dr. J. L. Chaboche, currently at ONERA (Office National d'Études et de Recherches Aérospatiales), and other excellent young researchers, and established the current foundation of damage mechanics. The basic theories and their application described in this book are largely due to their research results. Dr. Chaboche, in particular, has pursued the extension of the applicability of continuum damage mechanics, and derived a number of rigorous theoretical frameworks for this mechanics.

Professor D. R. Hayhurst, the University of Manchester, UK, also made a fundamental contribution, especially to the development of creep damage theory, and damage analysis of high temperature structures. His work in the late 1960s laid the foundations for the development of computational Continuum Damage Mechanics; and additionally, in the 1970s, he established with Professor F. A. Leckie important bounding theorems for structures. The author owes a considerable part of this book, especially those in [Chapter 8](#), to Professor Hayhurst's results.

Dr. Chaboche and Professor Hayhurst, in their very busy days of scientific activity, spent a lot of time in reading through the draft of this book, and gave a number of valuable suggestions for its improvements. The author is deeply grateful to them for their favor.

The author greatly acknowledges the contribution of Professor C. L. Chow, University of Michigan, Dearborn, USA. Working with able researchers, mainly from Asia, he established an accurate and firm basis for anisotropic elastic-plastic damage theory. Professor Chow's effort to start and to develop the *International Journal of Damage Mechanics* should be deeply appreciated. A number of his research results are referenced in this book.

The author pays his heartfelt respect and gratitude to the late Professor D. Krajcinovic, Arizona State University, USA, for his friendship and his contribution to damage mechanics. He made a magnificent contribution to the development of this discipline for geological materials, mainly from a micromechanics point of view. He left an everlasting excellent treatise of this subject.

In the course of writing and improving the manuscript, the author is indebted largely to a number of foreign colleagues and friends, especially to Professor P. Ladevèze, ENS/LMT, Professor K. Saanouni, Université de Tchnologie de Troyes and Professor J. Mazars, Institut National Polytechnique de Grenoble. Besides references to their outstanding research results, their invaluable comments and suggestions to improve the draft of this book are greatly appreciated.

Thanks are also due to a number of people in Japan for their cordial cooperation, support and favor. Professor E. Tanaka, Nagoya University, has kept supporting the author for a long time, and has given valuable suggestions in the whole process of preparing this book. Professor N. Ohno, Nagoya University, offered great deal of heartfelt support to the author for the period when the author started the damage mechanics research and prepared the basis for his international academic activity. Special thanks are due to both of them. The author is indebted also to his former colleagues and students, who collaborated with the author in his fruitful period of damage mechanic research.

Finally special thanks should be expressed to Springer-Verlag for their favor to undertake the publication of this book. Sincere gratitude is due to Ms. N. Jacobs, Publishing Editor, and Ms. J. Pot, Editor at Springer-Dordrecht for their cooperation and assistance in printing the book in this excellent form. The author gratefully acknowledges the favor and endeavor of Mr. K. Kimlica, Springer-Tokyo, who gave the author the unique chance to publish this book with the well established and prestigious publishing house of Springer.

This book is the enlarged and revised version of the Japanese book of the same title printed in Morikita Publishing Co. Ltd., Tokyo. The author is greatly obliged to the Executive Director, Dr. H. Morikita and to Editorial Manager, Mr. S. Ishida for their particular courtesy.

Sumio Murakami

Contents

Part I Foundations of Continuum Damage Mechanics

1 Material Damage and Continuum Damage Mechanics	3
1.1 Damage and Its Microscopic Mechanisms	3
1.1.1 Scales of Damage Phenomena	4
1.1.2 Physical Mechanisms of Damage	5
1.1.3 Damage in Fracture Problems	6
1.2 Representative Volume Element and Continuum Damage Mechanics	11
1.2.1 Representative Volume Element	11
1.2.2 Notion of Continuum Damage Mechanics	12
2 Mechanical Representation of Damage and Damage Variables	15
2.1 Mechanical Modeling of Damage	15
2.1.1 Modeling by Effective Area Reduction	16
2.1.2 Modeling by the Variation in Elastic Modulus	19
2.1.3 Modeling by Void Volume Fraction	20
2.2 Mechanical Representation of Three-Dimensional Damage State	21
2.2.1 Scalar Damage Variable	22
2.2.2 Plural Scalar Damage Variables	22
2.2.3 Vector Damage Variable	22
2.2.4 Damage State Defined by Effective Area Reduction, Damage Tensor of Second-Order	23
2.2.5 Damage State Defined by Geometrical Configuration of Microvoids	26
2.2.6 Damage State Defined by Directional Distribution of Microvoid Density	28
2.2.7 Damage Tensors of Fourth- and Eighth-Order	30
2.3 Effective Stress and Hypothesis of Mechanical Equivalence	32
2.3.1 Effective Stress Tensors	32
2.3.2 Damage Effect Tensors, Representation of Effective Stress Tensors	34
2.3.3 Hypothesis of Strain Equivalence	36

2.3.4	Hypothesis of Energy Equivalence 1 – Complementary Strain Energy Equivalence	38
2.3.5	Hypothesis of Energy Equivalence 2 – Strain Energy Equivalence	40
2.3.6	Hypothesis of Total Energy Equivalence	41
2.4	Elastic Constitutive Equation and Elastic Modulus Tensor of Damaged Material – Comparison Between Results by Different Effective Stresses and Equivalence Hypotheses	43
2.4.1	Elastic Constitutive Equations of Damaged Material . .	44
2.4.2	Matrix Representation of Damage Effect Tensors . . .	44
2.4.3	Matrix Representation of Elastic Constitutive Equation and Elastic Modulus Tensor	48
2.4.4	Elastic Constitutive Equation and Elastic Compliance Tensor 1 – By Hypothesis of Strain Equivalence	50
2.4.5	Elastic Constitutive Equation and Elastic Compliance Tensor 2 – By Hypothesis of Complementary Strain Energy Equivalence	52
2.4.6	Elastic Constitutive Equation and Elastic Compliance Tensor 3 – By Complementary Strain Energy Function and Representation Theorem .	53
2.5	Refinement of Continuum Damage Mechanics and Its Results .	54
3	Thermodynamics of Damaged Material	57
3.1	Thermodynamics of Continuum	57
3.1.1	State Variables and Principle of Local State	57
3.1.2	First Law of Thermodynamics	58
3.1.3	Second Law of Thermodynamics and Clausius-Duhem Inequality	61
3.1.4	Gibbs Relation and Thermodynamic Potentials	63
3.2	Thermodynamic Constitutive Theory of Inelasticity with Internal Variables	65
3.2.1	Thermodynamic Potentials and Constitutive Equations	66
3.2.2	Dissipation Potentials and Evolution Equations of Internal Variables	68
3.2.3	Constitutive Equations Expressed in Stress Space . .	71
3.3	Extension of Thermodynamic Constitutive Theory of Inelasticity	72
3.3.1	Generalized Standard Material	72
3.3.2	Thermodynamic Constitutive Theory Based on Multiple Dissipation Potentials – Quasi-Standard Thermodynamic Approach	73

4 Inelastic Constitutive Equation and Damage Evolution	
Equation of Material with Isotropic Damage	77
4.1 One-Dimensional Inelastic Constitutive Equation of Material with Isotropic Damage	77
4.1.1 Elastic-Plastic Deformation of Damaged Material	77
4.1.2 Viscoplastic Deformation of Damaged Material	79
4.2 Three-Dimensional Inelastic Constitutive Equations of Material with Isotropic Damage	81
4.2.1 Internal Variables and Thermodynamic Constitutive Theory	81
4.2.2 Thermodynamic Potential and Dissipation Potential . .	84
4.2.3 Elastic-Plastic Constitutive Equation of Damaged Material	88
4.2.4 Viscoplastic Constitutive Equation of Damaged Material	92
4.2.5 Evolution Equation of Elastic-Plastic Damage and Viscoplastic Damage	93
4.2.6 Threshold Value p_D of Plastic Strain for Damage Initiation – In the Case of Fatigue Damage .	94
4.3 Strain Energy Release Rate and Stress Criterion for Damage Development in Elastic-Plastic Damage	96
4.3.1 Strain Energy Release Rate Due to Damage Development	96
4.3.2 Energy Dissipation in Elastic-Plastic Damage	98
4.3.3 Stress Triaxiality and Stress Criterion for Damage Development	99
4.3.4 Effect of Stress Sign on Damage Development	101
4.3.5 Stress Criterion for Ductile Damage	105
4.4 Inelastic Damage Theory Based on Hypothesis of Total Energy Equivalence	106
4.4.1 Thermodynamic Potential and State Equation	107
4.4.2 Dissipation Potential and Evolution Equation of Plastic Damage	108
4.4.3 Dissipation Potential and Evolution Equation of Viscoplastic Damage	109
5 Inelastic Constitutive Equation and Damage Evolution	
Equation of Material with Anisotropic Damage	111
5.1 Elastic-Plastic Anisotropic Damage Theory Based on Second-Order Symmetric Damage Tensor	111
5.1.1 Internal Variables and Thermodynamic Constitutive Theory	111
5.1.2 Helmholtz Free Energy and Elastic Constitutive Equation	113

5.1.3	Dissipation Potential Functions of Plastic Deformation and Damage	115
5.1.4	Plastic Constitutive Equation and Damage Evolution Equation	117
5.2	Elastic-Plastic Anisotropic Damage Theory in Stress Space	119
5.2.1	Thermodynamic Constitutive Theory in Stress Space	119
5.2.2	Gibbs Potential and Elastic Constitutive Equation	120
5.2.3	Dissipation Potential Functions of Plastic Deformation and Damage	123
5.2.4	Plastic Constitutive Equation and Damage Evolution Equation	124
5.3	Fourth-Order Symmetric Damage Tensor and Its Application to Elastic-Plastic-Brittle Damage	126
5.3.1	Constitutive and Evolution Equations for Elastic-Brittle Damage	126
5.3.2	Opening-Closing Effect of Cracks in Brittle Damage Field and Its Mechanical Representation – Positive Projection Tensors for Strain and Stress	127
5.3.3	Effective Elastic Modulus Tensor in Opening and Closing States of Cracks in Brittle Material	132
5.3.4	Damage Variable Defined by the Elastic Modulus Tensor and Its Application to Elastic-Brittle Damage	134
5.3.5	Elastic-Plastic-Brittle Damage Theory Based on an Elastic Modulus Tensor as a Damage Variable	136

Part II Application of Continuum Damage Mechanics

6	Elastic-Plastic Damage	141
6.1	Constitutive and Evolution Equations of Elastic-Plastic Damage – Ductile Damage, Brittle Damage and Quasi-Brittle Damage	141
6.1.1	Constitutive and Evolution Equations of Elastic-Plastic Isotropic Damage	141
6.1.2	Ductile Damage and Brittle Damage	143
6.1.3	Quasi-Brittle Damage and Two-Scale Damage Model	144
6.1.4	Elaboration of Two-Scale Damage Model	147
6.1.5	Threshold Value of Damage Initiation p_D and Critical Value of Fracture D_C	153
6.2	Ductile Damage and Ductile Fracture	153
6.2.1	Mechanical Approaches to Ductile Damage Analysis	153
6.2.2	Ductile Damage Model of Lemaitre	155
6.2.3	Extension of Ductile Damage Model	158
6.2.4	Finite Element Analysis of Ductile Fracture Process	162

6.2.5	Effects of Stress Triaxiality on Damage Criteria and Damage Dissipation Potential	164
6.3	Application to Metal Forming Process	166
6.3.1	Fracture Limit of Sheet Metal Forming	167
6.3.2	Damage Analysis of Forging and Blanking Process	169
6.3.3	Fatigue Life Assessment of a Cold Working Tool	173
6.4	Analysis of Sheet Metal Forming Limit by Anisotropic Damage Theory	176
6.4.1	Elastic-Plastic Constitutive Equation, Evolution Equation of Damage	176
6.4.2	Criteria of Localized Necking and Fracture – Accumulated Damage Instability Criterion	179
6.4.3	Determination of Material Constants for Deformation and Damage	180
6.4.4	Numerical Results of Forming Limit Diagram	182
6.4.5	Other Damage Mechanics Analysis of Forming Limit	183
6.5	Constitutive Equations of Void-Containing Ductile Material	184
6.5.1	Constitutive Model of Gurson	184
6.5.2	Elaboration of Gurson Model—GTN Model	187
6.5.3	Constitutive Model of Rousselier	188
6.5.4	Application to Ductile Fracture Analysis of a Slab in Plane Strain	192
6.5.5	Modification of GTN Model	195
6.6	Continuum Damage Mechanics Theory with Plastic Compressibility	197
6.6.1	Thermodynamic Potential Function	197
6.6.2	Dissipation Potential Function	198
7	Fatigue Damage	201
7.1	High Cycle Fatigue	202
7.1.1	Analysis of High Cycle Fatigue by Two-Scale Damage Model	202
7.1.2	Analysis of High Cycle Fatigue by Elaborated Two-Scale Damage Model	204
7.2	Low Cycle Fatigue	207
7.2.1	Evolution Equation of Uniaxial Low Cycle Fatigue Damage, Fatigue Life Under Constant Strain Amplitude	207
7.2.2	Low Cycle Fatigue Under Variable Stain Amplitude	210
7.3	Uncoupled Numerical Analysis of Very Low Cycle Fatigue	212
8	Creep Damage and Creep-Fatigue Damage	217
8.1	Creep Damage and Phenomenological Theory of Creep Damage	217
8.1.1	Creep Damage	217
8.1.2	Kachanov-Rabotnov Theory	218
8.1.3	Three-Dimensional Creep Damage Theory, Stress Criteria of Creep Damage	221

8.1.4	Theory of Non-Steady State Creep Damage	222
8.1.5	Two-Damage Variable Model of Physics-Based Constitutive Equation	223
8.1.6	Anisotropic Creep Damage Theory	226
8.2	Viscoplastic Damage Theory of Creep Damage	230
8.2.1	Constitutive and Evolution Equations of Viscoplastic Damage Material	231
8.2.2	Creep Damage Under Uniaxial Tension	232
8.2.3	Viscoplastic Damage Theory by Hypothesis of Total Energy Equivalence	234
8.3	Creep-Fatigue Damage	234
8.3.1	Microscopic Mechanisms of Creep-Fatigue Damage and Its Modeling	234
8.3.2	Analysis of Uniaxial Creep-Fatigue Damage	236
8.3.3	Non-isothermal Multiaxial Creep-Fatigue Damage 1 – Modeling of Creep-Fatigue Interaction, Viscoplastic Damage Theory	240
8.3.4	Non-isothermal Multiaxial Creep-Fatigue Damage 2 – Coupled and Uncoupled Analyses by Viscoplastic Damage Theory	242
8.4	Effect of Damage Field on Stress Field at a Creep Crack Tip	247
9	Elastic-Brittle Damage	253
9.1	Damage of Elastic-Brittle Material	253
9.1.1	Damage of Brittle Material	253
9.1.2	Damage Behavior of Concrete	254
9.2	Isotropic Damage Theory of Concrete	257
9.2.1	Damage Variable and Gibbs Potential	258
9.2.2	Evolution Equation of Damage	260
9.3	Anisotropic Brittle Damage Theory by Second-Order Damage Tensor	262
9.3.1	Helmholtz Free Energy for Elastic-Brittle Material	262
9.3.2	Elastic Constitutive Equation, Damage Evolution Equation	264
9.3.3	Elastic-Brittle Damage Analysis of Concrete	266
9.4	Anisotropic Brittle Damage Theory with Elastic Modulus Tensor as Damage Variable	268
9.4.1	Helmholtz Free Energy and Elastic Constitutive Equation	268
9.4.2	Evolution Equation of Brittle Damage	268
9.4.3	Application to Elastic-Brittle Damage Analysis of Mortar	270
9.5	Anisotropic Brittle Damage Theory with Compliance Tensor as Damage Variable	270
9.5.1	Gibbs Potential, Evolution Equation of Damage	271

9.5.2	Unilateral Effect of Elastic Deformation	272
9.5.3	Damage Surface and Loading Criterion	274
9.5.4	Application to Elastic-Brittle Damage of Salem Limestone	275
10	Continuum Damage Mechanics of Composite Materials	277
10.1	Damage of Laminate Composites	277
10.1.1	Damage Variables and Thermodynamic Potential . . .	277
10.1.2	Evolution Equation of Damage Variables	280
10.1.3	Plastic Constitutive Equation of Damaged Material .	281
10.1.4	Application to Laminate Composites	282
10.1.5	Brittle Damage in Fiber Direction	285
10.1.6	Interlaminar Damage and Delamination of Laminate Composites	286
10.1.7	Damage Mesomodel of Laminates	287
10.2	Elastic-Brittle Damage of Ceramic Matrix Composites	288
10.2.1	Elastic-Brittle Damage Behavior of Ceramic Matrix Composites and Its Unilateral Effect	288
10.2.2	Damage Variable and Thermodynamic Potential . . .	289
10.2.3	Damage Potential and Evolution Equation of Damage .	291
10.2.4	Application to Ceramic Matrix Composites	291
10.3	Local Theory of Metal Matrix Composites	294
10.3.1	Local and Overall Configurations of Composites . . .	294
10.3.2	Local-Overall Relations of Stress and Strain	295
10.3.3	Strain- and Stress-Concentration Factors in Matrix and Fiber	296
10.3.4	Local-Overall Relations for Damage State	297
10.3.5	Stress- and Strain-Concentration Factors in Fictitious Undamaged and Current Damaged Configurations	298
10.3.6	Local Stress in Uniaxial Tension of Composites . . .	300
11	Local Approach to Damage and Fracture Analysis	305
11.1	Local Approach to Fracture Based on Continuum Damage Mechanics and Finite Element Method	305
11.1.1	Local Approach to Fracture, Modeling of Fracture . .	305
11.1.2	Mesh-Sensitivity in Local Approach to Fracture . . .	308
11.2	Mesh-Sensitivity in Time-Independent Deformation	308
11.2.1	Stain-Softening and Mesh-Sensitivity	308
11.2.2	Bifurcation of Deformation and Strain Localization .	310
11.3	Regularization of Strain and Damage Localization in Time-Independent Materials	313
11.3.1	Limitation of Mesh Size	313
11.3.2	Mesh-Dependent Softening Modulus – Modification of Material Property by Mesh-Size	314
11.3.3	Nonlocal Damage Theory	314

11.3.4	Gradient-Dependent Theory	316
11.3.5	Cosserat Continuum	317
11.3.6	Artificial Viscosity	317
11.4	Mesh-Sensitivity in Time-Dependent Deformation	317
11.4.1	Mesh-Sensitivity in Creep Crack Analysis	317
11.4.2	Bifurcation and Localization in Time- Dependent Deformation	320
11.5	Causes of Mesh-Sensitivity in Time-Dependent Deformation . .	320
11.5.1	Stress Singularity at Crack Tip	321
11.5.2	Stress-Sensitivity of Damage Evolution Equation and Damage Localization	322
11.5.3	Regularization of Mesh-Sensitivity in Time-Dependent Deformation	322
11.5.4	Analysis of Creep-Crack Extension by Means of Nonlocal Damage Theory	322

Appendix Foundations of Tensor Analysis

12	Foundations of Tensor Analysis – Tensor Algebra and Tensor Calculus	327
12.1	Vectors and Tensors	327
12.1.1	Euclidean Vector Spaces and Tensors	327
12.1.2	Product and Transpose of Tensors	330
12.2	Vector Product, Tensor Product and the Components of Tensors	332
12.2.1	Vector Product and Tensor Product	332
12.2.2	Tensor Components and Their Matrix Representation .	334
12.2.3	Axial Vector of Antisymmetric Tensor	335
12.2.4	Trace and Contraction of Tensors	336
12.2.5	Higher-Order Tensors and Their Tensor Operations .	336
12.3	Orthogonal Transformation, Invariants and Eigenvalues of Tensors	341
12.3.1	Orthogonal Transformation and Similar Tensors . . .	341
12.3.2	Transformation of Bases and that of Tensor Components	342
12.3.3	Trace and Determinant of Tensors	344
12.3.4	Eigenvalues, Eigenvectors and Principal Invariants of Tensors	345
12.3.5	Isotropic Tensor Functions and Orthogonal Invariants .	348
12.4	Differentiation and Integral of Tensor Fields	350
12.4.1	Euclidean Point Space and the Coordinate System . .	350
12.4.2	Differentiation of Tensor Fields	351
12.4.3	Integral of Tensor Fields and Gauss' Theorem	354
12.4.4	Material Time Derivative and Reynolds' Transport Theorem	356
12.5	Differential Calculus of Tensor Functions	358

Contents	xvii
12.5.1 Total Differential and Derivative	358
12.5.2 Derivative of Tensor Functions	359
12.5.3 Derivatives of Invariants	362
12.6 Representation Theorem for Tensor Functions	363
12.6.1 Scalar Invariants of Tensors and Vectors	364
12.6.2 Isotropic Tensor Functions of Tensors and Vectors . . .	364
12.6.3 Representation of Tensor Functions of Higher-Order .	366
12.7 Matrix Representation of Tensors and Tensor Relations	366
12.7.1 Voigt Notation of Hooke's Law	366
12.7.2 Matrix Representation of Tensors of Second- and Fourth-Order	368
12.7.3 Matrix Representation of Symmetric Tenors of Second- and Fourth-Order	369
12.7.4 Elastic Symmetry, Matrices of Elastic Modulus and Elastic Compliance	375
References	381
Bibliography	383
Index	395

List of Symbols

Symbols for Tensors

Light-face Letters	$a, b, \dots, A, B, \dots, \mathcal{A}, \mathcal{B}, \dots,$
Lowercase bold-face Latin letters	$\alpha, \beta \dots, \Gamma, \Delta, \dots$: scalars
Uppercase bold-face Latin letters	$\mathbf{a}, \mathbf{b}, \mathbf{c}, \dots$: vectors
Uppercase blackboard Latin letters	$\mathbb{A}, \mathbb{B}, \mathbb{C}, \dots$: second-order tensors
Uppercase calligraphic Latin letters	$\mathcal{A}, \mathcal{B}, \mathcal{C}, \dots$: fourth-order tensors
	$\mathcal{A}, \mathcal{B}, \mathcal{C}, \dots$: tensors of arbitrary-order

Symbols of Latin Letters

A

$\mathbb{A}^F, \mathbb{A}^M$:	tensors of strain-concentration factors in fiber and matrix of a composite
A :	kinematic hardening variable (or back stress tensor)
A_k :	generalized force vector
dA :	area of surface element
$d\tilde{A}$:	effective area of surface element
dA_D :	reduction in surface element due to voids
\mathbf{a}_p :	basis vectors of six-dimensional space

$$\{\mathbf{a}_p\} = \{\mathbf{e}_{ij}^S\} = \{(\mathbf{e}_i \otimes \mathbf{e}_j)^S\}$$

a :	crack length
-------	--------------

B

$\mathcal{B}^F, \mathcal{B}^M$:	stress-concentration factors in fiber and matrix of a composite
$\mathcal{B}^F, \mathcal{B}^M$:	tensors of stress-concentration factors in fiber and matrix of a composite
B :	body, region occupied by a body, configuration of a body, damage-strengthening variable associated with β

B_f, B_t : fictitious undamaged and current damaged configurations of a body
 ∂B : boundary, surface of body B

C

$C_0, \mathbb{C}(\mathcal{D})$: elastic modulus tensors of undamaged and damaged materials
 C_{AC} : activated elastic modulus tensor
 C_{EF} : effective elastic modulus tensor
 C_{pq} : components of elastic modulus matrix in Voigt notation
 C_{pq} : components of elastic modulus matrix in matrix representation of an elastic constitutive equation $[C_{pq}] = [C_{pr}] [W_{rq}]$
 c^F, c^M : volume fractions of fiber and matrix in a composite

D

$\mathcal{D}, \mathbb{D}, \mathbf{D}, D$: damage tensors of an arbitrary-order, fourth-, second- and 0th-order
 D_C : critical value of \mathcal{D} for fracture initiation
 D_1, D_2, D_F, D_S, D_T : scalar damage variables
 $D_0, D_{ij}, D_{ijkl}, \dots$: fabric tensors

E

\mathcal{E}^n : n-dimensional Euclidean vector space
 E : internal energy of a system
 E, E_0, E_i, E_{ij} : Young's modulus (or modulus of elasticity)
 e_i : orthonormal basis vectors
 e_{ij} : second-order basis tensors $e_{ij} = e_i \otimes e_j$
 e : internal energy per unit mass
 e_{ijk} : permutation tensor (or Eddington epsilon, or Levi-Civita symbol)

F

F : dissipation potential, force, load, yield function
 f : body force vector
 f : yield function, void volume fraction
 f_C : critical void volume fraction

G

G : damage variable
 G, G_i, G_{ij} : shear modulus
 g : temperature gradient $g = -\text{grad}T$

H

- H : strain hardening rate, damage variable
 $H(\cdot)$: Heaviside function $H(x) = 1$ for $x \geq 0$,
 $\quad\quad\quad H(x) = 0$ for $x < 0$
 h : enthalpy per unit mass
 $h(s - x)$: nonlocal weighting function

I

- $\mathbb{I}, \tilde{\mathbb{I}}$: forth-order identity tensors
 \mathbb{I}^S : fourth-order identity tensor transforming a second-order symmetric tensor to itself
 I : identity (or unit) linear transformation, second-order identity (or unit) tensor
 I_1, I_2, I_3 : principal invariants of a second-order tensor

J

- \mathbf{J} : generalized flux vector

K

- K : bulk modulus, kinetic energy of a system

L

- L : segment
 L_{KM} : coefficients in the phenomenological relation of Onsager
 ℓ : characteristic length

M

- \mathbb{M} : damage effect tensor
 M : microscopic volume element

N

- N_p : basis of six-dimensional vector space spanned by the dyad $\mathbf{n}_i \otimes \mathbf{n}_j$ of principal damage directions
 N : number of loading cycles
 N_C : number of cycles to fracture due to creep damage
 N_D : number of cycles to microcrack initiation

- N_F : crack extension life (number of cycles for a microcrack to grow to a crack of mesoscale)
 N_R : fatigue life (number of cycles to fatigue fracture)
 \mathbf{n} : unit normal vector
 \mathbf{n}_i : vectors of principal directions of a second-order tensor
 n : creep exponent, strain hardening exponent

O

- \mathbf{O} : zero linear transformation, zero tensor
 \mathbf{O} : origin of a coordinate system

P

- \mathcal{P}^3 : three-dimensional Euclidean point space
 \mathbb{P}_D : fourth-order projection tensor of a principal damage direction \mathbf{n}^D

$$\mathbb{P}_D = \mathbf{n}^D \otimes \mathbf{n}^D \otimes \mathbf{n}^D \otimes \mathbf{n}^D$$

- \mathbb{P}_i : fourth-order projection tensor of a direction \mathbf{n}_i

$$\mathbb{P}_i = \mathbf{n}_i \otimes \mathbf{n}_i \otimes \mathbf{n}_i \otimes \mathbf{n}_i$$

- \mathbb{P}_ε^+ : positive orthogonal projection tensor of strain tensor $\boldsymbol{\varepsilon}$

$$\mathbb{P}_\varepsilon^+ \equiv \sum_{i=1}^3 \sum_{j=1}^3 H(\varepsilon_i) H(\varepsilon_j) \delta_{ik} \delta_{jl} \mathbf{n}_i^{(\varepsilon)} \otimes \mathbf{n}_j^{(\varepsilon)} \otimes \mathbf{n}_k^{(\varepsilon)} \otimes \mathbf{n}_l^{(\varepsilon)}$$

- \mathbb{P}_ε^- : negative orthogonal projection tensor of strain tensor $\boldsymbol{\varepsilon}$

$$\mathbb{P}_\varepsilon^- = \mathbb{I} - \mathbb{P}_\varepsilon^+$$

- \mathbb{P}_σ^+ : positive orthogonal projection tensor of stress tensor $\boldsymbol{\sigma}$

$$\mathbb{P}_\sigma^+ \equiv \sum_{i=1}^3 \sum_{j=1}^3 H(\sigma_i) H(\sigma_j) \delta_{ik} \delta_{jl} \mathbf{n}_i^{(\sigma)} \otimes \mathbf{n}_j^{(\sigma)} \otimes \mathbf{n}_k^{(\sigma)} \otimes \mathbf{n}_l^{(\sigma)}$$

- \mathbb{P}_σ^- : negative orthogonal projection tensor of stress tensor $\boldsymbol{\sigma}$

$$\mathbb{P}_\sigma^- = \mathbb{I} - \mathbb{P}_\sigma^+$$

- \mathbf{P} : a material point, a point in Euclidean point space
 p : accumulated equivalent plastic strain $p = \int \dot{\varepsilon}_{EQ}^p dt$

- p_D : threshold of accumulated equivalent plastic strain for damage initiation
 p_R : accumulated equivalent plastic strain at fracture, equivalent plastic strain at fracture

Q

- Q : orthogonal tensor, orthogonal transformation
 Q : a material point, a point in Euclidean point space
 \dot{Q} : rate of heat supply to a system
 \mathbf{q} : heat flux vector

R

- R : a material point, a point in Euclidean point space
 R : isotropic hardening variable, average radius of spherical voids
 R_v : stress triaxiality function

$$R_v = (2/3)(1 + \nu) + 3(1 - 2\nu) (\sigma_H/\sigma_{EQ})^{1/2}$$

- r : isotropic hardening internal variable, heat generation rate per unit volume

S

- $\mathbb{S}, \mathbb{S}(\mathcal{D})$: elastic compliance tenors of undamaged and damaged materials
 S : boundary, surface, entropy of a system
 S_{pq} : components of elastic compliance matrix in Voigt notation
 S_{pq} : components of elastic compliance matrix in matrix representation of elastic constitutive equation $[S_{pq}] = [S_{pr}] [W_{rq}]$
 dS : surface element
 s : entropy per unit mass

T

- \mathbf{T}^v : surface force vector (or traction vector)
 T : absolute temperature
 t : surface force vector (or traction vector)
 t : time
 t_R : creep rupture time
 t_0 : time of creep damage initiation

U

- \mathbf{u} : displacement vector
 $\mathbf{u}^{(1)}, \mathbf{u}^{(2)}, \mathbf{u}^{(3)}$: eigen vectors (or principal directions) of a second-order tensor

V

$V_k:$	vector of internal variables
$\dot{V}_k:$	generalized flux vector
$V_p:$	internal variable of plastic deformation
$V:$	region occupied by a body, volume of a material
$V_0(\sigma, \alpha), V(\sigma, \mathcal{D}, \alpha):$	complementary strain energy functions of undamaged and damaged materials
$dV, dV_0, dV_\xi:$	volume elements
$v:$	velocity vector

W

$W:$	work done by external forces
$W^E:$	elastic strain energy per unit volume
$W_0(\varepsilon, \alpha), W(\varepsilon, \mathcal{D}, \alpha):$	strain energy functions of undamaged and damaged materials
$W_D:$	energy stored up to damage initiation
$W_S:$	energy stored in material
$W_{pq}:$	components of weighting matrix
$\dot{W}:$	rate of external mechanical work (or external mechanical power)
$\Delta W:$	energy per loading cycle

X

$X:$	generalized force vector
$x:$	position, position vector of a material point
$x_i:$	coordinates

Y

$\mathbb{Y}, Y, \mathcal{Y}:$	generalized forces associated with \mathbb{D}, \mathcal{D} and D (or damage-associated variables)
-------------------------------	---

Symbols of Greek Letters**A**

$\alpha:$	kinematic hardening internal variable (or associated variable of A)
-----------	--

B

β : damage-strengthening internal variable (or associated variable of B)

 Γ

Γ : Gibbs potential per unit mass

γ_p : components of column vector of engineering strain

γ_{ij} : shear strain

 Δ

δ_{ij} : Kronecker delta $\delta_{ij} = 1$ for $i = j$,
 $\delta_{ij} = 0$ for $i \neq j$

E

$\boldsymbol{\varepsilon}, \boldsymbol{\varepsilon}^e, \boldsymbol{\varepsilon}^D, \boldsymbol{\varepsilon}^v$: strain tensors
 $\boldsymbol{\varepsilon}^D$: deviatoric strain tensor $\boldsymbol{\varepsilon}^D = \boldsymbol{\varepsilon} - (1/3) (tr\boldsymbol{\varepsilon}) \mathbf{I}$
 $\boldsymbol{\varepsilon}^+$: positive-valued strain tensor $\boldsymbol{\varepsilon}^+ = \mathbb{P}_\varepsilon^+ : \boldsymbol{\varepsilon}$
 $\boldsymbol{\varepsilon}^-$: negative-valued strain tensor $\boldsymbol{\varepsilon}^- = \mathbb{P}_\varepsilon^- : \boldsymbol{\varepsilon}$
 ε_{EQ} : equivalent strain $\varepsilon_{EQ} = [(2/3) \varepsilon_{ij}^D \varepsilon_{ij}^D]^{1/2}$
 ε_H : mean strain $\varepsilon_H = (1/3) \varepsilon_{kk}$
 ε_p : strain components in Voigt notation
 $\Delta\varepsilon$: strain range

Z

ς : material constant

H

η : material constant characterizing the opening-closing effect of a crack

 Θ

θ : angle

 Λ

$\dot{\Lambda}$: indeterminate multiplier of plastic and/or damage evolution equation
 λ : stress singularity exponent at crack tip

λ : Lamé constant $\lambda = 2G\nu / (1 - 2\nu)$
 $\lambda_1, \lambda_2, \lambda_3$: eigen values (or principal values) of a second-order tensor

M

μ : Lamé constant $\mu = G$

N

ν : unit normal vector
 ν, ν_i, ν_{ij} : Poisson's ratio

E

ξ : void density, void volume fraction
 $\xi(\mathbf{n})$: distribution function of void density

P

ρ : mass density

Sigma

σ : stress tensor
 σ^D : deviatoric stress tensor $\sigma^D = \sigma - (1/3) (\text{tr}\sigma) \mathbf{I}$
 σ^+ : positive-valued stress tensor $\sigma^+ = \mathbb{P}_\sigma^+ : \sigma$
 σ^- : negative-valued stress tensor $\sigma^- = \mathbb{P}_\sigma^- : \sigma$
 σ_{EQ} : equivalent stress $\sigma_{EQ} = [(3/2) \sigma_{ij}^D \sigma_{ij}^D]^{1/2}$
 σ_F : fatigue limit
 σ_H : mean stress (or hydrostatic stress) $\sigma_H = (1/3) \sigma_{kk}$
 σ_R : fracture stress
 σ_U : tensile strength
 σ_V : viscous stress
 σ_Y : yield stress
 σ_a : stress amplitude
 σ_p : stress components in Voigt notation
 $\Delta\sigma$: stress range

T

τ : shear stress

Φ

Φ : dissipation per unit volume
 $\Phi(r, \theta)$: stress function of asymptotic stress field

 X

$\chi(\sigma_{ij})$: stress criterion of damage or fracture

 Ψ

ψ : Helmholtz free-energy per unit mass
 ψ : damage variable $\psi = 1 - D$

 Ω

Ω : solid angle, region of three-dimensional Euclidean point space
 Ω_C, Ω_F : damage variables of creep and fatigue

Symbols for Operation

(·): scalar product, contraction^{1*} $\mathbf{u} \cdot \mathbf{v} = u_i v_i$
(:): double contraction $\mathbf{A} : \mathbf{B} = A_{ij} B_{ij}$
(×): vector product $\mathbf{u} \times \mathbf{v} = e_{ijk} u_j v_k \mathbf{e}_i$
⊗: tensor product
tensor product of vectors $\mathbf{a} \otimes \mathbf{b} = a_i b_j \mathbf{e}_i \otimes \mathbf{e}_j$
tensor product of second-order tensors 1

$$\mathbf{A} \otimes \mathbf{B} = A_{ij} B_{kl} \mathbf{e}_i \otimes \mathbf{e}_j \otimes \mathbf{e}_k \otimes \mathbf{e}_l$$

⊗: tensor product of second-order tensor 2

$$\mathbf{A} \underline{\otimes} \mathbf{B} = A_{ik} B_{jl} \mathbf{e}_i \otimes \mathbf{e}_j \otimes \mathbf{e}_k \otimes \mathbf{e}_l$$

⊗: tensor product of second-order tensor 3

$$\mathbf{A} \overline{\otimes} \mathbf{B} = A_{il} B_{jk} \mathbf{e}_i \otimes \mathbf{e}_j \otimes \mathbf{e}_k \otimes \mathbf{e}_l$$

⊗: tensor product of second-order tensor 4

$$\mathbf{A} \underline{\overline{\otimes}} \mathbf{B} = \frac{1}{2} (A_{ik} B_{jl} + A_{il} B_{jk}) \mathbf{e}_i \otimes \mathbf{e}_j \otimes \mathbf{e}_k \otimes \mathbf{e}_l$$

¹ In the case of scalar product between a tensor and a vector, or between two tensors, the dot (·) representing scalar product is usually omitted by convention. See Eqs. (12.8) through (12.12) in Appendix and the related foot note

∂_i :	partial derivative with respect to coordinate x_i
∇ :	vector operator (or Nabla, or del operator)
$\text{grad}f$:	gradient of scalar field f
$\text{grad}f$:	gradient of vector f
$\text{div}f$:	divergence of vector f
$\text{curl}f$:	curl (or rotation) of vector f

$$\text{curl}f = \begin{cases} f \times \nabla = e_{ijk} (\partial f_i / \partial x_j) \mathbf{e}_k \\ \nabla \times f = e_{ijk} (\partial f_j / \partial x_i) \mathbf{e}_k \end{cases}$$

(\cdot) :	time derivative
(\cdot) :	material time derivative
$\det A$:	determinant of tensor A
$\text{tr}A$:	trace of tensor A
A^T :	transpose of tensor A
	$A\mathbf{u} \cdot \mathbf{v} = \mathbf{u} \cdot A^T \mathbf{v}$
	for arbitrary vectors \mathbf{u} and \mathbf{v}
$ \cdot $:	absolute value (or norm, or magnitude)
$[\cdot]$:	matrix
$\llbracket \cdot \rrbracket$:	discontinuity
$\langle \cdot \rangle$:	Macauley bracket
	$\langle x \rangle = H(x)x$

Symbols for Indices

$(\cdot)^A$:	antisymmetric (or skew-symmetric) part of a tensor
$(\cdot)^C$, $(\cdot)^c$:	creep
$(\cdot)^D$:	deviatoric tensor, damage
$(\cdot)^E$, $(\cdot)^e$:	elasticity
$(\cdot)^F$:	fiber of composites
$(\cdot)^I$:	isotropic hardening
$(\cdot)^{IN}$:	inelasticity
$(\cdot)^K$:	kinematic hardening
$(\cdot)^M$:	microscopic element, matrix of composites
$(\cdot)^P$, $(\cdot)^p$:	plasticity
$(\cdot)^S$:	symmetric part of a tensor
$(\cdot)^T$:	transpose of a tensor
$(\cdot)^{VP}$:	viscoplasticity
$(\cdot)^{-1}$:	inverse tensor, inverse transformation
$(\cdot)_C$:	creep
$(\cdot)_D$:	threshold for damage initiation
$(\cdot)_{EQ}$:	equivalent stress, equivalent strain
$(\cdot)_F$:	fatigue, fiber breakage

() _H :	mean stress, mean strain
() _R :	fracture, rupture
() _S :	shear, stored energy
() _T :	tension
() _U :	uniaxial state
([~]):	effective stress, effective strain, fictitious undamaged configuration
(⁻):	similar tensor $\bar{S} = QSQ^T$, similar vector $\bar{u} = Qu$

Part I

Foundations of Continuum

Damage Mechanics

Chapter 1

Material Damage and Continuum Damage Mechanics

Continuum damage mechanics is a mechanical theory for analyzing damage and fracture processes in materials from a continuum mechanics point of view. The present chapter starts with the notion of material damage and that of continuum damage mechanics. Section 1.1 is concerned with the definition of *damage*, its mechanical aspects observed in different scales, the physical mechanisms of damage development, and its examples encountered in the engineering problems of strength and fracture. In Section 1.2, furthermore, fundamental notion of continuum damage mechanics and of the mechanical procedures of its formulation and applications will be discussed.

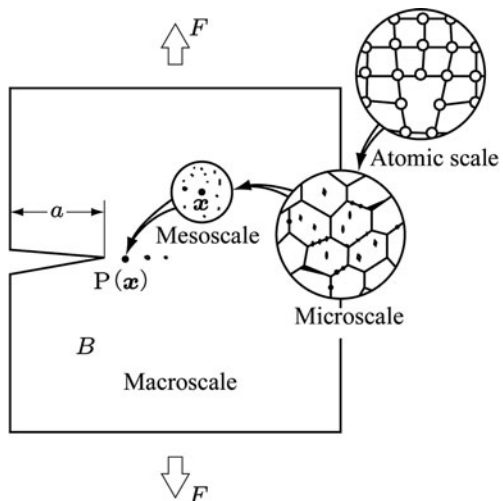
1.1 Damage and Its Microscopic Mechanisms

Consider a body B of Fig. 1.1, where a crack of length a has developed due to the action of an external load F . If we take an arbitrary point $P(x)$ near the crack tip, a number of microscopic cavities or microcracks would be observed in the region around the point $P(x)$. These cavities can be nucleated usually as a result of breakage of atomic bonds, or of some defects in atomic array.

The fracture of materials, therefore, is a process of the nucleation of microcavities or microcracks due to the breakage of atomic bonds from the *microscopic* view point. From the *macroscopic* point of view, however, it is a process of the extension of cracks brought about by the coalescence of these microcavities. Between these two processes, there exists a *mesoscopic* process where the nucleation, growth and the coalescence of the microscopic cavities leads to the initiation of a macroscopic crack.

The development of cavities in the microscopic, mesoscopic and the macroscopic processes of fracture in materials together with the resulting deterioration in their mechanical properties are called *damage* (Lemaitre and Chaboche 1978; Murakami 1983; Krajcinovic 1984). Continuum damage mechanics, in particular, aims at the analysis of the damage development in mesoscopic and macroscopic fracture processes in the framework of continuum mechanics.

Fig. 1.1 Scales of damage observation



We start this chapter by elucidating different scales of the damage observation, and by examining the mechanisms of the nucleation and the development of damage observed in these scales.

1.1.1 Scales of Damage Phenomena

As observed in Fig. 1.1, the phenomena of damage show different aspects according to the scales or the range of observation, and can be discussed on the following four scales:

(1) Atomic Scale

The mechanical properties of materials are determined by the constituent atoms or molecules, their array, and the kind of interatomic or intermolecular forces between them. The damage of materials in the atomic scale is induced by the separation of these interatomic or intermolecular bonds.

(2) Microscopic Scale

When a material is observed in a certain scale, though the visual field has a discontinuous structure as a whole, there may exist partly continuous regions in the material. This scale level is usually called the *microscale*. Thus damage in the microscale, i.e., microscopic damage, is found in *microcavities*, *microcracks*, or in the *decohesion* in microstructures of materials. Fiber breakage and decohesion of fiber-matrix interface in fiber-reinforced composites are examples of the last case.

(3) Mesoscopic Scale

Actual materials contain various microscopic discontinuities, e.g., microcavities, microcracks, crystal grains or inclusions. We consider a small region of an appropriate scale around an arbitrary point $P(x)$ of a material. If the value representing a mechanical property or a mechanical state of the material averaged over the small region can be expressed as a continuous function of the position x of the material point P , then the material can be idealized as a continuum. Then, the scale of the region is said to be *mesoscale*.

(4) Macroscopic Scale

If every point in a material can be viewed as a material point in a continuum, the scale of the observation is called *macroscale*. The material in this scale can be assumed to consist of material point distributed continuously in the material, and the material density as well as the relevant physical quantities can be defined in the material. An example of damage on the macroscale is a crack in the materials of sufficiently large size.

1.1.2 Physical Mechanisms of Damage

As observed in Fig. 1.2a, the separation of atomic bonds is induced by either *tensile* or *shear decohesion*. However, the separation of material at the microscopic level, i.e., the microscopic mechanism of material damage, consists of the four mechanisms shown in Fig. 1.2b:

(1) Cleavage

In crystalline materials like inorganic materials or body centered cubic metals, tensile decohesion is often observed in crystal planes intrinsic to the crystals. This

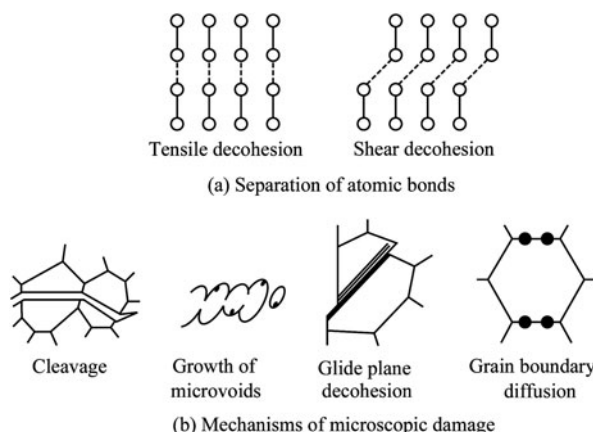


Fig. 1.2 Separation of atomic bonds and the mechanisms of microscopic damage

decohesion is called *cleavage*. Cleavage occurs preferentially on lattice planes of the weakest interatomic or intermolecular cohesive force, and is hardly accompanied by plastic deformation. Cleavage is induced usually by stress concentrations at defects in material. Cleavage may be brought about also on grain boundaries or in grains, due to the stress concentration induced by the constraint of the dislocation motion on the slip plane.

(2) Growth and Coalescence of Microvoids

When a ductile material is subject to large plastic deformation, decohesion of the interface between the matrix and inclusions, or fracture of inclusions may occur. The sites of the separation grow into microvoids. The cause of the decohesion or the fracture of inclusions is mainly due to the stress concentration induced by pile-up of dislocations to inclusions. In the fracture surface, furthermore, a number of *dimples*, i.e., dents produced by the growth and the coalescence of microvoids starting from inclusions, are observed.

Coalescence of voids due to plastic deformation proceeds either by the necking of materials among microvoids or by their shear fracture.

(3) Glide Plane Decohesion

Nucleation of new surfaces on specific slip planes due to large plastic deformation and the resulting fracture of crystalline material are called *glide plane decohesion*. In high purity metals, for example, there are no inclusions which furnish the nuclei for void formation. The shear stress induced by tension, however, gives large shear deformation in these metals. As a result of this large shear deformation, the cross sectional area of the material reduces almost to zero. This type of fracture is called *point fracture* or *chisel edge fracture*.

The glide plane decohesion is known also as the mechanism of nucleation and growth of fatigue cracks.

(4) Void Growth due to Grain-Boundary Diffusion

In metallic materials, thermal activation plays an important role at temperature higher than 1/3 of the absolute melting temperature T_m . When polycrystalline metals are subject to static load at high temperature for long time, diffusion of vacancies gives rise to cavities mainly on grain boundaries perpendicular to the tensile stress. The growth of these cavities leads to microscopic decohesion.

1.1.3 Damage in Fracture Problems

The development of cavities at microscopic, mesoscopic or macroscopic level and the resulting deterioration in mechanical properties are defined as *damage*. The

aspects of damage vary largely by the difference in materials and loading conditions. The damage may be classified phenomenologically as follows (Lemaitre 1992; Murakami 1993; François et al. 1998):

(1) Ductile Damage

Development of microvoids due to large plastic deformation is called *ductile damage*. In metallic material the damage is induced by the fracture of inclusions, or by the decohesion of inclusion-matrix interface as a result of large plastic deformation. The ductile damage, therefore, is one of the typical damage in engineering fracture problems. Figure 1.3 shows an example of ductile damage in copper.

(2) Brittle Damage

Nucleation of microvoids or microcracks and their coalescence can occur without plastic deformation not only in macroscopic but also in mesoscopic level. The deterioration of materials of this aspect is called *brittle damage*. This damage is observed mainly in rocks, concrete, ceramics and composite materials, where the cohesive strength is lower than the slip strength. Figure 1.4 is an example of brittle damage in a block of granite.

(3) Creep Damage

When polycrystalline metals are subject to static stress at temperature higher than $1/3$ of the absolute melting temperature T_m , microvoids or microcracks nucleate and grow mainly on grain boundaries perpendicular to the tensile stress, or at the grain boundary triple points (Evans 1984; François et al. 1998). This material deterioration is known as *creep damage*. Cavities of creep damage usually propagate and

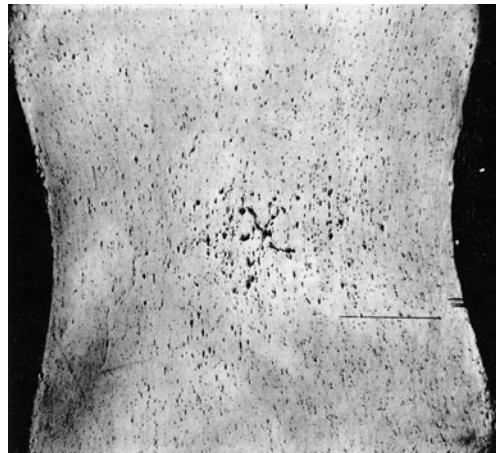


Fig. 1.3 Development of microvoids in ductile damage of copper

Source: Bluhm and Morrissey (1966, p. 1772, Fig. 31)

Fig. 1.4 Distribution of microcracks in Toki granite
Source: Yoshida and Ichikawa (2007)

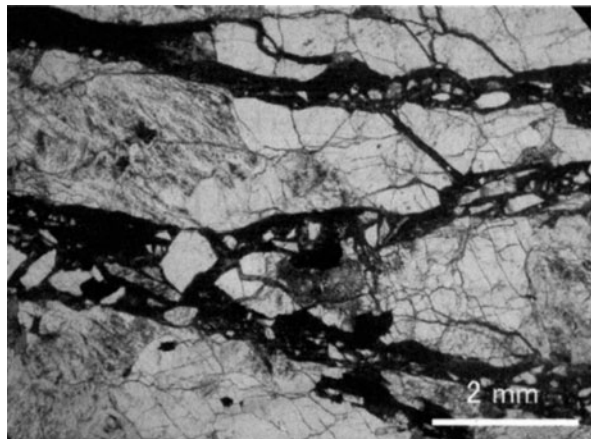
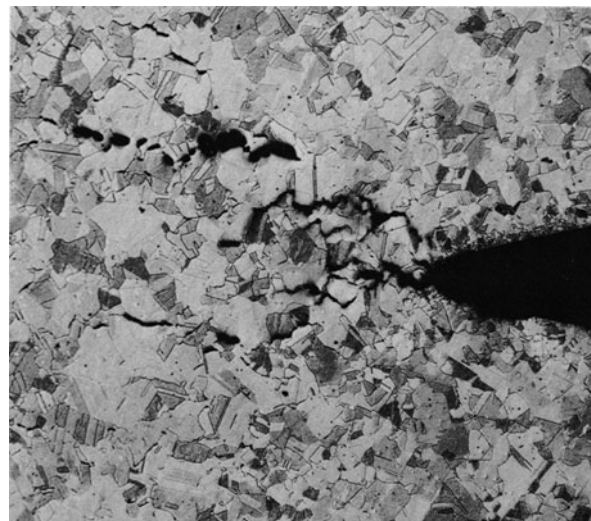


Fig. 1.5 Creep damage and creep cracks in copper at 250°C
Source: Hayhurst et al. (1984, plate 4, Fig. 11(b))



coalesce over the material with time into macroscopic cracks, and lead to eventual fracture called *creep rupture*. Figure 1.5 shows the grain boundary cavities in creep damage of copper.

(4) Low Cycle Fatigue

When cyclic load is applied to a material, microcavities may be induced as a result of irreversible plastic deformation. These cavities may grow to form cracks and give rise to final fracture of the material. The deterioration of the material in this process is called *fatigue damage*.

In the case of metals, in particular, cyclic load causes local transgranular slips. The accumulation of the slip on the material surface induces the glide plane decohesion on the surface, and leads to the initiation of microcracks. When the material is subject to cycles of large stress, transgranular slips are accumulated in a number of crystal grains on the material surface, and cause *fatigue fracture* in relatively small number of stress or strain cycles. The fatigue damage with the number of cycles to fracture $N_R < 10^4$ is classified as *low cycle fatigue*. Figure 1.6 shows an example of the low cycle fatigue of Inconel 718.

(5) Very Low Cycle Fatigue

In the category of low cycle fatigue, fatigue with the number of cycles to fracture $N_R < 10^2$, in particular, is said to be *very low cycle fatigue*. To this range of load, the life assessment rule for usual low cycle fatigue is not applicable any more; the fatigue fracture occurs at smaller number of cycles than predicted by the usual rule of low cycle fatigue (Dufailly and Lemaître 1995). This is an important fact for the assessment of the damage attained by the preliminary tests of heavy load apparatus or for the remaining life prediction of over stress structures.

(6) High Cycle Fatigue Damage

For fatigue under low level of cyclic load, on the other hand, plastic strain in mesoscale is so small that the transgranular slips occur only in limited number of grains on the material surface. Moreover, the damage growth in one cycle of strain is small, and a large number of cycles of load are needed for the fracture to occur. Fatigue with number of cycles to fracture $N_R > 10^5$ is called *high cycle fatigue*.

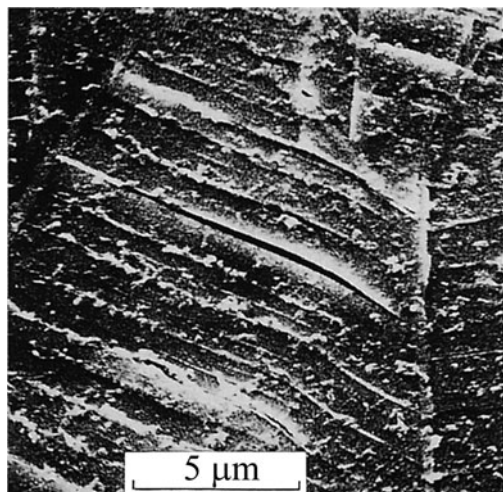


Fig. 1.6 Glide plane decohesion in low cycle fatigue damage of Inconel 718
Source: François et al. (1998, Vol. II, p. 93, Fig. 28(b))

Microcracks observed in high cycle fatigue start from small limited sites on the material surface, and develop along localized fracture surfaces.

(7) Very High Cycle Fatigue Damage

In high cycle fatigue of iron and steel, it has been supposed that the fatigue fracture would never occur if the applied load permits the repetition of loads up to $N = 10^6 \sim 10^7$ without fracture, and the corresponding magnitude of the load has been defied as *fatigue limit*.

In recent years, however, it was elucidated that, depending on the kind of materials or on the loading conditions, fatigue crack can nucleate from sites inside the material by the cyclic stress lower than the fatigue limit, by the number of stress cycles $N > 10^7$ (specifically $N = 10^8$ through 10^{10}). This kind of fatigue is known as *very high cycle fatigue* or *ultrahigh cycle fatigue* (Bathias and Paris 2005).

(8) Creep-Fatigue Damage

When polycrystalline metals are subject to cyclic load at elevated temperature, both creep damage and fatigue damage may occur at the same time. Creep damage develops, as already described, by the grain boundary cavitation throughout the metal. Fatigue damage, on the other hand, proceeds from transgranular microcracks on the surface of the material. Because of this difference in the physical mechanisms, interaction between both damages is not significant in early stage of damage. In the later stage of damage, however, these two kinds of damage start to influence each other. The damage in this stage is called *creep-fatigue damage* or *creep-fatigue interaction*. Since fatigue damage develops in more localized region, the effect of fatigue damage on creep damage is not as large as that of the creep damage on fatigue damage.

(9) Spall Damage

In a material subject to an intensive impact load, a number of microvoids may be nucleated and develop by the reflection and the interference of incident stress waves. This is referred to as *spall damage*. As the duration of the action of stress is quite short, the cavities cannot grow significantly. When the stress induced by the impact is large enough, the coalescence of cavities will give rise to a macrocrack, or a fracture surface called a *spall plane*.

The material damage described above are all brought about by the action of stress or strain. The ductile, brittle, fatigue and spall damage, among them, are caused as a result of elastic or elastic-plastic deformation, and are called *elastic damage* or *elastic-plastic damage*. Since the creep damage or creep-fatigue damage, on the other hand, are induced by the time-dependent deformation, they are sometimes called *viscous damage* or *viscoplastic damage*.

1.2 Representative Volume Element and Continuum Damage Mechanics

1.2.1 Representative Volume Element

In order to discuss the effects of microscopic discontinuities (e.g., voids, crystal grains, inclusions etc.) in materials by means of continuum mechanics, we must homogenize the mechanical effects of the microstructure, and represent them as a macroscopic continuous field in the material.

For this purpose, we take a small region V of a *mesoscale* around a material point $P(x)$ in a body B as shown in Fig. 1.7. We assume that the material with discontinuous structures in region V can be statistically homogeneous and the mechanical state of the material in V can be represented by the statistical average of the mechanical variables in V . If the volume element V is the smallest for which this condition is satisfied, the region V is said to be the *Representative Volume Element* (RVE) (Hill 1963; Hashin 1983).

Namely, if we can take an RVE of the proper size at each point of the body B , a material with microstructures can be idealized as a continuum by means of the statistical average of the mechanical state in the material. The mechanical state of the continuum is unique only if the RVE is the statistical representation of the actual material. For such RVE, the following two conditions should be satisfied:

- (1) For the material in the RVE to be statistically homogeneous, the RVE should be large enough to contain a sufficient number of discontinuities.

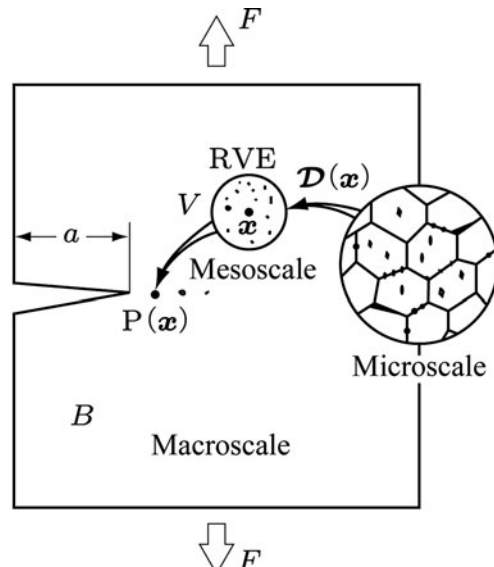


Fig. 1.7 Notion of representative volume element and continuum damage mechanics

- (2) In order to represent a non-uniform macroscopic mechanical field by means of a continuum, the size of RVE should be sufficiently small so that the variation of the macroscopic variable in it may be insignificantly small.

The size required for a volume to be an RVE depends on the microstructures of the relevant material, and their typical sizes are as follow (Lemaitre and Dufailly 1987; Lemaitre 1992):

(1) Metal and ceramics	$(0.1 \text{ mm})^3$
(2) Polymer and composites	$(1 \text{ mm})^3$
(3) Timber	$(10 \text{ mm})^3$
(4) Concrete	$(100 \text{ mm})^3$

The size of RVE depends also on the mechanical phenomena under discussion. Among damage phenomena, brittle damage and fatigue damage are much more localized than creep damage and ductile damage; the size of an RVE required to represent the brittle and the fatigue damage should be larger than that for creep damage and ductile damage.

1.2.2 Notion of Continuum Damage Mechanics

The mechanics in which material damage and its mechanical effects are discussed in the framework of continuum mechanics is referred to as *Continuum Damage Mechanics* (CDM) or simply as *Damage Mechanics* (Janson and Hult 1977; Kachanov 1986; Lemaitre 1992; Krajcinovic 1996). Namely, continuum damage mechanics is a branch of continuum mechanics used to describe the damage and fracture process ranging from the initiation of microcavities or microcracks to the final fracture in materials caused by the development of macrocracks.

Let us note Fig. 1.7 once more. Suppose that a number of microcavities have nucleated and developed in a material B shown in the figure. It is unrealistic and even impossible to describe the details of the evolution of each cavity. However, if we take the notion of a representative volume element (RVE) V at a point $P(x)$ sufficiently small in comparison with the body B , the mechanical effect of void distribution can be described by the continuum fields of mechanical variables defined in V .

According to the *principle of local state* (Kestin and Rice 1970; Germain 1973), the thermodynamic state at a point of a continuum can be described by *state variables* at the point. Damage state at a point is an internal state of material, which from mechanical point of view, can be represented by a properly defined internal variable, i.e., *damage variable* $\mathcal{D}(x)$. Since nucleation and development of microcracks depend on the direction of stress or strain acting in the volume element V , the internal variable $\mathcal{D}(x)$ in general should have the tensor character.

By means of continuum damage mechanics, therefore, a problem of damage and fracture caused by the development of distributed cavities can be analyzed in the framework of continuum mechanics by the following procedures:

- (1) Representing the damage state by means of a damage variable $\mathcal{D}(\mathbf{x})$.
- (2) Formulating an equation governing the development of the damage variable (i.e., evolution equation).
- (3) Formulating an equation describing the mechanical behavior of the damaged material (i.e., constitutive equation).
- (4) Solving the initial- and boundary-value problem by the use of these equations.

Procedure (1), i.e. mechanical representation of the damage state, will be discussed in detail in [Chapter 2](#). Procedures (2) and (3), i.e., the formulation of evolution and constitutive equations of a damaged material, on the other hand, can be performed systematically on the basis of the thermodynamic theory for constitutive equations to be explained in [Chapter 3](#).

Application of continuum damage mechanics to engineering problems of damage and fracture is discussed in [Chapter 4](#) and the subsequent chapters of this book.

Continuum damage mechanics has been formulated mainly in the mathematical framework of tensor algebra and tensor calculus. The foundations of tensor analysis are presented in some detail in [Chapter 12](#) for readers not familiar enough with this important subject.

Chapter 2

Mechanical Representation of Damage and Damage Variables

The procedure of the continuum damage mechanics is to represent first the damage state of a material in terms of properly defined *damage variables*, and then to describe the mechanical behavior of the damaged material and the further development of the damage by the use of these damage variables.

In Section 2.1, methods of the mechanical modeling of material damage are described in the case of uniaxial state of stress. Then Section 2.2 is concerned with extensive discussion of the three-dimensional modeling of material damage and the resulting damage variables, because this is one of the most important problems to secure the reliability of the continuum damage mechanics.

The mechanical behavior of a damaged material is usually described by using the notion of the *effective stress*, together with the *hypothesis of mechanical equivalence* between the damaged and the undamaged material. Different definitions of the effective stress (and/or effective mechanical variables) together with the concept of the mechanical equivalence will be discussed in Section 2.3.

In order to show the applicability of the notion of effective stress and the mechanical equivalence, variation of elastic properties caused by the damage development will be analyzed in Section 2.4 by the use of these methods. Finally, a few remarks will be given in Section 2.5 on criticisms about the theoretical rigor and the mechanical consistency of the current framework of continuum damage mechanics.

2.1 Mechanical Modeling of Damage

Proper modeling of material damage necessitates appropriate solutions to each of the following three procedures;

- (1) What a meso-mechanical effect is brought into focus for the definition of the damage?
- (2) What kind of mathematical (tensorial) property is prescribed to define the damage variable to describe the damage rate?
- (3) How can the magnitude of the damage variable be quantified?

Among these problems, the quantification of the damage variable of (3) can be solved by measuring the meso-mechanical effect of (1).

In this section, we will start with the one-dimensional model of damage, and discuss three fundamental methods of damage modeling.

2.1.1 Modeling by Effective Area Reduction

The notion of continuum damage mechanics was proposed first by Kachanov when he tried to predict the brittle creep rupture time of metals under constant tension (Kachanov 1958). By noting that the creep damage is brought about by the development of microscopic voids in creep process, he represented the damage state by a scalar damage variable ψ ($0 \leq \psi \leq 1$), where $\psi = 1$ and $\psi = 0$ signify the initial undamaged state and the final completely damaged state, respectively. In addition, Kachanov described the damage development by means of an evolution equation

$$\dot{\psi} = -A \left(\frac{\sigma}{\psi} \right)^m, \quad (2.1)$$

where (\cdot) and σ denote the time derivative and the stress, while A and m are material constants.

Later Rabotnov (1968, 1969) modified this *Kachanov theory* by introducing an alternative damage variable $D = 1 - \psi$ ($0 \leq D \leq 1$) and by postulating that the damage has the effect also on creep rate $\dot{\varepsilon}$ as follows:

$$\dot{D} = A \left(\frac{\sigma}{1 - D} \right)^m, \quad (2.2a)$$

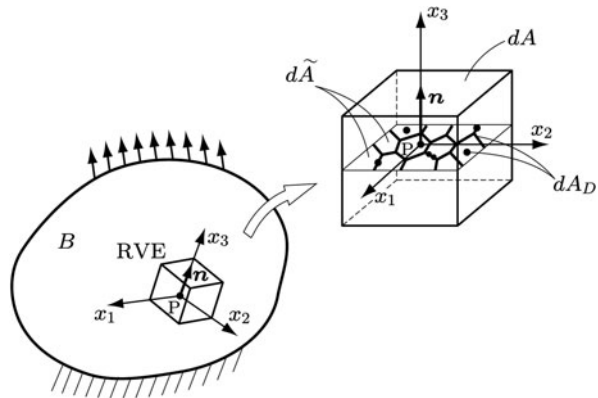
$$\dot{\varepsilon} = B \left(\frac{\sigma}{1 - D} \right)^n, \quad (2.2b)$$

where B and n as well as A and m are material constants. Equation (2.2) is known as *Kachanov-Rabotnov theory*, and has been the prototype of continuum damage mechanics model developed thereafter. The physical meaning of ψ and D is usually interpreted as the decrease in the *load carrying effective area* due to void development (Kachanov 1958, 1986; Rabotnov 1968).

Suppose a body B of Fig. 2.1. Let us take a representative volume element (RVE) at an arbitrary point $P(x)$ in B , and consider the *damage state* of a surface element dA of a unit normal vector \mathbf{n} at P . If the total void area in dA is dA_D , the mechanical effect of dA will be decreased by dA_D . Then the area

$$d\tilde{A} = dA - dA_D \quad (2.3)$$

Fig. 2.1 Effective area reduction due to void development



may be interpreted as the area which carries the internal force on the surface element dA , and is called *effective area*¹ (Kachanov 1986).

Thus, the damage variable ψ and D may be expressed by

$$\psi(\mathbf{x}, \mathbf{n}) = \frac{d\tilde{A}}{dA}, \quad (2.4a)$$

$$D(\mathbf{x}, \mathbf{n}) = 1 - \psi = \frac{dA - d\tilde{A}}{dA} = \frac{dA_D}{dA}, \quad (2.4b)$$

where the damage variable D is specified as

$$D = 0 \quad (\text{initial undamaged state}), \quad (2.5a)$$

$$D = 1 \quad (\text{final fractured state}), \quad (2.5b)$$

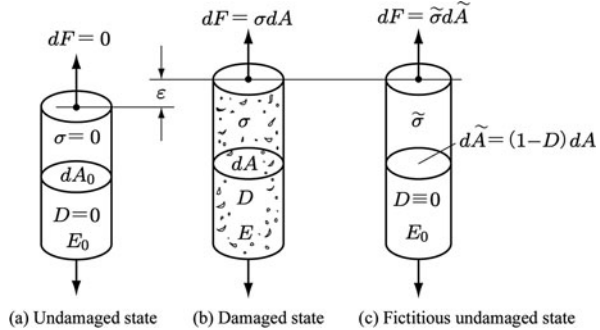
and may be interpreted as the fraction of decrease in the effective area due to damage development. The damage variable D can be applied not only to creep damage but also to a wide variety of damage.

Let us now consider the damage of a cylindrical bar of Fig. 2.2. Suppose that a bar of Fig. 2.2b with the cross-section area dA is subject to a tensile load dF and is in the damage state D . The actual load-carrying cross-sectional area is the effective area $d\tilde{A}$, rather than the apparent area dA . By the use of Eq. (2.4), the effective area $d\tilde{A}$ is given by

$$d\tilde{A} = (1 - D)dA. \quad (2.6)$$

¹ This area is usually interpreted as a net load-carrying area including the effect of microstress-concentration and/or that of the effect of mutual interaction of microcavities, rather than the rigorous geometrical area resulting from the microcavity distribution (Lemaître 1992).

Fig. 2.2 Deformation and damage of a bar under tensile load



The decrease in the load-carrying area magnifies the effect of the stress σ induced by the external force dF . Due to Eq. (2.6), the magnified stress $\tilde{\sigma}$ is given by

$$\tilde{\sigma} = \frac{dF}{d\tilde{A}} = \frac{\sigma}{1 - D}. \quad (2.7)$$

Since the stress $\tilde{\sigma}$ represents the effect of stress magnified by the net area reduction due to damage, it is named *effective stress*² (Kachanov 1958; Rabotnov 1968).

In view of Eqs. (2.6) and (2.7), we can postulate that the damaged cylindrical bar of Fig. 2.2b with the cross-section area dA and subject to the external force dF is mechanically equivalent to a fictitious undamaged bar of Fig. 2.2c, which is subject to the identical external force dF , has the cross-sectional area $d\tilde{A}$ and hence has the stress $\tilde{\sigma}$. Thus the state of Fig. 2.2c is referred to as the *fictitious undamaged state* or the *fictitious undamaged configuration* (Murakami 1988). This fictitious undamaged state or configuration gives an important notion for the damage modeling. Hereafter, the fictitious material in the fictitious undamaged state will also be called the *fictitious undamaged material*.

The effective stress defined by Eq. (2.7) can be understood so that it not only represents the effect of the decrease in the geometrical area due to damage, but also includes the effects of stress concentration at voids or the effects of interaction between voids.

The concept of Kachanov to model the damage state in terms of the decrease in the effective load-carrying area is quite clear from the mechanics point of view.

The actual phenomena of material damage, however, is much more complicated than that postulated in Kachanov's model, and the model may have limited validity (See, e.g., Rabier 1989; Lin et al. 2005). For more accurate description of damage, different models have been proposed thereafter, some of which will be discussed later.

² In order to distinguish from the effective stresses to be defined later by Eq. (2.9) and others, $\tilde{\sigma}$ of Eq. (2.7) is sometimes called also by the name of *net stress*. However, the reduced stresses introduced to describe the mechanical equivalence between the damaged and the undamaged states will be called “*effective stress*” throughout this book except the cases of special confusion.

2.1.2 Modeling by the Variation in Elastic Modulus

Since the development of microvoids induces the reduction in stiffness of materials, the damage state can be characterized also by the variation in elastic modulus (Chaboche 1977; Lemaitre and Chaboche 1978).

We now apply another concept of the effective stress to the bars of Fig. 2.2b and c. Let us suppose that the bars (b) and (c) are in the damaged and the fictitious undamaged state, respectively. Then the elastic strain ε in the bar (c) caused by the stress $\tilde{\sigma}$ should be equal to that ε of the bar (b) under stress σ ; i.e.,

$$\tilde{\sigma} = E_0 \varepsilon, \quad \sigma = E(D) \varepsilon, \quad (2.8a)$$

or

$$\varepsilon = \frac{\sigma}{E(D)} = \frac{\tilde{\sigma}}{E_0}, \quad (2.8b)$$

where E_0 and $E(D)$ denote Young's modulus of the material in the initial undamaged state and that in the damaged state after loading, respectively. Namely Eq. (2.8) defines another effective stress

$$\tilde{\sigma} = \frac{E_0}{E(D)} \sigma. \quad (2.9)$$

Equation (2.8) gives the basis of the *hypothesis of strain equivalence* discussed later in Section 2.3.3. Equation (2.9) defines the effective stress $\tilde{\sigma}$ by means of the variation in elastic modulus, and gives alternative notion to Eq. (2.7).

By combining Eqs. (2.7) and (2.9), we have

$$E(D) = (1 - D) E_0, \quad (2.10a)$$

or

$$D = 1 - \frac{E(D)}{E_0}. \quad (2.10b)$$

Thus, the damage variable D is characterized by the variation in Young's modulus $E(D)$.

The applicability of Eq. (2.10) can be examined by measuring the elastic modulus in the unloading process. Figure 2.3, for example, shows the variation in Young's modulus E and the corresponding evolution of the damage variable calculated by Eq. (2.10) in ductile damage of 99.9% copper. We see remarkable increase in damage after the plastic strain ε^p exceeds 30%.

Figure 2.4, on the other hands, shows the comparison between the measurements and the predictions of Young's modulus in creep damage of OFHC copper at 250°C. The symbols in the figure show the values of E measured during the unloading process in creep damage tests, while the solid line is the prediction of Eq. (2.10) and

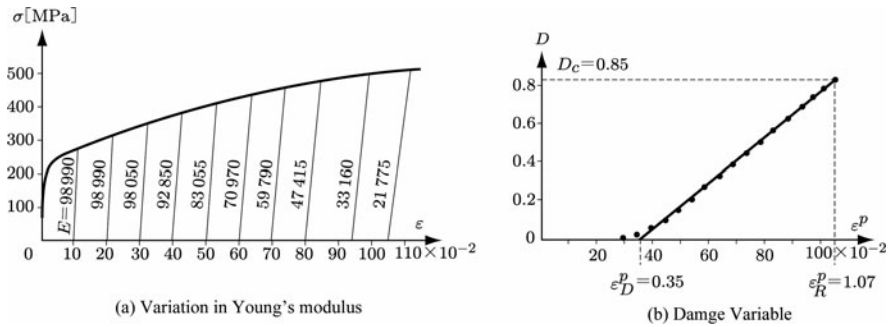
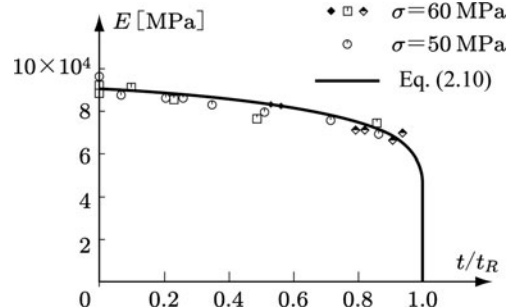


Fig. 2.3 Decrease in Young's modulus and ductile damage of copper (20°C , $E_0 = 99000 \text{ MPa}$)
Source: (Lemaitre 1985, p. 88, Fig. 3)

Fig. 2.4 Decrease in Young's modulus in creep damage of OFHC copper (250°C)
Source: Murakami et al. (1990, p. 2302, Fig. 4)



the values of D calculated from Eq. (8.6) later. The definition of Eq. (2.10) of D will be extended in Section 2.2 to tensor damage variables of fourth- and eighth-order.

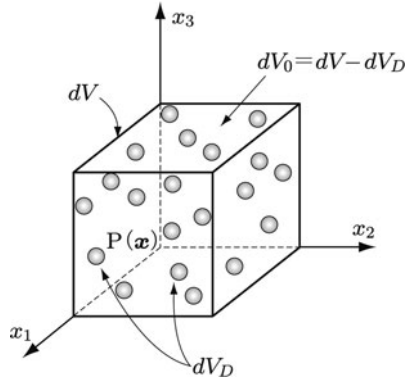
The modeling of damage states by means of the elastic modulus or the elastic compliance tensor have been applied also to the anisotropic damage of brittle materials like concrete and rocks, and will be discussed in Chapters 5 and 9 afterwards.

2.1.3 Modeling by Void Volume Fraction

The ductile damage of metals is brought about by the growth and the coalescence of microvoids. These microvoids may exist in materials from the beginning, or may be created by the plastic deformation due to different mechanisms; e.g., by the grain boundary sliding, by the decohesion of interfaces between the inclusions and the matrix, or by the fracture of the inclusions. Therefore the damage state of a ductile material can be described by the *void volume fraction* f in the material (Gurson 1977; Rousselier 1987).

Suppose a representative volume element (RVE) at point $P(x)$ in a material as shown in Fig. 2.5. Let dV , dV_D and dV_0 be the volume of RVE, total volume of the voids and the volume of the matrix of RVE, respectively. Then the void volume fraction f in RVE is given by

Fig. 2.5 RVE in material with microvoids



$$f = \frac{dV - dV_0}{dV} = \frac{dV_D}{dV} \quad (2.11)$$

It has been observed that the voids start to coalesce when they have grown to a size as large as the distance between them, and the void volume fraction at that stage is in the range of $f = 0.15$ through 0.25 (Goods and Brown 1979; Needleman and Tvergaard 1984).

Although direct measurement of the void volume fraction is difficult, it is rather easy to measure the density change of the material. Namely, if the initial and the damaged density of the material are denoted by ρ_0 and ρ , respectively, Eq. (2.11) can be expressed as

$$f = \frac{\rho_0 - \rho}{\rho_0} = 1 - \frac{\rho}{\rho_0}, \quad (2.12)$$

as far as f remains not too large.

In Section 6.5 of Chapter 6, the elastic-plastic constitutive equations of damaged materials will be discussed by representing the damage state by means of their void volume fraction.

Besides the methods mentioned above, the modeling of the damage states of materials can be performed also by other methods. For more detail, refer to Lemaitre and Dufailly (1987) and Lin, Liu, and Dean (2005).

2.2 Mechanical Representation of Three-Dimensional Damage State

The internal change of a material generally depends on the direction of applied stress or strain, and hence is an essentially anisotropic phenomenon. Thus, different theories have been developed for the modeling of anisotropic three-dimensional damage.

We now discuss some typical and fundamental theories to represent three-dimensional damage states and the relevant damage variables.

2.2.1 Scalar Damage Variable

In the case of random distribution of microvoids or of the isotropic distribution of spherical voids, the damage state is usually taken to be isotropic. The damage states in these cases may be represented by means of a scalar damage variable D or f of Eqs. (2.4), (2.10) or (2.11).

When micovoids have oriented geometry or when spherical cavities have oriented distribution, on the other hands, the damage states are anisotropic, and the scalar damage variable can not be applied accurately. However, when void density is small, even if the geometry or the configuration of voids is oriented, the global mechanical properties, above all the deformation property, can be viewed as nearly isotropic (Krajcinovic 1996). The scalar damage variable, moreover, is much easier in its mathematical procedure than that for the tensorial damage variables described hereafter. Thus, the *isotropic damage theory* based on an isotropic damage variable has been often applied also to three-dimensional problems of creep, elastic-plastic, ductile and fatigue damage (Lemaitre 1992).

2.2.2 Plural Scalar Damage Variables

A single scalar damage variable is often insufficient to describe the variation in mechanical properties of damaged materials, even if the resulting distribution of microcavities is isotropic. For example, modeling of the change in elastic properties due to damage development even in isotropic materials necessitates two independent scalar damage variables (Ju 1989; Rabier 1989; Cauvin and Testa 1999). Plural scalar damage variables are also employed to characterize several different microscopic mechanisms of the relevant damage development (See Sections 8.1, 9.2 and 10.1).

2.2.3 Vector Damage Variable

According to the discussion of Section 2.1.1, the damage state can be specified by the decrease in the load carrying effective area due to void development. Hence it would seem easy and natural to postulate a vector damage variable.

Kachanov (1974, 1986) tried to extend the definition of damage of Eq. (2.3) to the anisotropic damage. By noting a surface element in an arbitrary direction \mathbf{n} , he proposed a vector damage variable $\psi = \psi_n \mathbf{n}$, where ψ_n is the effective area fraction of Eq. (2.3).

However, as will be described in Section 2.2.6 afterwards, a damage variable $\mathcal{D}(\mathbf{n})$ representing the damage state of a plane with specific unit normal vector \mathbf{n}

should be unchanged irrespective of the change in the sense of \mathbf{n} , and hence we have the requirement

$$\mathcal{D}(\mathbf{n}) = \mathcal{D}(-\mathbf{n}). \quad (2.13)$$

The damage tensors of the odd-order, including the vector, have essential limitation not to satisfy the condition (2.13). Actually, when damage develops on planes of different orientations, the effect of total damage cannot be expressed by the sum of the damage vectors of each plane.

2.2.4 Damage State Defined by Effective Area Reduction, Damage Tensor of Second-Order

As observed above, proper description of an anisotropic damage state necessitates a damage variable of second or higher even-order tensor. We now discuss the extension of the one-dimensional damage model of Section 2.1.1 to general states of *three-dimensional anisotropic damage* (Murakami 1988).

The most essential aspect of Eq. (2.6) is that the damage state $(1 - D)$ is specified by the transformation of the surface element dA of Fig. 2.2b of the damaged state into the corresponding surface element $d\tilde{A}$ in the fictitious undamaged state of Fig. 2.2c. In the case of the general three-dimensional damage, however, the transformation between these surface elements depends on the direction of the surface elements in RVE.

For the three-dimensional extension of the concept of Fig. 2.2, we first take an arbitrary surface element PQR in RVE in the *current damaged configuration* B_t of Fig. 2.6a. The unit normal vector and the area of PQR are denoted by \mathbf{v} and dA . As in the case of Fig. 2.2, we further postulate the *fictitious undamaged configuration* B_f of Fig. 2.6b mechanically equivalent to B_t , and denote the corresponding surface element and its area vector by $\tilde{P}\tilde{Q}\tilde{R}$ and $\tilde{\mathbf{v}}d\tilde{A}$, respectively.

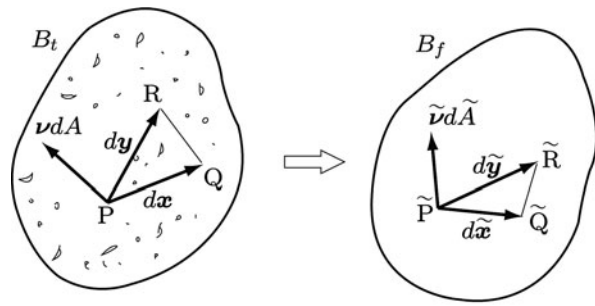


Fig. 2.6 Surface element in RVE of a damaged material

(a) Current damaged configuration

(b) Fictitious undamaged configuration

According to the notion of the load carrying effective area defined by Eq. (2.6), the damage variable of second-order tensor \mathbf{D} should be defined by a linear transformation from the area vector νdA in B_t into $\tilde{\nu} d\tilde{A}$ in B_f , i.e.,

$$\tilde{\nu} d\tilde{A} = (\mathbf{I} - \mathbf{D}) \nu dA, \quad (2.14)$$

where \mathbf{I} is the second-order identity tensor. Since the damage tensor \mathbf{D} can be shown to be symmetric, it can be expressed by its spectral decomposition (See Eq. (12.130) in Chapter 12)

$$\mathbf{D} = \sum_{i=1}^3 D_i \mathbf{n}_i \otimes \mathbf{n}_i, \quad (2.15)$$

where D_i and \mathbf{n}_i are the principal value and the principal direction of \mathbf{D} .

As will be observed in Section 12.3.4, a second-order symmetric tensor transforms an arbitrary vector in its principal direction (or eigen vector) \mathbf{n}_i into another vector in the same direction. Therefore, in order to express Eq. (2.14) by the use of the eigen vector \mathbf{n}_i of the damage tensor \mathbf{D} , we take principal coordinate systems $O-x_1x_2x_3$ and $\tilde{O}-\tilde{x}_1\tilde{x}_2\tilde{x}_3$ as shown in Fig. 2.7 so that the coordinate axes pass through the points P, Q, R and \tilde{P} , \tilde{Q} , \tilde{R} of Fig. 2.6; thus we have the tetrahedra OPQR and $\tilde{O}\tilde{P}\tilde{Q}\tilde{R}$. Then, substitution of Eq. (2.15) into Eq. (2.14) furnishes

$$\tilde{\nu} d\tilde{A} = \sum_{i=1}^3 (1 - D_i) dA_i \mathbf{n}_i$$

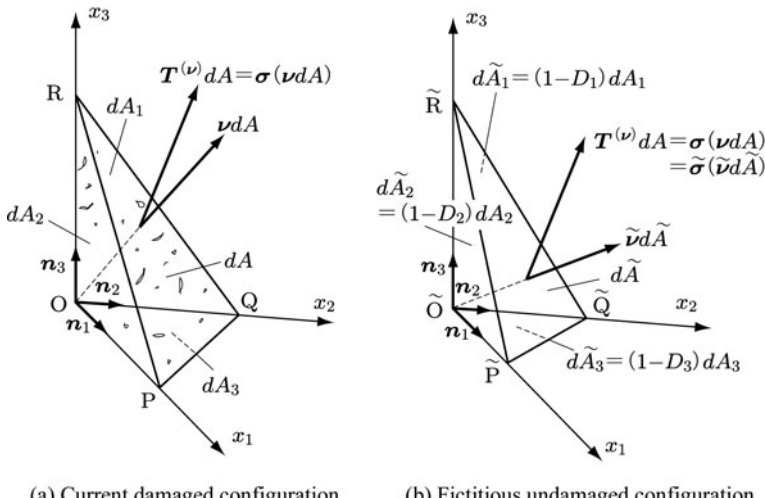


Fig. 2.7 Effective area reduction in the principal planes of the damage tensor \mathbf{D} , and asymmetric effective stress tensor $\tilde{\sigma}$

$$= d\tilde{A}_1 \mathbf{n}_1 + d\tilde{A}_2 \mathbf{n}_2 + d\tilde{A}_3 \mathbf{n}_3, \quad (2.16a)$$

$$d\tilde{A}_i = (1 - D_i) dA_i \quad (\text{no sum in } i; i = 1, 2, 3), \quad (2.16b)$$

where, $dA_i = v_i dA$, $d\tilde{A}_i = \tilde{v}_i d\tilde{A}$ ($i = 1, 2, 3$) are the areas of the coordinate planes of the tetrahedrons OPQR and $\tilde{O}\tilde{P}\tilde{Q}\tilde{R}$, respectively.

Equation (2.16b) signifies the reduction in load carrying effective areas from the principal area dA_i in B_t to those $d\tilde{A}_i$ in B_f . Namely, this equation implies that the principal values D_i ($i = 1, 2, 3$) of \mathbf{D} of Eq. (2.15) specifies the effective area reductions in the principal planes of \mathbf{D} in B_t , i.e., the void area fraction in B_t .

The above discussion has elucidated that when a material damage is characterized by the effective area reduction due to void development, the *damage state* induced by an arbitrary distribution of voids can be described by the second-order damage tensor of Eq. (2.15).

Then, how can the effective stress $\tilde{\sigma}$ of Eq. (2.7) be generalized to a state of three-dimensional stress in this case? According to the notion of Eq. (2.7), the effective stress tensor $\tilde{\sigma}$ of Fig. 2.7b can be defined as the stress induced in the fictitious undamaged configuration B_f when the surface element $\tilde{P}\tilde{Q}\tilde{R}$ in B_f is subject to the identical *surface force* vector $\mathbf{T}^{(v)} dA$ to that of the surface force vector acting on the surface element PQR in the current damage configuration of Fig. 2.7a.

Let the Cauchy stress tensor in the current damaged configuration B_t be σ (Fig. 2.7). Then, the stress vector $\mathbf{T}^{(v)}$ acting on a plane of unit normal vector \mathbf{v} in B_t is given by *Cauchy's formula*

$$\mathbf{T}^{(v)} = \sigma \mathbf{v}. \quad (2.17a)$$

Multiplying first the both-hand sides of this equation by dA and then by using Eq. (2.14), we have

$$\begin{aligned} \mathbf{T}^{(v)} dA &= \sigma (\mathbf{v} dA) = \tilde{\sigma} (\tilde{\mathbf{v}} d\tilde{A}) \\ &= \tilde{\sigma} (\mathbf{I} - \mathbf{D})(\mathbf{v} dA). \end{aligned} \quad (2.17b)$$

From this, the *effective stress tensor* $\tilde{\sigma}$ is given by

$$\tilde{\sigma} = (\mathbf{I} - \mathbf{D})^{-1} \sigma, \quad (2.18)$$

which is the extension of Eq. (2.7) to the general state of damage.

Since the effective stress tensor $\tilde{\sigma}$ of Eq. (2.18) is asymmetric, it is usually inconvenient to use it in the formulation of constitutive and evolution equations. A method of symmetrization is given by taking the symmetric part of its Cartesian decomposition

$$\begin{aligned}\tilde{\sigma}^S &= (\tilde{\sigma})^S = [(\mathbf{I} - \mathbf{D})^{-1} \boldsymbol{\sigma}]^S \\ &= \frac{1}{2} [(\mathbf{I} - \mathbf{D})^{-1} \boldsymbol{\sigma} + \boldsymbol{\sigma} (\mathbf{I} - \mathbf{D})^{-1}].\end{aligned}\quad (2.19)$$

As observed from the above argument on the effective stress, the mechanical effect of the Cauchy stress $\boldsymbol{\sigma}$ in the current damaged configuration is equivalent to that of the effective stress $\tilde{\boldsymbol{\sigma}}$ or $\tilde{\boldsymbol{\sigma}}^S$ in the corresponding fictitious undamaged configuration B_f . Then the constitutive and the evolution equations of a damaged material can be easily derived by the use of this equivalence, and thus the mechanical analyses of damaged materials can be largely simplified.

Equation (2.16b) specifies the damage state which is represented by the effective area reduction in the three principal planes. In other words, the second-order symmetric damage tensor \mathbf{D} of Eq. (2.15) can not represent the damage states more complex than *orthotropy*. Nevertheless, the elastic property of a damaged material due to distributed microcracks can be treated as orthotropic with sufficient accuracy even for materials with significant crack density (M. Kachanov 1987). Furthermore, it has been observed that the damage caused by the decohesion of the fiber-matrix interface in fiber-reinforced composites can also be represented as orthotropy (Raghavan and Ghosh 2005). Therefore the orthotropy characterized by the second-order damage variable \mathbf{D} of Eq. (2.15) usually does not give serious limitation in its application generally (Hansen and Schreyer 1994).

2.2.5 Damage State Defined by Geometrical Configuration of Microvoids

In the above section, the concepts of effective area and the related effective stress in one-dimension were extended into three-dimensional case, and the second-order symmetric damage tensor (2.15) was derived. A similar second-order symmetric damage tensor can be defined also by taking account of geometrical configuration of distributed microvoids.

In order to model the creep damage state in polycrystalline metals, Murakami and Ohno (1981) supposed an RVE of the volume element V shown by Fig. 2.8a. By representing the area and its unit normal vector of k th grain-boundary cavity by $dS_g^{(k)}$ and $\mathbf{n}^{(k)}$ ($k = 1, 2, \dots, N$), the mechanical effect of damage due to these microvoids may be expressed by

$$\mathbf{D} = \sum_{k=1}^N \int_{S^k} \frac{1}{S^k(V)} \mathbf{n}^{(k)} \otimes \mathbf{n}^{(k)} dS_g^{(k)}, \quad (2.20a)$$

where $S^k(V)$ denotes the cross sectional area of the volume element V cut by the plane containing the surface elements $dS_g^{(k)}$. Since the tensor \mathbf{D} of Eq. (2.20a) is symmetric, it can be expressed also in the form of Eq. (2.15)

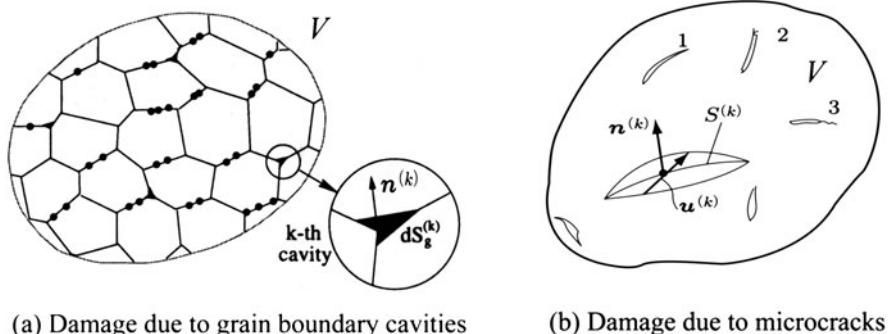


Fig. 2.8 Damage of material due to distributed microvoids

$$\mathbf{D} = \sum_{i=1}^3 D_i \mathbf{n}_i \otimes \mathbf{n}_i. \quad (2.20b)$$

Vakulenko and M. Kachanov (1971), on the other hand, proposed the following second-order crack-density tensor by taking account of the RVE of Fig. 2.8b:

$$\mathbf{D} = \frac{1}{V} \sum_k \int_{S(k)} \mathbf{u}^{(k)} \otimes \mathbf{n}^{(k)} dS^{(k)}, \quad (2.21)$$

where $S^{(k)}$ denotes the crack surface of the k th crack before crack-opening. The symbols $\mathbf{n}^{(k)}$ and $\mathbf{u}^{(k)}$, furthermore, are the unit normal vector of $S^{(k)}$ and the discontinuity in displacement at each point on $S^{(k)}$, respectively.

However, although the plane cracks without opening $\mathbf{u}^{(k)} = \mathbf{0}$ surely induce the material damage, Eq. (2.21) implies $\mathbf{D} = \mathbf{0}$ in this case. In order to obviate this anomaly, M. Kachanov (1980) postulated that the crack opening displacement has no much effect, and replaced $\mathbf{u}^{(k)}$ in Eq. (2.21) by $\mathbf{n}^{(k)}$:

$$\mathbf{D} = \frac{1}{V} \sum_k \int_{S(k)} \mathbf{n}^{(k)} \otimes \mathbf{n}^{(k)} dS^{(k)}. \quad (2.22)$$

In the particular case of penny shape cracks of radius $r^{(k)}$ in three-dimensional solids, or the case of slits of length $2a^{(k)}$ in two-dimensional plates, the crack density tensor (2.22) leads to

$$\mathbf{D} = \frac{1}{V} \sum_k \left(r^{(k)} \right)^3 \mathbf{n}^{(k)} \otimes \mathbf{n}^{(k)}, \quad (2.23a)$$

$$\mathbf{D} = \frac{1}{A} \sum_k \left(a^{(k)} \right)^2 \mathbf{n}^{(k)} \otimes \mathbf{n}^{(k)}, \quad (2.23b)$$

where V and A are the volume and the area to take average.

Equations (2.22) and (2.23) are essentially identical to the damage tensor of Eq. (2.15), and have been applied to the damage of elastic-brittle materials and composite materials.

2.2.6 Damage Sate Defined by Directional Distribution of Microvoid Density

More accurate representation of anisotropic damage can be given by the directional distribution of microvoid density (Kanatani 1984; Onat and Leckie 1988; Lubarda and Krajcinovic 1993).

We suppose a unit spherical surface S^2 around a point $P(\mathbf{x})$ in RVE (Fig. 2.9). Let us denote the direction in the material by a unit vector \mathbf{n} , the surface element on the unit surface around the tip of the vector \mathbf{n} by dA , and the solid angle of dA spanned at the point by $d\Omega$, respectively.

If the microvoid density is denoted by ξ , its directional distribution can be represented by a *distribution function* $\xi(\mathbf{n})$ on a unit sphere S^2 of Fig. 2.9. Since the magnitude of $\xi(\mathbf{n})$ is unchanged by the sense of \mathbf{n} , it should satisfy a relation

$$\xi(\mathbf{n}) = \xi(-\mathbf{n}). \quad (2.24)$$

Let us now derive the general representation of the function $\xi(\mathbf{n})$. For this purpose, we first expand the function $\xi(\mathbf{n})$ into a polynomial of \mathbf{n} on the unit sphere S^2

$$\xi(\mathbf{n}) = C_0 + C_{ij}n_i n_j + C_{ijkl}n_i n_j n_k n_l + \dots, \quad (2.25)$$

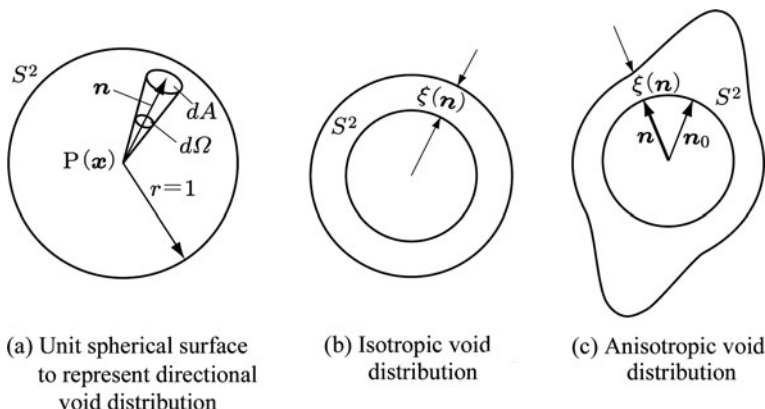


Fig. 2.9 Directional distribution of microvoid density

Source: Onat and Leckie (1988, p. 4, Fig. 2)

where n_i represents the Cartesian components of the vector \mathbf{n} , while $n_i n_j$, $n_i n_j n_k n_l$, ... are the components of the dyad and the polyad of \mathbf{n} . Furthermore, C_0 , C_{ij} , C_{ijkl} , ... are the coefficient tensors corresponding to the given function $\xi(\mathbf{n})$. In Eq. (2.25), the terms of odd-order tensor have been excluded due to Eq. (2.24).

In Eq. (2.25) the coefficients C_0 , C_{ij} , C_{ijkl} , ... can not be determined uniquely, because 1, $n_i n_j$, $n_i n_j n_k n_l$, ... are not linearly independent. To conform to this situation, we will expand Eq. (2.25) into a generalized Fourier series with respect to the irreducible tensor bases $f_{ij}(\mathbf{n})$, $f_{ijkl}(\mathbf{n})$, ... as follows (Onat and Leckie 1988):

$$\xi(\mathbf{n}) = D_0 + D_{ij} f_{ij}(\mathbf{n}) + D_{ijkl} f_{ijkl}(\mathbf{n}) + \dots, \quad (2.26a)$$

$$f_{ij}(\mathbf{n}) = n_i n_j - \frac{1}{3} \delta_{ij}, \quad (2.26b)$$

$$\begin{aligned} f_{ijkl}(\mathbf{n}) &= n_i n_j n_k n_l - \frac{1}{7} (\delta_{ij} n_k n_l + \delta_{ik} n_j n_l + \delta_{il} n_j n_k \\ &\quad + \delta_{jk} n_i n_l + \delta_{jl} n_i n_k + \delta_{kl} n_i n_j) \\ &\quad + \frac{1}{5 \times 7} (\delta_{ij} n_k n_l + \delta_{ik} n_j n_l + \delta_{il} n_j n_k) + \dots, \end{aligned} \quad (2.26c)$$

where D_0 , D_{ij} , D_{ijkl} , ... are the alternative coefficient tensors.

As will be observed in Section 12.3.5 of the Chapter 12, the representation of the distribution functions $\xi(\mathbf{n})$ of Eq. (2.26) is invariant as to the rotation of the orthogonal coordinate systems. The functional bases $f_{ij}(\mathbf{n})$, $f_{ijkl}(\mathbf{n})$, ... consist of the even-order tensor components, and are symmetric with respect to the indices. They further have vanishing trace, and are irreducible. Thus the number of the independent components of $f_{ij}(\mathbf{n})$, $f_{ijkl}(\mathbf{n})$, ... are five, nine,

The basis function of Eq. (2.26), furthermore, are orthogonal to each other, and we have

$$\int_{S^2} 1 \cdot f_{ij} d\Omega = \int_{S^2} 1 \cdot f_{ijkl} d\Omega = \int_{S^2} f_{ij} f_{klpq} d\Omega = \dots = 0. \quad (2.27)$$

This result can be confirmed by the use of the following relations (Krajcinovic 1996);

$$\int_{S^2} d\Omega = 4\pi, \quad \int_{S^2} n_i n_j d\Omega = \frac{4\pi}{3} \delta_{ij}, \quad (2.28a)$$

$$\int_{S^2} n_i n_j n_k n_l d\Omega = \frac{4\pi}{5} I_{ijkl}, \quad (2.28b)$$

$$I_{ijkl} = \frac{1}{3} (\delta_{ij} \delta_{kl} + \delta_{ik} \delta_{jl} + \delta_{il} \delta_{jk}),$$

$$\int_{S^2} n_i n_j n_k n_l n_p n_q d\Omega = \frac{4\pi}{7} I_{ijklpq}, \quad (2.28c)$$

$$\begin{aligned} I_{ijklpq} &= \frac{1}{15} (\delta_{ij} I_{klpq} + \delta_{ik} I_{jlpq} + \delta_{il} I_{jkpq} \\ &\quad + \delta_{ip} I_{jklq} + \delta_{iq} I_{jklp}), \end{aligned}$$

Finally, the coefficient tensors of the general representation (2.26) can be derived by calculating the following integrals for given $\xi(\mathbf{n})$ with the aids of Eq. (2.28);

$$D_0 = \frac{1}{4\pi} \int_{S^2} \xi(\mathbf{n}) d\Omega, \quad (2.29a)$$

$$D_{ij} = \frac{1}{4\pi} \frac{3 \times 5}{2} \int_{S^2} \xi(\mathbf{n}) f_{ij}(\mathbf{n}) d\Omega, \quad (2.29b)$$

$$D_{ijkl} = \frac{1}{4\pi} \frac{3 \times 5 \times 7 \times 9}{2 \times 3 \times 4} \int_{S^2} \xi(\mathbf{n}) f_{ijkl}(\mathbf{n}) d\Omega, \quad (2.29c)$$

.....

The tensors D_0 , D_{ij} , D_{ijkl} , . . . characterize the directional distribution of a given physical quantity, and are called *fabric tensors*.

Now let us recapitulate the signification of Eq. (2.26). Equation (2.26) means that

- (1) When directional distribution of the void density has been measured, Eq. (2.26) gives the analytical representation of the distribution $\xi(\mathbf{n})$, and then
- (2) the distribution is characterized by the set of even-order symmetric coefficient tensors D_0 , D_{ij} , D_{ijkl} , . . .

That is to say, the analytical representation of the void distribution as mentioned in (1) above can be derived, first by calculating the values of the coefficient tensors D_0 , D_{ij} , D_{ijkl} , . . . by the use of Eq. (2.29) and the measurement results of $\xi(\mathbf{n})$, and then by substituting them into Eq. (2.26).

On the other hands, when the values of the coefficient tensors are given beforehand, the cavity density $\xi(\mathbf{n}^*)$ in an arbitrary direction \mathbf{n}^* can be calculated by substituting the specified values (n_1^*, n_2^*, n_3^*) of the components of \mathbf{n}^* into Eq. (2.26). This implies that, as mentioned in (2) above, the even-order tensors D_0 , D_{ij} , D_{ijkl} , . . . represent completely the damage states of materials. Thus the tensors D_0 , D_{ij} , D_{ijkl} , . . . are exactly the damage variables, and have been utilized as the internal variables in the thermodynamic constitutive theories for creep and elastic-brittle damage (Onat and Leckie 1988; Lubarda and Krajcinovic 1993; Lacy et al. 1997).

2.2.7 Damage Tensors of Fourth- and Eighth-Order

The notion of Eq. (2.10) to represent the damage state in terms of the variation of an elastic modulus can be extended to the definition of damage tensor \mathcal{D} of the fourth- or eighth-order (Chaboche 1982, 1993).

Let the fourth-order elastic modulus tensor of an undamaged and the damaged material be denoted by \mathbb{C}_0 and $\mathbb{C}(\mathcal{D})$. Then the elastic constitutive equations of these materials are given by

$$\boldsymbol{\sigma} = \mathbb{C}_0 : \boldsymbol{\varepsilon}, \quad \boldsymbol{\sigma} = \mathbb{C}(\mathcal{D}) : \boldsymbol{\varepsilon}, \quad (2.30)$$

where (\cdot) denotes the double contraction defined by Eq. (12.74) of the Chapter 12. Since the elastic strain in a damaged material under stress σ is equal to that of the equivalent fictitious undamaged material subject to the effective stress $\tilde{\sigma}$, we have

$$\tilde{\sigma} = \mathbb{C}_0 : \boldsymbol{\varepsilon}. \quad (2.31)$$

Equations (2.30) and (2.31) lead to the effective stress

$$\tilde{\sigma} = [\mathbb{C}_0 : \mathbb{C}(\mathcal{D})^{-1}] : \boldsymbol{\sigma}. \quad (2.32)$$

In view of Eq. (2.30), the damage tensor \mathcal{D} may be viewed as an eighth-order tensor which transforms the fourth-order elasticity tensor \mathbb{C}_0 of an undamaged material to another fourth-order tensor $\mathbb{C}(\mathcal{D})$ of the damaged material. However, the mathematical operation of eighth-order tensors is highly complicated. Hence Chaboche (1982) employed an alternative fourth-order damage tensor \mathbb{D} , rather than \mathcal{D} , and supposed a transformation between elastic moduli;

$$\mathbb{C}(\mathbb{D}) = (\mathbb{I} - \mathbb{D}) : \mathbb{C}_0, \quad (2.33)$$

where \mathbb{I} denotes the fourth-order identity tensor. Thus the fourth-order damage tensor \mathbb{D} and the effective stress tensor $\tilde{\sigma}$ of Eq. (2.32) are given by the following relations, similar to Eqs. (2.10) and (2.7), respectively

$$\mathbb{D} = \mathbb{I} - \mathbb{C}(\mathbb{D}) : \mathbb{C}_0^{-1}, \quad (2.34a)$$

$$\tilde{\sigma} = (\mathbb{I} - \mathbb{D})^{-1} : \boldsymbol{\sigma}. \quad (2.34b)$$

As observed in Eq. (2.34a), the damage tensor is asymmetric. To overcome this difficulty, Chaboche (1993) later employed an alternative transformation

$$\mathbb{C}(\hat{\mathbb{D}}) = \frac{1}{2} \left[(\mathbb{I} - \hat{\mathbb{D}}) : \mathbb{C}_0 + \mathbb{C}_0 : (\mathbb{I} - \hat{\mathbb{D}}) \right], \quad (2.35)$$

and proposed a new fourth-order symmetric damage tensor $\hat{\mathbb{D}}$.

Equation (2.34) shows that the anisotropic damage state or the relevant fourth-order damage tensor can be defined by the variation in the stiffness of the material. Ortiz (1985) and Ju et al. (Simo and Ju 1987; Ju 1989), therefore, extended this idea further, and adopted the elastic modulus tensor \mathbb{C} itself as an internal variable of the damage state to develop another anisotropic damage theory.

The damage variable $\hat{\mathbb{D}}$ and \mathbb{C} have been applied to the damage with apparent opening-closing phenomena of cracks. The details of the application will be discussed in Sections 5.3 and 9.4 later.

2.3 Effective Stress and Hypothesis of Mechanical Equivalence

The constitutive and the evolution equations of damage mechanics can be derived by the use of the effective stress and other effective state variables, together with the hypotheses of mechanical equivalence between the damaged and the fictitious undamaged material. In this section we describe several definitions of the effective stress and the related hypotheses of mechanical equivalence.

2.3.1 Effective Stress Tensors

Mechanical representation of damage states and the resulting damage variables, together with the notion of the effective stress were discussed in Sections 2.1 and 2.2. These effective stresses, above all, are usually employed to describe the mechanical behavior of damaged materials. We now summarize and explain important notions of the effective stresses frequently postulated in damage mechanics.

(1) Effective Stress Tensor for Isotropic Damage (Lemaitre and Chaboche 1978)

Suppose that the state of damage is isotropic. Then extension of the effective stress of Eq. (2.7) to the effective stress tensor in three-dimensional state leads to

$$\tilde{\sigma} = (1 - D)^{-1} \sigma, \quad (2.36)$$

where D is the scalar damage variable of Eq. (2.4) or (2.10), while σ is the Cauchy stress tensor.

The effective stress of Eq. (2.36) simplifies the damage theory, and is employed in a number of damage problems, including ductile damage above all. This effective stress, however, cannot be applied to the damage of significant anisotropy, such as the case of the brittle damage due to microcrack distribution.

(2) Asymmetric Effective Stress Tensor for Anisotropic Damage (Murakami 1988)

In Section 2.2.4, the increase in stress effect caused by the net area reduction was represented by an effective stress tensor

$$\tilde{\sigma} = (\mathbf{I} - \mathbf{D})^{-1} \sigma, \quad (2.37)$$

where \mathbf{I} and \mathbf{D} are the second-order identity tensor and the second-order damage tensor given by Eq. (2.15). In the actual development of anisotropic damage, the stress induced in RVE of a damaged material is essentially asymmetric. However, an asymmetric stress tensor makes the mechanical analyses very complicated, and thus different schemes of symmetrization of Eq. (2.37) have been proposed as follows.

(3) Symmetrized Effective Stress Tensor for Anisotropic Damage 1 (Murakami and Ohno 1981; Murakami 1988)

As a simple symmetrization procedure of Eq. (2.37), the symmetric part of the Cartesian decomposition of Eq. (2.37) gives Eq. (2.19), i.e.,

$$\tilde{\sigma} = \frac{1}{2} \left[(\mathbf{I} - \mathbf{D})^{-1} \boldsymbol{\sigma} + \boldsymbol{\sigma} (\mathbf{I} - \mathbf{D})^{-1} \right]. \quad (2.38)$$

(4) Symmetrized Effective Stress Tensor for Anisotropic Damage 2 (Cordebois and Sidoroff 1982a, b)

Another form of the symmetrization was proposed by Cordebois and Sidoroff:

$$\tilde{\sigma} = (\mathbf{I} - \mathbf{D})^{-1/2} \boldsymbol{\sigma} (\mathbf{I} - \mathbf{D})^{-1/2}. \quad (2.39)$$

When $\boldsymbol{\sigma}$ and \mathbf{D} are co-axial, in particular, Eq. (2.39) is identical to Eq. (2.38). Moreover, unless the development of damage is large, the difference between these effective stress tensors was shown to be insignificant (Zheng and Betten 1996).

(5) Symmetrized Effective Stress Tensor for Anisotropic Damage 3 (Betten 1986)

Based on the representation theorem, Betten derived another effective stress tensor, i.e.,

$$\tilde{\sigma} = (\mathbf{I} - \mathbf{D})^{-1} \boldsymbol{\sigma} (\mathbf{I} - \mathbf{D})^{-1}. \quad (2.40)$$

Since tensors $(\mathbf{I} - \mathbf{D})^{-1}$ and $(\mathbf{I} - \mathbf{D})^{-1/2}$ are both second-order symmetric positive tensors, there is no essential difference between Eqs. (2.39) and (2.40).

Besides the above tensors, Chow et al. proposed the following two symmetric effective tensors.

(6) Symmetrized Effective Stress Tensor for Anisotropic Damage 4 (Chow and Lu 1989a; Chen and Chow 1995)

$$\tilde{\sigma} = \left\{ \frac{1}{2} [(\mathbf{I} - \mathbf{D}) \underline{\otimes} (\mathbf{I} - \mathbf{D}) + (\mathbf{I} - \mathbf{D}) \overline{\otimes} (\mathbf{I} - \mathbf{D})] \right\}^{-1/2} : \boldsymbol{\sigma}, \quad (2.41)$$

where $\underline{\otimes}$ and $\overline{\otimes}$ signify the tensor products defined in Eq. (12.82) of the Chapter 12, whereas $(:)$ represents the double contraction defined in Eq. (12.54).

(7) Symmetrized Effective Stress Tensor for Anisotropic Damage 5 (Chow and Lu 1989a; Chen and Chow 1995)

$$\tilde{\sigma} = \left[\mathbb{I} - \frac{1}{4} (\mathbf{I} \underline{\otimes} \mathbf{D} + \mathbf{I} \overline{\otimes} \mathbf{D} + \mathbf{D} \underline{\otimes} \mathbf{I} + \mathbf{D} \overline{\otimes} \mathbf{I}) \right]^{-1} : \boldsymbol{\sigma}, \quad (2.42)$$

where \mathbb{I} and (\cdot) are the fourth-order identity tensor and the double contraction defined by Eqs. (12.88) and (12.74).

2.3.2 Damage Effect Tensors, Representation of Effective Stress Tensors

Effective stress tensors $\tilde{\sigma}$ given by Eqs. (2.36) through (2.42) can be expressed in a unified form (Chaboche 1977; Cordebois and Sidoroff 1982a, b)

$$\tilde{\sigma} = \mathbb{M}(\mathcal{D}) : \boldsymbol{\sigma}, \quad (2.43)$$

where $\mathbb{M}(\mathcal{D})$ is a fourth-order tensor-valued tensor function which transforms the Cauchy stress tensor $\boldsymbol{\sigma}$ into the corresponding effective stress tensor $\tilde{\sigma}$, and is called a *damage effect tensor*. The tensor \mathcal{D} signifies an arbitrary even-order damage tensor among the zero-, second- and fourth-order tensors D , \mathbf{D} and \mathbb{D} .

In the discussion of damage mechanics, the effective stress tensors described in Section 2.3.1 are often represented conveniently in the form of Eq. (2.43). Then, the effective stress tensors of Eqs. (2.36) through (2.42) in the form of Eq. (2.43), together with their damage effect tensors, can be expressed as follows;

(1) **Effective Stress Tensor for Isotropic Damage** [Eq. (2.36)]

$$\tilde{\sigma} = \mathbb{M}^{(0)} : \boldsymbol{\sigma}, \quad \mathbb{M}^{(0)} = (1 - D)^{-1} \mathbb{I}, \quad (2.44a)$$

or

$$\tilde{\sigma} = M^{(0)} \boldsymbol{\sigma}, \quad M^{(0)} = (1 - D)^{-1}. \quad (2.44b)$$

(2) **Symmetrized Effective Stress Tensor for Anisotropic Damage 1** [Eq. (2.38)]
(Chow and Lu 1989a)

$$\tilde{\sigma} = \mathbb{M}^{(1)} : \boldsymbol{\sigma}, \quad (2.45a)$$

$$\begin{aligned} \mathbb{M}^{(1)} &= \frac{1}{4} (\boldsymbol{\Phi} \underline{\otimes} \mathbf{I} + \boldsymbol{\Phi} \overline{\otimes} \mathbf{I} + \mathbf{I} \underline{\otimes} \boldsymbol{\Phi} + \mathbf{I} \overline{\otimes} \boldsymbol{\Phi}), \\ \boldsymbol{\Phi} &= (\mathbf{I} - \mathbf{D})^{-1}, \end{aligned} \quad (2.45b)$$

or

$$M_{ijkl}^{(1)} = \frac{1}{4} (\Phi_{ik}\delta_{jl} + \Phi_{il}\delta_{jk} + \delta_{ik}\Phi_{jl} + \delta_{il}\Phi_{jk}). \quad (2.45c)$$

- (3) **Symmetrized Effective Stress Tensor for Anisotropic Damage 2** [Eq. (2.39)]
 (Chow and Wang 1987; Chaboche, Lesne, and Maire 1995)

$$\tilde{\sigma} = \mathbb{M}^{(2)} : \sigma, \quad (2.46a)$$

$$\begin{aligned} (\mathbb{M}^{(2)})^{-1} &= \frac{1}{2} (\Phi^{(2)} \underline{\otimes} \Phi^{(2)} + \Phi^{(2)} \overline{\otimes} \Phi^{(2)}), \\ \Phi^{(2)} &= (\mathbf{I} - \mathbf{D})^{1/2}, \end{aligned} \quad (2.46b)$$

or

$$(\mathbb{M}^{(2)})_{ijkl}^{-1} = \frac{1}{2} (\Phi_{ik}^{(2)} \Phi_{jl}^{(2)} + \Phi_{il}^{(2)} \Phi_{jk}^{(2)}). \quad (2.46c)$$

- (4) **Symmetrized Effective Stress Tensor for Anisotropic Damage 3** [Eq. (2.40)]
 (Zheng and Betten 1996)

The damage effect tensor $\mathbb{M}^{(3)}$ for the effective stress tensor of Eq. (2.40) is derived from Eq. (2.46) by replacing $\Phi^{(2)}$ in it by $\Phi^{(3)} = (\mathbf{I} - \mathbf{D})$.

- (5) **Symmetrized Effective Stress Tensor for Anisotropic Damage 4** [Eq. (2.41)]
 (Chen and Chow 1995)

$$\tilde{\sigma} = \mathbb{M}^{(4)} : \sigma, \quad (2.47a)$$

$$\begin{aligned} (\mathbb{M}^{(4)})^{-2} &= \frac{1}{2} (\Phi^{(4)} \underline{\otimes} \Phi^{(4)} + \Phi^{(4)} \overline{\otimes} \Phi^{(4)}), \\ \Phi^{(4)} &= \Phi^{(3)} = (\mathbf{I} - \mathbf{D}), \end{aligned} \quad (2.47b)$$

or

$$(\mathbb{M}^{(4)})_{ijkl}^{-2} = \frac{1}{2} (\Phi_{ik}^{(4)} \Phi_{jl}^{(4)} + \Phi_{il}^{(4)} \Phi_{jk}^{(4)}). \quad (2.47c)$$

- (6) **Symmetrized Effective Stress Tensor for Anisotropic Damage 5** [Eq. (2.42)]
 (Chen and Chow 1995)

$$\tilde{\sigma} = \mathbb{M}^{(5)} : \sigma, \quad (2.48a)$$

$$(\mathbb{M}^{(5)})^{-1} = \mathbb{I} - \frac{1}{4} (\mathbf{I} \underline{\otimes} \mathbf{D} + \mathbf{I} \overline{\otimes} \mathbf{D} + \mathbf{D} \underline{\otimes} \mathbf{I} + \mathbf{D} \overline{\otimes} \mathbf{I}), \quad (2.48b)$$

or

$$(\mathbb{M}^{(5)})_{ijkl}^{-1} = I_{ijkl} - \frac{1}{4} (\delta_{ik} D_{jl} + \delta_{il} D_{jk} + D_{ik} \delta_{jl} + D_{il} \delta_{jk}). \quad (2.48c)$$

In order to calculate the components of the above damage effect tensors, we need the components of the inverse and the square root of the tensors. Though the derivation of these components necessitates complicated tensor calculus in general, it can be performed easily by the use of symbolic manipulation programs (e.g., Maple, Mathematica, REDUCE) (Kreuzer 1994).

The matrix representation of the tensor $\Phi = (\mathbf{I} - \mathbf{D})^{-1}$ of Eq. (2.45b), the tensor $\Phi^{(2)} = (\mathbf{I} - \mathbf{D})^{1/2}$ of Eq. (2.46b), and those of the relevant damage effect tensors will be discussed afterward in Section 2.4.

2.3.3 Hypothesis of Strain Equivalence

The notion of the effective stress discussed in Figs. 2.2 and 2.7 can be generalized as shown in Fig. 2.10. Namely, the mechanical effect of the stress σ acting on RVE in the current damaged configuration B_t is equivalent to that of the equivalent stress $\tilde{\sigma}$ in the fictitious undamaged configuration B_f . Hence the deformation of the damaged material subject to σ should be equal to that of the fictitious undamaged material under $\tilde{\sigma}$. In fact, in the discussion of Sections 2.1.2 and 2.2.6, the equivalence of strain was assumed as regards the elastic strain.

Chaboche and Lemaitre extended this notion to the general state of inelastic deformation, and proposed the following hypothesis (Chaboche 1977, 1982; Lemaitre and Chaboche 1978):

Hypothesis of Strain Equivalence

The *inelastic constitutive equation* of a *damaged material* is given by the corresponding constitutive equation for an *undamaged material* by replacing the stress tensor σ in the equation with the corresponding effective stress tensor $\tilde{\sigma}$.

Suppose that the constitutive equation of an undamaged inelastic material is expressed by

$$\boldsymbol{\varepsilon} = \mathbf{F}_0(\sigma, \alpha), \quad (2.49a)$$

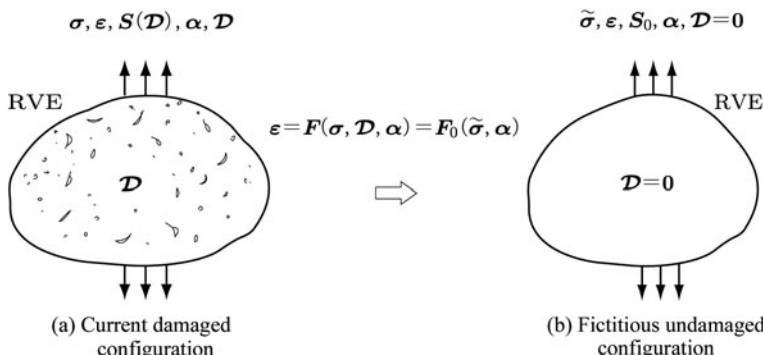


Fig. 2.10 Hypothesis of strain equivalence

or

$$\dot{\boldsymbol{\varepsilon}} = \mathbf{F}_0(\boldsymbol{\sigma}, \boldsymbol{\alpha}), \quad (2.49b)$$

where $\boldsymbol{\alpha}$ is an internal variable representing the internal structural change other than the damage, and (\cdot) denotes the material time derivative.

Then, the above hypothesis implies that the inelastic constitutive equation of the damaged material represented by a damage variable \mathcal{D} should be given by Eq. (2.49) by replacing $\boldsymbol{\sigma}$ in the equations with the relevant effective stress $\tilde{\boldsymbol{\sigma}}$ of Eq. (2.43), i.e.,

$$\boldsymbol{\varepsilon} = \mathbf{F}(\boldsymbol{\sigma}, \mathcal{D}, \boldsymbol{\alpha}) = \mathbf{F}_0(\tilde{\boldsymbol{\sigma}}, \boldsymbol{\alpha}), \quad (2.50a)$$

or

$$\dot{\boldsymbol{\varepsilon}} = \mathbf{F}(\boldsymbol{\sigma}, \mathcal{D}, \boldsymbol{\alpha}) = \mathbf{F}_0(\tilde{\boldsymbol{\sigma}}, \boldsymbol{\alpha}). \quad (2.50b)$$

In the case of elastic deformation, in particular, constitutive equations for an undamaged and the damaged material are given by

$$\boldsymbol{\varepsilon} = \mathbb{S}_0 : \boldsymbol{\sigma}, \quad (2.51)$$

$$\boldsymbol{\varepsilon} = \mathbb{S}(\mathcal{D}) : \boldsymbol{\sigma}, \quad (2.52)$$

where \mathbb{S}_0 and $\mathbb{S}(\mathcal{D})$ are the fourth-order elastic compliance tensors of the materials.

Then, according to the hypothesis of strain equivalence, the elastic constitutive equation (2.52) of the damaged material and the relevant compliance tensor $\mathbb{S}(\mathcal{D})$ are given by

$$\boldsymbol{\varepsilon} = \mathbb{S}_0 : \tilde{\boldsymbol{\sigma}} = [\mathbb{S}_0 : \mathbb{M}(\mathcal{D})] : \boldsymbol{\sigma} = \mathbb{S}(\mathcal{D}) : \boldsymbol{\sigma}, \quad (2.53a)$$

$$\mathbb{S}(\mathcal{D}) = \mathbb{S}_0 : \mathbb{M}(\mathcal{D}), \quad (2.53b)$$

where $\mathbb{M}(\mathcal{D})$ is the damage effect tensor of Eq. (2.43) discussed in Section 2.3.2. On the other hand, as a result of Eq. (2.53b), $\mathbb{M}(\mathcal{D})$ is related also to the compliance tensors

$$\mathbb{M}(\mathcal{D}) = \mathbb{S}_0^{-1} : \mathbb{S}(\mathcal{D}) \quad (2.54)$$

Though the notion of the strain equivalence is clear and simple to be applied, the resulting compliance tensor of Eq. (2.53b) has inconvenience of its asymmetry. However, this problem can be solved easily by noting that the damage variable \mathcal{D} is a state variable and can be quantified in a different way (Chaboche 1993; Besson et al. 2010). Namely, by taking another variable \mathcal{D}^* besides \mathcal{D} , we introduce a different definition of the compliance tensor $\mathbb{S}^*(\mathcal{D})$ in place of Eq. (2.53b):

$$\mathbb{S}^*(\mathcal{D}) = \frac{1}{2} [\mathbb{S}_0 : \mathbb{M}(\mathcal{D}^*) + \mathbb{M}^T(\mathcal{D}^*) : \mathbb{S}_0] \quad (2.55a)$$

Then $\mathbb{S}^*(\mathcal{D})$ is symmetric, and the damage variable \mathcal{D}^* is related to \mathcal{D} by means of a relation

$$\begin{aligned}\mathbb{M}(\mathcal{D}^*) &= \mathbb{S}_0^{-1} : \mathbb{S}^*(\mathcal{D}) \\ &= \frac{1}{2} \left[\mathbb{M}(\mathcal{D}^*) + \mathbb{S}_0^{-1} : \mathbb{M}^T(\mathcal{D}^*) : \mathbb{S}_0 \right],\end{aligned}\quad (2.55b)$$

where function $\mathbb{M}(\mathcal{D})$ is the same to that of Eq. (2.43).

2.3.4 Hypothesis of Energy Equivalence 1 – Complementary Strain Energy Equivalence

The existence of a strain energy function and/or a complementary strain energy function necessitates the symmetry of the elastic modulus and the compliance tensor. As observed in Eq. (2.53b), however, the hypothesis of the strain equivalence generally results in asymmetry of the compliance tensor, and does not satisfy this requirement. In Section 2.3.3, the symmetrization of Eq. (2.55) was employed to obviate this problem.

Cordebois and Sidoroff (1982a, b), on the other hand, proposed another hypothesis from the energy point of view, which satisfies the symmetry requirement for the elastic tensors as its intrinsic consequence.

Let us take an elastic-plastic material, and represent the internal change due to plastic deformation by an internal state variable α . Then the *complementary strain-energy functions* of the material at the undamaged and the damaged state are given, respectively, as follows:

$$V_0(\sigma, \alpha) = \frac{1}{2} \sigma : \mathbb{S}_0 : \sigma - \phi(\alpha), \quad (2.56)$$

$$V(\sigma, \mathcal{D}, \alpha) = \frac{1}{2} \sigma : \mathbb{S}(\mathcal{D}) : \sigma - \phi(\alpha). \quad (2.57)$$

Thus we have the elastic constitutive equations for the undamaged and the damaged material

$$\boldsymbol{\epsilon} = \frac{\partial V_0}{\partial \sigma} = \mathbb{S}_0 : \boldsymbol{\sigma}, \quad (2.58)$$

$$\boldsymbol{\epsilon} = \frac{\partial V}{\partial \sigma} = \mathbb{S}(\mathcal{D}) : \boldsymbol{\sigma}. \quad (2.59)$$

In order to derive the constitutive equation of a damaged material in the form of Eq. (2.59), Cordebois and Sidoroff (1982a, b) proposed the following hypothesis:

Hypothesis of Complementary Strain Energy Equivalence

Suppose a damaged material of Fig. 2.11a subject to stress σ , and represent the damage state and the internal state due to inelastic deformation by \mathcal{D} and α , respectively. Then the

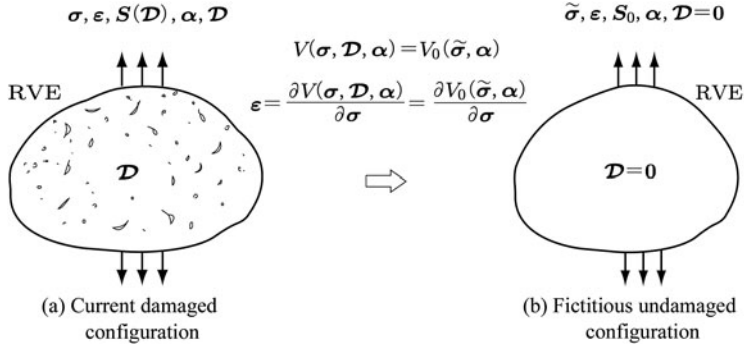


Fig. 2.11 Hypothesis of complementary strain energy equivalence

complementary strain energy function $V(\sigma, \mathcal{D}, \alpha)$ of the damaged material is given by the corresponding function $V_0(\sigma, \alpha)$ of the undamaged material of Fig. 2.11b by replacing the stress σ in $V_0(\sigma, \alpha)$ with the effective stress $\tilde{\sigma}$ of Eq. (2.43), i.e.,

$$V(\sigma, \mathcal{D}, \alpha) = V_0(\tilde{\sigma}, \alpha). \quad (2.60)$$

By the use of this hypothesis, the elastic strain of Eq. (2.59) leads to

$$\begin{aligned} \epsilon &= \frac{\partial V(\sigma, \mathcal{D}, \alpha)}{\partial \sigma} = \mathbb{S}(\mathcal{D}) : \sigma \\ &= \frac{\partial V_0(\tilde{\sigma}, \alpha)}{\partial \sigma} = \frac{\partial}{\partial \sigma} \left(\frac{1}{2} \tilde{\sigma} : \mathbb{S}_0 : \tilde{\sigma} \right) \\ &= \frac{1}{2} \frac{\partial}{\partial \sigma} [(\mathbb{M}(\mathcal{D}) : \sigma) : \mathbb{S}_0 : (\mathbb{M}(\mathcal{D}) : \sigma)] \\ &= [\mathbb{M}^T(\mathcal{D}) : \mathbb{S}_0 : \mathbb{M}(\mathcal{D})] : \sigma, \end{aligned} \quad (2.61)$$

where the symmetry of \mathbb{S}_0 was utilized. In view of Eq. (2.61), we have the elastic compliance tensor of the damaged material as follows:

$$\mathbb{S}(\mathcal{D}) = \mathbb{M}^T(\mathcal{D}) : \mathbb{S}_0 : \mathbb{M}(\mathcal{D}). \quad (2.62)$$

Namely, if the damage effect tensor $\mathbb{M}(\mathcal{D})$ is expressed by a proper fourth-order symmetric tensor, then the elastic compliance tensor $\mathbb{S}(\mathcal{D})$ comes to fourth-order symmetric tensor, and hence satisfies the thermodynamic requirement.

Equation (2.62), on the other hand, implies that the damage effect tensor $\mathbb{M}(\mathcal{D})$ is specified uniquely by the tensors \mathbb{S}_0 and $\mathbb{S}(\mathcal{D})$. If $\mathbb{M}(\mathcal{D})$ is symmetric, it can be given as (Zheng and Bettten 1996)

$$\mathbb{M}(\mathcal{D}) = \sqrt{\sqrt{\mathbb{S}_0^{-1}} : \mathbb{S}(\mathcal{D}) : \sqrt{\mathbb{S}_0^{-1}}}. \quad (2.63)$$

Furthermore, in relation to the effective stress tensor $\tilde{\sigma}$ of Eq. (2.43)

$$\tilde{\sigma} = M(D) : \sigma, \quad (2.64a)$$

we may define a new *effective strain tensor*

$$\tilde{\epsilon} = M^{-T}(D) : \epsilon. \quad (2.64b)$$

Then, the complementary strain energy function (2.57) and the elastic constitutive equation (2.59) can be written also in the following form (Cordebois and Sidoroff 1982a, b):

$$V = \frac{1}{2} \sigma : \epsilon - \phi(\alpha) = \frac{1}{2} \tilde{\sigma} : \tilde{\epsilon} - \phi(\alpha), \quad (2.65)$$

$$\tilde{\epsilon} = S_0 : \tilde{\sigma}. \quad (2.66)$$

Figure 2.12 shows the relations discussed above in the case of uniaxial stress. The symbols $\tilde{\sigma}^*$ and $\tilde{\epsilon}^*$ represent the values of the effective stress and the effective strain corresponding to the hypothesis of the complementary strain energy equivalence.

2.3.5 Hypothesis of Energy Equivalence 2 – Strain Energy Equivalence

The hypothesis of the energy equivalence can be formulated also for the strain energy in a damaged material (Cordebois and Sidoroff 1982a, b). In this case,

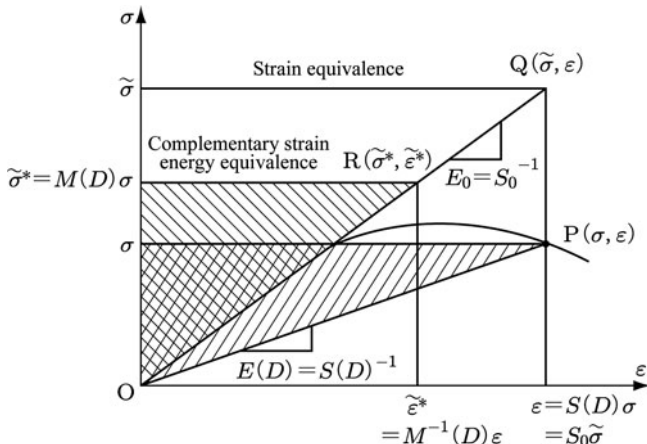


Fig. 2.12 Hypothesis of strain equivalence in elastic deformation and that of complementary strain energy equivalence

the strain energy functions for an undamaged and a damaged material are represented by

$$W_0(\boldsymbol{\epsilon}, \boldsymbol{\alpha}) = \frac{1}{2} \boldsymbol{\epsilon} : \mathcal{C}_0 : \boldsymbol{\epsilon} + \phi(\boldsymbol{\alpha}), \quad (2.67a)$$

$$W(\boldsymbol{\epsilon}, \mathcal{D}, \boldsymbol{\alpha}) = \frac{1}{2} \boldsymbol{\epsilon} : \mathcal{C}(\mathcal{D}) : \boldsymbol{\epsilon} + \phi(\boldsymbol{\alpha}), \quad (2.67b)$$

where \mathcal{C}_0 and $\mathcal{C}(\mathcal{D})$ are the elastic modulus tensors. Then, the elastic constitutive equations of the undamaged and the damaged material are given in the forms

$$\boldsymbol{\sigma} = \frac{\partial W_0}{\partial \boldsymbol{\epsilon}} = \mathcal{C}_0 : \boldsymbol{\epsilon}, \quad (2.68a)$$

$$\boldsymbol{\sigma} = \frac{\partial W}{\partial \boldsymbol{\epsilon}} = \mathcal{C}(\mathcal{D}) : \boldsymbol{\epsilon}. \quad (2.68b)$$

According to these relations, the hypothesis of strain energy equivalence can be expressed as follows:

Hypothesis of Strain Energy Equivalence

The *strain energy function* $W(\boldsymbol{\epsilon}, \mathcal{D}, \boldsymbol{\alpha})$ of a damaged material can be given by the strain energy function $W_0(\boldsymbol{\epsilon}, \boldsymbol{\alpha})$ of the corresponding undamaged material by replacing the strain $\boldsymbol{\epsilon}$ in the function with the effective strain $\tilde{\boldsymbol{\epsilon}}$ defined by Eq. (2.64b);

$$W(\boldsymbol{\epsilon}, \mathcal{D}, \boldsymbol{\alpha}) = W_0(\tilde{\boldsymbol{\epsilon}}, \boldsymbol{\alpha}). \quad (2.69)$$

2.3.6 Hypothesis of Total Energy Equivalence

The hypotheses of energy equivalence presented above not only assure the symmetry of the elastic modulus, and the compliance tensor, but they have also a favorable aspect that they define the equivalence between the damaged and the undamaged state by means of their energy state which reflect the each effect of stress and strain.

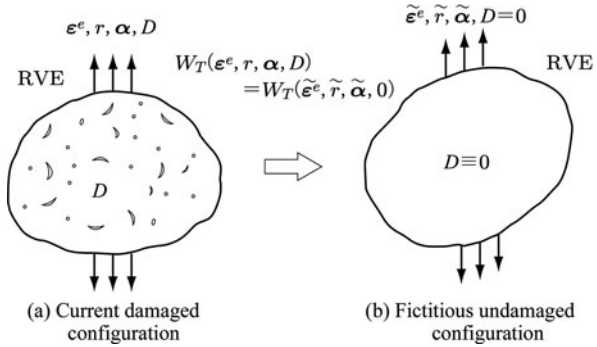
Strictly speaking, however, they are applicable only to the case of elastic state. In order to overcome this limitation, Saanouni, Forster, and Ben Hatira (1994) discussed this problem in the framework of irreversible thermodynamics with internal variables³. Then, they proposed a *hypothesis of total energy equivalence* for the thermoelastic deformation coupled with isotropic damage, and extended energy equivalence hypotheses of Cordebois and Sidoroff.

Let us suppose the representative volume element (RVE) in the current damaged configuration B_t of Fig. 2.13a, and assume that the inelastic damaged state can be specified by a set of state variables:

$$(\boldsymbol{\sigma}, \boldsymbol{\epsilon}^e), \quad (R, r), \quad (A, \boldsymbol{\alpha}), \quad (T, -s), \quad (Y, D), \quad (2.70)$$

³ As regards the constitutive theory based on the irreversible thermodynamics with internal variables, see the succeeding Chapter 3.

Fig. 2.13 Hypothesis of total energy equivalence



where σ , R , A , T and Y denote, respectively, the stress tensor, isotropic hardening variable, kinematic hardening variable, temperature and the associated thermodynamic variable³ with the isotropic damage variable D . The symbols ε^e , r , α and s , on the other hand, are respectively the elastic strain, the associated variables³ of R and A , and the entropy in the configuration B_t .

Then, we assume the existence of the fictitious undamaged configuration B_f of Fig. 2.13b, which has the identical total strain energy W_T to that of B_t and hence is mechanically equivalent to B_t . Let us assume further that the mechanical state of the RVE in B_f can be described by the following set of the effective variables corresponding to Eq. (2.70):

$$(\tilde{\sigma}, \tilde{\varepsilon}^e), (\tilde{R}, \tilde{r}), (\tilde{A}, \tilde{\alpha}), (T, -s), (Y = 0, D = 0). \quad (2.71)$$

The total energy W_T in the configurations B_t and B_f can be expressed as the sum of the reversible elastic energy W_E and those of the irreversible isotropic and kinematic hardening W_I and W_K

$$W_T(\varepsilon^e, r, \alpha, D) = W_T(\tilde{\varepsilon}^e, \tilde{r}, \tilde{\alpha}, D = 0) = W_E + W_I + W_K. \quad (2.72)$$

Since the RVE in B_t and B_f are mechanically equivalent to each other, the following relations should be satisfied for W_E , W_I and W_K :

$$W_E(\varepsilon^e, D) = W_E(\tilde{\varepsilon}^e, 0) = \frac{1}{2}\sigma : \varepsilon^e = \frac{1}{2}\tilde{\sigma} : \tilde{\varepsilon}^e, \quad (2.73a)$$

$$W_I(r, D) = W_I(\tilde{r}, 0) = \frac{1}{2}Rr = \frac{1}{2}\tilde{R}\tilde{r}, \quad (2.73b)$$

$$W_K(\alpha, D) = W_K(\tilde{\alpha}, 0) = \frac{1}{2}A : \alpha = \frac{1}{2}\tilde{A} : \tilde{\alpha}, \quad (2.73c)$$

where small strain is assumed.

The relations (2.73) are always satisfied if the effective state variables $\tilde{\sigma}$, $\tilde{\varepsilon}^e$, \tilde{R} , \tilde{r} , \tilde{A} and $\tilde{\alpha}$ are defined as follows:

$$\tilde{\sigma} = \frac{\sigma}{g(D)}, \quad \tilde{\epsilon}^e = g(D)\epsilon^e, \quad (2.74a)$$

$$\tilde{R} = \frac{R}{h_1(D)}, \quad \tilde{r} = h_1(D)r, \quad (2.74b)$$

$$\tilde{A} = \frac{A}{h_2(D)}, \quad \tilde{\alpha} = h_2(D)\alpha, \quad (2.74c)$$

where scalar functions $g(D)$, $h_1(D)$ and $h_2(D)$ are positive decreasing function of D . According to the results of experiments, these functions may be given:

$$g(D) = h_1(D) = h_2(D) = (1 - D)^{1/2}. \quad (2.75)$$

As a result of these discussions, Saanouni et al. (1994) proposed the following hypothesis:

Hypothesis of Total Energy Equivalence

The mechanical behavior of a damaged material in the current damaged configuration B_t of Fig. 2.13a is derived from the *state- and the dissipation-potential functions* of the equivalent material in the fictitious undamaged configuration B_f of Fig. 2.13b by replacing the state variables in them by the corresponding effective state variables of Eq. (2.74).

The proposed hypothesis is assumed to be applicable to general state- and dissipation-potential functions expressed in terms of the state variables of Eq. (2.70). As an example of its application, a constitutive and an evolution equation of an elastic-plastic-damaged material will be derived in Section 4.4 later. The usefulness and the validity of the hypothesis may be observed in these examples.

2.4 Elastic Constitutive Equation and Elastic Modulus Tensor of Damaged Material – Comparison Between Results by Different Effective Stresses and Equivalence Hypotheses

In the preceding sections, the notion of effective stress, that of effective state variables and the hypotheses of mechanical equivalence between the damaged and the undamaged material were described as a systematic method to formulate the constitutive equations of damaged materials. To elucidate the applicability of these hypotheses, we will derive elastic constitutive equations of damaged materials by these methods and compare the resulting elastic modulus tensors.

In order to facilitate the comparison of the results, tensor relations in this section are represented in the form of their matrix relations. Readers not familiar enough with the matrix representations of the tensors and the tensor relations are referred to Section 12.7 of the Chapter 12.

2.4.1 Elastic Constitutive Equations of Damaged Material

When the damage state of a material is described by the second-order symmetric damage tensor \mathbf{D} of Eq. (2.15), the constitutive equation of the damaged material can be expressed in one of the following forms:

$$(1) \quad \boldsymbol{\varepsilon} = \mathbb{S}(\mathbf{D}) : \boldsymbol{\sigma} \quad (2.76)$$

$$(2) \quad \boldsymbol{\varepsilon} = \frac{\partial V(\boldsymbol{\sigma}, \mathbf{D})}{\partial \boldsymbol{\sigma}}, \quad V = \frac{1}{2} \boldsymbol{\sigma} : \mathbb{S}(\mathbf{D}) : \boldsymbol{\sigma} \quad (2.77)$$

$$(3) \quad \boldsymbol{\sigma} = \mathbb{C}(\mathbf{D}) : \boldsymbol{\varepsilon} \quad (2.78)$$

$$(4) \quad \boldsymbol{\sigma} = \frac{\partial W(\boldsymbol{\varepsilon}, \mathbf{D})}{\partial \boldsymbol{\varepsilon}}, \quad W = \frac{1}{2} \boldsymbol{\varepsilon} : \mathbb{C}(\mathbf{D}) : \boldsymbol{\varepsilon} \quad (2.79)$$

where $\mathbb{S}(\mathbf{D})$ and $\mathbb{C}(\mathbf{D})$ are the elastic compliance tensor and the elastic modulus tensor of the fourth-order, while $V(\boldsymbol{\sigma}, \mathbf{D})$ and $W(\boldsymbol{\varepsilon}, \mathbf{D})$ denote the complementary strain energy and the strain energy function, respectively.

Hence, the general procedure to formulate the elastic behavior of a damaged material is to represent one of the functions of $\mathbb{S}(\mathbf{D})$, $\mathbb{C}(\mathbf{D})$, $V(\boldsymbol{\sigma}, \mathbf{D})$ and $W(\boldsymbol{\varepsilon}, \mathbf{D})$ as a pertinent function of the damage tensor \mathbf{D} .

2.4.2 Matrix Representation of Damage Effect Tensors

In Section 2.3.2, the general form of an effective stress tensor $\tilde{\boldsymbol{\sigma}}$ was given by Eq. (2.43) in terms of the damage effect tensor \mathbb{M} and the corresponding Cauchy stress tensor $\boldsymbol{\sigma}$, i.e.,

$$\tilde{\boldsymbol{\sigma}} = \mathbb{M} : \boldsymbol{\sigma}. \quad (2.80)$$

For the tensor operation of this relation, it is often convenient to express the tensors in the form of the matrices of their components, and then to execute the tensor operation as a matrix calculus. To simplify this procedure, we take an orthonormal basis $\{\mathbf{n}_i\}$ with the principal directions \mathbf{n}_i of the second-order symmetric damage tensor \mathbf{D} , and represent the tensor in terms of their components as to this basis.

According to the Voigt notation described in Section 12.7 of the Chapter 12, a second-order symmetric stress tensor $\boldsymbol{\sigma}$ and the related effective stress tensor $\tilde{\boldsymbol{\sigma}}$ are expressed by the column vectors of six-dimension:

$$\begin{aligned} [\sigma_p] &\equiv [\sigma_{11} \ \sigma_{22} \ \sigma_{33} \ \sigma_{23} \ \sigma_{31} \ \sigma_{12}]^T \\ &\equiv [\sigma_1 \ \sigma_2 \ \sigma_3 \ \sigma_4 \ \sigma_5 \ \sigma_6]^T, \end{aligned} \quad (2.81)$$

$$\begin{aligned} [\tilde{\sigma}_p] &\equiv [\tilde{\sigma}_{11} \ \tilde{\sigma}_{22} \ \tilde{\sigma}_{33} \ \tilde{\sigma}_{23} \ \tilde{\sigma}_{31} \ \tilde{\sigma}_{12}]^T \\ &\equiv [\tilde{\sigma}_1 \ \tilde{\sigma}_2 \ \tilde{\sigma}_3 \ \tilde{\sigma}_4 \ \tilde{\sigma}_5 \ \tilde{\sigma}_6]^T. \end{aligned} \quad (2.82)$$

As regards the damage effect tensor \mathbb{M} of Eq. (2.80), we suppose a symmetric tensor in particular. By representing the first two indices ij and those of the succeeding two indices kl of the tensor by p and q ($p, q = 1, 2, \dots, 6$), respectively, the components of \mathbb{M} are expressed by a six by six matrix

$$\begin{aligned} [M_{pq}] &\equiv \begin{bmatrix} M_{1111} & M_{1122} & M_{1133} & M_{1123} & M_{1131} & M_{1112} \\ M_{2211} & M_{2222} & M_{2233} & M_{2223} & M_{2231} & M_{2212} \\ M_{3311} & M_{3322} & M_{3333} & M_{3323} & M_{3331} & M_{3312} \\ M_{2311} & M_{2322} & M_{2333} & M_{2323} & M_{2331} & M_{2312} \\ M_{3111} & M_{3122} & M_{3133} & M_{3123} & M_{3131} & M_{3112} \\ M_{1211} & M_{1222} & M_{1233} & M_{1223} & M_{1231} & M_{1212} \end{bmatrix} \\ &\equiv \begin{bmatrix} M_{11} & M_{12} & M_{13} & M_{14} & M_{15} & M_{16} \\ M_{21} & M_{22} & M_{23} & M_{24} & M_{25} & M_{26} \\ M_{31} & M_{32} & M_{33} & M_{34} & M_{35} & M_{36} \\ M_{41} & M_{42} & M_{43} & M_{44} & M_{45} & M_{46} \\ M_{51} & M_{52} & M_{53} & M_{54} & M_{55} & M_{56} \\ M_{61} & M_{62} & M_{63} & M_{64} & M_{65} & M_{66} \end{bmatrix}. \end{aligned} \quad (2.83)$$

By means of the matrix representation of Eq. (12.262), we have the matrix form of Eq. (2.80):

$$[\tilde{\sigma}_p] \equiv [M_{pr}] [W_{rq}] [\sigma_q], \quad (2.84)$$

where $[W_{rq}]$ is the weighting matrix of Eq. (12.256).

As will be observed in Section 12.7.3, the transformation matrix $[M_{pr}] [W_{rq}]$ of Eq. (2.84) is different from the matrix $[M_{pq}]$ of the tensor \mathbb{M} in the tensor relation (2.80). To obviate this complexity, we introduce a new roman type symbol $[\mathbf{M}_{pq}]$ and rewrite Eq. (2.84) in the form

$$[\tilde{\sigma}_p] \equiv [\mathbf{M}_{pq}] [\sigma_q], \quad [\mathbf{M}_{pq}] \equiv [M_{pr}] [W_{rq}]. \quad (2.85)$$

Thus, by applying the matrix operation of Eq. (2.85) to the matrices of the damage effect tensors $\mathbb{M}^{(1)}$ through $\mathbb{M}^{(5)}$ discussed in Section 2.3.2, we have the corresponding transformation matrices $[\mathbf{M}_{pq}^{(i)}]$ ($i = 1, 2, \dots, 5$) as shown below.

For the matrix representation of $\mathbb{M}^{(5)}$ of Eq. (2.48), in particular, the fourth-order identity tensor \mathbb{I} should be replaced by the fourth-order symmetric identity tensor \mathbb{I}^S .

(1) **Damage Effect Tensor 1** [Eq. (2.45)]

$$\begin{aligned} \left[M_{pq}^{(1)} \right] &\equiv \left[M_{pr}^{(1)} \right] \left[W_{rq} \right] \\ &= \begin{bmatrix} \Phi_1 & 0 & 0 & 0 & 0 & 0 \\ 0 & \Phi_2 & 0 & 0 & 0 & 0 \\ 0 & 0 & \Phi_3 & 0 & 0 & 0 \\ 0 & 0 & 0 & (\Phi_2 + \Phi_3)/2 & 0 & 0 \\ 0 & 0 & 0 & 0 & (\Phi_3 + \Phi_1)/2 & 0 \\ 0 & 0 & 0 & 0 & 0 & (\Phi_1 + \Phi_2)/2 \end{bmatrix}, \end{aligned} \quad (2.86a)$$

$$\Phi_i = (1 - D_i)^{-1}, \quad (i = 1, 2, 3), \quad (2.86b)$$

or

$$M_{11}^{(1)} = \frac{1}{1 - D_1}, \dots, M_{66}^{(1)} = \frac{1}{2} \left(\frac{1}{1 - D_1} + \frac{1}{1 - D_2} \right). \quad (2.86c)$$

(2) **Damage Effect Tensor 2** [Eq. (2.46)]

$$\begin{aligned} \left[M_{pq}^{(2)} \right]^{-1} &\equiv \left\{ \left[M_{pr}^{(2)} \right] \left[W_{rq} \right] \right\}^{-1} \\ &= \begin{bmatrix} \left(\Phi_1^{(2)} \right)^2 & 0 & 0 & 0 & 0 & 0 \\ 0 & \left(\Phi_2^{(2)} \right)^2 & 0 & 0 & 0 & 0 \\ 0 & 0 & \left(\Phi_3^{(2)} \right)^2 & 0 & 0 & 0 \\ 0 & 0 & 0 & \Phi_2^{(2)} \Phi_3^{(2)} & 0 & 0 \\ 0 & 0 & 0 & 0 & \Phi_3^{(2)} \Phi_1^{(2)} & 0 \\ 0 & 0 & 0 & 0 & 0 & \Phi_1^{(2)} \Phi_2^{(2)} \end{bmatrix}, \end{aligned} \quad (2.87a)$$

$$\Phi_i^{(2)} = (1 - D_i)^{1/2}, \quad (i = 1, 2, 3), \quad (2.87b)$$

or

$$M_{11}^{(2)} = \frac{1}{1 - D_1}, \dots, M_{66}^{(2)} = \frac{1}{\sqrt{(1 - D_1)(1 - D_2)}}. \quad (2.87c)$$

(3) Damage Effect Tensor 3

The matrix representation of $M^{(3)}$ of Eq. (2.40) is derived by replacing $\Phi^{(2)}$ in Eq. (2.87) by $\Phi^{(3)} = (\mathbf{I} - \mathbf{D})$.

(4) Damage Effect Tensor 4 [Eq. (2.47)]

$$\begin{aligned} [M_{pq}^{(4)}]^{-2} &\equiv \left\{ \left[M_{pr}^{(4)} \right] \left[W_{rq} \right] \right\}^{-2} \\ &= \begin{bmatrix} \left(\Phi_1^{(4)} \right)^2 & 0 & 0 & 0 & 0 & 0 \\ 0 & \left(\Phi_2^{(4)} \right)^2 & 0 & 0 & 0 & 0 \\ 0 & 0 & \left(\Phi_3^{(4)} \right)^2 & 0 & 0 & 0 \\ 0 & 0 & 0 & \Phi_2^{(4)} \Phi_3^{(4)} & 0 & 0 \\ 0 & 0 & 0 & 0 & \Phi_3^{(4)} \Phi_1^{(4)} & 0 \\ 0 & 0 & 0 & 0 & 0 & \Phi_1^{(4)} \Phi_2^{(4)} \end{bmatrix}, \end{aligned} \quad (2.88a)$$

$$\Phi_i^{(4)} = 1 - D_i, \quad (i = 1, 2, 3) \quad (2.88b)$$

or

$$M_{11}^{(4)} = \frac{1}{1 - D_1}, \dots, M_{66}^{(4)} = \frac{1}{\sqrt{(1 - D_1)(1 - D_2)}} \quad (2.88c)$$

It should be noted from Eqs. (2.87c) and (2.88c) that the damage effect tensors $M^{(2)}$ of Eqs. (2.46) and $M^{(4)}$ of Eq. (2.47) have the same components as far as the principal coordinates of the damage tensor are concerned.

(5) **Damage Effect Tensor 5** [Eq. (2.48)]

$$\left[M_{pq}^{(5)} \right] \equiv \left[M_{pr}^{(5)} \right] \left[W_{rq} \right]$$

$$= \begin{bmatrix} \frac{1}{1-D_1} & 0 & 0 & 0 & 0 & 0 \\ 0 & \frac{1}{1-D_2} & 0 & 0 & 0 & 0 \\ 0 & 0 & \frac{1}{1-D_3} & 0 & 0 & 0 \\ 0 & 0 & 0 & \frac{1}{1-\frac{D_2+D_3}{2}} & 0 & 0 \\ 0 & 0 & 0 & 0 & \frac{1}{1-\frac{D_3+D_1}{2}} & 0 \\ 0 & 0 & 0 & 0 & 0 & \frac{1}{1-\frac{D_1+D_2}{2}} \end{bmatrix} \quad (2.89)$$

In the discussion throughout this section, all the tensor components are concerned with the orthonormal basis in the principal direction \mathbf{n}_i of the damage tensor \mathbf{D} , and every damage effect tensor has the form of the diagonal matrix. In the case of a general coordinate systems, however, the derivation of the matrices of the damage effect tensors necessitates complicated matrix calculus including the inverse or the square root matrix. These calculi may be performed by the use of symbolic manipulation softwares.

2.4.3 Matrix Representation of Elastic Constitutive Equation and Elastic Modulus Tensor

According to the hypotheses of mechanical equivalence discussed in Section 2.3, the elastic constitutive equation of a damaged material can be derived by replacing the Cauchy stress tensor $\boldsymbol{\sigma}$ in the equation or in the strain energy function of the undamaged material by the corresponding effective stress tensor $\tilde{\boldsymbol{\sigma}}$.

Prior to the derivation of constitutive equations of damaged materials, we first discuss the matrix representation of the elastic constitutive equation of an undamaged material.

As observed in Section 12.7.4, the elastic constitutive equation of an isotropic undamaged material is given by Eqs. (12.224) and (12.278), and has the form

$$\boldsymbol{\sigma} = \mathbb{C}_0 : \boldsymbol{\epsilon} \quad \text{or} \quad \sigma_{ij} = C_{ijkl}^0 \epsilon_{kl}, \quad (2.90)$$

$$\mathbb{C}_0 = \lambda \mathbf{I} \otimes \mathbf{I} + 2\mu \mathbb{I}^S, \quad (2.91a)$$

or

$$C_{ijkl}^0 = \lambda \delta_{ij} \delta_{kl} + \mu (\delta_{ik} \delta_{jl} + \delta_{il} \delta_{jk}). \quad (2.91b)$$

By the use of the matrix representation of Eq. (12.273) for σ , ϵ and C_0 , and taking account of the relations of Eqs. (12.276) and (12.280), the elastic constitutive equation of Eq. (2.90) is expressed as follows:

$$[\sigma_p] = [C_{pq}^0][\epsilon_q], \quad (2.92a)$$

$$[C_{pq}^0] = [C_{pr}^0][W_{rq}]$$

$$= \frac{E}{(1+\nu)(1-2\nu)} \begin{bmatrix} 1-\nu & \nu & \nu & 0 & 0 & 0 \\ \nu & 1-\nu & \nu & 0 & 0 & 0 \\ \nu & \nu & 1-\nu & 0 & 0 & 0 \\ 0 & 0 & 0 & 1-2\nu & 0 & 0 \\ 0 & 0 & 0 & 0 & 1-2\nu & 0 \\ 0 & 0 & 0 & 0 & 0 & 1-2\nu \end{bmatrix}. \quad (2.92b)$$

The elastic constitutive equation (2.58) expressed in terms of σ , on the other hand, is expressed for an undamaged isotropic material as

$$\epsilon = S_0 : \sigma \quad \text{or} \quad \epsilon_{ij} = S_{ijkl}^0 \sigma_{kl}, \quad (2.93)$$

$$S_0 = \frac{1+\nu}{E} I^S - \frac{\nu}{E} I \otimes I, \quad (2.94a)$$

or

$$S_{ijkl}^0 = \frac{1+\nu}{2E} (\delta_{ik}\delta_{jl} + \delta_{il}\delta_{jk}) - \frac{\nu}{E} \delta_{ij}\delta_{kl}. \quad (2.94b)$$

By means of Eqs. (12.277) and (12.281), Eq. (12.93) is expressed in the matrix form

$$[\epsilon_p] = [S_{pq}^0][\sigma_q], \quad (2.95a)$$

$$[S_{pq}^0] = [S_{pr}^0][W_{rq}]$$

$$= \begin{bmatrix} \frac{1}{E} & \frac{-\nu}{E} & \frac{-\nu}{E} & 0 & 0 & 0 \\ \frac{-\nu}{E} & \frac{1}{E} & \frac{-\nu}{E} & 0 & 0 & 0 \\ \frac{-\nu}{E} & \frac{-\nu}{E} & \frac{1}{E} & 0 & 0 & 0 \\ 0 & 0 & 0 & \frac{1}{2G} & 0 & 0 \\ 0 & 0 & 0 & 0 & \frac{1}{2G} & 0 \\ 0 & 0 & 0 & 0 & 0 & \frac{1}{2G} \end{bmatrix} \quad (2.95b)$$

2.4.4 Elastic Constitutive Equation and Elastic Compliance Tensor 1 – By Hypothesis of Strain Equivalence

The preceding subsections were concerned with the matrix representation of the elastic constitutive equations and that of damage effect tensors. Applying these results, together with the hypotheses of mechanical equivalence described in Section 2.3, we now discuss the variation of elastic properties of materials due to damage development.

We suppose first the damage effect tensor $\mathbb{M}^{(1)}$ of Eq. (2.45) defined by the second-order symmetric damage tensor \mathbf{D} . Applying the hypothesis of strain equivalence and the effective stress of Eq. (2.85) in the matrix form to the elastic constitutive equation (12.277), we have

$$\begin{aligned} [\varepsilon_p] &= [S_{pq}(\mathbf{D})][\sigma_q] = \left[S_{pq}^0 \right] [\tilde{\sigma}_q] \\ &= \left[S_{pr}^0 \right] \left[M_{rq}^{(1)}(\mathbf{D}) \right] [\sigma_q]. \end{aligned} \quad (2.96)$$

Thus the elastic constitutive equation and the corresponding compliance matrix of a damaged material specified by the damage effect tensor $\mathbb{M}^{(1)}$ are given by

$$[\varepsilon_p] = \left[S_{pq}^{(1)}(\mathbf{D}) \right] [\sigma_q], \quad (2.97)$$

$$\left[S_{pq}^{(1)}(\mathbf{D}) \right] = \left[S_{pr}^0 \right] \left[M_{rq}^{(1)}(\mathbf{D}) \right], \quad (2.98)$$

where $\left[S_{pr}^0 \right]$ and $\left[M_{rq}^{(1)}(\mathbf{D}) \right]$ are the compliance matrix of an undamaged elastic material and the matrix of the damage effect tensor $\mathbb{M}^{(1)}$, respectively, and are given explicitly by Eqs. (2.95) and (2.86). Note that Eqs. (2.97) and (2.98) above are the matrix representation of Eqs. (2.53).

Let us now derive the explicit representation of the compliance matrix of Eq. (2.98) in some detail. By substituting Eqs. (2.95) and (2.86) into Eq. (2.98), we have

$$\left[S_{pq}^{(1)}(\mathbf{D}) \right] = \left[S_{pr}^0 \right] \left[M_{rq}^{(1)}(\mathbf{D}) \right] = \begin{bmatrix} \frac{1}{\tilde{E}_1} & \frac{-\tilde{v}_{21}}{\tilde{E}_2} & \frac{-\tilde{v}_{31}}{\tilde{E}_3} & 0 & 0 & 0 \\ -\frac{\tilde{v}_{12}}{\tilde{E}_1} & \frac{1}{\tilde{E}_2} & \frac{-\tilde{v}_{32}}{\tilde{E}_3} & 0 & 0 & 0 \\ -\frac{\tilde{v}_{13}}{\tilde{E}_1} & -\frac{\tilde{v}_{23}}{\tilde{E}_2} & \frac{1}{\tilde{E}_3} & 0 & 0 & 0 \\ 0 & 0 & 0 & \frac{1}{2\tilde{G}_{23}} & 0 & 0 \\ 0 & 0 & 0 & 0 & \frac{1}{2\tilde{G}_{31}} & 0 \\ 0 & 0 & 0 & 0 & 0 & \frac{1}{2\tilde{G}_{12}} \end{bmatrix}, \quad (2.99)$$

where \tilde{E}_i , \tilde{G}_{ij} and $\tilde{\nu}_{ij}$ denote the Young's modulus in i -direction, the shear modulus in $i-j$ plane and Poisson's ratio representing the transverse strain in j -direction induced by the uniaxial stress in i -direction, respectively, and are expressed as

$$\begin{aligned} \frac{1}{\tilde{E}_i} &= \frac{1}{E} \Phi_i, \quad \frac{1}{2\tilde{G}_{ij}} = \frac{1}{2G} \Phi_{ij}, \quad \frac{\tilde{\nu}_{ij}}{\tilde{E}_i} = \frac{\nu}{2E} \Phi_i, \\ \Phi_i &= (1 - D_i)^{-1}, \quad \Phi_{ij} = \frac{1}{2} (\Phi_i + \Phi_j). \end{aligned} \quad (2.100a)$$

(no sum for i ; $i, j = 1, 2, 3$)

As observed from Eqs. (2.99) and (2.100a), the compliance matrix $[S_{pq}^{(1)}(\mathbf{D})]$ thus obtained is asymmetric. A simple procedure to symmetrize this matrix is to take the symmetric part of the Cartesian decomposition of Eq. (2.100a):

$$\frac{1}{\tilde{E}_i} = \frac{1}{E} \Phi_i, \quad \frac{1}{2\tilde{G}_{ij}} = \frac{1}{2G} \Phi_{ij}, \quad \frac{\tilde{\nu}_{ij}}{\tilde{E}_i} = \frac{\nu}{2E} (\Phi_i + \Phi_j) \quad (2.100b)$$

However, as described in Section 2.3.3, asymmetry of the resulting compliance matrix is not the intrinsic consequence of the hypothesis of strain equivalence. In fact, by the use of the $\mathbb{M}(\mathbf{D}^*)$ of Eq. (2.55b) in place of $\mathbb{M}^{(1)}$, the relevant compliance tensor is given by Eq. (2.55a):

$$S_{pq}^{(1)*}(\mathbf{D}) = \frac{1}{2} [S_0 : \mathbb{M}^{(1)}(\mathbf{D}^*) + \mathbb{M}^{(1)\top}(\mathbf{D}^*) : S_0] \quad (2.101a)$$

In view of Eq. (12.272), the matrix representation of this relation leads to

$$\begin{aligned} [S_{pq}^{(1)*}(\mathbf{D})] &= \frac{1}{2} \left\{ [S_{pr}^0] [W_{rs}] [M_{sq}^{(1)}(\mathbf{D}^*)] + [M_{pr}^{(1)\top}(\mathbf{D}^*)] [W_{rs}] [S_{sq}^0] \right\} \\ &= \frac{1}{2} \left\{ [S_{pr}^0] [M_{rq}^{(1)}(\mathbf{D}^*)] + [M_{pr}^{(1)\top}(\mathbf{D}^*)] [S_{rq}^0] \right\} \\ &= \frac{1}{2} \left\{ [S_{pq}^{(1)}(\mathbf{D}^*)] + [S_{pq}^{(1)}(\mathbf{D}^*)]^T \right\}, \end{aligned} \quad (2.101b)$$

where the matrix $[S_{pq}^{(1)}(\mathbf{D}^*)]$ is identical to Eqs. (2.99) and (2.100a), and its argument \mathbf{D}^* is related to the damage tensor \mathbf{D} by means of Eq. (2.55b). It should be noted that Eq. (2.101b) is exactly identical to the symmetrized compliance matrix of Eqs. (2.99) and (2.100b).

As observed in the results of Eqs. (2.99) and (2.100b) or in Eq. (2.101b), the development of damage in this case reduces an initially isotropic elastic material to an orthotropic elastic material with respect to the principal directions of the damage tensor \mathbf{D} . Furthermore, it is ascertained that the elastic constants of this damaged material satisfy *Saint-Venant's condition* for orthotropy, i.e., the condition of planar isotropy for the shear modulus

$$\frac{1}{\tilde{G}_{ij}} = \frac{1 + \tilde{\nu}_{ij}}{\tilde{E}_i} + \frac{1 + \tilde{\nu}_{ji}}{\tilde{E}_j}. \quad (2.102)$$

2.4.5 Elastic Constitutive Equation and Elastic Compliance Tensor 2 – By Hypothesis of Complementary Strain Energy Equivalence

As an alternative method to secure the symmetry of the elastic compliance tensor $\mathbb{S}(\mathbf{D})$, Cordebois and Sidoroff (1982a, b) employed the hypothesis of complementary strain energy equivalence of Section 2.3.4 together with the corresponding effective stress $\tilde{\sigma}$ of Eq. (2.39).

By the use of the damage effect tensor $M^{(2)}(\mathbf{D})$ of Eq. (2.46b), the effective stress tensor $\tilde{\sigma}$ of Eq. (2.39) was expressed in the form of Eq. (2.46a). Then, the matrix representation of $M^{(2)}(\mathbf{D})$ is given by Eq. (2.87), i.e.,

$$\left[M_{pq}^{(2)} \right] = \begin{bmatrix} \Phi_1 & 0 & 0 & 0 & 0 & 0 \\ 0 & \Phi_2 & 0 & 0 & 0 & 0 \\ 0 & 0 & \Phi_3 & 0 & 0 & 0 \\ 0 & 0 & 0 & (\Phi_2 \Phi_3)^{\frac{1}{2}} & 0 & 0 \\ 0 & 0 & 0 & 0 & (\Phi_3 \Phi_1)^{\frac{1}{2}} & 0 \\ 0 & 0 & 0 & 0 & 0 & (\Phi_1 \Phi_2)^{\frac{1}{2}} \end{bmatrix}, \quad (2.103a)$$

$$\Phi_i = \left(\Phi_i^{(2)} \right)^{-2} = (1 - D_i)^{-1}. \quad (2.103b)$$

Thus, the elastic constitutive equation and its compliance tensor $\mathbb{S}^{(2)}(\mathbf{D})$ of a damaged material derived by the hypothesis of complementary strain energy equivalence are expressed in matrix form by the use of Eqs. (2.61) and (2.62):

$$[\varepsilon_p] = [\mathbb{S}_{pq}^{(2)}(\mathbf{D})] [\sigma_q], \quad (2.104)$$

$$[\mathbb{S}_{pq}^{(2)}(\mathbf{D})] = [M_{rp}^{(2)}(\mathbf{D})]^T [\mathbb{S}_{rs}^0] [M_{sq}^{(2)}(\mathbf{D})]. \quad (2.105)$$

The compliance matrix of the damaged material, therefore, is derived by substituting Eqs. (2.95b) and (2.103) into Eq. (2.105), i.e.,

$$\left[S_{pq}^{(2)}(\mathbf{D}) \right] = \begin{bmatrix} \frac{1}{\tilde{E}_1} & \frac{-\tilde{\nu}_{21}}{\tilde{E}_2} & \frac{-\tilde{\nu}_{31}}{\tilde{E}_3} & 0 & 0 & 0 \\ \frac{-\tilde{\nu}_{12}}{\tilde{E}_1} & \frac{1}{\tilde{E}_2} & \frac{-\tilde{\nu}_{32}}{\tilde{E}_3} & 0 & 0 & 0 \\ \frac{-\tilde{\nu}_{13}}{\tilde{E}_1} & \frac{-\tilde{\nu}_{23}}{\tilde{E}_2} & \frac{1}{\tilde{E}_3} & 0 & 0 & 0 \\ 0 & 0 & 0 & \frac{1}{2\tilde{G}_{23}} & 0 & 0 \\ 0 & 0 & 0 & 0 & \frac{1}{2\tilde{G}_{31}} & 0 \\ 0 & 0 & 0 & 0 & 0 & \frac{1}{2\tilde{G}_{12}} \end{bmatrix}, \quad (2.106)$$

where \tilde{E}_i , \tilde{G}_{ij} and $\tilde{\nu}_{ij}$ are given by

$$\frac{1}{\tilde{E}_i} = \frac{1}{E} \Phi_i^2, \quad \frac{1}{2\tilde{G}_{ij}} = \frac{1}{2G} \Phi_i \Phi_j, \quad \frac{\tilde{\nu}_{ij}}{\tilde{E}_i} = \frac{\nu}{E} \Phi_i \Phi_j, \quad (2.107a)$$

$$\Phi_i = (1 - D_i)^{-1}, \quad (\text{no sum for } i; \quad i, j = 1, 2, 3). \quad (2.107b)$$

As observed from Eqs. (2.106) and (2.107), the hypothesis of complementary strain energy equivalence provides a symmetric compliance tensor. Equation (2.107), furthermore, satisfies Saint-Venant's condition of Eq. (2.102).

Equation (2.107) shows that the effect of damage on the elastic property in this case is expressed in the square of $\Phi_i = (1 - D_i)^{-1}$. However, it should be noted that this result differs from other results that the variation of elastic constants is proportional to Φ_i in the range of small damage (M. Kachanov 1980; Hayakawa and Murakami 1997).

2.4.6 Elastic Constitutive Equation and Elastic Compliance Tensor 3 – By Complementary Strain Energy Function and Representation Theorem

The elastic constitutive equation of a damaged material, or the change in elastic property due to damage, can be formulated also from the appropriate representation of the strain energy function $V(\boldsymbol{\sigma}, \mathbf{D}, \boldsymbol{\alpha})$ or $W(\boldsymbol{\epsilon}, \mathbf{D}, \boldsymbol{\alpha})$ of Eq. (2.57) or (2.67), besides the derivation due to hypotheses of mechanical equivalence described above.

M. Kachanov (1980), by describing the damage state of an elastic material by a second-order crack-density tensor \mathbf{D} of Eq. (2.28), represented the complementary strain energy function $V(\boldsymbol{\sigma}, \mathbf{D}, \boldsymbol{\alpha})$ in terms of a scalar valued isotropic tensor function of Eq. (12.215). Then he formulated the orthotropic elastic constitutive equation of a material damaged by distributed microcracks.

In the analysis, Kachanov expressed $V(\boldsymbol{\sigma}, \mathbf{D}, \boldsymbol{\alpha})$ as a function of basic invariants of two symmetric second-order tensors $\boldsymbol{\sigma}$ and \mathbf{D}

$$\begin{aligned} V(\boldsymbol{\sigma}, \mathbf{D}) = & -\frac{\nu}{2E} (\text{tr}\boldsymbol{\sigma})^2 + \frac{1+\nu}{2E} \text{tr}\boldsymbol{\sigma}^2 \\ & + \eta_1 \text{tr}\boldsymbol{\sigma} \text{tr}(\boldsymbol{\sigma}\mathbf{D}) + \eta_2 \text{tr}(\boldsymbol{\sigma}^2 \mathbf{D}). \end{aligned} \quad (2.108)$$

Substitution of this equation into Eq. (2.78b) gives the compliance matrix of the damaged material:

$$[S_{pq}(\mathbf{D})] = \begin{bmatrix} \frac{1}{\tilde{E}_1} & \frac{-\tilde{\nu}_{21}}{\tilde{E}_2} & \frac{-\tilde{\nu}_{31}}{\tilde{E}_3} & 0 & 0 & 0 \\ \frac{-\tilde{\nu}_{12}}{\tilde{E}_1} & \frac{1}{\tilde{E}_2} & \frac{-\tilde{\nu}_{32}}{\tilde{E}_3} & 0 & 0 & 0 \\ \frac{-\tilde{\nu}_{13}}{\tilde{E}_1} & \frac{-\tilde{\nu}_{23}}{\tilde{E}_2} & \frac{1}{\tilde{E}_3} & 0 & 0 & 0 \\ 0 & 0 & 0 & \frac{1}{2\tilde{G}_{23}} & 0 & 0 \\ 0 & 0 & 0 & 0 & \frac{1}{2\tilde{G}_{31}} & 0 \\ 0 & 0 & 0 & 0 & 0 & \frac{1}{2\tilde{G}_{12}} \end{bmatrix}, \quad (2.109)$$

where \tilde{E}_i , \tilde{G}_{ij} and $\tilde{\nu}_{ij}$ are given as follows:

$$\frac{1}{\tilde{E}_i} = \frac{1}{E} + 2(\eta_1 + \eta_2)D_i, \quad (2.110a)$$

$$\frac{1}{2\tilde{G}_{ij}} = \frac{1}{2G} + 2\eta_2(D_i + D_j), \quad (2.110b)$$

$$\frac{\tilde{\nu}_{ij}}{\tilde{E}_i} = \frac{\nu}{E} - \eta_1(D_i + D_j). \quad (2.110c)$$

The symbols η_1 and η_2 in these equations are indeterminate constants. Equations (2.109) and (2.110) satisfy Saint-Venant's condition (2.102), and are in agreement with the compliance of Eqs. (2.99), and (2.100b), or Eq. (2.101b) within the accuracy of the second-order of D_i .

In this section, as the application of the notion of the effective stress and the hypotheses of mechanical equivalence, we described the elastic constitutive equations of damaged materials by postulating a second-order symmetric damage tensor \mathbf{D} . Afterwards, in Chapters 5 and 9, anisotropic elastic-brittle damage theories for brittle materials, like ceramics, concrete and rock, will be formulated by postulating the fourth-order damage tensors and by including the effect of opening-closing behavior of cracks.

2.5 Refinement of Continuum Damage Mechanics and Its Results

As observed so far, continuum damage mechanics has been constructed mainly on the basis of the following premises:

- (1) The damage state of a material caused by its microstructural change can be described by means of macroscopic damage variables,

- (2) The mechanical behavior of a damaged material can be described by a set of constitutive and evolution equations for the state variables.
- (3) The mechanical formulation of these equations can be performed by the use of the notion of effective state variables and the hypotheses of mechanical equivalence between the damage and the undamaged states.

As will be found in the subsequent chapters, these premises and the resulting simplified procedure have facilitated the solutions of complicated engineering problems of damage and fracture, and helped the development of this field of mechanics.

With respect to this framework of CDM, however, the rigor and the consistency of the above simplified notion and hypothesis, in addition to the rationality of the selection of damage variables, have been often subjected to the criticisms and the remarks together with the proposed refinement (e.g., Rabier 1989; He and Curnier 1995; Lacy et al. 1997; Yang et al. 2005).

At the end of this chapter, a short comment on the development of CDM from this point of view will be described here.

In order to obviate the simplified notion and the hypothesis of the continuum damage mechanics, He and Curnier (1995), for example, developed a precise theoretical framework of the damage theory, and showed the resulting aspects in the case of the elastic constitutive equation of damaged materials. Lacy and others (1997), on the other hand, based on the two-dimensional micromechanics analysis of cracked elastic-brittle materials with a few uniformly distributed crack patterns, compared their results of the effective elastic modulus and the crack evolution force with those of continuum damage mechanics. Then, they extended detailed discussion on the implication and the limitations of the continuum damage mechanics approach.

Comparison of their results with those of Section 2.4, however, will show the complexity and the lack of flexibility of the elaborated approaches to damage problems. In view of the insignificant difference between these results, at least as far as the cases of low to moderate density of voids is concerned, the simplicity and the effectiveness of the traditional theory of damage mechanics presented in the subsequent chapters of this book will be recognized.

Chapter 3

Thermodynamics of Damaged Material

In the preceding chapter, we discussed the mechanical modeling of the damaged state of materials by means of internal variables, and called them damage variables. The present chapter is concerned with the thermodynamic constitutive theory with internal variables, which furnishes a consistent basis to formulate the mechanical behavior of damaged materials.

In Section 3.1, the fundamental principles and the basic laws of the non-equilibrium continuum thermodynamics are presented as the foundations for the succeeding discussions. In Section 3.2, the notion and the procedure of the thermodynamic constitutive theory with internal variables will be described in detail. It is shown that the inelastic constitutive equations and the evolution equations for internal variables are formulated as a set of generalized normality rule defined by a dissipation potential function and a common multiplier. Finally in Section 3.3, the extension of this standard thermodynamic constitutive theory by the use of multiple damage potentials will be described briefly.

3.1 Thermodynamics of Continuum

3.1.1 State Variables and Principle of Local State

A set of particles surrounded by a boundary in a space is called a *system*, and the region occupied by the particles and the boundary of the region are denoted by B and ∂B , respectively. A system consisting of a fixed set of particles is said to be a *closed system*. In the following, we suppose a closed system, and the collection of the particles, or the fixed amount of mass occupying the region B will be called a *system B* .

The thermodynamic state of a system can be described by a set of macroscopic variables which pertinently characterize the state. Among these variables, those specified only by the current state of the system are called *state variables*. The state variables, furthermore, are divided into the *external variables* (or *observable variables*) and *internal variables* (or *hidden variables*), depending on whether they are observable from the outside or not.

When the thermodynamic state (hence the state variables) of a system does not vary with time, the system is said to be in *thermodynamic equilibrium*. On the other hand, if the state of a system undergoes a change under the action of some agencies, the change in the state is called a *thermodynamic process*. If the state of a system changes in the reverse direction of the process by reversing the action of the agencies and returns to the initial thermodynamic state, the thermodynamic process is said to be *reversible*. Otherwise, the process is said to be *irreversible*.

The state variables which govern independently the change of the state are referred to as *independent variables*. The variables which are given by single-valued functions of these independent variables are called *dependent variables*. The choice of the independent variables is not unique.

When a continuum undergoes a process of deformation, the internal states, such as strain and temperature, may differ from a location to another in the continuum and vary with time. In other words, the thermodynamic state of a continuum in general is non-uniform and is in a non-equilibrium state, and the thermodynamic process is irreversible. Such a non-equilibrium process, however, cannot be discussed by the use of the classical thermodynamics (i.e., thermostatics) which was developed under the assumption of uniform and equilibrium states. In order to solve this essential problem, quite a number of notions and theories have been proposed hitherto.¹ Among them, one of the most well-developed and the most frequently employed theories in continuum thermodynamics is given by the following *principle of local state* (Kestin and Rice 1970; Germain 1973) or *hypothesis of local equilibrium* (De Groot and Mazur 1962; Glansdorff and Prigogine 1971):

We take a small material element at a given point of a body, and suppose that the thermodynamic state of the element at any time is completely specified by a set of state variables. Then, even if the element is in a non-equilibrium state, the state variables of the element at any instant are determined by the same thermodynamic relations as for the equilibrium case.

This hypothesis postulates that a material element in a continuum in non-equilibrium state show the identical thermodynamic response to that in the corresponding equilibrium state. Thus this postulate holds always if the response time of the material element to attain to its equilibrium state should be short in comparison with the characteristic time of the kinematic and thermodynamic evolution of the continuum. Namely this hypothesis implies that the thermodynamic process of a material element of a moving continuum proceeds as a succession of its equilibrium state.

3.1.2 First Law of Thermodynamics

The energy-balance postulate as a fundamental axiom of mechanics has been formulated in the form of the first law of thermodynamics. By means of this law, we

¹ Excellent review of the development of the non-equilibrium thermodynamics and its major results are found in Germain et al. (1983) and Chaboche (1997).

can define the internal energy of a system, and can represent the thermodynamic state of the system. Namely, the *first law of thermodynamics* states:

The rate of the internal energy plus that of the kinetic energy of a thermodynamic system is equal to the rate of external mechanical work plus the rate of heat supply to the system due to the heat flux and the heat source.

If a thermodynamic system B is a continuum as shown in Fig. 3.1, the *internal energy* E and the *kinetic energy* K of B are given by

$$E = \int_B \rho e dV, \quad (3.1)$$

$$K = \frac{1}{2} \int_B \rho v \cdot v dV, \quad (3.2)$$

where ρ , e and v signify the mass density, the internal energy per unit mass and the velocity.

If the *surface force* per unit area (or *traction*) and the *body force* per unit mass acting on B are denoted by t and f , the *external mechanical power* done by these forces (i.e., rate of external mechanical work) are expressed as

$$\dot{W} = \int_B \rho f \cdot v dV + \int_{\partial B} t \cdot v dS, \quad (3.3)$$

where (\cdot) is the material time derivative defined by Eq. (12.172) in Chapter 12. Furthermore, let r and q be the rate of *heat generation* per unit volume in B and the outward *heat flux vector* on ∂B . Then we have the *rate of heat supply* to B :

$$\dot{Q} = \int_B r dV - \int_{\partial B} q \cdot n dS, \quad (3.4)$$

where n is the outward unit normal vector on ∂B .

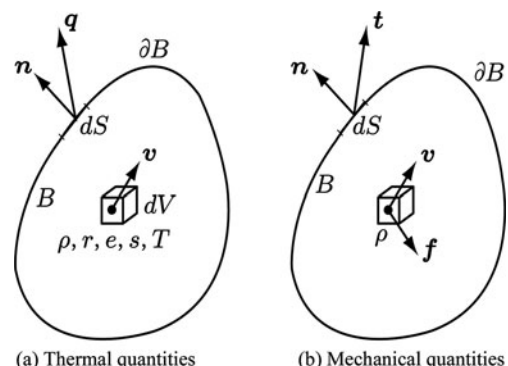


Fig. 3.1 Heat flux and heat generation in a body, the forces acting on the body and the velocity of the material point

With Eqs. (3.1) through (3.4), one has the first law of thermodynamics

$$\dot{K} + \dot{E} = \dot{W} + \dot{Q}, \quad (3.5a)$$

or

$$\begin{aligned} \frac{D}{Dt} \int_B \rho \left(\frac{1}{2} \mathbf{v} \cdot \mathbf{v} + e \right) dV &= \int_B (\rho f \cdot \mathbf{v} + r) dV \\ &\quad + \int_{\partial B} (\mathbf{t} \cdot \mathbf{v} - \mathbf{q} \cdot \mathbf{n}) dS. \end{aligned} \quad (3.5b)$$

According to Reynolds' transport theorem (12.180), the left-hand side of Eq. (3.5b) leads to

$$\begin{aligned} &\frac{D}{Dt} \int_B \rho \left(\frac{1}{2} \mathbf{v} \cdot \mathbf{v} + e \right) dV \\ &= \int_B \left\{ \frac{D}{Dt} \left[\rho \left(\frac{1}{2} \mathbf{v} \cdot \mathbf{v} + e \right) \right] + \left[\rho \left(\frac{1}{2} \mathbf{v} \cdot \mathbf{v} + e \right) \right] \operatorname{div} \mathbf{v} \right\} dV \\ &= \int_B \left[\left(\frac{1}{2} \mathbf{v} \cdot \mathbf{v} + e \right) \frac{D\rho}{Dt} + \rho \frac{D}{Dt} \left(\frac{1}{2} \mathbf{v} \cdot \mathbf{v} + e \right) + \rho \left(\frac{1}{2} \mathbf{v} \cdot \mathbf{v} + e \right) \operatorname{div} \mathbf{v} \right] dV \\ &= \int_B \rho (\mathbf{v} \cdot \dot{\mathbf{v}} + \dot{e}) dV, \end{aligned} \quad (3.6)$$

where the expression of the fourth line was derived by the use of the *law of conservation of mass* (or the *equation of continuity*)

$$\frac{D\rho}{Dt} + \rho \operatorname{div} \mathbf{v} = 0. \quad (3.7)$$

The second terms on the right-hand side of Eq. (3.5b), on the other hand, takes the following form by the use of *Cauchy's formula* $\mathbf{t} = \sigma \mathbf{n}$ of Eq. (2.17a) and Gauss' divergence theorem (12.168):

$$\begin{aligned} \int_{\partial B} (\mathbf{t} \cdot \mathbf{v} - \mathbf{q} \cdot \mathbf{n}) dS &= \int_{\partial B} (\mathbf{v} \cdot \sigma \mathbf{n} - \mathbf{q} \cdot \mathbf{n}) dS \\ &= \int_{\partial B} (\sigma^T \mathbf{v} - \mathbf{q}) \cdot \mathbf{n} dS \\ &= \int_B \operatorname{div}(\sigma \mathbf{v} - \mathbf{q}) dV. \end{aligned} \quad (3.8)$$

Substitution of Eqs. (3.6) and (3.8) into Eq. (3.5b) gives

$$\int_B \rho(\mathbf{v} \cdot \dot{\mathbf{v}} + \dot{e}) dV = \int_B [(\rho\mathbf{f} \cdot \mathbf{v} + r) + \operatorname{div}(\boldsymbol{\sigma}\mathbf{v} - \mathbf{q})] dV,$$

from which we have

$$\begin{aligned} \int_B [\boldsymbol{\sigma} : \operatorname{grad} \mathbf{v} - \operatorname{div} \mathbf{q} + r - \rho\dot{e}] dV \\ + \int_B [\mathbf{v} \cdot (\operatorname{div} \boldsymbol{\sigma} + \rho\mathbf{f} - \rho\dot{\mathbf{v}})] dV = 0. \end{aligned} \quad (3.9)$$

In view of the *momentum balance principle* (or *equation of motion*)

$$\rho\dot{\mathbf{v}} = \rho\mathbf{f} + \operatorname{div} \boldsymbol{\sigma}, \quad (3.10)$$

the second term of Eq. (3.9) vanishes, and hence the first law of the thermodynamics (3.5) is finally given as

$$\int_B \rho\dot{e} dV = \int_B (\boldsymbol{\sigma} : \operatorname{grad} \mathbf{v} - \operatorname{div} \mathbf{q} + r) dV. \quad (3.11a)$$

Since the choice of the region B is arbitrary, Eq. (3.11a) may lead to the local form

$$\rho\dot{e} = \boldsymbol{\sigma} : \operatorname{grad} \mathbf{v} - \operatorname{div} \mathbf{q} + r. \quad (3.11b)$$

In the particular case of small strain, by the use of strain rate $\dot{\epsilon}$, Eq. (3.11b) is expressed also in the form

$$\rho\dot{e} = \boldsymbol{\sigma} : \dot{\boldsymbol{\epsilon}} - \operatorname{div} \mathbf{q} + r. \quad (3.11c)$$

3.1.3 Second Law of Thermodynamics and Clausius-Duhem Inequality

Equation (3.11) gives the *law of energy conservation* in a thermodynamic process. However, in order to describe the non-equilibrium thermodynamics of a continuum, the permissible direction of the process should be also specified. Thus we now consider the concept and the consequence of the second law of thermodynamics.

Let us first assume that two further thermodynamic variables, i.e., *entropy* s per unit mass and the *absolute temperature* T of a positive value, can be defined (Fig. 3.1). The entropy S of the system B is given by

$$S = \int_B \rho s dV. \quad (3.12)$$

Then, the *second law of thermodynamics* states:

The rate of increase in the entropy of a system is never less than the rate of increase in the entropy due to the heat source and the heat flux.

According to the second law of thermodynamics postulated above, the rate of change of entropy in a system B always satisfies the inequality

$$\frac{DS}{Dt} \geq \int_B \frac{r}{T} dV - \int_{\partial B} \frac{\mathbf{q} \cdot \mathbf{n}}{T} dS, \quad (3.13)$$

where the terms r/T and \mathbf{q}/T on the right-hand side denote the entropy increase due to heat generation and heat flow, and are called an *entropy source* and the *entropy flux*, respectively. The equality in this relation holds for a reversible process.

By the use of Gauss' divergence theorem of Eq. (12.168) together with Reynold's transport theorem (12.180), Eq. (3.13) leads to

$$\int_B \left[\rho \dot{s} + \operatorname{div}\left(\frac{\mathbf{q}}{T}\right) - \frac{r}{T} \right] dV \geq 0. \quad (3.14)$$

Since this relation holds for an arbitrary region B , we have the local form of Eq. (3.14):

$$\rho \dot{s} + \operatorname{div}\left(\frac{\mathbf{q}}{T}\right) - \frac{r}{T} \geq 0. \quad (3.15)$$

Substitution of r from Eq. (3.11c) into this relation gives

$$\rho \dot{s} + \operatorname{div}\left(\frac{\mathbf{q}}{T}\right) - \frac{1}{T}(\rho \dot{e} - \boldsymbol{\sigma} : \dot{\boldsymbol{\epsilon}} + \operatorname{div} \mathbf{q}) \geq 0. \quad (3.16)$$

In view of a relation $\operatorname{div}(\mathbf{q}/T) = (\operatorname{div} \mathbf{q})/T - (\mathbf{q} \cdot \operatorname{grad} T)/T^2$, and by multiplying $T \geq 0$ to both-hand side of Eq. (3.16), we have

$$\boldsymbol{\sigma} : \dot{\boldsymbol{\epsilon}} + \rho(T \dot{s} - \dot{e}) - \mathbf{q} \cdot \frac{\operatorname{grad} T}{T} \geq 0. \quad (3.17)$$

By using the *Helmholtz free energy* (or simply *free energy*) per unit mass to be defined in Section 3.1.4 afterward

$$\psi = e - Ts, \quad (3.18)$$

and by eliminating the internal energy e from Eq. (3.17), we finally have the following relation

$$\boldsymbol{\sigma} : \dot{\boldsymbol{\epsilon}} - \rho(\dot{\psi} + \dot{T}s) - \mathbf{q} \cdot \frac{\operatorname{grad} T}{T} \geq 0. \quad (3.19)$$

Equation (3.19) is known as the *Clausius-Duhem inequality*, and must be satisfied for every possible process (Truesdell and Noll 1965; Malvern 1969; Germain 1973).

Thus, this inequality imposes essential restrictions on constitutive equations, and gives the foundation of the thermodynamic constitutive theory for the dissipative process of a continuum. Besides Eq. (3.19), Eqs. (3.15) and (3.17) are often referred to as Clausius-Duhem inequality.

3.1.4 Gibbs Relation and Thermodynamic Potentials

According to the basic assumption of thermodynamics, the local internal energy e per unit mass is determined by the entropy s per unit mass and n *thermodynamic substate variables* χ_i ($i = 1, 2, \dots, n$), and is given by a function (Truesdell and Toupin 1960; Malvern 1969)

$$e = e(s, \chi_i). \quad (3.20)^2$$

By means of this equation, temperature T and the additional thermodynamic variables η_i associated to the state variables χ_i can be defined as follows:

$$T = \frac{\partial e}{\partial s}, \quad \eta_i = \frac{\partial e}{\partial \chi_i}. \quad (3.21)$$

Thus, for any change in the thermodynamic state of a given material point, we have

$$de = Tds + \eta_i d\chi_i. \quad (i = 1, 2, \dots, n) \quad (3.22)$$

This relation is known as the *Gibbs relation*, and gives a basic relation to discuss the *entropy balance*.

In particular, when the strain $\boldsymbol{\epsilon}$ and the *internal variables* of the material element \mathbf{V}_k ($k = 1, 2, \dots$) are taken as its substate variables χ_i , Eqs. (3.22) and (3.20) are

$$de = Tds + \frac{1}{\rho} \boldsymbol{\sigma} : d\boldsymbol{\epsilon} - \mathbf{A}_k \cdot d\mathbf{V}_k, \quad (3.23)$$

$$\mathbf{A}_k = -\frac{\partial e}{\partial \mathbf{V}_k} \quad (k = 1, 2, \dots)$$

$$e = e(s, \boldsymbol{\epsilon}, \mathbf{V}_k) \quad (3.24)$$

where $\boldsymbol{\sigma}$, ρ and \mathbf{A}_k are the stress, material density and the associated variables to \mathbf{V}_k .

The internal energy e and the entropy s are the state variables. Thus, by the use of Eqs. (3.23) and (3.24), the following three *state functions* per unit mass, besides the internal energy function of Eq. (3.24), can be introduced:

² This equation together with the analogous equations, e.g., $s = s(e, \chi_i)$, $e = e(T, \mathbf{F})$, $s = s(T, \mathbf{F})$, describes the thermodynamic property of the material, and thus they are called *caloric equations of state* (Truesdell and Toupin 1960; Coleman and Mizel 1964), where \mathbf{F} is the deformation gradient.

(1) *Helmholtz free energy*

$$\psi(T, \boldsymbol{\epsilon}, \mathbf{V}_k) = e - Ts. \quad (3.25)$$

(2) *Gibbs potential*³

$$\begin{aligned} \Gamma(T, \boldsymbol{\sigma}, \mathbf{V}_k) &= e - Ts - \frac{1}{\rho} \boldsymbol{\sigma} : \boldsymbol{\epsilon} \\ &= \psi - \frac{1}{\rho} \boldsymbol{\sigma} : \boldsymbol{\epsilon}. \end{aligned} \quad (3.26)$$

(3) *Enthalpy*

$$\begin{aligned} h = h(s, \boldsymbol{\sigma}, \mathbf{V}_k) &= e - \frac{1}{\rho} \boldsymbol{\sigma} : \boldsymbol{\epsilon} \\ &= \Gamma + Ts. \end{aligned} \quad (3.27)$$

By the use of Eq. (3.23), the total differentials of Eqs. (3.25) through (3.27) are given as follow:

$$\begin{aligned} d\psi &= de - Tds - sdT \\ &= -sdT + \frac{1}{\rho} \boldsymbol{\sigma} : d\boldsymbol{\epsilon} - \mathbf{A}_k \cdot d\mathbf{V}_k, \end{aligned} \quad (3.28)$$

$$\begin{aligned} d\Gamma &= d\psi - \frac{1}{\rho} \boldsymbol{\sigma} : d\boldsymbol{\epsilon} - \frac{1}{\rho} \boldsymbol{\epsilon} : d\boldsymbol{\sigma} \\ &= -sdT - \frac{1}{\rho} \boldsymbol{\epsilon} : d\boldsymbol{\sigma} - \mathbf{A}_k \cdot d\mathbf{V}_k, \end{aligned} \quad (3.29)$$

$$\begin{aligned} dh &= de - \frac{1}{\rho} \boldsymbol{\sigma} : d\boldsymbol{\epsilon} - \frac{1}{\rho} \boldsymbol{\epsilon} : d\boldsymbol{\sigma} \\ &= Tds - \frac{1}{\rho} \boldsymbol{\epsilon} : d\boldsymbol{\sigma} - \mathbf{A}_k \cdot d\mathbf{V}_k. \end{aligned} \quad (3.30)$$

So far we defined four thermodynamic state functions e , ψ , Γ and h as functions of the three independent variables s or T , $\boldsymbol{\epsilon}$ or $\boldsymbol{\sigma}$ besides the internal variable \mathbf{V}_k , and derived their total differentials in the form of Eqs. (3.23) and (3.28) through (3.30).

Then let us examine the thermodynamic features of these state functions in some detail. First, the total differential of the internal energy function e of Eq. (3.24) with respect to its arguments is derived as

$$de = \frac{\partial e}{\partial s} \Big|_{\boldsymbol{\epsilon}, \mathbf{V}_k} ds + \frac{\partial e}{\partial \boldsymbol{\epsilon}} \Big|_{s, \mathbf{V}_k} : d\boldsymbol{\epsilon} + \frac{\partial e}{\partial \mathbf{V}_k} \Big|_{s, \boldsymbol{\epsilon}} \cdot d\mathbf{V}_k. \quad (3.31)$$

Comparison of this relation with the Gibbs relation (3.23) gives the relations

³ Called also *Gibbs function*, or *Gibbs free energy*.

$$T = \frac{\partial e}{\partial s} |_{\boldsymbol{\varepsilon}, V_k}, \quad \sigma = \rho \frac{\partial e}{\partial \boldsymbol{\varepsilon}} |_{s, V_k}, \quad A_k = -\frac{\partial e}{\partial V_k} |_{s, \boldsymbol{\varepsilon}}. \quad (3.32)$$

As regards the state functions of Eqs. (3.25) through (3.27), by deriving the total differentials as to their independent variables and by comparing the results with Eqs. (3.28) through (3.30), we have similar relations

$$s = -\frac{\partial \psi}{\partial T} |_{\boldsymbol{\varepsilon}, V_k}, \quad \sigma = \rho \frac{\partial \psi}{\partial \boldsymbol{\varepsilon}} |_{T, V_k}, \quad A_k = -\frac{\partial \psi}{\partial V_k} |_{T, \boldsymbol{\varepsilon}}, \quad (3.33)$$

$$s = -\frac{\partial \Gamma}{\partial T} |_{\sigma, V_k}, \quad \boldsymbol{\varepsilon} = -\rho \frac{\partial \Gamma}{\partial \sigma} |_{T, V_k}, \quad A_k = -\frac{\partial \Gamma}{\partial V_k} |_{T, \sigma}, \quad (3.34)$$

$$T = \frac{\partial h}{\partial s} |_{\sigma, V_k}, \quad \boldsymbol{\varepsilon} = -\rho \frac{\partial h}{\partial \sigma} |_{s, V_k}, \quad A_k = -\frac{\partial h}{\partial V_k} |_{s, \sigma}. \quad (3.35)$$

It will be observed from Eqs. (3.32) through (3.35) that the thermodynamic state functions e , ψ , Γ and h determine a set of three state variables T or s , σ or $\boldsymbol{\varepsilon}$ and V_k by their partial derivatives with respect to their respective associated variables, and thus specify the thermodynamic properties of the system. For example, Eq. (3.32) and the internal energy function e give the temperature-entropy relation in a constant strain process, as well as the stress-strain relation in iso-entropy process; i.e., Eq. (3.32) gives the thermal and the mechanical *constitutive equations*⁴ of a material.

Since the thermodynamic state functions e , ψ , Γ and h determine the thermal and mechanical properties of the system by the partial derivatives with respect to their independent variables, they are called *thermodynamic potentials*, *state potentials* or *thermodynamic characteristic functions*. Equations (3.32) through (3.35) give the fundamental relations of the *thermodynamic constitutive theory*.⁴

3.2 Thermodynamic Constitutive Theory of Inelasticity with Internal Variables

Inelastic deformation usually is accompanied with microstructural internal change in the material, and the process is irreversible. We will now represent this internal change in terms of the *internal variables* of thermodynamics. Then, by postulating the *principle of local state*, the consistent constitutive theories for wide variety of inelastic materials will be discussed on the basis of the thermodynamic potential functions and the Clausius-Duhem inequality described in the preceding section.

⁴ Thermal and mechanical behavior of a material is governed not only by various conservation laws of general validity but also by material relations specifying the intrinsic response of the material. In a broad sense, equations characterizing the individual material are called *constitutive equations*. Thus the state functions of Eqs. (3.24) through (3.27) are called *state equations*, or *constitutive equations*.

3.2.1 Thermodynamic Potentials and Constitutive Equations

We first assume that the deformation is small, and the total strain $\boldsymbol{\epsilon}$ is divided into the sum of the elastic strain $\boldsymbol{\epsilon}^e$ and the plastic strain $\boldsymbol{\epsilon}^p$, i.e.,

$$\boldsymbol{\epsilon} = \boldsymbol{\epsilon}^e + \boldsymbol{\epsilon}^p. \quad (3.36)$$

Derivation of inelastic constitutive equations by the thermodynamic theory of Section 3.1 necessitates pertinent selection of internal variables. As the external variables, we adopt the total strain $\boldsymbol{\epsilon}$ and the temperature T :

$$\{\boldsymbol{\epsilon}, T\}. \quad (3.37)$$

By the use of these two variables, we can elucidate a number of mechanical phenomena, such as elastic, viscoelastic and plastic deformation as well as damage and fracture.

The internal variables, on the other hand, must be selected so that they can represent adequately the change of internal state of the relevant material, such as the atomic and molecular array, the configuration of dislocations and the geometry and distribution of microvoids, etc. Though the internal variables affect the observable external variables, the values of the internal variables cannot be measured directly from the outside.

Thus the selection of the internal variables depends on the phenomena to be described. We will assume that the internal variables here can be represented by a set of tensor variables:

$$\{V_k; k = 1, 2, \dots, n\}. \quad (3.38)$$

In the application of the Clausius-Duhem inequality (3.19), one must specify first the independent variables governing the *Helmholtz free energy function* ψ . Helmholtz free energy in a material undergoing irreversible process is affected by the internal structural change of the material, such as the development of the inelastic strain and microvoids. Thus we postulate that the Helmholtz free energy ψ per unit mass of the material can be expressed as a function of inelastic strain $\boldsymbol{\epsilon}^p$ and internal variables V_k , besides the total strain $\boldsymbol{\epsilon}$ and the temperature T :

$$\psi = \psi(\boldsymbol{\epsilon}, T, \boldsymbol{\epsilon}^p, V_k), \quad (3.39)$$

where ψ is a continuous scalar function concave as regards the temperature and convex in other variables (Germain 1973; Lemaitre and Chaboche 1985).

Since the effect of $\boldsymbol{\epsilon}^p$ on the Helmholtz free energy ψ may be expressed in terms of the internal variable V_k , one can eliminate $\boldsymbol{\epsilon}^p$ from the argument of ψ , and hence Eq. (3.39) leads to

$$\psi = \psi(\boldsymbol{\epsilon}^e, T, V_k). \quad (3.40)$$

Time derivative of this equation gives

$$\dot{\psi} = \frac{\partial\psi}{\partial\boldsymbol{\epsilon}^e} : \dot{\boldsymbol{\epsilon}}^e + \frac{\partial\psi}{\partial T} \dot{T} + \frac{\partial\psi}{\partial \mathbf{V}_k} : \dot{\mathbf{V}}_k. \quad (3.41)$$

By substituting Eq. (3.41) together with Eq. (3.36) into the Clausius-Duhem inequality (3.19), we obtain

$$\begin{aligned} & \left(\boldsymbol{\sigma} - \rho \frac{\partial\psi}{\partial\boldsymbol{\epsilon}^e} \right) : \dot{\boldsymbol{\epsilon}}^e + \boldsymbol{\sigma} : \dot{\boldsymbol{\epsilon}}^p - \rho \left(s + \frac{\partial\psi}{\partial T} \right) \dot{T} \\ & - \rho \frac{\partial\psi}{\partial \mathbf{V}_k} : \dot{\mathbf{V}}_k - \frac{\text{grad}T}{T} \cdot \mathbf{q} \geq 0. \end{aligned} \quad (3.42)$$

This relation should be satisfied for every thermodynamic process described by the function (3.40).

Let us suppose first elastic deformation in a uniform temperature field. Since the internal state in this case remains unchanged, we have

$$\text{grad}T = 0, \quad \dot{\boldsymbol{\epsilon}}^p = 0, \quad \dot{\mathbf{V}}_k = 0. \quad (3.43)$$

Then Eq. (3.42) leads to

$$\left(\boldsymbol{\sigma} - \rho \frac{\partial\psi}{\partial\boldsymbol{\epsilon}^e} \right) : \dot{\boldsymbol{\epsilon}}^e - \rho \left(s + \frac{\partial\psi}{\partial T} \right) \dot{T} \geq 0. \quad (3.44)$$

This inequality should be satisfied for any choice of $\dot{\boldsymbol{\epsilon}}^e$ and \dot{T} , and hence we have the following *state equations*, or the *constitutive equations*:

$$\boldsymbol{\sigma} = \rho \frac{\partial\psi}{\partial\boldsymbol{\epsilon}^e}, \quad s = - \frac{\partial\psi}{\partial T}. \quad (3.45)$$

Namely, the stress $\boldsymbol{\sigma}$ and the entropy s are derived by differentiating the Helmholtz free energy function ψ with respect to the elastic strain $\boldsymbol{\epsilon}^e$ and the temperature T .

Let us now substitute Eq. (3.45) into Eq. (3.42). Then we have the inequality

$$\boldsymbol{\sigma} : \dot{\boldsymbol{\epsilon}}^p - \rho \frac{\partial\psi}{\partial \mathbf{V}_k} : \dot{\mathbf{V}}_k - \frac{\text{grad}T}{T} \cdot \mathbf{q} \geq 0. \quad (3.46)$$

By defining new variables

$$A_k \equiv -\rho \frac{\partial\psi}{\partial \mathbf{V}_k}, \quad (3.47)^5$$

⁵ In the definitions (3.47) and (3.48) of A_k and \mathbf{g} (e.g., Maugin 1992), we have arbitrariness in the selection of the sign on their right-hand sides. In Chapter 4 and thereafter, the definition of Eq. (3.47) without the minus sign “–” will be used for a part of the associated variables A_k .

$$\mathbf{g} \equiv -\text{grad}T, \quad (3.48)^5$$

and substituting them into Eq. (3.46), the Clausius-Duhem inequality (3.42) eventually reduces to

$$\Phi = \boldsymbol{\sigma} : \dot{\boldsymbol{\epsilon}}^p + A_k : \dot{V}_k + (\mathbf{g}/T) \cdot \mathbf{q} \geq 0. \quad (3.49)$$

The symbols Φ in this relation denotes the *dissipation* per unit volume of the material, while A_k is an associated variable with V_k . Equation (3.49) is called *dissipation inequality*, and states that the dissipation brought about by the change of internal state is always non-negative.

The Clausius-Duhem inequality (3.19) can be expressed also by the use of thermodynamic potentials other than the Helmholtz free energy ψ . The constitutive equations derived from Gibbs potential will be presented in 3.2.3.

3.2.2 Dissipation Potentials and Evolution Equations of Internal Variables

It was shown above that the thermoelastic constitutive equation and the thermal state equation of a continuum undergoing irreversible process are given by a thermodynamic potential ψ and Eq. (3.45). However, the description of the change in the internal state necessitates the *evolution equations*⁶ of the internal variables $\dot{\boldsymbol{\epsilon}}^p$ and \dot{V}_k .

Equation (3.49) shows that the dissipation Φ is expressed by the products of the generalized flux vector and the generalized force vector. However, between the vector of the internal variable rates $\{\dot{\boldsymbol{\epsilon}}^p, \dot{V}_k, \mathbf{q}\}$ and that of their *associated variables* $\{\boldsymbol{\sigma}, A_k, \mathbf{g}/T\}$, the selection which will be taken for generalized flux vector and which for the generalized force vector is not unique. Conventionally, it may be easier to understand that the force is the cause of the flux. Therefore we will define hereafter the *generalized force vector* X and the associated *generalized flux vector* J , respectively, as follows:

$$X \equiv \{\boldsymbol{\sigma}, A_k, \mathbf{g}/T\}, \quad (3.50)$$

$$J \equiv \{\dot{\boldsymbol{\epsilon}}^p, \dot{V}_k, \mathbf{q}\}, \quad (3.51)$$

⁶ The equation which governs the change of internal state is a material function, and is called a *constitutive equation* as already described in Section 3.1.4. However the equation which describes the progress of an irreversible process, in particular, is usually termed an *evolution equation* or a *complementary equation*.

and express Eq. (3.49) in the form

$$\Phi = X \cdot J \geq 0. \quad (3.52)$$

In this case, the generalized flux J represents the rate of change of the internal variables, while the generalized force X stands for their cause.

When the dissipation Φ can be expressed in the form of Eq. (3.52), in particular, the evolution equations of J can be derived from a potential function defined as a function of X (Rice 1971, 1975; Germain 1973; Lemaitre and Chaboche 1985).

Then we postulate the existence of a scalar function of the generalized force X , i.e., a *dissipation potential function*

$$F = F(X; V_k, T), \quad (3.53)$$

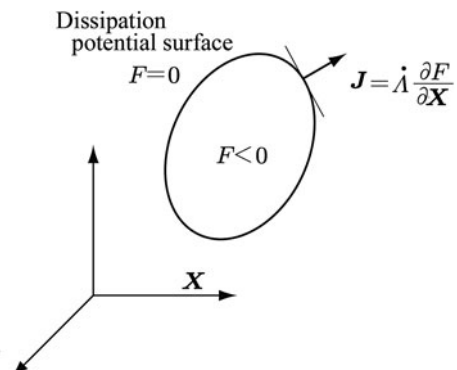
such that the generalized flux J is derived from F (Fig. 3.2):

$$J = \dot{\lambda} \frac{\partial F}{\partial X}. \quad (3.54)$$

The function F of Eq. (3.53) has been assumed to be a non-negative convex function of X and to be $F = 0$ for $X = 0$. Moreover, in the function F , the current state variable V_k and T have been included as parameters after the semicolon “;”. The symbol $\dot{\lambda}$ in Eq. (3.54), on the other hand, is an indeterminate multiplier. Explicit expressions of Eq. (3.54) are given as

$$\dot{\epsilon}^p = \dot{\lambda} \frac{\partial F}{\partial \sigma}, \quad \dot{V}_k = \dot{\lambda} \frac{\partial F}{\partial A_k}, \quad q = \dot{\lambda} \frac{\partial F}{\partial (g/T)}. \quad (3.55)$$

Fig. 3.2 Dissipation potential surface and the generalized flux vector in the space of the generalized force



In other words, the *constitutive equations* of plastic strain rate $\dot{\epsilon}^P$ and the heat flux vector \mathbf{q} , together with the *evolution equations* of the internal variable V_k are specified by the outward normal vectors to the potential surface $F = 0$ in the space of generalized force, i.e., by a *normality law*.

For the existence of the dissipation potential function F of Eq. (3.53), the differential $J_K dX_K$ should be exact differential. This requirement is satisfied in the following two cases.

As a first case, we assume the irreversible process discussed by Onsager (1931), and suppose the vicinity of the equilibrium state $\mathbf{J} = 0$. Then we have the linear relation between \mathbf{J} and \mathbf{X} , and can write

$$J_K = L_{KM} X_M. \quad (3.56)$$

This relation is called the *phenomenological relation* or the *phenomenological equation*, and the coefficients L_{KM} have the symmetry

$$L_{KM} = L_{MK}. \quad (3.57)$$

Equation (3.57) was derived by means of the statistical mechanics, and is known as *Onsager reciprocity relation*.

When Eqs. (3.56) and (3.57) are satisfied, $J_K dX_K$ is proved to be the exact differential, and the dissipation potential F is given by a homogeneous quadratic function (Germain 1973; Maugin 1992):

$$F(\mathbf{X}; V_k, T) = \frac{1}{2} L_{KM} X_K X_M. \quad (3.58)$$

This function together with Eq. (3.54) provides the evolution equation for internal variables

$$J_K = L_{KM} X_M. \quad (3.59)$$

The second example of the existence of the dissipation potential F is the case where the component J_K of the generalized flux \mathbf{J} depends only on the corresponding component X_K of the generalized force \mathbf{X} , and can be expressed as (Rice 1971, 1975)

$$J_K = J_K(X_K; V_k, T). \quad (3.60)$$

This property in the dependence of J_K on X_K is called *local dependence* of the internal structural change in material. In the case of Eq. (3.60), $J_K dX_K$ is the exact differential and hence existence of the potential $F(\mathbf{X}; V_k, T)$ is certified.

3.2.3 Constitutive Equations Expressed in Stress Space

Derivation of constitutive equations on the basis of Helmholtz free energy function $\psi(\boldsymbol{\varepsilon}^e, T, V_k)$ was discussed in Section 3.2.1. In that case, elastic strain $\boldsymbol{\varepsilon}^e$ was taken as the independent variable, and the constitutive equation (3.45) and the dissipation function (3.52) are specified as the functions of $\boldsymbol{\varepsilon}^e$.

In inelastic and damaged processes, however, elastic strain cannot be measured directly. Moreover, elastic property itself varies with damage, and it is often inconvenient to choose elastic strain as the independent variable. In other words, one would like to formulate mechanical behavior of materials in the stress space.

Let us now derive the alternative relations in stress space on the basis of the Gibbs potential.

We first assume that the internal variables of an elastic-plastic-damaged material are given as

$$\{\boldsymbol{\varepsilon}^p, V_k; k = 1, 2, \dots, n\}. \quad (3.61)$$

In view of Eq. (3.26) the Gibbs potential per unit mass is

$$\rho\Gamma(\boldsymbol{\sigma}, T, V_k) = \rho\psi(\boldsymbol{\varepsilon}^e, T, V_k) - \boldsymbol{\sigma} : \boldsymbol{\varepsilon}^e. \quad (3.62)$$

Substitution of this relation into the Clausius-Duhem inequality (3.19) leads to

$$\begin{aligned} \boldsymbol{\sigma} : \dot{\boldsymbol{\varepsilon}}^p - \left(\boldsymbol{\varepsilon}^e + \rho \frac{\partial\Gamma}{\partial\boldsymbol{\sigma}} \right) : \dot{\boldsymbol{\sigma}} - \rho \left(s + \frac{\partial\Gamma}{\partial T} \right) \dot{T} \\ - \rho \frac{\partial\Gamma}{\partial V_k} \dot{V}_k - \frac{\text{grad}T}{T} \cdot \mathbf{q} \geq 0. \end{aligned} \quad (3.63)$$

From this relation we have the elastic and the thermal constitutive equations:

$$\boldsymbol{\varepsilon}^e = -\rho \frac{\partial\Gamma}{\partial\boldsymbol{\sigma}}, \quad s = -\frac{\partial\Gamma}{\partial T}. \quad (3.64)$$

Then we introduce new variables

$$\mathbf{A}_k \equiv -\rho \frac{\partial\Gamma}{\partial V_k}, \quad \mathbf{g} \equiv -\text{grad}T. \quad (3.65)^7$$

By the use of Eqs. (3.64) and (3.65), the Clausius-Duhem inequality (3.63) can be expressed in the similar forms to Eqs. (3.50) through (3.52)

$$\Phi = \mathbf{X} \cdot \mathbf{J} \geq 0, \quad (3.66)$$

⁷ \mathbf{A}_k defined here is identical to that of Eq. (3.47), and has the same value.

$$\mathbf{X} = \{\boldsymbol{\sigma}, \mathbf{A}_k, \mathbf{g}/\mathbf{T}\}, \quad (3.67a)$$

$$\mathbf{J} = \{\dot{\boldsymbol{\epsilon}}^p, \dot{\mathbf{V}}_k, \mathbf{q}\}. \quad (3.67b)$$

Finally, if the existence of a dissipation potential function

$$F = F(\mathbf{X}; \mathbf{V}_k, T) \quad (3.68)$$

can be postulated, the evolution equation of the *generalized flux vector*, i.e., the inelastic constitutive equation together with the evolution equation of the internal variable can be derived by the similar procedure as in Section 3.2.2 as follows:

$$\mathbf{J} = \dot{\Lambda} \frac{\partial F}{\partial \mathbf{X}}. \quad (3.69)$$

In the present case, as observed from Eqs. (3.62), (3.65) and (3.67), the *generalized force* \mathbf{X} is given as a function of the stress $\boldsymbol{\sigma}$, and hence the resulting constitutive and evolution equation are expressed in the stress space.

3.3 Extension of Thermodynamic Constitutive Theory of Inelasticity

Thermodynamic constitutive theory described above provides a unified procedure to formulate constitutive equations of inelasticity and damage. However, for accurate modeling of complicated behavior of wide range of material, the theory has its own limitations. We now describe briefly the extension of the applicability of the preceding constitutive theories.

3.3.1 Generalized Standard Material

According to the derivation of Section 3.2.2, the evolution equations of the generalized flux vector $\mathbf{J} \equiv \{\dot{\boldsymbol{\epsilon}}^p, \dot{\mathbf{V}}_k\}$ are given by Eq. (3.55) by the use of the dissipation potential function F of Eq. (3.53). This fact implies that the evolution equation (3.55) may be taken as the generalization of the flow law of plastic deformation to include the evolution equations of the related internal variables.

In the framework of the thermodynamic constitutive theory, therefore, if there exists a dissipation potential $F = F(\boldsymbol{\sigma}, \mathbf{A}_k; \mathbf{V}_k)$ in the space of the generalized force $\mathbf{X} \equiv \{\boldsymbol{\sigma}, \mathbf{A}_k\}$, and if the constitutive law of inelastic deformation and the evolution equations of internal variables are given by a *generalized normality law*

$$\dot{\boldsymbol{\epsilon}}^p = \dot{\Lambda} \frac{\partial F}{\partial \boldsymbol{\sigma}}, \quad \dot{\mathbf{V}}_k = \dot{\Lambda} \frac{\partial F}{\partial \mathbf{A}_k}, \quad (3.70)$$

then this particular class of material is called a *generalized standard material* (Halphen and Nguyen 1975; Chaboche 1997; Besson et al. 2010). In other words, in

a generalized standard material, the flow law and the hardening law are completely defined once its yield function is specified.

An important aspect of the generalized standard material exists in the fact that the existence of the generalized flux vector $\mathbf{J} \equiv \{\dot{\epsilon}^p, V_k\}$ and the non-negative requirement of their dissipation, or the second law of the thermodynamics, can be assured in the framework of the irreversible thermodynamics. As in the case of Eq. (3.70), furthermore, when the inelastic deformation and the ensuing evolution of internal variables are all specified by *a single* potential F and *a single* multiplier λ , the formulation is called *standard thermodynamic approach*.

3.3.2 Thermodynamic Constitutive Theory Based on Multiple Dissipation Potentials – Quasi-Standard Thermodynamic Approach

The standard thermodynamic approach described above implies the simultaneous evolution of the inelastic deformation and the damage. As regards actual materials, however, ductile damage usually starts after significant inelastic deformation, whereas the brittle damage occurs without remarkable deformation. Thus the postulate of a single potential and a single multiplier in the standard thermodynamic approach may impose severe restrictions on the material modeling.

This restriction can be overcome by employing plural independent dissipation potentials together with the corresponding multipliers for specific physical mechanisms for deformation and damage (Chow and Wang 1987; Hansen and Schreyer 1994; Chaboche 1997).

For this purpose, the internal variables V_k defined by Eq. (3.38) are divided into the strain-hardening variables $\{\alpha_j (j = 1, 2, 3, \dots, m)\}$ and those of the current damage state and the accumulated effect of damage $\{D, \beta\}$ as follows

$$\{V_k\} = \{\alpha_j, D, \beta\}. \quad (3.71)$$

Then the free energy function of Eq. (3.40) has the form

$$\psi = \psi(\epsilon^e, \alpha_j, D, \beta), \quad (3.72)$$

and the thermodynamic associated variables of α_j, D, β are given by Eq. (3.47):

$$A_j = -\rho \frac{\partial \psi}{\partial \alpha_j}, \quad Y = -\rho \frac{\partial \psi}{\partial D}, \quad B = -\rho \frac{\partial \psi}{\partial \beta}. \quad (3.73)^8$$

⁸ Note that the associated variables A_j , Y and B are defined by Eq. (3.47) in this chapter. However, in Chapter 4 and thereafter, the different sign is used in the right hand side of the definition of these variables for the expedience of the argument.

Then, the dissipation potential F of Eq. (3.53) is assumed to be divided into two independent potentials F^P and F^D , respectively, for the inelastic deformation and the damage. By assuming the independent development of these phenomena, the evolution equations of their dissipation processes are derived as follow, for the cases of the rate-independent and the rate-dependent materials, respectively (Besson et al. 2010).

(1) Rate-Independent Material

Let us postulate that the development of the plastic deformation and the damage are described by the following two sets of the criterion functions and the dissipation potentials:

$$f^P(\sigma, A_j, \mathbf{D}) \leq 0, \quad (3.74a)$$

$$\begin{aligned} F^P &= F^P(\sigma, A_j, \mathbf{D}) \\ &= f^P + f^H(A_j, \mathbf{D}), \end{aligned} \quad (3.74b)$$

$$f^D(Y, B; \mathbf{D}, \beta) \leq 0, \quad (3.75a)$$

$$F^D = F^D(Y, B; \mathbf{D}, \beta), \quad (3.75b)$$

where f^P and f^D stand for the elastic and the undamaged region in the space of stress and that of the associated damage variables, respectively. The function f^H , furthermore, is an additional function to represent the dynamic recovery effect of strain-hardening.

The evolution equations of plastic strain and damage are derived from Eq. (3.55), and are expressed in the form of the generalized normality rule:

$$\dot{\boldsymbol{\epsilon}}^P = \dot{\Lambda}^P \frac{\partial F^P}{\partial \sigma}, \quad \dot{\boldsymbol{\alpha}}_j = \dot{\Lambda}^P \frac{\partial F^P}{\partial A_j}, \quad (3.76)$$

$$\dot{\mathbf{D}} = \dot{\Lambda}^D \frac{\partial F^D}{\partial Y}, \quad \dot{\beta} = \dot{\Lambda}^D \frac{\partial F^D}{\partial B}, \quad (3.77)$$

where two multipliers $\dot{\Lambda}^P$ and $\dot{\Lambda}^D$ are determined independently by the use of the consistency conditions⁹ for the respective dissipation process as follows:

$$\dot{f}^P = f^P = 0, \quad (3.78)$$

$$\dot{f}^D = f^D = 0. \quad (3.79)$$

⁹ As regards the consistency condition, see the footnote of Section 4.2.3 afterward.

Namely, Eqs. (3.76) and (3.77) enable the description of the independent evolution of the deformation and the damage in the elastic-plastic damage process.

(2) Rate-Dependent Material

As in the above case of the rate-independent material, we assume that the internal state variables, the free energy function and the associated variables to the internal state variables are given by Eqs. (3.71) through (3.73).

In the case of rate-dependent material, however, the evolution rate of deformation and damage do not subject to the restriction of the criteria f^P, f^D of Eqs. (3.74a) and (3.75a). Thus description of deformation and damage necessitates the following two independent potential functions F^P and F^D together with two independent multiplier functions $\dot{\Lambda}^P$ and $\dot{\Lambda}^D$ specifying their rates:

$$\begin{aligned} F^P &= F^P(\sigma, A_j, D) \\ &= f^P + f^H(A_j, D), \end{aligned} \quad (3.80a)$$

$$\dot{\Lambda}^P = \dot{\Lambda}^P(\sigma, A_j, D), \quad (3.80b)$$

$$F^D = F^D(Y, B; D) = f^D, \quad (3.81a)$$

$$\dot{\Lambda}^D = \dot{\Lambda}^D(Y, B; D), \quad (3.81b)$$

where f^P and f^D are functions similar to Eqs. (3.74a) and (3.75a).

Finally, the evolution equations are given by a generalized normality rule:

$$\dot{\epsilon}^P = \dot{\Lambda}^P \frac{\partial F^P}{\partial \sigma}, \quad \dot{\alpha}_j = \dot{\Lambda}^P \frac{\partial F^P}{\partial A_j}, \quad (3.82)$$

$$\dot{D} = \dot{\Lambda}^D \frac{\partial F^D}{\partial Y}. \quad (3.83)$$

By postulating the power-law evolution rate, the above multiplier functions $\dot{\Lambda}^P$ and $\dot{\Lambda}^D$ are given, respectively, by

$$\dot{\Lambda}^P = \left\langle \frac{f^P}{K} \right\rangle^r, \quad \dot{\Lambda}^D = \left\langle \frac{f^D}{L} \right\rangle^s, \quad (3.84)$$

where $\langle \rangle$ denotes Macauley bracket, while r, s, L, K are material constants.

The above extension of the thermodynamic constitutive theory for the generalized standard material is called *quasi-standard thermodynamic approach*. This extension can be applied also to the case of the multiple dissipation potentials

$F^{(I)}$ ($I = 1, 2, 3, \dots, N$). In this case, the evolution of the inelastic strain and the internal variables are expressed as follow (Chaboche 1997; Besson et al. 2010):

$$\dot{\boldsymbol{\epsilon}}^p = \sum_{I=1}^N \dot{A}_I^{(0)} \frac{\partial F^{(I)}}{\partial \boldsymbol{\sigma}}, \quad (I = 1, 2, 3, \dots, N), \quad (3.85)$$

$$\dot{V}_k = \sum_{I=1}^N \dot{A}_I^{(k)} \frac{\partial F^{(I)}}{\partial A_k}, \quad (k = 1, 2, 3, \dots, n). \quad (3.86)$$

Chapter 4

Inelastic Constitutive Equation and Damage Evolution Equation of Material with Isotropic Damage

The thermodynamic constitutive theory described in the preceding chapter is applied to inelastic materials with isotropic damage. In Section 4.1, one-dimensional elastic-plastic and elastic-viscoplastic constitutive equations of damaged materials will be described as the basis for the succeeding sections. The application of the constitutive theory of Chapter 3 to the three-dimensional case will be discussed in Section 4.2. The strain energy release rate due to damage development and the stress criterion for elastic-plastic damage growth will be considered in Section 4.3, while Section 4.4 is concerned with the inelastic damage theories based on the hypothesis of mechanical equivalence.

4.1 One-Dimensional Inelastic Constitutive Equation of Material with Isotropic Damage

Material damage induced by microvoids in isotropic distribution or by microcracks of random distribution can be characterized by *isotropic damage*. Even when the cavities have apparent orientation in their geometry and distribution, their mechanical effect may be assumed to be isotropic if their size and density are sufficiently small. The damage state in these cases can be represented by a scalar damage variable D as already described in Section 2.2.

4.1.1 Elastic-Plastic Deformation of Damaged Material

Let us suppose uniaxial tension of a strain-hardening elastic-plastic material shown in Fig. 4.1. As observed in Fig. 4.1b, the damage starts when plastic strain ε^p attains to a limit ε_D^p , and the damage variable D increases with the increase in ε^p . The value ε_D^p is called a *threshold plastic strain* for the damage initiation.

When the plastic strain ε^p attains to the *fracture plastic strain* ε_R^p , the damage variable D attains to the *critical value of fracture* D_C and the material starts to fracture:

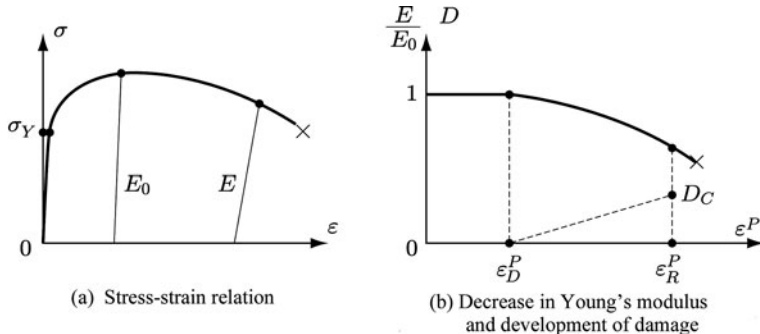


Fig. 4.1 Stress-strain relation and damage development of a strain-hardening elastic-plastic material

$$D = 0, \quad \varepsilon^P \leq \varepsilon_D^P, \quad (4.1a)$$

$$0 \leq D \leq D_C \leq 1, \quad \varepsilon_D^P \leq \varepsilon^P \leq \varepsilon_R^P. \quad (4.1b)$$

In some material, the threshold value of the damage initiation is $\varepsilon_D^P = 0$, and thus damage occurs from the beginning of the plastic deformation. For metallic materials, the critical value of fracture mostly has $D_C = 0.2 \sim 0.8$.

As observed in Fig. 4.1b, Young's modulus $E(D)$ of the damaged material decreases with damage. Hence the damage variable D increases with the decrease of $E(D)$, and may be given by Eq. (2.10)

$$D = 1 - \frac{E(D)}{E_0}. \quad (4.2)$$

Let us first consider the elastic-plastic deformation in the undamaged state $\varepsilon^P \leq \varepsilon_D^P$ of Fig. 4.1. In the case of a strain hardening plastic material, the *subsequent yield stress* σ (i.e., the stress necessary to induce the succeeding plastic strain) increases with the plastic strain ε^P . This increase in the subsequent yield stress σ is called *strain-hardening*. In the general case of the three-dimensional elastic-plastic deformation, this phenomenon of strain-hardening is usually described in terms of the *isotropic hardening* and/or the *kinematic hardening*, which are depicted schematically by the expansion of the *yield surface* $f = 0$ (see Eq. (4.65) in Section 4.2) and/or the translation of its center, respectively.

In the present case of uniaxial state of stress, we postulate that the subsequent yield stress σ is expressed by the sum of the initial yield stress σ_Y , *isotropic hardening variables* $R(\varepsilon^P)$ and the *kinematic hardening variable* (or *back stress*) $A(\varepsilon^P)$, i.e.,

$$\sigma = \sigma_Y + R(\varepsilon^P) + A(\varepsilon^P). \quad (4.3)$$

By the use of the *yield function* or the *loading function* f , Eq. (4.3) can be written in an alternative form, i.e., in the form of *yield condition*:

$$f = |\sigma - A| - R - \sigma_Y = 0. \quad (4.4)$$

Then the function f specifies the development of the plastic strain ε^p in the material:

$$\begin{aligned} \dot{\varepsilon}^p &= 0, & \text{for } f < 0 \quad \text{or} \quad \dot{f} < 0, \\ \dot{\varepsilon}^p &\neq 0, & \text{for } f = 0 \quad \text{and} \quad \dot{f} = 0. \end{aligned} \quad (4.5)$$

In the damaged state $\varepsilon^p \geq \varepsilon_D^p$ in Fig. 4.1b, on the other hand, the mechanical effect of damage on the subsequent yield stress σ of Eq. (4.3) is given by the effective stress $\tilde{\sigma}$ of Eq. (2.7). Thus, by means of the hypothesis of the strain equivalence (2.50), we have

$$\begin{aligned} \tilde{\sigma} &= \frac{\sigma}{1 - D} \\ &= \sigma_Y + R(\varepsilon^p) + A(\varepsilon^p), \end{aligned} \quad (4.6)$$

or

$$f = |\tilde{\sigma} - A| - R - \sigma_Y = 0. \quad (4.7)$$

Equations (4.6) and (4.7) describe the plastic behavior of a damaged material in one-dimensional state of stress. Hence Eqs. (4.6) and (4.7) may be called a one-dimensional elastic-plastic constitutive equation of a damaged material, and provides the basis for the three-dimensional constitutive equations.

In the particular case of the strain-hardening metallic material, the functions $R(\varepsilon^p)$ and $A(\varepsilon^p)$ of Eqs. (4.3) and (4.6) are often given by (Lemaitre 1992)

$$R = R_\infty [1 - \exp(-b\varepsilon^p)], \quad (4.8a)$$

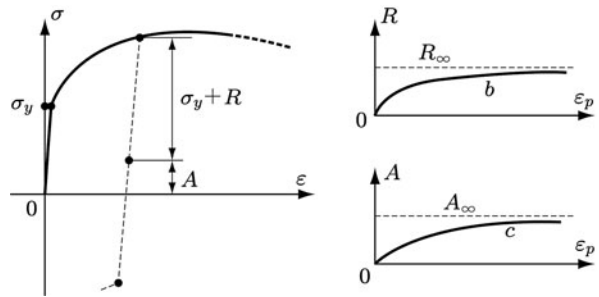
$$A = A_\infty [1 - \exp(-c\varepsilon^p)], \quad (4.8b)$$

where R_∞ , b , A_∞ and c are material constants. Figure 4.2 shows schematically the stress-strain curve calculated by Eqs. (4.6) and (4.8). The material constants σ_Y , R_∞ , b , A_∞ and c can be identified by the comparison between the experimental curve and the corresponding numerical results.

4.1.2 Viscoplastic Deformation of Damaged Material

When the value of temperature or the magnitude of stress is increased, the plastic deformation described above usually starts to increase with time. In the case of metals, for example, the time-dependent deformation is markedly observed in

Fig. 4.2 Stress-strain curve given by Eqs. (4.6) and (4.8)
Source: Lemaître (1992,
p. 59, Fig. 2.7)



the temperature range higher than 1/3 of their melting temperature in the absolute temperature.

The phenomenon of time-dependent irreversible deformation, increasing even under constant stress, is called *viscous deformation*. The irreversible deformation occurring only in the stress range larger than a threshold (i.e., the irreversible deformation with yielding) is called the *plastic deformation*. Therefore the time-dependent plastic deformation is called *viscoplastic deformation*,¹ whereas the time-dependent irreversible deformation without yielding is usually called *creep*.

Now let us consider the constitutive equation of viscoplastic deformation. We first suppose the case of undamaged material. The viscoplastic deformation starts when the applied stress attains to the threshold stress to induce the plastic deformation, i.e., to the subsequent yield stress of Eq. (4.3). The difference between the applied stress and this threshold stress

$$\sigma_V = \sigma - [\sigma_Y + R(\varepsilon^p) + A(\varepsilon^p)] \quad (4.9a)$$

is called *viscous stress*. Hence the yield function of Eq. (4.4) leads to

$$f = |\sigma - A| - R - \sigma_Y = \sigma_V. \quad (4.9b)$$

In the case of damaged material, by replacing the stress σ of Eq. (4.9) by the corresponding effective stress $\tilde{\sigma}$, we have

$$\tilde{\sigma}_V = \tilde{\sigma} - [\sigma_Y + R(\varepsilon^p) + A(\varepsilon^p)], \quad (4.10a)$$

$$\tilde{f} = |\tilde{\sigma} - A| - R - \sigma_Y = \sigma_V. \quad (4.10b)$$

The viscous strain rate (or creep rate) $\dot{\varepsilon}^v$ under a constant stress σ is often described by the *Norton law*

¹ Time-dependence (or rate-dependence) of plastic deformation is observed markedly not only in the quasi-static case due to elevated temperature or due to high level of stress discussed here, but also in the case of high rate of strain due to dynamic loading. Viscoplastic deformation at high rate of strain and its constitutive equations are referred to the excellent reference of Perzyna (1966).

$$\dot{\varepsilon}^v = \left(\frac{\sigma_V}{K_V} \right)^n, \quad (4.11)$$

or by the *logarithmic law*

$$\dot{\varepsilon}^v = \ln \left(1 - \frac{\sigma_V}{K_\infty} \right)^{-N}, \quad (4.12)$$

where n , K_V and N , K_∞ are material constants. While the Norton law is applied mainly to the case of relatively low level of stress, the logarithmic law is employed to the case of larger stress leading to failure in relatively short time.

By applying the viscous stress or the yield stress function of Eq. (4.10), Eqs. (4.11) and (4.12), respectively, lead to the viscoplastic constitutive equations of damaged material under uniaxial state of stress:

$$\dot{\varepsilon}^{vp} = \left(\frac{\tilde{\sigma}_V}{K_V} \right)^n = \left(\frac{\tilde{f}}{K_V} \right)^n, \quad (4.13)$$

$$\dot{\varepsilon}^{vp} = \ln \left(1 - \frac{\sigma_V}{K_\infty} \right)^{-N} = \ln \left(1 - \frac{\tilde{f}}{K_\infty} \right)^{-N}. \quad (4.14)$$

4.2 Three-Dimensional Inelastic Constitutive Equations of Material with Isotropic Damage

Let us now apply the thermodynamic constitutive theory of Section 3.2 and the one-dimensional inelastic constitutive equation described above, and derive the three-dimensional constitutive equations of inelastic and damaged material.

We postulate first that the deformation is small, and that the total strain $\boldsymbol{\varepsilon}$ is decomposed into the sum of the elastic strain $\boldsymbol{\varepsilon}^e$ and the plastic strain $\boldsymbol{\varepsilon}^p$:

$$\boldsymbol{\varepsilon} = \boldsymbol{\varepsilon}^e + \boldsymbol{\varepsilon}^p, \quad (4.15)$$

or

$$\dot{\boldsymbol{\varepsilon}} = \dot{\boldsymbol{\varepsilon}}^e + \dot{\boldsymbol{\varepsilon}}^p. \quad (4.16)$$

4.2.1 Internal Variables and Thermodynamic Constitutive Theory

According to the *principle of local state* described in Section 3.1.1, a non-equilibrium process in a continuum can be described as a succession of its equilibrium state, and hence by the process of the change in its state variables. Thus,

the thermodynamic state of a strain-hardening material in three-dimensional deformation is specified by the total strain $\boldsymbol{\epsilon}$ and the temperature T , in addition to the pertinently defined internal variables V_k ($k = 1, 2, 3, \dots$) representing the states of damage and strain-hardening.

By assuming the isotropy of damage, the damage state can be described by a scalar damage variable D . Strain-hardening of the material is assumed to consist of the isotropic and the kinematic hardening, and we represent these states in terms of a scalar r and a tensor α , respectively. The internal variables r and α are referred to as the *isotropic hardening variable* and the *kinematic hardening variable* (or the *back stress*), respectively.

Then the internal variables of the strain-hardening damaged material are specified as follows:

$$V_k = \{r, \alpha, D\}. \quad (4.17)^2$$

In view of Eq. (3.40), the Helmholtz free energy function per unit mass is now given by

$$\psi = \psi(\boldsymbol{\epsilon}^e, T, r, \alpha, D), \quad (4.18)$$

where the function ψ is a scalar-valued continuous function, concave with respect to T and convex as to the other variables.

Substitution of Eqs. (4.18) and (4.15) into the Clausius-Duhem inequality (3.19) provides

$$\begin{aligned} & \left(\boldsymbol{\sigma} - \rho \frac{\partial \psi}{\partial \boldsymbol{\epsilon}^e} \right) : \dot{\boldsymbol{\epsilon}}^e - \rho \left(s + \frac{\partial \psi}{\partial T} \right) \dot{T} + \boldsymbol{\sigma} : \dot{\boldsymbol{\epsilon}}^p \\ & - \rho \frac{\partial \psi}{\partial r} \dot{r} - \rho \frac{\partial \psi}{\partial \alpha} \dot{\alpha} - \rho \frac{\partial \psi}{\partial D} \dot{D} - \frac{\text{grad}T}{T} \cdot \boldsymbol{q} \geq 0, \end{aligned} \quad (4.19)$$

which must be satisfied by any change of the state.

In order that the inequality (4.19) may be satisfied by any change of the elastic strain $\boldsymbol{\epsilon}^e$ and the temperature T , the coefficients of the first and the second term of the inequality must be zero. From this requirement we have the elastic constitutive equation and the thermal state equation

$$\boldsymbol{\sigma} = \rho \frac{\partial \psi}{\partial \boldsymbol{\epsilon}^e}, \quad s = - \frac{\partial \psi}{\partial T}. \quad (4.20)$$

² Besides these internal variables, another scalar internal variable β , called *damage-strengthening variable* may be introduced to represent the effect of damage history on its further evolution. As regards the detail of the procedure, see Chapter 5.

By the use of these relations, Eq. (4.19) results in

$$\boldsymbol{\sigma} : \dot{\boldsymbol{\epsilon}}^p - \rho \frac{\partial \psi}{\partial r} \dot{r} - \rho \frac{\partial \psi}{\partial \boldsymbol{\alpha}} : \dot{\boldsymbol{\alpha}} - \rho \frac{\partial \psi}{\partial D} \dot{D} - \frac{\text{grad}T}{T} \cdot \boldsymbol{q} \geq 0. \quad (4.21)$$

Then, for the second through the fifth term of this inequality, we define the associated variables with the internal variables $r, \boldsymbol{\alpha}, D$ and the heat flux \boldsymbol{q} :

$$R \equiv \rho \frac{\partial \psi}{\partial r}, \quad A \equiv \rho \frac{\partial \psi}{\partial \boldsymbol{\alpha}}, \quad Y \equiv -\rho \frac{\partial \psi}{\partial D}, \quad \boldsymbol{g} \equiv -\text{grad}T. \quad (4.22)^3$$

In view of Eqs. (4.21) and (4.22), the Clausius-Duhem inequality (4.19) can be expressed eventually in the form

$$\Phi = \boldsymbol{\sigma} : \dot{\boldsymbol{\epsilon}}^p - R \dot{r} - A : \dot{\boldsymbol{\alpha}} + Y \dot{D} + (\boldsymbol{g}/T) \cdot \boldsymbol{q} \geq 0, \quad (4.23)$$

where R and A are exactly the isotropic and the kinematic hardening variables described in Section 4.1.1.

For the dissipation process of Eq. (4.23), we define a generalized flux vector \boldsymbol{J} and a generalized force vector \boldsymbol{X} as follows:

$$\boldsymbol{J} \equiv \{\dot{\boldsymbol{\epsilon}}^p, \dot{r}, \dot{\boldsymbol{\alpha}}, \dot{D}, \boldsymbol{q}\}, \quad (4.24)$$

$$\boldsymbol{X} \equiv \{\boldsymbol{\sigma}, -R, -A, Y, \boldsymbol{g}/T\}. \quad (4.25)$$

Then, Eq. (4.23) is expressed in a compact form

$$\Phi = \boldsymbol{X} \cdot \boldsymbol{J} \geq 0, \quad (4.26)$$

which is a specific expression of Eq. (3.49).

As already shown in Section 3.2.2, when the dissipation Φ is expressed in the form of Eq. (4.26), the evolution equation for the generalized flux vector \boldsymbol{J} can be derived from a potential function F of the generalized force \boldsymbol{X} . Then, we now postulate a dissipation potential function $F(\boldsymbol{X})$ in the form

$$F(\boldsymbol{X}) = F(\boldsymbol{\sigma}, R, A, Y, \boldsymbol{g}/T; \boldsymbol{\epsilon}^p, r, \boldsymbol{\alpha}, D, T), \quad (4.27a)$$

$$F = 0, \quad \text{for } \boldsymbol{X} = 0. \quad (4.27b)$$

³ For the expedience in the discussion hereafter, the generalized forces R and A of Eq. (4.22) have been defined by eliminating the minus sign “-” from the right hand side of the generalized definition (3.47) (e.g., Lemaître 1992; Lemaître and Desmorat 2005).

By means of Eq. (3.54), the evolution equation of the flux vector \mathbf{J} is given by

$$\mathbf{J} = \dot{\Lambda} \frac{\partial F}{\partial \mathbf{X}}, \quad (4.28)$$

where $\dot{\Lambda}$ is an indeterminate scalar multiplier whose value is identified by the consistency condition described later in Section 4.2.3.

Finally the explicit expressions of Eq. (4.28) are given as follows:

$$\dot{\boldsymbol{\epsilon}}^p = \dot{\Lambda} \frac{\partial F}{\partial \boldsymbol{\sigma}}, \quad \dot{r} = -\dot{\Lambda} \frac{\partial F}{\partial R}, \quad \dot{\boldsymbol{\alpha}} = -\dot{\Lambda} \frac{\partial F}{\partial \mathbf{A}}, \quad (4.29a)$$

$$\dot{D} = \dot{\Lambda} \frac{\partial F}{\partial Y}, \quad \mathbf{q} = \dot{\Lambda} \frac{\partial F}{\partial (\mathbf{g}/T)}. \quad (4.29b)$$

4.2.2 Thermodynamic Potential and Dissipation Potential

The derivation of the constitutive equations of damaged materials from Eqs. (4.20) and (4.29) necessitates the pertinent expression of the Helmholtz free energy function ψ and the dissipation potential function F . Let us now consider this problem mainly for the isothermal process of metallic materials.

(1) Helmholtz Free Energy Function

The magnitude of free energy stored in a damaged material depends on the state of strain, that of damage, and the state of dislocation structure, etc. Then the Helmholtz free energy function ψ per unit mass in an isothermal process may be postulated as

$$\psi(\boldsymbol{\epsilon}^e, r, \boldsymbol{\alpha}, D) = \psi^E(\boldsymbol{\epsilon}^e, D) + \psi^I(r) + \psi^K(\boldsymbol{\alpha}), \quad (4.30)^4$$

where $\psi^E(\boldsymbol{\epsilon}^e, D)$ denotes the elastic strain energy affected by damage, while $\psi^I(r)$ and $\psi^K(\boldsymbol{\alpha})$ stand for the free energies due to the isotropic and the kinematic hardening in plastic deformation.

If the material shows isotropic linear elasticity, the elastic constitutive equation in the undamaged state is given by Eqs. (2.90) and (2.91):

$$\sigma_{ij} = C_{ijkl}^0 \epsilon_{kl}^e, \quad (4.31)$$

$$C_{ijkl}^0 = \lambda \delta_{ij} \delta_{kl} + \mu (\delta_{ik} \delta_{jl} + \delta_{il} \delta_{jk}), \quad (4.32a)$$

⁴ As regards the specific expressions of the Helmholtz free energy function ψ of Eq. (4.30) and the dissipation potential F of Eq. (4.44) later, especially those of the coupled effect between strain-hardening and damage, refer to Section 3.3, and Besson et al. (2010).

$$\lambda = \frac{Ev}{(1+\nu)(1-2\nu)}, \quad \mu = \frac{E}{2(1+\nu)}, \quad (4.32b)$$

where C_{ijkl}^0 and λ, μ signify the elastic modulus tensor and Lamé constants, while E and ν are Young's modulus and Poisson's ratio.

In the case of damaged material, on the other hand, by the use of the effective stress of Eq. (2.36) together with the hypothesis of strain equivalence (2.50), the constitutive equation of elasticity is derived as

$$\sigma_{ij} = C_{ijkl}(D)\varepsilon_{kl}^e, \quad (4.33)$$

$$C_{ijkl}(D) = (1 - D)C_{ijkl}^0. \quad (4.34)$$

Thus the Helmholtz free energy ψ^E or the strain energy of the damaged material is given by

$$\rho\psi^E(\boldsymbol{\varepsilon}^e, D) = \frac{1}{2}C_{ijkl}^0\varepsilon_{ij}^e\varepsilon_{kl}^e(1 - D). \quad (4.35)$$

As regards the functions $\psi^I(r)$ and $\psi^K(\boldsymbol{\alpha})$, they can be determined so that they may represent the isotropic and the kinematic hardening phenomena observed in the uniaxial test of Fig. 4.1. For example they are given by (Lemaitre 1992)

$$\rho\psi^I(r) = R_\infty \left[r + \frac{1}{b} \exp(-br) \right], \quad (4.36)$$

$$\rho\psi^K(\boldsymbol{\alpha}) = \frac{1}{3}A_\infty c\alpha_{ij}\alpha_{ij}, \quad (4.37)$$

where R_∞ , b , A_∞ and c are material constants. By putting together Eqs. (4.35) through (4.37), the Helmholtz free energy function has the form

$$\begin{aligned} \rho\psi(\boldsymbol{\varepsilon}^e, r, \boldsymbol{\alpha}, D) &= \frac{1}{2}C_{ijkl}^0\varepsilon_{ij}^e\varepsilon_{kl}^e(1 - D) \\ &\quad + R_\infty \left[r + \frac{1}{b} \exp(-br) \right] + \frac{1}{3}A_\infty c\alpha_{ij}\alpha_{ij}. \end{aligned} \quad (4.38)$$

Equation (4.38) finally provides the elastic constitutive equation and the generalized forces associated with the internal variables. Substitution of Eq. (4.38) into Eq. (4.20) gives the elastic constitutive equation of a damaged material:

$$\begin{aligned} \sigma_{ij} &= \rho \frac{\partial \psi}{\partial \varepsilon_{ij}^e} = C_{ijkl}^0\varepsilon_{kl}^e(1 - D) \\ &= \frac{E(1 - D)}{1 + \nu} \left(\frac{\nu}{1 - 2\nu} \varepsilon_{kk}^e \delta_{ij} + \varepsilon_{ij}^e \right), \end{aligned} \quad (4.39)$$

or

$$\varepsilon_{ij}^e = \frac{1+\nu}{E} \frac{\sigma_{ij}}{1-D} - \frac{\nu}{E} \frac{\sigma_{kk}}{1-D} \delta_{ij}. \quad (4.40)$$

The generalized forces associated with the internal variables are derived from Eqs. (4.22) and (4.38) as follows:

$$R = \rho \frac{\partial \psi}{\partial r} = R_\infty [1 - \exp(-br)], \quad (4.41)$$

$$A_{ij} = \rho \frac{\partial \psi}{\partial \alpha_{ij}} = \frac{2}{3} A_\infty c \alpha_{ij}, \quad (4.42)$$

$$Y = -\rho \frac{\partial \psi}{\partial D} = \frac{1}{2} C_{ijkl}^0 \varepsilon_{ij}^e \varepsilon_{kl}^e. \quad (4.43)^5$$

(2) Dissipation Potential Function

Assuming the standard thermodynamic approach of Section 3.3, we now determine the dissipation potential F of Eq. (4.27). The dissipation Φ of Eq. (4.23) was derived by postulating four dissipation mechanisms in the isothermal inelastic damage process, i.e., plastic deformation, isotropic and kinematic hardening and the damage development. Thus the dissipation potential function F of Eq. (4.27) may be divided into the dissipation potential due to the plastic deformation F^P , that due to strain-hardening F^H and that due to damage F^D :

$$F(\sigma, R, A, Y) = F^P(\sigma, R, A; D) + F^H(R, A) + F^D(Y; r, D). \quad (4.44)$$

In the potential F^P postulated above, the damage variable D has been included as a parameter. This is because the development of damage may bring about the contraction of the yield surface.

As observed in Eq. (4.29), the plastic dissipation potential F^P plays the role of the *plastic potential surface* in the space of the generalized forces:

$$F^P(\sigma, R, A; D) = 0. \quad (4.45)$$

By assuming the generalized standard material, we use the associated flow rule and identify the yield function f with the plastic potential function F^P . Then, the specific

⁵ As will be described in Section 4.3.1 later, the generalized force Y associated with the damage variable D represents the release rate of elastic strain energy per unit volume caused by the damage development. Hereafter the generalized force Y will be called the *damage-associated variable*, or the *strain energy density release rate*.

form of the function F^P can be determined by extending the function f of Eq. (4.4) to the three-dimensional state of stress.

By the use of von Mises yield condition for the undamaged material, the relevant equivalent stress σ_{EQ} is given as

$$\sigma_{EQ} = \left[\frac{3}{2} \sigma_{ij}^D \sigma_{ij}^D \right]^{1/2}, \quad \sigma_{ij}^D = \sigma_{ij} - \frac{1}{3} \sigma_{kk} \delta_{ij}, \quad (4.46)$$

where σ_{ij}^D signify the deviatoric stress tensor.

In view of the yield function of Eq. (4.4), the strain hardening induced by the plastic deformation can be represented by the increase in the size R of the yield surface (i.e., the isotropic hardening) and the translation A of the center of the surface $f = 0$ (i.e., the kinematic hardening). Then by means of the hypothesis of strain-equivalence of Eq. (2.50) and the effective stress tensor $\tilde{\sigma}$ of Eq. (2.36), the plastic dissipation potential of Eq. (4.45) for a damaged material leads to

$$F^P = (\tilde{\sigma} - A)_{EQ} - R - \sigma_Y, \quad (4.47a)^6$$

$$(\tilde{\sigma} - A)_{EQ} = \left[\frac{3}{2} (\tilde{\sigma}_{ij}^D - A_{ij}^D) (\tilde{\sigma}_{ij}^D - A_{ij}^D) \right]^{1/2}, \quad (4.47b)$$

where $\tilde{\sigma}$, $\tilde{\sigma}_{ij}^D$ and A_{ij}^D are the effective stress, the components of the deviatoric tensors of stress $\tilde{\sigma}$ and the kinematic hardening variable A , which are expressed by

$$\tilde{\sigma} = \frac{\sigma}{1 - D}, \quad \tilde{\sigma}_{ij}^D = \tilde{\sigma}_{ij} - \frac{1}{3} \tilde{\sigma}_{kk} \delta_{ij}, \quad A_{ij}^D = A_{ij} - \frac{1}{3} A_{kk} \delta_{ij}. \quad (4.47c)$$

As regards the strain-hardening dissipation potential F^H , on the other hand, the dissipation due to the non-linear kinematic hardening gives

$$F^H(R, A) = \frac{3}{4A_\infty} A_{ij}^D A_{ij}^D, \quad (4.49)$$

⁶ In the plastic potential of this expression, the center of the elastic region in stress space deviates from the point A as damage develops, except the case of the isotropic damage. In order to avoid this aspect, another plastic potential function

$$F^P = (\tilde{\sigma} - \tilde{A})_{EQ} - R - \sigma_Y \quad (4.48)$$

derived by replacing the kinematic variable A of Eq. (4.47) with its effective variable $\tilde{A} = M^{-1} : A$ is often employed (Lemaitre and Chaboche 1985). In the most standard form of the plastic potential, i.e., Eq. (4.48), the point A remains at the center of the elastic region throughout the damage process. The difference between the results of calculation by Eqs. (4.47) and (4.48), however, is ascertained to be small (Besson et al. 2010).

where A_∞ signifies the asymptotic value of the kinematic hardening variable in uniaxial deformation, while the coefficient 3/4 has been employed for the simplification of further expression.

The evolution of the damage variable D depends on the internal variables r and D in addition to the generalized force Y . Thus one may write the damage dissipation potential as

$$F^D = F^D(Y; r, D). \quad (4.50)$$

Since the function F^D depends on various factors, e.g., the class of damage, mechanical property of the material, details of the function will be discussed in Section 4.2.5 afterward.

By putting together Eqs. (4.47) through (4.50), the dissipation potential F of Eq. (4.44) is given by (Lemaître 1990)

$$F = (\tilde{\sigma} - A)_{EQ} - R - \sigma_Y + \frac{3}{4A_\infty} A_{ij}^D A_{ij}^D + F^D(Y; r, D). \quad (4.51)$$

4.2.3 Elastic-Plastic Constitutive Equation of Damaged Material

The evolution equations of the internal variables ϵ^p , r , α and D are derived by substituting F of Eq. (4.51) into Eq. (4.29). Firstly the constitutive equation of the plastic strain rate $\dot{\epsilon}_{ij}^p$ is obtained in the form

$$\begin{aligned} \dot{\epsilon}_{ij}^p &= \dot{A} \frac{\partial F}{\partial \sigma_{ij}} = \dot{A} \frac{\partial F^P}{\partial \sigma_{ij}} = \dot{A} \frac{\partial (\tilde{\sigma} - A)_{EQ}}{\partial \sigma_{ij}} \\ &= \dot{A} \frac{\partial}{\partial \sigma_{ij}} \left[\frac{3}{2} \left(\frac{\sigma_{ij}^D}{1-D} - A_{ij}^D \right) \left(\frac{\sigma_{ij}^D}{1-D} - A_{ij}^D \right) \right]^{1/2} \\ &= \frac{3}{2} \frac{\tilde{\sigma}_{ij}^D - A_{ij}^D}{(\tilde{\sigma} - A)_{EQ}} \frac{\dot{A}}{1-D}. \end{aligned} \quad (4.52)$$

By defining the equivalent plastic strain rate

$$\dot{\epsilon}_{EQ}^p = \left[\frac{2}{3} \dot{\epsilon}_{ij}^p \dot{\epsilon}_{ij}^p \right]^{1/2}, \quad (4.53)$$

we take its integral along the strain trajectory

$$p = \int \dot{p} dt = \int \dot{\epsilon}_{EQ}^p dt, \quad (4.54)$$

or

$$\dot{p} = \dot{\epsilon}_{EQ}^p. \quad (4.55)$$

The physical quantity p is called the *accumulated plastic strain*. Since p increases monotonously with the progress of plastic deformation, it is utilized as a measure of internal change of materials brought about by the plastic deformation. By the use of Eqs. (4.52) and (4.53), \dot{p} of Eq. (4.55) leads to

$$\dot{p} = \dot{\varepsilon}_{EQ}^p = \frac{\dot{\Lambda}}{1 - D}. \quad (4.56)$$

The evolution equation of the isotropic hardening variable r , on the other hand, is derived from Eqs. (4.29) and (4.51):

$$\dot{r} = -\dot{\Lambda} \frac{\partial F}{\partial R} = -\dot{\Lambda} \frac{\partial F^P}{\partial R} = -\dot{\Lambda} \frac{\partial (-R)}{\partial R} = \dot{\Lambda}. \quad (4.57)$$

In view of Eq. (4.56), we further have the expression

$$\dot{r} = \dot{\Lambda} = \dot{p}(1 - D). \quad (4.58)$$

Namely, the evolution equation of the isotropic hardening variable r is given by \dot{p} and D . In the particular case of undamaged material, we have $\dot{r} = \dot{p}$.

The evolution equations of the kinematic and the damage variables α_{ij} and D are derived in a similar way as follows:

$$\begin{aligned} \dot{\alpha}_{ij} &= -\dot{\Lambda} \frac{\partial F}{\partial A_{ij}} = -\dot{\Lambda} \left(\frac{\partial F^P}{\partial A_{ij}} + \frac{\partial F^H}{\partial A_{ij}} \right) \\ &= \frac{3}{2} \dot{\Lambda} \left[\frac{(\tilde{\sigma}_{ij}^D - A_{ij}^D)}{(\tilde{\sigma} - A)_{EQ}} - \frac{A_{ij}^D}{A_\infty} \right] \\ &= \dot{\varepsilon}_{ij}^p (1 - D) - \frac{3}{2A_\infty} A_{ij}^D \dot{\Lambda}, \end{aligned} \quad (4.59)$$

$$\dot{D} = \dot{\Lambda} \frac{\partial F}{\partial Y} = \dot{\Lambda} \frac{\partial F^D}{\partial Y}. \quad (4.60)$$

In order to calculate the specific values of $\dot{\varepsilon}_{ij}^p$, \dot{r} and $\dot{\alpha}_{ij}$, one needs the values of the generalized forces R and A_{ij} associated with r and α_{ij} , together with that of the indeterminate multiplier $\dot{\Lambda}$. The values of R and A_{ij} are given by Eqs. (4.41) and (4.42), respectively, by

$$R = R_\infty [1 - \exp(-br)], \quad (4.61)$$

$$A_{ij}^D = \frac{2}{3} A_\infty c \alpha_{ij}^D. \quad (4.62)$$

The rates of these variables are also needed for the calculation of the indeterminate multiplier $\dot{\Lambda}$, and are derived as follows:

$$\dot{R} = R_\infty b \exp(-br) \dot{r} = b(R_\infty - R) \dot{\Lambda}, \quad (4.63)$$

$$\dot{A}_{ij}^D = \frac{2}{3} A_\infty c \dot{\alpha}_{ij}^D = c \left[A_\infty \frac{(\tilde{\sigma}_{ij}^D - A_{ij}^D)}{(\tilde{\sigma} - A)_{EQ}} - A_{ij}^D \right] \dot{\Lambda}. \quad (4.64)$$

Finally, the multiplier $\dot{\Lambda}$ can be determined by different ways (Malvern 1969).

For instance, for the plastic deformation to occur successively, the yield condition should be satisfied throughout the loading process.⁷ In the case of the plastic potential of Eq. (4.47), the yield condition is given as

$$f = F^P(\sigma, R, A; D) = (\tilde{\sigma} - A)_{EQ} - R - \sigma_Y = 0. \quad (4.65)^7$$

By differentiating this relation with respect to time, we have

$$\begin{aligned} \dot{f} &= \frac{\partial f}{\partial \sigma_{ij}} \dot{\sigma}_{ij} + \frac{\partial f}{\partial A_{ij}} \dot{A}_{ij} + \frac{\partial f}{\partial R} \dot{R} + \frac{\partial f}{\partial D} \dot{D} \\ &= \frac{3}{2} \frac{(\tilde{\sigma}_{ij}^D - A_{ij}^D)}{(\tilde{\sigma} - A)_{EQ}} \left[\frac{\dot{\sigma}_{ij}}{1 - D} - \dot{A}_{ij}^D + \frac{\sigma_{ij}^D}{(1 - D)^2} \dot{D} \right] - \dot{R} \\ &= 0. \end{aligned} \quad (4.66)$$

By substituting Eqs. (4.60), (4.63) and (4.64) into this relation, the multiplier $\dot{\Lambda}$ can be derived after some operations:

$$\begin{aligned} \dot{\Lambda} &= \frac{3}{2} \left(\tilde{\sigma}_{ij}^D - A_{ij}^D \right) \dot{\sigma}_{ij}^D / \left\{ (\tilde{\sigma} - A)_{EQ} (1 - D) \left[b(R_\infty - R) + cA_\infty \right. \right. \\ &\quad \left. \left. - \frac{3}{2} \frac{\tilde{\sigma}_{kl}^D - A_{kl}^D}{(\tilde{\sigma} - A)_{EQ}} \left(cA_{kl}^D + \frac{\tilde{\sigma}_{kl}^D}{(1 - D)^2} \frac{\partial F^D}{\partial Y} \right) \right] \right\}. \end{aligned} \quad (4.67)$$

In the case of the plastic deformation, the *loading-unloading condition* of Eq. (4.5) must be also extended to the state of three-dimensional stress. By replacing f and \dot{e}^p of Eq. (4.5) by f of Eq. (4.65) and $\dot{\Lambda}$ of Eq. (4.67) respectively, this condition now is expressed by

$$\dot{\Lambda} = 0, \quad f < 0 \quad \text{or} \quad \dot{f} < 0, \quad (4.68a)$$

$$\dot{\Lambda} \neq 0, \quad f = 0 \quad \text{and} \quad \dot{f} = 0. \quad (4.68b)$$

⁷ This condition is known as *Prager's consistency condition*, and given by $f = 0$ and $\dot{f} = 0$.

In summary, the three-dimensional elastic-plastic constitutive equations of isotropic damaged material are given as follows:

$$\varepsilon_{ij} = \varepsilon_{ij}^e + \dot{\varepsilon}_{ij}^p, \quad (4.69)$$

$$\varepsilon_{ij}^e = \frac{1+\nu}{E} \frac{\sigma_{ij}}{1-D} - \frac{\nu}{E} \frac{\sigma_{kk}}{1-D} \delta_{ij}, \quad (4.70)$$

$$\dot{\varepsilon}_{ij}^p = \frac{3}{2} \frac{\tilde{\sigma}_{ij}^D - A_{ij}^D}{(\tilde{\sigma} - A)_{EQ}} \frac{1}{1-D} \dot{\Lambda}, \quad (4.71)$$

$$\dot{r} = \dot{\Lambda} = (1-D)\dot{p}, \quad (4.72)$$

$$\dot{\alpha}_{ij} = \dot{\varepsilon}_{ij}^p(1-D) - \frac{3}{2A_\infty} A_{ij}^D \dot{\Lambda}, \quad (4.73)$$

$$f = (\tilde{\sigma} - A)_{EQ} - R - \sigma_Y = 0, \quad (4.74)$$

$$R = R_\infty [1 - \exp(-br)], \quad (4.75)$$

$$A_{ij}^D = \frac{2}{3} A_\infty c \alpha_{ij}^D, \quad (4.76)$$

$$\dot{D} = \dot{\Lambda} \frac{\partial F^D}{\partial Y}, \quad (4.77)$$

$$\dot{\Lambda} = 0, \quad f < 0 \quad \text{or} \quad \dot{f} < 0, \quad (4.78a)$$

$$\begin{aligned} \dot{\Lambda} &= \frac{3}{2} (\tilde{\sigma}_{ij}^D - A_{ij}^D) \dot{\sigma}_{ij} / \\ &\left\{ (\tilde{\sigma} - A)_{EQ} (1-D) \left[b(R_\infty - R) + cA_\infty \frac{3}{2} \frac{\tilde{\sigma}_{kl}^D - A_{kl}^D}{(\tilde{\sigma} - A)_{EQ}} \left(cA_{kl}^D + \frac{\tilde{\sigma}_{kl}^D}{(1-D)^2} \frac{\partial F^D}{\partial Y} \right) \right] \right\}, \\ f &= 0 \quad \text{and} \quad \dot{f} = 0, \end{aligned} \quad (4.78b)$$

where $(\tilde{\sigma} - A)_{EQ}$ denotes the equivalent stress for $(\tilde{\sigma} - A)$.

The details of the identification of the values of the material constants included in the above elastic-plastic constitutive equations together with those in the viscoplastic constitutive equations discussed later will be found in the relevant references (for example, Lemaître 1992; Lemaître and Chaboche 1985; Lemaître and Desmorat 2005).

In the above derivation, both the constitutive equation (4.71) and the evolution equation (4.77) are governed by an identical multiplier $\dot{\Lambda}$, and the values of $\dot{\Lambda}$ is given by Eq. (4.78). This fact implies that the plastic deformation and the damage develop concurrently, and gives significant restriction in the modeling of elastic-plastic damage process.

As described in Section 3.3, in order to overcome this restriction, the *quasi-standard thermodynamic approach* of the generalized standard material employs an independent dissipation function and the independent multiplier for each

mechanism of the inelastic deformation and the damage. Then, the independent multipliers are determined separately by applying the consistency conditions to them. The specific application of this methods is shown in [Chapter 5](#).

4.2.4 Viscoplastic Constitutive Equation of Damaged Material⁸

The strain rate in viscoplastic deformation is governed only by the current state of stress and the current internal state, and is independent of the sign of the rate of yield function \dot{f} . Hence the *loading-unloading condition* of the viscoplastic constitutive equations is given differently from Eq. (4.78).

By the use of the thermodynamic and the dissipation potentials of Eqs. (4.38) and (4.51), the viscoplastic constitutive equation of a damaged material is given by Eq. (4.52), just as in the case of elastic-plastic deformation discussed in Section 4.2.3. In the present case, however, the multiplier $\dot{\lambda}$ is given by Eq. (4.56) as

$$\dot{\lambda} = (1 - D)\dot{p}. \quad (4.79)$$

In particular, if the Norton law of Eq. (4.13) is adopted as the viscoplastic constitutive equation in uniaxial state of stress, the accumulated plastic strain rate \dot{p} is given by

$$\dot{p} = \dot{\varepsilon}_{EQ}^{vp} = \left(\frac{f}{K_V} \right)^n. \quad (4.80)$$

Extension of Eq. (4.10) into the three-dimensional state of stress provides

$$f = (\tilde{\sigma} - A)_{EQ} - R - \sigma_Y. \quad (4.81)$$

Substitution of Eq. (4.80) into Eq. (4.79) provides the multiplier

$$\dot{\lambda} = (1 - D) \left(\frac{f}{K_V} \right)^n. \quad (4.82)$$

According to the results derived above, the elastic-viscoplastic constitutive equation of the damaged material is given by Eqs. (4.69) through (4.77) together with

$$\dot{\lambda} = 0, \quad f < 0, \quad (4.83a)$$

$$\dot{\lambda} = (1 - D) \left(\frac{f}{K_V} \right)^n, \quad f \geq 0, \quad (4.83b)$$

$$f = (\tilde{\sigma} - A)_{EQ} - R - \sigma_Y. \quad (4.84)$$

⁸ As regards more detailed formulation based on the standard and the quasi-standard thermodynamic approach to plastic and viscoplastic deformation, refer to Chaboche (1997) and Besson et al. (2010).

When the viscoplastic strain under uniaxial stress is represented by the logarithmic creep law of Eq. (4.14), on the other hand, the multiplier $\dot{\lambda}$ of Eq. (4.83) is replaced by

$$\dot{\lambda} = (1 - D) \ln \left(1 - \frac{f}{K_V} \right)^{-N}, \quad f \geq 0. \quad (4.85)$$

4.2.5 Evolution Equation of Elastic-Plastic Damage and Viscoplastic Damage⁸

In Sections 4.2.3 and 4.2.4, the derivation of the specific elastic-plastic and the elastic-viscoplastic constitutive equations of damaged material were elucidated. Let us now discuss the formulation of the damage dissipation potential F^D and the resulting evolution equations.

By the use of Eq. (4.29), together with Eqs. (4.44) and (4.58), we have the evolution equation of the isotropic damage:

$$\dot{D} = \dot{\lambda} \frac{\partial F}{\partial Y} = \dot{\lambda} \frac{\partial F^D}{\partial Y}, \quad (4.86)$$

$$\dot{\lambda} = \dot{r} = (1 - D)\dot{p}, \quad (4.87)$$

$$F^D = F^D(Y; r, D). \quad (4.88)$$

As already described in Section 4.1, the development of material damage is governed by the accumulation of the local and microscopic plastic strain in material, and starts to develop when the accumulated plastic strain attains to its *threshold value*. In the case of the multiaxial state of stress, the damage starts when the accumulated plastic strain p gets to its threshold p_D . Then, the multiplier $\dot{\lambda}$ of Eq. (4.87) is expressed as

$$\dot{\lambda} = (1 - D)\dot{p}H(p - p_D), \quad (4.89)$$

where $H(\)$ denotes the Heaviside function.

By examining the microscopic mechanisms of ductile and brittle damage from micromechanics point of view, Lemaître (1987) derived the following damage dissipation potential F^D and the resulting damage evolution equation:

$$F^D(Y; r, D) = \frac{Y^2}{2S(1 - D)}, \quad (4.90)$$

$$\dot{D} = \dot{\lambda} \frac{\partial F^D}{\partial Y} = \frac{Y}{S}\dot{p}H(p - p_D), \quad (4.91)$$

where S is a material constant. Then the initiation of a crack or the onset of the fracture was assumed to occur when the damage variable D attains to its *critical value*

$$D = D_C. \quad (4.92)$$

The above evolution equations can be generalized further by means of a power function of the strain energy density release rate Y instead of F^D of Eq. (4.90):

$$F^D(Y; r, D) = \frac{S}{(s+1)(1-D)} \left(\frac{Y}{S}\right)^{s+1}, \quad (4.93)$$

$$\dot{D} = \dot{\Lambda} \frac{\partial F^D}{\partial Y} = \left(\frac{Y}{S}\right)^s \dot{p} H(p - p_D), \quad (4.94)$$

where s and S are material constants.

Equations (4.91) and (4.94) have been applied to the analyses of a wide variety of damage, e.g., elastic-plastic damage, creep damage and low cycle fatigue. For further details, refer to Lemaitre (1992) and Lemaitre and Desmorat (2005).

4.2.6 Threshold Value p_D of Plastic Strain for Damage Initiation – In the Case of Fatigue Damage

The value of threshold p_D for damage initiation in Eqs. (4.91) and (4.94) varies largely with the loading condition and the stress state. For example, the threshold value p_D in the case of uniaxial monotonous loading is several per cent, while it amounts to several hundred per cent for fatigue damage. In general, it is not obvious how to identify the value of p_D . In the particular case of fatigue damage, however, the value of p_D can be obtained as follows (Lemaitre 1992; Lemaitre, Desmorat, and Sauzay 2000).

Initiation of a microvoid due to damage is governed by the magnitude of energy W_S stored in the material. In the case of cyclic loading, the energy is stored in the form of the dislocation network and other microdefects as well as the microstructural change in their vicinity. From a mechanics point of view, the stored energy W_S is given by the total plastic work supplied to the material subtracted by the energy dissipated in the form of heat during the deformation, i.e.,

$$W_S = \int_0^t \sigma_{ij} \dot{\epsilon}_{ij}^p dt - \int_0^t \Phi dt, \quad (4.95)$$

where Φ is the dissipation defined in Section 4.2.1. Since $D = \dot{D} = 0$ before the initiation of damage and the value of Φ is given by Eq. (4.23), W_S of Eq. (4.95) leads to

$$\begin{aligned} W_S &= \int_0^t \sigma_{ij} \dot{\varepsilon}_{ij}^p dt - \int_0^t (\sigma_{ij} \dot{\varepsilon}_{ij}^p - R\dot{r} - A_{ij} \dot{\alpha}_{ij}) dt \\ &= \int_0^t (R\dot{r} + A_{ij} \dot{\alpha}_{ij}) dt, \end{aligned} \quad (4.96)$$

where the fatigue process has been assumed to be isothermal.

In the case of fatigue damage under symmetric cyclic loading, kinematic hardening of the material can be disregarded and we have $A_{ij} = 0$. Furthermore, it has been observed that the rate \dot{W}_S of the stored strain energy W_S decreases markedly with the increase of the accumulated plastic strain p . Thus, by the use of a new decreasing function $z(p)$, the expression of W_S of Eq. (4.96) may be further elaborated as

$$W_S = \int_0^p R(p) z(p) dp, \quad z(\infty) = 0, \quad (4.97a)$$

$$z(p) = \frac{B}{\varsigma} p^{(1-\varsigma)/\varsigma}, \quad \varsigma \geq 1, \quad (4.97b)$$

where B and ς are material functions.

We now take the particular case of Fig. 4.3 where a perfectly plastic material is subject to symmetric cyclic loading. The energy W_D stored up to the onset of damage as the internal structural change of material is given by substituting the yield function (4.74) into the function $R(p)$ of Eq. (4.97), i.e.,

$$\begin{aligned} W_D &= \int_0^{p_D} < \sigma_{EQ} - \sigma_Y > \frac{B}{\varsigma} p^{(1-\varsigma)/\varsigma} dp \\ &= B(\sigma_{EQ}^{\max} - \sigma_Y) p_D^{1/\varsigma}, \end{aligned} \quad (4.98)$$

where $< >$ signifies the Macauley bracket to be defined by Eq. (4.127) afterward, and σ_{EQ}^{\max} denotes the maximum value of the effective stress.

On the other hand, if Eq. (4.98) is applied to the case of uniaxial monotonous tension, the energy $(W_D)_T$ stored up to the microcrack initiation may be expressed as

$$(W_D)_T = B(\sigma_U - \sigma_Y)(\varepsilon_D^p)^{1/\varsigma}, \quad (4.99)$$

where σ_U is the tensile strength of the material.

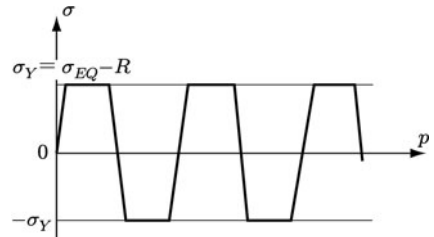


Fig. 4.3 Symmetric cyclic loading of perfectly plastic material

Let us suppose that the amount of the stored energy before the microvoid initiation is the same irrespective of the loading condition. Then the threshold value p_D for the fatigue damage initiation may be derived by equating Eqs. (4.98) and (4.99):

$$p_D = \varepsilon_D^p \left(\frac{\sigma_U - \sigma_Y}{\sigma_{EQ}^{max} - \sigma_Y} \right)^{\varsigma}. \quad (4.100)$$

In Section 8.3.4 later, Eq. (4.100) will be extended so that it may be applicable not only to the fatigue damage but also to the creep damage due to monotonous tension.

4.3 Strain Energy Release Rate and Stress Criterion for Damage Development in Elastic-Plastic Damage

4.3.1 Strain Energy Release Rate Due to Damage Development

In Section 4.2.2, by postulating the Helmholtz free energy function ψ of an elastic-plastic material with isotropic damage in the form of Eq. (4.38), the generalized force Y associated with D was derived as

$$Y = -\rho \frac{\partial \psi}{\partial D} = \frac{1}{2} C_{ijkl}^0 \varepsilon_{ij}^e \varepsilon_{kl}^e. \quad (4.101)$$

We now consider the physical significance of this *damage-associated variable* of Y (Chaboche 1977, 1988).

According to Eq. (4.39), the elastic constitutive equation of a damaged material is expressed by

$$\sigma_{ij} = C_{ijkl}^0 \varepsilon_{kl}^e (1 - D), \quad (4.102)$$

Then the increment of the elastic strain energy W^E per unit volume is given by

$$dW^E = \sigma_{ij} d\varepsilon_{ij}^e = C_{ijkl}^0 (1 - D) \varepsilon_{kl}^e d\varepsilon_{ij}^e. \quad (4.103)$$

Integration of this relation under the condition $D = \text{const.}$ gives

$$\begin{aligned} W^E &= \int C_{ijkl}^0 (1 - D) \varepsilon_{kl}^e d\varepsilon_{ij}^e \\ &= \frac{1}{2} C_{ijkl}^0 \varepsilon_{ij}^e \varepsilon_{kl}^e (1 - D). \end{aligned} \quad (4.104)$$

By the use of this relation, Eq. (4.101) leads to

$$Y = \frac{W^E}{1 - D}. \quad (4.105)$$

This relation states that the damage-associated variable Y is proportional to the elastic strain energy W^E , and its proportionality coefficient $1/(1 - D)$ increases with the damage D .

In the particular case of $\sigma_{ij} = \text{const.}$, Eq. (4.102) gives

$$d\varepsilon_{kl}^e = \frac{\varepsilon_{kl}^e}{1 - D} dD. \quad (4.106)$$

Substitution of this relation into Eq. (4.103) provides

$$\begin{aligned} (dW^E)_{\sigma=\text{const.}} &= \sigma_{ij} d\varepsilon_{ij}^e = C_{ijkl}^0 \varepsilon_{kl}^e \varepsilon_{ij}^e dD \\ &= 2YdD, \end{aligned} \quad (4.107)$$

from which we have

$$Y = \frac{1}{2} \left(\frac{\partial W^E}{\partial D} \right)_{\sigma=\text{const.}}. \quad (4.108)$$

In view of this relation, Y implies the release rate of the elastic strain energy caused by the development of damage D . In other words, the damage-associated variable Y plays a role similar to the strain energy release rate in fracture mechanics (Chaboche 1977). Thus the damage-associated variable Y is called also *strain energy density release rate*.

Figure 4.4 illustrates this relation. Let us suppose a state A on a stress-strain diagram under uniaxial tension. Then we postulate that the damage proceeds by dD under the condition of $\sigma = \text{const.}$, and that the elastic strain accordingly increases by $d\varepsilon^e$ to attain to the state B. In view of Eq. (4.108) or (4.107), the area ΔABC represents the amount of the strain energy release YdD due to the damage growth. Thus it will be observed that the variable Y gives the *elastic strain release rate* caused by the development of damage D .

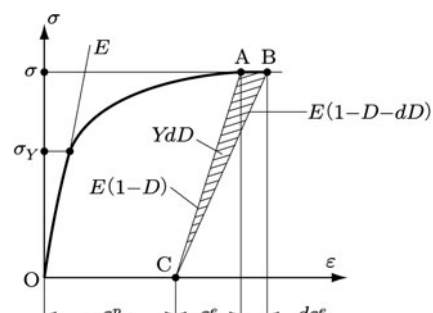


Fig. 4.4 Strain energy release caused by damage development

Then let us now discuss the value of the critical damage D_C for the fracture initiation. As already observed in Fig. 4.1, the material starts to fracture when D attains to D_C . According to the above interpretation of the damage-associated variable Y , the fracture criterion of a damaged material may be described also by means of Y :

$$Y = Y_C. \quad (4.109)$$

By denoting the uniaxial fracture stress by σ_R and by using Eq. (4.104), Eq. (4.105) may be expressed also in the form

$$Y_C = \frac{W^E}{1 - D} = \frac{(\sigma_R)^2}{2E(1 - D_C)^2}. \quad (4.110)$$

Hence the value of the critical damage D_C at the fracture of a damaged material is derived as

$$D_C = 1 - \frac{\sigma_R}{(2EY_C)^{1/2}}. \quad (4.111)$$

The value of the critical damage D_C has been ascertained to be $0.2 < D_C < 0.8$ in a number of experiments.

4.3.2 Energy Dissipation in Elastic-Plastic Damage

Let us discuss in some detail the causes of the energy dissipation observed in an elastic-plastic-damaged material. We suppose the uniaxial tension of a strain-hardening elastic-plastic-damaged material of Fig. 4.5.

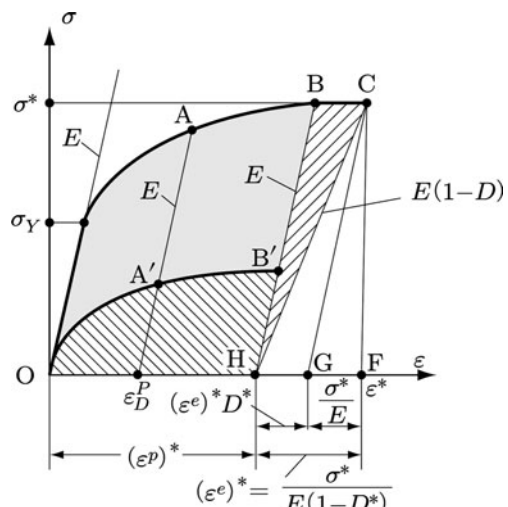


Fig. 4.5 Energy dissipation due to elastic-plastic damage

We assume that the plastic strain ε^p attains to its threshold ε_D^p at a point A on the stress-strain curve, and then damage starts to develop. After that point Young's modulus E decreases with the increase in D by $E(1 - D)$, and the curve leads to the point C. Moreover the material is assumed to show isotropic hardening only.

In the light of Fig. 4.5, the total work W supplied to the material before the point C by the external force is expressed as

$$\begin{aligned} W &= \text{Area OABCFO} = \int_0^{(\varepsilon^e)^*} \sigma d\varepsilon \\ &= \int_0^{(\varepsilon^e)^*} \sigma(\varepsilon^e) d\varepsilon^e + \int_0^{(\varepsilon^p)^*} \sigma(\varepsilon^p) d\varepsilon^p, \end{aligned} \quad (4.112)$$

where the asterisk “*” denotes the values of variables at the point C. By rewriting the second term on the right hand-side of Eq. (4.112) by the use of Eqs. (4.6) and (4.58), we have

$$\begin{aligned} W &= \int_0^{(\varepsilon^e)^*} \sigma(\varepsilon^e) d\varepsilon^e + \int_0^{(\varepsilon^p)^*} [(1 - D)\sigma_Y + (1 - D)R] d\varepsilon^p \\ &= \int_0^{(\varepsilon^e)^*} \sigma(\varepsilon^e) d\varepsilon^e + \int_0^{(\varepsilon^p)^*} (1 - D)\sigma_Y d\varepsilon^p - \int_0^{r^*} R dr. \end{aligned} \quad (4.113)$$

From this relation, the *energy dissipation* Φ during the above mechanical process is derived as follows:

$$\begin{aligned} \Phi &= \text{Area OABCHO} = W - \frac{1}{2}\sigma^*(\varepsilon^e)^* \\ &= \left[\int_0^{(\varepsilon^e)^*} \sigma d\varepsilon^e - \frac{1}{2}\sigma^*(\varepsilon^e)^* \right] \\ &\quad + \int_0^{(\varepsilon^p)^*} (1 - D)\sigma_Y d\varepsilon^p - \int_0^{r^*} R dr. \end{aligned} \quad (4.114)$$

The first, second and the third term of the right-hand side of this relation represent the elastic strain energy released by the damage growth, the energy dissipated in the form of heat, and the dissipated energy consumed by the strain hardening, respectively. The energies dissipated by these mechanisms can be represented schematically by the areas BCHB, OBB'O and OB'HO in Fig. 4.5.

4.3.3 Stress Triaxiality and Stress Criterion for Damage Development

As described in Section 4.2, the damage-associated variable Y is a generalized force to induce damage. Thus, by examining the expression (4.105) of the associated

variable Y , we can derive the effective stress and the stress criterion for the damage development (Lemaître 1985).

Let us first decompose the stress and the elastic strain tensors σ_{ij} and ε_{ij}^e into the sum of their deviatoric parts σ_{ij}^D , ε_{ij}^{eD} and the spherical parts σ_H , ε_H^e :

$$\sigma_{ij} = \sigma_{ij}^D + \sigma_H \delta_{ij}, \quad (4.115a)$$

$$\varepsilon_{ij}^e = \varepsilon_{ij}^{eD} + \varepsilon_H^e \delta_{ij}, \quad (4.115b)$$

where the *deviatoric stress tensor* σ_{ij}^D and the *deviatoric elastic strain tensor* ε_{ij}^{eD} are given by

$$\sigma_{ij}^D = \sigma_{ij} - (1/3)\sigma_{kk}\delta_{ij}, \quad \varepsilon_{ij}^{eD} = \varepsilon_{ij}^e - (1/3)\varepsilon_{kk}^e\delta_{ij}. \quad (4.115c)$$

The quantities σ_H and ε_H^e in Eq. (4.115), on the other hand, are called the *mean stress* and the *mean elastic strain* respectively, and are given by

$$\sigma_H = (1/3)\sigma_{kk}, \quad \varepsilon_H^e = (1/3)\varepsilon_{kk}^e. \quad (4.115d)$$

The mean stress σ_H is called also the *hydrostatic stress*.

Then by the use of the elastic constitutive equation (4.39), W^E of Eq. (4.104) can be expressed as

$$\begin{aligned} W^E &= \frac{1}{2}(1-D) \left[\frac{Ev}{(1+\nu)(1-2\nu)} \delta_{ij}\delta_{kl} + 2 \frac{E}{2(1+\nu)} \delta_{il}\delta_{jk} \right] \varepsilon_{ij}^e \varepsilon_{kl}^e \\ &= \frac{1}{2}(1-D) \left[\frac{E}{1+\nu} \varepsilon_{ij}^{eD} \varepsilon_{ij}^{eD} + \frac{3E}{1-2\nu} (\varepsilon_H^e)^2 \right]. \end{aligned} \quad (4.116)$$

The elastic constitutive equation (4.40), on the other hand, provides

$$\varepsilon_{ij}^{eD} = \frac{1+\nu}{E} \frac{\sigma_{ij}^D}{1-D}, \quad \varepsilon_H^e = \frac{1-2\nu}{E} \frac{\sigma_H}{1-D}. \quad (4.117)$$

If one substitutes Eqs. (4.116) and (4.117) into Eq. (4.105) and utilizes the effective stress of Eq. (2.36), the damage-associated variable Y is written in an alternative form

$$\begin{aligned} Y &= \frac{W^E}{1-D} \\ &= \frac{2}{3} \frac{1+\nu}{2E} (\tilde{\sigma}_{EQ})^2 + 3 \frac{1-2\nu}{2E} (\tilde{\sigma}_H)^2 \\ &= \frac{(\tilde{\sigma}_{EQ})^2}{2E} \left[\frac{2}{3}(1+\nu) + 3(1-2\nu) \left(\frac{\sigma_H}{\sigma_{EQ}} \right)^2 \right], \end{aligned} \quad (4.118)$$

where the term σ_H/σ_{EQ} is called the *stress triaxiality*. The stress triaxiality is an important quantity governing the fracture mode of material, and the larger the value of σ_H/σ_{EQ} the more brittle is the fracture.

The quantity in the brackets on the right-hand side of Eq. (4.118) is denoted by

$$R_v \equiv \frac{2}{3}(1 + \nu) + 3(1 - 2\nu) \left(\frac{\sigma_H}{\sigma_{EQ}} \right)^2, \quad (4.119)$$

and is called the *stress triaxiality function*. Then Eq (4.118) may be expressed also in the form

$$Y = \frac{(\tilde{\sigma}_{EQ})^2}{2E} R_v. \quad (4.120)$$

If we apply this relation to the particular case of uniaxial tension under $\sigma = \sigma^*$, we have

$$Y = \frac{(\sigma^*)^2}{2E(1 - D)^2}. \quad (4.121)$$

Comparison between Eqs. (4.120) and (4.121) gives the relation

$$\begin{aligned} \sigma^* &= \sigma_{EQ}(R_v)^{1/2} \\ &= \left[\frac{2}{3}(1 + \nu)(\sigma_{EQ})^2 + 3(1 - 2\nu)(\sigma_H)^2 \right]^{1/2}. \end{aligned} \quad (4.122)$$

This relation represents the equivalence between the uniaxial and the multiaxial states of stress as to their effect on the damage development, and corresponds to the von Mises equivalent stress for the plastic deformation. Then the quantity σ^* defined by the Eq. (4.122) is called *damage equivalent stress*. Furthermore, the relation

$$\sigma^* = \sigma_{EQ}(R_v)^{1/2} = \text{const.} \quad (4.123)$$

gives the stress criterion governing the development of damage in multiaxial state of stress, i.e., stress criterion for damage, or *damage stress criterion*.

4.3.4 Effect of Stress Sign on Damage Development

So far we have postulated that the material damage develops in the same way under the tensile and the compressive stress. In materials such as concrete and rocks, however, the crack closure effect due to compressive stress can not be disregarded. Moreover, the mechanisms of damage development in metals and composite materials depend saliently on the sign of stress. Namely the development of damage and its mechanical effect generally have different aspects between the cases of tensile and

compressive stress. In order to elucidate the effect of stress sign on damage behavior, Ladevèze and Lemaître (1984) extended the argument of Section 4.3.3 as follows.

The discussion in the stress space necessitates the specific expression of the Gibbs potential function of Eq. (3.62). For this purpose we first postulate the Helmholtz free energy function of Eq. (4.35):

$$\rho\psi^E(\boldsymbol{\varepsilon}^e, D) = \frac{1}{2}C_{ijkl}^0\varepsilon_{ij}^e\varepsilon_{kl}^e(1-D). \quad (4.124)$$

In the case of isotropic elastic material, by means of Eq. (4.32), Eq. (4.124) is expressed as

$$\begin{aligned} & \rho\psi^E(\boldsymbol{\varepsilon}^e, D) \\ &= \frac{1}{2}(1-D)\left[\frac{E}{1+\nu}\varepsilon_{ij}^e\varepsilon_{ij}^e + \frac{Ev}{(1+\nu)(1-2\nu)}(\varepsilon_{kk}^e)^2\right]. \end{aligned} \quad (4.125)$$

By substituting this relation together with the elastic constitutive equation (4.40) into Eq. (3.62), the Gibbs potential Γ^E is derived as

$$\rho\Gamma^E(\boldsymbol{\sigma}, D) = \frac{-1}{2E(1-D)}\left[(1+\nu)\sigma_{ij}\sigma_{ij} - \nu(\sigma_{kk})^2\right]. \quad (4.126)$$

We now introduce the *Macaulay bracket*

$$\langle x \rangle = H(x)x, \quad (4.127a)$$

i.e.,

$$\langle x \rangle = x \quad \text{for } x \geq 0, \quad (4.127b)$$

$$\langle x \rangle = 0 \quad \text{for } x < 0, \quad (4.127c)$$

where $H(\)$ is the *Heaviside function*. Then the matrix of the principal stress

$$[\boldsymbol{\sigma}] = \begin{bmatrix} \sigma_1 & 0 & 0 \\ 0 & \sigma_2 & 0 \\ 0 & 0 & \sigma_3 \end{bmatrix} \quad (4.128)$$

can be expressed in the form

$$[\boldsymbol{\sigma}] = \begin{bmatrix} \langle \sigma_1 \rangle & 0 & 0 \\ 0 & \langle \sigma_2 \rangle & 0 \\ 0 & 0 & \langle \sigma_3 \rangle \end{bmatrix} - \begin{bmatrix} \langle -\sigma_1 \rangle & 0 & 0 \\ 0 & \langle -\sigma_2 \rangle & 0 \\ 0 & 0 & \langle -\sigma_3 \rangle \end{bmatrix}. \quad (4.129)$$

Likewise the stress components σ_{ij} can be separated into the positive and the negative components:

$$\sigma_{ij} = <\sigma_{ij}> - <-\sigma_{ij}>. \quad (4.130)$$

Thus the Gibbs potential (4.126) can be rewritten in terms of $<\sigma_{ij}>$ and $<-\sigma_{ij}>$. In view of the relation $<x><-x> \equiv 0$, one has the following relations:

$$\sigma_{ij}\sigma_{ij} = <\sigma_{ij}><\sigma_{ij}> + <-\sigma_{ij}><-\sigma_{ij}>, \quad (4.131a)$$

$$\sigma_{kk} = <\sigma_{kk}> - <-\sigma_{kk}>, \quad (4.131b)$$

$$<\sigma_{kk}><-\sigma_{kk}> = <\sigma_{kk}><-\sigma_{ll}> = 0, \quad (4.131c)$$

$$(\sigma_{ij})^2 = \sigma_{kk}\sigma_{ll} = <\sigma_{kk}>^2 + <-\sigma_{kk}>^2. \quad (4.131d)$$

By the aid of these relations, Eq. (4.126) leads to

$$\begin{aligned} \rho\Gamma^E(\sigma, D) = & \frac{-1}{2E(1-D)} \left\{ \left[(1+\nu) <\sigma_{ij}><\sigma_{ij}> - \nu <\sigma_{kk}>^2 \right] \right. \\ & \left. + \left[(1+\nu) <-\sigma_{ij}><-\sigma_{ij}> - \nu <-\sigma_{kk}>^2 \right] \right\}. \end{aligned} \quad (4.132)$$

By substituting this relation into the elastic constitutive equation of Eq. (3.64), we have the constitutive equation of elastic material with isotropic damage:

$$\begin{aligned} \varepsilon_{ij}^e &= -\rho \frac{\partial \Gamma^E}{\partial \sigma_{ij}} \\ &= \left[\frac{1+\nu}{E(1-D)} <\sigma_{ij}> - \frac{\nu}{E(1-D)} <\sigma_{kk}> \delta_{ij} \right] \\ &\quad - \left[\frac{1+\nu}{E(1-D)} <-\sigma_{ij}> - \frac{\nu}{E(1-D)} <-\sigma_{kk}> \delta_{ij} \right] \\ &= \frac{1+\nu}{E(1-D)} \sigma_{ij} - \frac{\nu}{E(1-D)} \sigma_{kk} \delta_{ij}. \end{aligned} \quad (4.133)$$

In the derivation of this relation, the following differential operations have been employed:

$$\frac{\partial}{\partial \sigma_{ij}} <\sigma_{kl}> = \frac{\partial}{\partial \sigma_{ij}} [H(\sigma_{kl}) \sigma_{kl}] = H(\sigma_{kl}) \delta_{ik} \delta_{jl}, \quad (4.134a)$$

$$\frac{\partial}{\partial \sigma_{ij}} <-\sigma_{kl}> = \frac{\partial}{\partial \sigma_{ij}} [-H(-\sigma_{kl}) \sigma_{kl}] = -H(-\sigma_{kl}) \delta_{ik} \delta_{jl}, \quad (4.134b)$$

$$\frac{\partial}{\partial \sigma_{ij}} \langle \sigma_{kk} \rangle = \frac{\partial}{\partial \sigma_{ij}} [H(\sigma_{kk}) \sigma_{kk}] = H(\sigma_{kk}) \delta_{ij}, \quad (4.134c)$$

$$\frac{\partial}{\partial \sigma_{ij}} [\langle \sigma_{kl} \rangle \langle \sigma_{kl} \rangle] = \frac{\partial H(\sigma_{kl}) H(\sigma_{kl}) \sigma_{kl} \sigma_{kl}}{\partial \sigma_{ij}} \\ (4.134d)$$

$$= 2H(\sigma_{kl}) \sigma_{kl} \delta_{ik} \delta_{jl} = 2H(\sigma_{ij}) \sigma_{ij},$$

$$\frac{\partial}{\partial \sigma_{ij}} [\langle \sigma_{kk} \rangle^2] = \frac{\partial H(\sigma_{kk}) H(\sigma_{ll}) \sigma_{kk} \sigma_{ll}}{\partial \sigma_{ij}} \\ (4.134e)$$

$$= 2H(\sigma_{kk}) \sigma_{kk} \delta_{il} \delta_{jl} = 2H(\sigma_{kk}) \sigma_{kk} \delta_{ij}.$$

The mechanical effect of the compressive stress on damage growth is usually smaller than that of the tensile stress. The expression of this feature is facilitated by using a new parameter η ($0 \leq \eta \leq 1$), and by postulating that the effect of damage is D for the tensile stress whereas that of the compressive stress is ηD . Then function Γ^E of Eq. (4.132) is rewritten in the alternative form:

$$\rho \Gamma^E(\sigma, D) = \frac{-1}{2E(1-D)} [(1+\nu) \langle \sigma_{ij} \rangle \langle \sigma_{ij} \rangle - \nu \langle \sigma_{kk} \rangle^2] \\ - \frac{1}{2E(1-\eta D)} [(1+\nu) \langle -\sigma_{ij} \rangle \langle -\sigma_{ij} \rangle - \nu \langle -\sigma_{kk} \rangle^2]. \quad (4.135)$$

The cases of $\eta = 0$ and $\eta = 1$ in this function represent the crack behavior of Fig. 4.6a and b, respectively. Namely the case $\eta = 0$ shows a crack completely closing under the compressive stress, while the case $\eta = 1$ corresponds to a crack without closing under the compressive stress. These mechanical effects of crack behavior are called the *unilateral* and the *bilateral effect* of cracks, respectively. Furthermore, the case of $0 < \eta < 1$ is often called the *quasi-unilateral effect* of cracks.

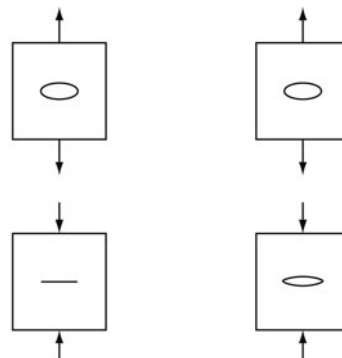


Fig. 4.6 Unilateral and bilateral effect in crack behavior

(a) Unilateral crack effect
($\eta = 0$)

(b) Bilateral crack effect
($\eta = 1$)

Finally by substituting Eq. (4.135) into the elastic constitutive equation (3.64) and the associated generalized forces of Eq. (3.65), we have the corresponding relations for the unilateral damaged material. The damage equivalent stress σ^* for this material, furthermore, can be derived from Eq. (4.121). All the resulting relations are summarized as follows

$$\begin{aligned}\varepsilon_{ij}^e &= -\rho \frac{\partial \Gamma^E}{\partial \sigma_{ij}} \\ &= \frac{1+\nu}{E(1-D)} \left[<\sigma_{ij}> - \frac{\nu}{1+\nu} <\sigma_{kk}> \delta_{ij} \right] \\ &\quad - \frac{1+\nu}{E(1-\eta D)} \left[<-\sigma_{ij}> - \frac{\nu}{1+\nu} <-\sigma_{kk}> \delta_{ij} \right],\end{aligned}\tag{4.136}$$

$$\begin{aligned}Y &= -\rho \frac{\partial \Gamma^E}{\partial D} \\ &= \frac{1+\nu}{2E} \left[\frac{<\sigma_{ij}><\sigma_{ij}>}{(1-D)^2} + \frac{\eta <-\sigma_{ij}><-\sigma_{ij}>}{(1-\eta D)^2} \right] \\ &\quad - \frac{\nu}{2E} \left[\frac{<\sigma_{kk}>^2}{(1-D)^2} + \frac{\eta <-\sigma_{kk}>^2}{(1-\eta D)^2} \right],\end{aligned}\tag{4.137}$$

$$\begin{aligned}\sigma^* &= \left\{ \left[(1+\nu) <\sigma_{ij}><\sigma_{ij}> - \nu <\sigma_{kk}>^2 \right] \right. \\ &\quad \left. + \frac{(1-D)^2 \eta}{(1-\eta D)^2} \left[(1+\nu) <-\sigma_{ij}><-\sigma_{ij}> - \nu <-\sigma_{kk}>^2 \right] \right\}^{1/2}.\end{aligned}\tag{4.138}$$

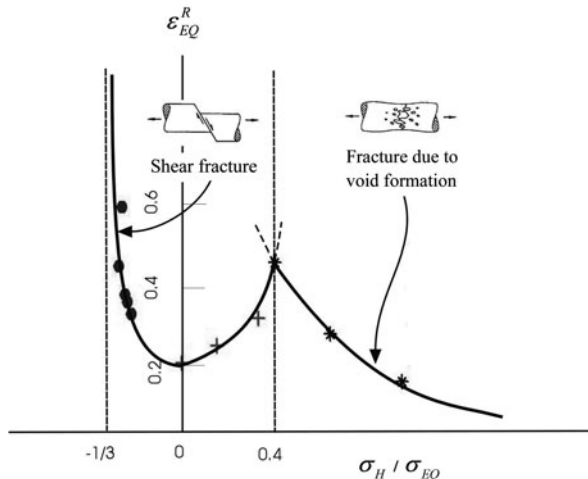
The above argument on the unilateral damage due to Ladevèze and Lemaitre (1984) is clear, and has been applied to the analyses of the elastic-plastic and the fatigue damage of metals and composites. The thermodynamic theory of Eqs. (4.135) through (4.138) representing crack-closure effect in isotropic damage was extended thereafter to the case of anisotropic damage based on the second-order damage tensor (Desmorat and Cantournet 2008).

More consistent theory to decompose the effect of stress and strain into their positive and negative parts will be discussed in detail in Section 5.3 afterward.

4.3.5 Stress Criterion for Ductile Damage

The damage stress criterion (4.123) was derived by assuming that the damage growth under multiaxial state of stress is governed by the damage-associated variable, i.e., strain energy release rate Y . Then, the damage equivalent stress σ^* of this relation was specified as a function of the stress triaxiality σ_H/σ_{EQ} .

Fig. 4.7 Dependence of the equivalent strain to fracture on the stress triaxiality
Source: Bao and Wierzbicki (2005, p. 1060, Fig. 11: by the courtesy of the authors)



In the case of a ductile material, however, it has been observed that the time of damage initiation and the rate of damage growth depend largely on σ_H/σ_{EQ} , and hence the mechanism of the damage and fracture vary markedly with σ_H/σ_{EQ} . That is to say, the damage and the fracture of ductile material sometimes cannot be described accurately by a single criterion of Eq. (4.123). In the case of 2024-T351 aluminum alloy, for example, the mode of the ductile fracture varies largely with the stress triaxiality range of $-1/3 \leq \sigma_H/\sigma_{EQ} \leq 0$, $0 \leq \sigma_H/\sigma_{EQ} \leq 1/\sqrt{3}$ and $1/\sqrt{3} \leq \sigma_H/\sigma_{EQ}$, and the predominant damage mechanisms in these ranges are the shear mechanism, mixed shear and void-growth mechanism and the void-growth mechanism, respectively (Bao and Wierzbicki 2004, 2005). Figure 4.7 shows the relation between the fracture strain and the stress triaxiality. In Chapter 6 afterward, the damage stress criteria besides Eq. (4.123) will be discussed in some detail.

4.4 Inelastic Damage Theory Based on Hypothesis of Total Energy Equivalence

On the basis of the hypothesis of the total energy equivalence described in Section 2.3.6, Saanouni et al. (1994) proposed a general thermodynamic constitutive theory for thermoelastic damage materials.

Let us first suppose a current damaged configuration B_t of RVE and a fictitious undamaged configuration B_f mechanically equivalent to B_t , as shown in Fig. 2.13. We postulate that the deformation is small and the total strain $\boldsymbol{\varepsilon}$ is expressed as the sum of the elastic strain $\boldsymbol{\varepsilon}^e$ and the inelastic strain $\boldsymbol{\varepsilon}^{in}$. The inelastic strain $\boldsymbol{\varepsilon}^{in}$ signifies either the plastic strain $\boldsymbol{\varepsilon}^p$ or the viscoplastic strain $\boldsymbol{\varepsilon}^{vp}$. It is assumed further that the inelastic deformation of the material follows the von Mises yield condition, and its internal state is described by the isotropic and the kinematic hardening variables r , α and the damage variable D .

Then the internal variables V_k , \tilde{V}_k , and the associated generalized forces A_k , \tilde{A}_k of the inelastic-damaged material in the configurations B_t and B_f are given by

$$V_k = \{\boldsymbol{\epsilon}^{in}, r, \boldsymbol{\alpha}, D\}, \quad A_k = \{\sigma, -R, -A, Y\}, \quad (4.139)$$

$$\tilde{V}_k = \{\tilde{\boldsymbol{\epsilon}}^{in}, \tilde{r}, \tilde{\boldsymbol{\alpha}}, 0\}, \quad \tilde{A}_k = \{\tilde{\sigma}, -\tilde{R}, -\tilde{A}, 0\}, \quad (4.140)$$

where the effective state variables \tilde{V}_k , \tilde{A}_k are defined by Eqs. (2.74) and (2.75):

$$\tilde{V}_k = (1 - D)^{1/2} V_k, \quad \tilde{A}_k = (1 - D)^{-1/2} A_k. \quad (4.141)$$

4.4.1 Thermodynamic Potential and State Equation

According to the hypothesis of total energy equivalence described in Section 2.3, the Helmholtz free energy function ψ of a damaged material can be expressed by the sum of the elastic ψ^E and the inelastic part ψ^{IN} of the free energy function in the fictitious undamaged configuration, i.e.,

$$\psi(\boldsymbol{\epsilon}^e, r, \boldsymbol{\alpha}, T, D) = \psi^E(\tilde{\boldsymbol{\epsilon}}^e, T) + \psi^{IN}(\tilde{r}, \tilde{\boldsymbol{\alpha}}, T). \quad (4.142a)$$

If the material shows the isotropic linear elasticity and the isotropic-kinematic hardening plasticity, the functions ψ^E and ψ^{IN} of Eq. (4.142a) can be expressed by

$$\begin{aligned} \rho \psi^E(\tilde{\boldsymbol{\epsilon}}^e, T) &= (1/2) \tilde{\boldsymbol{\epsilon}}^e : \mathbb{C}_0 : \tilde{\boldsymbol{\epsilon}}^e - (T - T_0) \mathbf{k} : \tilde{\boldsymbol{\epsilon}}^e \\ &\quad - \rho c_v T [\ln(T/T_0) - 1], \end{aligned} \quad (4.142b)$$

$$\rho \psi^{IN}(\tilde{r}, \tilde{\boldsymbol{\alpha}}, T) = (1/2) Q \tilde{r}^2 + (1/3) P \tilde{\boldsymbol{\alpha}} : \tilde{\boldsymbol{\alpha}}, \quad (4.142c)$$

where \mathbb{C}_0 and \mathbf{k} are the fourth-order elastic modulus tensor and the second-order thermal expansion tensor, while ρ and c_v denote the mass density and the isochoric specific heat. The symbols Q , P and T_0 are the isotropic and the kinematic hardening coefficients and the initial temperature, respectively.

Substitution of Eq. (4.142) into Eqs. (4.20) and (4.22) provides the stress σ , entropy s and the associated thermodynamic variables with r , $\boldsymbol{\alpha}$ and D :

$$\sigma = \rho \frac{\partial \psi}{\partial \boldsymbol{\epsilon}^e} = (1 - D) \mathbb{C}_0 : \boldsymbol{\epsilon}^e - (T - T_0) (1 - D)^{1/2} \mathbf{k}, \quad (4.143)$$

$$s = -\frac{\partial \psi}{\partial T} = (1/\rho) (1 - D)^{1/2} \mathbf{k} : \boldsymbol{\epsilon}^e + c_v \ln(T/T_0), \quad (4.144)$$

$$R = \rho \frac{\partial \psi}{\partial r} = (1 - D) Q r, \quad (4.145)$$

$$A = \rho \frac{\partial \psi}{\partial \boldsymbol{\alpha}} = \frac{2}{3} (1 - D) P \boldsymbol{\alpha}, \quad (4.146)$$

$$Y = -\rho \frac{\partial \psi}{\partial D} = Y^E + Y^{IN}, \quad (4.147a)$$

$$\begin{aligned} Y^E &= (1/2)\boldsymbol{\epsilon}^e : \mathbb{C}_0 : \boldsymbol{\epsilon}^e \\ &\quad -(1/2)(T - T_0)(1 - D)^{-1/2}\mathbf{k} : \boldsymbol{\epsilon}^e, \end{aligned} \quad (4.147b)$$

$$Y^{IN} = (1/2)Qr^2 + (1/3)P\boldsymbol{\alpha} : \boldsymbol{\alpha}. \quad (4.147c)$$

As observed in Eq. (4.147), the generalized force Y associated with D in this theory includes not only the elastic strain energy release rate $Y^E = W^E/(1 - D)$ but also the release rate Y^{IN} of energy stored by the strain hardening. This is the marked difference from the preceding theories. Moreover, according to Eqs. (4.143) through (4.146), the values of σ , R and A tend to 0 when D tends to its critical value D_{cr} . This is an important aspect for the numerical stability in the local approach of fracture in damage mechanics described later.

4.4.2 Dissipation Potential and Evolution Equation of Plastic Damage

As an example of the above inelastic theory, we now consider the case of plastic damage. The von Mises yield condition is assumed, and a non-negative convex dissipation potential function for strain hardening and damage development is postulated as follows:

$$\begin{aligned} F(\sigma, R, A, T; D) &= f + \frac{1}{2} \frac{a}{Q} \tilde{R}^2 + \frac{1}{2} \frac{b}{P} \left[(3/2) \tilde{A}^D : \tilde{A}^D \right] \\ &\quad + \frac{S}{s+1} \frac{1}{(1-D)^q} \left(\frac{Y}{S} \right)^{s+1}, \end{aligned} \quad (4.148)$$

$$f = (\tilde{\sigma} - \tilde{A})_{EQ} - \tilde{R} - \sigma_Y, \quad (4.149)$$

where σ_Y denotes the yield stress under simple tension, and a, b, q, s, P, Q, S are material constants. The symbols \tilde{A}^D and $(\tilde{\sigma} - \tilde{A})_{EQ}$, furthermore, signify the deviatoric tensors of \tilde{A} and the equivalent stress of $(\tilde{\sigma} - \tilde{A})$.

By means of Eq. (4.148) and (4.29), we have the constitutive equation of $\dot{\boldsymbol{\epsilon}}^p$ together with the evolution equations of r , $\boldsymbol{\alpha}$ and D , i.e.,

$$\dot{\boldsymbol{\epsilon}}^p = \dot{A} \frac{\partial F}{\partial \sigma} = \frac{3}{2}(1 - D)^{-1/2} \frac{\sigma^D - A^D}{(\sigma - A)_{EQ}} \dot{A}, \quad (4.150)$$

$$\dot{r} = -\dot{A} \frac{\partial F}{\partial R} = (1 - D)^{-1/2} \left[1 - a(1 - D)^{1/2} r \right] \dot{A}, \quad (4.151)$$

$$\dot{\alpha} = -\dot{A} \frac{\partial F}{\partial A} = \dot{\epsilon}^p - b\alpha \dot{A}, \quad (4.152)$$

$$\dot{D} = \dot{A} \frac{\partial F}{\partial Y} = \frac{1}{(1-D)^q} \left(\frac{Y}{S} \right)^s \dot{A}. \quad (4.153)$$

The accumulated plastic strain rate \dot{p} can be calculated by Eq. (4.150):

$$\dot{p} = (1-D)^{-1/2} \dot{A}. \quad (4.154)$$

Finally the loading-unloading condition for Eqs. (4.150) through (4.153) are given by the condition that all of the following *Kuhn-Tucker relation* should be satisfied (Ju 1989):

$$\dot{A} \geq 0, \quad f \leq 0, \quad \dot{A}f = 0. \quad (4.155)$$

The damage-associated variable Y of Eq. (4.147) includes also the effect of the release rate of the energy stored by the strain hardening, and hence the evolution equation (4.153) of damage is expressed not only by Y but also by the damage variable D itself; i.e., this is an extended feature of Eq. (4.153) in comparison with the evolution equation developed in Section 4.3.

The above constitutive modeling of plastic damage based on the hypothesis of the total strain energy equivalence will be applied in Section 6.3 later to the damage analysis of the metal forming process.

4.4.3 Dissipation Potential and Evolution Equation of Viscoplastic Damage

As another example of the inelastic damage, we will now consider the viscoplastic damage.

Creep rate or visoplastic strain rate usually shows significant nonlinear hardening. Saanouni et al. (1994), therefore, assumed that the dissipation potential F in this case consists of two nonlinear functions, i.e., the visoplastic part F^{VP} and the damage part F^D :

$$F(\sigma, R, A, Y, T; D) = F^{VP}(\tilde{\sigma}, \tilde{R}, \tilde{A}, T) + F^D(Y, T; D), \quad (4.156)^9$$

where the functions F^{VP} and F^D are expressed as the following power functions

⁹ When the viscoplastic strain rate $\dot{\epsilon}^{vp}$ is calculated by differentiating the dissipation potential function F with respect to the stress σ , the damage part F^D of F should not affect $\dot{\epsilon}^{vp}$. Thus σ should be excluded from a set of the independent variables of F^D . Then the term σ in Eq. (4.158) is interpreted as a parameter (or a function of a parameter ϵ^e) of F^D .

$$\begin{aligned} F^{VP} &= \frac{K}{n+1} < \frac{1}{K} \left[f(\sigma, R, A; D) + \frac{1}{2} \frac{a}{Q} \tilde{R}^2 \right. \\ &\quad \left. - \frac{1}{2} a Q \tilde{r}^2 + \frac{3}{4} \frac{b}{P} \tilde{A} : \tilde{A} - \frac{1}{3} b P \tilde{\alpha} : \tilde{\alpha} \right] >^{n+1}, \end{aligned} \quad (4.157)$$

$$F^D = Y \frac{1}{(1-D)^q} \left[\frac{\chi(\sigma)}{B} \right]^s, \quad (4.158)^9$$

$$f = (\tilde{\sigma} - \tilde{A})_{EQ} - \tilde{R} - \sigma_Y, \quad (4.159)$$

$$\chi(\sigma) = \alpha \sigma_1 + \beta \sigma_{EQ} + 3(1 - \alpha - \beta) \sigma_H. \quad (4.160)$$

The symbols a , b , n , q , s and B , K , P , Q , α , β in these relations signify the material constants, while $< >$ and $\chi(\sigma)$ denote the Macauley bracket and the stress criterion for the viscoplastic damage. Furthermore, σ_1 and $\sigma_H = (1/3)\sigma_{kk}$ in Eq. (4.160) are the maximum principle stress and the mean stress.

The evolution equations of viscoplastic strain, strain hardening variables and the damage variable are derived by substituting Eq. (4.156) into Eq. (4.29), in similar forms as Eqs. (4.150) through (4.153):

$$\dot{\epsilon}^{vp} = \dot{A}^{VP} \frac{\partial F}{\partial \sigma} = \frac{3}{2} (1-D)^{-1/2} \frac{\sigma^D - A^D}{(\sigma - A)_{EQ}} \dot{A}^{VP}, \quad (4.161)$$

$$\dot{r} = -\dot{A}^{VP} \frac{\partial F}{\partial R} = (1-D)^{-1/2} \left[1 - a(1-D)^{1/2} r \right] \dot{A}^{VP}, \quad (4.162)$$

$$\dot{\alpha} = -\dot{A}^{VP} \frac{\partial F}{\partial A} = \dot{\epsilon}^{vp} \dot{\alpha} - b \alpha \dot{A}^{VP}, \quad (4.163)$$

$$\dot{D} = \dot{A}^{VP} \frac{\partial F}{\partial Y} = \frac{1}{(1-D)^q} \left[\frac{\chi(\sigma)}{B} \right]^s \dot{A}^{VP}. \quad (4.164)$$

By the use of the Norton law of Eq. (4.13), the multiplier in the above relations is given as follows:

$$\dot{A}^{VP} = < \frac{f}{K} >^n. \quad (4.165)$$

The above argument throughout this chapter is developed in the framework of the standard thermodynamic approach based on a single dissipation potential function F and a corresponding multiplier \dot{A} . As discussed in Section 3.3, the applicability of this method of constitutive modeling can be extended by the use of plural independent dissipation potentials (Chaboche 1997; Besson et al. 2010).

Chapter 5

Inelastic Constitutive Equation and Damage Evolution Equation of Material with Anisotropic Damage

The development of microvoids in materials usually depends on the direction of the applied stress, and hence the material damage is essentially anisotropic. In this chapter we consider the damage mechanics theories of the constitutive and the evolution equations of materials with anisotropic damage.

In Section 5.1, the thermodynamic constitutive theory described in Section 3.2 is applied to material with anisotropic damage characterized by a second-order symmetric damage tensor D . Then the anisotropic damage theory expressed in stress space is developed in Section 5.2, by applying the thermodynamic constitutive theory of Section 3.2.3 and by postulating the second-order damage tensor D .

In Section 5.3, the anisotropic damage theory for the elastic-brittle and the elastic-plastic-brittle materials is discussed by employing the fourth-order damage tensor D and the elastic modulus tensor C as another kind of damage tensor. The mechanical representation and the effects of the crack-closure phenomena in brittle material are discussed in some detail.

5.1 Elastic-Plastic Anisotropic Damage Theory Based on Second-Order Symmetric Damage Tensor

We mainly consider polycrystalline materials, and represent their damage state by means of a second-order symmetric damage tensor D . It is assumed that the total strain ϵ consists of the elastic ϵ^e and the plastic strain ϵ^p , and the elastic-plastic-damage process is isothermal.

5.1.1 Internal Variables and Thermodynamic Constitutive Theory

We suppose that the strain-hardening state is represented by an isotropic hardening variable r and a kinematic hardening variable α . The size of the damage dissipation potential surface may vary with the development of damage. Thus we introduce a new scalar internal variable β to represent the effect of damage development. This

variable β plays a role similar to that of the strain hardening variable r in the plastic deformation, and will be called a *damage-strengthening variable*.

Then we assume that the internal variable vector of the elastic-plastic material with anisotropic damage is expressed by

$$\mathbf{V}_k = \{\boldsymbol{\varepsilon}^p, r, \boldsymbol{\alpha}, \mathbf{D}, \beta\}. \quad (5.1)$$

Then the Helmholtz free energy function ψ of Eq. (3.40) per unit mass of the material can be given by

$$\psi = \psi(\boldsymbol{\varepsilon}^e, r, \boldsymbol{\alpha}, \mathbf{D}, \beta). \quad (5.2)$$

The constitutive and the evolution equations of the material can be derived in the similar procedure as in Sections 3.2 and 4.2. Namely substitution of Eq. (5.2) into the Clausius-Duhem inequality (3.19) gives

$$\begin{aligned} & \left(\boldsymbol{\sigma} - \rho \frac{\partial \psi}{\partial \boldsymbol{\varepsilon}^e} \right) : \dot{\boldsymbol{\varepsilon}}^e + \boldsymbol{\sigma} : \dot{\boldsymbol{\varepsilon}}^p - \rho \frac{\partial \psi}{\partial r} \dot{r} - \rho \frac{\partial \psi}{\partial \boldsymbol{\alpha}} \dot{\boldsymbol{\alpha}} \\ & - \rho \frac{\partial \psi}{\partial \mathbf{D}} : \dot{\mathbf{D}} - \rho \frac{\partial \psi}{\partial \beta} \dot{\beta} \geq 0. \end{aligned} \quad (5.3)$$

In view of the requirement that this inequality must be satisfied by any change in $\boldsymbol{\varepsilon}^e$, we have the elastic constitutive equation:

$$\boldsymbol{\sigma} = \rho \frac{\partial \psi}{\partial \boldsymbol{\varepsilon}^e}. \quad (5.4)$$

By introducing new variables

$$R \equiv \rho \frac{\partial \psi}{\partial r}, \quad \mathbf{A} \equiv \rho \frac{\partial \psi}{\partial \boldsymbol{\alpha}}, \quad \mathbf{Y} \equiv -\rho \frac{\partial \psi}{\partial \mathbf{D}}, \quad B \equiv \rho \frac{\partial \psi}{\partial \beta}, \quad (5.5)$$

and by using Eq. (5.4), the inequality (5.3) is expressed in the form

$$\Phi = \mathbf{X} \cdot \mathbf{J} \geq 0, \quad (5.6)$$

$$\mathbf{X} = \{\boldsymbol{\sigma}, -R, -\mathbf{A}, \mathbf{Y}, -B\}, \quad (5.7)$$

$$\mathbf{J} = \{\dot{\boldsymbol{\varepsilon}}^p, \dot{r}, \dot{\boldsymbol{\alpha}}, \dot{\mathbf{D}}, \dot{\beta}\}, \quad (5.8)$$

where Φ denotes the dissipation per unit volume, while \mathbf{X} and \mathbf{J} are the vectors of the generalized force and the generalized flux.

As already described in Section 3.2, if Φ is expressed in the form of Eq. (5.6), we can postulate the existence of a dissipation potential function

$$F = F(\boldsymbol{\sigma}, R, \mathbf{A}, \mathbf{Y}, B; r, \boldsymbol{\alpha}, \mathbf{D}, \beta), \quad (5.9)$$

from which the generalized flux vector \mathbf{J} of Eq. (5.8) are derived as follows:

$$\begin{aligned}\dot{\boldsymbol{\varepsilon}}^P &= \dot{\Lambda} \frac{\partial F}{\partial \boldsymbol{\sigma}}, \quad \dot{r} = -\dot{\Lambda} \frac{\partial F}{\partial R}, \quad \dot{\boldsymbol{\alpha}} = -\dot{\Lambda} \frac{\partial F}{\partial A}, \\ \dot{\mathbf{D}} &= \dot{\Lambda} \frac{\partial F}{\partial \mathbf{Y}}, \quad \dot{\beta} = -\dot{\Lambda} \frac{\partial F}{\partial B}\end{aligned}\tag{5.10}$$

5.1.2 Helmholtz Free Energy and Elastic Constitutive Equation

In the application of the above thermodynamic constitutive theory, the specific form of the Helmholtz free energy function ψ of Eq. (5.2) and that of the dissipation potential function F of Eq. (5.9) should be derived first. We discuss this problem with reference to Chow and his coworkers (Chow and Wang 1987, 1988; Chow and Lu 1989b).

As regards the Helmholtz free energy function ψ , we assume that it consists of the free energy ψ^E caused by the elastic deformation, the energy ψ^P due to plastic deformation and of the free energy ψ^D related to damage. Then the function ψ^E is subject to the effect of the material damage as a result of the change in elastic property of the material. Though the functions ψ^P and ψ^D , on the other hand, may be affected by the strain energy of the crystal lattice due to dislocation motion and by the surface energy related to void growth, the damage effects on ψ^P and ψ^D are usually limited. The effect of the kinematic hardening is assumed to be small. Then, the free energy function per unit mass ψ can be expressed in the form

$$\psi(\boldsymbol{\varepsilon}^e, r, \mathbf{D}, \beta) = \psi^E(\boldsymbol{\varepsilon}^e, \mathbf{D}) + \psi^P(r) + \psi^D(\beta).\tag{5.11}^1$$

Let us first derive the specific expression of the function ψ^E . According to the hypotheses of the energy equivalence discussed in Sections 2.3.4 and 2.3.5, the effective stress $\tilde{\boldsymbol{\sigma}}$ and the effective strain $\tilde{\boldsymbol{\varepsilon}}$ are given by Eq. (2.64):

$$\tilde{\boldsymbol{\sigma}} = \mathbb{M}(\mathbf{D}) : \boldsymbol{\sigma},\tag{5.12a}$$

$$\tilde{\boldsymbol{\varepsilon}} = \mathbb{M}(\mathbf{D})^{-T} : \boldsymbol{\varepsilon},\tag{5.12b}$$

where $\mathbb{M}(\mathbf{D})$ is the fourth-order damage effect tensor, whose explicit expressions were discussed in Section 2.3.2.

Let the elastic modulus and the elastic compliance tensors of the undamaged and the damaged material be denoted, respectively, by \mathcal{C}_0 , $\mathcal{C}(\mathbf{D})$ and \mathbb{S}_0 , $\mathbb{S}(\mathbf{D})$. Then, by the use of Eq. (2.62), we have the relations

$$\mathcal{C}(\mathbf{D}) = \mathbb{M}(\mathbf{D})^{-1} : \mathcal{C}_0 : \mathbb{M}(\mathbf{D})^{-T},\tag{5.13a}$$

¹ As regards the formulation taking account of the kinematic hardening, refer to Besson et al. (2010).

$$\mathbb{S}(\mathbf{D}) = \mathbb{M}(\mathbf{D})^T : \mathbb{S}_0 : \mathbb{M}(\mathbf{D}). \quad (5.13b)$$

In view of Eqs. (5.12b) and (5.13a), the Helmholtz free energy function for elastic deformation is expressed as

$$\begin{aligned} \rho\psi^E(\boldsymbol{\epsilon}^e, \mathbf{D}) &= \frac{1}{2}\boldsymbol{\epsilon}^e : \mathbb{C}(\mathbf{D}) : \boldsymbol{\epsilon}^e \\ &= \frac{1}{2}\tilde{\boldsymbol{\epsilon}}^e : \mathbb{C}_0 : \tilde{\boldsymbol{\epsilon}}^e. \end{aligned} \quad (5.14)$$

As regards the free energy $\psi^P(r)$ of Eq. (5.11), we recall Eq. (4.36) as a pertinent expression of the effect of isotropic hardening. As to $\psi^D(\beta)$, on the other hand, we assume the linear relationship between the damage-strengthening variable β and its associated variable B . Then we have the following expressions for ψ^P and ψ^D :

$$\rho\psi^P(r) = R_\infty \left[r + \frac{1}{b} \exp(-br) \right], \quad (5.15)$$

$$\rho\psi^D(\beta) = \frac{1}{2}K_d\beta^2, \quad (5.16)$$

where R_∞ , b and K_d are material constants.

By the use of these relations, the Helmholtz free energy function of Eq. (5.11) leads to the following explicit expression for the elastic-plastic material with anisotropic damage:

$$\begin{aligned} \rho\psi(\boldsymbol{\epsilon}^e, r, \mathbf{D}, \beta) &= \frac{1}{2}\boldsymbol{\epsilon}^e : \mathbb{C}(\mathbf{D}) : \boldsymbol{\epsilon}^e \\ &\quad + R_\infty \left[r + \frac{1}{b} \exp(-br) \right] + \frac{1}{2}K_d\beta^2. \end{aligned} \quad (5.17)$$

Substitution of this relation into Eqs. (5.4) and (5.5) provides the elastic constitutive equation and the thermodynamically associated variables \mathbf{Y} , R and B as follows:

$$\sigma = \frac{\partial(\rho\psi^E)}{\partial\boldsymbol{\epsilon}^e} = \mathbb{C}(\mathbf{D}) : \boldsymbol{\epsilon}^e, \quad (5.18)$$

$$Y = -\frac{\partial(\rho\psi^E)}{\partial\mathbf{D}} \quad (5.19)$$

$$= \frac{1}{2}\boldsymbol{\epsilon}^e : \left[\mathbb{M}^{-1} : \frac{\partial\mathbb{M}}{\partial\mathbf{D}} : \mathbb{C}(\mathbf{D}) + \mathbb{C}(\mathbf{D}) : \frac{\partial\mathbb{M}^T}{\partial\mathbf{D}} : \mathbb{M}^{-T} \right] : \boldsymbol{\epsilon}^e,$$

$$R = \frac{\partial(\rho\psi^P)}{\partial r} = R_\infty [1 - \exp(-br)], \quad (5.20)$$

$$B = \frac{\partial(\rho\psi^D)}{\partial\beta} = K_d\beta, \quad (5.21)$$

where the differentiation of Eq. (5.19) was performed by the following procedure. Namely, we first take the identities

$$\mathbb{M}^{-1} : \mathbb{M} = \mathbb{I}, \quad \mathbb{M}^T : \mathbb{M}^{-T} = \mathbb{I}. \quad (5.22)$$

Then, by differentiating these relations, we have

$$\frac{\partial \mathbb{M}^{-1}}{\partial \mathbf{D}} : \mathbb{M} = -\mathbb{M}^{-1} : \frac{\partial \mathbb{M}}{\partial \mathbf{D}}, \quad (5.23a)$$

$$\mathbb{M}^T : \frac{\partial \mathbb{M}^{-T}}{\partial \mathbf{D}} = -\frac{\partial \mathbb{M}^T}{\partial \mathbf{D}} : \mathbb{M}^{-T}. \quad (5.23b)$$

By applying these relations to the differential calculus of $\partial \mathbb{C}(\mathbf{D})/\partial \mathbf{D}$, we have the expression of the right-hand side of Eq. (5.19).

5.1.3 Dissipation Potential Functions of Plastic Deformation and Damage

By taking account of the dissipation mechanisms postulated in Eqs. (5.6) through (5.8), we employ the quasi-standard approach of [Section 3.3](#). Then the total dissipation potential F of Eq. (5.9) is expressed by the sum of the plastic and the damage dissipation potentials F^P and F^D , i.e.,

$$F(\boldsymbol{\sigma}, R, Y, B; r, \mathbf{D}, \beta) = F^P(\boldsymbol{\sigma}, R; \mathbf{D}) + F^D(Y, B; \beta). \quad (5.24)$$

The bounds of the initiation of the plastic deformation and the damage can be specified by the equi-dissipation (or equi-potential) surface in the space of the generalized forces $\{\boldsymbol{\sigma}, -R, Y, -B\}$. Then, the evolution equation (5.10) of the generalized flux vectors $\{\dot{\boldsymbol{\epsilon}}^P, \dot{r}, \dot{\mathbf{D}}, \dot{\beta}\}$ implies the *principle of maximum dissipation*, or *generalized normality law*. Hence, the yield surface and the *damage surface* (or damage loading surface) can be given by $F^P = 0$ and $F^D = 0$ by the use of the potential functions F^P and F^D of Eq. (5.24) (See Fig. 5.1).

As regards the plastic dissipation potential function, we will assume a simple loading path, and postulate the following yield function of isotropic hardening (Chow and Wang 1987, 1988):

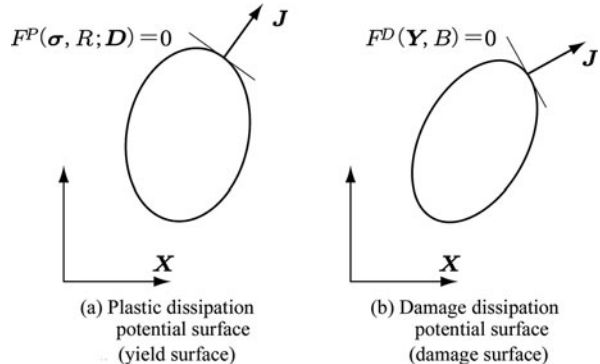
$$F^P(\boldsymbol{\sigma}, R; \mathbf{D}) = \tilde{\sigma}_{EQ} - (\sigma_Y + R) = 0, \quad (5.25a)$$

$$\tilde{\sigma}_{EQ} = \left[\frac{1}{2} \tilde{\boldsymbol{\sigma}} : \mathbb{H} : \tilde{\boldsymbol{\sigma}} \right]^{1/2} = \left[\frac{1}{2} \boldsymbol{\sigma} : \tilde{\mathbb{H}} : \boldsymbol{\sigma} \right]^{1/2}, \quad (5.25b)$$

$$\tilde{\mathbb{H}} = \mathbb{M}^T(\mathbf{D}) : \mathbb{H} : \mathbb{M}(\mathbf{D}). \quad (5.25c)$$

The tensor \mathbb{H} in these relations is a positive semi-definite tensor of the fourth-order characterizing the yield condition of orthotropic materials, whose matrix representation with respect to the principal directions of the orthotropy is given by

Fig. 5.1 The surfaces of the plastic and the damage dissipation potentials



$$[\mathbb{H}] = \begin{bmatrix} G + H & -H & -G & 0 & 0 & 0 \\ H + F & -F & 0 & 0 & 0 & 0 \\ F + G & 0 & 0 & 0 & 0 & 0 \\ 2L & 0 & 0 & 0 & 0 & 0 \\ Sym. & & & 2M & 0 & 0 \\ & & & & & 2N \end{bmatrix}, \quad (5.26)$$

where F , G , H , L , M and N are parameters characterizing the anisotropy of the material, and are called *anisotropy parameters*. In the particular case of isotropy, they have the values

$$F = G = H = 1, \quad L = M = N = 3. \quad (5.27)$$

As to the evolution equation of a damage variable, on the other hand, the existence of the damage dissipation potential surface $F^D = 0$ in the space of the generalized force $\{\sigma, -\mathbf{R}, \mathbf{Y}, -B\}$ has been ascertained for some materials (Chow and Lu 1989b; Murakami, Hayakawa, and Liu 1998). Then, if we postulate that the evolution of the damage tensor \mathbf{D} depends linearly on \mathbf{D} itself and its associated variable \mathbf{Y} , the damage dissipation potential F^D can be expressed by a homogeneous scalar function of order two in the components of \mathbf{Y} :

$$F^D(\mathbf{Y}, B) = Y_{EQ} - (B_0 + B) = 0, \quad (5.28a)$$

$$Y_{EQ} = \left[\frac{1}{2} \mathbf{Y} : \mathbb{L}(\mathbf{D}) : \mathbf{Y} \right]^{1/2}, \quad (5.28b)$$

where B_0 is a material constant specifying the size of the initial damage surface. The function $\mathbb{L}(\mathbf{D})$, on the other hand, is a positive semi-definite tensor function of fourth-order with the argument \mathbf{D} , and is expressed as

$$L_{ijkl} = \frac{1}{2}(\delta_{ik}\delta_{jl} + \delta_{il}\delta_{jk}) + \frac{1}{2}c^d(\delta_{ik}D_{jl} + D_{ik}\delta_{jl} \\ + \delta_{il}D_{jk} + D_{il}\delta_{jk}), \quad (5.29)$$

where c^d is a material constant.

By recapitulating the above results, the dissipation potential (5.24) of an elastic-plastic material with anisotropic damage is given by Eqs. (5.25) and (5.28) as follows:

$$F(\boldsymbol{\sigma}, R, Y, B; r, \mathbf{D}, \beta) = F^P(\boldsymbol{\sigma}, R; \mathbf{D}) + F^D(Y, B) \\ = \tilde{\sigma}_{EQ} - (\sigma_Y + R) + Y_{EQ} - (B_0 + B). \quad (5.30)$$

Besides Eq. (5.28), if the damage surface is defined in the space of the generalized forces and the damage-strengthening is governed by the elastic strain energy W^E , the damage potential function F^D may be given in the form (Chow and Lu 1989b)

$$F^D = Y_D - [B_0 + B(W^E)] = 0, \quad (5.31)$$

$$Y_D = \left[\frac{1}{2} \mathbf{Y} : \mathbb{K} : \mathbf{Y} \right]^{1/2}, \quad (5.32a)$$

$$W^E = \frac{1}{2} \boldsymbol{\sigma} : \boldsymbol{\varepsilon}^e. \quad (5.32b)$$

5.1.4 Plastic Constitutive Equation and Damage Evolution Equation

By substituting the dissipation potential F of Eq. (5.30) above into Eq. (5.10), the plastic constitutive equation and the evolution equation of the internal variables would be derived with an indeterminate multiplier $\dot{\Lambda}$. However, as already described in Section 3.3.2, the framework of the standard thermodynamic approach gives significant restriction to the mechanical behavior of a material.

In order to avoid this restriction, we now take the quasi-standard approach, and postulate two independent multipliers $\dot{\Lambda}^P$ and $\dot{\Lambda}^D$, respectively, for the dissipation potential functions of Eqs. (5.25) and (5.28) (Chow and Wang 1987; Hansen and Schreyer 1994).

By substituting the dissipation function F^P of Eq. (5.25) into Eq. (5.10), we first have the constitutive equations of the plastic strain $\dot{\boldsymbol{\varepsilon}}^p$ together with the evolution equation of the isotropic hardening variable r (Fig. 5.2):

$$\dot{\boldsymbol{\varepsilon}}^p = \dot{\Lambda}^P \frac{\partial F^P}{\partial \boldsymbol{\sigma}} = \frac{1}{2} \frac{\dot{\Lambda}^P}{\tilde{\sigma}_{EQ}} \tilde{\mathbb{H}} : \boldsymbol{\sigma}, \quad (5.33)$$

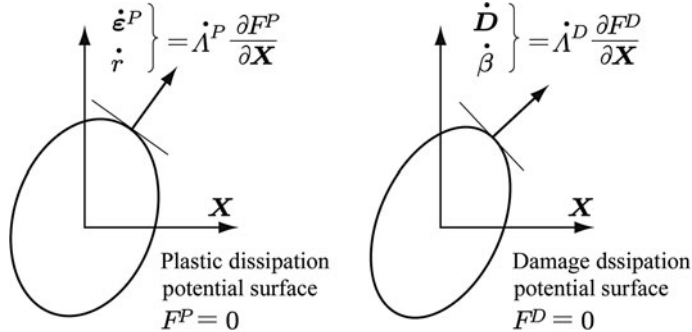


Fig. 5.2 Plastic and damage dissipation potential surfaces and generalized flux vector $\{\dot{\epsilon}^P, \dot{r}, \dot{D}, \dot{\beta}\}$

$$\dot{r} = -\dot{\Lambda}^P \frac{\partial F^P}{\partial R} = -\dot{\Lambda}^P \frac{\partial(-R)}{\partial R} = \dot{\Lambda}^P, \quad (5.34)$$

where the explicit value of the indeterminate multiplier $\dot{\Lambda}^P$ can be derived from the consistency condition $\dot{F}^P = 0$ of Eq. (5.25), i.e.,

$$\dot{\Lambda}^P = \frac{1}{2\tilde{\sigma}_{EQ}} (\boldsymbol{\sigma} : \tilde{\mathbb{H}} : \dot{\boldsymbol{\sigma}}) / \left(\frac{\partial R}{\partial r} \right). \quad (5.35)$$

The loading-unloading condition of Eqs. (5.33) and (5.34) is given by the condition that all of the following *Kuhn-Tucker relation* should be satisfied (Ju 1989):

$$\dot{\Lambda}^P \geq 0, \quad F^P \leq 0, \quad \dot{\Lambda}^P F^P = 0. \quad (5.36)$$

The evolution equations of the damage variable D and the damage-strengthening variable β , on the other hand, are derived by substituting F^D of Eq. (5.28) into Eq. (5.10) as follows (Fig. 5.2):

$$\dot{D} = \dot{\Lambda}^D \frac{\partial F^D}{\partial Y} = \frac{1}{2Y_{EQ}} (\mathbb{L} : Y) \dot{\Lambda}^D, \quad (5.37)$$

$$\dot{\beta} = -\dot{\Lambda}^D \frac{\partial F^D}{\partial B} = -\dot{\Lambda}^D \frac{\partial(-B)}{\partial B} = \dot{\Lambda}^D. \quad (5.38)$$

The explicit value of the multiplier $\dot{\Lambda}^D$ of these equations, furthermore, is obtained from the *consistency condition* $\dot{F}^D = 0$ as to Eq. (5.28):

$$\dot{\Lambda}^D = \frac{1}{2Y_{EQ}} \left[Y : \mathbb{L} : \dot{Y} + \frac{1}{2} Y : \left(\frac{\partial \mathbb{L}}{\partial D} : Y \right) : \dot{D} \right] / \left(\frac{\partial B}{\partial \beta} \right). \quad (5.39)$$

The loading-unloading condition of Eqs. (5.37) and (5.38) is given by the Kuhn-Tucker relation

$$\dot{\Lambda}^D \geq 0, \quad F^D \leq 0, \quad \dot{\Lambda}^D F^D = 0. \quad (5.40)$$

The application of the constitutive equation of elasticity (5.18), that of plasticity (5.33) through (5.36) and the evolution equation of damage (5.37) through (5.40) will be discussed later in [Chapter 6](#). The extension of the above theory to incorporate the unilateral effect due to microcrack closure together with its experimental verification are found in a reference (Hayakawa, Murakami, and Liu [1998](#)).

5.2 Elastic-Plastic Anisotropic Damage Theory in Stress Space

In the anisotropic damage theory developed in the preceding section, the Helmholtz free energy function ψ and hence the resulting generalized forces $\{\sigma, -R, Y, -B\}$ were defined in terms of the elastic strain $\boldsymbol{\epsilon}^e$. As described already in [Section 3.2.3](#), the selection of stress as an independent variable is often convenient for the experimental discussion of the damage behavior. In this section we develop another anisotropic damage theory expressed in the independent variable space of stress σ .

5.2.1 Thermodynamic Constitutive Theory in Stress Space

Let us first apply the constitutive theory of [Section 3.2.3](#) developed in stress space to the anisotropically damaged material represented by a second-order symmetric damage variable \mathbf{D} . Then, the Gibbs potential function Γ per unit mass is given by the use of the Helmholtz free energy function ψ :

$$\rho\Gamma(\sigma, r, \mathbf{D}, \beta) = \rho\psi(\boldsymbol{\epsilon}^e, r, \mathbf{D}, \beta) - \sigma : \boldsymbol{\epsilon}^e, \quad (5.41)$$

where β is the damage-strengthening variable.

Substitution of this relation into the Clausius-Duhem inequality (3.19) leads to

$$\begin{aligned} \sigma : \dot{\boldsymbol{\epsilon}}^e - \left(\boldsymbol{\epsilon}^e + \rho \frac{\partial \Gamma}{\partial \sigma} \right) : \dot{\boldsymbol{\sigma}} - \rho \frac{\partial \Gamma}{\partial r} \dot{r} \\ - \rho \frac{\partial \Gamma}{\partial \mathbf{D}} : \dot{\mathbf{D}} - \rho \frac{\partial \Gamma}{\partial \beta} \dot{\beta} \geq 0, \end{aligned} \quad (5.42)$$

from which we have the elastic constitutive equation:

$$\boldsymbol{\epsilon}^e = -\rho \frac{\partial \Gamma}{\partial \sigma}. \quad (5.43)$$

By defining new associated variables

$$R \equiv \rho \frac{\partial \Gamma}{\partial r}, \quad Y \equiv -\rho \frac{\partial \Gamma}{\partial \mathbf{D}}, \quad B \equiv \rho \frac{\partial \Gamma}{\partial \beta} \quad (5.44)$$

and by the use of Eq. (5.43), the Clausius-Duhem inequality (5.42) can be expressed in the form

$$\Phi = \mathbf{X} \cdot \mathbf{J} \geq 0, \quad (5.45)$$

$$\mathbf{X} = \{\boldsymbol{\sigma}, -R, \mathbf{Y}, -B\}, \quad (5.46)$$

$$\mathbf{J} = \{\dot{\boldsymbol{\epsilon}}^p, \dot{r}, \dot{\mathbf{D}}, \dot{\beta}\}. \quad (5.47)$$

Similarly to the discussion of Section 3.2.3, by postulating the existence of the dissipation potential

$$F = F(\boldsymbol{\sigma}, R, \mathbf{Y}, B; r, \mathbf{D}, \beta), \quad (5.48)$$

the evolution equation of the generalized flux vector \mathbf{J} , i.e., the inelastic constitutive equation and the evolution equations of the internal variables are derived as follows:

$$\dot{\boldsymbol{\epsilon}}^p = \dot{\Lambda} \frac{\partial F}{\partial \boldsymbol{\sigma}}, \quad \dot{r} = -\dot{\Lambda} \frac{\partial F}{\partial R}, \quad \dot{\mathbf{D}} = \dot{\Lambda} \frac{\partial F}{\partial \mathbf{Y}}, \quad \dot{\beta} = -\dot{\Lambda} \frac{\partial F}{\partial B}. \quad (5.49)$$

As observed in Eqs. (5.41) and (5.44), the generalized force \mathbf{Y} associated with the damage variable \mathbf{D} has been specified as a function of the stress $\boldsymbol{\sigma}$ in this case.

5.2.2 Gibbs Potential and Elastic Constitutive Equation

In Section 5.1, the explicit forms of the Helmholtz free energy function ψ and the dissipation function F were determined on the basis of effective stress tensor $\tilde{\boldsymbol{\sigma}}$ and the hypothesis of the strain energy equivalence. In this section, however, we show another way to derive the thermodynamic functions by the use of the representation theorem of tensor functions explained in Chapter 12.

As described in Section 4.3, the opening and closing behavior of microcracks may be induced by the change of stress sign. Thus we will incorporate the unilateral effect (see Section 4.3.4) in the mechanical behavior due to crack opening.

Let us first assume that the Gibbs potential function Γ per unit mass is expressed by the sum of the elastic complementary strain energy Γ^E , the potential related to the plastic deformation Γ^P and that of damage Γ^D :

$$\Gamma(\boldsymbol{\sigma}, r, \mathbf{D}, \beta) = \Gamma^E(\boldsymbol{\sigma}, \mathbf{D}) + \Gamma^P(r) + \Gamma^D(\beta). \quad (5.50)$$

If the initial undamaged material is isotropic, the complementary strain energy function Γ^E of the material can be given by a scalar-valued tensor function of the two symmetric tensors $\boldsymbol{\sigma}$ and \mathbf{D} . In view of Eq. (12.215) in Chapter 12, the most

general form of the function can be represented by a scalar function of ten basic invariants (i.e., simultaneous orthogonal invariants) of the tensors σ and D .

Though the elastic response of the material in the initial undamaged state is linear, the ensuing rigidity of the material decreases with the damage development. Then, by taking account of the crack closure effect due to compressive stress together with the continuity condition of stress and strain (Chaboche 1993), the function Γ^E can be expressed as follows (Hayakawa and Murakami 1997):

$$\rho \Gamma^E(\sigma, D) = \frac{v_0}{2E_0} (\text{tr}\sigma)^2 - \frac{1+v_0}{2E_0} \text{tr}(\sigma^2) - \vartheta_1 (\text{tr}D)(\text{tr}\sigma)^2 \\ - \vartheta_2 (\text{tr}D)(\text{tr}\bar{\sigma}^2) - \vartheta_3 (\text{tr}\sigma)(\text{tr}\sigma D) - \vartheta_4 (\text{tr}\bar{\sigma}^2 D), \quad (5.51)^2$$

where E_0 and v_0 denote Young's modulus and Poisson's ratio in the initial undamaged state, and ϑ_1 through ϑ_4 are material constants. The symbol $\bar{\sigma}$ denotes the modified stress tensor representing the unilateral effects, and are defined as follows:

$$\bar{\sigma} = <\sigma> - \eta <-\sigma>, \quad (0 \leq \eta \leq 1), \quad (5.52)$$

$$[<\sigma>] = \begin{bmatrix} <\sigma_1> & 0 & 0 \\ 0 & <\sigma_2> & 0 \\ 0 & 0 & <\sigma_3> \end{bmatrix}, \quad (5.53a)$$

$$[<-\sigma>] = \begin{bmatrix} <-\sigma_1> & 0 & 0 \\ 0 & <-\sigma_2> & 0 \\ 0 & 0 & <-\sigma_3> \end{bmatrix}, \quad (5.53b)$$

where $<>$ and σ_i ($i = 1, 2, 3$), respectively, are Macauley bracket and the principal value of the tensor σ . The symbol η ($0 \leq \eta \leq 1$), furthermore, is a material constant representing the crack closure effect due to compressive stress.

The function Γ^P and Γ^D of Eq. (5.50), on the other hand, are determined so that Γ^P may represent pertinently the isotropic hardening due to plastic deformation, while Γ^D are determined so that it may give a linear relationship between the damage strengthening variable β and its associated variable B :

$$\rho \Gamma^P(r) = R_\infty \left[r + \frac{1}{b} \exp(-br) \right], \quad (5.54)$$

$$\rho \Gamma^D(\beta) = (1/2)K_d \beta^2, \quad (5.55)$$

where R_∞ , b and K_d are material constants.

The elastic constitutive equation of this material can be derived by substituting the Gibbs potential function (5.51) into Eq. (5.43). In the derivation, the differential

² According to the definition (3.26), the Gibbs potential Γ is usually a negative-valued function.

calculus of the scalar valued tensor function $\Gamma^E(\sigma, D)$ with respect to σ can be performed by the procedure mentioned in [Section 12.5](#). For example, as regards the differentiation of the sixth term in the right hand side of Eq. (5.51), we first apply the chain rule and have the relation

$$\frac{\partial \text{tr}(\bar{\sigma}^2 D)}{\partial \sigma} = \frac{\partial \text{tr}(\bar{\sigma} \bar{\sigma} D)}{\partial \bar{\sigma}} : \frac{\partial \bar{\sigma}}{\partial \sigma}. \quad (5.56a)$$

By taking an arbitrary tensor C belonging to the same tensor space as $\bar{\sigma}$ and a scalar h of a real value, we replace $\bar{\sigma}$ in $\text{tr}(\bar{\sigma} \bar{\sigma} D)$ with $(\bar{\sigma} + hC)$. By expanding it with respect to h , we have

$$\begin{aligned} \text{tr}[(\bar{\sigma} + hC)(\bar{\sigma} + hC)D] &= \text{tr}[(D\bar{\sigma} + hDC)(\bar{\sigma} + hC)] \\ &= \text{tr}(D\bar{\sigma} \bar{\sigma}) + h[\text{tr}(D\bar{\sigma} C) + \text{tr}(DC\bar{\sigma})] + O(h^2). \end{aligned} \quad (5.56b)$$

Then by applying the same operation as that of [Eq. \(12.203\)](#) of the Appendix, we have the total differential:

$$\begin{aligned} \text{tr}\left[\left(\frac{\partial \text{tr}(D\bar{\sigma} \bar{\sigma})}{\partial \bar{\sigma}}\right)^T C\right] \\ = \lim_{h \rightarrow 0} \frac{1}{h} \{\text{tr}[D(\bar{\sigma} + hC)(\bar{\sigma} + hC)] - \text{tr}(D\bar{\sigma} \bar{\sigma})\} \\ = \text{tr}(D\bar{\sigma} C) + \text{tr}(DC\bar{\sigma}) = \text{tr}(D\bar{\sigma} C) + \text{tr}(\bar{\sigma} DC) \\ = \text{tr}[(D\bar{\sigma} + \bar{\sigma} D)C]. \end{aligned} \quad (5.56c)$$

Since this relation should hold for an arbitrary value of C , we have

$$\frac{\partial \text{tr}(\bar{\sigma} \bar{\sigma} D)}{\partial \bar{\sigma}} = (D\bar{\sigma} + \bar{\sigma} D)^T = \bar{\sigma} D + D\bar{\sigma}, \quad (5.56d)$$

and hence the derivative of Eq. (5.56a) leads to

$$\frac{\partial \text{tr}(\bar{\sigma}^2 D)}{\partial \sigma} = (\bar{\sigma} D + D\bar{\sigma}) : \frac{\partial \bar{\sigma}}{\partial \sigma}. \quad (5.56e)$$

The derivative of the other terms in the right hand side of Eq. (5.51) can be derived in the similar procedure, and hence the elastic constitutive equation of this damaged material is finally obtained as follows:

$$\begin{aligned}\boldsymbol{\varepsilon}^e &= -\rho \frac{\partial \Gamma^E}{\partial \boldsymbol{\sigma}} \\ &= -\frac{\nu_0}{E_0} (\text{tr} \boldsymbol{\sigma}) \mathbf{I} + \frac{1 + \nu_0}{E_0} \text{tr} \boldsymbol{\sigma} \\ &\quad + 2\vartheta_1(\text{tr} \mathbf{D})(\text{tr} \boldsymbol{\sigma}) \mathbf{I} + 2\vartheta_2(\text{tr} \mathbf{D}) \bar{\boldsymbol{\sigma}} : \frac{\partial \bar{\boldsymbol{\sigma}}}{\partial \boldsymbol{\sigma}} \\ &\quad + \vartheta_3 [(\text{tr} \boldsymbol{\sigma} \mathbf{D}) \mathbf{I} + (\text{tr} \boldsymbol{\sigma}) \mathbf{D}] + \vartheta_4 (\bar{\boldsymbol{\sigma}} \mathbf{D} + \mathbf{D} \bar{\boldsymbol{\sigma}}) : \frac{\partial \bar{\boldsymbol{\sigma}}}{\partial \boldsymbol{\sigma}},\end{aligned}\tag{5.57}$$

where $\bar{\boldsymbol{\sigma}}$ is the modified stress tensor defined by Eq. (5.52), and represents the unilateral effect due to crack closure.

The generalized forces of Eq. (5.46), furthermore, are derived by substituting Eqs. (5.54) and (5.55) into Eq. (5.44) as follows:

$$\mathbf{Y} = -\rho \frac{\partial \Gamma^E}{\partial \mathbf{D}} = \left[\vartheta_1(\text{tr} \boldsymbol{\sigma})^2 + \vartheta_2 \text{tr} \bar{\boldsymbol{\sigma}}^2 \right] \mathbf{I} + \vartheta_3(\text{tr} \boldsymbol{\sigma}) \boldsymbol{\sigma} + \vartheta_4 \bar{\boldsymbol{\sigma}}^2,\tag{5.58}$$

$$R = \rho \frac{\partial \Gamma^P}{\partial r} = R_\infty [1 - \exp(-br)],\tag{5.59}$$

$$B = \rho \frac{\partial \Gamma^D}{\partial \beta} = K_d \beta.\tag{5.60}$$

5.2.3 Dissipation Potential Functions of Plastic Deformation and Damage

By recalling the internal structural change postulated in the formulation of the generalized flux (5.47), the dissipation potential function F of Eq. (5.48) may be expressed as the sum of the dissipation potentials F^P and F^D related to plastic deformation and damage:

$$F(\boldsymbol{\sigma}, R, Y, B; r, \mathbf{D}, \beta) = F^P(\boldsymbol{\sigma}, R; \mathbf{D}) + F^D(Y, B; \mathbf{D}, r).\tag{5.61}$$

Suppose that, as in the case of Section 5.1.3, the yield surface and the damage loading surface exist in the space of the generalized forces $\{\boldsymbol{\sigma}, -R, Y, -B\}$, and that these surfaces are specified by the potential functions F^P and F^D of Eq. (5.61).

Concerning the plastic dissipation potential F^P , we extend the von Mises yield function to the damaged material, and assume the following yield condition of isotropic hardening:

$$F^P(\boldsymbol{\sigma}, R; \mathbf{D}) = \tilde{\sigma}_{EQ} - (\sigma_Y + R) = 0,\tag{5.62a}$$

$$\tilde{\sigma}_{EQ} = \left[\frac{1}{2} \boldsymbol{\sigma} : \mathbb{K}(\mathbf{D}) : \boldsymbol{\sigma} \right]^{1/2},\tag{5.62b}$$

where $\mathbb{K}(\mathbf{D})$ denotes a fourth-order symmetric tensor function of \mathbf{D} , and are expressed:

$$K_{ijkl} = \frac{1}{2}(\delta_{ik}\delta_{jl} + \delta_{il}\delta_{jk}) + \frac{1}{2}c^p(\delta_{ik}D_{jl} + D_{ik}\delta_{jl} + \delta_{il}D_{jk} + D_{il}\delta_{jk}), \quad (5.62c)$$

where c^p is a material constant.

As regards the damage development, on the other hand, the existence of the damage potential surface $F^D = 0$ in the space of the generalized forces can be assumed as will be described in Section 5.2.4. Hence we assume a damage potential surface of a similar form as Eq. (5.62), i.e., a second-order homogeneous function of \mathbf{Y} as follows:

$$F^D(\mathbf{Y}, B; \mathbf{D}, r) = Y_{EQ} + c^r r(\text{tr}\mathbf{D})(\text{tr}\mathbf{Y}) - (B_0 + B) = 0, \quad (5.63a)$$

$$Y_{EQ} = \left[\frac{1}{2} \mathbf{Y} : \mathbb{L}(\mathbf{D}) : \mathbf{Y} \right]^{1/2}, \quad (5.63b)$$

where c^r is a material constant and B_0 is a material constant signifying the size of the initial damage surface. The function $\mathbb{L}(\mathbf{D})$, furthermore, is a fourth-order tensor-valued function of \mathbf{D} :

$$L_{ijkl} = \frac{1}{2}(\delta_{ik}\delta_{jl} + \delta_{il}\delta_{jk}) + \frac{1}{2}c^d(\delta_{ik}D_{jl} + D_{ik}\delta_{jl} + \delta_{il}D_{jk} + D_{il}\delta_{jk}), \quad (5.63c)$$

where c^d is a material constant. The term with c^r in Eq. (5.63a) has been introduced in order to represent the effect of isotropic damage on the damage development.

5.2.4 Plastic Constitutive Equation and Damage Evolution Equation

We now apply the quasi-standard thermodynamic approach described in Section 3.3.2, and postulate the dissipation potentials F^P and F^D of Eqs. (5.62) and (5.63) together with two independent multiplier λ^P and λ^D .

Substitution of the yield function F^P of Eq. (5.62) into Eq. (5.49) gives the constitutive equations of the plastic strain $\boldsymbol{\epsilon}^P$ and the isotropic hardening variable r as follows (Fig. 5.2):

$$\dot{\boldsymbol{\epsilon}}^P = \dot{\Lambda}^P \frac{\partial F^P}{\partial \boldsymbol{\sigma}} = \frac{1}{2} \dot{\Lambda}^P \frac{\mathbb{K}(\mathbf{D}) : \boldsymbol{\sigma}}{\tilde{\sigma}_{EQ}}, \quad (5.64)$$

$$\dot{r} = -\dot{\Lambda}^P \frac{\partial F^P}{\partial R} = \dot{\Lambda}^P, \quad (5.65)$$

where the indeterminate multiplier $\dot{\Lambda}^P$ is determined by the consistency condition $\dot{F}^P = 0$:

$$\dot{\Lambda}^P = \frac{1}{2\tilde{\sigma}_{EQ}} [\boldsymbol{\sigma} : \mathbb{K}(\mathbf{D}) : \dot{\boldsymbol{\sigma}}] / \left(\frac{\partial R}{\partial r} \right). \quad (5.66)$$

Furthermore, the loading-unloading condition is specified by the Kuhn-Tucker relation of Eq. (5.36).

The evolution equation of the damage tensor \mathbf{D} and the damage-strengthening internal variable β , on the other hand, are derived from Eq. (5.49) and the damage dissipation potential function F^D of Eq. (5.63) as follows (Fig. 5.2):

$$\dot{\mathbf{D}} = \dot{\Lambda}^D \frac{\partial F^D}{\partial \mathbf{Y}} = \dot{\Lambda}^D \left[\frac{1}{2Y_{EQ}} (\mathbb{L} : \mathbf{Y}) + c^r r (\text{tr} \mathbf{D}) \mathbf{I} \right], \quad (5.67)$$

$$\dot{\beta} = -\dot{\Lambda}^D \frac{\partial F^D}{\partial B} = \dot{\Lambda}^D, \quad (5.68)$$

where $\dot{\Lambda}^D$ is given by the consistency condition $\dot{F}^D = 0$:

$$\dot{\Lambda}^D = \left(\frac{\partial F^D}{\partial \mathbf{Y}} : \dot{\mathbf{Y}} + \frac{\partial F^D}{\partial r} \dot{r} \right) / \left(\frac{\partial B}{\partial \beta} - \frac{\partial F^D}{\partial \mathbf{D}} : \frac{\partial F^D}{\partial \mathbf{Y}} \right). \quad (5.69)$$

The loading-unloading condition is specified by the Kuhn-Tucker relation of Eq. (5.40).

Figure 5.3 shows the comparison between the results of elastic-plastic damage tests on spheroidized graphite cast iron tubes and the corresponding prediction of the elastic-plastic anisotropic damage theory described above (Hayakawa and Murakami 1997). The spheroidized cast iron was selected here as a typical material showing both of moderate ductility and apparent damage anisotropy.

Firstly, Fig. 5.3a shows the experimental results and the predictions of Eq. (5.63) on the damage loading surface (d.s.) in the combined tension-torsion stress space. The symbols \circlearrowleft , \square and \triangle show the critical states of damage initiation defined by the threshold event frequency $N = 10 \text{ sec}^{-1}$ of the acoustic emission (AE) signals.

Figure 5.3b, on the other hand, represent the initial and the succeeding damage potential surface (p.s.) in the space of the damage associated variable \mathbf{Y} . The points A_0 , B_0 , C_0 and A_1 , B_1 , C_1 in this figure show the stress points in Fig. 5.3a. This figure certifies the existence of the damage dissipation potential for the damage development, and ascertains the normality assumption of the damage increment to the damage surface.

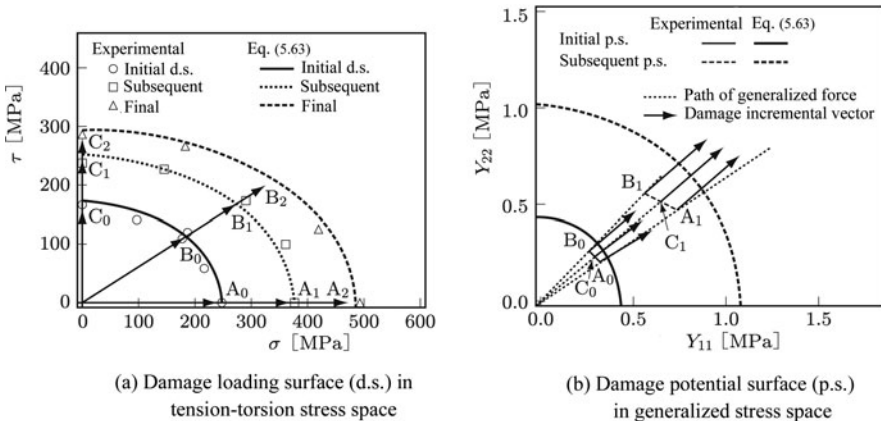


Fig. 5.3 Damage surface in the stress space, and damage potential surface in the generalized stress space

5.3 Fourth-Order Symmetric Damage Tensor and Its Application to Elastic-Plastic-Brittle Damage

The anisotropic damage theory based on the second-order symmetric damage tensor \mathbf{D} discussed in Sections 5.1 and 5.2 can not be applied to damage states more complicated than the orthotropy.

However, in elastic-brittle materials such as concrete and rocks, or in fiber-reinforced composite materials with complex initial anisotropy, a number of distributed microcracks develop with specific anisotropy corresponding to the material structure and the loading condition. Hence the damage states may be much more complicated than the orthotropy. For the accurate description of these complicated damage states and their development, several damage theories based on a fourth-order symmetric damage tensor have been proposed.

We now discuss a few important damage theories for elastic-brittle and elastic-plastic-brittle material of complicated anisotropy.

5.3.1 Constitutive and Evolution Equations for Elastic-Brittle Damage

For the sake of simplicity, small deformation in isothermal process is postulated. The internal state of the material, furthermore, is assumed to be represented by a fourth-order symmetric damage tensor \mathbb{D} and a damage-strengthening variable β .

According to the thermodynamic theory of Sections 5.1 and 5.2, the Helmholtz free energy function ψ per unit mass in this case can be written as

$$\rho\psi(\boldsymbol{\varepsilon}, \mathbb{D}, \beta) = \frac{1}{2}\boldsymbol{\varepsilon} : \mathbb{C}(\mathbb{D}) : \boldsymbol{\varepsilon} + \frac{1}{2}\beta^2, \quad (5.70)$$

where $\boldsymbol{\varepsilon}$ and $\mathbb{C}(\mathbb{D})$ denote the elastic strain and the elastic modulus tensor of the damaged material (or the secant modulus tensor).

By means of the Clausius-Duhem inequality (5.3), one can obtain the expressions of the stress $\boldsymbol{\sigma}$ and the generalized forces \mathbb{Y} and B associated with \mathbb{D} and β :

$$\boldsymbol{\sigma} = \rho \frac{\partial \psi}{\partial \boldsymbol{\varepsilon}} = \mathbb{C}(\mathbb{D}) : \boldsymbol{\varepsilon}, \quad (5.71)$$

$$\mathbb{Y} = -\rho \frac{\partial \psi}{\partial \mathbb{D}} = -\frac{1}{2}\boldsymbol{\varepsilon} : \frac{\partial \mathbb{C}(\mathbb{D})}{\partial \mathbb{D}} : \boldsymbol{\varepsilon}, \quad (5.72)$$

$$B = \rho \frac{\partial \psi}{\partial \beta} = \beta. \quad (5.73)$$

Let us now consider the evolution equation of the damage variable \mathbb{D} . According to the discussion of Section 3.2 or 5.1, the evolution equation of \mathbb{D} and β can be derived from a damage dissipation potential function $F^D(\mathbb{Y}, B)$. By postulating the potential function F^D of the form

$$F^D(\mathbb{Y}, B) = g(\mathbb{Y}) - B \leq 0, \quad (5.74)$$

we have the evolution equations of \mathbb{D} and β from Eq. (5.10):

$$\dot{\mathbb{D}} = \dot{\Lambda}^D \frac{\partial F^D}{\partial \mathbb{Y}}, \quad (5.75)$$

$$\dot{\beta} = -\dot{\Lambda}^D \frac{\partial F^D}{\partial B} = \dot{\Lambda}^D, \quad (5.76)$$

where $\dot{\Lambda}^D$ is the indeterminate scalar multiplier, whose value can be determined by the consistency condition $\dot{F}^D = 0$. The loading-unloading condition for damage development is given by the Kuhn-Tucker relation:

$$\dot{\Lambda}^D \geq 0, \quad F^D \leq 0, \quad \dot{\Lambda}^D F^D = 0. \quad (5.77)$$

5.3.2 Opening-Closing Effect of Cracks in Brittle Damage Field and Its Mechanical Representation – Positive Projection Tensors for Strain and Stress

Cracks in a *brittle-damage material* are effective only when they are open; they usually have no mechanical effect when they are closed. The state of cracks which are perfectly open is called *active*, while the state of cracks which are perfectly closed is said to be *passive*. A phenomenon in which the mechanical effects differ according to the sign of stress or strain is called *unilateral*.

Fig. 5.4 Unilateral mechanical behavior of elastic-brittle-damage material

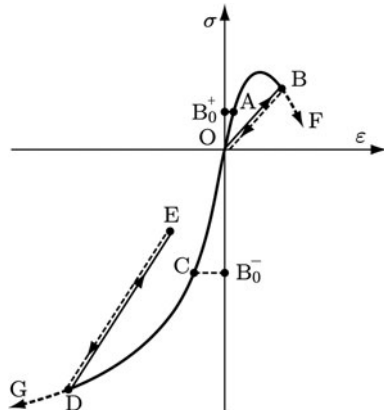


Figure 5.4 is the schematic representation of the mechanical behavior of an elastic-brittle-damage material under tension-compression loading. As observed in the figure, material damage starts at the points A and C. The succeeding region ABF and CDG are the loading processes where damage develops. The region OA, OC or BO, DE, on the other hand, show the elastic response before damage initiation or in the unloading process. The unilateral effect observed in such brittle damage is an essential phenomenon for the description of the mechanical behavior of brittle material, e.g., the damage development and the resulting change in rigidity, above all. This feature is one of the most complicated problems in damage mechanics. We will discuss first the mechanical representation of the opening-closing effect of microcracks.

Opening or closing of a single crack is specified by the condition whether the normal strain or the normal stress acting on the crack plane is tensile or compressive. In the case of the distributed cracks, however, which set of cracks is opening, and which set is closing are governed by the relative relation between the state of crack distribution and that of stress and strain, and are not apparent. Therefore, in damage mechanics of unilateral material, we must represent appropriately the effect of stress and strain states on the opening-closing behavior of microcracks. A simple description of the effect of tensile or compressive stress on the crack-opening in elastic-brittle damage field was already discussed in Sections 4.3.4 and 5.2.2. The reduction of damage effects due to microcrack closure is generally called *damage deactivation*.

So far several *projection tensors* have been proposed in order to represent the strain or the stress effect on the crack opening behavior in brittle damage fields (Ortiz 1985; Simo and Ju 1987; Yazdani and Schreyer 1988; Lubarda, Krajcinovic, and Mastilovic 1994). These projection tensors were employed in the subsequent damage theories. Here we show some important projection tensors and their application in the case of elastic-damage material.

(1) Positive Projection Tensor for Strain Tensor

Opening-closing behavior of a crack is governed mainly by the strain component normal to the crack plane. We take the elastic strain $\boldsymbol{\varepsilon}$, and express it by its spectral decomposition

$$\boldsymbol{\varepsilon} = \sum_{i=1}^3 \varepsilon_i \mathbf{n}_i^{(\boldsymbol{\varepsilon})} \otimes \mathbf{n}_i^{(\boldsymbol{\varepsilon})}, \quad (5.78)$$

where ε_i and $\mathbf{n}_i^{(\boldsymbol{\varepsilon})}$ denote i th principle strain (i th proper value) and the corresponding proper vector (eigenvector).

Let us suppose that the crack opening is induced by the positive part of the principal strain. In order to express this assumption, the following *positive-valued strain tensor* is defined:

$$[\varepsilon_{ij}^+] = \begin{bmatrix} < \varepsilon_1 > & 0 & 0 \\ 0 & < \varepsilon_2 > & 0 \\ 0 & 0 & < \varepsilon_3 > \end{bmatrix}, \quad (5.79a)$$

or

$$\boldsymbol{\varepsilon}^+ = \sum_{i=1}^3 \varepsilon_i^+ \mathbf{n}_i^{(\boldsymbol{\varepsilon})} \otimes \mathbf{n}_i^{(\boldsymbol{\varepsilon})}, \quad \varepsilon_i^+ = < \varepsilon_i > = H(\varepsilon_i) \varepsilon_i, \quad (5.79b)$$

where $< >$ and $H()$ are the Macauley bracket and the Heaviside function.

For the consistent discussion of the opening-closing behavior of distributed cracks, it is expedient to express the positive-valued strain tensor $\boldsymbol{\varepsilon}^+$ as a transformation from the strain tensor $\boldsymbol{\varepsilon}$. For this purpose, we first define the following two projection tensors of the second-order (Lubarda et al. 1994):

$$\mathbf{Q}_{\boldsymbol{\varepsilon}} \equiv \mathbf{n}_i^{(\boldsymbol{\varepsilon})} \otimes \mathbf{e}_i = \delta_{ij} \mathbf{n}_i^{(\boldsymbol{\varepsilon})} \otimes \mathbf{e}_j, \quad (5.80)$$

$$\mathbf{Q}_{\boldsymbol{\varepsilon}}^+ \equiv \sum_{i=1}^3 H(\varepsilon_i) \mathbf{n}_i^{(\boldsymbol{\varepsilon})} \otimes \mathbf{e}_i, \quad (5.81)$$

where \mathbf{e}_i denotes the orthonormal basis of the relevant coordinate system. The tensors $\mathbf{Q}_{\boldsymbol{\varepsilon}}$ and $\mathbf{Q}_{\boldsymbol{\varepsilon}}^+$ of Eqs. (5.80) and (5.81) denote, respectively, the dyad of the eigenvector $\mathbf{n}_i^{(\boldsymbol{\varepsilon})}$ and the basis vector \mathbf{e}_i , and that of the vector $H(\varepsilon_i) \mathbf{n}_i^{(\boldsymbol{\varepsilon})}$ and \mathbf{e}_i .

By applying the similar transformation by $\mathbf{Q}_{\boldsymbol{\varepsilon}}$ onto $\boldsymbol{\varepsilon}$, we have a tensor

$$\begin{aligned}
\bar{\boldsymbol{\epsilon}} &= \mathbf{Q}_{\boldsymbol{\epsilon}}^T \boldsymbol{\epsilon} \mathbf{Q}_{\boldsymbol{\epsilon}} = \left(\sum_{i=1}^3 \mathbf{n}_i^{(\boldsymbol{\epsilon})} \otimes \mathbf{e}_i \right)^T \boldsymbol{\epsilon} \left(\sum_{j=1}^3 \mathbf{n}_j^{(\boldsymbol{\epsilon})} \otimes \mathbf{e}_j \right) \\
&= \left(\sum_{i=1}^3 \mathbf{e}_i \otimes \mathbf{n}_i^{(\boldsymbol{\epsilon})} \right) \left(\sum_{k=1}^3 \varepsilon_k \mathbf{n}_k^{(\boldsymbol{\epsilon})} \otimes \mathbf{n}_k^{(\boldsymbol{\epsilon})} \right) \left(\sum_{j=1}^3 \mathbf{n}_j^{(\boldsymbol{\epsilon})} \otimes \mathbf{e}_j \right) \\
&= \sum_{i=1}^3 \varepsilon_i \mathbf{e}_i \otimes \mathbf{e}_i.
\end{aligned} \tag{5.82}$$

Furthermore, one more application of the similar transformation by $\mathbf{Q}_{\boldsymbol{\epsilon}}^+$ to this $\bar{\boldsymbol{\epsilon}}$ leads to

$$\begin{aligned}
&\mathbf{Q}_{\boldsymbol{\epsilon}}^+ \bar{\boldsymbol{\epsilon}} (\mathbf{Q}_{\boldsymbol{\epsilon}}^+)^T \\
&= \left[\sum_{i=1}^3 H(\varepsilon_i) \mathbf{n}_i^{(\boldsymbol{\epsilon})} \otimes \mathbf{e}_i \right] \left[\sum_{j=1}^3 \varepsilon_j \mathbf{e}_j \otimes \mathbf{e}_j \right] \left[\sum_{k=1}^3 H(\varepsilon_k) \mathbf{n}_k^{(\boldsymbol{\epsilon})} \otimes \mathbf{e}_k \right]^T \\
&= \sum_{i=1}^3 H(\varepsilon_i) \varepsilon_i \mathbf{n}_i^{(\boldsymbol{\epsilon})} \otimes \mathbf{n}_i^{(\boldsymbol{\epsilon})} = \sum_{i=1}^3 \varepsilon_i^+ \mathbf{n}_i^{(\boldsymbol{\epsilon})} \otimes \mathbf{n}_i^{(\boldsymbol{\epsilon})} \\
&= \boldsymbol{\epsilon}^+,
\end{aligned}$$

or

$$\boldsymbol{\epsilon}^+ = \sum_{i=1}^3 H(\varepsilon_i) \varepsilon_i \mathbf{n}_i^{(\boldsymbol{\epsilon})} \otimes \mathbf{n}_i^{(\boldsymbol{\epsilon})} \tag{5.83}$$

As will be observed from this relation, if we define a new fourth-order projection tensor

$$\mathbb{P}_{\boldsymbol{\epsilon}}^+ \equiv \sum_{i=1}^3 H(\varepsilon_i) \mathbf{n}_i^{(\boldsymbol{\epsilon})} \otimes \mathbf{n}_i^{(\boldsymbol{\epsilon})} \otimes \mathbf{n}_i^{(\boldsymbol{\epsilon})} \otimes \mathbf{n}_i^{(\boldsymbol{\epsilon})}, \tag{5.84}$$

the positive-valued strain tensor $\boldsymbol{\epsilon}^+$ of Eq. (5.79) or Eq. (5.83) can be expressed as follows:

$$\boldsymbol{\epsilon}^+ = \mathbb{P}_{\boldsymbol{\epsilon}}^+ : \boldsymbol{\epsilon}, \tag{5.85a}$$

or

$$\varepsilon_{ij}^+ = (\mathbb{P}_{\boldsymbol{\epsilon}}^+)_{ijkl} \varepsilon_{kl}. \tag{5.85b}$$

The tensor $\mathbb{P}_{\boldsymbol{\epsilon}}^+$ of Eq. (5.84) is called a *positive orthogonal projection tensor* of the strain tensor $\boldsymbol{\epsilon}$ with respect to its principal directions.

Finally the negative part of the strain tensor $\boldsymbol{\epsilon}^-$, i.e., the *negative-valued strain tensor* and the *negative orthogonal projection tensor* of strain are given by the relations

$$\begin{aligned}\boldsymbol{\varepsilon}^- &= \boldsymbol{\varepsilon} - \boldsymbol{\varepsilon}^+ \\ &= \mathbb{P}_{\boldsymbol{\varepsilon}}^- : \boldsymbol{\varepsilon},\end{aligned}\tag{5.86}$$

$$\mathbb{P}_{\boldsymbol{\varepsilon}}^- = \mathbb{I} - \mathbb{P}_{\boldsymbol{\varepsilon}}^+, \tag{5.87}$$

where \mathbb{I} is the identity tensor of fourth-order.

(2) Positive Projection Tensor for Stress Tensor

The above argument for the strain tensor $\boldsymbol{\varepsilon}$ is applicable also to the stress tensor $\boldsymbol{\sigma}$. First of all, the positive part of the stress tensor $\boldsymbol{\sigma}$ are given as

$$\left[\sigma_{ij}^+ \right] = \begin{bmatrix} < \sigma_1 > & 0 & 0 \\ 0 & < \sigma_2 > & 0 \\ 0 & 0 & < \sigma_3 > \end{bmatrix}, \tag{5.88a}$$

or

$$\boldsymbol{\sigma}^+ = \sum_{i=1}^3 \sigma_i^+ \mathbf{n}_i^{(\sigma)} \otimes \mathbf{n}_i^{(\sigma)}, \quad \sigma_i^+ = < \sigma_i > = H(\sigma_i) \sigma_i, \tag{5.88b}$$

where σ_i and $\mathbf{n}_i^{(\sigma)}$ denote the i th principal stress and the corresponding eigenvectors.

By rewriting Eqs. (5.84) through (5.87) for the case of the stress tensor $\boldsymbol{\sigma}$, the *positive-valued stress tensor* $\boldsymbol{\sigma}^+$, *positive orthogonal projection tensor* $\mathbb{P}_{\boldsymbol{\sigma}}^+$, *negative-valued stress tensor* $\boldsymbol{\sigma}^-$, and the *negative orthogonal projection tensor* $\mathbb{P}_{\boldsymbol{\sigma}}^-$ are given as follows:

$$\boldsymbol{\sigma}^+ = \mathbb{P}_{\boldsymbol{\sigma}}^+ : \boldsymbol{\sigma}, \tag{5.89}$$

$$\mathbb{P}_{\boldsymbol{\sigma}}^+ \equiv \sum_{i=1}^3 H(\sigma_i) \mathbf{n}_i^{(\sigma)} \otimes \mathbf{n}_i^{(\sigma)} \otimes \mathbf{n}_i^{(\sigma)} \otimes \mathbf{n}_i^{(\sigma)}, \tag{5.90}$$

$$\begin{aligned}\boldsymbol{\sigma}^- &= \boldsymbol{\sigma} - \boldsymbol{\sigma}^+ \\ &= \mathbb{P}_{\boldsymbol{\sigma}}^- : \boldsymbol{\sigma},\end{aligned}\tag{5.91}$$

$$\mathbb{P}_{\boldsymbol{\sigma}}^- = \mathbb{I} - \mathbb{P}_{\boldsymbol{\sigma}}^+. \tag{5.92}$$

As observed from Eqs. (5.84) and (5.90), the positive projection tensors $\mathbb{P}_{\boldsymbol{\varepsilon}}^+$, $\mathbb{P}_{\boldsymbol{\sigma}}^+$ for strain and stress have the identical symmetry to each other, e.g., symmetry between the first two indices and the last two

$$(P_{\boldsymbol{\varepsilon}}^+)_{ijkl} = (P_{\boldsymbol{\varepsilon}}^+)_{klji}, \quad (P_{\boldsymbol{\sigma}}^+)_{ijkl} = (P_{\boldsymbol{\sigma}}^+)_{klji}. \tag{5.93}$$

However, these projection tensors themselves, in general, are different from each other

$$\mathbb{P}_{\boldsymbol{\varepsilon}}^+ \neq \mathbb{P}_{\boldsymbol{\sigma}}^+, \quad \mathbb{P}_{\boldsymbol{\varepsilon}}^- \neq \mathbb{P}_{\boldsymbol{\sigma}}^-. \tag{5.94}$$

5.3.3 Effective Elastic Modulus Tensor in Opening and Closing States of Cracks in Brittle Material

The elastic modulus of a material with elastic-brittle damage has marked unilateral effect due to opening-closing behavior of cracks. The magnitude of the elastic modulus, furthermore, varies largely with the strain or the stress state in the material.

Then, in the general state of brittle damage, how does the elastic modulus tensor of a material at a specific state of damage vary with the change in the strain and stress state? Now we discuss two different approaches to this problem.

(1) Effective Elastic Modulus Tensor in Crack-Opening State Specified by the Strain State

Let us represent the elastic modulus tensors of an elastic-brittle material in the undamaged and the damaged state of \mathcal{D} by \mathbb{C}_0 and $\mathbb{C}(\mathcal{D})$. Then, the reduction \mathbb{C}^D of the elastic modulus tensor caused by the damage development is given by

$$\mathbb{C}^D = \mathbb{C}_0 - \mathbb{C}(\mathcal{D}). \quad (5.95)^3$$

Note that this decrease in an elastic modulus tensor is relevant to the fully active state of the distributed cracks. In general, however, open cracks are only a part of the cracks developed so far.

The reduction in the rigidity caused by the actual distribution of the opening cracks in a specific strain state $\boldsymbol{\epsilon}$, i.e., the reduction in *activated elastic modulus tensor* \mathbb{C}_{AC}^D , is derived by applying the positive orthogonal projection tensor $\mathbb{P}_{\boldsymbol{\epsilon}}^+$ of Eq. (5.84) as follows:

$$\begin{aligned} \mathbb{C}_{AC}^D &= \mathbb{P}_{\boldsymbol{\epsilon}}^+ : \mathbb{C}^D : \mathbb{P}_{\boldsymbol{\epsilon}}^+ \\ &= \mathbb{P}_{\boldsymbol{\epsilon}}^+ : [\mathbb{C}_0 - \mathbb{C}(\mathcal{D})] : \mathbb{P}_{\boldsymbol{\epsilon}}^+. \end{aligned} \quad (5.96)$$

Finally, by the use of this relation, the *effective elastic modulus tensor* \mathbb{C}_{EF} relevant to the actual state of crack-opening at the strain $\boldsymbol{\epsilon}$ can be derived:

$$\begin{aligned} \mathbb{C}_{EF} &= \mathbb{C}_0 - \mathbb{C}_{AC}^D \\ &= \mathbb{C}_0 - \mathbb{P}_{\boldsymbol{\epsilon}}^+ : [\mathbb{C}_0 - \mathbb{C}(\mathcal{D})] : \mathbb{P}_{\boldsymbol{\epsilon}}^+. \end{aligned} \quad (5.97)$$

³ Since the description of (1) and (2) in this Subsection is applicable also to damage tensor \mathcal{D} of an arbitrary even-order, the elastic modulus tensor in damaged state will be denoted here by $\mathbb{C}(\mathcal{D})$ with the argument \mathcal{D} .

(2) Effective Elastic Modulus Tensor in Crack-Opening State Specified by the Strain and the Damage State

The unilateral property of the elastic modulus tensors arises from the dependence of the damage effect on the strain state. Chaboche and others (Chaboche 1993; Chaboche, Lesne, and Maire 1995) postulated that the damage effect on the elastic property of materials is governed by the relative relation between the strain tensor $\boldsymbol{\varepsilon}$ and the principal direction $\mathbf{n}^{(D)}$ of the damage tensor \mathcal{D} . Then, for a given principal direction $\mathbf{n}^{(D)}$, they defined another fourth-order projection tensor

$$\mathbb{P}_D = \mathbf{n}^{(D)} \otimes \mathbf{n}^{(D)} \otimes \mathbf{n}^{(D)} \otimes \mathbf{n}^{(D)}. \quad (5.98)$$

If the normal strain $\varepsilon_{n^{(D)}}$ in the direction $\mathbf{n}^{(D)}$ is positive, i.e.

$$\varepsilon_{n^{(D)}} = \mathbf{n}^{(D)} \cdot \boldsymbol{\varepsilon} \cdot \mathbf{n}^{(D)} = \text{tr}(\mathbb{P}_D : \boldsymbol{\varepsilon}) > 0, \quad (5.99)$$

then we can assume that the damage state in the direction $\mathbf{n}^{(D)}$ may be fully *active*.

The elastic modulus tensor \mathcal{C}_0 in the initial undamaged state leads to $\mathcal{C}(\mathcal{D})$ at the damaged state \mathcal{D} . However, the actual mechanical effect of $\mathcal{C}(\mathcal{D})$ depends on the strain state $\boldsymbol{\varepsilon}$ as a result of the crack-opening phenomena. For example, for the damage principal direction $\mathbf{n}^{(D)}$ in which the normal strain $\varepsilon_{n^{(D)}}$ is negative, the damage state is *passive*, and the reduction in the rigidity $\mathcal{C}_0 - \mathcal{C}(\mathcal{D})$ does not occur. Thus, the effective elastic modulus tensor \mathcal{C}_{EF} in such strain state $\boldsymbol{\varepsilon}$ can be expressed by

$$\mathcal{C}_{EF} = \mathcal{C}(\mathcal{D}) + H(-\varepsilon_{n^{(D)}}) \mathbb{P}_D : [\mathcal{C}_0 - \mathcal{C}(\mathcal{D})] : \mathbb{P}_D. \quad (5.100)$$

The above argument is applicable also to the three principal directions of damage $\mathbf{n}_i^{(D)} (i = 1, 2, 3)$. Then, instead of \mathbb{P}_D of Eq. (5.98), the projection tensors with respect to the respective principal direction $\mathbf{n}_i^{(D)}$ can be defined:

$$\mathbb{P}_{Di} = \mathbf{n}_i^{(D)} \otimes \mathbf{n}_i^{(D)} \otimes \mathbf{n}_i^{(D)} \otimes \mathbf{n}_i^{(D)} \quad (i = 1, 2, 3). \quad (5.101)$$

The effective elastic modulus tensor \mathcal{C}_{EF} of Eq. (5.100), in this case, can be generalized in the form (Chaboche 1993)

$$\mathcal{C}_{EF} = \mathcal{C}(\mathcal{D}) + \eta \sum_{i=1}^3 H(-\varepsilon_i) \mathbb{P}_{Di} : [\mathcal{C}_0 - \mathcal{C}(\mathcal{D})] : \mathbb{P}_{Di}, \quad (5.102a)$$

$$\varepsilon_i = \mathbf{n}_i^{(D)} \cdot \boldsymbol{\varepsilon} \cdot \mathbf{n}_i^{(D)} = \text{tr}(\mathbb{P}_{Di} : \boldsymbol{\varepsilon}), \quad (5.102b)$$

where $\eta (0 \leq \eta \leq 1)$ denotes a material constant representing the degree of the unilateral properties. It should be noted that the unilateral effects described by Eq. (5.102) affect only the principal diagonal terms ($C_{1111}, C_{2222}, C_{3333}$) of the elastic modulus tensor with respect to the principal strain coordinates. The fact that the off-diagonal terms of the tensor are not affected by the damage deactivation ensures the

symmetry of the elastic modulus tensor together with the continuity of the stress-strain response under any change of loading (Besson et al. 2010).

5.3.4 Damage Variable Defined by the Elastic Modulus Tensor and Its Application to Elastic-Brittle Damage

In order to describe the significant opening-closing effect of cracks in elastic-brittle damage, Chaboche (1993) introduced the following fourth-order damage tensor \mathbb{D} of Eq. (2.35):

$$\mathcal{C}(\mathbb{D}) = \frac{1}{2}[(\mathbb{I} - \mathbb{D}) : \mathcal{C}_0 + \mathcal{C}_0 : (\mathbb{I} - \mathbb{D})], \quad (5.103)$$

where \mathcal{C}_0 and $\mathcal{C}(\mathbb{D})$ are the fourth-order elastic modulus tensor in the initial undamaged state and that in the damaged state with fully opening cracks (i.e., the secant modulus tensor). The symbol \mathbb{I} , furthermore, is the fourth-order identity tensor.

According to the hypothesis of strain equivalence, the effective stress tensor $\tilde{\sigma}$ is given by Eqs. (2.43) and (2.55):

$$\tilde{\sigma} = M(\mathbb{D}) : \sigma, \quad M(\mathbb{D}) = \mathcal{C}_0 : \mathcal{C}(\mathbb{D})^{-1}, \quad (5.104)$$

where $M(\mathbb{D})$ is the damage effect tensor, and is expressed by the use of Eq. (5.103) as follows:

$$M(\mathbb{D})^{-1} = \frac{1}{2} \left[(\mathbb{I} - \mathbb{D}) + \mathcal{C}_0 : (\mathbb{I} - \mathbb{D}) : \mathcal{C}_0^{-1} \right]. \quad (5.105)$$

On the basis of the damage variable \mathbb{D} defined by these relations, Chaboche (1993) developed accurate modeling of the three-dimensional unilateral damage of an elastic-brittle material.

In the application of the thermodynamic theory of Section 5.3.1 to the unilateral damage, we adopt the effective elastic tensor \mathcal{C}_{EF} of Eq. (5.102), and represent the free energy function ψ of the elastic-brittle material:

$$\rho\psi(\boldsymbol{\epsilon}, \mathbb{D}, \beta) = \frac{1}{2}\boldsymbol{\epsilon} : \mathcal{C}_{EF} : \boldsymbol{\epsilon}. \quad (5.106)$$

Then the elastic constitutive equation of this material is given by Eqs. (5.71) and (5.106):

$$\sigma = \mathcal{C}_{EF} : \boldsymbol{\epsilon}. \quad (5.107)$$

The evolution equation of damage, on the other hand, can be derived from Eqs. (5.74) through (5.76). For this purpose, we first introduce a fourth-order indeterminate tensor \mathbb{Q} to represent the direction of damage development, and define the function $g(\mathbb{Y})$ of Eq. (5.74):

$$g(\mathbb{Y}) = \text{tr}(\mathbb{Q}; \mathbb{Y}), \quad (5.108a)$$

where \mathbb{Y} is the associated variable with the damage variable D . Then, the damage loading surface of Eq. (5.74) is expressed:

$$\begin{aligned} F^D(\mathbb{Y}, B) &= g(\mathbb{Y}) - B \\ &= \text{tr}(\mathbb{Q} : \mathbb{Y}) - B \leq 0. \end{aligned} \quad (5.108b)$$

The evolution equation of the internal variables are derived from this relation together with Eqs. (5.75) and (5.76):

$$\dot{D} = \dot{\Lambda}^D \frac{\partial F^D}{\partial \mathbb{Y}} = \dot{\Lambda}^D \mathbb{Q}, \quad (5.109)$$

$$\dot{\beta} = -\dot{\Lambda}^D \frac{\partial F^D}{\partial B} = \dot{\Lambda}^D, \quad (5.110)$$

from which we have

$$\dot{D} = \mathbb{Q} \dot{\beta}. \quad (5.111)$$

For the determination of the indeterminate tensor \mathbb{Q} of Eq. (5.108), Chaboche examined the features of the microcrack development under different loading conditions. As shown in Fig. 5.5, the crack development in a brittle damage material under uniaxial tension is characterized by the *planar transverse isotropy* perpendicular to the loading direction, while the crack development under uniaxial compression shows *cylindrical transverse isotropy* in planes containing the loading direction. Chaboche showed specific tensor expressions that represent the essential feature of the damage development (Chaboche 1993).

The above argument was extended afterward to the case of the fiber-reinforced ceramic composites, and its unilateral elastic-brittle damage was elucidated

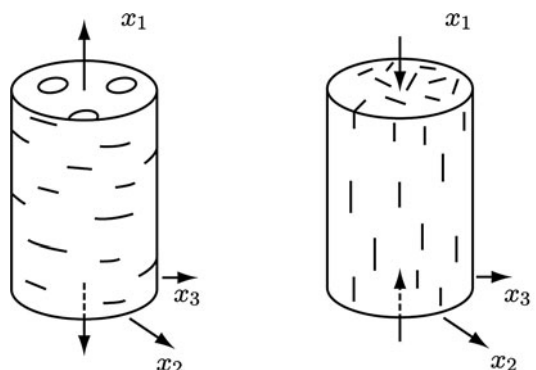


Fig. 5.5 Crack development in elastic-brittle damage material
Source: Chaboche (1993; p. 323, Fig. 2)

(a) Planarily transverse-isotropic cracks by uniaxial tension

(b) Cylindrically transverse-isotropic cracks by uniaxial compression

(Chaboche, Lesne, and Maire 1995; Chaboche, Lesne, and Pottier 1998). A part of the results of the analysis will be described in [Section 10.2](#).

5.3.5 Elastic-Plastic-Brittle Damage Theory Based on an Elastic Modulus Tensor as a Damage Variable

In view of [Eq. \(2.34\)](#) or [\(5.103\)](#), the damage variable of a material can be defined also by the change in its elasticity tensor. Ju and his coworker (Simo and Ju 1987; Ju 1989), therefore, extended this idea and discussed the damage process of a material by describing its damage state by the use of the elastic modulus tensor of the material itself. We now discuss an elastic-plastic-brittle damage theory of a plasticity-damage coupled material by employing its elastic modulus tensor \mathcal{C} as a damage variable.

As observed in [Eqs. \(4.30\)](#) and [\(5.11\)](#), so far we assumed that plastic deformation and damage do not affect each other. Thus it has been assumed that the generalized force associated with the damage variable, or the energy release rate due to damage development, depends only on its elastic strain energy.

Ju (1989), on the other hand, postulated that the nucleation and the growth of microcracks are influenced by the plastic deformation and that the damage state of the material can be described by its elasticity tensor \mathcal{C} . Then he expressed the Helmholtz free energy function ψ of an elastic-plastic material with anisotropic damage:

$$\begin{aligned}\rho\psi(\boldsymbol{\epsilon}^e, \mathbf{V}_p, \mathcal{C}) &= \rho\psi^{ED}(\boldsymbol{\epsilon}^e, \mathcal{C}) + \rho\psi^{PD}(\mathbf{V}_p, \mathcal{C}) \\ &= \frac{1}{2}\boldsymbol{\epsilon}^e : \mathcal{C} : \boldsymbol{\epsilon}^e + \rho\psi^{PD}(\mathbf{V}, \mathcal{C}),\end{aligned}\quad (5.112)$$

where ψ^{ED} and ψ^{PD} are the damage affected free energy functions related to elastic and the plastic deformation, while \mathbf{V}_p denotes an internal state variable related to plasticity.

If we apply the thermodynamic theory of [Section 5.3.1](#) to the free energy function of [Eq. \(5.112\)](#), the stress tensor $\boldsymbol{\sigma}$ of the elastic-plastic-damaged material, together with the generalized forces \mathbb{Y} and \mathbf{A}_p associated with internal variables \mathcal{C} and \mathbf{V}_p , are given as follows:

$$\boldsymbol{\sigma} = \rho \frac{\partial \psi}{\partial \boldsymbol{\epsilon}^e} = \mathcal{C} : \boldsymbol{\epsilon}^e, \quad (5.113)$$

$$\mathbb{Y} = -\rho \frac{\partial \psi}{\partial \mathcal{C}} = -\frac{1}{2}\boldsymbol{\epsilon}^e \otimes \boldsymbol{\epsilon}^e - \rho \frac{\partial \psi^{PD}}{\partial \mathcal{C}}, \quad (5.114)$$

$$\mathbf{A}_p = -\rho \frac{\partial \psi}{\partial \mathbf{V}_p} = -\rho \frac{\partial \psi^{PD}}{\partial \mathbf{V}_p}. \quad (5.115)$$

Since the dependence of the function $\psi^{PD}(\mathbf{V}_p, \mathcal{C})$ on \mathcal{C} is not significant, it can be expressed by a linear function

$$\psi^{PD}(\mathbf{V}_p, \mathbb{C}) = \mathbb{C} : \mathbb{C}_0^{-1} \psi^{P0}(\mathbf{V}_p), \quad (5.116)$$

where $\psi^{P0}(\mathbf{V}_p)$ signifies the free energy function related to the plastic deformation of the undamaged material, and \mathbb{C}_0 is the elastic modulus tensor of the undamaged material. In this case Eq. (5.114) leads to

$$\mathbb{Y} = -\rho \frac{\partial \psi}{\partial \mathbb{C}} = -\frac{1}{2} \boldsymbol{\epsilon}^e \otimes \boldsymbol{\epsilon}^e - \psi^{P0}(\mathbf{V}_p) \mathbb{C}_0^{-1}. \quad (5.117)$$

As regards the damage development, on the other hand, the existence of the following damage loading surface was assumed:

$$F^D(\mathbb{Y}, B) = g(\mathbb{Y}) - B \leq 0, \quad (5.118)$$

where B is the threshold value of the damage initiation. In the derivation of Eq. (5.118), furthermore, it is assumed that the damage develops only when the damage-associated variable \mathbb{Y} remains on this loading surface. By means of the principle of maximum dissipation of damage together with Eq. (5.118), the damage evolution equation of \mathbb{C} can be derived

$$\dot{\mathbb{C}} = \dot{\Lambda}^D \frac{\partial F^D}{\partial \mathbb{Y}}, \quad (5.119)$$

where $\dot{\Lambda}^D$ is an indeterminate multiplier. The loading-unloading condition for the damage development, moreover, is given by the Kuhn-Tucker relation:

$$\dot{\Lambda}^D \geq 0, \quad F^D \leq 0, \quad \dot{\Lambda}^D F^D = 0. \quad (5.120)$$

As already described in Section 5.3.3, the effective elastic modulus tensor \mathbb{C}_{EF} of the damaged material varies with the crack-opening state and hence varies with the strain field $\boldsymbol{\epsilon}$ in the material, even for a specific damaged state. Since the effective elastic modulus tensor \mathbb{C}_{EF} has been defined as the elastic modulus tensor of the undamaged material subtracted by its reduction caused by crack opening, it is given as follows:

$$\mathbb{C}_{EF} = \mathbb{C}_0 - \tilde{\mathbb{C}}_{AC}, \quad (5.121a)$$

$$\tilde{\mathbb{C}}_{AC} = \mathbb{P}_{\boldsymbol{\epsilon}}^+ : \mathbb{C} : \mathbb{P}_{\boldsymbol{\epsilon}}^+. \quad (5.121b)$$

It should be noted that the above activated elastic modulus tensor $\tilde{\mathbb{C}}_{AC}$ has been defined with respect to the elastic modulus tensor \mathbb{C} for the damaged material. The stress-strain relation in this state is given finally by

$$\boldsymbol{\sigma} = \mathbb{C}_{EF} : \boldsymbol{\epsilon}. \quad (5.122)$$

As regards the above elastic-plastic and unilateral-brittle-damage theory of Ju, it has been pointed out that the discontinuity in the stress-strain relation may occur due to the change in sign of stress or strain components (Chaboche 1992). The application of Ju's theory to the brittle damage analysis of concrete cylindrical specimens will be discussed in [Section 9.4](#).

The above discussions in this chapter were concerned with the development of anisotropic damage in initially isotropic materials. The assumption of initial isotropy, however, may sometimes give significant restrictions on the damage analyses of materials with significant initial anisotropy, e.g., in sedimentary rocks or brittle composite materials. Halm and others (Halm, Dragon, and Charles 2002), therefore, discussed a damage mechanics theory of anisotropic damage developed in initially anisotropic materials.

Part II

**Application of Continuum
Damage Mechanics**

Chapter 6

Elastic-Plastic Damage

The preceding chapters were concerned with the notion and the fundamental theories of *continuum damage mechanics* (CDM). Hereafter we will discuss the application of CDM to damage and fracture phenomena encountered in wide range of engineering problems.

The present chapter starts with the modeling of elastic-plastic damage and its application. In Section 6.1, we summarized the constitutive and the evolution equations of elastic-plastic isotropic damage of materials developed in Chapter 4, and discuss their application to the problems of ductile damage, brittle damage and quasi-brittle damage. Section 6.2, on the other hand, is concerned with the detailed discussion of ductile damage process, i.e., the discussion of physical and mechanical aspects of ductile damage, their mechanical modeling and its analysis.

In Sections 6.3 and 6.4, furthermore, we elucidate the applications of isotropic and anisotropic damage theories to some important metal forming processes. The ductile damage theories from micromechanics point of view by the use of the void volume fractions as a damage variable are discussed in Section 6.5. Finally in Section 6.6, we consider the essential role of plastic compressibility in ductile damage analyses, and develop a continuum damage theory incorporating this effect.

6.1 Constitutive and Evolution Equations of Elastic-Plastic Damage – Ductile Damage, Brittle Damage and Quasi-Brittle Damage

6.1.1 *Constitutive and Evolution Equations of Elastic-Plastic Isotropic Damage*

As described in Section 4.1, the damage state in an elastic-plastic material can be mostly supposed isotropic. To facilitate the discussion in the following sections, we summarize and explain here the constitutive and the evolution equations of elastic-plastic isotropic damaged material derived in Sections 4.1 and 4.2.

In the case of elastic-plastic deformation under uniaxial or under proportional loading, the strain-hardening of the material can be described usually by the isotropic-hardening theory of plasticity. Thus the elastic-plastic constitutive equation of an isotropic-hardening material with isotropic damage is given by Eqs. (4.69) through (4.78) of Section 4.2.3 as follows:

$$\varepsilon_{ij} = \varepsilon_{ij}^e + \varepsilon_{ij}^p q, \quad (6.1)$$

$$\varepsilon_{ij}^e = \frac{1+\nu}{E} \tilde{\sigma}_{ij} - \frac{\nu}{E} \tilde{\sigma}_{kk} \delta_{ij}, \quad (6.2)$$

$$f = \tilde{\sigma}_{EQ} - (R + \sigma_Y) = 0, \quad (6.3)$$

$$\dot{\varepsilon}_{ij}^p = \frac{3}{2} \frac{\tilde{\sigma}_{ij}^D}{\tilde{\sigma}_{EQ}} \dot{p}, \quad (6.4)$$

$$\dot{R} = R_\infty b \exp(-br)(1-D)\dot{p}, \quad (6.5)$$

$$\dot{r} = (1-D)\dot{p}, \quad (6.6a)$$

$$\dot{p} = \dot{\varepsilon}_{EQ}^p, \quad (6.6b)$$

where ε_{ij}^e and ε_{ij}^p are the elastic and the plastic strain tensor, while $\tilde{\sigma}_{ij}$ and $\tilde{\sigma}_{ij}^D$ denote the effective stress tensor of Eq. (2.36) and its deviatoric tensor. Symbols f , R and σ_Y , on the other hand, signify the yield function, isotropic-hardening variable and the initial yield stress, respectively.

In Eqs. (6.4) and (6.6), furthermore, $\tilde{\sigma}_{EQ}$ and $\dot{\varepsilon}_{EQ}^p$ are the equivalent effective stress and the equivalent plastic strain rate, and are defined:

$$\tilde{\sigma}_{EQ} = \left(\frac{3}{2} \tilde{\sigma}_{ij}^D \tilde{\sigma}_{ij}^D \right)^{1/2}, \quad \dot{\varepsilon}_{EQ}^p = \left(\frac{2}{3} \dot{\varepsilon}_{ij}^p \dot{\varepsilon}_{ij}^p \right)^{1/2}. \quad (6.7)$$

The symbol \dot{p} in these relations denotes the accumulated plastic strain rate. Equation (6.5) was derived by the use of Eqs. (4.58) and (4.75), where R_∞ and b are material constants characterizing the strain-hardening of the material.

The development of material damage, on the other hand, were discussed in Section 4.2.5, and the evolution equation of damage variable is given by Eq. (4.91) as

$$\dot{D} = \frac{Y}{S} \dot{p} H(p - p_D), \quad (6.8)$$

where Y is the generalized force associated with the damage variable D (i.e., the damage-associated variable), and can be interpreted as the release rate of the strain energy density due to the damage development. The symbols p_D and S denote the

threshold value of the accumulated plastic strain for the damage initiation and a material constant, while $H(\cdot)$ signifies the Heaviside function.

As we learned in [Section 4.3](#), the damage-associated variable Y is given as

$$Y = \frac{(\tilde{\sigma}_{EQ})^2}{2E} R_v, \quad R_v \equiv \frac{2}{3}(1 + \nu) + 3(1 - 2\nu) \left(\frac{\sigma_H}{\sigma_{EQ}} \right)^2, \quad (6.9)$$

where σ_H/σ_{EQ} and R_v are the stress triaxiality and the stress triaxiality function.

Substitution of Eq. (6.9) into Eq. (6.8) provides the evolution equation of the damage variable D

$$\dot{D} = \frac{(\tilde{\sigma}_{EQ})^2}{2ES} R_v \dot{p} H(p - p_D). \quad (6.10)$$

As we described in [Section 4.2.5](#), by the use of a power function of Y , the evolution equation (6.8) can be extended also to the form

$$\dot{D} = \left(\frac{Y}{S} \right)^s \dot{p} H(p - p_D), \quad (6.11)$$

where s and S are material constants. The damage evolution equations (6.8) and (6.11) can be elaborated further by incorporating the effects of damage variables and accumulated plastic strain, the detail of which will be shown in [Section 6.2.3](#).

The material constants in the above Eqs. (6.1) through (6.11) can all be identified by elastic-plastic ductile fracture tests in simple tension ([Lemaitre 1992](#); [Lemaitre and Desmorat 2005](#)).

In some cases of special reliability, we often need precise prediction of fracture lifetime under non-proportional cyclic loading. The deformation and the damage state in these cases are influenced largely by anisotropic stain-hardening of the material. The analyses of these damage and fracture processes can be performed by the use of the elastic-plastic constitutive equations (4.69) through (4.78) of combined isotropic-kinematic hardening together with the evolution equations (4.90) thorough (4.94) of isotropic damage. They were discussed, respectively, in [Sections 4.2.3](#) and [4.2.5](#).

6.1.2 Ductile Damage and Brittle Damage

The nucleation and the growth of spherical and ellipsoidal microvoids in materials caused by plastic deformation are called *ductile damage* ([Fig. 1.3](#)). The development of ductile damage leads to *ductile fracture*.

When the ductile damage state is described by an isotropic damage variable D , the damage process can be analyzed by applying the elastic-plastic constitutive equations (6.1) through (6.7) and the damage evolution equations (6.10) and (6.11). The detail of the analysis will be presented in [Section 6.2](#) and thereafter.

In some cases, on the other hand, microcracks may develop without involving plastic deformation, not only in the macroscopic scale but also in the mesoscale (see Fig. 1.4). This type of damage is called *brittle damage*. The brittle damage is observed, for example, in rocks, concrete, glass, and ceramics, and the mesocracks develop with apparent orientation. However, in the particular case of an incipient damage state, or of the damage under proportional loading, for example, the damage process in these materials can be analyzed by postulating isotropic damage (Mazars 1986).

Since brittle damage cannot be characterized by the accumulated plastic strain rate $\dot{\gamma}$, the evolution equations (6.10) and (6.11) of elastic-plastic damage cannot be applied in these circumstances.

For these materials, if the damage is assumed to start when the damage-associated variable Y of Eq. (6.9) attains to the fracture criterion of Eq. (4.110), we have the relation

$$\begin{aligned} Y &= \frac{(\sigma_{EQ})^2}{2E} R_v \\ &= Y_C = \frac{(\sigma_R)^2}{2E}, \end{aligned} \quad (6.12)$$

where σ_R is the brittle fracture stress under uniaxial tension. Equation (6.12) implies that the brittle fracture starts when the material is subject to the equivalent stress

$$\sigma_{EQ} = \frac{\sigma_R}{(R_v)^{1/2}}. \quad (6.13)$$

Thus, the relevant value of σ_{EQ} is specified by the magnitude of σ_R and the value of the stress triaxiality function R_v .

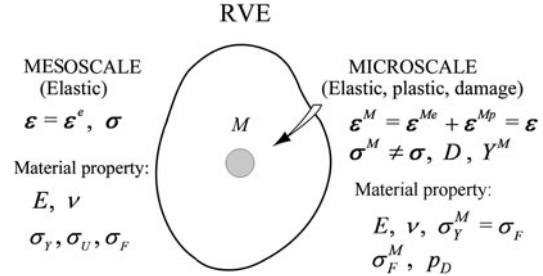
The application of continuum damage mechanics to the problem of brittle damage will be discussed in detail in Chapter 9 later.

6.1.3 Quasi-Brittle Damage and Two-Scale Damage Model

In a certain type of damage, although it may have brittle aspects not only in the macroscale but also in the mesoscale, the occurrence and the development of the damage are governed by the plastic deformation in microscopic regions of a material. This type of damage is called *quasi-brittle damage* (for more detail, refer to Chapter 9 later). Since this damage is highly localized in general, it is difficult to define a proper representative volume element (RVE) described in Section 1.2. Thus it is necessary to characterize the damage state of a material by the use of a procedure different from that discussed hitherto.

In the quasi-brittle damage, the localized microscopic voids or cracks lead to macroscopic fracture. This implies that we should suppose further a volume element of *microscale* within an RVE of mesoscale (Fig. 6.1), and should define pertinently the damage states in the volume elements of these two scales. We now consider

Fig. 6.1 Two-scale damage model based on Lin-Taylor hypothesis



the *two-scale damage model* (Lemaitre 1990, 1992) proposed for the quasi-brittle damage observed in damage processes, e.g., brittle fracture, and fatigue fracture.

We suppose first the RVE of Fig. 6.1 as the volume element of mesoscale, within which the material is elastic throughout except the microscopic volume element M . The yield stress, tensile strength and the fatigue limit of the RVE will be denoted by σ_Y , σ_U and σ_F .

The microscopic volume element M is assumed to be elastic-perfectly plastic. We postulate that, even when the volume element RVE of mesoscale is elastic, the element M is subject to plastic deformation and damage development due to the defects in the material. In other words, we may understand that the element M is a microscopic inclusion with lower yield stress existing in the RVE. Then the threshold stress for the plastic deformation (i.e., yield stress) and the fatigue limit of the element M are denoted by σ_Y^M and σ_F^M , respectively.

The damage in M should be induced when stress σ ($\sigma_Y \gg \sigma \geq \sigma_F$) is applied to the element RVE. Thus the yield stress σ_Y^M of the element M is given by the fatigue limit σ_F of the RVE:

$$\sigma_Y^M = \sigma_F. \quad (6.14)$$

We assume further that the fatigue limit σ_F^M of the element M is specified by σ_F in proportion to the ratio σ_Y^M/σ_Y between the yield stresses of these two elements:

$$\sigma_F^M = \frac{\sigma_Y^M}{\sigma_Y} \sigma_F. \quad (6.15)$$

The damage evolution equation of the inclusion M is given by Eq. (6.8), i.e.,

$$\dot{D} = \frac{Y^M}{S} \dot{p}^M H(p^M - p_D), \quad (6.16)$$

where p^M and p_D are the accumulated equivalent plastic strain and its threshold for damage initiation in the element M . In order to calculate Eq. (6.16), the values of

Y^M and \dot{p}^M need to be related to the values of stress σ and strain ϵ of the RVE element.

If we employ the Lin-Taylor hypothesis, the strain ϵ is uniform within the RVE. Then the strain ϵ^M of the element M also is equal to ϵ :

$$\epsilon = \epsilon^M. \quad (6.17)$$

Since the elastic strain ϵ^{Me} in M may be disregarded in comparison with its plastic strain ϵ^{Mp} , the accumulated equivalent plastic strain rate \dot{p}^M is given by

$$\dot{p}^M = \left[\frac{2}{3} \dot{\epsilon}_{ij}^{Mp} \dot{\epsilon}_{ij}^{Mp} \right]^{1/2} = \left[\frac{2}{3} \dot{\epsilon}_{ij}^M \dot{\epsilon}_{ij}^M \right]^{1/2} = \dot{\epsilon}_{EQ}. \quad (6.18)$$

Since the element M is perfectly-plastic, its yield condition is given by

$$\frac{\sigma_{EQ}^M}{1 - D} = \tilde{\sigma}_{EQ}^M = \sigma_Y^M, \quad (6.19)$$

where σ_{EQ}^M and $\tilde{\sigma}_{EQ}^M$ are, respectively, the equivalent stress and the effective equivalent stress of the element M . Thus, the damage-associated variable Y^M in Eq. (6.16) is furnished by Eq. (4.120), i.e.,

$$Y^M = \frac{\left(\tilde{\sigma}_{EQ}^M\right)^2}{2E} R_v^M = \frac{\left(\sigma_Y^M\right)^2}{2E} R_v^M, \quad (6.20)$$

where R_v^M is the stress triaxiality function of M , and is given by Eq. (6.9):

$$R_v^M = \frac{2}{3}(1 + \nu) + 3(1 - 2\nu) \left(\frac{\sigma_H^M}{\sigma_{EQ}^M} \right)^2. \quad (6.21)$$

By the use of Eq. (4.117), the mean stress σ_H^M in Eq. (6.21) leads to

$$\begin{aligned} \sigma_H^M &= \frac{E(1 - D)}{1 - 2\nu} \epsilon_H^{Me} = \frac{E(1 - D)}{1 - 2\nu} \epsilon_H \\ &= \frac{E(1 - D)}{1 - 2\nu} \frac{1 - 2\nu}{E} \sigma_H = (1 - D)\sigma_H, \end{aligned} \quad (6.22)$$

where σ_H and ϵ_H are the mean stress and the mean strain. In view of Eqs. (6.19) and (6.22), Eq. (6.21) is expressed in an alternative form

$$R_v^M = \frac{2}{3}(1 + \nu) + 3(1 - 2\nu) \left(\frac{\sigma_H}{\sigma_Y^M} \right)^2. \quad (6.23)$$

By substituting Eqs. (6.18), (6.20) and (6.23), the damage evolution equations (6.16) of the microscopic volume element eventually has the form

$$\begin{aligned}\dot{D} &= \frac{(\sigma_Y^M)^2 R_v^M}{2ES} \dot{\varepsilon}_{EQ} H(\varepsilon_{EQ} - p_D) \\ &= \frac{(\sigma_Y^M)^2}{2ES} \left[\frac{2}{3}(1 + \nu) + 3(1 - 2\nu) \left(\frac{\sigma_H}{\sigma_Y^M} \right)^2 \right] \dot{\varepsilon}_{EQ} H(\varepsilon_{EQ} - p_D),\end{aligned}\quad (6.24)$$

where ε_{EQ} is the accumulated plastic strain in the element M (i.e., the accumulated equivalent strain in RVE), and p_D is the threshold value of p defined in Eq. (4.100):

$$p_D = \varepsilon_D^p \frac{\sigma_U - \sigma_F}{\sigma_Y^M - \sigma_F^M}. \quad (6.25)$$

According to the two-scale damage model described above, once the mean stress σ_H and equivalent strain ε_{EQ} in the mesoscale are determined by the macroscopic stress analysis, Eq. (6.24) enables the calculation of the damage rate \dot{D} in the element M , and hence the development of damage D in the mesoscopic volume element RVE. The application of this two-scale damage model to the high-cycle fatigue analysis will be discussed in Section 7.1.

6.1.4 Elaboration of Two-Scale Damage Model

The two-scale damage model discussed in Section 6.1.3 was elaborated further by the use of the self-consistent theory of micromechanics (Lemaître and Doghri 1994; Lemaître, Sermage, and Desmorat 1999; Lemaître and Desmorat 2005).

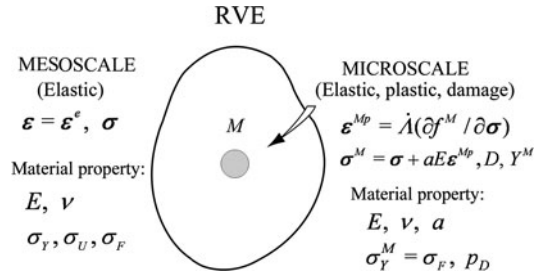
Suppose a mesoscale volume element of RVE in a body (Fig. 6.2). We postulate that the volume element RVE includes a microscopic inclusion subject to damage, and represent this inclusion by a volume element M of *microscale*. We further assume that though the deformation property of the RVE is not affected by the elastic-plastic damage in the microscopic volume element M , the failure of the RVE is induced by the damage of the element M .

Let the elastic property of the RVE be specified by Young's modulus E and Poisson ratio ν , and the fatigue limit be σ_F . As regards the volume element M , we assume that the elastic property is represented by E and ν just as in the RVE, and the yield stress σ_Y^M is given by the fatigue limit σ_F of the RVE, i.e.,

$$\sigma_Y^M = \sigma_F. \quad (6.26)$$

The plastic deformation of the microscopic element M , furthermore, is assumed to show kinematic hardening, but no isotropic hardening.

Fig. 6.2 Two-scale damage model based on self-consistent theory



(1) Elastic-Plastic Constitutive Equation and Damage Evolution Equation of the Microscopic Volume Element M

Suppose that the mechanical state of the mesoscopic element RVE is known. The calculation of damage development in the microscopic volume element M necessitates the stress or strain state of M . Then we employ the Eshelby-Kröner localization law of micromechanics, and assume that the microscopic stress σ_{ij}^M of the element M is related to the mesoscopic stress σ_{ij} in RVE:

$$\sigma_{ij}^M = \sigma_{ij} - aE\epsilon_{ij}^{Mp}, \quad (6.27a)$$

where ϵ_{ij}^{Mp} is the plastic strain of the element M whereas a denotes a localization parameter. In the case of the spherical inclusion, a is given by

$$a = \frac{1 - \beta}{1 + \nu}, \quad \beta = \frac{2(4 - 5\nu)}{15(1 - \nu)}. \quad (6.27b)$$

However, it is sometimes convenient to take it as a material constant of the element M .

When the material constants and the stress σ_{ij}^M of the element M are given by Fig. 6.2 and Eqs. (6.26) and (6.27), its elastic-plastic constitutive equation is furnished by Eqs. (4.69) through (4.78) as follow:

$$\epsilon_{ij}^M = \epsilon_{ij}^{Me} + \epsilon_{ij}^{Mp}, \quad (6.28)$$

$$\epsilon_{ij}^{Me} = \frac{1 + \nu}{E} \tilde{\sigma}_{ij}^M - \frac{\nu}{E} \tilde{\sigma}_{kk}^M \delta_{ij}, \quad \tilde{\sigma}_{ij}^M = \frac{\sigma_{ij}^M}{1 - D}, \quad (6.29)$$

$$f^M = (\tilde{\sigma}^M - A^M)_{EQ} - \sigma_F = 0, \quad (6.30a)$$

$$(\tilde{\sigma}^M - A^M)_{EQ} = \left[\frac{3}{2} \left(\tilde{\sigma}_{ij}^{MD} - A_{ij}^{MD} \right) \left(\tilde{\sigma}_{ij}^{MD} - A_{ij}^{MD} \right) \right]^{1/2}, \quad (6.30b)$$

$$\tilde{\sigma}_{ij}^{MD} = \tilde{\sigma}_{ij}^M - \frac{1}{3} \tilde{\sigma}_{kk}^M \delta_{ij}, \quad A_{ij}^{MD} = A_{ij}^M - \frac{1}{3} A_{kk}^M \delta_{ij}, \quad (6.30c)$$

$$\dot{\varepsilon}_{ij}^{Mp} = \dot{A} \frac{\partial f^M}{\partial \sigma_{ij}} = \frac{3}{2} \frac{\tilde{\sigma}_{ij}^{MD} - A_{ij}^{MD}}{(\tilde{\sigma}^M - A^M)_{EQ}} \frac{1}{1-D} \dot{A}, \quad (6.31)$$

$$\begin{aligned} \dot{A}_{ij}^{MD} &= \frac{2}{3} c A_\infty \dot{\alpha}_{ij}^D \\ &= \frac{2}{3} C \dot{\varepsilon}_{ij}^{Mp} (1-D), \quad C = c A_\infty, \end{aligned} \quad (6.32)$$

$$\dot{A} = 0, \quad \text{for } f^M < 0 \text{ or } \dot{f}^M < 0, \quad (6.33a)$$

$$\dot{A} \neq 0, \quad \text{for } f^M = 0 \text{ and } \dot{f}^M = 0. \quad (6.33b)$$

In the above relations, the element M was assumed to be an elastic-plastic material obeying the linear kinematic hardening, and A_{ij}^M represents the kinematic hardening variable. The value of the indeterminate multiplier \dot{A} of Eq. (6.33) can be determined by the consistency condition $\dot{f}^M = 0$, and its explicit expression was given by Eq. (4.67).

As regards the damage development in the element M , we postulate that it is governed by the damage-associated variable (i.e., energy release rate due to damage) Y^M and the accumulated plastic strain p^M in M . Then, by the use of Eqs. (6.11), (6.20) and (6.25), we have

$$\dot{D} = \left(\frac{Y^M}{S} \right)^s p^M H(p^M - p_D), \quad (6.34)$$

$$Y^M = \frac{\left(\sigma_{EQ}^M \right)^2 R_v^M}{2E(1-D)^2}, \quad (6.35a)$$

$$R_v^M = \frac{2}{3}(1+\nu) + 3(1-2\nu) \left(\frac{\sigma_H^M}{\sigma_{EQ}^M} \right)^2, \quad (6.35b)$$

$$p_D = \varepsilon_D^p \frac{\sigma_U - \sigma_F}{\sigma_{EQ}^M - \sigma_F}. \quad (6.36)$$

The condition of fracture in M , and therefore the condition of mesocrack initiation in RVE is given by

$$D = D_C, \quad (6.37)$$

where D_C is the critical value of the damage variable D in M .

When the unilateral effect due to the opening-closing of microcracks cannot be disregarded, in particular, the damage-associated variable Y^M in Eq. (6.35) can be replaced, by means of Eq. (4.135), as follows:

$$Y^M = \frac{1+\nu}{2E} \left[\frac{<\sigma_{ij}^M>^2}{(1-D)^2} + \frac{\eta <-\sigma_{ij}^M>^2}{(1-Dh)^2} \right] - \frac{\nu}{2E} \left[\frac{<\sigma_{kk}^M>^2}{(1-D)^2} + \frac{\eta <-\sigma_{kk}^M>^2}{(1-Dh)^2} \right]. \quad (6.38)$$

According to the *elaborated two-scale damage model* discussed here, the stress state of the microscopic element M can be specified by Eq. (6.27) if the stress and strain in RVE have been known. Thus the elastic-plastic damage process of the element M can be calculated by Eqs. (6.28) through (6.38). We suppose that the mesoscale cracks start when the damage state of the element M , i.e., the damage variable D in microscopic scale, attains to its critical value D_C .

(2) Analytical Solution of the Elaborated Two-Scale Damage Model

The damage analysis of the microscopic volume element M described above should be performed numerically in general. By simplifying the model, however, the analytical solution of the damage variable in the element M can be derived as the function of stress in the mesoscale (Lemaitre, Sermage, and Desmorat 1999). For this purpose, we assume the following simplifications:

- 1) The unilateral effect resulting from microcrack closure is disregarded.
- 2) The threshold value p_D for the damage initiation and the critical value D_C for the crack start are given, respectively, by

$$p_D = 0, \quad D_C = 1. \quad (6.39)$$

- 3) The damage effect on the elastic-plastic deformation of the element M is disregarded.
- 4) The element M is subject to proportional loading. Thus we postulate that the rates of stress, strain and the kinematic-hardening variable are given by

$$\dot{\sigma}_{ij}^M = T_{ij}\dot{\sigma}^M, \quad \dot{\varepsilon}_{ij}^{Mp} = T_{ij}^D\dot{\varepsilon}^{Mp}, \quad \dot{A}_{ij}^M = T_{ij}\dot{A}^M, \quad (6.40)$$

where T_{ij} and T_{ij}^D are the time-independent constants.

According to this simplification, the yield function and the plastic strain rate of the element M are given by substituting $D = 0$ into Eqs. (6.30) through (6.32):

$$f^M = \left[\frac{3}{2} \left(\sigma_{ij}^{MD} - A_{ij}^{MD} \right) \left(\sigma_{ij}^{MD} - A_{ij}^{MD} \right) \right]^{1/2} - \sigma_F = 0, \quad (6.41)$$

$$\dot{\varepsilon}_{ij}^{Mp} = \frac{3}{2} \frac{\sigma_{ij}^{MD} - A_{ij}^{MD}}{\left(\sigma^M - A^M \right)_{EQ}} \dot{A} = \frac{3}{2} \frac{\sigma_{ij}^{MD} - A_{ij}^{MD}}{\sigma_F} \dot{A}, \quad (6.42a)$$

$$\dot{A}_{ij}^{MD} = \frac{2}{3} C \dot{\varepsilon}_{ij}^{Mp}. \quad (6.42b)$$

As regards Eq. (6.33) and the value of the multiplier \dot{A} , by assuming $(R_\infty - R) = 0$, $D = 0$, $\partial F/\partial \sigma = 0$ and $A_{kl}^D/A_\infty \ll 1$ in Eq. (4.67), we have

$$\dot{A} = 0, \quad \text{for } f^M < 0 \text{ or } \dot{f}^M < 0, \quad (6.43a)$$

$$\dot{A} = \frac{3}{2C\sigma_F} (\sigma_{kl}^{MD} - A_{kl}^{MD}) \dot{\sigma}_{kl}^M,$$

$$\text{for } f^M = 0 \text{ and } \dot{f}^M = 0. \quad (6.43b)$$

From Eqs. (6.42) and (6.43) we have

$$\dot{\varepsilon}_{ij}^{Mp} = \frac{9}{4C(\sigma_F)^2} < (\sigma_{kl}^{MD} - A_{kl}^{MD}) \dot{\sigma}_{kl}^{MD} > > (\sigma_{ij}^{MD} - A_{ij}^{MD}). \quad (6.44)$$

In view of the condition of proportional loading of (6.40), Eq. (6.44) leads to

$$\dot{\varepsilon}_{ij}^{Mp} = \frac{3}{2C} < \dot{\sigma}_{ij}^{MD} >, \quad (6.45a)$$

$$\varepsilon_{ij}^{Mp} = \frac{3}{2C} < \sigma_{ij}^{MD} >. \quad (6.45b)$$

Since the hydrostatic stress of mesoscopic element RVE is equal to that of the microscopic element M , Eq. (6.27) is expressed also in the form

$$\sigma_{ij}^{MD} = \sigma_{ij}^D - aE\varepsilon_{ij}^{Mp}. \quad (6.46)$$

The equivalent stress of the mesoscale element can be calculated from Eqs. (6.45b) and (6.46) as follows:

$$\begin{aligned} \sigma_{EQ} &= \left[\frac{3}{2} (\sigma_{ij}^{MD} + aE\varepsilon_{ij}^{Mp}) (\sigma_{ij}^{MD} + aE\varepsilon_{ij}^{Mp}) \right]^{1/2} \\ &= \sigma_{EQ}^M \left(1 + \frac{3aE}{2C} \right). \end{aligned} \quad (6.47a)$$

By differentiating this relation with respect to time, we have

$$\dot{\sigma}_{EQ} = (1 + k) \dot{\sigma}_{EQ}^M, \quad k = \frac{3aE}{2C}, \quad (6.47b)$$

integration of which gives us

$$\sigma_{EQ}^M = \sigma_{EQ}, \quad \text{for } \sigma_{EQ} < \sigma_F, \quad (6.48a)$$

$$\begin{aligned}\sigma_{EQ}^M &= \sigma_F + \frac{1}{1+k} \int_{\sigma_F}^{\sigma} d\sigma_{EQ} \\ &= \frac{\sigma_{EQ} + k\sigma_F}{1+k}, \quad \text{for } \sigma_{EQ} \geq \sigma_F.\end{aligned}\tag{6.48b}$$

The accumulated plastic strain of the element M , on the other hand, can be obtained by Eq. (6.45a) together with the condition of proportional loading:

$$\begin{aligned}\dot{p}^M &= \left(\frac{2}{3} \dot{\varepsilon}_{ij}^{Mp} \dot{\varepsilon}_{ij}^{Mp} \right)^{1/2} = \left[\frac{2}{3} \left(\frac{3}{2C} \right)^2 \frac{2}{3} \frac{3}{2} \dot{\sigma}_{ij}^{MD} \dot{\sigma}_{ij}^{MD} \right]^{1/2} \\ &= \frac{\dot{\sigma}_{EQ}}{C(1+k)}, \quad \text{for } \sigma_{EQ} \geq \sigma_F.\end{aligned}\tag{6.49}$$

Finally, by the use of Eqs. (6.47) and (6.48), the damage evolution equation of the microelement M can be derived from Eqs. (6.34) and (6.35):

$$\begin{aligned}\dot{D} &= \left(\frac{Y^M}{S} \right)^s \dot{p}^M = \left[\frac{(\sigma_{EQ})^2 R_v^M}{2E(1-D)^2} \right]^s \dot{p}^M \\ &= \left[\frac{(\sigma_{EQ} + k\sigma_F)^2 R_v^M}{2ES(1+k)^2(1-D)^2} \right]^s \frac{\dot{\sigma}_{EQ}}{C(1+k)}, \quad \text{for } \sigma_{EQ} \geq \sigma_F,\end{aligned}\tag{6.50a}$$

$$R_v^M = \frac{2}{3}(1+\nu) + 3(1-2\nu) \left[\frac{\sigma_H(1+k)}{\sigma_{EQ} + k\sigma_F} \right]^2.\tag{6.50b}$$

The elaborated two-scale damage model described above can represent the effects of mean stress and variable stress history on high cycle fatigue, as well as the effects of the non-proportional loading on multi-axial fatigue. Thus this model is applicable to damage problems of wider variety than the two-scale model of Section 6.1.3. Lemaitre and others (1999) elucidated also the procedure of identification of ten material constants contained in the model, and discussed its application to specific problems. In Section 7.2 later, we will analyze the high cycle fatigue under variable stress amplitude.

(3) Improvement of the Elaborated Two-Scale Damage Model

The elaborated two-scale damage model described above was improved further by including plastic strain $\boldsymbol{\epsilon}^p$ also in the mesoscale volume element and by rewriting the localization law of Eq. (6.27) in the form

$$\boldsymbol{\epsilon}^M = \boldsymbol{\epsilon} + \beta(\boldsymbol{\epsilon}^{Mp} - \boldsymbol{\epsilon}^p),\tag{6.51}$$

where β is given by Eq. (6.27b). For details of the derivation and its application, refer to Lemaitre and Desmorat (2005) and Desmorat and others (2007). As regards the application of Eq. (6.51), see Section 7.1.2 later.

6.1.5 Threshold Value of Damage Initiation p_D and Critical Value of Fracture D_C

Damage initiation in a representative volume element RVE (namely, the start of increase in D) is usually specified by the threshold value p_D of the accumulated plastic strain p . The local fracture of material (i.e., the fracture in the mesoscale), furthermore, is postulated to start when D attains to its critical value D_C . The values of p_D and D_C , however, vary largely depending on the material and the loading condition. For example, the threshold values of p_D in the cases of uniaxial monotonic loading and fatigue were already discussed in Section 4.2.6.

As regards the critical value D_C of fracture, by analyzing the strain energy release rate of elastic-plastic damaged material, we already showed in Section 4.3.1:

$$D_C = 1 - \frac{\sigma_R}{(2EY_C)^{1/2}}. \quad (6.52)$$

It was shown also that, the value of D_C has $D_C = 0.2 \sim 0.8$ in many cases.

The fracture in the mesoscale can be supposed to occur also as a result of unstable ductile fracture in the matrix of RVE. In this case, the critical damage D_C of ductile fracture under monotonic uniaxial tension is given as

$$D_C = 1 - \frac{\sigma_R}{\sigma_U}, \quad (6.53)$$

where σ_U and σ_R are the uniaxial tensile strength and the stress at the final fracture, respectively. Thus the value of this D_C may be interpreted as a characteristic fracture property of a material, and has the values of $D_C = 0.2 \sim 0.5$ for usual ductile fracture.

Bonora, Gentile and others (2005), furthermore, measured the damage variable D of steels by the use of their stiffness decrease, and found that the values of D_C attain to $D_C = 0.4 \sim 0.5$ before the necking starts. They measured the value of $D_C \simeq 0.8$ in the case of copper.

6.2 Ductile Damage and Ductile Fracture

6.2.1 Mechanical Approaches to Ductile Damage Analysis

Ductile damage is induced by the void development due to plastic deformation in materials. In the case of metals, in particular, this sort of damage is involved in a number of important engineering problems, such as the fracture of structural

elements and the damage induced in plastic forming processes. Thus the process of the initiation and the development of ductile damage has been discussed extensively from the theoretical as well as the experimental point of view.

In the tensile test of a ductile metal, microscopic voids are usually observed in rather small strain range. It is well known that these voids are initiated, mainly by the *decohesion* at the inclusion-matrix interfaces, fracture of inclusions, or by fracture of the matrix surrounding the inclusions (Hancock and Mackenzie 1976; Thomason 1990). These voids grow and coalesce by the necking and the shearing of the *ligaments* (matrices between neighboring voids) around the voids, and give rise to damage and fracture of materials. The development of these voids, furthermore, is subject to significant influence of the hydrostatic stress (Brownrigg et al. 1983). Thus the feature of the damage development and their dependence on the hydrostatic stress in shear and compression tests are largely different from those in tension (Bao and Wierzbicki 2004, 2005).

The continuum mechanics approach to ductile damage problems may be divided mainly into the following two. In the first approach, the mechanical effects of damage is represented by the *void volume fraction* f discussed in [Section 2.1.3](#). Then the plastic constitutive equation of voided material and the evolution law of the void development are derived by means of micromechanics analysis (Gurson 1977; Needleman and Tvergaard 1984; Rousselier 1987). This approach has been applied to a wide range of engineering problems, such as ductile fracture analysis of structural elements, and the damage and the fracture analyses in metal forming processes. Though this procedure is based on the microscopic mechanism of ductile damage process, it has the difficulty in the identification of the material constants together with the complexity in the mechanical representation of the damage anisotropy. In [Section 6.5](#) later, the constitutive equation of Gurson and that of Rousselier for void damage material will be discussed, and the intrinsic properties of these equations will be elucidated by comparing their numerical results. The limitation of the applicability of these micromechanics approaches and their further elaboration will be also presented.

The second approach to the ductile damage analysis is given by the *continuum damage mechanics*. In this approach, a systematic procedure based on continuum mechanics and irreversible thermodynamics has been established for the formulations of the damage evolution equation and the constitutive equation of damaged materials. Therefore, the continuum damage mechanics has been applied to the analysis of extensive range of damage and fracture problems. However, this approach also has limitations in its ability to properly describe the plastic volumetric strain. The extension of the damage mechanics in this respect will be discussed in [Section 6.6](#).

In the subsequent part of this section, we first discuss some important analytical models of ductile damage analysis, and then show the application of the isotropic damage theory to the finite element analysis of some ductile damage processes. As regards more details of the damage mechanics models of ductile damage and fracture, together with the computational procedures for their application, refer to the comprehensive and excellent review of Besson ([2010](#)).

6.2.2 Ductile Damage Model of Lemaître

We begin with the plastic-ductile damage model of Lemaître (1985). Since ductile damage occurs in large strain range, elastic strain may be disregarded. Thus the accumulated plastic strain p can be expressed in terms of the total strain ϵ

$$p = \left(\frac{2}{3} \epsilon_{ij} \epsilon_{ij} \right)^{1/2}. \quad (6.54)$$

By postulating *Ramberg-Osgood hardening law* and isotropic hardening of plastic deformation, the equivalent stress-equivalent strain relation of a damaged material in multiaxial state may be expressed by

$$p = \left[\frac{\sigma_{EQ}}{(1-D)K} \right]^n, \quad (6.55)$$

where n and K are material constants.

The evolution equation of damage is given by Eqs. (6.9) and (6.11)

$$\dot{D} = \left(\frac{Y}{S} \right)^s \dot{p} H(p - p_D), \quad Y = \frac{(\sigma_{EQ})^2}{2E(1-D)^2} R_v, \quad (6.56)$$

where R_v is the stress triaxiality function. By the use of the accumulated plastic strain p of Eq. (6.55), Eq. (6.56) further has the form

$$\dot{D} = \left(\frac{K^2 R_v}{2ES} p^{2/n} \right)^s \dot{p} H(p - p_D). \quad (6.57)$$

Development of ductile damage under arbitrary loading condition can be obtained by integrating Eq. (6.57) along its loading history.

(1) Damage Process under Proportional Loading, Linear Ductile Damage Model

Engineering problems of damage can be often analyzed by postulating proportional loading. Then Eq. (6.57) can be readily integrated to give

$$D = \left(\frac{K^2 R_v}{2ES} \right)^s \frac{n}{2s+n} \left(p^{(2s+n)/n} - p_D^{(2s+n)/n} \right). \quad (6.58)$$

Local fracture at every point of a material starts when the damage variable D attains to its critical value D_C . Then if we represent the strain at the start of fracture by p_R , Eq. (6.58) leads to

$$D_C = \left(\frac{K^2 R_v}{2ES} \right)^s \frac{n}{2s+n} \left(p_R^{(2s+n)/n} - p_D^{(2s+n)/n} \right). \quad (6.59)$$

In view of this relation, Eq. (6.58) has the alternative form

$$D = D_C \left[\frac{p^{(2s+n)/n} - p_D^{(2s+n)/n}}{p_R^{(2s+n)/n} - p_D^{(2s+n)/n}} \right]. \quad (6.60)$$

In metals under large plastic deformation, the *strain-hardening exponent* n is very large in general (e.g., $n = \infty$ for a perfectly plastic material), and the results of damage experiment show that the exponent s is nearly 1. Hence Eq. (6.60) can be expressed with sufficient accuracy as

$$D = D_C \left(\frac{p - p_D}{p_R - p_D} \right). \quad (6.61)$$

Though the threshold of damage initiation p_D as well as the rupture strain p_R depends on the stress triaxiality function R_v , the dependence of their ratio p_D/p_R on R_v is not significant. Hence the value of p_D/p_R may be approximated by its value in the uniaxial case:

$$\frac{p_D}{p_R} = \frac{\varepsilon_D}{\varepsilon_R}. \quad (6.62)$$

By the use of this relation, Eq. (6.61) may be expressed in the form

$$D = D_C \left[\frac{p(\varepsilon_R/p_R) - \varepsilon_D}{\varepsilon_R - \varepsilon_D} \right]. \quad (6.63)$$

As will be observed in Eq. (6.77) later, the validity of the assumption (6.62) is not always obvious, and may sometimes necessitate its confirmation.

On the other hand, in view of the approximate relations $(2s + n)/n \simeq 1$ and $s \simeq 1$, Eq. (6.59) can be further simplified. From the resulting relation, we can derive p_R as follows

$$p_R = \frac{2ESD_C}{K^2 R_v} \frac{1}{1 - (p_D/p_R)}. \quad (6.64)$$

For the particular case of uniaxial state, this relation leads to

$$\begin{aligned} (p_R)_U &= \varepsilon_R = \frac{2ESD_C}{K^2 (R_v)_U} \frac{1}{1 - (\varepsilon_D/\varepsilon_R)} \\ &= \frac{2ESD_C}{K^2} \frac{1}{1 - (p_D/p_R)}, \end{aligned} \quad (6.65)$$

where $()_U$ signifies the uniaxial state, and Eq. (6.62) and the relation $(R_v)_U = 1$ have been employed in the derivation.

By substituting Eqs. (6.64) and (6.65) into the term ε_R/p_R on the right-hand side of Eq. (6.63), we have the damage evolution for the proportional loading

$$D = D_C \left(\frac{pR_v - \varepsilon_D}{\varepsilon_R - \varepsilon_D} \right). \quad (6.66)$$

For the particular case of uniaxial loading, this relation leads to

$$D = D_C \left(\frac{\varepsilon - \varepsilon_D}{\varepsilon_R - \varepsilon_D} \right). \quad (6.67)$$

(2) Damage Evolution Equation for General Loading Conditions

By deriving D_C from Eq. (6.65) and using Eq. (6.62), we have

$$\begin{aligned} D_C &= \frac{K^2}{2ES} \varepsilon_R \left(1 - \frac{p_D}{p_R} \right) \\ &= \frac{K^2}{2ES} (\varepsilon_R - \varepsilon_D). \end{aligned} \quad (6.68)$$

By means of this relation, the evolution equation (6.57) of plastic ductile damage under a general loading path is expressed in a simple form

$$\dot{D} = \frac{D_C R_v}{\varepsilon_R - \varepsilon_D} p^{2/n} \dot{p} H(p - p_D). \quad (6.69)$$

Equations (6.66) and (6.67), as well as Eq. (6.69) with $n \simeq \infty$, represent a linear relation between damage development and plastic strain increase. This feature is observed in the experiments for a number of metallic material as shown in Fig. 6.3 (Lemaitre 1985). However, depending on the material and the condition of loading, the linear damage model described above cannot be always applicable. Thus the

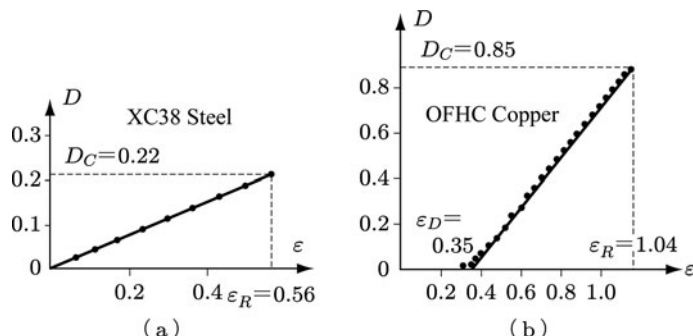


Fig. 6.3 Development of ductile damage in XC38 steel and OFHC copper
Source: Lemaitre (1985, p. 88, Fig. 4)

limitation of the aforementioned models and the improved nonlinear ductile damage model will be discussed in Section 6.2.3 below.

6.2.3 Extension of Ductile Damage Model

The linear ductile damage model of Section 6.2.2 has been extended to describe more extensive ductile damage processes (Tai and Yang 1986; Chandrakanth and Pandey 1993; Bonora 1997). We now consider the *non-linear ductile damage model* of Bonora (1997).

(1) Extension of Damage Evolution Equation

The development of ductile damage is governed not only by the damage- associated variable (i.e., strain energy release rate) Y , but also by the states of plastic strain and damage. Moreover mechanical effect of material damage may depend on the relative relation between the current values of damage D and its critical value D_C . If these two effects may be represented by power functions of p and $(D_C - D)$, the damage dissipation potential F^D of Eq. (4.90) has an elaborated form

$$F^D = \frac{1}{2} \frac{S}{1-D} \left(\frac{Y}{S} \right)^2 \frac{(D_C - D)^{(\alpha-1)/\alpha}}{p^{(2+n)/n}}, \quad (6.70)$$

where n is the strain-hardening exponent of Ramberg-Osgood law, while α is an exponent characterizing the damage development.

By substituting Eq. (6.70) into Eq. (4.86) and employing Eqs. (4.89), (6.9) and (6.55), the evolution equation of the damage variable D is derived as follows

$$\dot{D} = \dot{A} \frac{\partial F^D}{\partial Y} = \frac{K^2}{2ES} R_v (D_C - D)^{(\alpha-1)/\alpha} \left(\frac{\dot{p}}{p} \right) H(p - p_D). \quad (6.71)$$

Integration of this relation under uniaxial tension with the initial condition of $p = \varepsilon_D$ and $D = D_0$ gives

$$D = D_C - \left[(D_C - D_0)^{1/\alpha} - \frac{1}{\alpha} \frac{K^2}{2ES} \ln(\varepsilon/\varepsilon_D) \right]^\alpha. \quad (6.72)$$

By applying the fracture condition $\varepsilon = \varepsilon_R$ and $D = D_C$ to this relation, we have

$$\frac{K^2}{2ES} = \frac{\alpha(D_C - D_0)^{1/\alpha}}{\ln(\varepsilon_R/\varepsilon_D)}. \quad (6.73)$$

By means of this relation, the damage evolution equation (6.71) eventually has the form

$$\dot{D} = \frac{\alpha(D_C - D_0)^{1/\alpha}}{\ln(\varepsilon_R/\varepsilon_D)} R_v (D_C - D)^{(\alpha-1)/\alpha} \left(\frac{\dot{p}}{p} \right) H(p - p_D). \quad (6.74)$$

A variety of ductile damage processes, including those in structural elements and metal forming, can be elucidated by integrating this equation along the given loading history.

In the particular cases of the uniaxial loading and the multiaxial proportional loading, Eq. (6.74) can be integrated analytically, and leads, respectively, to the relations

$$D = D_0 + (D_C - D_0) \left\{ 1 - \left[1 - \frac{\ln(\varepsilon/\varepsilon_D)}{\ln(\varepsilon_R/\varepsilon_D)} \right]^\alpha \right\}, \quad (6.75)$$

$$D = D_0 + (D_C - D_0) \left\{ 1 - \left[1 - \frac{\ln(p/p_D)}{\ln(\varepsilon_R/\varepsilon_D)} R_v \right]^\alpha \right\}. \quad (6.76)$$

Equations (6.74) through (6.76) are applicable to more wide range of metallic materials in comparison with Eqs. (6.8) and (6.11). Table 6.1 shows the material constants in these relations for some materials.

(2) Comparison with Experimental Results

As observed in Eqs. (6.75) and (6.76), the damage exponent α characterizes the aspects of damage development expressed as a function of equivalent plastic strain. Thus, depending on the magnitude of the exponent α , the modes of ductile damage development under uniaxial loading may be divided into three typical cases shown in Fig. 6.4. The curves of Type 1, 2 and 3 in the figure correspond to $\alpha = 0.05$, 0.25 and 0.90, respectively. The insertions in the figure show schematically the development of microvoids started from the microscopic inclusions.

Figure 6.5a, b show the damage development in 1090 steel and 2024-T3 aluminium alloy as the examples of types 2 and 3 of Fig. 6.4. The comparison between the experimental results and the predictions of Eq. (6.75) ascertains the effectiveness of the present model.

Table 6.1 Material constants in damage evolution equations

Material	ε_D	ε_R	D_C	D_0	α
Alloy A12024-T3	0.0092	0.33	0.188	0.0	0.679
Alloy Al-Li 2091	0.0077	0.1	0.140	0.0	0.446
Low carbon steel A3	0.202	1.0	0.1	0.0	0.198
Steel 1015	0.259	1.4	0.065	0.0	0.2175
Steel 1045	0.223	0.95	0.065	0.0	0.2173
Steel 1090	0.129	0.64	0.065	0.0	0.2
Copper 99.9%	0.34	1.04	0.85	0.0	0.631
Steel E24	0.5	0.88	0.17	0.0	–
Steel 304 CD4	0.02	0.37	0.24	0.0	–
Alloy INCO 718	0.02	0.29	0.24	0.0	–

(Bonora 1997, p. 18 Table 2)

Fig. 6.4 Three types of damage development
Source: Bonora (1997, p. 19
Fig. 3)

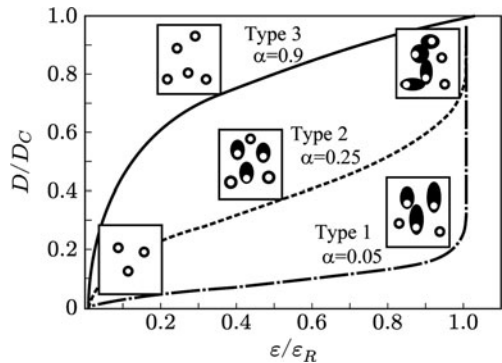
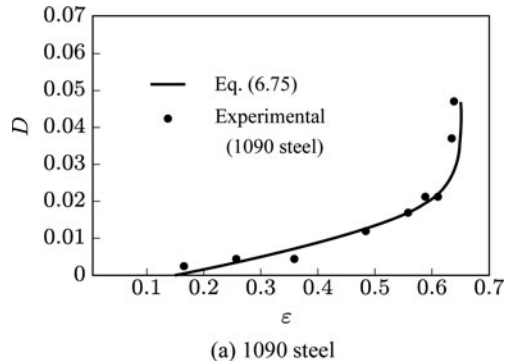
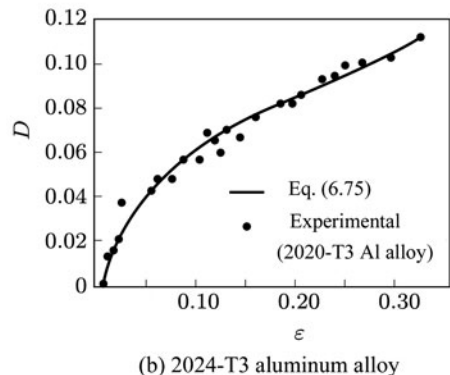


Fig. 6.5 Damage development in 1090 steel and 2024-T3 aluminum alloy
Source: Bonora (1997, p. 22
Fig. 10; p. 23 Fig. 12)



(a) 1090 steel



(b) 2024-T3 aluminum alloy

(3) Effects of the Stress Triaxiality in Ductile Damage

In order to elucidate the damage process under multiaxial loading on the basis of the experimental results of uniaxial fracture tests, we need the values of the threshold equivalent strain p_D for damage occurrence and the equivalent fracture strain p_R . In other words, we must elucidate the effects of stress triaxiality on the damage threshold strain p_D and the fracture strain p_R .

Comparing Eq. (6.75) with Eq. (6.76) at the fracture state, we have

$$\ln\left(\frac{\varepsilon_R}{\varepsilon_D}\right) = R_v \ln\left(\frac{p_R}{p_D}\right). \quad (6.77)$$

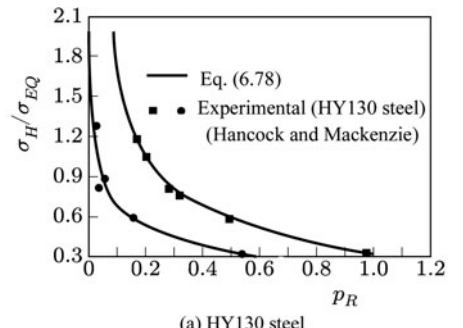
Since the effect of stress triaxiality on the damage threshold strain ε_D can be assumed insignificant (Thomson and Hancock 1984), we have $p_R = \varepsilon_R$, and thus Eq. (6.77) leads to

$$p_R = \varepsilon_D \left(\frac{\varepsilon_R}{\varepsilon_D} \right)^{1/R_v}. \quad (6.78)$$

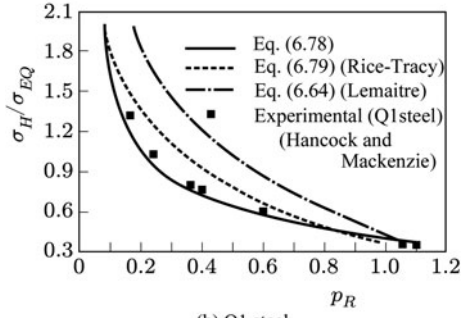
Namely, the equivalent fracture strain under multiaxial state of stress is given by a power function of the uniaxial fracture strain ε_R with the exponent $1/R_v$.

Figure 6.6 shows the comparison of Eq. (6.78) with the experiments of two kinds of steels and other theories. The dashed and the chain line in (b) are the results based on Rice and Tracy model (1969)

$$\varepsilon_R = C_0 \exp\left(-\frac{3\sigma_H}{2\sigma_{EQ}}\right), \quad (6.79)$$



(a) HY130 steel



(b) Q1 steel

Fig. 6.6 Influence of stress triaxiality on fracture strain

Source: Bonora (1997, p. 26, Fig. 19; p. 25, Fig. 16)

and that of Lemaitre model of Eq. (6.64), where C_0 is a material constant. Figure 6.6 shows marked influence of stress triaxiality σ_H/σ_{EQ} on the magnitude of fracture strain p_R .

6.2.4 Finite Element Analysis of Ductile Fracture Process

Since ductile damage is accompanied by large plastic deformation, the development of damage induces significant change in the stress and the strain distribution in materials. Besides, the ductile damage processes are influenced largely by the stress triaxiality. Therefore, for the accurate discussion of the damage, stress, strain and the stress triaxiality induced in the damage processes, we often should have recourse to the finite element analysis. We will now consider this problem by referring to the work of Bonora, Gentile and others (2005).

(1) Constitutive and Damage Evolution Equations of Damaged Material

The macroscopic stress-strain relation of most metals hardly show the softening due to damage (Pirondi and Bonora 2003). Hence, the effect of damage softening on the plastic constitutive equation may be disregarded.

We suppose that the strain hardening of materials obeys the Ramberg-Osgood law. Then the elastic-plastic constitutive equations of isotropic-hardening materials Eqs. (6.1) through (6.6) are given:

$$\varepsilon_{ij} = \varepsilon_{ij}^e + \varepsilon_{ij}^p, \quad (6.80)$$

$$\varepsilon_{ij}^e = \frac{1+\nu}{E} \frac{\sigma_{ij}}{1-D} - \frac{\nu}{E} \frac{\sigma_{kk}}{1-D} \delta_{ij}, \quad (6.81)$$

$$\dot{\varepsilon}_{ij}^p = \dot{\Lambda} \frac{\partial F^P}{\partial \sigma_{ij}} = \frac{3}{2} \frac{\sigma_{ij}^D}{\sigma_{EQ}} \dot{\Lambda}, \quad (6.82)$$

$$\dot{r} = \dot{\Lambda} \frac{\partial F^P}{\partial R} = \dot{\Lambda} = \dot{p}, \quad (6.83)$$

$$p = \left(\frac{\sigma_{EQ}}{K} \right)^n. \quad (6.84)$$

As regards the evolution equation of damage, on the other hand, we postulate Eq. (6.74) described in the previous subsection:

$$\dot{D} = \frac{\alpha(D_C - D_0)^{1/\alpha}}{\ln(\varepsilon_R/\varepsilon_D)} R_v (D_C - D)^{(\alpha-1)/\alpha} \left(\frac{\dot{p}}{p} \right) H(p - p_D). \quad (6.85)$$

(2) Finite Element Analysis of Ductile Damage Process

Equations (6.80) through (6.84) were applied to the three-dimensional finite element analysis of ductile fracture process. The analysis was performed for a smooth and an externally notched rectangular specimens of A533B low alloy steel. The material constants employed in the calculation are shown in Table 6.2.

Figure 6.7 shows the stress triaxiality in the damage process of a flat rectangular specimen of 5 mm thick and 12 mm wide. Figure 6.7a shows the change in the stress triaxiality σ_H/σ_{EQ} at the locations O, A and B shown in (b). The necking of the specimen starts at the equivalent plastic strain $\varepsilon_{EQ}^p \simeq 0.4$. As observed in (a), the variation of the stress triaxiality over the cross-section is less than 30% before the start of necking. After that, the stress triaxiality at the center of the cross-section O increases monotonously, and attains to $\sigma_H/\sigma_{EQ} \simeq 0.6$. Figure 6.7b, on the other hand, shows the distribution of the stress triaxiality in the necking part of the specimen at $\varepsilon_{EQ}^p = 0.4$.

Figure 6.8, on the other hand, shows the damage development in a rectangular specimen with semicircular external notches of radius 2 mm (width and thickness of the minimum section are 8 mm and 5 mm, respectively). The ductile damage in a notched specimen is induced by the concurrent effects of plastic strain concentration due to notch effect and the resulting stress triaxiality. The incipient fracture starts at

Table 6.2 Material constants employed in the analysis

Constitutive Eqs. (6.81) (6.84)	E [GPa] 200	ν 0.3	σ_Y [MPa] 400	K [MPa] 9.754×10^2	n 4.739
Evolution Eq. (6.85)	α 0.535	ε_D, p_D 0.0195	ε_R 1.75	D_0 0	D_C 1.0

Note: A533B low alloy steel at room temperature

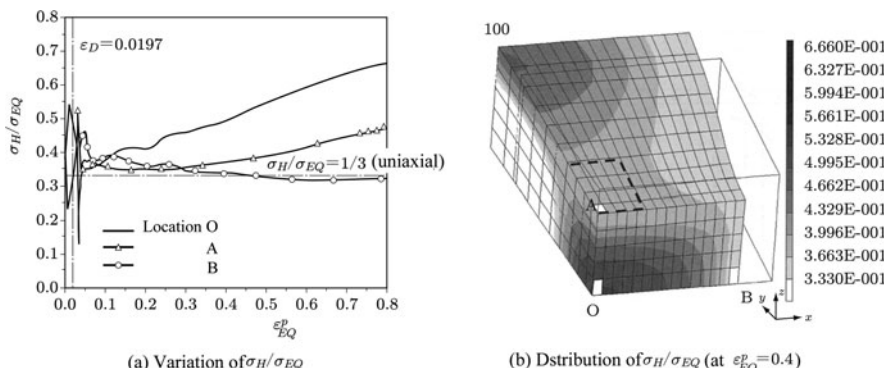


Fig. 6.7 Ductile damage process of a rectangular specimen. (A533B low alloy steel at room temperature)

Source: Bonora et al. (2005, p. 995, Fig. 4)

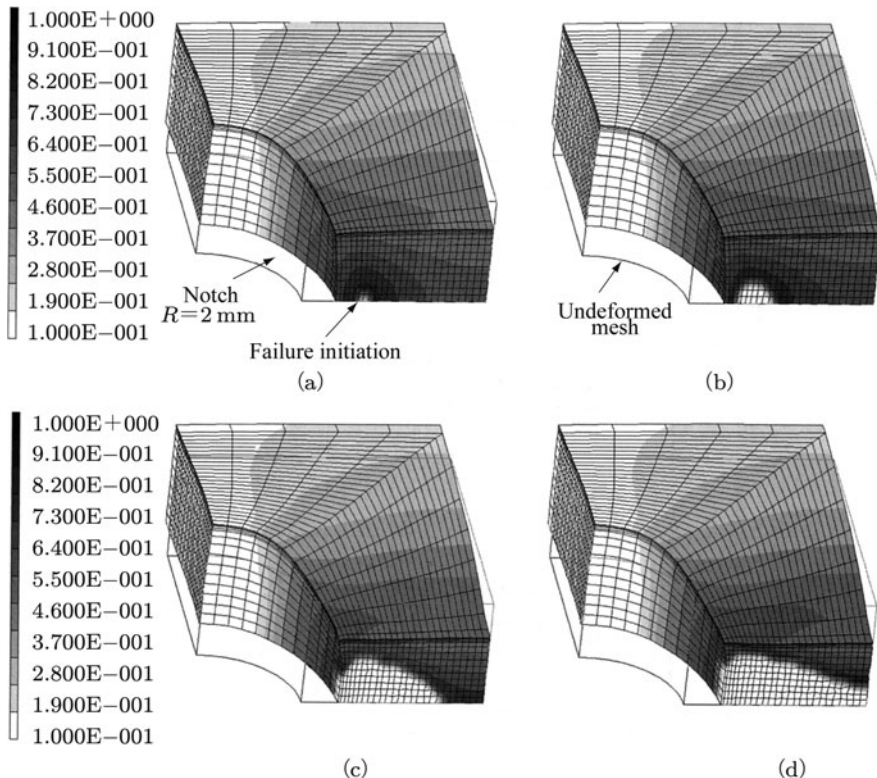


Fig. 6.8 Damage development in a rectangular specimen with semicircular notches (white regions on the minimum cross-section indicate the fractured elements)

Source: Bonora et al. 2005, p. 1002, Fig. 14)

a location just inside the minimum section, rather than on the notch surface. This was confirmed also by SEM observation on the fractured surface of the specimen. The white regions on the minimum cross-section of (a) through (d) indicate the fractured elements. These figures clearly show the *cup and cone fracture* characteristic to ductile fracture. According to the analysis, the microcrack which had started in the minimum section extended rapidly over the whole section after a few load increments, and leaded to the final ductile fracture.

6.2.5 Effects of Stress Triaxiality on Damage Criteria and Damage Dissipation Potential

The discussion extended hitherto, for example, the derivation of the ductile fracture models of Sections 6.2.2 and 6.2.3, was performed on the basis of the damage evolution equations, respectively of Eqs. (6.56) and (6.74). This implies that the occurrence and the development of damage in these cases are governed by the damage-associated variable

$$Y = \frac{(\tilde{\sigma}_{EQ})^2}{2E} R_v, \quad R_v = \frac{2}{3}(1 + v) + 3(1 - 2v) \left(\frac{\sigma_H}{\sigma_{EQ}} \right)^2. \quad (6.86)$$

As we learned in Section 6.2.1, in the case of ductile damage, not only the threshold of damage occurrence, but also the rate of damage development and its microscopic mechanisms depend largely on the value of stress triaxiality σ_H/σ_{EQ} .

Strictly speaking, therefore, the effects of stress triaxiality σ_H/σ_{EQ} on ductile damage development cannot be described by a single expression of Eq. (6.86). For example, in the case of metal forming processes to be discussed in Section 6.3, we have $\sigma_H/\sigma_{EQ} < 0$ in the forging and the rolling, while $\sigma_H/\sigma_{EQ} \simeq 0$ in the shearing and the thin plate forming; they have different aspects from the cases of $\sigma_H/\sigma_{EQ} > 0$ shown in Figs. 6.3 through 6.6.

In order to develop an anisotropic damage theory for large deformation applicable to accurate analyses of ductile damage problems, Brüning and others (2008) discussed the damage evolution equation and the stress criterion for damage initiation by incorporating the effect of wide range of stress triaxiality. By performing shear and tensile tests on smooth and notched flat specimens to realize wide range of stress triaxiality and by taking account of Bao and Wierzbicki's results (2004, 2005) described in Section 4.3.5, they proposed the following damage criteria and damage dissipation potentials.

(1) Damage Criterion

$$\chi(\sigma, \sigma_D) = \left(\frac{3}{2} \sigma_{ij}^D \sigma_{ij}^D \right)^{1/2} - \sigma_D = 0, \quad (6.87a)$$

for $-\frac{1}{3} \leq \frac{\sigma_H}{\sigma_{EQ}} \leq 0$,

$$\chi(\sigma, \sigma_D) = \frac{1}{3} \sigma_{kk} + \alpha \left(\frac{3}{2} \sigma_{ij}^D \sigma_{ij}^D \right)^{1/2} - \sigma_D = 0, \quad (6.87b)$$

$$\alpha = 1 - \left(\frac{\varsigma \sigma_H}{\sigma_{EQ}} \right)^m,$$

$$\chi(\sigma, \sigma_D) = \frac{1}{3} \sigma_{kk} - \sigma_D = 0, \quad (6.87c)$$

for $0 < \frac{\sigma_H}{\sigma_{EQ}} < \frac{1}{\sqrt{3}}$,

$$\frac{1}{\sqrt{3}} \leq \frac{\sigma_H}{\sigma_{EQ}},$$

where σ_D and α denote the threshold value for damage onset and a parameter characterizing damage aspect, while ς and m are material constants.

(2) Damage Dissipation Potential

$$F^D(\sigma, \bar{\alpha}) = \bar{\alpha} \left(\frac{3}{2} \tilde{\sigma}_{ij}^D \tilde{\sigma}_{ij}^D \right)^{1/2}, \quad \text{for } -\frac{1}{3} \leq \frac{\sigma_H}{\sigma_{EQ}} \leq 0, \quad (6.88a)$$

$$F^D(\sigma, \bar{\alpha}) = \frac{1}{3} (1-f)^{-1} \tilde{\sigma}_{kk} + \bar{\alpha} \left(\frac{3}{2} \tilde{\sigma}_{ij}^D \tilde{\sigma}_{ij}^D \right)^{1/2}, \\ \text{for } 0 < \frac{\sigma_H}{\sigma_{EQ}} < \frac{1}{\sqrt{3}} \text{ or } f_D \leq f, \quad (6.88b)$$

$$F^D(\sigma, \bar{\alpha}) = \frac{1}{3} (1-f)^{-1} \tilde{\sigma}_{kk}, \quad \text{for } \frac{1}{\sqrt{3}} \leq \frac{\sigma_H}{\sigma_{EQ}} \text{ and } f < f_D, \quad (6.88c)$$

where $\bar{\alpha}$ and f are the parameter of damage anisotropy and the void volume fraction, while f_D is the damage threshold value of f .

As already mentioned in Section 6.2.1, besides the significant effects of the stress triaxiality, the continuum damage mechanics applied to accurate analyses of ductile damage process has another limitation that it usually does not represent the plastic compressibility. The improvement in this respect will be discussed in Section 6.6 later.

6.3 Application to Metal Forming Process

The metal forming process is one of the most typical problems of predominant elastic-plastic damage. As a result of large plastic deformation, or of plastic instability, microscopic defects may occur and develop on the surface or inside the workpiece of plastic forming. In the metal forming tools, furthermore, fatigue damage is induced by the repeated action of high level of stress or cyclic thermal loading.

In the present section, we first describe the analytical prediction of the fracture limit in sheet metal forming. Then, the application of elastic-plastic isotropic damage theory to some three-dimensional metal forming processes, e.g., forging and blanking, will be discussed. The fatigue life prediction of cold forming tools will be also presented.

Besides the coupled inelastic and damage phenomena at large deformation, the analysis of the metal forming process involves the generation and the conduction of heat in works and tools, together with complicated boundary conditions between them. As to the details of the computational procedure for this problem, refer to the relevant references (Saanouni 2003, 2006; Saanouni and Chaboche 2003). The computational aspects in the damage and fracture analysis based on damage mechanics and the finite element method will be discussed briefly in Chapter 11.

6.3.1 Fracture Limit of Sheet Metal Forming

Fracture limit in sheet metal forming is an important objective of the ductile damage theory. Referring to Lemaitre (1992), we will now consider this problem.

Let us suppose that a work of sheet metal forming is subject to proportional loading in plane-stress state. Then the stress triaxiality function R_v of Eq. (6.9) remains constant throughout the process. The elastic-plastic damage will be noticeable only after sufficient strain-hardening and after the isotropic hardening variable R tends to its asymptotic value. Therefore if the subsequent yield stress is denoted by σ_s , the yield condition (6.3) has the form

$$\begin{aligned}\tilde{\sigma}_{EQ} &= \sigma_Y + R \\ &\equiv \sigma_s \quad (= \text{const.}),\end{aligned}\tag{6.89}$$

where σ_Y denotes the initial yield stress. Then by noting Eq. (6.9), the evolution equation of damage (6.8) can be readily integrated to give

$$D = \frac{(\sigma_s)^2}{2ES} R_v (p - p_D),\tag{6.90}$$

where p_D is the threshold of the accumulated equivalent plastic strain p for the damage development.

In the special case of uniaxial and monotonic loading, we have $R_v = 1$ and $p = \varepsilon^p$, and thus Eq. (6.90) leads to

$$D = \frac{(\sigma_s)^2}{2ES} (\varepsilon^p - \varepsilon_D^p).\tag{6.91}$$

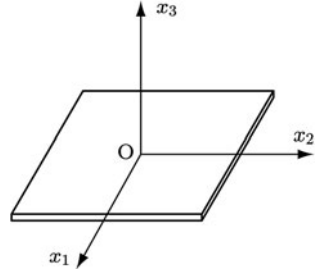
Let the plastic strain at fracture in one- and three-dimensional damage be ε_R^p and p_R , respectively. Then, comparison between Eqs. (6.90) and (6.91) at the states of fracture limit gives

$$\begin{aligned}\frac{p_R - p_D}{\varepsilon_R^p - \varepsilon_D^p} &= \frac{1}{R_v} \\ &= \left[\frac{2}{3}(1 + \nu) + 3(1 - 2\nu) \left(\frac{\sigma_H}{\sigma_{EQ}} \right)^2 \right]^{-1}.\end{aligned}\tag{6.92}$$

This relation implies that the value of the equivalent fracture plastic strain p_R in three-dimensional states is governed explicitly by the stress triaxiality σ_H/σ_{EQ} or the stress triaxiality function R_v .

The forming limit in sheet metal forming is usually discussed in the plastic strain space. Then, the right hand side of Eq. (6.92) should be expressed in terms of the plastic strain ε_{ij}^p . We first take an orthogonal coordinate system $O-x_1x_2x_3$ on a sheet metal as shown in Fig. 6.9.

Fig. 6.9 A sheet metal in plane-stress state and an orthogonal coordinate system



In view of the plastic incompressibility condition, the plastic strain tensor of a sheet in plane state of stress is given by

$$[\boldsymbol{\varepsilon}^p] = \begin{bmatrix} \varepsilon_1^p & 0 & 0 \\ 0 & \varepsilon_2^p & 0 \\ 0 & 0 & -(\varepsilon_1^p + \varepsilon_2^p) \end{bmatrix}, \quad (6.93)$$

from which we have the equivalent plastic strain at fracture p_R , i.e.,

$$p_R = \left(\frac{2}{3} \varepsilon_{ij}^p \varepsilon_{ij}^p \right)_R^{1/2} = \frac{2}{\sqrt{3}} \left[(\varepsilon_1^p)^2 + (\varepsilon_2^p)^2 + \varepsilon_1^p \varepsilon_2^p \right]_R^{1/2}. \quad (6.94)$$

On the other hand, the deviatoric stress tensor in plane stress state is given by Eq. (4.46):

$$[\sigma^D] = \frac{1}{3} \begin{bmatrix} 2\sigma_1 - \sigma_2 & 0 & 0 \\ 0 & 2\sigma_2 - \sigma_1 & 0 \\ 0 & 0 & -\sigma_1 - \sigma_2 \end{bmatrix}. \quad (6.95)$$

Since we have assumed that the forming process is subject to proportional loading, the plastic constitutive equation of Eq. (6.4) can be integrated to give

$$\frac{\varepsilon_2^p}{\varepsilon_1^p} = \frac{\sigma_2^D}{\sigma_1^D} = \frac{2\sigma_2 - \sigma_1}{2\sigma_1 - \sigma_2}, \quad (6.96a)$$

from which we have a relation

$$\frac{\sigma_H}{\sigma_{EQ}} = \frac{(\varepsilon_2^p / \varepsilon_1^p) + 1}{\sqrt{3} \left[(\varepsilon_2^p / \varepsilon_1^p)^2 + (\varepsilon_2^p / \varepsilon_1^p) + 1 \right]^{1/2}}. \quad (6.96b)$$

Since the elastic strain ε_{ij}^e and the threshold strain ε_D^p for damage start are sufficiently small in comparison with the fracture strain ε_R , we can postulate the

approximate relations of $\varepsilon_{ij}^e = 0$ and $\varepsilon_D^p = p_D = 0$. Then, by substituting Eqs. (6.94) and (6.96b) into Eq. (6.92), we finally have the fracture limit in sheet metal forming as follows

$$\left(\frac{\varepsilon_1}{\varepsilon_R}\right)^2 + \frac{\varepsilon_1 \varepsilon_2}{\varepsilon_R^2} + \left(\frac{\varepsilon_2}{\varepsilon_R}\right)^2 - \frac{3}{4} \left\{ \frac{2}{3}(1+\nu) + (1-2\nu) \frac{[(\varepsilon_2/\varepsilon_1) + 1]^2}{(\varepsilon_2/\varepsilon_1)^2 + (\varepsilon_2/\varepsilon_1) + 1} \right\}^{-2} = 0. \quad (6.97)$$

Figure 6.10 shows the fracture limits calculated by Eq. (6.97) for a few values of Poisson ratio ν .

In the process of sheet metal forming, *diffused necking* and/or *localized necking* are observed in advance of sheet fracture. Thus the onset of the localized necking is usually focused as the *forming limit* of sheet metals, and the limit of their occurrence is represented by the use of a *forming limit diagram* (FLD).

Occurrence of the localized necking is subject to large influence of plastic- and damage-anisotropy. In Section 6.4, more accurate analysis of this problem will be discussed on the basis of anisotropic plasticity-anisotropic damage theory.

6.3.2 Damage Analysis of Forging and Blanking Process

Let us now consider the application of elastic-plastic damage theory to more complicated forming processes. We consider here the results of finite element analysis of the lateral forging of a circular cylinder and the blanking of a sheet metal as shown in Figs. 6.11 and 6.12 later (Saanouni, Nesnas, and Hammi 2000).

By assuming the infinitesimal elastic and the finite plastic deformation, the deformation rate tensor \mathbf{d} is expressed in the form

$$\mathbf{d} = \dot{\mathbf{\epsilon}}^e + \mathbf{d}^p, \quad (6.98)$$

where $\dot{\mathbf{\epsilon}}^e$ and \mathbf{d}^p are the Jaumann derivative of the elastic strain tensor and the plastic deformation rate tensor.

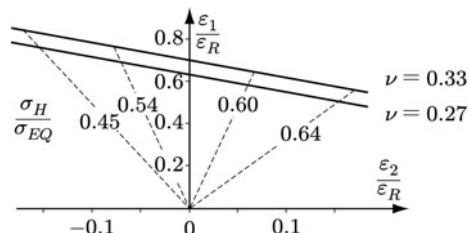


Fig. 6.10 Fracture limit in sheet metal forming

Source: Lemaitre (1992, p. 123, Fig. 3.14)

(1) Helmholtz Free Energy Function and Constitutive Equations

By representing the damage state by a scalar damage variable D and disregarding the kinematic hardening of plasticity, the Helmholtz free energy function ψ per unit volume is given by

$$\begin{aligned}\rho\psi(\boldsymbol{\varepsilon}^e, r, D, T) &= \rho\psi^E(\boldsymbol{\varepsilon}^e, D, T) + \rho\psi^{IN}(r, D, T) \\ &= (1 - D) \left[\frac{1}{2} \lambda (\text{tr}\boldsymbol{\varepsilon}^e)^2 + \mu (\text{tr}\boldsymbol{\varepsilon}^e \boldsymbol{\varepsilon}^e) \right] + (3\lambda + 2\mu)\alpha\sqrt{1 - D}(T - T_0)\text{tr}\boldsymbol{\varepsilon}^e \\ &\quad - \frac{1}{2}\rho \frac{c_v}{T_0}(T - T_0)^2 + \frac{1}{2}R_0(1 - D)r^2,\end{aligned}\tag{6.99}$$

where r and T denote the internal variable of isotropic hardening and the temperature. The symbols α , c_v and λ , μ , furthermore, are the linear expansion coefficient, the specific heat and the Lamé constants of the material. The symbols T_0 and R_0 are the reference temperature and a material constant of isotropic hardening. Then, the thermodynamic variables associated with the state variables $\boldsymbol{\varepsilon}^e$, T , r and D are given by substituting Eq. (6.99) into Eqs. (4.20) and (4.22) as follow:

$$\begin{aligned}\sigma &= \rho \frac{\partial \psi}{\partial \boldsymbol{\varepsilon}^e} = (1 - D) [\lambda(\text{tr}\boldsymbol{\varepsilon}^e)\mathbf{I} + 2\mu\boldsymbol{\varepsilon}^e] \\ &\quad + \sqrt{1 - D}(3\lambda + 2\mu)\alpha(T - T_0)\mathbf{I},\end{aligned}\tag{6.100a}$$

$$s = -\frac{\partial \psi}{\partial T} = \frac{1}{\rho}(3\lambda + 2\mu)\sqrt{1 - D}\alpha\text{tr}\boldsymbol{\varepsilon}^e + \frac{c_v}{T_0}(T - T_0)R,\tag{6.100b}$$

$$R = \rho \frac{\partial \psi}{\partial r} = (1 - D)R_0r,\tag{6.100c}$$

$$\begin{aligned}Y &= -\rho \frac{\partial \psi}{\partial D} = \frac{1}{2}R_0r^2 + \frac{1}{2}\lambda(\text{tr}\boldsymbol{\varepsilon}^e)^2 + \mu(\text{tr}\boldsymbol{\varepsilon}^e \boldsymbol{\varepsilon}^e) \\ &\quad + \frac{1}{2}\frac{\alpha}{\sqrt{1 - D}}(3\lambda + 2\mu)(T - T_0)\text{tr}\boldsymbol{\varepsilon}^e.\end{aligned}\tag{6.100d}$$

(2) Dissipation Potential and Evolution Equations

The dissipation potential F of the plastic deformation and damage development, on the other hand, are given by

$$\begin{aligned}F(\tilde{\boldsymbol{\sigma}}, \tilde{R}; T) &= F^P(\tilde{\boldsymbol{\sigma}}, \tilde{R}; T) + F^H(\tilde{R}) + F^D(\tilde{\boldsymbol{\sigma}}, Y; D) \\ &= \tilde{\sigma}_{EQ} - \tilde{R} - \sigma_Y + \frac{1}{2} \frac{B}{R_0} \tilde{R}^2 + Y \left[\frac{\chi(\tilde{\boldsymbol{\sigma}})}{A} \right]^a \frac{1}{(1 - D)^b},\end{aligned}\tag{6.101}$$

where a , b , A and B are material constants. The effective stress $\tilde{\sigma}$ and the effective isotropic hardening variable \tilde{R} in the above equation and their associated variables $\tilde{\epsilon}^e$, \tilde{r} are defined by the hypothesis of total energy equivalence of [Section 2.3.6](#), and are given by

$$\tilde{\sigma} = \frac{\sigma}{\sqrt{1-D}}, \quad \tilde{\epsilon}^e = \sqrt{1-D}\epsilon^e, \quad (6.102a)$$

$$\tilde{R} = \frac{R}{\sqrt{1-D}}, \quad \tilde{r} = \sqrt{1-Dr}. \quad (6.102b)$$

Finally, the symbol $\chi(\tilde{\sigma})$ in Eq. (6.101) denotes a ductile damage criteria, and is given by

$$\begin{aligned} \chi(\tilde{\sigma}) &= \frac{(\sigma_{EQ})^2}{2E(1-D)^2} \left[\frac{2}{3}(1+\nu) + 3(1-2\nu) \left(\frac{\sigma_H}{\sigma_{EQ}} \right)^2 \right] \\ &+ \frac{1}{2} \frac{R^2}{R_0(1-D)} - \frac{3}{2} \frac{\alpha}{(1-D)^{3/2}} (T - T_0) \sigma_H. \end{aligned} \quad (6.102c)$$

Then the constitutive equation of d^p and the evolution equations of r and D are provided by Eqs. (4.29) and (6.101) as follow:

$$d^p = \dot{A} \frac{\partial F}{\partial \sigma} = \frac{3}{2} (1-D)^{-1/2} \frac{\sigma^D}{\sigma_{EQ}} \dot{A}, \quad (6.103a)$$

$$\dot{r} = \dot{A} \frac{\partial F}{\partial R} = (1-D)^{-1/2} \left[1 - b(1-D)^{-1/2} r \right] \dot{A}, \quad (6.103b)$$

$$\dot{D} = \dot{A} \frac{\partial F}{\partial Y} = (1-D)^{-b} \left[\frac{\chi(\tilde{\sigma})}{A} \right]^a \dot{A}. \quad (6.103c)$$

The analysis of a forming process necessitates the specification of the conditions of the contact and the friction between work and tool. The accuracy of the analysis depends largely on the pertinence of this modeling.

The friction condition is usually expressed as a relation among the normal stress σ_n , shear stress τ_s and the relative tangential velocity v_s between work and tool. The friction condition in this analysis is postulated to be rate-independent and to be given by the generalized Coulomb friction model.

$$\tau_s = -\mu(\sigma_n) |v_s|^{q-1} v_s, \quad (6.104)$$

where μ and q are temperature dependent material constants. It is assumed, furthermore, that the friction law is not affected by damage.

The numerical simulation of metal forming process can be performed by incorporating the above coupled deformation and damage theory into a large deformation finite element program.

(3) Examples of Damage Analysis in Forging and Blanking Process

As the application of the coupled damage theory developed above, Figs. 6.11 and 6.12 show the damage and fracture development in a forging and a blanking process of metal (Saanouni, Nesnas and Hammi 2000). The figures were obtained by the two-dimensional fully adaptive finite element analysis performed by deleting the completely damaged elements.

Figure 6.11 shows the final fracture observed in the side pressing of an aluminum alloy cylinder of the diameter $d = 30$ mm. The punch displacement in the figure was $u = 9$ mm, and the fracture of the work has been induced by the cross-linked shear bands starting from the ends of the contact surfaces between the punch and the cylinder.

Figure 6.12, on the other hand, shows a damage state in blanking of a DP 600 steel circular plate of 1 mm thick at the punch displacement $u = 0.14$ mm. Two damaged zones first appear in the blank; i.e., the one induced closely to the punch flank at the beginning of the cutting edge radius and the second appearing closely to the cutting edge of the lower die flank. Then, these two damaged zones extend rapidly to form a narrow shear band or a macroscopic crack, and give rise to the final blanking at the punch displacement of $u = 0.22$ mm.

(4) Elaboration and Extension of the Metal Forming Analysis

The coupled ductile-damage and thermoelastic-plastic theory of Eqs. (6.99) through (6.103) was extended thereafter to include the combined isotropic-kinematic hardening viscoplasticity, and was applied to the plastic and damage analyses in wide range of metal forming processes, e.g., axisymmetric forging, cold extrusion, orthogonal cutting by chip formation, three-dimensional splitting of thin sheets (Saanouni 2006; Saanouni et al. 2011).

One of the important difficulties encountered in metal forming analysis is the local instability in damage development. Figure 6.13 elucidates one of these examples, and shows the discontinuous *central burst* (or the occurrence of the *chevron-shaped cracks*) appearing in the axisymmetric cold forward extrusion in a commercial steel, together with the two-dimensional finite element simulation based on the refined fully coupled analysis. The initial radius R_b and the initial

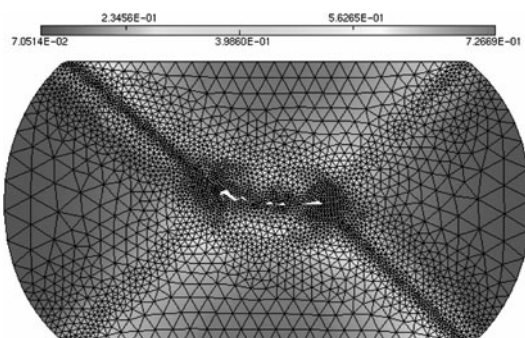


Fig. 6.11 Damage and fracture in an aluminum alloy cylinder subject to lateral compression

Source: Saanouni et al. (2000, p. 226, Fig. 9) (Elaborated figure by courtesy of K. Saanouni)

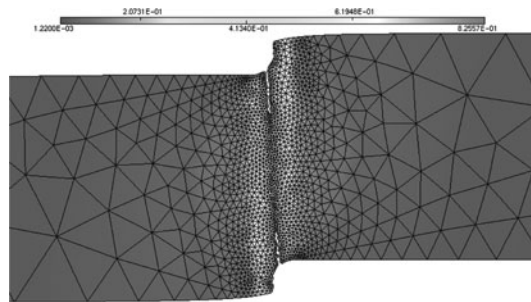
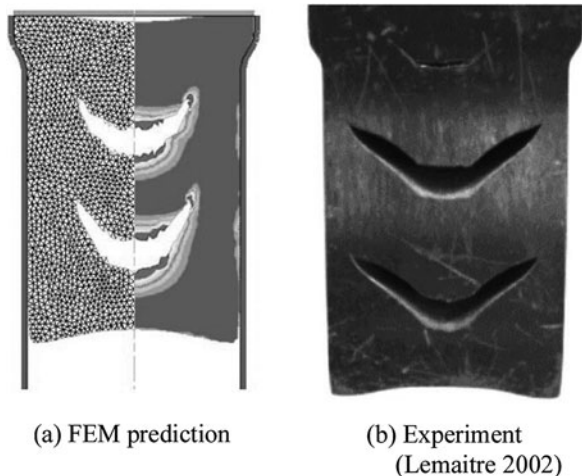


Fig. 6.12 Damage and fracture in blanking of a circular steel plate at the punch displacement of $u = 0.14$ mm (The diameter and the cutting edge radius of the punch are $d = 20$ mm and $r = 0.1$ mm)

Source: Saanouni et al. (2000, p. 235, Fig. 14) (Elaborated figure by courtesy of K. Saanouni)

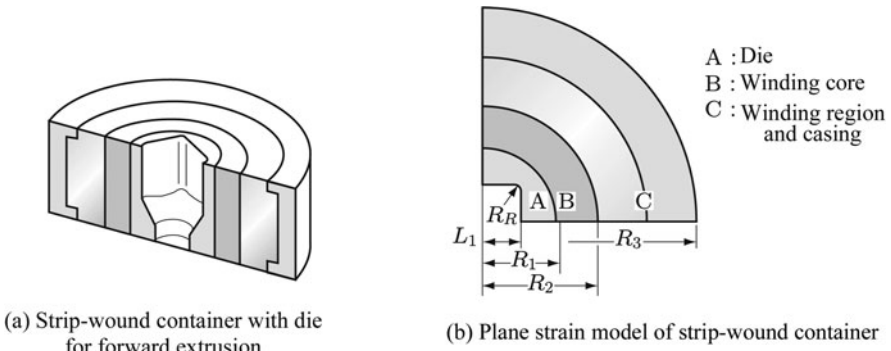
Fig. 6.13 Discontinuous chevron cracks in axisymmetric cold forward extrusion and its finite element simulation (die-billet friction coefficient and material ductility, i.e., fracture strain, are $\xi_f = 0.15$ and $\varepsilon_r = 19\%$)
Source: Saanouni et al. (2004, p. 2330, Fig. 21)



length L of the billet are 35 mm and 75 mm, while the areal reduction A_r and the die semi-angle α_d are 10% and 30° , respectively. The occurrence of the chevron cracks is not only sensitive to the parameters of the extrusion process, but also is governed essentially by the damage-induced change in the stress distribution in the billet. Thus its accurate prediction is possible only by means of the fully coupled nonlinear hardening-ductile damage analysis.

6.3.3 Fatigue Life Assessment of a Cold Working Tool

Metal forming tools are subject to repeated and high rate action of large working stress. The prolongation of the fracture life of these tools and the accurate prediction of their fracture life are essential problems for the development of efficient forging



(a) Strip-wound container with die

for forward extrusion

(b) Plane strain model of strip-wound container

Fig. 6.14 Die for forward-extrusion and plane strain model for damage analysis

Source: Pedersen (2000, p. 800, Fig. 1; p. 807, Fig. 2)

processes. We now consider the continuum damage mechanics procedure of the fatigue damage assessment of a cold working die shown in Fig. 6.14 (Pedersen 2000).

Complicated three-dimensional cyclic plastic strain as a result of repeated action of the forging load may induce significant elastic-plastic damage in the dies. For a proper description of the cyclic hardening behavior under multiaxial loading, we postulate a scalar damage variable D and assume the following plastic constitutive equation

$$\dot{\epsilon}^p = \dot{A} \frac{\partial F^p}{\partial \sigma}, \quad (6.105)$$

$$F^p = (\tilde{\sigma} - A)_{EQ} - R - \sigma_Y = 0, \quad (6.106)$$

where $\tilde{\sigma}$, σ_Y , A and R are the effective stress, the initial yield stress, the kinematic and the isotropic hardening variables, respectively. Cyclic hardening in multiaxial state of loading depends largely not only on the magnitude of the cyclic strain range (or the cyclic stress range) and the maximum strain in the loading path, but also on the geometry and non-proportionality of the path. An accurate description of this loading path dependence can be facilitated by the following *Armstrong-Frederick evolution equation* for the hardening variables R and A (Chaboche 1986; Ohno and Wang 1994; Tanaka 1994)

$$\dot{R} = b(R_\infty - R)\dot{A}, \quad (6.107)$$

$$\dot{A} = \sum_{n=1}^3 \dot{A}^{(n)}, \quad (6.108)$$

$$\dot{A}^{(n)} = c^{(n)} \left[A_\infty^{(n)} (1 - D) \dot{\epsilon}^p - d^{(n)} \left(A_{EQ}^{(n)} \right)^{m^{(n)}} A^{(n)} \dot{A} \right], \quad (6.109)$$

where b , $c^{(n)}$, $d^{(n)}$, R_∞ , $A_\infty^{(n)}$ and $m^{(n)}$ are material constants.

The evolution equation of damage variable D , on the other hand, is given by Eq. (6.8), i.e.,

$$\dot{D} = \frac{Y}{S} \dot{p} H(p - p_D), \quad (6.110)$$

where $H(\cdot)$ and Y are the Heaviside function and the damage-associated variable given by Eq. (6.9). Furthermore, since the fatigue damage process depends largely on the sign of the average stress σ_H , Eq. (6.9) is modified here as follows

$$Y = \frac{(\sigma_{EQ})^2}{2E(1-D)^2} \left\{ \left[1 + \varsigma \frac{\sigma_H}{\sigma_Y} \right] H(\sigma_H) + \left[\exp\left(\varsigma \frac{\sigma_H}{\sigma_Y}\right) \right] H(-\sigma_H) \right\}, \quad (6.111)^1$$

where ς is a material constant.

The simulation of the fatigue damage process was performed by incorporating the above equations into a finite element program, and by simplifying the forward-extrusion die reinforced by strip winding of Fig. 6.14a by a plane strain die model of Fig. 6.14b. The die A in the center of (a) is inserted into the winding core B radially compressed by the strip-wound ring C.

Figure 6.15 shows the damage development at the critical corner of the inner surface of the die A calculated for three different pre-stressing systems. The die A is subject to cyclic uniform pressure $p_{max}/E = 0.005$ at the inner surface. The pre-stressed die I is the conventional stress ring where die A is inserted into the unified

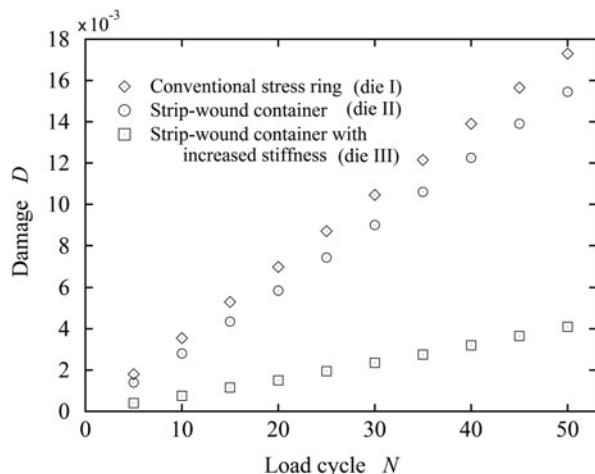


Fig. 6.15 Damage development in pre-stressed dies for forward-extrusion
Source: Pedersen (2000, p. 815, Fig. 10)

¹We should note that the variable Y thus defined, strictly speaking, has not the thermodynamically associated relation with the damage variable D of Eq. (6.110).

press ring BC, while the die II consists of a winding core B pre-stressed by the strip-wound ring C. In the die III, the core B is replaced by an increased-stiffness core made of cemented carbide WC/Co. Figure 6.15 shows that the amount of damage varies markedly depending on the pre-stressing systems, and the damage in the die III is less than 1/4 of that in the conventional pre-stressing system.

6.4 Analysis of Sheet Metal Forming Limit by Anisotropic Damage Theory

Another important subject of metal forming process is the prediction of sheet metal forming limit. The condition of the onset of the localized necking is usually estimated in the principal plastic strain space, with the first and the second principal plastic strain ε_1 and ε_2 as the abscissa and the ordinate, respectively. The locus of the onset of the localized necking in this plane is called a *forming limit diagram*.

In this diagram, the region of the negative strain ratio $\alpha = \varepsilon_2/\varepsilon_1 \leq 0$ and that of the positive one $\alpha > 0$ have different mechanisms of the necking. In the conventional scheme, however, the necking in both of these regions has been supposed as the instability of the plastic deformation, and analyzed in the framework of classical plasticity theory. Thus, in these analyses, the anisotropic cavity development and significant plastic anisotropy induced in the forming processes have been disregarded, and could not provide accurate prediction of the experimental results.

Let us now discuss this problem in some detail by applying the anisotropic damage theory described in [Chapter 5](#) and by referring to the work of Chow and others (Chow, Yu, and Demeri [1997, 2001](#)).

6.4.1 Elastic-Plastic Constitutive Equation, Evolution Equation of Damage

(1) Damage Tensor, Damage Effect Tensor and Elastic Constitutive Equation

Suppose that a sheet of metal is initially orthotropic elastic-plastic, and that its damage state is represented by a second-order symmetric damage tensor \mathbf{D} of Eq. (2.15).

By postulating the hypothesis of complementary strain energy equivalence, the elastic constitutive equation of the damaged material is given by Eqs. (2.61) and (2.62):

$$\boldsymbol{\varepsilon}^e = \mathbb{S}(\mathbf{D}) : \boldsymbol{\sigma}, \quad (6.112a)$$

$$\mathbb{S}(\mathbf{D}) = \mathbb{M}(\mathbf{D})^T : \mathbb{S}_0 : \mathbb{M}(\mathbf{D}), \quad (6.112b)$$

where $\boldsymbol{\varepsilon}^e$ and \mathbb{S}_0 denote the elastic strain and the elastic compliance tensor of the undamaged material.

In view of the effective stress $\tilde{\sigma}$ and the effective strain $\tilde{\epsilon}$ defined by Eq. (2.64)

$$\tilde{\sigma} = \mathbb{M}(\mathbf{D}) : \boldsymbol{\sigma}, \quad \tilde{\epsilon} = \mathbb{M}(\mathbf{D})^{-T} : \boldsymbol{\epsilon}, \quad (6.113a)$$

Equation (6.112a) may be written in an alternative form

$$\tilde{\epsilon}^e = \mathbb{S}_0 : \tilde{\sigma}. \quad (6.113b)$$

For the matrix representation of the elastic constitutive equation (6.112), we must derive the matrices of the damage effect tensor $\mathbb{M}(\mathbf{D})$ and of the elastic compliance tensor \mathbb{S}_0 of the undamaged material. We first represent the damage state by the damage effect tensor $\mathbb{M}^{(2)}(\mathbf{D})$ of Eq. (2.46). By recalling Eq. (2.103), the matrix representation of $\mathbb{M}^{(2)}(\mathbf{D})$ is furnished by

$$\left[\mathbb{M}_{pq}^{(2)} \right] = \left[M_{pr}^{(2)} \right] \left[W_{rq} \right] = \begin{bmatrix} \Phi_1 & 0 & 0 & 0 & 0 & 0 \\ 0 & \Phi_2 & 0 & 0 & 0 & 0 \\ 0 & 0 & \Phi_3 & 0 & 0 & 0 \\ 0 & 0 & 0 & (\Phi_2 \Phi_3)^{1/2} & 0 & 0 \\ 0 & 0 & 0 & 0 & (\Phi_3 \Phi_1)^{1/2} & 0 \\ 0 & 0 & 0 & 0 & 0 & (\Phi_1 \Phi_2)^{1/2} \end{bmatrix}, \quad (6.114a)$$

$$\Phi_i = (1 - D_i)^{-1}, \quad (i = 1, 2, 3). \quad (6.114b)$$

The elastic compliance matrix $\left[\mathbb{S}_{pq}^0 \right]$ of undamaged orthotropic elastic material is given by Eq. (12.286) in the Chapter 12. Then, by substituting Eqs. (6.114) and (12.286) into Eq. (2.105), the matrix $\left[\mathbb{S}_{pq}^{(2)}(\mathbf{D}) \right]$ of the elastic compliance tensor (6.112b) of this material in the damaged state is given:

$$\begin{aligned} \left[\mathbb{S}_{pq}^{(2)}(\mathbf{D}) \right] &= \left[M_{rp}^{(2)}(\mathbf{D}) \right]^T \left[\mathbb{S}_{rs}^0 \right] \left[M_{sq}^{(2)}(\mathbf{D}) \right] \\ &= \begin{bmatrix} 1/\tilde{E}_1 & -\tilde{v}_{21}/\tilde{E}_2 & -\tilde{v}_{31}/\tilde{E}_3 & 0 & 0 & 0 \\ -\tilde{v}_{12}/\tilde{E}_1 & 1/\tilde{E}_2 & -\tilde{v}_{32}/\tilde{E}_3 & 0 & 0 & 0 \\ -\tilde{v}_{13}/\tilde{E}_1 & -\tilde{v}_{23}/\tilde{E}_2 & 1/\tilde{E}_3 & 0 & 0 & 0 \\ 0 & 0 & 0 & 1/2\tilde{G}_{23} & 0 & 0 \\ 0 & 0 & 0 & 0 & 1/2\tilde{G}_{31} & 0 \\ 0 & 0 & 0 & 0 & 0 & 1/2\tilde{G}_{12} \end{bmatrix}, \end{aligned} \quad (6.115a)$$

$$\tilde{E}_i = E_i(\Phi_i)^{-2}, \quad 2\tilde{G}_{ij} = 2G_{ij}(\Phi_i\Phi_j)^{-1}$$

$$\tilde{v}_{ij} = v_{ij}\Phi_j(\Phi_i)^{-1}, \quad \Phi_i = (1 - D_i)^{-1}. \quad (6.115b)$$

In the particular case of initial isotropic elastic material, Eq. (6.115) leads to Eq. (2.106).

(2) Dissipation Potential and Plastic Constitutive Equation

The plastic constitutive equation and the evolution equation of the anisotropic damaged material were discussed in Sections 5.1 and 5.2. As in the case of Eq. (5.24), we postulate that the total dissipation potential F consists of the plastic dissipation potential F^P and the damage one F^D

$$F(\sigma, R, Y, B; r, D, \beta) = F^P(\sigma, R; D) + F^D(Y, B; \beta), \quad (6.116)$$

where R , Y and B are the isotropic hardening variable, damage-associated variable and damage strengthening variable, respectively, and were defined by Eq. (6.5). Furthermore, r and β in Eq. (6.116) denote the strain-hardening and the damage-strengthening internal variable.

By means of Eq. (5.25), the plastic dissipation potential F^P may be expressed as

$$F^P(\sigma, R; D) = \tilde{\sigma}_{EQ} - [\sigma_Y + R(r)], \quad (6.117a)$$

$$\tilde{\sigma}_{EQ} = \left(\frac{1}{2} \tilde{\sigma} : \mathbb{H} : \tilde{\sigma} \right)^{1/2} = \left(\frac{1}{2} \sigma : \tilde{\mathbb{H}} : \sigma \right)^{1/2}, \quad (6.117b)$$

$$\tilde{\mathbb{H}} = M(D)^T : \mathbb{H} : M(D), \quad (6.117c)$$

where σ_Y and $\tilde{\sigma}_{EQ}$ are the initial yield stress and the equivalent effective stress. The symbol \mathbb{H} , furthermore, is a fourth-order positive semi-definite tensor of plastic anisotropy, whose components are given by Eq. (5.26).

The plastic constitutive equations of the damaged material can be derived by substituting F^P of Eq. (6.117) into the evolution equation of Eq. (5.10); they have the following forms, similarly to Eqs. (5.33) through (5.36)

$$\dot{\epsilon}^P = \dot{\Lambda}^P \frac{\partial F^P}{\partial \sigma} = \frac{\dot{\Lambda}^P}{2\tilde{\sigma}_{EQ}} \tilde{\mathbb{H}} : \sigma, \quad (6.118a)$$

$$\dot{r} = -\dot{\Lambda}^P \frac{\partial F^P}{\partial R} = -\dot{\Lambda}^P \frac{\partial (-R)}{\partial R} = \dot{\Lambda}^P, \quad (6.118b)$$

$$\dot{\Lambda}^P = \frac{1}{2\tilde{\sigma}_{EQ}} \frac{\sigma : \mathbb{H} : \dot{\sigma}}{\partial R / \partial r}, \quad (6.118c)$$

$$\dot{p} = 2 \left(\frac{1}{2} \dot{\tilde{\epsilon}}^p : \mathbb{H}^{-1} : \dot{\tilde{\epsilon}}^p \right)^{1/2} = 2 \left(\frac{1}{2} \dot{\epsilon}^p : \tilde{\mathbb{H}}^{-1} : \dot{\epsilon}^p \right)^{1/2}, \quad (6.118d)$$

where Eq. (6.118d) was derived from Eqs. (6.117c) and (6.118a).

(3) Damage Dissipation Potential and Evolution Equation of Damage

As to the damage dissipation potential F^D of Eq. (6.116), we will assume Eq. (5.28):

$$F^D(\mathbf{Y}, B; \beta) = Y_{EQ} - [B_0 + B(\beta)] = 0, \quad (6.119a)$$

$$Y_{EQ} = \left(\frac{1}{2} \mathbf{Y} : \mathbb{L} : \mathbf{Y} \right)^{1/2}, \quad (6.119b)$$

$$L_{ijkl} = \frac{1}{2} \varsigma \delta_{ij} \delta_{kl} + \frac{1}{2} (1 - \varsigma) (\delta_{ik} \delta_{jl} + \delta_{il} \delta_{jk}), \quad (6.119c)$$

where B_0 and B denote the threshold value of Y_{EQ} for the damage initiation and the damage-strengthening variable, respectively. The tensor \mathbb{L} of Eq. (6.119) characterizes the anisotropy of damage development, and is a fourth-order isotropic tensor with a material constant ς .

Finally the evolution equations of β and \mathbf{D} are derived by substituting Eq. (6.119) into Eq. (5.10) as follow (similarly to Eqs. (5.37) through (5.40)):

$$\dot{\mathbf{D}} = \dot{\Lambda}^D \frac{\partial F^D}{\partial \mathbf{Y}} = \frac{1}{2(Y_{EQ})^{1/2}} (\mathbb{L} : \mathbf{Y}) \dot{\Lambda}^D, \quad (6.120a)$$

$$\dot{\beta} = -\dot{\Lambda}^D \frac{\partial F^D}{\partial B} = -\dot{\Lambda}^D \frac{\partial (-B)}{\partial B} = \dot{\Lambda}^D, \quad (6.120b)$$

$$\dot{\Lambda}^D = \frac{1}{2(Y_{EQ})^{1/2}} \frac{\mathbf{Y} : \mathbb{L} : \dot{\mathbf{Y}}}{\partial B / \partial \beta}. \quad (6.120c)$$

6.4.2 Criteria of Localized Necking and Fracture – Accumulated Damage Instability Criterion

The aspect of the development of localized necking differs largely depending on whether the principal plastic strain ratio $\alpha (= \varepsilon_2 / \varepsilon_1)$ is non-positive $\alpha \leq 0$ or positive $\alpha > 0$. Namely, in the case of $\alpha \leq 0$, the reduction in plate thickness is accompanied by the corresponding reduction in its width, and large material damage is induced. In the case of $\alpha > 0$, on the other hand, both strains in the sheet plane are positive, and the damage development is not significant. However, we may assume that the onset of the localized necking in sheets in these cases is governed by the damage variable \mathbf{D} , the damage-strengthening internal variable β and the principal plastic strain ratio α . Thus, by defining a new parameter

$$\beta_L \equiv \beta - \alpha \varsigma G(D_1 + D_2 + D_3), \quad (6.121a)$$

or

$$d\beta_L \equiv d\beta - \alpha \varsigma G(dD_1 + dD_2 + dD_3), \quad (6.121b)$$

the condition for the start of localized necking can be expressed by (Chow et al. 2001; Chow and Yang 2004):

$$\beta_L = \beta_{LCR}, \quad (6.121c)$$

where β_{LCR} signifies a material constant identified by the tests. The symbol ς in Eq. (6.121) denotes a material constant employed in Eq. (6.119c), while G is a component of the orthotropic tensor \mathbb{H} of Eq. (6.117c).

Finally, by postulating that the fracture of the material is governed by the damage state, the final fracture condition of the sheet can be expressed by the use of the damage-strengthening internal variable β

$$\beta = \beta_{CR}, \quad (6.122)$$

where β_{CR} is another material constant whose value is determined by uniaxial tension tests.

6.4.3 Determination of Material Constants for Deformation and Damage

Let us now consider the evaluation of the material constants in the accumulated damage instability criterion developed above. Suppose that the material is an elastic material of initial orthotropy, and that the principal axes of the applied stress coincide with those of the orthotropy of the material. Then the damage caused in the material under proportional loading also has the principal directions identical to those of the stress.

In view of Eq. (6.115), the elastic compliance matrices in the undamaged and the damaged states are given as follow:

$$\left[S_{pq}^0 \right] = \begin{bmatrix} \frac{1}{E_1} & -\frac{\nu_{21}}{E_2} & -\frac{\nu_{31}}{E_3} \\ -\frac{\nu_{12}}{E_1} & \frac{1}{E_2} & -\frac{\nu_{32}}{E_3} \\ -\frac{\nu_{13}}{E_1} & -\frac{\nu_{23}}{E_2} & \frac{1}{E_3} \end{bmatrix}, \quad (6.123)$$

$$[\mathbf{S}_{pq}(\mathbf{D})] = \begin{bmatrix} \frac{1}{\tilde{E}_1} & -\frac{\tilde{\nu}_{21}}{\tilde{E}_2} & -\frac{\tilde{\nu}_{31}}{\tilde{E}_3} \\ -\frac{\tilde{\nu}_{12}}{\tilde{E}_1} & \frac{1}{\tilde{E}_2} & -\frac{\tilde{\nu}_{32}}{\tilde{E}_3} \\ -\frac{\tilde{\nu}_{13}}{\tilde{E}_1} & -\frac{\tilde{\nu}_{23}}{\tilde{E}_2} & \frac{1}{\tilde{E}_3} \end{bmatrix}, \quad (6.124a)$$

$$\tilde{E}_i = E_i(1 - D_i)^2, \quad \tilde{\nu}_{ij} = \nu_{ij} \frac{1 - D_i}{1 - D_j}, \quad (\text{no sum for } i, j; i, j = 1, 2, 3). \quad (6.124b)$$

From Eq. (6.124) the damage variables D_1 and D_2 can be identified to be

$$D_1 = 1 - \left(\frac{\tilde{E}_1}{E_1} \right)^{1/2}, \quad D_2 = 1 - (1 - D_1) \frac{\nu_{12}}{\tilde{\nu}_{12}}. \quad (6.125)$$

Concerning the damage rates, on the other hand, Eqs. (6.119) and (6.120) provide

$$\begin{aligned} \dot{\mathbf{D}} &= \frac{\dot{\mathcal{A}}^D}{2(Y_{EQ})^{1/2}} (\mathbb{L} : \mathbf{Y}) = \frac{\dot{\mathcal{A}}^D}{2(Y_{EQ})^{1/2}} \begin{bmatrix} 1 & \varsigma & \varsigma \\ \varsigma & 1 & \varsigma \\ \varsigma & \varsigma & 1 \end{bmatrix} \begin{bmatrix} Y_1 \\ Y_2 \\ Y_3 \end{bmatrix} \\ &= \frac{\dot{\mathcal{A}}^D}{2(Y_{EQ})^{1/2}} \begin{bmatrix} Y_1 + \varsigma(Y_2 + Y_3) \\ Y_2 + \varsigma(Y_3 + Y_1) \\ Y_3 + \varsigma(Y_1 + Y_2) \end{bmatrix}. \end{aligned} \quad (6.126)$$

This relation applied to the case of uniaxial tension $\sigma_{22} = \sigma_{33} = 0$ and $Y_2 = Y_3 = 0$ gives

$$\frac{\dot{D}_2}{\dot{D}_1} = \frac{\dot{D}_3}{\dot{D}_1} = \varsigma, \quad (6.127)$$

and thus for the proportional loading we have

$$\frac{D_2}{D_1} = \frac{D_3}{D_1} = \varsigma. \quad (6.128)$$

In the particular case of initial isotropic elasticity, Eqs. (6.125) and (6.128) give the value of ς :

$$\varsigma = \frac{1 - (\tilde{E}/E)^{1/2}(\nu/\tilde{\nu})}{1 - (\tilde{E}/E)^{1/2}}. \quad (6.129)$$

Finally, the plastic anisotropy of the material must be identified. Then, we take the principal directions of the plastic anisotropy 1, 2 and 3 in the rolling direction, the transverse direction and the thickness direction of the plate, respectively. From Eqs. (6.117) and (5.26), the initial plastic yield condition is written as

$$f = \frac{1}{G+H} \left[F(\sigma_{22} - \sigma_{33})^2 + G(\sigma_{33} - \sigma_{11})^2 + H(\sigma_{11} - \sigma_{22})^2 \right] - (\sigma_{Y11})^2 = 0, \quad (6.130)$$

where σ_{Y11} denotes the yield stress in simple tension in the rolling direction. By deriving the flow rule for plane state of stress from this relation, we evaluate the *Lankford values* for the uniaxial tension in the rolling and the transverse directions,

$$R_0 = \frac{\varepsilon_{22}}{\varepsilon_{33}} = \frac{H}{G}, \quad R_{90} = \frac{\varepsilon_{11}}{\varepsilon_{33}} = \frac{H}{F}. \quad (6.131)$$

Then the anisotropy parameters of Eq. (6.130) are determined as follow

$$F = \frac{R_0}{R_{90}(1+R_0)}, \quad G = \frac{1}{1+R_0}, \quad H = \frac{R_0}{1+R_0}. \quad (6.132)$$

The material constants for plasticity and damage in the above relations were determined for the 6111-T4 aluminum alloy, and are given as follow (Chow et al. 2001)

$$E = 70.1 \text{ GPa}, \quad \nu = 0.33, \quad \sigma_Y = 177 \text{ MPa}, \quad (6.133a)$$

$$n = 0.22, \quad R_0 = 0.662, \quad R_{90} = 0.787,$$

$$\varsigma = 0.375, \quad \beta_{LCR} = 0.0865, \quad \beta_{CR} = 0.117, \quad \varsigma G = 0.225. \quad (6.133b)$$

6.4.4 Numerical Results of Forming Limit Diagram

Figure 6.16 shows the calculated and the experimental results of the *forming limit diagram* (FLD), where the strain stands for the plastic strain. The calculation was performed by integrating Eqs. (6.118) and (6.120) for the principal plastic strain ratio $\alpha = \varepsilon_{22}/\varepsilon_{11} = \text{const.}$ until the localized necking criterion (6.121) is attained. The experimental results (Graf and Hosford 1994), on the other hand, were evaluated by performing bulge tests by the use of a semi-sphere punch on rectangular sheets with different width-length ratios. The strain ratio α was measured from the square grids printed on the specimens. Figure 6.16a shows the forming limit diagram for proportional loading, and the experimental and the calculated results are in good correlation.

Figure 6.16b, on the other hand, is the results of the bulge tests on specimens cut out in the same direction to the prestrain of $\varepsilon_{11} = 0.18$ in the rolling direction. Figure 6.16c, furthermore, shows the results of the tests on specimens cut out

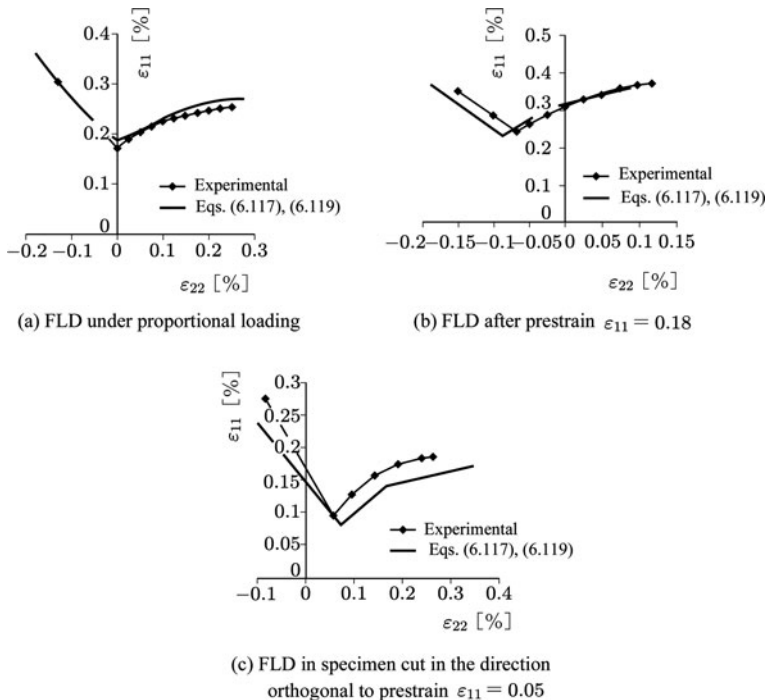


Fig. 6.16 Forming limit diagram for 6111-T4 aluminum alloy sheet
Source: Chow et al. (2001, p. 480, Fig. 3; p. 481, Fig. 5; p. 483, Fig. 11)

perpendicularly to the prestrain $\varepsilon_{11} = 0.05$ in the rolling direction. It is observed that the discrepancy between the experimental and the predicted results can not be disregarded any more for strain paths largely deviated from the proportional loading.

6.4.5 Other Damage Mechanics Analysis of Forming Limit

The localized necking criteria of Eq. (6.121) is expressed in terms of the accumulated damage state parameters, and hence can be applicable to the sheet metal forming under arbitrary paths of loading. The mechanisms of the start of localized necking are mainly governed by the bifurcation and instability of their inelastic deformation. Thus the forming limit analysis can be performed directly by the bifurcation and instability analysis in the damaged sheets.

Chow and Jie (2004), for example, derived a damage-coupled localized necking criteria by applying the elastic-plastic anisotropic damage theory of Section 6.4.1 to the modified vertex theory. The criteria leads to explicit expression of the localized necking criteria on both side of the principal plastic strain ratio α on the forming limit diagram (FLD), i.e., for $\alpha \leq 0$ and $0 < \alpha$. Strictly speaking, however, they

are applicable only to the case of the proportional loading and rate-independent strain-hardening material.

The anisotropic damage theory of Section 6.4.1 was applied also to the bifurcation analysis of strain-softening damaged material encountered in warm and heat working (Chow, Jie, and Wu 2007), and facilitates the derivation of the forming limit criteria in this condition.

6.5 Constitutive Equations of Void-Containing Ductile Material

Ductile damage in metals develops as a result of initiation, growth and coalescence of microscopic voids in the material. These voids are brought about by the decohesion of the interfaces between microscopic inclusions and the matrix, or by cracking of the inclusions. The growth and the coalescence of the voids are caused by the large plastic deformation or by the localization of plastic deformation in the neighboring ligaments.

In the present section, we consider the constitutive model of Gurson and that of Rousselier which describe the process of nucleation, growth and coalescence of spherical voids in metals. The application and the elaboration of these models are also discussed.

6.5.1 Constitutive Model of Gurson

(1) Gurson's Yield Function

Gurson (1977) approximated a continuum containing microvoids by a rigid-plastic sphere containing a concentric spherical cavity, and performed a rigid-plastic analysis of its axisymmetric deformation. On the basis of this analysis, Gurson proposed an approximate yield function of a void-containing damaged material by the use of a void volume fraction f as follows:

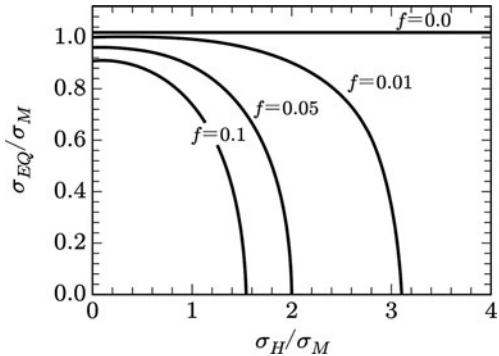
$$F(\sigma_{ij}, \sigma_M, f) = \left(\frac{\sigma_{EQ}}{\sigma_M} \right)^2 + 2f \cosh \left(\frac{3}{2} \frac{\sigma_H}{\sigma_M} \right) - f^2 - 1 = 0, \quad (6.134)$$

where σ_{ij} , σ_{EQ} and $\sigma_H = \sigma_{kk}/3$ are the macroscopic stress, equivalent stress and the mean stress acting on the void-containing damaged material, and σ_M denotes the yield stress of matrix of the material. In the particular case of $f = 0$, Eq. (6.134) is reduced to the von Mises yield criterion. Figure 6.17 shows the dependence of the yield function (6.134) on the void volume fraction f .

(2) Evolution Equation of Void Volume Fraction

For the application of the yield function of Eq. (6.134), we should first derive the evolution equation of the void volume fraction f during the damage process.

Fig. 6.17 Effect of void volume fraction on Gurson's yield function
Source: Gurson (1977, p. 12, Fig. 11)



The rate of the void volume fraction \dot{f} may be divided into the void growth rate \dot{f}_{grow} and the nucleation rate of new voids \dot{f}_{nucl}

$$\dot{f} = \dot{f}_{grow} + \dot{f}_{nucl}. \quad (6.135a)$$

Since the material matrix can be assumed incompressible, the void growth rate should be equal to the macroscopic volumetric strain rate (Needleman and Rice 1978)

$$\dot{f}_{grow} = (1 - f) \dot{\varepsilon}_{kk}^p. \quad (6.135b)$$

The nucleation of new voids occurs mainly by the cracking of inclusions together with the decohesion of the interfaces between the inclusions and matrix, and thus we have

$$\dot{f}_{nucl} = A_1 (\dot{\sigma}_M + \dot{\sigma}_H) + A_2 \dot{\varepsilon}_M^p, \quad (6.135c)$$

where $\dot{\varepsilon}_M^p$ is the equivalent plastic strain of the matrix. If the voids nucleate according to the probability distributions with the stress σ_N and the strain ε_N as their mean values together with s_N as their standard deviation, the coefficients A_1 and A_2 in Eq. (6.135c) can be given as follows (Chu and Needleman 1980):

$$A_1 = \frac{f_N}{s_N \sqrt{2\pi}} \exp \left[-\frac{1}{2} \left(\frac{\sigma_M + (\sigma_{kk}/3) - \sigma_N}{s_N} \right)^2 \right], \quad (6.136a)$$

$$A_2 = \frac{f_N}{s_N \sqrt{2\pi}} \exp \left[-\frac{1}{2} \left(\frac{\dot{\varepsilon}_M^p - \dot{\varepsilon}_N}{s_N} \right)^2 \right], \quad (6.136b)$$

where f_N is the volume fraction of void nucleating particles.

(3) Plastic Constitutive Equation of Void-Containing Damaged Material

When matrix material obeys the normality rule based on the von Mises yield function, the macroscopic plastic strain rate is also given by the relation (Berg 1970)

$$\dot{\varepsilon}_{ij}^p = \dot{A} \frac{\partial F}{\partial \sigma_{ij}}, \quad (6.137)$$

where \dot{A} is an indeterminate multiplier, which can be determined from the *consistency condition* for Eq. (6.134), i.e.,

$$\dot{F} = \frac{\partial F}{\partial \sigma_{ij}} \dot{\sigma}_{ij} + \frac{\partial F}{\partial \sigma_M} \dot{\sigma}_M + \frac{\partial F}{\partial f} \dot{f} = 0. \quad (6.138)$$

For the calculation of this relation, the rates $\dot{\sigma}_M$ and \dot{f} must be related to the macroscopic variables σ_{ij} and $\dot{\varepsilon}_{ij}^p$.

Since the plastic work proceeds only in the matrix material, the macroscopic work rate of the damaged material is given by

$$\sigma_{ij} \dot{\varepsilon}_{ij}^p = (1-f) \sigma_M \dot{\varepsilon}_M^p. \quad (6.139)$$

By designating the *strain-hardening rate* of the material matrix by H , we have a relation

$$H = \frac{d\sigma_M}{d\varepsilon_M^p}, \quad \text{or} \quad \dot{\varepsilon}_M^p = \frac{1}{H} \dot{\sigma}_M. \quad (6.140)$$

Then, Eq. (6.139) has an alternative form

$$\dot{\varepsilon}_M^p = \frac{\sigma_{ij} \dot{\varepsilon}_{ij}^p}{(1-f)\sigma_M}, \quad \dot{\sigma}_M = H \frac{\sigma_{ij} \dot{\varepsilon}_{ij}^p}{(1-f)\sigma_M}. \quad (6.141)$$

Thus the variables $\dot{\varepsilon}_M^p$ and $\dot{\sigma}_M$ of the matrix material are related to the macroscopic variables of σ_{ij} and $\dot{\varepsilon}_{ij}^p$.

By means of Eq. (6.141), the evolution equation of the void volume fraction f of Eq. (6.135) leads to

$$\begin{aligned} \dot{f} &= (1-f) \dot{\varepsilon}_{kk}^p + A_1 (\dot{\sigma}_M + \dot{\sigma}_H) + A_2 \dot{\varepsilon}_M^p \\ &= (1-f) \dot{\varepsilon}_{kk}^p + \frac{(A_1 H + A_2)}{(1-f)\sigma_M} \sigma_{ij} \dot{\varepsilon}_{ij}^p + \frac{1}{3} A_1 \dot{\sigma}_{kk}. \end{aligned} \quad (6.142)$$

Then, from Eqs. (6.137), (6.141) and (6.142), the consistency condition (6.138) leads to the form

$$\begin{aligned}
\dot{F} &= \frac{\partial F}{\partial \sigma_{ij}} \dot{\sigma}_{ij} + \frac{\partial F}{\partial \sigma_M} \frac{H \sigma_{ij}}{(1-f) \sigma_M} \dot{\varepsilon}_{ij}^p + \frac{\partial F}{\partial f} \left[(1-f) \dot{\varepsilon}_{kk}^p + \frac{(A_1 H + A_2)}{(1-f) \sigma_M} \sigma_{ij} \dot{\varepsilon}_{ij}^p + \frac{1}{3} A_1 \dot{\sigma}_{kk} \right] \\
&= \left(\frac{\partial F}{\partial \sigma_{ij}} + \frac{\partial F}{\partial f} \frac{A_1}{3} \delta_{ij} \right) \dot{\sigma}_{ij} + \left\{ \left[H \frac{\partial F}{\partial \sigma_M} + \frac{\partial F}{\partial f} (A_1 H + A_2) \right] \frac{\sigma_{ij}}{(1-f) \sigma_M} \right. \\
&\quad \left. + (1-f) \frac{\partial F}{\partial f} \delta_{ij} \right\} \dot{\lambda} \frac{\partial F}{\partial \sigma_{ij}} = 0,
\end{aligned} \tag{6.143}$$

from which the multiplier $\dot{\lambda}$ are determined as follows

$$\dot{\lambda} = \frac{1}{M} \left(\frac{\partial F}{\partial \sigma_{ij}} + \frac{\partial F}{\partial f} \frac{A_1}{3} \delta_{ij} \right) \dot{\sigma}_{ij}, \tag{6.144a}$$

$$M = - \left\{ \left[H \frac{\partial F}{\partial \sigma_M} + \frac{\partial F}{\partial f} (A_1 H + A_2) \right] \frac{\sigma_{ij}}{(1-f) \sigma_M} + (1-f) \frac{\partial F}{\partial f} \delta_{ij} \right\} \frac{\partial F}{\partial \sigma_{ij}}. \tag{6.144b}$$

Finally, substitution of Eq. (6.144) into Eq. (6.137) furnishes the plastic constitutive equations of void-containing damaged materials

$$\dot{\varepsilon}_{ij}^p = \frac{1}{M} \left(\frac{\partial F}{\partial \sigma_{kl}} + \frac{\partial F}{\partial f} \frac{A_1}{3} \delta_{kl} \right) \dot{\sigma}_{kl} \frac{\partial F}{\partial \sigma_{ij}}. \tag{6.145}$$

6.5.2 Elaboration of Gurson Model—GTN Model

The Gurson model was elaborated thereafter by incorporating the effect of void coalescence in damage process (Tvergaard and Needleman 1984). Namely, the yield function (6.134) was revised by replacing the void volume fraction f with the corresponding *effective void volume fraction* f^* as follows

$$F(\sigma_{ij}, \sigma_M, f) = \left(\frac{\sigma_{EQ}}{\sigma_M} \right)^2 + 2f^* q_1 \cosh \left(\frac{3}{2} \frac{q_2 \sigma_H}{\sigma_M} \right) - q_3 (f^*)^2 - 1 = 0. \tag{6.146}$$

The variable $f^* = f^*(f)$ in this relation has been introduced in order to represent the significant loss of load-carrying capacity due to the void coalescence at the final stage of the fracture, and is defined:

$$f^*(f) = f, \quad \text{for } f \leq f_C, \tag{6.147a}$$

$$f^*(f) = f_C + \left(\frac{1}{q_1} - f_C \right) \frac{f - f_C}{f_F - f_C}, \quad \text{for } f > f_C, \tag{6.147b}$$

where f_C and f_F designate the critical void volume fraction at the onset of void coalescence, and the void volume fraction at the stage of complete loss of load-carrying capacity, respectively. The symbols q_1 , q_2 and q_3 , furthermore, are parameters to enhance the accuracy of the model, and are usually assumed:

$$q_1 = 1.5, \quad q_2 = 1.0, \quad q_3 = (q_1)^2. \quad (6.147c)$$

In view of Eq. (6.147), when the void volume fraction f attains to the value f_F of the fractured state, the yield function of Eq. (6.146) leads to the sum of two independent terms $(\sigma_{EQ}/\sigma_M)^2$ and $2[\cosh(3\sigma_H/2\sigma_M) - 1]$. This implies that, for the plastic deformation to occur at this state, the yield condition $F = 0$ requires $\sigma_{EQ} = \sigma_H = 0$, and hence $\sigma_{ij} = 0$. Namely the elaborated Gurson model of Eqs. (6.146) and (6.147) furnishes always vanishing stress components at the final state of fracture, which conforms to the results of the usual damage mechanics prediction (e.g., Besson et al. 2010).

The plastic constitutive equation associated with the modified yield function F of Eq. (6.146) is called *GTN model* (Gurson-Tvergaard-Needleman model), and has been applied to wide variety of ductile fracture problems, ranging from the ductile fracture mechanics and crack extension analysis (Tvergaard 1990; Xia et al. 1995; Mahnken 2002; Besson et al. 2003) to the void development and the strain localization in metal forming processes (Needleman and Triantafyllidis 1978); Oñate et al. 1988).

Since Gurson yield function (GTN model) postulates isotropic hardening of plasticity, it is applicable only to the problems of proportional loading. Then, in order to facilitate the analyses of non-proportional and cyclic loading processes, the extension of Gurson model to incorporate the kinematic hardening was also proposed (Leblond, Perrin, and Devaux 1995; Besson and Guillemer-Neel 2003).

In Sections 6.5.4 and 6.5.5 later, the application, limitation and further extension of Gurson model will be described.

6.5.3 Constitutive Model of Rousselier

By postulating damage isotropy, and by relating the damage-strengthening internal variable β with the growth rate of spherical voids, Rousselier (1987) derived a simple elastic-plastic constitutive model of voided ductile material. This constitutive model has been extended also to the case of finite deformation (Rousselier 1981).

(1) Constitutive and Evolution Equations of Void-Containing Damaged Material

Rousselier postulated first the constitutive theory of Section 5.1.1, and represented the internal state of the ductile damaged material by means of an isotropic hardening

internal variable² p and the damage-strengthening internal variable β . The damage state was assumed to be isotropic. Then, according to Eq. (5.11), he expressed the Helmholtz free energy function of the material in the form

$$\psi(\varepsilon_{ij}, p, \beta) = \psi^E(\varepsilon_{ij}^e) + \psi^P(p) + \psi^D(\beta). \quad (6.148)^2$$

By the use of ψ of this equation, the elastic constitutive equation and the generalized forces² P and B associated with the internal variables p, β are given by Eqs. (5.4) and (5.5):

$$\sigma_{ij} = \rho \frac{\partial \psi^E}{\partial \varepsilon_{ij}^e}, \quad (6.149)$$

$$P(p) = \rho \frac{\partial \psi^P}{\partial p}, \quad B(\beta) = \rho \frac{\partial \psi^D}{\partial \beta}, \quad (6.150)^2$$

where ρ denotes the mass density as a function of the damage-strengthening internal variable

$$\rho = \rho(\beta). \quad (6.151)$$

The mass density ρ , on the other hand, is related also to the void volume fraction f

$$\frac{\rho}{\rho_0} = \frac{1-f}{1-f_0}, \quad (6.152)$$

where ρ_0 and f_0 are the initial values of the density and the void volume fraction of the material. By assuming the linear elasticity, the function $\psi^E(\varepsilon_{ij}^e)$ in Eq. (6.148) has the expression

$$\psi^E = \frac{1}{2} C_{ijkl} \varepsilon_{ij}^e \varepsilon_{kl}^e, \quad (6.153)$$

where C_{ijkl} is the elastic modulus tensor of the voided material.

As regards the functions $\psi^P(p)$ and $\psi^D(\beta)$ in Eq. (6.148), instead of prescribing them at first, the generalized forces $P(p)$ and $B(\beta)$ associated with the internal variables p and β will be determined directly. Namely, since $P(p)$ is the strain-hardening function, it can be determined by experiments. The damage-strengthening function $B(\beta)$, on the other hand, can be derived by the analysis of spherical void growth in the form of Eq. (6.160) later.

According to Eq. (5.30), the dissipation potentials for plastic deformation and damage development may have the expressions

² In the argument of this subsection, the symbol R will be reserved to signify the average radius of spherical voids. Hence to avoid the repeated use of the symbol, the isotropic hardening variable R and its associated internal variable r will be replaced here by different symbols P and p .

$$F\left(\frac{\sigma_{ij}}{\rho}, P, B\right) = F^P\left(\frac{\sigma_{EQ}}{\rho}, P\right) + F^D\left(\frac{\sigma_H}{\rho}, B\right), \quad (6.154a)$$

$$F^P = \frac{\sigma_{EQ}}{\rho} - P(p), \quad F^D = B(\beta)g\left(\frac{\sigma_H}{\rho}\right), \quad (6.154b)$$

where $\sigma_H = (1/3)\sigma_{kk}$, $\sigma_{EQ} = [(3/2)\sigma_{ij}^D \sigma_{ij}^D]^{1/2}$ and $\sigma_{ij}^D = \sigma_{ij} - \sigma_H \delta_{ij}$ are the mean stress, equivalent stress and the deviatoric stress, respectively.

Substitution of the dissipation potentials of Eq. (6.154) into Eq. (5.10) furnishes the following constitutive and evolution equations of plastic deformation and damage development

$$\dot{\varepsilon}_{ij}^p = \dot{A} \frac{\partial F^P}{\partial (\sigma_{ij}/\rho)} = \frac{3}{2} \dot{A} \frac{\sigma_{ij}^D}{\sigma_{EQ}}, \quad (6.155a)$$

$$\dot{\varepsilon}_H^p = \frac{1}{3} \text{tr} \left[\dot{A} \frac{\partial F^D}{\partial (\sigma_{ij}/\rho)} \right] = \frac{1}{3} \dot{A} B(\beta) g'(\sigma_H/\rho), \quad (6.155b)$$

$$\dot{p} = -\dot{A} \frac{\partial F^P}{\partial P} = \dot{A} = \dot{\varepsilon}_{EQ}^p, \quad (6.155c)$$

$$\dot{\beta} = -\dot{A} \frac{\partial F^D}{\partial B} = \dot{A} g(\sigma_H/\rho), \quad (6.155d)$$

where $\dot{\varepsilon}_H^p$ and $(\cdot)'$ denote the mean plastic strain and the differentiation with respect to its argument.

(2) Determination of Functions of $\rho(\beta)$, $B(\beta)$ and $g(\sigma_H/\rho)$

For the derivation of the specific expressions of these equations, we need to determine the functions of $\rho(\beta)$, $B(\beta)$ and $g(\sigma_H/\rho)$ of Eqs. (6.151) and (6.154).

Rousselier first substituted Eqs. (6.155b) and (6.155d) into the law of conservation of mass for the matrix material

$$\dot{\rho} + 3\rho \dot{\varepsilon}_H^p = 0, \quad (6.156a)$$

or

$$3\rho \dot{\varepsilon}_H^p = -\rho'(\beta) \dot{\beta}, \quad (6.156b)$$

and derived a relation

$$\frac{g'(\sigma_H/\rho)}{g(\sigma_H/\rho)} = -\frac{\rho'(\beta)}{B(\beta)\rho(\beta)}. \quad (6.156c)$$

Since the left and the right hand side of this relation, respectively, are functions of different variables σ_H/ρ and β , this relation holds only when the both hand sides

have a constant of identical value. If one designates this constant value by $1/\sigma^*$, Eq. (6.156) furnishes a relation

$$g\left(\frac{\sigma_H}{\rho}\right) = C \exp\left(\frac{\sigma_H}{\rho\sigma^*}\right), \quad (6.157)$$

where C and σ^* are material constants.

The functions $\rho(\beta)$ and $B(\beta)$, on the other hand, can be determined by supposing a spherical void nucleated in incompressible matrix of unit volume. Namely, let the average radius of the spherical voids be R , then the void volume fraction f is given by

$$f = \frac{(4/3)\pi R^3}{1 + (4/3)\pi R^3}, \quad (6.158a)$$

from which we have

$$\frac{\dot{f}}{f(1-f)} = 3\frac{\dot{R}}{R}. \quad (6.158b)$$

We first substitute Eq. (6.152) into f and \dot{f} of this relation and note the functional relation of Eq. (6.151). Then, by applying the evolution equations (6.155d) and (6.157) to the resulting equation, we have a relation

$$\begin{aligned} 3\frac{\dot{R}}{R} &= -\frac{\rho'\dot{\beta}}{\rho(1-\rho+\rho f_0)} \\ &= -\frac{\rho'}{\rho(1-\rho+\rho f_0)} C \dot{\varepsilon}_{EQ}^p \exp\left(\frac{\sigma_H}{\rho\sigma^*}\right), \end{aligned} \quad (6.159a)$$

where we have defined the mass density ρ as the relative density with respect to its initial density, and thus specified $\rho_0 = 1$.

If we suppose a special case of

$$-\frac{\rho'}{\rho(1-\rho+\rho f_0)} \equiv 1, \quad (6.159b)$$

Equation (6.159a) leads to

$$3\frac{\dot{R}}{R} = C \dot{\varepsilon}_{EQ}^p \exp\left(\frac{\sigma_H}{\rho\sigma^*}\right), \quad (6.159c)$$

i.e., a relation similar to Eq. (6.79) of Rice and Tracy (1969).

Integration of Eq. (6.159b) furnishes the indeterminate function $\rho(\beta)$ of Eq. (6.151) in the form

$$\rho(\beta) = \frac{1}{1 - f_0 + f_0 \exp \beta}. \quad (6.160a)$$

If we further recall that Eq. (6.156c) has a constant value of $1/\sigma^*$ and substitute ρ and ρ' from Eq. (6.160a) into its right-hand side, we have the other indeterminate function $B(\beta)$ of Eq. (6.154b):

$$B(\beta) = \frac{\sigma^* f_0 \exp \beta}{1 - f_0 + f_0 \exp \beta}, \quad (6.160b)$$

By means of Eq. (6.157), the dissipation potential of Eq. (6.154) has a simple expression

$$F = \frac{\sigma_{EQ}}{\rho} + CB(\beta) \exp\left(\frac{\sigma_H}{\rho \sigma^*}\right) - P(p). \quad (6.161)$$

Finally, the constitutive and the evolution equations of a voided ductile material are given as follows

$$\dot{\varepsilon}_{ij}^p = \frac{3}{2} \frac{\sigma_{ij}^D}{\sigma_{EQ}} \dot{p}, \quad (6.162a)$$

$$\dot{\varepsilon}_H^p = \frac{1}{3} \frac{C}{\sigma^*} B(\beta) \left[\exp\left(\frac{\sigma_H}{\rho \sigma^*}\right) \right] \dot{p}, \quad (6.162b)$$

$$\dot{p} = \dot{\varepsilon}_{EQ}^p, \quad (6.162c)$$

$$\dot{\beta} = C \left[\exp\left(\frac{\sigma_H}{\rho \sigma^*}\right) \right] \dot{p}. \quad (6.162d)$$

In the particular case of $B(\beta) = \sigma^* f$, Eq. (6.161) leads to

$$F = \frac{\sigma_{EQ}}{\rho} + C \sigma^* f \exp\left(\frac{\sigma_H}{\rho \sigma^*}\right) - P(p), \quad (6.163)$$

and has the analogous form with the Gurson's yield function of Eq. (6.134).

6.5.4 Application to Ductile Fracture Analysis of a Slab in Plane Strain

As an application of the constitutive model of Gurson (GTN mode) and that of Rousselier, let us discuss the finite element analysis of the *slant fracture* of a slab in plane strain state (Besson, Steglich, and Brocks 2003). It has been ascertained that this problem consists of two separate processes of the crack initiation and its extension, and that the plane of crack extension differs from the direction perpendicular to the applied load.

(1) The Constitutive and the Evolution Equation

The analysis was performed by the use of the constitutive models of Gurson (GTN model) and Rousselier of the following equations.

1) Gurson Model (GTN Model)

$$F(\sigma_{ij}, \sigma_M, f) = \left(\frac{\sigma_{EQ}}{\sigma_M} \right)^2 + 2q_1 f^* \cosh \left(\frac{3}{2} \frac{q_2 \sigma_H}{\sigma_M} \right) - q_1^2 (f^*)^2 - 1 = 0, \quad (6.164)$$

$$f^* = f, \quad \text{for } f \leq f_C, \quad (6.165a)$$

$$f^* = f_C + \delta(f - f_C), \quad \text{for } f > f_C, \quad (6.165b)$$

$$\dot{f} = (1-f)\dot{\varepsilon}_{kk}^p + A\dot{p}, \quad (6.166)$$

$$\dot{\varepsilon}_{ij}^p = (1-f) \frac{\partial \sigma_M}{\partial \sigma_{ij}} \dot{p} = \frac{3}{2} \frac{\sigma_{ij}^D}{\sigma_M} \dot{p}, \quad (6.167a)$$

$$\dot{p} = \frac{\dot{\varepsilon}_{ij}^p \sigma_{ij}}{(1-f)\sigma_M}, \quad (6.167b)$$

$$\sigma_M = R(p) = K(p + \varepsilon_0)^n, \quad (6.168a)$$

$$\sigma_{EQ} = \frac{1}{1-f} \left[\frac{3}{2} \sigma_{kl}^D \sigma_{kl}^D \right]^{1/2}, \quad (6.168b)$$

where σ_M and p denote the equivalent stress in matrix material and the equivalent plastic strain governing the strain-hardening of the matrix. In Eq. (6.167), differently from Section 6.5.1, von Mises flow rule has been assumed.

2) Rousselier Model

$$F(\sigma_{ij}, \sigma_M, f) = \frac{\sigma_{EQ}}{1-f} + C \sigma^* f \exp \left(\frac{1}{1-f} \frac{\sigma_H}{\sigma^*} \right) - \sigma_M = 0, \quad (6.169)$$

$$\rho = \frac{1}{1-f_0 + f_0 \exp \beta}, \quad \frac{\rho}{\rho_0} = \frac{1-f}{1-f_0}, \quad (6.170)$$

$$\dot{\beta} = C \left[\exp \left(\frac{\sigma_H}{\rho \sigma^*} \right) \right] \dot{p}, \quad (6.171)$$

$$\dot{\varepsilon}_{ij}^p = \frac{3}{2} \frac{\sigma_{ij}^D}{\sigma_M} \dot{p}, \quad \dot{p} = \dot{\varepsilon}_{EQ}^p, \quad (6.172)$$

$$\dot{\varepsilon}_H^p = \frac{1}{3} \frac{C}{\sigma^*} B(\beta) \exp \left(\frac{1}{1-f} \frac{\sigma_H}{\sigma^*} \right) \dot{p}, \quad (6.173)$$

$$\sigma_M = P(p) = K(p + \varepsilon_0)^n. \quad (6.174)$$

Though the Gurson and the Rousselier model have similar construction, they have some significant differences in their predictions. In the case of pure shear $\sigma_H = 0$, for example, while the Rousselier model predicts $\dot{\beta} > 0$ and $\dot{f} > 0$, the Gurson model of Eq. (6.166) with $A = 0$ leads to $\dot{f} = 0$, and does not give any increase in void volume fraction.

(2) Conditions of Calculation and its Results

Besson et al. (2003) applied the above equations to the finite element analysis of the fracture process in a low alloy steel X70 HSLA slab of 5mm thick under plane-strain tension. The material constants as to the elastic-plastic deformation and damage were indentified by the usual tension tests as follow:

$$E = 210 \text{ GPa}, \quad \nu = 0.3, \quad (6.175a)$$

$$K = 795 \text{ MPa}, \quad \varepsilon_0 = 0.002, \quad n = 0.13, \quad f_0 = 1.5 \times 10^{-4}. \quad (6.175b)$$

Besides the material constants of Eq. (6.175), parameters included in the Gurson model of Eqs. (6.164) through (6.168) and those in the Rousselier model of Eqs. (6.169) through (6.174) were taken as in the following cases of R , G_* , G_n and G :

Rousselier Model

$$R : \quad C = 1.4, \quad \sigma^* = 450 \text{ MPa}, \quad (6.176)$$

Gurson Model

$$G_* : \quad q_1 = 1.5, \quad q_2 = 1.0, \quad f_C = 0.005, \quad \delta = 3, \quad A = 0, \quad (6.177a)$$

$$G_n : \quad q_1 = 1.5, \quad q_2 = 1.0, \quad f_C = 0.005, \quad (6.177b)$$

$$A = 0 \quad f \leq f_C; \quad A = 0.2 \quad f > f_C,$$

$$G : \quad q_1 = 1.5, \quad q_2 = 1.15, \quad f_C = 0.005, \quad \delta = 3, \quad A = 0.2. \quad (6.177c)$$

The analysis was carried out mainly by the use of the finite strain finite element software ABAQUS. Figure 6.18 shows the numerical results of the fracture process under plane strain tension obtained for four different cases of R , G_* , G_n and G . The symbols F and S_0 in the figure denote the tensile force and the initial cross-section area, while e_0 and Δe are the initial thickness of the slab and the reduction in the thickness. The dark part in the figure indicates the cracked region defined by $f > 0.1$.

As observed in the figure, the reduction ratios of the plate thickness at fracture are $0.52 < \Delta e/e_0 < 0.58$, and its dependence on the constitutive models and the material parameters is not significant. As regards the fracture mode, however, though the

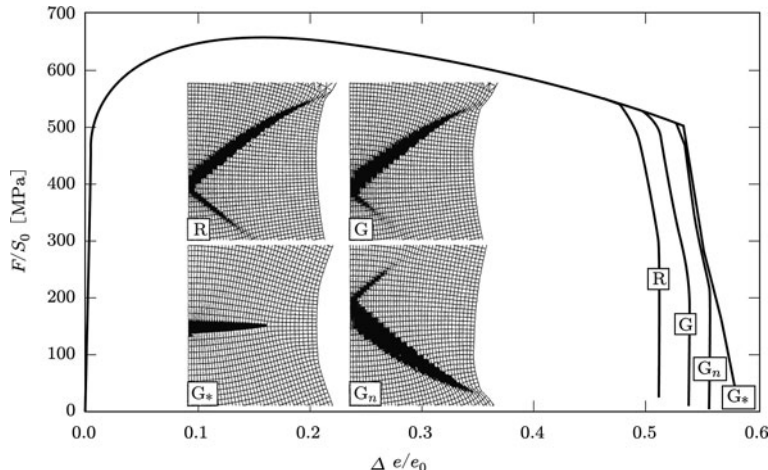


Fig. 6.18 Reduction in plate thickness and contours of cracks under plane-strain tension
Source: Besson, Steglich, and Brocks (2003, p. 1532, Fig. 8)

cases of R, G_n and G predict the slant fracture as observed in the corresponding experiments, the crack extension perpendicular to the tensile load was predicted in the case of G^* . This implies that the Gurson model (GTN model) may give significant difference in the fracture aspects depending on a small difference in the prescribed values of material constants.

6.5.5 Modification of GTN Model

The constitutive model of Gurson (GTN model) described above represents the isotropic damage state by the use of the volume fraction f of spherical voids, and has been applied mainly to the problems with large stress triaxiality σ_H/σ_{EQ} , such as tensile fracture or crack extension in ductile material.

The metal forming process, however, is concerned mainly with shear deformation, and hence is related to low range of the stress triaxiality. Voids in this condition are usually stretched in their maximum strain directions, and are subject not only to the change in their aspect ratios but also to the rotation of their principal axes. This change in the void configuration has significant influence on the processes of void growth and their coalescence. Namely, the Gurson model developed on the premise of spherical voids cannot describe properly the void growth and the resulting material softening in the case of shear dominant deformation.

Thus by taking account of these geometrical changes of voids, Gurson model (GTN model) has been extended to be applicable not only to anisotropic damage but also to damage in low range of stress triaxiality (Gologanu et al. 1993, 1994; Benzerga 2002; Benzerga et al. 2004a, 2004b; Pardoen 2006).

From phenomenological point of view, on the other hand, as described in Sections 4.3.5 and 6.2.5, the damage development and its microscopic mechanism depend largely on its stress triaxiality, and the feature of its dependence is not regular. This fact implies that the triaxiality is not a sufficient parameter to characterize the ductile damage process of materials. Nahshon and others (Nahshon and Hutchinson 2008; Nahshon and Xue 2009), therefore, modified the Gurson model by employing the Lode parameter³ of stress state, or equivalently the third invariant of deviatoric stress tensor J_3 , in addition to the triaxiality parameter.

In order to discriminate between the axisymmetric (equi-biaxial) state of stress and the state of pure shear (and pure shear combined with the hydraulic stress σ_H), they introduced a new parameter

$$\omega(\boldsymbol{\sigma}) = 1 - \left[\frac{27J_3}{2(\sigma_{EQ})^3} \right]^2, \quad J_3 = \det(\boldsymbol{\sigma}^D) = \frac{1}{3}\sigma_{ij}^D\sigma_{jk}^D\sigma_{ki}^D. \quad (6.178a)$$

Then the parameter $\omega(\boldsymbol{\sigma})$ has the following values:

$$\omega(\boldsymbol{\sigma}) = 0 \quad (\text{axisymmetric state of stress}), \quad (6.178b)$$

$$\omega(\boldsymbol{\sigma}) = 1 \quad (\text{state of pure shear}). \quad (6.178c)$$

As described in Section 6.5.4, the Gurson model (GTN model) in the case of pure shear cannot predict the increase of voids, or it cannot properly describe the damage evolution. Then, they modified the evolution equation of Eq. (6.135) by the use of the parameter $\omega(\boldsymbol{\sigma})$ of Eq. (6.178) as follows:

$$\dot{f} = \dot{f}_{growth} + \dot{f}_{nucle.}, \quad (6.179a)$$

$$\dot{f}_{growth} = (1-f)\dot{\varepsilon}_{kk}^p + k_\omega\omega(\boldsymbol{\sigma})f\frac{\sigma_{ij}^D\dot{\varepsilon}_{ij}^p}{\sigma_{EQ}}, \quad (6.179b)$$

$$\dot{f}_{nucle.} = \frac{f_N}{s_N\sqrt{2\pi}} \exp \left[-\frac{1}{2} \left(\frac{\varepsilon_M^p - \varepsilon_N}{s_N} \right)^2 \right] H(\sigma_H)\dot{\varepsilon}_M^p, \quad (6.179c)$$

where k_ω and $H(\cdot)$ are a new material constant and Heaviside function, while ε_M^p denotes the equivalent plastic strain of the material matrix. The yield function in this case is given again by Eq. (6.146). Thus as observed from Eqs. (6.178b) and (6.179b), the modified GTN model of Eq. (6.179) coincides with the ordinary one in the case of axisymmetric deformation.

³ A parameter $\mu = (2\sigma_2 - \sigma_1 - \sigma_3)/(\sigma_1 - \sigma_3)$ is called *Lode (stress) parameter*, where $\sigma_1 \geq \sigma_2 \geq \sigma_3$ are principal stresses.

Nahshon and Xue (2009) applied this extended model to the FEM analysis of quasi-static blanking process of HD36 steel sheet, and assured its applicability by comparing them with those of experiments.

6.6 Continuum Damage Mechanics Theory with Plastic Compressibility

Though the damage theories of the preceding section developed by the use of void volume fraction have been applied to a wide range of ductile fracture problems, they have some obvious limitations as described above. The continuum damage mechanic theory discussed so far, on the other hand, not only facilitates systematic argument in the framework continuum thermodynamics, but also describes pertinently the general features of damage; i.e., the effects of anisotropic damage, opening- closing effect of microcracks, mechanical effect of stress triaxiality, etc.

This damage mechanic theory, however, is usually formulated by the use of von Mises plastic potential, and does not represent the plastic volumetric strain. In other words, this theory cannot represent the effect of mass density variation in material, and hence it cannot be applied to the accurate analysis of ductile damage process with void development.

At the end of this chapter, the extension of the isotropic damage theory to incorporate the effect of *plastic compressibility* into plastic potential function will be briefly discussed (Chaboche, Boudifa, and Saanouni 2006).

6.6.1 Thermodynamic Potential Function

Let us suppose an elastic-plastic damaged material described by internal variables $\{r, D\}$, where r and D denote the isotropic hardening variables and the isotropic damage variable, respectively. Then, we assume that the Helmholtz free energy function per unit mass ψ of Eq. (4.18) can be expressed in terms of a function ψ_I with respect to its initial state

$$\psi = \frac{1}{\rho_0} \psi_I(\varepsilon_{ij}^e, r, D). \quad (6.180)$$

Substitution of this equation into the Clausius-Duhem inequality (3.19) furnishes the elastic constitutive equation

$$\sigma = \rho \frac{\partial \psi}{\partial \varepsilon^e} = \frac{\rho}{\rho_0} \frac{\partial \psi_I}{\partial \varepsilon^e}. \quad (6.181)$$

By defining the thermodynamic variables associated with r and D

$$R = \rho_0 \frac{\partial \psi}{\partial r} = \frac{\partial \psi_I}{\partial r}, \quad Y = -\rho_0 \frac{\partial \psi}{\partial D} = -\frac{\partial \psi_I}{\partial D}, \quad (6.182)$$

we have the dissipation (4.23) as regards the initial state

$$\Phi_I = \frac{\rho_0}{\rho} \boldsymbol{\sigma} : \dot{\boldsymbol{\epsilon}}^p - R\dot{r} + Y\dot{D}. \quad (6.183)$$

If the free energy function (6.180) is expressed in a specific form

$$\psi = \frac{1}{2\rho_0}(1-D)\boldsymbol{\epsilon}^e : \mathcal{C} : \boldsymbol{\epsilon}^e + \frac{1}{2\rho_0}bQr^2, \quad (6.184)$$

the elastic constitutive equation of Eq. (6.181) is expressed as

$$\boldsymbol{\sigma} = \frac{\rho}{\rho_0}(1-D)\mathcal{C} : \boldsymbol{\epsilon}^e, \quad (6.185)$$

where b , Q and \mathcal{C} denote material constants and the elastic modulus tensor of order four.

We suppose that the volume change induced by the deformation is a manifestation of the damage effect, and thus we represent it by another damage variable D_V . Then we have the relation

$$\frac{\rho}{\rho_0} = 1 - D_V. \quad (6.186)$$

The variable D_V , therefore, may be interpreted as the void volume fraction in the void-containing damaged material.

In view of this relation, Eq. (6.185) may be expressed as

$$\boldsymbol{\sigma} = (1 - D_V)(1 - D)\mathcal{C} : \boldsymbol{\epsilon}^e. \quad (6.187)$$

By the use of Eq. (6.184), the associated variables of Eq. (6.182) have the following expressions

$$R = \rho_0 \frac{\partial \psi}{\partial r} = bQr, \quad (6.188)$$

$$Y = Y^e = -\rho_0 \frac{\partial \psi}{\partial D} = \frac{1}{2}\boldsymbol{\epsilon}^e : \mathcal{C} : \boldsymbol{\epsilon}^e. \quad (6.189)$$

6.6.2 Dissipation Potential Function

Concerning the dissipation potential function of Eq. (4.44), by postulating the coupling of plastic deformation with damage and void development, we assume the following expression

$$F(\boldsymbol{\sigma}, R, Y) = F^P\left(\frac{\rho_0}{\rho}\boldsymbol{\sigma}, R; D, D_V\right) + F^H(R; D) + F^D(Y; D), \quad (6.190)$$

where F^P , F^H and F^D denote the dissipation functions related to plasticity, strain-hardening and damage, respectively. The specific forms of these functions are given as

$$F^P = \frac{\rho_0}{\rho} \frac{\sigma_{EQ}^*}{1 - D} - R - \sigma_Y, \quad (6.191a)$$

$$\sigma_{EQ}^* = \left[(\sigma_{EQ})^2 + 9\alpha D^*(D, D_V)(\sigma_H)^2 \right]^{1/2}, \quad (6.191b)$$

$$\sigma_{EQ} = [\boldsymbol{\sigma} : \mathbb{H} : \boldsymbol{\sigma}]^{1/2}, \quad (6.191c)$$

$$F^H = \frac{1}{2Q} R^2, \quad (6.192)$$

$$F^D = \frac{S}{s+1} \left(\frac{Y}{S} \right)^{s+1} (1 - D)^{-(m+1)}, \quad (6.193)$$

where \mathbb{H} denotes the fourth-order anisotropy tensor specifying Hill's yield criterion for orthotropic plasticity, and its components were given in Eq. (5.26). The symbols m , s , Q , S and α , furthermore, are material constants.

Substitution of these relations into Eq. (4.29) of the generalized flux vector provides the evolution equations of plastic strain $\dot{\boldsymbol{\epsilon}}^p$ and internal variables r and D . Namely, by the use of Eqs. (6.191) and (4.29), we first have

$$\begin{aligned} \dot{\boldsymbol{\epsilon}}^p &= \dot{\Lambda} \frac{\partial F}{\partial (\rho_0 \boldsymbol{\sigma} / \rho)} = \dot{\Lambda} \frac{1}{1 - D} \frac{\partial \sigma_{EQ}^*}{\partial \boldsymbol{\sigma}} = \dot{\Lambda} \frac{1}{1 - D} N, \\ N &= \frac{\mathbb{H} : \boldsymbol{\sigma}}{\sigma_{EQ}^*} + 27\alpha D^* \frac{\sigma_H}{\sigma_{EQ}^*} \mathbf{I}. \end{aligned} \quad (6.194)$$

By representing the equivalent plastic strain rate in the form

$$\dot{p} = \left[\dot{\boldsymbol{\epsilon}}^p : (\mathbb{H} + \alpha D^* \mathbf{I} \otimes \mathbf{I})^{-1} : \dot{\boldsymbol{\epsilon}}^p \right]^{1/2}, \quad (6.195)$$

Equation (6.194) readily leads to

$$\dot{\boldsymbol{\epsilon}}^p = \frac{\dot{\Lambda}}{1 - D} N = \dot{p} N, \quad \dot{\Lambda} = \dot{p}(1 - D). \quad (6.196)$$

The evolution equations of the strain-hardening internal variable r and the damage variable D , on the other hand, are derived by substituting Eqs. (6.192) and (6.193) into Eq. (4.29) and by employing Eqs. (6.188) and (6.196) as follows:

$$\begin{aligned} \dot{r} &= -\dot{\Lambda} \frac{\partial F}{\partial R} = \dot{\Lambda} \left(\frac{\partial F^P}{\partial R} + \frac{\partial F^H}{\partial R} \right) = \dot{\Lambda} \left(1 - \frac{R}{Q} D \right) \\ &= (1 - D)(1 - br)\dot{p}, \end{aligned} \quad (6.197)$$

$$\dot{D} = \dot{\Lambda} \frac{\partial F}{\partial Y} = \dot{\Lambda} \frac{\partial F^D}{\partial Y} = \left(\frac{Y}{S} \right)^s (1 - D)^{-m} \dot{p}. \quad (6.198)$$

Finally, the evolution equation of the plastic volumetric strain is derived from Eq. (6.186)

$$\dot{D}_V = -(1 - D_V)(\dot{\rho}/\rho) = (1 - D_V)\text{tr}\dot{\epsilon}^P. \quad (6.199)$$

It should be noted that, unlike the Gurson model, the damage evolution equation (6.198) describes the damage development in low range of stress triaxiality, e.g., that in shear deformation process. Equation (6.199), furthermore, represents the volumetric change in ductile damage process in the framework of continuum damage mechanics.

Chapter 7

Fatigue Damage

Fatigue damage in polycrystalline metals is caused by the microcrack formation in accumulated slip bands due to repeated loading. These slip bands develop in favorably oriented grains located on the material surface as a result of irreversible dislocation glide process.

As observed in Table 7.1, however, the aspect of fatigue damage development, e.g., the number of load cycles up to failure N_R , the plastic strain range vs. elastic strain range ratio $\Delta\varepsilon^p/\Delta\varepsilon^e$, the dissipated plastic energy vs. elastic strain energy ratio per cycle $\Delta W^p/\Delta W^e$, etc., vary largely depending on the magnitude of the cyclic load. Fatigue damage, therefore, is usually classified into four classes as shown in Table 7.1.

The present chapter is concerned with the continuum damage mechanics theory applied to the analysis of the three classes of fatigue except very high cycle fatigue. In Section 7.1, the two-scale and the elaborated two-scale damage model described in Section 6.1 will be applied to analyze the high cycle fatigue process. In Sections 7.2 and 7.3, ductile damage theory of Section 6.2 will be applied to the problems of low cycle fatigue and very low cycle fatigue.

Table 7.1 Classification of fatigue damage

Fatigue	Failure cycles N_R	Pertinent stress	Strain ratio $\Delta\varepsilon^p/\Delta\varepsilon^e$	Energy ratio $\Delta W^p/\Delta W^e$
Very high cycle fatigue	$> 10^7$	$< \sigma_F$	≈ 0	≈ 0
High cycle fatigue	10^5 to 10^6	$< \sigma_Y$	≈ 0	≈ 0
Low cycle fatigue	10^2 to 10^4	σ_Y to σ_U	1 to 10	1 to 10
Very low cycle fatigue	1 to 20	$\approx \sigma_U$	10 to 100	10 to 100

Source: Dufailly and Lemaître (1995)

7.1 High Cycle Fatigue

7.1.1 Analysis of High Cycle Fatigue by Two-Scale Damage Model

Microcracks in high cycle fatigue are brought about only in limited number of crystal grains in material. Hence the plastic strain of material in mesoscale is very small, and may be disregarded. The elastic-plastic damage theory discussed in [Chapter 4](#), therefore, cannot be applied to the analysis of this kind of fatigue.

In the two-scale damage model of [Section 6.1.3](#), a microscopic volume element M has been postulated inside the representative volume element (RVE), and the development of elastic-plastic damage is allowed for in the element M . Therefore, we analyze here the high cycle fatigue process by the use of this two-scale damage model (Lemaitre 1992).

In the derivation of the evolution equation (6.24) of the two-scale model, it was assumed that the microscopic volume element M in [Fig. 6.1](#) is an elastic-perfectly plastic material with yield stress σ_Y^M , and that σ_Y^M is equal to the fatigue limit σ_F of RVE as shown in [Eq. \(6.14\)](#). Then, the damage evolution equation (6.24) for the mesoscopic RVE can be expressed

$$\dot{D} = \frac{(\sigma_F)^2}{2ES} \left[\frac{2}{3}(1+\nu) + 3(1-2\nu) \left(\frac{\sigma_H}{3\sigma_F} \right)^2 \right] \dot{\varepsilon}_{EQ} H(\varepsilon_{EQ} - p_D), \quad (7.1)$$

where ε_{EQ} is the accumulated equivalent plastic strain in the element M ; i.e., the accumulated equivalent strain in RVE. The symbol p_D in Eq. (7.1) denotes the threshold value of p for damage initiation, and is given by [Eq. \(6.25\)](#).

Now, let us consider the particular case of high cycle fatigue under uniaxial tension-compression of a constant stress range $\Delta\sigma = \text{const.}$ (i.e., constant stress amplitude $\sigma_a = \text{const.}$) shown in [Fig. 7.1](#). Then, since we have

$$\frac{\sigma_H}{\sigma_F} = \frac{\sigma}{3\sigma_F}, \quad \dot{\varepsilon}_{EQ} = \frac{\dot{\sigma}}{E}, \quad (7.2)$$

Equation (7.1) has the form

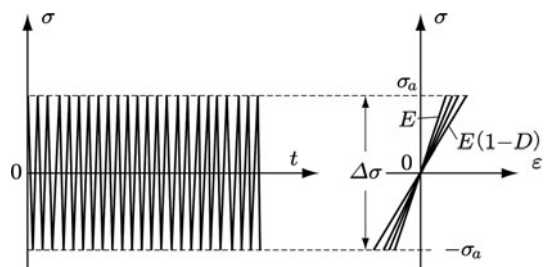


Fig. 7.1 High cycle fatigue under constant stress range

$$\dot{D} = \frac{(\sigma_F)^2}{2E^2S} \left[\frac{2}{3}(1+\nu) + 3(1-2\nu) \left(\frac{\sigma}{3\sigma_F} \right)^2 \right] \dot{\sigma} H(\varepsilon_{EQ} - p_D). \quad (7.3)$$

By integrating this equation along one cycle, we have

$$\begin{aligned} \frac{\delta D}{\delta N} &= 4 \times \frac{(\sigma_F)^2}{2E^2S} \int_{\sigma_F}^{\sigma_a} \left[\frac{2}{3}(1+\nu) + 3(1-2\nu) \left(\frac{\sigma}{3\sigma_F} \right)^2 \right] H(\varepsilon_{EQ} - p_D) d\sigma \\ &= \frac{2(\sigma_F)^2}{E^2S} \left\{ (1+\nu)(\sigma_a - \sigma_F) + \frac{1-2\nu}{9(\sigma_F)^2} [(\sigma_a)^3 - (\sigma_F)^3] \right\}. \end{aligned} \quad (7.4)$$

Let N_D denote the number of stress cycles at the damage start (or at the microcrack nucleation), namely the number of stress cycles when the accumulated cyclic strain ε_{EQ} attains to the threshold p_D of fatigue damage initiation. Then, by means of Eq. (6.25), N_D is given:

$$N_D = \frac{p_D}{4\varepsilon_{EQ}} = \frac{Ep_D}{4\sigma_a} = \frac{E\varepsilon_D^P}{4\sigma_a} \frac{\sigma_U - \sigma_F}{\sigma_{EQ} - \sigma_F}. \quad (7.5)$$

By the use of the initial condition

$$D = 0 \quad \text{at} \quad N = N_D, \quad (7.6)$$

integration of Eq. (7.4) with respect to the cycle number N furnishes

$$D = \frac{2(\sigma_F)^2}{E^2S} \left\{ (1+\nu)(\sigma_a - \sigma_F) + \frac{1-2\nu}{9(\sigma_F)^2} [(\sigma_a)^3 - (\sigma_F)^3] \right\} (N - N_D). \quad (7.7)$$

Fatigue fracture, on the other hand, is brought about when the damage variable D attains to its critical value D_C . Then, designating the fracture cycle number (i.e., *fatigue life*) by N_R , we have

$$D_C = \frac{2(\sigma_F)^2}{E^2S} \left\{ (1+\nu)(\sigma_a - \sigma_F) + \frac{1-2\nu}{9(\sigma_F)^2} [(\sigma_a)^3 - (\sigma_F)^3] \right\} (N_R - N_D), \quad (7.8)$$

or

$$N_R = N_D + \frac{D_C}{\frac{2(\sigma_F)^2}{E^2S} \left\{ (1+\nu)(\sigma_a - \sigma_F) + \frac{1-2\nu}{9(\sigma_F)^2} [(\sigma_a)^3 - (\sigma_F)^3] \right\}}. \quad (7.9)$$

Dividing Eq. (7.7) by Eq. (7.8), we obtain the evolution equation of fatigue damage expressed in terms of the stress cycle N as follows

$$D = D_C \frac{N - N_D}{N_R - N_D}, \quad (7.10)$$

which represents the linear increase in damage with the number of stress cycle.

Fig. 7.2 S-N curve of the structural steel S45C

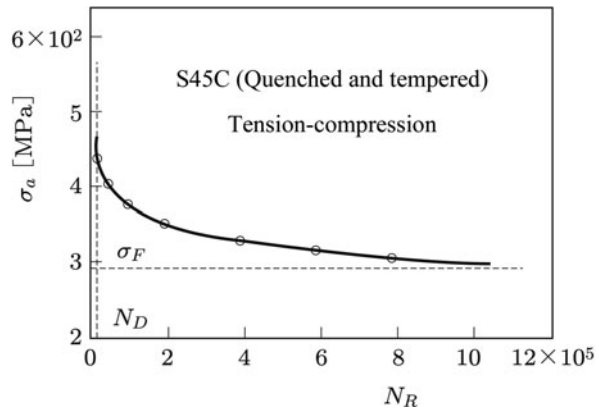


Figure 7.2 shows the S-N curve of tension-compression high cycle fatigue of the structural steel S45C. Equation (7.9) represents a quasi-hyperbola with the asymptotes of $N_R = N_D$ and $\sigma_a = \sigma_F$, and describes the S-N curve of Fig. 7.2.

7.1.2 Analysis of High Cycle Fatigue by Elaborated Two-Scale Damage Model

The analysis of high cycle fatigue under complicated loading conditions should have recourse to a more refined model. We now discuss this problem by the use of the elaborated two-scale damage model described in Section 6.1.4.

(1) Tension-Compression Fatigue under Constant Stress Amplitude

Let us first apply Eq. (6.50) of the elaborated two-scale model to high cycle fatigue under constant stress amplitude σ_a . Since we have

$$\sigma_H = \frac{1}{3}\sigma_a, \quad \sigma_{EQ} = \sigma_a, \quad (7.11)$$

Equation (6.50) leads to

$$\dot{D} = \frac{(R_v^M)^s(\sigma_a + k\sigma_F)^{2s}}{C(1+k)[2ES(1+k)^2(1-D)^2]^s} \dot{\sigma}, \quad (7.12a)$$

$$R_v^M = \frac{2}{3}(1+\nu) + 3(1-2\nu) \left\{ \frac{1+k}{3[1+k(\sigma_F/\sigma_a)]} \right\}^2. \quad (7.12b)$$

Integration of this relation throughout a cycle provides

$$\begin{aligned}\frac{\delta D}{\delta N} &= 2 \times \frac{(R_v^M)^s}{C(1+k)[2ES(1+k)^2(1-D)^2]^s} \int_{\sigma_F}^{\sigma_a} (\sigma + k\sigma_F)^{2s} d\sigma \\ &= \frac{2(R_v^M)^s \{(\sigma_a + k\sigma_F)^{2s+1} - [\sigma_F(1+k)]^{2s+1}\}}{C(1+k)(2s+1)[2ES(1+k)^2(1-D)^2]^s}.\end{aligned}\quad (7.13)$$

By integrating this relation under the initial and the fracture condition

$$N = 0, \quad D = 0; \quad N = N_R, \quad D = D_C = 1, \quad (7.14)$$

the number of cycles to fracture is derived as follows

$$N_R = \frac{(2ES)^s C}{2(R_v^M)^s \left\{ \left[\sigma_a \frac{1 + k(\sigma_F/\sigma_a)}{1 + k} \right]^{2s+1} - (\sigma_F)^{2s+1} \right\}}. \quad (7.15)$$

In comparison with Eq. (7.9), Eq. (7.15) includes not only the non-linearity s of the damage evolution equation, but also the local strain-hardening property C defined by Eq. (6.32), the micromechanics property k of the inclusion, etc. Thus, Eq. (7.15) can describe more complicated fatigue problems than Eq. (7.9). The material constants s and S of Eq. (7.15) can be identified by comparing its predictions with the corresponding fatigue test results.

(2) Application to Fatigue Damage under General Loading

By incorporating the elaborated two-scale damage model of Eqs. (6.28) through (6.38) into computer programs of numerical calculation, wide range of fatigue phenomena, including multiaxial fatigue, can be analyzed.

Figure 7.3 shows the numerical results for mean stress effects in tension-compression and in cyclic-torsion fatigue tests on a steel at room temperature. The symbols σ_a and τ_a denote the stress amplitudes corresponding to a specific fracture

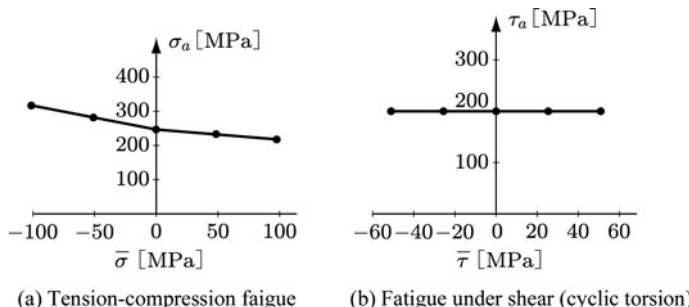


Fig. 7.3 Effect of mean stress in fatigue under tension-compression and under cyclic torsion ($N_R = 10^5$)

Source: Lemaitre et al. (1999, p. 76, Fig. 6)

cycle number of $N_R = 10^5$, while $\bar{\sigma}$ and $\bar{\tau}$ are their mean stresses. The symbol of black dot \bullet in the figure signifies the numerical results of Eqs. (6.28) through (6.38) together with the following material constants:

$$\begin{aligned} E &= 200 \text{ GPa}, \quad \nu = 0.3, \quad \sigma_F = 200 \text{ MPa}, \quad \sigma_U = 600 \text{ MPa}, \\ C &= 2000 \text{ MPa}, \quad S = 0.3 \text{ MPa}, \quad s = 2, \quad D_C = 1, \quad \varepsilon_D^p = 0.05. \end{aligned} \quad (7.16)$$

As observed in the figure, salient mean stress effect as a result of unilateral behavior of microcracks is predicted in the case of tension-compression fatigue, whereas the fatigue by shear has no mean stress effect. These results coincides with the generally observed feature in experiments.

Figure 7.4, on the other hand, shows the prediction of the amplitude history effect in two-level loading fatigue at zero mean stress. The symbol $n_i (i = 1, 2)$ denotes the number of cycles under a stress amplitude σ_{ai} , while N_{Ri} is the number of cycles to fracture at a constant amplitude σ_{ai} . The small square \blacksquare in the figure designates the numerical predictions of Eqs. (6.28) through (6.38), while a straight line represents the *linear cumulative damage law*, or *Miner-Palmgren law* (also *Palmgren-Miner law*)

$$\frac{n_1}{N_{R1}} + \frac{n_2}{N_{R2}} = 1. \quad (7.17)$$

As observed in the figure, the elaborated two-scale damage model can describe pertinently the markedly non-linear phenomena of damage accumulation.

(3) Fatigue Damage Analysis by Means of Improved Elaborated Two-Scale Damage Model

As described in Section 6.1.4, the elaborated two-scale damage model employed in the above analysis has been improved further by rewriting the localization law of Eq. (6.27) into the form of Eq. (6.51) and by taking account of the plastic

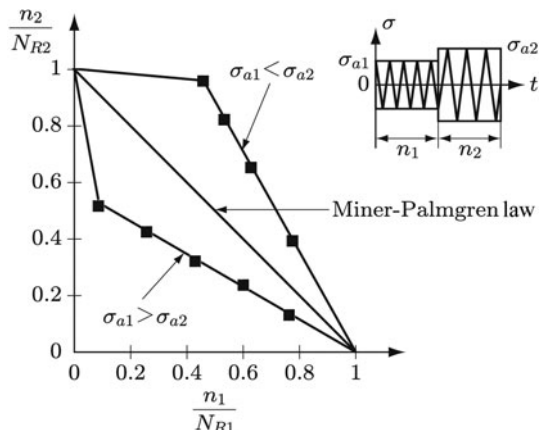


Fig. 7.4 Effect of amplitude history in fatigue under two-amplitude tension-compression loading
Source: Lemaitre et al. (1999, p. 77, Fig. 7)

deformation also in the mesoscopic volume element. This improved elaborated two-scale damage model has been applied to the numerical analysis of high-cycle thermo-mechanical fatigue under multiaxial state of stress. For the detail of the analysis, see the reference (Lemaitre and Desmorat 2005; Desmorat et al. 2007).

7.2 Low Cycle Fatigue

Let us now consider the analysis of low cycle fatigue. Since the low cycle fatigue is caused by the accumulation of the plastic damage discussed in [Section 6.1](#), the damage development is described by the evolution [equation \(6.10\)](#):

$$\dot{D} = \frac{(\sigma_{EQ})^2 R_v}{2ES(1-D)^2} \dot{p} H(p - p_D), \quad (7.18)$$

where σ_{EQ} , R_v , p and p_D denote, respectively, the equivalent stress, stress triaxiality function, accumulated plastic strain and the threshold value of p for damage initiation. The symbol $H(\cdot)$, furthermore, is the Heaviside function.

The low cycle fatigue process under general loading history can be analyzed by integrating Eq. (7.18) according to the given history of plastic strain $\varepsilon_{ij}^p(t)$, and/or of stress $\sigma_{ij}(t)$.

The application of Eq. (7.18) in such procedure necessitate to overcome some related problems. One of the most essential aspects is the proper description of cyclic behavior of material under multiaxial repeated loading coupled with damage. As regards the determination of the cyclic plastic constitutive equations for this purpose, refer to the references in the relevant field (Chaboche 1989; Lemaitre and Chaboche 1985; Ohno and Wang 1994; Pineau, Cailletaud, and Lindley 1996; Lemaitre and Desmorat 2005).

As the cases where the analytical integration of Eq. (7.18) is feasible, we first consider in this section the low cycle fatigue under uniaxial tension-compression with a constant and a lump-wise variable range of plastic strain (Lemaitre 1992; Lemaitre and Desmorat 2005).

7.2.1 Evolution Equation of Uniaxial Low Cycle Fatigue Damage, Fatigue Life Under Constant Strain Amplitude

[Equation \(8.18\)](#) above has the following form for a uniaxial state

$$\dot{D} = \frac{\sigma^2}{2ES(1-D)^2} |\dot{\varepsilon}^p| H(\varepsilon^p - p_D). \quad (7.19)$$

The number of cycles to fracture, or *fatigue life* N_R , is expressed as the sum of the number of cycles to microcrack initiation N_D and the number of cycles for these

microcracks to grow into cracks of mesoscale (i.e., *crack extension life*) N_F :

$$N_R = N_D + N_F. \quad (7.20)$$

(1) Number of Cycles to Microcrack Nucleation N_D

As shown in Fig. 7.5, the cyclic elastic-plastic behavior in low cycle fatigue rapidly attains to the stage of steady state with the repetition of strain cycles. After the steady state is attained, stress amplitude σ_a remains nearly constant until the start of damage initiation due to microcrack formation. Since the increase in the accumulated plastic strain in one cycle is $2\Delta\varepsilon^p$, the number of cycles to microcrack initiation N_D is given by

$$N_D = \frac{p_D}{2\Delta\varepsilon^p}. \quad (7.21)$$

(2) Number of Cycles to Mesoscopic Fracture N_R

In order to derive the number of cycles N_R to fracture, Eq. (7.19) should be integrated over $N_D \leq N \leq N_R$. The integration could be easily achieved by numerical calculation. For the derivation of an analytical solution, however, we simplify the integration of Eq. (7.19) by employing the following assumptions:

- (1) Variation of the damage variable D during one cycle is small. Hence $(1 - D)$ is supposed to be constant.
- (2) Strain-hardening in one cycle is small. Therefore, the material is supposed to be perfectly plastic with the yield stress σ_Y as shown in Fig. 7.5, where σ_Y is the yield stress of the damaged material.

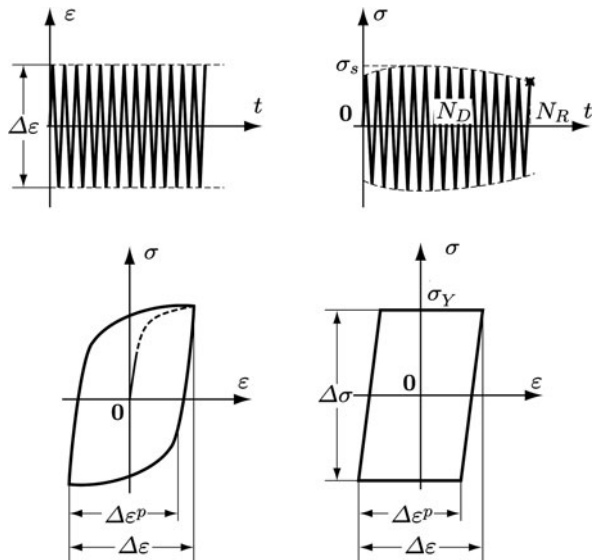


Fig. 7.5 Low cycle fatigue under a constant strain range

On the basis of these assumptions, Eq. (7.19) can be integrated along a cycle of loading:

$$\begin{aligned}\frac{\delta D}{\delta N} &= \int \frac{(\sigma_a)^2}{2ES(1-D)^2} \dot{\varepsilon}^p dt = \frac{(\sigma_Y)^2}{2ES(1-D)^2} \times 2 \int_0^{\Delta\varepsilon^p} \dot{\varepsilon}^p dt \\ &= \frac{(\Delta\sigma)^2}{4ES(1-D)^2} \Delta\varepsilon^p.\end{aligned}\quad (7.22)$$

The integration of this relation necessitates a relation between the plastic strain range $\Delta\varepsilon^p$ and the stress range $\Delta\sigma$. Then we postulate a cyclic stress-strain relation between $\Delta\varepsilon^p$ and $\Delta\sigma$ as follows

$$\Delta\varepsilon^p = \left[\frac{\Delta\sigma}{K(1-D)} \right]^M, \quad (7.23)^1$$

where K and M are material constants.

Substitution of $\Delta\sigma$ from Eq. (7.23) into Eq. (7.22) gives the damage increase in one cycle

$$\frac{\delta D}{\delta N} = \frac{K^2}{4ES} (\Delta\varepsilon^p)^{(M+2)/M}. \quad (7.24)$$

In the case of low cycle fatigue, plastic strain range $\Delta\varepsilon^p$ can be assumed to be constant throughout the fatigue process. Then, Eq. (7.24) is integrated to give

$$\begin{aligned}D &= \int_{N_D}^N \frac{\delta D}{\delta N} \delta N \\ &= \frac{K^2}{4ES} (\Delta\varepsilon^p)^{(M+2)/M} (N - N_D).\end{aligned}\quad (7.25)$$

Fatigue fracture occurs when D attains to its critical value D_C . In view of Eq. (7.21), Eq. (7.25) leads to

$$D_C = \frac{K^2}{4ES} (\Delta\varepsilon^p)^{(M+2)/M} \left(N_R - \frac{P_D}{2\Delta p} \right), \quad (7.26)$$

from which we obtain the number of cycles to fracture in low cycle fatigue

¹ In the calculation of damage increments, material can be simplified to be perfectly plastic. In reality, however, material shows strain-hardening to a certain extent, and hence increments of stress and strain can be related uniquely.

$$N_R = N_D + N_F \\ = \frac{p_D}{2\Delta\varepsilon^p} + \frac{4ESD_C}{K^2} (\Delta\varepsilon^p)^{-(M+2)/M}. \quad (7.27)$$

In the particular case of $p_D = 0$, Eq. (7.27) leads to

$$N_R = \frac{4ESD_C}{K^2} (\Delta\varepsilon^p)^{-(M+2)/M}, \quad (7.28a)$$

or

$$N_R = \left(\frac{\Delta\varepsilon^p}{C} \right)^{-\alpha}, \quad (7.28b)$$

where C and α are material constants.

Equation (7.28) represents a power relation between a plastic strain range $\Delta\varepsilon^p$ and the fatigue life N_R , and is called *Coffin-Manson law* (or *Manson-Coffin law*). In a number of metallic material, the exponent $\alpha = (M + 2)/M$ of Eq. (7.28) takes the value of 1.5 through 2.

Figure 7.6 shows the results of tension-compression low cycle fatigue tests of UDIMET 700 alloy under constant strain range. This figure confirms the validity of the relation of Eq. (7.28).

7.2.2 Low Cycle Fatigue Under Variable Stain Amplitude

High-cycle fatigue life under two-amplitude tension-compression loading was calculated numerically in Section 7.1.2 by the use of two-scale damage model. In the

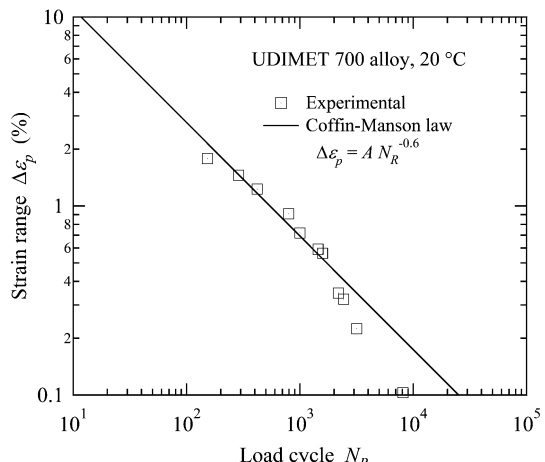


Fig. 7.6 Results of tension-compression low cycle fatigue tests of UDIMET 700 alloy at 20°C and the predictions of Coffin-Manson law
Source: Lemaitre and Chaboche (1985, p. 373, Fig. 7.15(b))

case of low cycle fatigue, however, the closed form model of the preceding section can be easily extended also to the case of two-level fatigue loading (Lemaitre and Desmorat 2005).

In the particular case of low cycle fatigue with constant plastic strain range $\Delta\varepsilon^p$, the critical state of damage at fracture is given by Eq. (7.25):

$$D_C = \frac{K^2}{4ES} (\Delta\varepsilon^p)^{\frac{M+2}{M}} (N_R - N_D). \quad (7.29)$$

Then we consider two-level tension-compression cyclic loading as shown in Fig. 7.4 previously, and represent the strain range, stress range and the relevant cycles of these stages by $\Delta\varepsilon_1^p$, $\Delta\sigma_1$, n_1 and $\Delta\varepsilon_2^p$, $\Delta\sigma_2$, n_2 , respectively.

By expressing the number of cycle at damage initiation under a constant strain range $\Delta\varepsilon_1^p$ by N_{D1} , the damage brought about by n_1 cycles of $\Delta\varepsilon_1^p$ is given by Eq. (7.25)

$$D(n_1) = \frac{K^2}{4ES} (\Delta\varepsilon_1^p)^{\frac{M+2}{M}} (n_1 - N_{D1}), \quad (7.30)$$

which together with Eq. (7.29) furnishes a relation

$$D(n_1) = \frac{n_1 - N_{D1}}{N_{R1} - N_{D1}} D_C, \quad (7.31)$$

where N_{R1} is the fatigue life due to constant $\Delta\varepsilon_1^p$.

Suppose that the fatigue fracture is attained by the succeeding application of n_2 cycles of constant range $\Delta\varepsilon_2^p$. Then we have the following relation:

$$\begin{aligned} D_C(N_R) &= D(n_1) + D(n_2) \\ &= \frac{n_1 - N_{D1}}{N_{R1} - N_{D1}} D_C + \frac{K^2}{4ES} (\Delta\varepsilon_2^p)^{\frac{M+2}{M}} n_2. \end{aligned} \quad (7.32)$$

By applying Eq. (7.29), furthermore, to the case of constant strain range $\Delta\varepsilon_2^p$, and by eliminating $\Delta\varepsilon_2^p$ from the resulting relation and Eq. (7.32), we have

$$D_C(N_R) = \frac{n_1 - N_{D1}}{N_{R1} - N_{D1}} D_C + \frac{n_2}{N_{R2} - N_{D2}} D_C, \quad (7.33a)$$

or

$$\frac{n_1}{N_{R1}} + \frac{n_2}{N_{R2}} \frac{1 - (N_{D1}/N_{R1})}{1 - (N_{D2}/N_{R2})} = 1. \quad (7.33b)$$

Thus we finally have the relations

$$\frac{n_1}{N_{R1}} + \frac{n_2}{N_{R2}} < 1 \quad \text{for} \quad \frac{N_{D1}}{N_{R1}} > \frac{N_{D2}}{N_{R2}}, \quad (7.34a)$$

$$\frac{n_1}{N_{R1}} + \frac{n_2}{N_{R2}} > 1 \quad \text{for} \quad \frac{N_{D1}}{N_{R1}} < \frac{N_{D2}}{N_{R2}}. \quad (7.34b)$$

Equations (7.34a) and (7.34b) imply, respectively, the case of first larger strain range followed by smaller one and the case of the opposite sequence, and show the analogous feature to that of high-cycle fatigue observed already in Fig. 7.4.

The particular case of Eq. (7.33)

$$\frac{n_1}{N_{R1}} + \frac{n_2}{N_{R2}} = 1 \quad (7.35)$$

recovers Miner-Plamgren law of Eq. (7.17).

The derivation in this section is based on the damage evolution equation of Eq. (7.18), or Eq. (6.10). Exactly same results are derived also from the power damage law of Eq. (6.11) in place of Eq. (6.10).

7.3 Uncoupled Numerical Analysis of Very Low Cycle Fatigue

The quantitative estimation of a damage state in a rocket motor subject to preliminary tests before launching, or of the residual life of structural elements suffered from accidental overload, for example, necessitates accurate analyses of the fatigue damage process characterized by the fracture life of the order $N_R = 10$. Fatigue with this order of fracture life is called *very low cycle fatigue*, and the Coffin-Manson law of Eq. (7.28) is not applicable any more with required accuracy.

We now consider the uncoupled finite element analysis of the very low cycle fatigue of circumferentially notched tubular specimens of Inconel 718 at 630°C under cyclic tension-compression shown in Fig. 7.7 (Dufailly and Lemaître 1995).

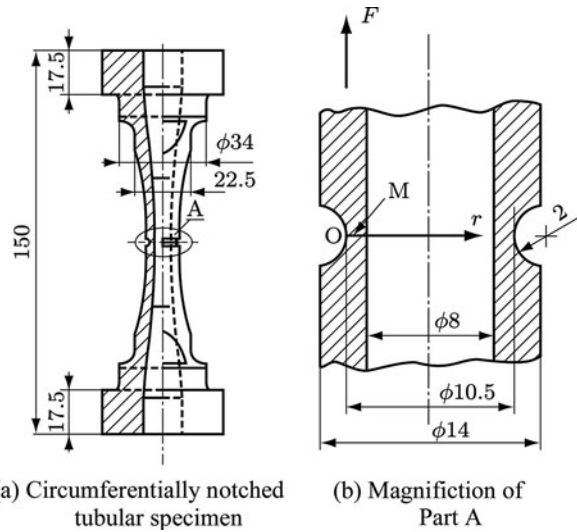
(1) Damage Evolution Equation and Fracture Cycles

We first postulate the power law damage evolution equation of Eq. (6.56):

$$\dot{D} = \left[\frac{(\sigma_{EQ})^2 R_v}{2ES(1-D)^2} \right]^s \dot{\epsilon}. \quad (7.36)$$

In the case of very low cycle fatigue of Inconel 718, the plastic strain at each cycle is very large, and thus its plastic behavior can be modelled by perfect plasticity. Denoting the yield stress in undamaged state by σ_Y , the effective stress in Eq. (7.36) is expressed by

Fig. 7.7 Circumferentially notched hollow cylindrical specimen of Inconel 718
Source: Dufailly and Lemaitre (1995, p. 164, Fig. 9)



$$\frac{\sigma_{EQ}}{1 - D} = \sigma_Y = \text{const.} \quad (7.37)$$

In view of this relation, integration of Eq. (7.36) over one cycle leads to

$$\frac{\delta D}{\delta N} = \left[\frac{(\sigma_Y)^2 R_v}{2ES} \right]^s \Delta p. \quad (7.38)$$

For cyclic loading of constant plastic strain range $\Delta p = \text{const.}$, by the use of the initial and the final fracture conditions

$$N = 0, \quad D = 0, \quad (7.39a)$$

$$N = N_R, \quad D = 1, \quad (7.39b)$$

further integration of Eq. (7.38) gives

$$N_R = \left[\frac{2ES}{(\sigma_Y)^2 R_v} \right]^s (\Delta p)^{-1}. \quad (7.40)$$

In the particular case of uniaxial tension-compression cycles, the yield stress σ_Y is 1/2 of the stress range $\Delta\sigma$, Eq. (7.40) is reduced to

$$N_R = \frac{1}{2} (8ES)^s (\Delta p)^{-2s} (\Delta \varepsilon^p)^{-1}. \quad (7.41)$$

The material constants s and S can be identified by comparing Eq. (7.41) with the experiment.

(2) Uncoupled Damage-Deformation Analysis of Very Low Cycle Fatigue Process, Comparison with Experiment

Since the plastic deformation in each cycle in the relevant specimen under cyclic loading is very large, the plastic behavior of every part of the specimen can be assumed to be perfectly plastic. Thus the stress range, the plastic strain range and the stress state at each point of the specimen under cyclic loading can be estimated from the results of elastic-plastic analysis of the undamaged specimen under monotonic loading.

For this uncoupled analysis, Dufailly and Lemaître postulated the elastic-plastic constitutive equation based on the power hardening law

$$\varepsilon^P = \left(\frac{\sigma - \sigma_Y}{K_P} \right)^{M_P}, \quad (7.42)$$

and performed FEM elastic-plastic analysis of the specimen of Fig. 7.7 under simple tension by employing ABAQUS code, where K_P and M_P are material constants. By the use of the states of stress and plastic strain, they estimated the damage state of the specimen under cyclic loading.

Figure 7.8 shows the results of the elastic-plastic analysis and the location of crack initiation predicted in the specimen subject to cyclic loading of $F = \pm 22.3 \times 10^3$ N predicted by the uncoupled analysis. Namely, the values of σ_{EQ} , σ_H , Δp and R_v were obtained from the results of elastic-plastic FEM analysis under simple tension, while the fracture life N_R in each point is estimated by these results and Eq. (7.40). In

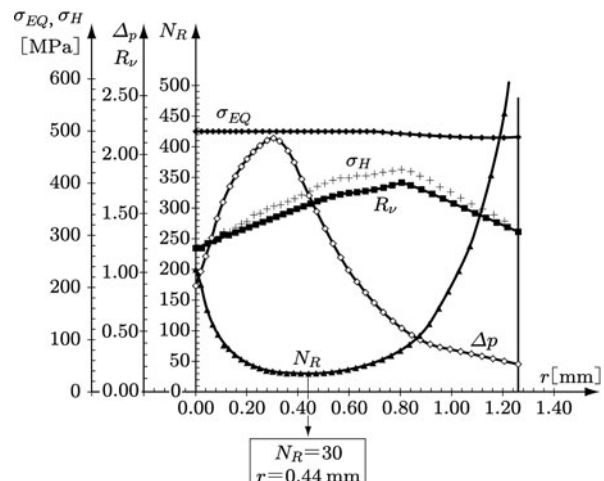


Fig. 7.8 Results of the elastic-plastic finite element analysis and the location of crack initiation predicted by Eq. (7.41)

Source: Dufailly and Lemaître (1995, p. 167, Fig. 15)

the experiment, the fatigue crack started at $N_R = 16$ at the location of $r = 0.41\text{mm}$ on the minimum cross-section. This location of crack initiation coincides well with the point $r = 0.44\text{mm}$ of the smallest fatigue life N_R predicted by the analysis. This location is not the notch root, nor the location of the largest strain range Δp , nor of the largest stress triaxiality R_v .

Chapter 8

Creep Damage and Creep-Fatigue Damage

A time-dependent deformation occurring in a material subject to load for a prolonged period of time is called *creep*. In a narrower sense, creep means a time-dependent deformation caused by a constant stress or a constant load. Materials undergoing creep for long time are often accompanied by time dependent internal deterioration. This deterioration is called *creep damage*.

When metals and alloys are subject to a variable load at elevated temperature, the materials are deteriorated by combined damage of creep and fatigue. This damage is called *creep-fatigue damage*. Creep damage and creep-fatigue damage, therefore, give essential failure modes of high temperature components.

The present chapter is concerned with the continuum damage mechanics approach to these problems. In Section 8.1, we review the phenomenological theory of creep damage which has given the prototype of continuum damage mechanics, and we describe its later refinement. Sections 8.2 and 8.3 are concerned with the application of the viscoplastic damage theory of Section 4.2 to the problems of creep and creep-fatigue damage. The application of the resulting theory to the analysis of non-isothermal creep-fatigue problems is also discussed. In Section 8.4, finally, the stress and the damage field at a creep crack tip will be discussed as another application of the creep damage theory.

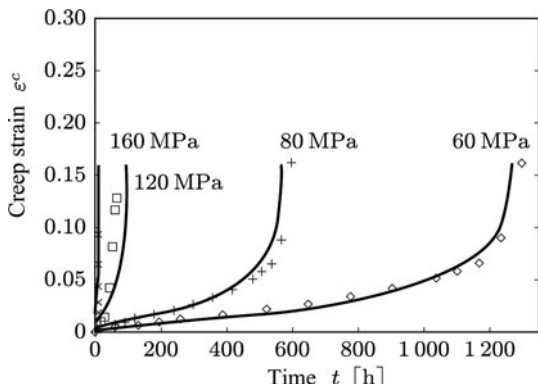
8.1 Creep Damage and Phenomenological Theory of Creep Damage

8.1.1 Creep Damage

Creep properties of materials are usually identified by creep tests, in which increase of creep strain in specimens subjected to a constant tensile load or constant tensile stress is observed. The relation between the observed creep strain ε^c versus the corresponding time t of a specimen is plotted as a *creep curve*.

Figure 8.1 shows a creep curve of 0.5Cr-0.5Mo-0.25V ferritic steel at 640°C. As observed in the figure, the creep rate $\dot{\varepsilon}^c$ decreases with the time t at first, remains constant, increases again and finally leads to the *creep rupture*. Therefore, a creep

Fig. 8.1 Creep curve of 0.5Cr-0.5Mo-0.25V steel at 640°C
Source: Perrin and Hayhurst (1999, p. 607, Fig. 4)



process can be divided into three stages from a phenomenological point of view; the *primary creep stage*, *secondary creep stage* and the *tertiary creep stage* (Odqvist and Hult 1962; Boyle and Spence 1983). The creep deformation occurring in these three stages is called *transient creep*, *steady state creep* and *accelerating creep*, respectively.

Polycrystalline metals generally show salient creep at a temperature higher than 1/3 of their melting temperatures in the absolute scale. In this range of temperature, creep is usually accompanied by material damage. This creep damage accelerates creep, and gives rise to tertiary creep stage. The microscopic mechanism of creep damage consists mainly of the nucleation, growth and the coalescence of microvoids on grain boundaries. Creep damage may be induced also by the change in metallographic structures of the metals, as will be described later.

Creep at high temperature under low level of stress, in particular, is accompanied by the salient *microvoid diffusion* in crystal grains rather than by the deformation due to dislocation motion. Materials in such condition may lead to rupture after small creep strain without obvious tertiary creep stage.

Figure 8.2 shows the micrographs of grain boundary cavities (voids) in copper, together with grain boundary cracks in type 304 austenitic stainless steel. These voids appear mainly on grain boundaries perpendicular to the direction of the maximum tensile stress, and their nucleation necessitates *grain boundary sliding* (Evans 1984).

Which one of these two types of cavities actually appears depends on the material, stress state, temperature and other factors. For example, *w-type cracks* tend to appear at lower temperature and higher stress than *r-type voids*. However, they may frequently occur in the same material; in that case w-type cracks tend to appear at lower temperature and under higher stress than the r-type voids.

8.1.2 Kachanov-Rabotnov Theory

In order to predict the creep rupture time of polycrystalline metals under uniaxial tension, Kachanov (1958) proposed a new damage theory by representing the internal damage state of the material by the use of a macroscopic variable.

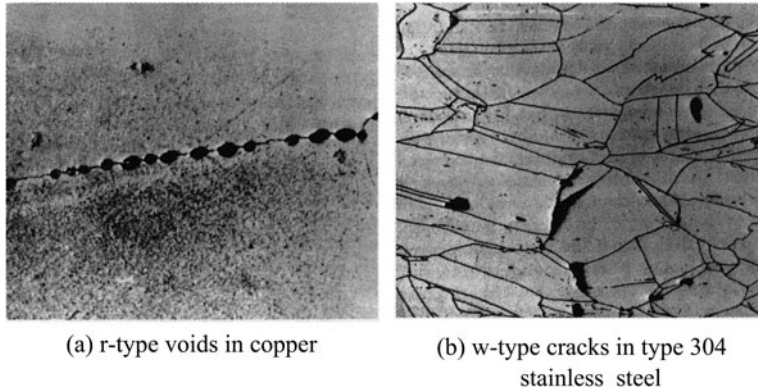


Fig. 8.2 Grain boundary cavities associated with creep damage

Source: (a) Needham, Wheatley and Greenwood (1975, p. 26, Fig. 6), (b) Matera and Rustichelli (1979, p. 398, Fig. 4)

Thereafter, Rabotnov (1969) extended this *Kachanov theory* by allowing for the increase in creep rate $\dot{\epsilon}^c$ due to creep damage, and expressed the *damage evolution equation* and the *creep constitutive equation* as follow:

$$\dot{D} = A \frac{\sigma^m}{(1 - D)^p}, \quad (8.1)$$

$$\dot{\epsilon}^c = B \frac{\sigma^n}{(1 - D)^q}, \quad (8.2)$$

where D , σ and (\cdot) denote damage variable, stress and the differentiation with respect to time t , respectively. Moreover m , n , p , q , A and B are material constants. Equations (8.1) and (8.2) are called *Kachanov-Rabotnov theory*, and have provided the prototype of the continuum damage mechanics developed thereafter.

Since $D = 0$ in the initial undamaged state, Eq. (8.2) leads to

$$\dot{\epsilon}_0^c = B\sigma^n. \quad (8.3)$$

This equation represents the steady state creep of a material, and is known as *Norton law*.

Evolution of creep damage can be calculated by Eq. (8.1) independently of the deformation. In the case of constant stress $\sigma = \text{const.}$, integration of Eq. (8.1) with the initial condition $D = 0$ at $t = 0$ gives

$$(1 - D)^{p+1} = 1 - A(p + 1)\sigma^m t. \quad (8.4)$$

Then, the *creep rupture time* t_R under a constant stress σ is obtained from Eq. (8.4) and the fracture condition $D = 1$ at $t = t_R$:

$$t_R = \frac{1}{A(p + 1)\sigma^m}. \quad (8.5)$$

The material constants m , p and A can be determined by comparing Eq. (8.5) with the results of creep tests. By eliminating $A(p + 1)\sigma^m$ from Eqs. (8.4) and (8.5), we have the evolution equation of the damage variable D

$$D = 1 - \left(1 - \frac{t}{t_R}\right)^{1/(p+1)}. \quad (8.6)$$

The creep strain ε^c , on the other hand, is derived by substituting Eq. (8.6) into Eq. (8.2) and then by integrating the resulting relation as follows:

$$\varepsilon^c = \lambda \dot{\varepsilon}_0^c t_R \left[1 - \left(1 - \frac{t}{t_R}\right)^{1/\lambda} \right], \quad (8.7a)$$

$$\lambda = \frac{1+p}{1+p-q}, \quad (8.7b)$$

where $\dot{\varepsilon}_0^c$ is the initial creep rate at the undamaged state, i.e., steady state creep rate given by Eq. (8.3).

By substituting $t = t_R$ into Eq. (8.7), we have the creep strain at rupture, i.e., *creep rupture strain*

$$\varepsilon_R^c = \lambda \dot{\varepsilon}_0^c t_R. \quad (8.8)$$

The relation of Eq. (8.8) is depicted in Fig. 8.3. As observed in the figure, increase in creep strain during the tertiary creep stage is characterized by the material constant λ of Eq. (8.7).

By introducing a new parameter $\eta = m/n$, and by using Eqs. (8.3) and (8.5), we have a relation

$$(\dot{\varepsilon}_0^c)^\eta t_R = \frac{B^{m/n}}{A(p+1)},$$

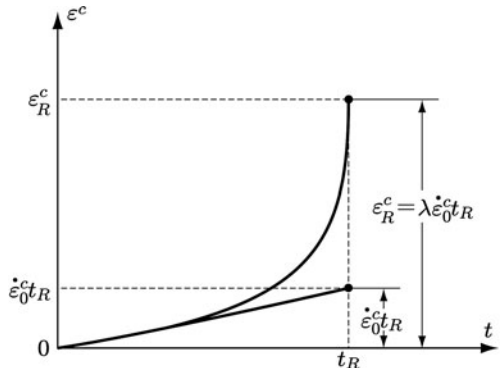


Fig. 8.3 Creep rupture time and creep rupture strain under a constant stress

or

$$(\dot{\varepsilon}_0^c)^\eta t_R = \text{const.} \quad (8.9)$$

This relation implies that there exist a relationship, which is independent of the magnitude of stress, between the steady state creep rate and the creep rupture time, and is called *Monkman-Grant relationship* (Evans 1984).

Finally, by substituting Eqs. (8.3) and (8.5), the creep rupture strain of Eq. (8.8) is expressed in an alternative form

$$\varepsilon_R^c = \frac{B}{(1+p-q)A} \sigma^{n-m}. \quad (8.10)$$

The creep exponent n in metallic materials is usually larger than the exponent m . Hence, Eq. (8.10) implies that the larger the applied stress σ the larger the resulting creep rupture strain ε_R^c , which has been ascertained by experiments. The material constants n , q and B of Eq. (8.2) are usually identified by fitting Eqs. (8.3) and (8.10) to the results of creep tests.

8.1.3 Three-Dimensional Creep Damage Theory, Stress Criteria of Creep Damage

In order to extend the evolution equation (8.1) to multiaxial states of stress, we must elucidate the dependence of damage development on the state of stress. Figure 8.4 shows the *isochronous creep rupture curves* of copper, aluminum alloy and heat-resisting alloys. As observed in the figure, the isochronous creep rupture curve of copper is governed by the maximum principal stress σ_1 or σ_2 , while that of aluminum alloy is expressed by the equivalent stress σ_{EQ} of Eq. (4.46). The isochronous creep rupture curve of some heat-resisting alloys potted in Fig. 8.4c shows the

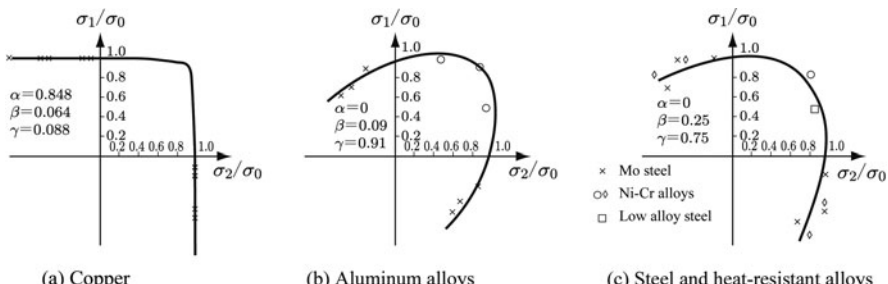


Fig. 8.4 Isochronous creep rupture curves of metallic materials

Source: Hayhurst (1972, p. 388, Fig. 11; p. 389, Fig. 13; p. 389, Fig. 12)

intermediate dependence between Fig. 8.4a and b. On the basis of these results, Hayhurst (1972) expressed the *damage stress criterion* $\chi(\sigma_{ij})$ for creep rupture as follows:

$$\chi(\sigma_{ij}) = \alpha\sigma_1 + \beta\sigma_{EQ} + 3(1 - \alpha - \beta)\sigma_H, \quad (8.11)$$

where $\sigma_H = (1/3)\sigma_{kk}$ and α , β are mean stress and material constants. The values of constants α and β for copper, aluminum alloy, Ni-Cr steel, low alloy steels, etc. can be found in the literature of Hayhurst and his coworkers (Hayhurst 1972; Hayhurst, Brown, and Morrison 1984).

In view of the stress criterion of Eq. (8.11), the evolution equation of creep damage (8.1) may be extended to the multiaxial state of stress, i.e.,

$$\dot{D} = A \frac{\chi^m}{(1 - D)^p}. \quad (8.12)$$

According to the experiments of multiaxial creep, on the other hand, it has been ascertained that the creep deformation is isochoric $\dot{\varepsilon}_{kk}^c = 0$ and the creep rate tensor $\dot{\varepsilon}_{ij}^c$ is coaxial with the deviatoric stress tensor $\sigma_{ij}^D = \sigma_{ij} - (1/3)\sigma_{kk}\delta_{ij}$. Moreover, it has been found that the equivalent creep rate $\dot{\varepsilon}_{EQ}^c = [(2/3)\dot{\varepsilon}_{ij}^c\dot{\varepsilon}_{ij}^c]^{1/2}$ is governed by the equivalent stress σ_{EQ} . Thus, on the basis of von Mises equivalent stress and the associated flow rule, the creep constitutive equation (8.2) may be extended to the form

$$\dot{\varepsilon}_{ij}^c = \frac{3}{2}B \frac{\sigma_{EQ}^n}{(1 - D)^q} \frac{\sigma_{ij}^D}{\sigma_{EQ}}. \quad (8.13)$$

The details of the microscopic mechanisms of creep, creep damage and their modeling can be found in Evans (1984), Cocks and Leckie (1987) and Cadek (1988).

8.1.4 Theory of Non-Steady State Creep Damage

The creep constitutive equation (8.13) of isotropically damaged materials was derived by postulating that the uniaxial creep rate at the undamaged state is represented by the steady state creep rate of Eq. (8.3). As shown in Fig. 8.1, however, transient increase in creep rate caused by the increase in load is usually observed in high temperature creep of metallic materials.

In the case of non-steady state creep (or transient creep) in an undamaged state, the increase in creep strain ε^c after the application of a constant stress σ can be represented by *Bailey-Norton law*

$$\varepsilon^c = B\sigma^n t^s, \quad (8.14)$$

where n , s and B are material constants. By differentiating both hand side of Eq. (8.14) with respect to time t , we have non-steady state creep rate

$$\dot{\varepsilon}^c = sB\sigma^n t^{s-1}, \quad (\text{time hardening theory}). \quad (8.15a)$$

Elimination of the time t from this relation by means of t in Eq. (8.14) provides an alternative expression of $\dot{\varepsilon}^c$:

$$\dot{\varepsilon}^c = sB^{1/s}\sigma^{n/s}(\varepsilon^c)^{(s-1)/s}, \quad (\text{strain hardening theory}). \quad (8.15b)$$

Equations (8.15a) and (8.15b) are called, respectively, *time hardening theory* and *strain hardening theory* of unsteady state creep rate (Kraus 1980; Boyle and Spence 1983).

As regards the creep rate in a damage state, on the other hand, by applying the hypothesis of strain equivalence described in Section 2.3.3 to Eq. (8.15), we have

$$\dot{\varepsilon}^c = sB\left(\frac{\sigma}{1-D}\right)^n t^{s-1}, \quad (\text{time hardening theory}), \quad (8.16a)$$

$$\dot{\varepsilon}^c = sB^{1/s}\left(\frac{\sigma}{1-D}\right)^{n/s}(\varepsilon^c)^{(s-1)/s}, \quad (\text{strain hardening theory}), \quad (8.16b)$$

where the material constant q in Eq. (8.2) has been specified as $q = n$.

Finally, by employing von Mises equivalent stress and the associated flow law, Eq. (8.16) can be extended to the multiaxial state of stress:

$$\dot{\varepsilon}_{ij}^c = \frac{3}{2}sBt^{s-1}\left(\frac{\sigma_{EQ}}{1-D}\right)^n \frac{\sigma_{ij}^D}{\sigma_{EQ}}, \quad (\text{time hardening theory}), \quad (8.17a)$$

$$\dot{\varepsilon}_{ij}^c = \frac{3}{2}sB^{1/s}\left(\varepsilon_{EQ}^c\right)^{(s-1)/s}\left(\frac{\sigma_{EQ}}{1-D}\right)^{n/s} \frac{\sigma_{ij}^D}{\sigma_{EQ}}, \quad (\text{strain hardening theory}), \quad (8.17b)$$

where ε_{EQ}^c is the equivalent creep strain defined by

$$\varepsilon_{EQ}^c = \int_0^t \left(\frac{2}{3} \dot{\varepsilon}_{ij}^c \dot{\varepsilon}_{ij}^c \right) dt. \quad (8.18)$$

8.1.5 Two-Damage Variable Model of Physics-Based Constitutive Equation

Kachanov-Rabotnov theory mentioned above represents damage states in a material by means of a scalar damage variable D , and describes the development of creep damage and the creep deformation in a damaged material. This theory,

therefore, cannot be applied accurately except to the cases where damage proceeds only in one physical mechanism, or to the cases where one specific mechanism is predominant among several mechanisms. As regards the creep rate, moreover, there are cases where the hardening and the softening behavior of a material caused by deformation are governed by several physical mechanisms. Thus the Kachanov-Rabotnov theory cannot be applied to these cases with required accuracy.

The first example of these cases is the creep damage of the nickel base superalloys. Creep damage or the deterioration of the material is caused by the softening due to multiplication of dislocation sub-structures, in addition to the nucleation of grain boundary cavities shown in Fig. 8.2. The second example can be found in ferritic low alloy steels; besides the increase in creep rate due to grain boundary cavities, salient material softening is induced also by the coarsening of precipitated particles in crystal grains.

Dyson, Hayhurst and others, therefore, postulated two damage variables D_1 and D_2 to remove the limitation of the Kachanov-Rabotnov theory, and proposed some creep constitutive equations by allowing for plural physical mechanisms for damage and deformation (Dyson, Hayhurst, and Lin 1996; Othman et al. 1993; Kowalewski et al. 1994). These equations can be summarized as follow (Hayhurst 2001).

(1) Creep Constitutive Equation

$$\frac{d\varepsilon_{ij}^c}{dt} = \frac{3}{2} \frac{A}{1 - D_2} \sinh \left[\frac{B\sigma_{EQ}(1 - H)}{(1 - G)(1 - D_1)} \right] \frac{\sigma_{ij}^D}{\sigma_{EQ}}, \quad (8.19)$$

$$\frac{dH}{dt} = \lambda_1 \frac{hA}{1 - D_2} \sinh \left[\frac{B\sigma_{EQ}(1 - H)}{(1 - G)(1 - D_1)} \right] \left(1 - \frac{H}{H^*}\right) \frac{1}{\sigma_{EQ}}, \quad (8.20)$$

$$\frac{dG}{dt} = \lambda_2 \frac{C}{3} (1 - G)^4. \quad (8.21)$$

(2) Damage Evolution Equation

$$\frac{dD_1}{dt} = \lambda_3 \frac{PA}{1 - D_2} \sinh \left[\frac{B\sigma_{EQ}(1 - H)}{(1 - G)(1 - D_1)} \right] \left(\frac{\sigma_I}{\sigma_{EQ}} \right)^n, \quad (8.22)$$

$$\frac{dD_2}{dt} = \lambda_4 QA (1 - D_2) \sinh \left[\frac{B\sigma_{EQ}(1 - H)}{(1 - G)(1 - D_1)} \right] \left(1 - \frac{H}{H^*}\right), \quad (8.23)$$

where D_1 , D_2 and G , H denote the internal variables representing the damage state and the strain-hardening state, respectively. The symbols σ_{ij}^D , σ_{EQ} and σ_I

designate the deviatoric stress, equivalent stress and the maximum principal stress, while h , n , A , B , H^* , P and Q are the material constants. The symbols λ_1 through λ_4 are parameters representing the governing mechanisms of deformation and damage, and they each have the value of 1 or 0.

Among four internal variables D_1 through H , the variable H denotes the state of strain-hardening of the primary creep, and its evolution equation (8.20) describes the increase in dislocation density in primary creep. The internal variable G , on the other hand, signifies the creep softening due to coarsening of precipitated particles in crystal grains, and the relevant evolution equation (8.21) describes monotonous increase in G from $G = 0$ to 1. The damage variable D_1 of Eq (8.22), furthermore, represents the development of creep-constrained grain boundary cavitation caused by the creep of the matrix. Finally, the damage variable D_2 of Eq. (8.23) models material softening caused by the multiplication of dislocation sub-structures.

Equations (8.19) through (8.23) furnish the creep constitutive equations and the damage evolution equations of the following materials by selecting the relevant values of λ_1 through λ_4 (Hayhurst 2001):

- (1) Aluminum Alloy: $\lambda_4 = 0$
- (2) Nickel Base Superalloy: $\lambda_1 = \lambda_2 = 0$
- (3) Ferritic Low Alloy Steel: $\lambda_4 = 0$

Figure 8.5 shows the results of a three-dimensional finite element analysis of creep damage in a branch pipe connection of a ferritic low alloy steel. While Fig. 8.5a

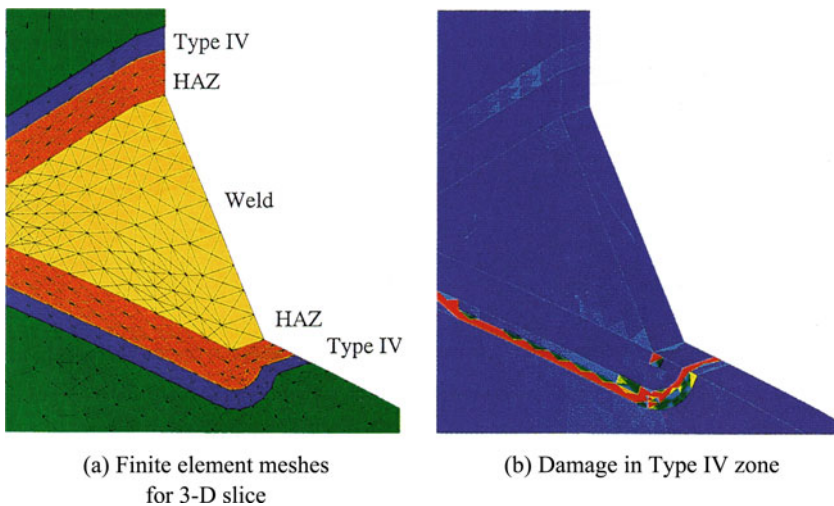


Fig. 8.5 Creep damage analysis of a welded T-branch pipe connection subject to internal pressure at elevated temperature

Source: Hayhurst (2001, p. 184, Fig. 9 (c), (d))

depicts finite element meshes, Fig. 8.5b represents the damage distribution at the failure time of 18,254 h. The pipe material and the weld metal were 0.5Cr-0.5Mo-0.25V steel and 2.25Cr-1.0Mo steel, and the working temperature and the working pressure were 590°C and 4 MPa.

As observed in Fig. 8.5b, the fracture region of $D = 0.99$ is prevailed largely in *Type IV zone*.¹ The creep constitutive equation and the damage evolution equation are given by prescribing $\lambda_4 = 0$ in Eqs. (8.19) through (8.23). The material constants for the pipe, weld metal and the materials of HAZ¹ and Type IV zone are given in literature (Hayhurst 2001; Perrin and Hayhurst 1999; Kowalewski et al. 1994).

8.1.6 Anisotropic Creep Damage Theory

As described in Section 8.1.1, creep damage in polycrystalline material usually shows salient anisotropic features. The evolution equations and the related constitutive equations of such materials can be derived in the general framework of the anisotropic damage theory described in Chapters 2 and 5.

We now consider two typical anisotropic creep damage theories developed by means of the second and the fourth order damage tensors.

(1) Creep Damage Theory Based on a Second Order Damage Tensor

Creep damage of polycrystalline material is characterized by the effective area reduction caused by the development of grain boundary cavities on planes perpendicular, or nearly perpendicular to the maximum tensile stress. By postulating a representative volume element (RVE) of volume V shown in Fig. 8.6, the damage

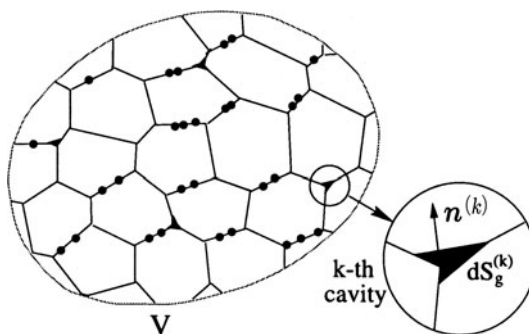


Fig. 8.6 Representative volume element and grain boundary cavities in creep damage
Source: Murakami and Ohno (1981)

¹ In weld parts of steel, the heat affected zone between the weld metal and the matrix material is called HAZ (heat affected zone). HAZ is classified into several types by their metallographic structures. Among them, there is a case where a softening layer of minute grains is formed between the weld metal and the matrix, and the zone is called Type IV zone. Type IV zone is usually noted because the triaxiality stress may be induced in this zone by the constraint of the relatively hard layers outside this zone (Viswanathan 1989).

state in the RVE can be represented by the procedure discussed in [Section 2.2.4](#). Then the state of damage and the related magnified stress can be represented, respectively, by a second-order symmetric damage tensor of [Eq. \(2.15\)](#) and the effective stress tensor of [Eq. \(2.19\)](#):

$$\mathbf{D} = \sum_{i=1}^3 D_i \mathbf{n}_i \otimes \mathbf{n}_i, \quad (8.24)$$

$$\tilde{\boldsymbol{\sigma}} = \frac{1}{2} \left[(\mathbf{I} - \mathbf{D})^{-1} \boldsymbol{\sigma} + \boldsymbol{\sigma} (\mathbf{I} - \mathbf{D})^{-1} \right], \quad (8.25)$$

where D_i and \mathbf{n}_i denote the principal value and the principal direction of the damage tensor \mathbf{D} .

As regards the development of creep damage, we postulate the effective area reduction on the plane perpendicular to the maximum principal direction $\mathbf{n}^{(1)}$ of the effective stress tensor $\tilde{\boldsymbol{\sigma}}$, in addition to the accompanying isotropic damage due to the development of spherical grain boundary voids.

Then we may write the evolution equation of the creep damage in the form ([Murakami and Ohno 1981](#)):

$$\dot{\mathbf{D}} = A\chi(\tilde{\boldsymbol{\sigma}})^m \left[\zeta \mathbf{I} + (1 - \zeta) \mathbf{n}^{(1)} \otimes \mathbf{n}^{(1)} \right], \quad (8.26a)$$

$$\chi(\tilde{\boldsymbol{\sigma}}) = \alpha \tilde{\sigma}^{(1)} + \beta \tilde{\sigma}_{EQ} + (1 - \alpha - \beta) (\text{tr} \tilde{\boldsymbol{\sigma}}), \quad (8.26b)$$

where $\tilde{\sigma}^{(1)}$ and $\tilde{\sigma}_{EQ}$ denote the maximum effective principal stress and the equivalent stress of the effective stress tensor $\tilde{\boldsymbol{\sigma}}$, whereas A , m , α , β and ζ are material constants.

The simplest expression of the anisotropic *evolution equation* is furnished by taking $\alpha = 1$ and $\beta = \zeta = 0$ in Eq. (8.26):

$$\dot{\mathbf{D}} = A \left(\tilde{\sigma}^{(1)} \right)^m \mathbf{n}^{(1)} \otimes \mathbf{n}^{(1)}. \quad (8.27)$$

As regards the constitutive equation of creep, the strain-hardening hypothesis of [Section 8.1.4](#) is postulated. If the equivalent creep rate $\dot{\varepsilon}_{EQ}^c$ can be expressed in the form

$$\dot{\varepsilon}_{EQ}^c = B \left(\varepsilon_{EQ}^c \right)^s \left(\tilde{\sigma}_{EQ} \right)^n, \quad (8.28)$$

the creep *constitutive equations* is given as follows:

$$\dot{\boldsymbol{\varepsilon}}^c = \frac{3}{2} \Lambda \frac{\tilde{\boldsymbol{\sigma}}^D}{\tilde{\sigma}_{EQ}}, \quad (8.29a)$$

$$\Lambda = \dot{\varepsilon}_{EQ}^c, \quad (8.29b)$$

where n , s and B are material constants.

(2) Creep Damage Theory Based on a Fourth Order Damage Tensor

As described in [Section 2.2.7](#), the anisotropic damage state of material can be expressed also by the variation of the elastic modulus caused by damage. Then, by employing a fourth-order asymmetric damage tensor \mathbb{D} and an effective stress tensor $\tilde{\sigma}$ of [Eq. \(2.34\)](#)

$$\mathbb{D} = \mathbb{I} - \mathcal{C}(\mathbb{D}) : \mathbb{C}_0^{-1}, \quad (8.30)$$

$$\tilde{\sigma} = (\mathbb{I} - \mathbb{D})^{-1} : \sigma, \quad (8.31)$$

Chaboche ([1982](#), [1984](#)) developed the following anisotropic creep damage theory.

By postulating a process of proportional loading, the anisotropic features of the damage may remain unchanged. Then, the damage rate can be described by

$$\dot{\mathbb{D}} = \mathcal{Q}\dot{D}, \quad (8.32)$$

where \mathcal{Q} is a fourth-order constant tensor characterized by the principal directions $\mathbf{n}^{(i)}$ of the effective stress tensor $\tilde{\sigma}$, and by the intrinsic material property. The symbol \dot{D} , on the other hand, denotes a scalar variable specifying the damage rate.

If the material damage is induced by the distributed plane microcracks perpendicular to the maximum principal stress, in addition to the isotropic development of grain boundary voids, [Eq. \(8.32\)](#) is expressed in an explicit form:

$$\dot{\mathbb{D}} = [\gamma\mathbb{I} + (1 - \gamma)\mathbb{G}]\dot{D}, \quad (8.33a)$$

$$\dot{D} = <\frac{\chi(\tilde{\sigma}, D)}{A}>^k \left[\frac{\chi(\sigma)}{A} \right]^{r-k}, \quad (8.33b)$$

where \mathbb{G} is a fourth-order tensor representing the rigidity variation due to damage development. If damaged material can be modeled by an elastic body containing a number of periodically distributed plane microcracks, the tensor \mathbb{G} can be represented by the following matrix in Voigt notation (see [Section 12.7.1](#)):

$$\mathbb{G} = \begin{bmatrix} 1 & 0 & 0 & 0 & 0 & 0 \\ v/(1-v) & 0 & 0 & 0 & 0 & 0 \\ v/(1-v) & 0 & 0 & 0 & 0 & 0 \\ 0 & 0 & 0 & 0 & 0 & 0 \\ 0 & 0 & 0 & 0 & \eta & 0 \\ 0 & 0 & 0 & 0 & 0 & \eta \end{bmatrix}, \quad (8.34)$$

where v and η denote the Poisson's ratio and a material constant. The function $\chi(\tilde{\sigma}, D)$ of [Eq. \(8.33b\)](#) is a damage stress criterion expressed in the effective stress $\tilde{\sigma}$, and has a similar form to [Eq. \(8.26\)](#):

$$\chi(\tilde{\sigma}, D) = \alpha\tilde{\sigma}^{(1)} + \beta H(D)\tilde{\sigma}_{EQ} + (1 - \alpha - \beta)J(D)(\text{tr}\tilde{\sigma}), \quad (8.35)$$

where $H(D)$ and $J(D)$ are properly identified material functions.

Finally, by postulating a viscoplastic potential

$$F = \frac{K}{n+1} \left[\frac{\tilde{\sigma}_{EQ}}{K} \right]^{n+1} p^{-n/m}, \quad p = \varepsilon_{EQ}^c, \quad (8.36)$$

the creep rate of the damaged material is expressed as follows:

$$\begin{aligned} \dot{\varepsilon}^c &= \frac{\partial F}{\partial \sigma} \\ &= \frac{3}{2} \left[\frac{\tilde{\sigma}_{EQ}}{K} \right]^n \frac{(\mathbb{I} - \mathbb{D})^{-1} : \tilde{\sigma}^D}{\tilde{\sigma}_{EQ}}, \end{aligned} \quad (8.37)$$

where $\tilde{\sigma}^D$, m , n and K are material constants.

(3) Validation and Comparison between Two Anisotropic Damage Theories

The essential difference between the above two anisotropic damage theories exists in the definition of the effective stresses and the equivalence hypotheses between damaged and undamaged materials.

Systematic experimental results applicable to the validation of the above anisotropic creep damage theories have been hardly available. Murakami and Imaizumi (1982), therefore, performed a series of model tests by the use of plate specimens deteriorated by two-dimensional periodic distribution of small circular holes subject to tension in different directions. Then Murakami and Imaizumi (1982) and Chaboche (1984) discussed this problem based on the results of these tests.

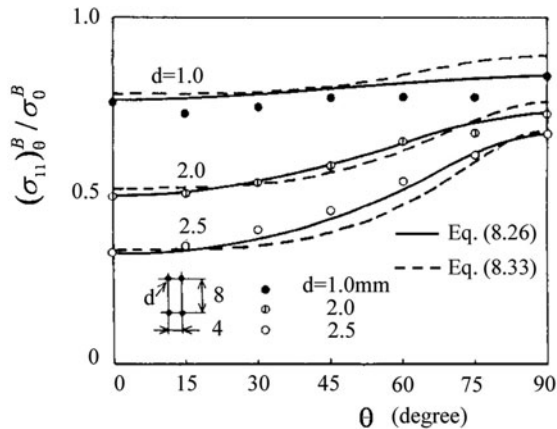
Figure 8.7 shows examples of the results of this validation, and demonstrates the orientation dependence of the strength and the strain response of the damaged specimens. The abscissae of these figures are the angle θ between the principal directions of the orthotropic perforation arrangement entered in the figures and the tensile direction of the specimens. The solid and the dashed lines represent the prediction of Eqs. (8.26) and (8.33), respectively.

Figure 8.7a firstly represents the orientation dependence of the fracture strength of the damaged specimens, where σ_0^B and $(\sigma_{11})_\theta^B$ denote the tensile strength of the undamaged isotropic material and that of the perforated specimens under tension in the θ direction. Thus Fig. 8.7a may represent the isochronous creep damage stress for different states of damage.

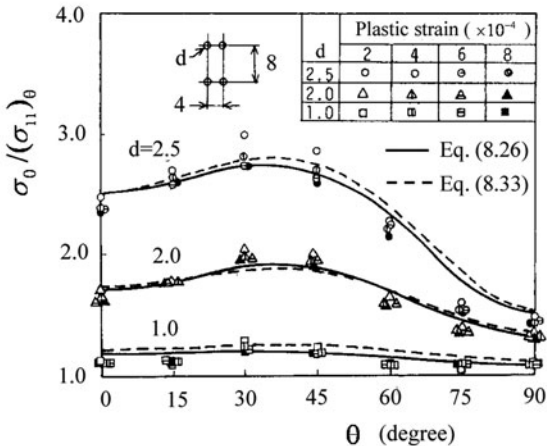
Figure 8.7b, on the other hand, represents the orientation dependence of the effective stress ratio $\sigma_0 / (\sigma_{11})_\theta$ which furnishes the identical magnitudes of the strains. The symbol $(\sigma_{11})_\theta$ represents the magnitude of the tensile stress in the θ specimen which furnishes the strain of the identical magnitude to that induced in the undamaged specimen by the stress σ_0 .

It should be noted in the figure that, as far as the present model tests are concerned, any significant difference was not observed between two anisotropic damage theories. In the case of more complicated anisotropy, e.g., fiber-reinforced

Fig. 8.7 Comparison between two anisotropic damage tensors
Source: Murakami and Imaizumi (1982) and Chaboche (1984)



(a) Orientation dependence of the fracture strength



(b) Orientation dependence of the effective stress

composites, or geological materials under complicated loading history, the applicability of the second-order damage tensor may have its limitation. The example of these cases will be described in Chapters 9 and 10 later.

8.2 Viscoplastic Damage Theory of Creep Damage

In a number of metals, including the stainless steel and the nickel base alloy, viscoplastic deformation is frequently observed when they are subject to load at elevated temperature. In these cases, marked creep deformation is induced when the stress exceeds their yield limit, and creep damage ensues from it.

In the present section, we first apply the thermodynamic constitutive theory of viscoplastic damage discussed in [Section 4.2](#) to derive the constitutive and the evolution equation of creep damage. Then we consider some related problems of the resulting theory.

8.2.1 Constitutive and Evolution Equations of Viscoplastic Damage Material

The constitutive and the evolution equation of the viscoplastic isotropic damage theory developed in [Sections 4.2.3](#) through [4.2.5](#) are summarized as follow:

(1) Constitutive Equation of Viscoplasticity

$$\dot{\varepsilon}_{ij}^{vp} = \frac{3}{2} \frac{1}{1-D} \frac{\tilde{\sigma}_{ij}^D - A_{ij}^D}{(\tilde{\sigma} - A)_{EQ}} \dot{\Lambda}, \quad (8.38)$$

$$\dot{\Lambda} = (1-D) < \frac{f}{K_V} >^n, \quad (8.39)$$

$$\dot{p} = \dot{\varepsilon}_{EQ}^{vp} = \frac{\dot{\Lambda}}{1-D} = < \frac{f}{K_V} >^n, \quad (8.40)$$

$$\dot{r} = \dot{\Lambda}, \quad (8.41)$$

$$\dot{\alpha}_{ij} = \frac{3}{2} \left[\frac{\tilde{\sigma}_{ij}^D - A_{ij}^D}{(\tilde{\sigma} - A)_{EQ}} - \frac{1}{A_\infty} A_{ij}^D \right] \dot{\Lambda}, \quad (8.42)$$

$$f = (\tilde{\sigma} - A)_{EQ} - R - \sigma_Y, \quad (8.43)$$

$$\dot{R} = R_\infty [1 - \exp(-br)], \quad (8.44)$$

$$A_{ij}^D = \frac{2}{3} A_\infty \gamma \alpha_{ij}^D, \quad (8.45)$$

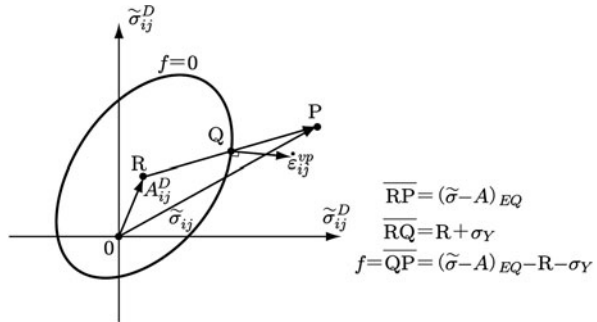
where $< >$ of Eq. (8.39) is the Macauley bracket.

(2) Evolution Equation of Isotropic Viscoplastic Damage

$$\dot{D} = \left(\frac{Y}{S} \right)^m \dot{p} H(p - p_D), \quad (8.46)$$

$$Y = \frac{(\tilde{\sigma}_{EQ})^2}{2E} R_v, \quad (8.47)$$

Fig. 8.8 Loading surface and viscoplastic strain rate



When viscoplastic strain in uniaxial state is expressed by the logarithmic creep law of Eq. (4.14) rather than the Norton law of Eq. (4.13), \dot{p} in the above equations is given, instead of Eq. (8.40), as follows:

$$\dot{p} = \dot{\varepsilon}_{EQ}^{vp} = \frac{\dot{A}}{1-D} = \ln \left(1 - \frac{f}{K_\infty} \right)^{-N}. \quad (8.48)$$

Equation (8.38) describes time dependent strain rate $\dot{\varepsilon}_{ij}^{vp}$, and its magnitude is specified by \dot{A} of Eq. (8.39). Figure 8.8 shows schematically the loading surface $f = 0$ and the associated viscoplastic strain rate $\dot{\varepsilon}_{ij}^{vp}$. The viscoplastic strain rate $\dot{\varepsilon}_{ij}^{vp}$ occurs when $f = \overline{QP} > 0$ holds in this figure, and the damage rate \dot{D} of Eq. (8.46) is induced when the accumulated viscoplastic strain p exceeds its threshold p_D .

The creep deformation, i.e., viscoplastic deformation without yield phenomenon, is frequently observed in high polymer materials as well as in metallic materials subjected to quasi-static load at elevated temperature. By prescribing $\sigma_Y = 0$, Eqs. (8.38) through (8.48) furnish the constitutive equations of combined isotropic and kinematic hardening creep, together with the evolution equation of the resulting isotropic creep damage.

8.2.2 Creep Damage Under Uniaxial Tension

Let us examine the uniaxial case of Eqs. (8.38) through (8.48). If we take $\sigma_Y = 0$, $R = 0$ and $A_{ij}^D = 0$, Eqs. (8.38) and (8.46) are reduced, respectively, to

$$\dot{\varepsilon}^c = (K_V)^{-n} \left(\frac{\sigma}{1-D} \right)^n, \quad (8.49)$$

$$\dot{D} = (2ES)^{-m} (K_V)^{-n} \left(\frac{\sigma}{1-D} \right)^{2m+n} H(\varepsilon^c - \varepsilon_D^c), \quad (8.50)$$

i.e., we have the Kachanov-Rabotnov equations (8.1) and (8.2) for uniaxial steady state creep.

In order to examine the effect of the threshold strain ε_D^c on the creep rupture behavior of a material, we rewrite Eqs. (8.49) and (8.50) in the forms of Eqs. (8.1) and (8.2):

$$\dot{\varepsilon}^c = B \left(\frac{\sigma}{1 - D} \right)^n, \quad (8.51)$$

$$\dot{D} = A \left(\frac{\sigma}{1 - D} \right)^m H(\varepsilon^c - \varepsilon_D^c). \quad (8.52)$$

Let t_0 denote the time of creep damage initiation under a constant stress σ . Then, the threshold creep strain ε_D^c for creep damage initiation is given by Eq. (8.51):

$$\varepsilon_D^c = B\sigma^n t_0. \quad (8.53)$$

Evolution of creep damage variable D , on the other hand, can be derived by integrating Eq. (8.52) with the initial condition of $t = t_0$ and $D = 0$ as follows:

$$D = 1 - [1 - (m+1)A\sigma^m(t - t_0)]^{1/(m+1)}. \quad (8.54)$$

By applying the fracture condition of $D = D_C = 1$ to this equation, we have the creep rupture time t_R :

$$t_R - t_0 = \frac{1}{(m+1)A\sigma^m}. \quad (8.55)$$

Then, the evolution of creep damage is expressed in the form

$$D = 1 - \left(1 - \frac{t - t_0}{t_R - t_0} \right)^{1/(m+1)}. \quad (8.56)$$

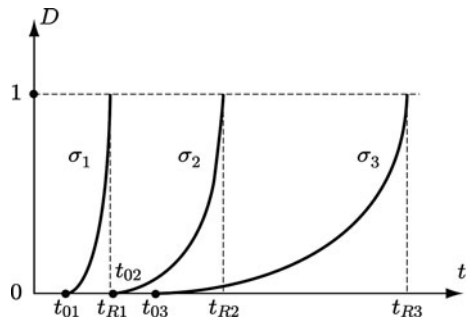
Finally, the development of creep strain ε^c is obtained by substituting Eq. (8.56) into Eq. (8.51), and by integrating the resulting equation as follows:

$$\varepsilon^c - \varepsilon_D^c = \lambda \dot{\varepsilon}_0^c (t_R - t_0) \left[1 - \left(1 - \frac{t - t_0}{t_R - t_0} \right)^{1/\lambda} \right], \quad (8.57a)$$

$$\lambda = \frac{1+m}{1+m-n}, \quad \dot{\varepsilon}_0^c = B\sigma^n. \quad (8.57b)$$

Figure 8.9 shows schematically the creep damage process caused by three constant magnitudes of stress σ_1 , σ_2 and σ_3 ($\sigma_1 > \sigma_2 > \sigma_3$) in the case of a given strain threshold $\varepsilon_D^c = \text{const.}$ for the damage initiation. In the particular case of $t_0 = 0$ and $\varepsilon_D^c = 0$, the above results are reduced to those of Kachanov-Rabotnov theory described in Section 8.1.2.

Fig. 8.9 Creep damage process for a given damage threshold $\varepsilon_D^c = \text{const.}$
 $(\sigma_1 > \sigma_2 > \sigma_3)$



8.2.3 Viscoplastic Damage Theory by Hypothesis of Total Energy Equivalence

In Section 4.4.3, a nonlinear hardening viscoplastic constitutive equation was derived on the basis of the hypothesis of total energy equivalence (Saanouni et al. 1994). Then, the constitutive equation of viscoplastic strain $\boldsymbol{\epsilon}^{vp}$ and the evolution equations of the internal state variables r , α and D were expressed by Eqs. (4.161) through (4.165).

In comparison with the constitutive theory of viscoplastic damage in Section 8.2.1, the evolution equations of Section 4.4.3 have explicit coupling between isotropic hardening variable r and damage variable D . In other words, the viscoplastic damage theory based on the hypothesis of total energy equivalence can describe creep damage phenomena over a broader range without restrictions mentioned in the preceding section.

8.3 Creep-Fatigue Damage

When a polycrystalline metal is subject to a cyclic loading at an elevated temperature, the material undergoes creep damage and fatigue damage at the same time. Since the microscopic mechanisms of these two kinds of damage differ from each other, they essentially develop independently. However, depending on the loading conditions, they may affect each other and accelerate the material damage.

This type of damage is called *creep-fatigue damage*, or *creep-fatigue interaction*, and gives one of the most important problems in the fracture-life evaluation of high temperature components.

8.3.1 Microscopic Mechanisms of Creep-Fatigue Damage and Its Modeling

While creep damage in polycrystalline metals develops mainly by the development of grain boundary cavities in the material, fatigue damage is caused by

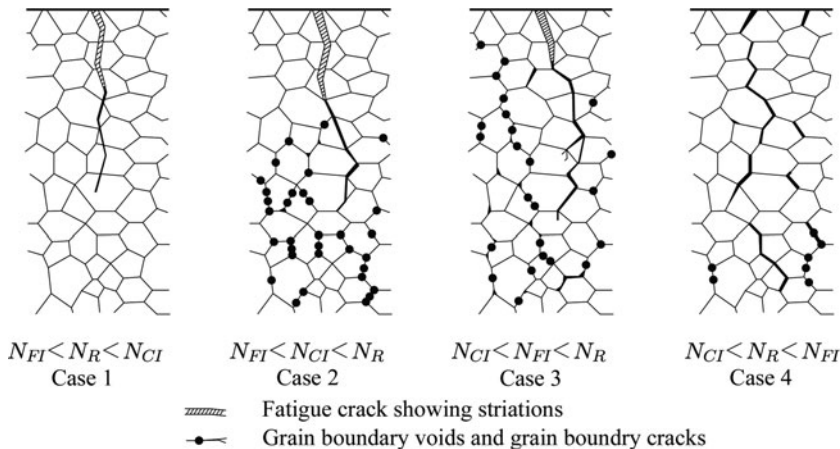


Fig. 8.10 Modes of damage in creep-fatigue damage

Source: Goodall et al. (1981, p. 119, Fig. 11)

the occurrence and growth of microcracks on the surface of the material due to intra-granular sliding.

Figure 8.10 shows schematically the four damage modes observed in creep-fatigue damage. The symbols N_R , N_{FI} and N_{CI} in the figure denote the fracture cycle number due to creep-fatigue damage, the cycle number of fatigue crack initiation and that of creep void nucleation, respectively. Because of the difference in the mechanisms of creep and fatigue, the interaction between these two types of damage is not salient in the early stage of damage. In the stage of developed damage, however, creep damage usually accelerates fatigue damage, whereas the effect of fatigue damage on creep damage is not significant.

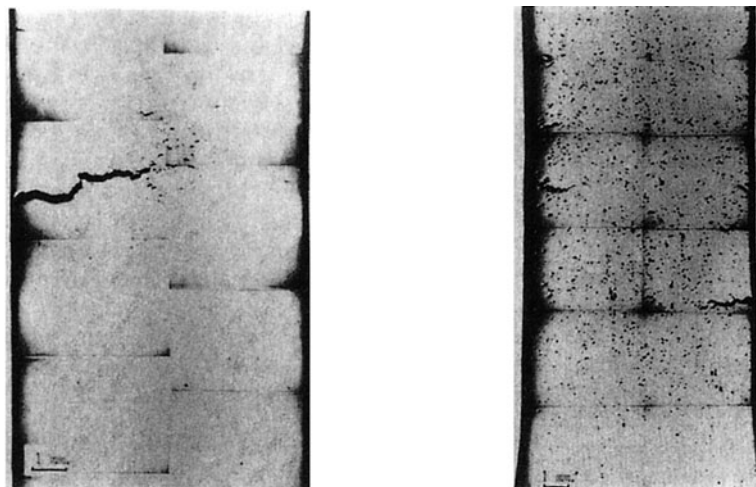
Figure 8.11 shows micrographs of creep-fatigue damage in 316L stainless steel at 600°C, where figures (a) and (b) correspond to the cases of 2 and 3 of Fig. 8.10. Namely the fatigue crack of Fig. 8.11a accelerates the development of grain boundary voids at its crack tip, and these voids facilitate the extension of the fatigue crack. In Fig. 8.11b, on the other hand, the effect of surface fatigue cracks on the creep damage inside the material is small.

The most straightforward method to analyze the creep fatigue damage by means of damage mechanics is to express the damage increase dD in terms of the sum of the creep damage increase dD_C and the fatigue damage increase dD_F :

$$\begin{aligned} dD &= dD_C + dD_F, \\ &= F_C(\sigma, D_C, D_F, T) dN + F_F(\sigma, D_C, D_F, T) dN, \end{aligned} \quad (8.58)$$

where F_C and F_F are the functions specifying the development of the creep and the fatigue damage in one cycle.

Specification of Eq. (8.58) will be discussed in the following sections.



(a) Load cycles of 1.2% total strain range. First 500 cycles with 10 min. tensile hold, then 100 cycles with 5 hr. tensile hold, and again 55 cycles with 10 min. tensile hold.
(b) 373 loading cycles of 1.2 % total stain range, with 24 hr. tensile hold in each cycle.

Fig. 8.11 Creep-fatigue damage in 316L stainless steel at 600°C

Source: Cailletaud and Levaillant (1984, p. 281, Fig. 6; p. 282, Fig. 7)

8.3.2 Analysis of Uniaxial Creep-Fatigue Damage

A specific form of Eq. (8.58) can be formulated (Lemaitre 1992) by the use of the creep damage theory of Section 8.2 together with the low cycle fatigue theory of Section 7.2. Let us first suppose the creep-fatigue damage process under uniaxial loading shown in Fig. 8.12.

The effect of such creep-fatigue interaction can be depicted as in Fig. 8.13. The symbol N_R in the figure denotes the fracture cycle number of the creep-fatigue damage, i.e., the cycle number at fracture due to the strain range $\Delta\varepsilon^p$ in Fig. 8.12b.

Fig. 8.12 Loading cycle in creep-fatigue damage
Source: Lemaitre (1992, p. 133, Fig. 3.23)

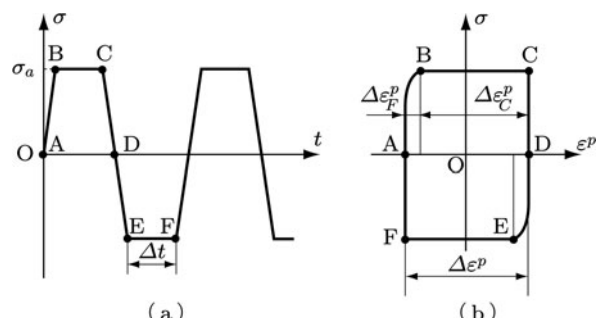
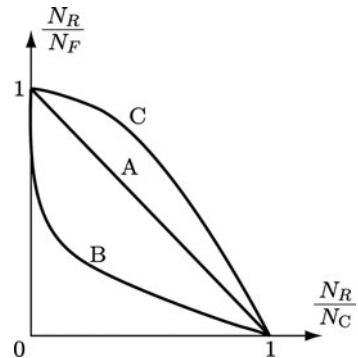


Fig. 8.13 Fracture life in creep-fatigue damage



The symbol N_F , on the other hand, is the fracture cycle number when the fatigue damage of strain range $\Delta\varepsilon_F^p$ alone would develop in the cycle, whereas N_C is the fracture cycle number when the creep damage due to $\Delta\varepsilon_C^p$ alone would proceed. The curves, A, B and C in the figure show schematically the damage processes represented, respectively, by the relations

$$\frac{N_R}{N_F} + \frac{N_R}{N_C} = 1, \quad (8.59a)$$

$$\frac{N_R}{N_F} + \frac{N_R}{N_C} < 1, \quad (8.59b)$$

$$\frac{N_R}{N_F} + \frac{N_R}{N_C} > 1. \quad (8.59c)$$

While Eq. (8.59a) represents a *linear creep-fatigue damage law*, Eq. (8.59b) and (8.59c) describe *nonlinear creep-fatigue damage laws*. The case of Eq. (8.59b), in particular, represents the decrease in fatigue life as a result of creep-fatigue interaction.

Now we analyze the creep-fatigue damage process caused by the loading cycles of Fig. 8.12, and elucidate their interaction in some detail. For this purpose, we postulate that the loading cycle can be divided into a fatigue part AB + DE and a creep part BC + EF. Furthermore, we suppose that the total plastic strain range $\Delta\varepsilon^p$ consists of the strain range of a fatigue part $\Delta\varepsilon_F^p$ and that of a creep part $\Delta\varepsilon_C^p$, as shown in Fig. 8.12b.

Let us first derive the number of cycles at fracture N_R of the creep-fatigue damage process. As regards one cycle of the creep-fatigue damage of Fig. 8.12, i.e., one cycle of plastic strain range $\Delta\varepsilon^p$, Eq. (7.22) gives

$$\frac{\delta D}{\delta N} = \frac{(\sigma_a)^2}{ES(1-D)^2} \Delta\varepsilon^p, \quad (8.60a)$$

where σ_a signifies the stress amplitude. In order to determine the damage development due to loading cycles, we assume that the change in damage variable during one cycle is small. Then integration of Eq. (8.60a) gives

$$\int (1 - D)^2 dD = \int \frac{(\sigma_a)^2}{ES} \Delta\varepsilon^p dN. \quad (8.60b)$$

By employing the condition of microcrack initiation of Eq. (7.21) together with the condition of final fracture of $D = D^C$ at $N = N_F$, the calculation of Eq. (8.60b) leads to the relation:

$$N_R = (\Delta\varepsilon^p)^{-1} \left\{ \frac{p_D}{2} + \frac{ES \left[1 - (1 - D^C)^3 \right]}{3(\sigma_a)^2} \right\}. \quad (8.61)$$

In this section, subscript C has been employed to signify the creep damage. To avoid the confusion, the critical value of the damage variable D will be represented by D^C by using superscript C hereafter.

Now, we consider the fracture cycle number N_F of fatigue damage subject only to the cyclic plastic strain amplitude $\Delta\varepsilon_F^p$. Then, the fatigue damage development in one cycle is given by Eq. (7.22) as follows

$$\frac{\delta D_F}{\delta N} = \frac{(\sigma_a)^2}{ES(1 - D_F)^2} \Delta\varepsilon_F^p. \quad (8.62)$$

Integration of this relation with the condition (7.21) for microcrack initiation and the fatigue fracture condition of $D_F = D_F^C$ at $N = N_F$ furnishes the following relation, similarly to Eq. (8.61):

$$N_F = (\Delta\varepsilon_F^p)^{-1} \left\{ \frac{p_D}{2} + \frac{ES \left[1 - (1 - D_F^C)^3 \right]}{3(\sigma_a)^2} \right\}. \quad (8.63)$$

Concerning the creep damage, on the other hand, the damage growth in one cycle of cyclic creep due to strain range $\Delta\varepsilon_C^p$ alone can be derived from Eqs. (8.46) and (8.47):

$$\frac{\delta D_C}{\delta N} = \frac{(\sigma_a)^2}{2ES(1 - D_C)^2} \Delta\varepsilon_C^p, \quad (8.64)$$

where we assumed $m = 1$ in Eq. (8.46), and that no creep damage occurs in the compressive part EF of Fig. 8.12. Integration of this relation with the crack initiation condition (7.21) and the fracture condition of $D_C = D_C^C$ at $N = N_C$ gives

$$N_C = (\Delta\varepsilon_C^p)^{-1} \left\{ \frac{p_D}{2} + \frac{2ES}{(\sigma_a)^2} \frac{1 - (1 - D_C^C)^3}{3} \right\}. \quad (8.65)$$

Finally, by the use of Eqs. (8.61) through (8.65), the terms of $N_R/N_F + N_R/N_C$ in Eq. (8.59) is derived

$$\frac{N_R}{N_F} + \frac{N_R}{N_C} = \left(\frac{\Delta\varepsilon_F^p}{\Delta\varepsilon^p} \right) \frac{\frac{p_D}{2} + \frac{ES[1 - (1 - D^C)^3]}{3(\sigma_a)^2}}{\frac{p_D}{2} + \frac{ES[1 - (1 - D_F^C)^3]}{3(\sigma_a)^2}} + \left(\frac{\Delta\varepsilon_C^p}{\Delta\varepsilon^p} \right) \frac{\frac{p_D}{2} + \frac{ES[1 - (1 - D^C)^3]}{3(\sigma_a)^2}}{\frac{p_D}{2} + \frac{2ES}{(\sigma_a)^2} \frac{1 - (1 - D_C^C)^3}{3}}. \quad (8.66)$$

According to the relative values of D^C , D_F^C and D_C^C among them, the left hand side of Eq. (8.66) has the specific values corresponding to any one of the right hand side of Eq. (8.59), and thus describes the phenomena of creep-fatigue interaction. Because of the complexity of Eq. (8.66), however, it is not easy to clarify its functional feature. Then, by considering the particular case of

$$p_D = 0, \quad \Delta\varepsilon_F^p = \Delta\varepsilon_C^p = \frac{1}{2}\Delta\varepsilon^p, \quad (8.67)$$

and by disregarding the terms higher than the second-order of D^C , D_F^C and D_C^C , Eq. (8.66) is reduces to

$$\frac{N_R}{N_F} + \frac{N_R}{N_C} = \frac{1}{2} \frac{D^C (D_F^C + D_C^C)}{D_F^C D_C^C}. \quad (8.68)$$

In view of this relation, it will be observed that each of Eq. (8.59) corresponds to the cases

$$\frac{D^C}{2} \left(\frac{1}{D_F^C} + \frac{1}{D_C^C} \right) = 1, \quad (8.69a)$$

$$\frac{D^C}{2} \left(\frac{1}{D_F^C} + \frac{1}{D_C^C} \right) < 1, \quad (8.69b)$$

$$\frac{D^C}{2} \left(\frac{1}{D_F^C} + \frac{1}{D_C^C} \right) > 1. \quad (8.69c)$$

Equation (8.69) shows that whether the creep-fatigue interaction reduces or prolongs the fracture life depends on whether the critical value of fracture D^C is smaller than the values of D_F^C and D_C^C or not. The present analysis is concerned with the

combined damage of creep and fatigue. However, as observed from Eqs. (8.62) and (8.64), the interaction between the creep damage D_C and the fatigue damage D_F has not been taken into account.

8.3.3 Non-isothermal Multiaxial Creep-Fatigue Damage I – Modeling of Creep-Fatigue Interaction, Viscoplastic Damage Theory

For the accurate analysis of creep-fatigue damage process of high temperature components, the discussion of Section 8.3.2 should be extended to non-isothermal multiaxial state. We now consider a non-isothermal multiaxial creep-fatigue damage theory based on the evolution equation of Eq. (8.58) and the nonlinear hardening viscoplastic constitutive equation.

(1) Mechanical Effect of Damages in Creep-Fatigue Damage

Let us first assume that the state of creep and fatigue damage can be represented by a scalar damage variable Ω_C and Ω_F , respectively. Since creep damage and fatigue damage influence each other, subsequent development of creep damage Ω_C and fatigue damage Ω_F is affected not only by their own current states Ω_C and Ω_F but also by the state of the other damage Ω_F and Ω_C . Then, we shall represent the overall effect of the current damage state on the damage Ω_C and Ω_F by the use of new damage variables D_C and D_F , and shall discuss their specific expressions.

As described in Section 8.3.1, the effect of creep damage on the subsequent development of fatigue damage is larger than that of fatigue damage on creep damage. Moreover, this interaction will be significant only after the sufficient development of damage.

By taking account of this aspect, Dunne and Hayhurst (1992a) expressed the damage variable D_C and D_F :

$$D_C = \Omega_C + \alpha_1 Z(\Omega_C) \Omega_F, \quad (8.70a)$$

$$D_F = \Omega_F + \alpha_2 Z(\Omega_C) \Omega_C, \quad (8.70b)$$

where α_1 , α_2 ($>> \alpha_1$) and $Z(\Omega_C)$ are material constants and a material function characterizing the creep-fatigue interaction of the material.

As regards the damage effect on the viscoplastic deformation of the material, on the other hand, there is little difference between the effect of creep damage and that of fatigue damage. Then, the damage effect on the deformation may be expressed by a damage variable

$$D = \Omega_C + \Omega_F. \quad (8.70c)$$

(2) Evolution and Constitutive Equations of Multiaxial Creep-Fatigue Damage

Let us now consider the evolution equation and the constitutive equation of cyclic viscoplastic deformation. As regards the creep damage in multiaxial states, Eqs. (8.11) and (8.12) give the following evolution equation

$$\frac{d\Omega_C}{dt} = A \frac{[\alpha\sigma_1 + (1 - \alpha)\sigma_{EQ}]^m}{(1 - D_C)^p}, \quad (8.71)$$

where σ_1 and σ_{EQ} are the maximum principal stress and the von Mises equivalent stress. The symbols A , m , p and α are temperature dependent material constants.

Concerning the fatigue damage, on the other hands, the evolution equation of multiaxial cyclic plastic damage (Chaboche 1988) may be employed:

$$\frac{d\Omega_F}{dN} = B \left[1 - (1 - D_F)^{q+1} \right]^\ell \left[\frac{A_{EQ}}{M(1 - D_F)} \right]^q, \quad (8.72a)$$

$$A_{EQ} = \frac{1}{2} \max(t) \left\{ \max(t') \left[\frac{3}{2} (\sigma^D(t) - \sigma^D(t')) : (\sigma^D(t) - \sigma^D(t')) \right]^{1/2} \right\}, \quad (8.72b)$$

where A_{EQ} signifies the maximum range of equivalent stress variation during one cycle. Furthermore, ℓ and M denote a function of A_{EQ} and that of mean stress, respectively, whereas q and B are temperature dependent material constants. Symbols t and t' in Eq. (8.72b) signify arbitrary time in one cycle.

Finally, the constitutive equation of multiaxial cyclic deformation is given by the nonlinear hardening viscoplastic constitutive equation of Chaboche and Rousselier (1983) as follows:

$$\dot{\epsilon}^p = \frac{3}{2} < \frac{(\sigma - A)_{EQ} / (1 - D) - \sigma_Y}{K} >_n \frac{\sigma^D - A^D}{(\sigma - A)_{EQ}}, \quad (8.73a)$$

$$A = A_1 + A_2, \quad (8.73b)$$

$$\dot{A}_1 = \frac{2}{3} C_1 (1 - D) \dot{\epsilon}^p - \gamma_1 A_1 \dot{p} + \frac{C'_1}{C_1} A_1 \dot{T}, \quad (8.73c)$$

$$\dot{A}_2 = \frac{2}{3} C_2 (1 - D) \dot{\epsilon}^p - \gamma_2 A_2 \dot{p} + \frac{C'_2}{C_2} A_2 \dot{T}, \quad (8.73d)$$

$$(\sigma - A)_{EQ} = \left[\frac{3}{2} (\sigma^D - A^D) : (\sigma^D - A^D) \right]^{1/2}, \quad (8.73e)$$

$$\dot{p} = \left(\frac{2}{3} \dot{\epsilon}^p : \dot{\epsilon}^p \right)^{1/2}, \quad (8.73f)$$

$$C'_1 = \frac{dC_1}{dT}, \quad C'_2 = \frac{dC_2}{dT}, \quad (8.73g)$$

$$\sigma = \mathbb{C} (1 - D) : (\epsilon - \epsilon^p - \epsilon^T), \quad (8.74)$$

where A , T , C , σ_Y and $\boldsymbol{\epsilon}^T$ denote, respectively, kinematic hardening variable, temperature, elastic modulus tensor, yield stress and thermal strain. Moreover, symbols n , K , C_1 , C_2 , γ_1 and γ_2 are temperature dependent material constants.

The method of the identification of the material constants involved in the evolution equations (8.70) through (8.72) and those in constitutive equations (8.73) and (8.74) together with their results for copper at 20°C through 500°C are shown in Dunne and Hayhurst (1992a). These equations were applied to finite element analysis of creep-fatigue damage due to thermal stress cycles in a slag-tap of a gasification equipment of coal.

8.3.4 Non-isothermal Multiaxial Creep-Fatigue Damage 2 – Coupled and Uncoupled Analyses by Viscoplastic Damage Theory

Analyses of non-isothermal multiaxial creep-fatigue damage necessitate not only pertinent constitutive and evolution equations but also efficient analytical methods to deal with a huge amount of computation.

According to Sermage and others (2000), we now show that the viscoplastic damage theory described in Chapter 4 can be applicable to the analyses not only of the ductile and the fatigue damage, but also of the multiaxial creep-fatigue damage. Then, by comparing their results of a coupled and an uncoupled analysis of viscoplastic damage process with the results of experiments, we show that an uncoupled analysis can give sufficiently accurate evaluation of their failure life.

(1) Evolution Equation and Threshold Values for Damage Initiation

The analyses of the ductile damage and the fatigue damage of Chapters 6 and 7 were performed based on the evolution equation (6.11) or (8.46) of isotropic damage and the related crack initiation condition, i.e.,

$$\dot{D} = \left(\frac{Y}{S} \right)^s \dot{p} H(p - p_D), \quad (8.75a)$$

$$D = D^C, \quad (8.75b)$$

where p_D is the threshold of the accumulated plastic strain p for damage initiation given by Eq. (4.100). As to its value, however, while it is $p_D = \varepsilon_D^p$ in the case of a monotonic uniaxial test, the value determined by fatigue tests is $p_D = \varepsilon_D^p (\sigma_U - \sigma_Y)^\zeta / (\sigma_{EQ}^{Max} - \sigma_Y)^\zeta$ as given by Eq. (4.100), and has significant difference between them.

In order to obviate this inconsistency, we suppose the rate of stored energy in the material

$$\dot{W}_S = (\sigma_{EQ} - \sigma_Y) \dot{p}, \quad (8.76)$$

which was employed for the derivation of Eq. (4.100). Since dW_S/dp tends to 0 with the increase of p , Eq. (8.76) may be modified to be

$$\dot{W}_S = (\sigma_{EQ} - \sigma_Y) \frac{\varepsilon_D^p}{p + \varepsilon_D^p} \dot{p}. \quad (8.77)$$

Let the maximum value of σ_{EQ} in the course of the deformation be σ_{EQ}^{Max} . Then, integration of Eq. (8.77) from $p = 0$ to $p = p_D$ provides

$$W_S = \left(\sigma_{EQ}^{Max} - \sigma_Y \right) \varepsilon_D^p \ln \left(\frac{p_D + \varepsilon_D^p}{\varepsilon_D^p} \right). \quad (8.78)$$

In the case of a simple tension, this relation leads to

$$(W_S)_T = (\sigma_U - \sigma_Y) \varepsilon_D^p \ln 2. \quad (8.79)$$

The stored energy for the damage initiation must be identical in the cases of the variable stress and the monotonic simple tension. Then, Eqs. (8.78) and (8.79) together with the relation $W_S = (W_S)_T$ give the threshold p_D for damage initiation:

$$p_D = \varepsilon_D^p \left[\exp \left(\frac{\sigma_U - \sigma_Y}{\sigma_{EQ}^{Max} - \sigma_Y} \ln 2 \right) - 1 \right]. \quad (8.80)$$

(2) Elastic-Viscoplastic Constitutive Equation

Concerning the constitutive equation of coupled multiaxial creep-fatigue damage, by the use of effective stress

$$\tilde{\sigma} = \frac{\sigma}{1 - D}, \quad (8.81)$$

and the elastic-viscoplastic constitutive equation of Eqs. (4.69) through (4.76) together with Norton law of Eq. (4.80), we have the following expressions:

$$\dot{\epsilon} = \dot{\epsilon}^e + \dot{\epsilon}^p, \quad (8.82)$$

$$\epsilon^e = \frac{1 + \nu}{E} \tilde{\sigma} - \frac{\nu}{E} (\text{tr} \tilde{\sigma}) I, \quad (8.83)$$

$$\dot{\epsilon}^p = \frac{3}{2} \frac{\tilde{\sigma}^D - A^D}{(\tilde{\sigma}^D - A^D)_{EQ}} \dot{p} H(f), \quad (8.84)$$

$$(\tilde{\sigma} - A)_{EQ} = \left[\frac{3}{2} (\tilde{\sigma}^D - A^D) : (\tilde{\sigma}^D - A^D) \right]^{1/2}, \quad (8.85)$$

$$\dot{p} = \left\langle \frac{f}{K} \right\rangle^N, \quad (8.86)$$

$$f = (\tilde{\sigma} - A)_{EQ} - R - \sigma_Y, \quad (8.87)$$

$$R = R_\infty [1 - \exp(-br)], \quad (8.88)$$

$$\dot{r} = (1 - D) \dot{p}, \quad (8.89)$$

$$\dot{A} = \frac{2}{3} \gamma A_\infty (1 - D) \dot{\epsilon}^p - \gamma A (1 - D) \dot{p}, \quad (8.90)$$

where R, A and $(\cdot)^D$ denote isotropic hardening variable, kinematic hardening variable and the deviatoric part of tensors. Moreover, yield stress σ_Y , the parameters of plastic hardening b , A_∞ , γ and the parameters of Norton law K and N are all temperature dependent material constants.

The specific values of the above material constants have been identified for 2.25Cr-1Mo steel by cyclic tension-compression tests at 20, 300, 400, 500 and 600°C (Sermage et al. 2000).

As examples of the results of these tests, the threshold ε_D^p for damage initiation and the critical value D^C for crack nucleation in simple tension are shown in Fig. 8.14.

(3) Damage Analysis of Maltese-Cross Specimen

Damage and fracture analyses of structural components are usually performed on various level of elaboration depending on the required accuracy and permissible costs of the calculation.

Let us now examine the accuracy and the time needed for the calculation on two levels of elaboration, with respect to the case of finite element analysis of biaxial creep-fatigue damage in Maltese-cross specimen shown in Fig. 8.15 (Sermage et al.

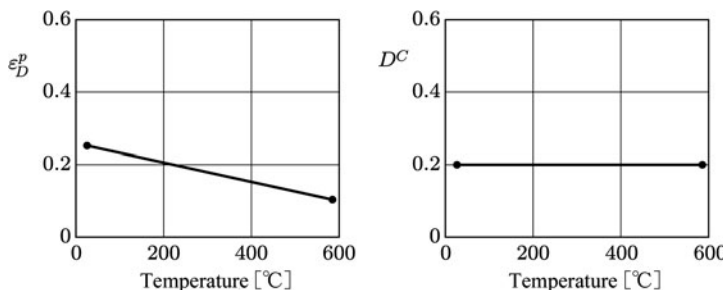


Fig. 8.14 Threshold for damage initiation ε_D^p and critical value for crack nucleation D^C in uniaxial tension

Source: Sermage et al. (2000, p. 245, Fig. 5)

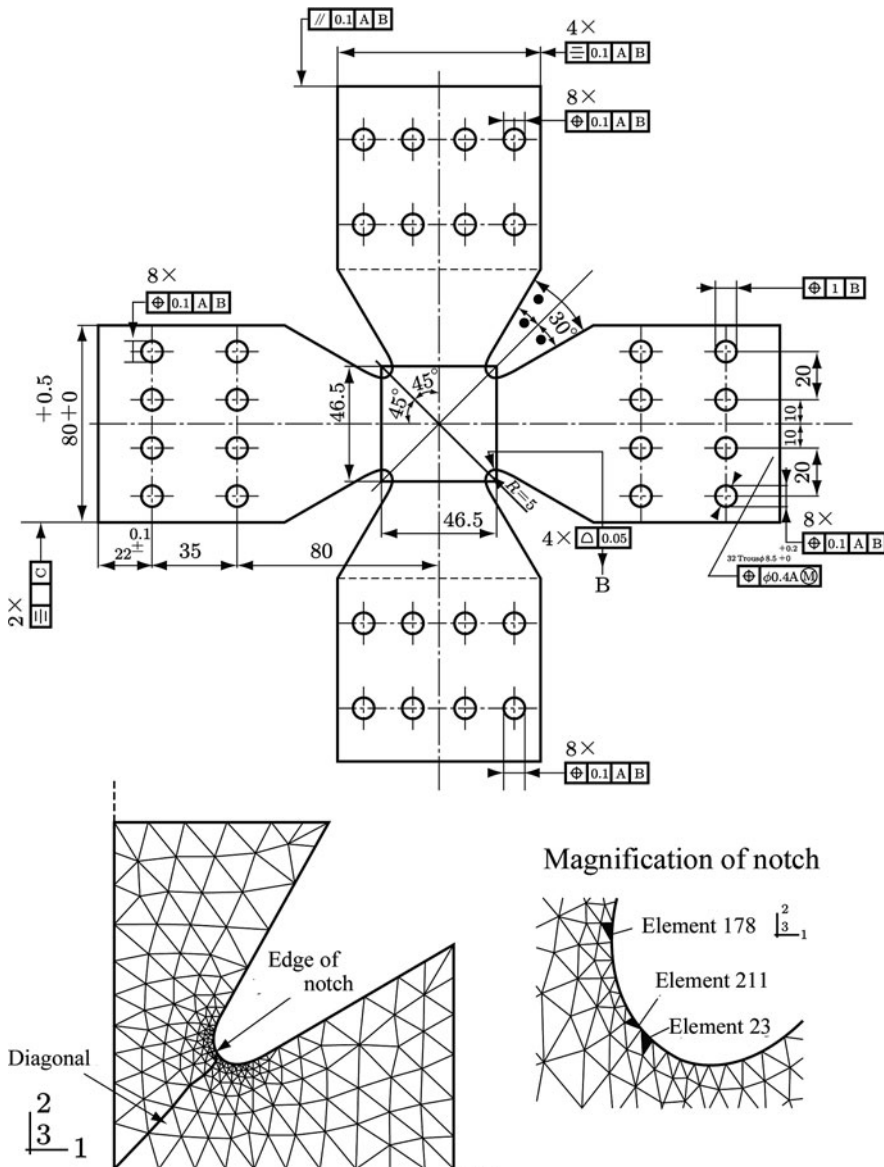


Fig. 8.15 Maltese-cross specimen (thickness 4.5 mm) and finite element meshes (320 six-node triangles)

Source: Sermage et al. (2000, p. 248, Fig. 7)

2000): the one is the coupled analysis of deformation and damage, while the other is the case of uncoupled analysis. The analyses are performed by the use of the evolution equation of viscoplastic damage of Eqs. (8.75) through (8.80) together with the elastic-viscoplastic constitutive equation of Eqs. (8.81) through (8.90).

In the coupled analysis, the evolution and the constitutive equation are calculated at the same time to determine the stress, plastic strain and the damage as functions of time. The uncoupled analysis, on the other hand, is carried out in two steps. In the first step, by postulating undamaged state of $D = 0$, one performs elastic-viscoplastic analysis of undamaged material to obtain the stress and the plastic strain history. In the second step, furthermore, the evolution equation of damage is integrated by the use of the resulting stress and plastic strain histories to calculate the evolution equation of damage.

The calculation and the corresponding experiments were executed for six conditions shown in Table 8.1. Table 8.2 summarizes the results of these experiments and analyses. The time of calculation for the uncoupled analysis was less than 1/50 of that of the coupled analysis.

As observed in Table 8.2, the difference in the numerical results of N_R for the uncoupled and the coupled analysis was 47% at most. Moreover, the difference between the result of N_R for the uncoupled analysis and those of experiments is less than a factor of two, and this difference may be permissible from the practical point of view. That is to say, though the damage evolution equation of Eq. (8.75) has been derived for the purpose of the ductile and the fatigue damage analyses, it can

Table 8.1 Condition of creep-fatigue tests (Sermage et al. 2000, p. 249, Table 1)

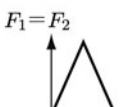
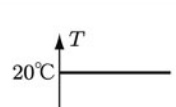
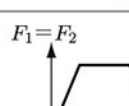
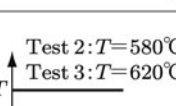
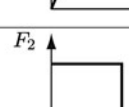
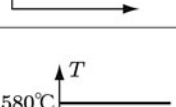
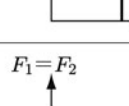
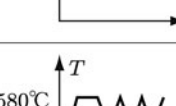
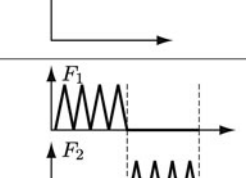
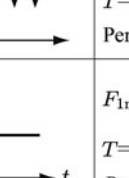
Test 1 Pure fatigue	 	Inspection of test procedures
Tests 2&3 Creep-fatigue	 	$F_{1\max} = F_{2\max} = 28 \text{ kN}$ Hold time 40 s
Test 4 Out of phase, nonproportional	 	$F_{1\max} = F_{2\max} = 28 \text{ kN}$ Hold time 40 s
Test 5 Thermal fatigue	 	$F_{1\max} = F_{2\max} = 32 \text{ kN}$ $T = 350 \sim 580^\circ\text{C}$ Period 600 s
Test 6 Sequential, nonproportional	 	$F_{1\max} = F_{2\max} = 35 \text{ kN}$ $T = 580^\circ\text{C}$ Period 160 s

Table 8.2 Comparison between the results of experiments and analyses (Sermage et al. 2000, p. 249, Table 2)

Test	Results of tests	Comparison	
		Coupled analysis	Uncoupled analysis
Tests 2, 3 Creep-fatigue	$N_R (580^\circ C) = 331$ $N_R (620^\circ C) = 100$	$N_R = 420$ $N_R = 115$	$N_R = 266$
Test 4 Out of phase, non-proportional	$N_R = 2356$	$N_R = 2135$	$N_R = 1130$
Test 5 Thermal fatigue	$N_R = 56$	$N_R = 48$	$N_R = 27$
Test 6 Sequential, non-proportional	$N_R = 196$	$N_R = 230$	$N_R = 273$

be applicable also to the analyses of creep-fatigue damage with sufficient accuracy by the use of the threshold p_D of Eq. (8.80) for the damage initiation.

8.4 Effect of Damage Field on Stress Field at a Creep Crack Tip

Damage field around a crack tip affects the surrounding stress field, and hence governs the crack extension behavior in the material. This effect of the damage field is an important problem also in the discussion of stability and convergence in crack extension analysis.

At the end of this chapter, we shall show briefly the approximate analysis of the effect of damage field on the stress field around a mode I creep crack in steady state growth (Murakami, Hirano, and Liu 2000, 2001). The analysis of mode III creep crack can be performed in a similar way (Murakami and Hirano 2000).

Let us first consider a Cartesian coordinate system $O-x_1x_2x_3$ and a polar coordinate system $O-r\theta z$ of Fig. 8.16a with their origin O at the tip of a creep crack which is in steady state growth at a constant velocity v . Then, the governing equations for the analysis of creep crack extension in the state of plane strain or plane stress are given as follow:

(1) Creep Damage Evolution Equation and Creep Constitutive Equation

According to the Kachanov-Rabotnov creep damage theory, the evolution and the constitutive equation of creep damage are given by Eqs. (8.12) and (8.13) as follow:

$$\dot{D} = A \left(\frac{\sigma_{EQ}}{1 - D} \right)^m, \quad (8.91)$$

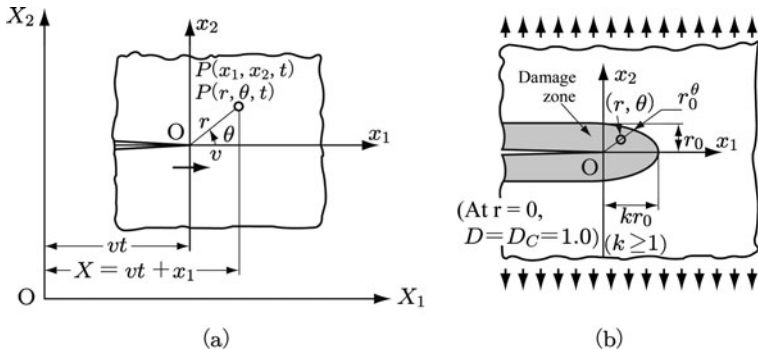


Fig. 8.16 Mode I creep crack in steady state growth

$$\dot{\varepsilon}_{ij}^c = \frac{3}{2}B \left(\frac{\sigma_{EQ}}{1-D} \right)^n \frac{\sigma_{ij}^D}{1-D}, \quad (8.92)$$

where (\cdot) denotes the material derivative with respect to time t , and is given as

$$(\cdot) = \frac{\partial}{\partial t} - \left(\cos \theta \frac{\partial}{\partial r} - \frac{\sin \theta}{r} \frac{\partial}{\partial \theta} \right) v. \quad (8.93)$$

Since the damage field $D(r, \theta, z, t)$ around the creep crack tip in steady growth at a constant velocity v is unchanged with respect to the moving coordinate system $O-r\theta z$, we have the relation

$$\frac{\partial D}{\partial t} \equiv 0. \quad (8.94)$$

Hence, the evolution equation (8.91) has the following form

$$-\cos \theta \frac{\partial D}{\partial r} + \frac{\sin \theta}{r} \frac{\partial D}{\partial \theta} = \frac{A}{v} \left(\frac{\sigma_{EQ}}{1-D} \right)^m. \quad (8.95)$$

(2) Compatibility Equation of Creep Strain Rate

$$r \frac{\partial}{\partial r} \left[\frac{\partial (r \dot{\varepsilon}_{\theta\theta})}{\partial r} \right] + \frac{\partial^2 \dot{\varepsilon}_{rr}}{\partial \theta^2} - r \frac{\partial \dot{\varepsilon}_{rr}}{\partial r} - 2 \frac{\partial}{\partial r} \left(r \frac{\partial \dot{\varepsilon}_{r\theta}}{\partial \theta} \right) = 0. \quad (8.96)$$

(3) Stress Components

By postulating Airy stress function $\Phi(r, \theta)$ expressed in the polar coordinate system, the stress components in the plane strain and in the plane stress state are expressed:

$$\begin{aligned}\sigma_{rr} &= \frac{1}{r^2} \frac{\partial^2 \Phi}{\partial \theta^2} + \frac{1}{r} \frac{\partial \Phi}{\partial r}, & \sigma_{\theta\theta} &= \frac{\partial^2 \Phi}{\partial r^2}, \\ \sigma_{r\theta} &= -\frac{\partial}{\partial r} \left(\frac{1}{r} \frac{\partial \Phi}{\partial \theta} \right).\end{aligned}\tag{8.97}$$

(4) Airy Stress Function

As for the *asymptotic stress field* at the crack tip, we can postulate the following Airy stress function

$$\Phi(r, \theta) = Kr^\varsigma F(\theta),\tag{8.98}$$

where K , ς and $F(\theta)$ are an indeterminate coefficient, an indeterminate exponent and an indeterminate function of θ , respectively. From this relation together with Eq. (8.97), the asymptotic stress field at the crack tip is derived as follows:

$$\sigma_{rr}(r, \theta) = Kr^\lambda [sF(\theta) + F''(\theta)],\tag{8.99a}$$

$$\sigma_{\theta\theta}(r, \theta) = Kr^\lambda [s(s-1)F(\theta)],\tag{8.99b}$$

$$\sigma_{r\theta}(r, \theta) = Kr^\lambda [(1-s)F'(\theta)],\tag{8.99c}$$

where $\lambda = \varsigma - 2$ denotes the exponent representing the singularity of the stress field, and will be called the *stress singularity exponent* hereafter. The indeterminate coefficient K corresponds to the *stress intensity factor* of nonlinear material, and hence depends on the stress exponent n of the creep constitutive equation.

By substituting the stress components of Eq. (8.99) into creep constitutive equation (8.92) and damage evolution equation (8.95), and by employing the resulting equation together with the compatibility equation (8.96), we could have a set of nonlinear simultaneous partial differential equations of the damage variable D and the indeterminate function $F(\theta)$. It is not easy, however, to derive the rigorous solutions of $D(r, \theta)$ and $F(\theta)$ for the whole domain of analysis (Benallal and Siad 1997, 2001). Hence the problem was solved by deriving an asymptotic damage field shown in Fig. 8.16b which satisfies the damage evolution equation (8.95) in the region around the crack tip. The detail of the analysis should be referred to the literature (Murakami, Hirano, and Liu 2000, 2001).

Figure 8.17 shows the relation between the stress singularity exponent λ of the asymptotic stress field (8.99) at the crack tip and the creep and the damage properties

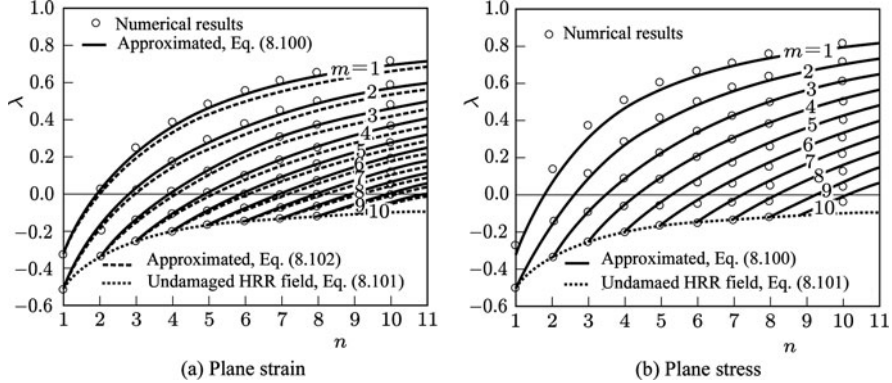


Fig. 8.17 Stress singularity at the tip of Mode I creep crack in steady state growth

of the material. The analysis was performed for the case of the semicircular crack tip field ($k = 1$) (see Fig. 8.16b). The small circles in the figure are the results of the numerical analysis by means of the semi-inverse method, whereas the solid lines represent the following approximate expression to the numerical results (Murakami, Hirano, and Liu 2000):

$$\lambda = \frac{n^{(1+c/n)} - (m+1)}{n + m[1 + n - n^{(1+c/n)}] + 1}, \quad (8.100a)$$

$$c = 0.100 \quad (\text{plane strain state}), \quad (8.100b)$$

$$c = 0.370 \quad (\text{plane stress state}). \quad (8.100c)$$

The dotted lines in the figure, on the other hand, represent the HRR (Hutchinson-Rice-Rosengren) stress fields for an undamaged nonlinear hardening material

$$\lambda = -\frac{1}{n+1}. \quad (8.101)$$

Since the stress singularity exponent $\lambda < 0$ represents the singular stress at the crack tip $r = 0$, HRR stress field is singular at the crack tip for all the finite value of stress exponent n . As observed in Fig. 8.17, however, the existence of a damage field increases largely the value of λ , and hence may furnish nonsingular (regular) stress field for finite value of n . This is a very important aspect in the damage field effect on the stress singularity of the crack tip field.

In the case of plane strain state, in particular, the numerical results shown by small circles in Fig. 8.17 can be approximated by a more simple relation than Eq. (8.100):

$$\lambda = \frac{n - (m + 1)}{n + m + 1}. \quad (8.102)$$

The dashed lines in Fig. 8.17a indicate the relation of Eq. (8.102). In the vicinity of the singularity limit $\lambda = 0$, above all, Eq. (8.102) describes the numerical results within the error of 5%.

As already mentioned in Section 8.1.1, usual metals have the property $n \geq m$, and hence gives an inequality

$$n \geq m - 1. \quad (8.103)$$

In view of this inequality together with Eqs. (8.102) and (8.103), the value of the stress singularity exponent λ is specified as

$$\lambda < 0 \quad \text{for} \quad m - 1 \leq n < m + 1. \quad (8.104a)$$

$$\lambda \geq 0 \quad \text{for} \quad m + 1 \leq n. \quad (8.104b)$$

According to these relations, we may predict that the stress field in front of a mode I creep crack in steady state growth is singular or regular, depending on whether the exponent n and m are in the range of Eq. (8.104a) or in Eq. (8.104b).

The relation of Eq. (8.100) or (8.102) gives important information not only for the discussion of creep crack behavior in structural components, but also for the discussion of the stability and the convergence in numerical analysis of creep fracture process.²

Similar results have been obtained also for a mode III creep crack in steady state growth (Murakami and Hirano 2000).

² When λ given by Eq. (8.100) or (8.102) is $\lambda < 0$, the stress field in front of the creep crack tip is singular, and a stable convergent solution is not assured. The procedures to obviate the stress singularity or the damage localization in the local approach to fracture based on the continuum damage mechanics and the finite element method are described later in Chapter 11.

Chapter 9

Elastic-Brittle Damage

Besides ductile materials considered hitherto, a variety of brittle materials, like concrete, rocks and ceramics, are widely employed in engineering practice. Their mechanical behavior can not be described by the elastic-plastic damage theory or by the viscoplastic damage theory discussed already.

The present chapter is concerned with the damage and the deformation behavior of elastic-brittle materials, and the related continuum damage mechanics theory to describe them. In Section 9.1, the microscopic mechanisms of damage and the related mechanical behavior of microcracks in concrete will be discussed. Application of the simplest theory of isotropic damage to the damage process of concrete with unilateral crack effect is described in Section 9.2.

The damage of brittle materials is generally accompanied by salient anisotropy and unilateral effects. In Section 9.3, therefore, this problem is discussed by the use of anisotropic damage theory based on a second-order damage tensor. Finally, in order to elucidate the effect of anisotropy which is more complex than the orthotropy, the anisotropic damage theories employing the elastic modulus tensor and the elastic compliance tensor as a damage variable will be discussed in Sections 9.4 and 9.5, respectively.

9.1 Damage of Elastic-Brittle Material

9.1.1 Damage of Brittle Material¹

In ductile materials, such as metals, large irreversible deformation can develop without any material damage. That is to say, as regards dislocation motion in crystalline

¹ Concrete, rocks and ceramics are usually called brittle materials. Observed in more detail, however, these materials may be accompanied by certain amount of dissipation prior to fracture.

Thus, more rigorous definition of the material is sometimes employed for this reason. Namely, a material is defined a *brittle material* if it has no dissipation before the crack initiation and its fracture does not result in any irreversible strain (e.g., glass and ceramics). On the other hand, a material is said a *quasi-brittle material* if a certain amount of dissipation occurs before crack initiation although it shows no irreversible strain in its whole process (e.g., concrete).

Hereafter, a term “brittle material” will be used both for the brittle and the quasi-brittle material, unless their distinction is particularly needed.

metals, the breakage and the connection of atomic bonds equilibrate with each other, and the elastic properties of metals are hardly changed by their plastic deformation. The irreversible deformation in brittle materials, on the other hand, is caused mainly by the occurrence and development of microcracks in the material, and is accompanied by marked decrease in elastic rigidity.

The aspects of initiation and growth of *microcracks* in brittle materials differ largely by the difference in microstructures of the materials, stress and strain states, and their loading rates, etc. For example, in a brittle material including a number of microscopic voids or microscopic inclusions, the mesoscopic cracks are nucleated by the tensile stress acting on void surfaces, on inclusions or in their interfaces. In brittle materials which hardly include voids and inclusions, on the other hand, microcracks of kink or of wing shape can be induced by the relative slide on the crack surfaces existing initially (Horii and Nemat-Nassar 1985; Krajcinovic 1996).

Concrete, in particular, is one of the most important construction materials, and is a heterogeneous composite consisting of cement mortar and aggregates. Hence the mechanisms of damage and deformation of concrete are even more complex. Namely, in concrete, by a stress that is not only tensile but is compressive, microcracks are induced at the interfaces between mortar and aggregate, or in the mortar between aggregates. These microcracks bring about the initiation and the extension of macroscopic cracks.

With regards to the modeling of damage in brittle materials, and in particular the mechanical behavior of microcracks in brittle materials, see a comprehensive exposition of Krajcinovic (1989, 1996).

9.1.2 Damage Behavior of Concrete

Concerning the modeling of concrete as a brittle material, a considerable number of damage theories are available. Let us first consider here the microscopic structures of concrete and the associated feature of damage and fracture for the expedience of the subsequent discussion.

(1) Nucleation of Microcracks

Concrete is a composite of cement mortar and aggregate. Its microscopic structure consists of three phases, i.e., *mortar*, *aggregate* and the *interface layers* between them (Mehta 1986). In the interface layers, crystals of hydrated cement have specific orientation. This part includes a large number of microcracks and other defects, has large void ratio, and constitutes the weakest phase.

Damage of concrete starts mainly from the interface layers or from the mortar phase, because there exist a plenty of microvoids. The aspects of the damage development, however, differ largely depending on the condition of loading. In the case of uniaxial tension, a number of *microcracks* of the *mixed mode* (I+II) originate from the initial defects in interface layers in the vicinity of aggregate. These microcracks propagate into the mortar layers, and leads to a macroscopic crack perpendicular to the loading direction.

In the case of uniaxial compression, on the other hand, microcracks of mode II start in the interface layers around aggregate particles of complicated geometry. These microcracks induce decohesion of the planes perpendicular to the loading direction, and gives rise to mode I cracks around the aggregate particles. After that, these microcracks develop into cracks of the mixed mode (I+II) in the mortar phase, and finally bring about a crack parallel to the compressive direction. More simply, we may say that due to a uniaxial compressive loading, the aggregate particles move apart in the lateral direction, and this displacement of aggregate causes lateral tensile stress in mortar to induce the mode I cracks.

In the case of hydrostatic pressure, increase of the stress causes the collapse of microvoids in the porous region, and brings about the nucleation of microcracks. Then, by the further increase of the hydrostatic pressure, consolidation proceeds in the material including microcracks. The rigidity of the materials, therefore, decreases at the beginning, then starts to increase. As typical examples of the macroscopic effects of damage, Fig. 9.1 shows the deformation behavior of concrete under a uniaxial compression and a uniaxial tension.

(2) Activation of Microcracks and their Damage Effect

Opening-closing behavior of cracks in brittle materials was described in Section 5.3.2. Now we focus on a single microcrack, and elucidate its behavior and the resulting mechanical effects in some detail. Then, let us consider first in what condition the state of a crack is *active*, and in what condition it is *passive*. Here,

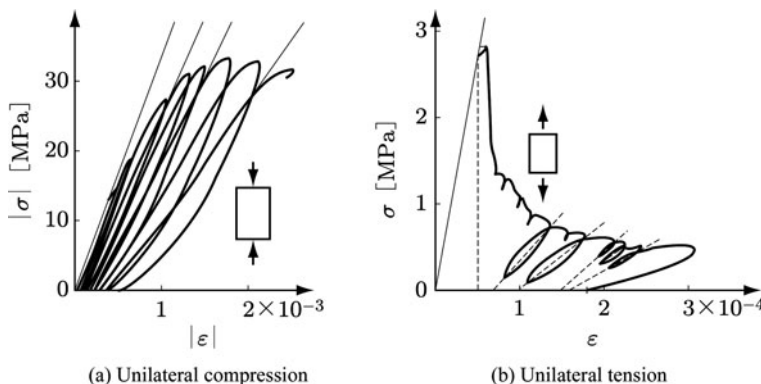


Fig. 9.1 Deformation behavior of concrete under a uniaxial compression and a uniaxial tension
Source: Mazars and Pijaudier-Cabot (1989, p. 347, Fig. 1)

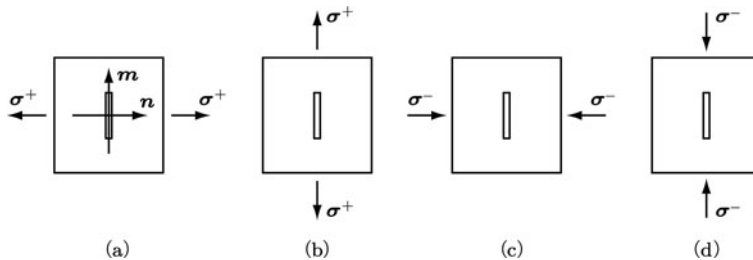


Fig. 9.2 A plane crack subject to a tensile and a compressive stress

by “*activation of a crack*” we mean the state in which relative discontinuous displacement across the crack surface is induced by the local stress or the local strain field.

The state of activation, or the opening behavior, of a microcrack differs significantly by the state of acting stress. Suppose a plane microcrack shown in Fig. 9.2, and consider four cases of loading; i.e., a tensile stress σ^+ or a compressive stress σ^- acts in the perpendicular or in the parallel direction to this crack surface (Ortiz 1985). Symbols n and m in the figure denote, respectively, the unit vectors perpendicular and parallel to the crack surface.

In the case of Fig. 9.2a, a normal tensile stress of $n \cdot \sigma^+ \cdot n > 0$ acts on the crack surface, and crack behavior of mode I, or split failure mode is observed (Fig. 9.3a). In the cases of Fig. 9.2b and c, on the other hand, the normal stresses on these crack surfaces are $n \cdot \sigma^+ \cdot n = 0$ and $n \cdot \sigma^- \cdot n < 0$, respectively. In these cases, therefore, no relative displacement occurs on these crack surfaces, and the crack state is passive.

Finally, what is the response to the case of Fig. 9.2d? In this situation, the normal stress acting on the crack plane is $n \cdot \sigma^+ \cdot n = 0$, and no crack opening occurs if the crack surface is perfectly plane. The actual crack surface, however, is not a perfect plane, but has local tilts as shown in Fig. 9.3b. In this case, a compressive stress σ^- parallel to the average plane of the crack induces crack opening of the mode II, and the crack is active.

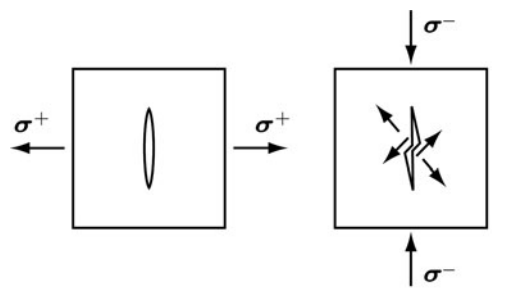


Fig. 9.3 Plane cracks activated by a tensile and a compressive stress

(a) Tensile stress

(b) Compressive stress

In summary, among the four cases of stress states acting on the plane cracks of Fig. 9.2, only those of (a) and (d) activate the cracks, and give rise to the crack opening.

(3) Bilateral and Unilateral Effects of Damage

As observed in Figs. 9.2 and 9.3, the mechanical behavior of microcracks, or the effects of damage, in a brittle material differs markedly depending on whether they are subject to a tensile stress or a compressive stress. A phenomenon in which the damage effect differs depending on the sign of the local normal stress is called a *unilateral effect* of the damage. On the other hand, a phenomenon in which the damage effect is independent of the sign of the stress is called a *bilateral effect* of damage. The unilateral behavior of a material with brittle damage was already shown in Fig. 5.4.

(4) Mesoscopic Mechanical Behavior of Concrete

As observed above, damage in concrete is brought about by the nucleation of microcracks and/or by the relative slide on the microcrack surfaces. Though the resulting mesoscopic mechanical behavior has wide variety of aspects, the following general features have been observed in it (Ortiz 1985; Mazars 1986; Yazdani and Schreyer 1988):

- (1) In comparison with tensile stress, compressive strength is much larger, and the ratio between them amounts to 8 through 13.
- (2) Lateral hydraulic stress applied to a specimen increases its strength and ductility.
- (3) In a uniaxial compression test, though the volume of a specimen decreases (contracts) at first, it starts to increase (expand) rapidly² with the initiation of microcracks.
- (4) Development of damage is accompanied by marked anisotropy in materials.
- (5) A stress-strain curve depicts a salient hysteresis curve in unloading process.

9.2 Isotropic Damage Theory of Concrete

As described above, one of the characteristic aspects of the brittle damage is the development of microcracks and the anisotropy of their mechanical effects. In the analysis of a damage process, however, the isotropy of damage can be postulated adequately in an early stage of damage or in the case of proportional loading.

² This increase in volume is caused by shear deformation in addition to microcrack initiation due to compressive stress, and is called *dilatancy*.

Referring to Mazars and Pijaudier-Cabot (Mazars 1986; Mazars and Pijaudier-Cabot 1989), we now consider the application of the isotropic damage theory to brittle materials.

9.2.1 Damage Variable and Gibbs Potential

We postulate first that the material is elastic-brittle and its damage state can be represented by a scalar damage variable D . Though the constitutive equation of isotropic damage cannot describe the anisotropic property of material, it can describe its unilateral behavior. Moreover, the related theory is easy to understand, and the procedure of application is simple.

As we learned in Section 9.1, the damage effect in brittle materials differs largely between the tensile and the compressive state of stress. Thus we assume that the damage variable D in multiaxial states of stress can be expressed by dividing it into D_t due to a tensile stress and D_c by a compressive stress:

$$D = \alpha_t D_t + \alpha_c D_c, \quad (9.1)$$

where coefficients α_t and α_c ($\alpha_t + \alpha_c = 1$) are functions of the strain states.

In order to represent the unilateral effects of brittle damage, we divide a stress σ into a positive part of the principal stress σ^+ and a negative one σ^- as described in Section 5.3.2

$$\sigma = \sigma^+ + \sigma^-, \quad (9.2a)$$

$$\sigma^+ = \mathbb{P}_\sigma^+ : \sigma, \quad \sigma^- = \sigma - \sigma^+, \quad (9.2b)$$

where \mathbb{P}_σ^+ denotes a positive orthotropic projection tensor defined by Eq. (5.90).

By assuming that the damage process is isothermal, Gibbs potential for an elastic-brittle material is given by Eq. (4.126):

$$\begin{aligned} \rho \Gamma(\sigma, D) &= \Gamma \rho(\sigma^+, D) + \rho \Gamma(\sigma^-, D) \\ &= -\frac{1}{2} \left\{ \frac{1}{E_0(1-D_t)} \left[(1+\nu_0) \text{tr}(\sigma^+ \sigma^+) - \nu_0 (\text{tr} \sigma^+)^2 \right] \right. \\ &\quad \left. - \frac{1}{E_0(1-D_c)} \left[(1+\nu_0) \text{tr}(\sigma^- \sigma^-) - \nu_0 (\text{tr} \sigma^-)^2 \right] \right\}, \end{aligned} \quad (9.3)^3$$

where ρ , E_0 and ν_0 are the mass density, Young's modulus and Poisson's ratio of the undamaged material. Then, by means of the thermodynamic theory of

³ According to the definition of Eq. (3.26), Gibbs potential Γ is negative in general.

[Section 3.2](#), the elastic constitutive equation, damage-associated variables Y_t , Y_c and the dissipation inequality are derived as follow:

$$\boldsymbol{\varepsilon} = -\rho \frac{\partial \Gamma}{\partial \boldsymbol{\sigma}} = \boldsymbol{\varepsilon}_t + \boldsymbol{\varepsilon}_c, \quad (9.4a)$$

$$\boldsymbol{\varepsilon}_t = \frac{1}{E_0(1-D_t)} [(1+\nu_0) \boldsymbol{\sigma}^+ - \nu_0 (\text{tr} \boldsymbol{\sigma}^+) \mathbf{I}], \quad (9.4b)$$

$$\boldsymbol{\varepsilon}_c = \frac{1}{E_0(1-D_c)} [(1+\nu_0) \boldsymbol{\sigma}^- - \nu_0 (\text{tr} \boldsymbol{\sigma}^-) \mathbf{I}], \quad (9.4c)$$

$$\begin{aligned} Y_t &= -\rho \frac{\partial \Gamma}{\partial D_t} \\ &= \frac{1}{2E_0(1-D_t)^2} [(1+\nu_0) \text{tr}(\boldsymbol{\sigma}^+ \boldsymbol{\sigma}^+) - \nu_0 (\text{tr} \boldsymbol{\sigma}^+)^2], \end{aligned} \quad (9.5a)$$

$$\begin{aligned} Y_c &= -\rho \frac{\partial \Gamma}{\partial D_c} \\ &= \frac{1}{2E_0(1-D_c)^2} [(1+\nu_0) \text{tr}(\boldsymbol{\sigma}^- \boldsymbol{\sigma}^-) - \nu_0 (\text{tr} \boldsymbol{\sigma}^-)^2], \end{aligned} \quad (9.5b)$$

$$\Phi = Y_t \dot{D}_t + Y_c \dot{D}_c \geq 0, \quad (9.6)$$

where \mathbf{I} denotes the identity tensor of the second-order, and Φ is the dissipation per unit volume due to damage.

The constitutive equation of a damaged material with unilateral effects must be continuous for a change in the sign of stress and strain components. The constitutive equation of Eq. (9.4) can be proved to satisfy this condition.

Namely, by expressing Eq. (9.4) in terms of the principal stress components in the plane stress state, the resulting stress-strain relation is divided into the following four cases (Chaboche 1992):

(1) $\sigma_1 > 0, \sigma_2 > 0$:

$$\begin{aligned} \varepsilon_1 &= \frac{1}{E_0(1-D_t)} (\sigma_1 - \nu_0 \sigma_2), \\ \varepsilon_2 &= \frac{1}{E_0(1-D_t)} (-\nu_0 \sigma_1 + \sigma_2). \end{aligned} \quad (9.7a)$$

(2) $\sigma_1 < 0, \sigma_2 > 0, \sigma_1 + \sigma_2 > 0$:

$$\begin{aligned} \varepsilon_1 &= \left[\frac{1+\nu_0}{E_0(1-D_c)} - \frac{\nu_0}{E_0(1-D_t)} \right] \sigma_1 - \frac{\nu_0}{E_0(1-D_t)} \sigma_2, \\ \varepsilon_2 &= -\frac{\nu_0}{E_0(1-D_t)} \sigma_1 + \frac{1}{E_0(1-D_t)} \sigma_2. \end{aligned} \quad (9.7b)$$

(3) $\sigma_1 < 0, \sigma_2 > 0, \sigma_1 + \sigma_2 < 0$:

$$\begin{aligned}\varepsilon_1 &= \frac{1}{E_0(1-D_c)}\sigma_1 - \frac{\nu_0}{E_0(1-D_c)}\sigma_2, \\ \varepsilon_2 &= -\frac{\nu_0}{E_0(1-D_c)}\sigma_1 + \left[\frac{1+\nu_0}{E_0(1-D_t)} - \frac{\nu_0}{E_0(1-D_c)} \right] \sigma_2.\end{aligned}\quad (9.7c)$$

(4) $\sigma_1 < 0, \sigma_2 < 0$:

$$\begin{aligned}\varepsilon_1 &= \frac{1}{E_0(1-D_c)} (\sigma_1 - \nu_0\sigma_2), \\ \varepsilon_2 &= \frac{1}{E_0(1-D_c)} (-\nu_0\sigma_1 + \sigma_2).\end{aligned}\quad (9.7d)$$

Furthermore, it is readily confirmed that for $\sigma_{12} = 0$ Eq. (9.4) furnishes $\varepsilon_{12} = 0$.

As observed in Eq. (9.7), the present stress-strain relations are always continuous for any change in stress. For example, in the stress ranges of (1) and (2), Eqs. (9.7a) and (9.7b) give the identical results in the case of $\sigma_1 = 0$; i.e., the stress-strain relation is continuous for the change in the sign of σ_1 . Moreover, by the use of Eq. (9.7), the symmetry of the elastic compliance tensor is also confirmed.

9.2.2 Evolution Equation of Damage

The evolution equations of the damage variables D_t and D_c can be readily derived from Eq. (4.29), if the dissipation potential functions $F_t(Y_t; D_t)$ and $F_c(Y_c; D_c)$ are determined adequately as the functions of the damage-associated variables Y_t and Y_c . However, since it is not easy to derive the pertinent functions F_t and F_c , we adopt here another procedure.

The progress of micocracks in brittle materials is brought about mainly by tensile strain. This implies that damage evolution can be specified also in a strain space.

Let us first define the effective strain governing the evolution of damage as

$$\tilde{\varepsilon} = \left[(H(\varepsilon_i) \varepsilon_i)^2 \right]^{1/2} = \left[\text{tr}(\mathbb{P}_\varepsilon^+ : \boldsymbol{\varepsilon})^2 \right]^{1/2}, \quad (9.8)$$

where ε_i is a principal strain component, and \mathbb{P}_ε^+ is the fourth-order positive orthogonal projection tensor defined by Eq. (5.84).

In order to specify the start of damage, we next suppose two *damage surfaces* in the strain space

$$f_t(\boldsymbol{\varepsilon}_t) = \tilde{\varepsilon}_t - K_t(D_t), \quad f_c(\boldsymbol{\varepsilon}_c) = \tilde{\varepsilon}_c - K_c(D_c), \quad (9.9)$$

where $\tilde{\varepsilon}_t$ and $\tilde{\varepsilon}_c$ are given by Eqs. (9.4b), (9.4c) and (9.8). Furthermore, the damage hardening parameters $K_t(D_t)$ and $K_c(D_c)$ in Eq. (9.9) signify the largest equivalent strain which material element has undergone in their loading history.

Then, on the basis of the experimental results, Mazars and Pijaudier-Cabot (Mazars 1986; Mazars and Pijaudier-Cabot 1989) derived the following equations of material damage in finite form

$$D = \alpha_t D_t + \alpha_c D_c, \quad (9.10a)$$

$$D_t = 1 - \frac{(1 - A_t)K_0}{\tilde{\varepsilon}} - \frac{A_t}{\exp[B_t(\tilde{\varepsilon} - K_0)]}, \quad (9.10b)$$

$$D_c = 1 - \frac{(1 - A_c)K_0}{\tilde{\varepsilon}} - \frac{A_c}{\exp[B_c(\tilde{\varepsilon} - K_0)]}, \quad (9.10c)$$

$$\alpha_t = \sum_{i=1}^3 H(\varepsilon_{ti}) \frac{\varepsilon_{ti}(\varepsilon_{ti} + \varepsilon_{ci})}{\tilde{\varepsilon}^2}, \quad (9.10d)$$

$$\alpha_c = \sum_{i=1}^3 H(\varepsilon_{ci}) \frac{\varepsilon_{ci}(\varepsilon_{ti} + \varepsilon_{ci})}{\tilde{\varepsilon}^2}, \quad (9.10e)$$

where K_0 , A_t , B_t , A_c and B_c are material constants which can be determined by uniaxial compression tests of cylindrical specimens and bending tests of beams.

Figure 9.4 shows the stress-strain curve for uniaxial tension-compression and the initial damage surface of concrete calculated by the above relations.

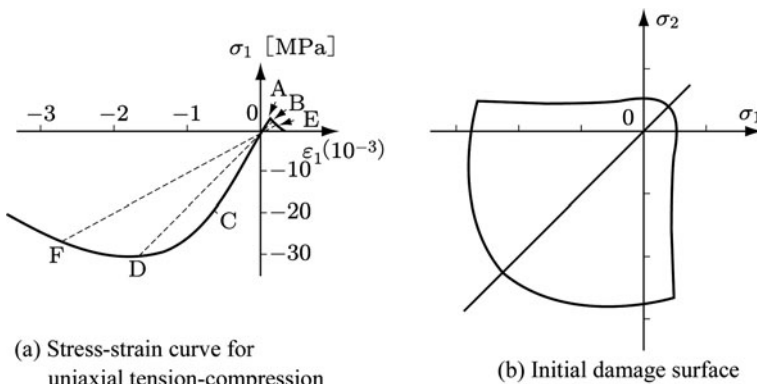


Fig. 9.4 Predictions of the brittle damage theory by the use of a scalar damage variable
Source: Mazars and Pijaudier-Cabot (1989, p. 350, Fig. 2)

9.3 Anisotropic Brittle Damage Theory by Second-Order Damage Tensor

Though the theory discussed in the preceding section is simple and easy to understand, it cannot be applied to the cases of marked anisotropy. Now we apply the anisotropic damage theory based on the second-order damage variable \mathbf{D} discussed in [Section 5.1](#) to a unilateral elastic-brittle damage material (Murakami and Kamiya 1997).

9.3.1 Helmholtz Free Energy for Elastic-Brittle Material

Consider an isothermal anisotropic damage process of an elastic-brittle material. As discussed in [Section 5.1](#), Helmholtz free energy function per unit mass of this material is expressed as

$$\psi = \psi(\boldsymbol{\epsilon}, \mathbf{D}, \beta), \quad (9.11)$$

where $\boldsymbol{\epsilon}$, \mathbf{D} and β are elastic strain, a second-order symmetric damage tensor and a damage-strengthening internal variable.

According to [Eqs. \(5.4\)](#) and [\(5.5\)](#), the elastic constitutive equation and the generalized forces $\{Y, -B\}$ associated with the internal variable $\{\mathbf{D}, \beta\}$ are given as follows:

$$\boldsymbol{\sigma} = \rho \frac{\partial \psi}{\partial \boldsymbol{\epsilon}}, \quad Y = -\rho \frac{\partial \psi}{\partial \mathbf{D}}, \quad B = \rho \frac{\partial \psi}{\partial \beta}, \quad (9.12)$$

where ρ denotes the mass density of the material.

The free energy function ψ of Eq. (9.11) can be divided into the energy $\psi^E(\boldsymbol{\epsilon}, \mathbf{D})$ due to elastic deformation and that of $\psi^D(\beta)$ related to damage development:

$$\psi(\boldsymbol{\epsilon}, \mathbf{D}, \beta) = \psi^E(\boldsymbol{\epsilon}, \mathbf{D}) + \psi^D(\beta). \quad (9.13)$$

Let us first consider the specific representation of the function $\psi^E(\boldsymbol{\epsilon}, \mathbf{D})$ of the elastic-brittle damage material without unilateral effects. The general representation of a scalar-valued isotropic tensor function of $\boldsymbol{\epsilon}$ and \mathbf{D} is given by ten simultaneous invariants of [Eq. \(12.215\)](#) in [Chapter 12](#). Moreover, the material is isotropic linearly elastic, and the elastic strain energy in damaged state $\psi^E(\boldsymbol{\epsilon}, \mathbf{D})$ decreases with the development of damage \mathbf{D} . Hence the most general expression of the free energy function $\rho\psi^E(\boldsymbol{\epsilon}, \mathbf{D})$ is given by

$$\begin{aligned} \rho\psi^E(\boldsymbol{\epsilon}, \mathbf{D}) &= \frac{1}{2}\lambda(\text{tr}\boldsymbol{\epsilon})^2 + \mu\text{tr}(\boldsymbol{\epsilon}^2) + \eta_1(\text{tr}\mathbf{D})(\text{tr}\boldsymbol{\epsilon})^2 + \eta_2(\text{tr}\mathbf{D})\text{tr}(\boldsymbol{\epsilon}^2) \\ &\quad + \eta_3(\text{tr}\boldsymbol{\epsilon})(\text{tr}\boldsymbol{\epsilon}\mathbf{D}) + \eta_4(\text{tr}\boldsymbol{\epsilon}^2\mathbf{D}), \end{aligned} \quad (9.14)$$

where λ , μ and η_1 through η_4 denote Lamé constants and material constants.

Since the unilateral effect of crack behavior manifests itself as the influence of damage \mathbf{D} on the deformation behavior, it should be represented by the third to sixth terms on the right hand side of Eq. (9.14). The state of activation of these cracks can be expressed by means of the positive-valued strain tensor of Eq. (5.85)

$$\boldsymbol{\varepsilon}^+ = \mathbb{P}_\varepsilon^+ : \boldsymbol{\varepsilon}, \quad (9.15a)$$

$$(\mathbb{P}_\varepsilon^+)^{ijkl} = H(\varepsilon_i) H(\varepsilon_j) \delta_{ij} \delta_{kl}, \quad (9.15b)$$

(no sum for i and j),

where $H()$ denotes the Heaviside function. Thus, the elastic strain energy function of a unilateral damaged material will be furnished by Eq. (9.14), if the strain tensor $\boldsymbol{\varepsilon}$ in the third to sixth terms of its right hand side is replaced by the positive strain tensor $\boldsymbol{\varepsilon}^+$ of Eq. (9.15), i.e.,

$$\begin{aligned} \rho \psi^E (\boldsymbol{\varepsilon}, \mathbf{D}) &= \frac{1}{2} \lambda (\operatorname{tr} \boldsymbol{\varepsilon})^2 + \mu \operatorname{tr} (\boldsymbol{\varepsilon}^2) \\ &\quad + \eta_1 (\operatorname{tr} \mathbf{D}) (\operatorname{tr} \boldsymbol{\varepsilon}^+)^2 + \eta_2 (\operatorname{tr} \mathbf{D}) \operatorname{tr} (\boldsymbol{\varepsilon}^+)^2 \\ &\quad + \eta_3 (\operatorname{tr} \boldsymbol{\varepsilon}^+) (\operatorname{tr} \boldsymbol{\varepsilon}^+ \mathbf{D}) + \eta_4 \operatorname{tr} [(\boldsymbol{\varepsilon}^+)^2 \mathbf{D}]. \end{aligned} \quad (9.16)$$

Let us examine here the condition of continuity of the stress-strain relation derived from the elastic constitutive equations of Eqs. (9.12) and (9.16). By denoting the stress resulting from the third term in the right hand side of Eq. (9.16) by $\sigma_{\eta 1}$, we have the following expression from Eqs. (9.12) and (9.15):

$$\begin{aligned} \sigma_{\eta 1} &= \rho \frac{\partial (\psi^E)_{\eta 1}}{\partial \boldsymbol{\varepsilon}} = \frac{\partial}{\partial \boldsymbol{\varepsilon}} \left[\eta_1 (\operatorname{tr} \mathbf{D}) (\operatorname{tr} \boldsymbol{\varepsilon}^+)^2 \right] \\ &= 2 \eta_1 (\operatorname{tr} \mathbf{D}) (\operatorname{tr} \boldsymbol{\varepsilon}^+) \mathbf{I} : \mathbb{P}_\varepsilon^+, \end{aligned} \quad (9.17a)$$

or

$$\begin{aligned} (\sigma_{\eta 1})_{ij} &= 2 \eta_1 (\operatorname{tr} \mathbf{D}) \left(\varepsilon_{pp}^+ \right) \delta_{kl} (\mathbb{P}_\varepsilon^+)^{klj} \\ &= 2 \eta_1 (\operatorname{tr} \mathbf{D}) \left(\varepsilon_{pp}^+ \right) H(\varepsilon_i) H(\varepsilon_j) \delta_{ij}, \end{aligned} \quad (9.17b)$$

(no sum for i and j),

where the derivative of the scalar-valued tensor function was derived according to the procedure of Section 12.5.

We now consider Eq. (9.17) with respect to the isotropic deformation in $x_2 - x_3$ plane, for example. In this case, if ε_{11} changes its sign at $\varepsilon_{11} = 0$ in the condition $\varepsilon_{22} = \varepsilon_{33} \neq 0$, the resulting change in the stress $(\sigma_{\eta 1})_{11}$ becomes discontinuous.

Thus, the requirement of the continuity in ε_{11} at $\varepsilon_{11} = 0$ necessitates the following relation

$$\eta_1 = 0. \quad (9.18)$$

As to the constant η_3 of Eq. (9.16), we have by a similar reasoning

$$\eta_3 = 0. \quad (9.19)$$

In view of the above results of Eqs. (9.18) and (9.19), Helmholtz free energy function (9.16) for a unilateral damage material eventually leads to

$$\begin{aligned} \rho\psi^E(\boldsymbol{\varepsilon}, \mathbf{D}) &= \frac{1}{2}\lambda(\text{tr}\boldsymbol{\varepsilon})^2 + \mu\text{tr}(\boldsymbol{\varepsilon}^2) + \eta_2(\text{tr}\mathbf{D})\text{tr}(\boldsymbol{\varepsilon}^+)^2 \\ &\quad + \eta_4\text{tr}[(\boldsymbol{\varepsilon}^+)^2 \mathbf{D}]. \end{aligned} \quad (9.20)$$

We consider next the specific form of the function $\psi^D(\beta)$ of Eq. (9.13). This function $\psi^D(\beta)$ represents the effects of damage history on the subsequent evolution of the damage via its associated variable B of Eq. (9.12). Thus an assumption of a linear relation between β and B , similarly to Eq. (5.16), furnishes

$$\rho\psi^D(\beta) = \frac{1}{2}K_d\beta^2, \quad (9.21)$$

where K_d is a material constant.

From Eqs. (9.20) and (9.21), the Helmholtz free energy function of an elastic-brittle damage material with unilateral anisotropic damage is expressed finally as follows:

$$\begin{aligned} \rho\psi(\boldsymbol{\varepsilon}, \mathbf{D}, \beta) &= \rho\psi^E(\boldsymbol{\varepsilon}, \mathbf{D}) + \rho\psi^D(\beta) \\ &= \frac{1}{2}\lambda(\text{tr}\boldsymbol{\varepsilon})^2 + \mu\text{tr}(\boldsymbol{\varepsilon}^2) + \eta_2(\text{tr}\mathbf{D})\text{tr}(\boldsymbol{\varepsilon}^+)^2 \\ &\quad + \eta_4\text{tr}[(\boldsymbol{\varepsilon}^+)^2 \mathbf{D}] + \frac{1}{2}K_d\beta^2. \end{aligned} \quad (9.22)$$

9.3.2 Elastic Constitutive Equation, Damage Evolution Equation

By substituting the Helmholtz free energy function (9.22) into Eq. (9.12) and by applying the differential calculus of Section 12.5 to the resulting relations, we have the stress tensor and the generalized forces:

$$\begin{aligned} \boldsymbol{\sigma} &= \rho \frac{\partial \psi}{\partial \boldsymbol{\varepsilon}} = \rho \frac{\partial \psi^E}{\partial \boldsymbol{\varepsilon}} \\ &= \lambda(\text{tr}\boldsymbol{\varepsilon}) \mathbf{I} + 2\mu\boldsymbol{\varepsilon} + 2\eta_2(\text{tr}\mathbf{D})\boldsymbol{\varepsilon}^+ + 2\eta_4\boldsymbol{\varepsilon}^+\mathbf{D}, \end{aligned} \quad (9.23)$$

$$\begin{aligned} \mathbf{Y} &= -\rho \frac{\partial \psi}{\partial \mathbf{D}} = -\rho \frac{\partial \psi^E}{\partial \mathbf{D}} \\ &= -\eta_2 \left[\text{tr}(\boldsymbol{\varepsilon}^+)^2 \right] \mathbf{I} - \eta_4 (\boldsymbol{\varepsilon}^+)^2, \end{aligned} \quad (9.24)$$

$$B = \rho \frac{\partial \psi}{\partial \beta} = \rho \frac{\partial \psi^D}{\partial \beta} = K_d \beta. \quad (9.25)$$

In order to calculate the above relations, we need to formulate specific evolution equations of the damage variable \mathbf{D} and the damage strengthening internal variable β . If we suppose that, as in [Section 5.1](#), the rate of the damage variable \mathbf{D} depends linearly on its associated variable \mathbf{Y} and on \mathbf{D} itself, the surface of the damage potential can be expressed as

$$F^D(\mathbf{Y}, B) = Y_{EQ} - (B_0 + B) = 0, \quad (9.26a)$$

$$Y_{EQ} = \left(\frac{1}{2} \mathbf{Y} : \mathbf{Y} \right)^{1/2}, \quad (9.26b)$$

where B_0 is a material constant specifying the size of the initial damage surface.

Substitution of Eq. (9.26) into [Eq. \(5.10\)](#) gives the evolution equations of the damage variable \mathbf{D} and the damage strengthening internal variable β :

$$\dot{\mathbf{D}} = \dot{\Lambda}^D \frac{\partial F^D}{\partial \mathbf{Y}} = \dot{\Lambda}^D \frac{\mathbf{Y}}{2Y_{EQ}}, \quad (9.27a)$$

$$\dot{\beta} = -\dot{\Lambda}^D \frac{\partial F^D}{\partial B} = \dot{\Lambda}^D, \quad (9.27b)$$

where $\dot{\Lambda}^D$ is an indeterminate multiplier, whose value can be given by means of the consistency condition for the damage surface (9.26a) as follows

$$\dot{\Lambda}^D = \alpha \frac{\partial F^D}{\partial \mathbf{Y}} : \dot{\mathbf{Y}} / \left(\frac{\partial B}{\partial \beta} \right) = \alpha \frac{1}{2K_d Y_{EQ}} \mathbf{Y} : \dot{\mathbf{Y}}, \quad (9.28a)$$

$$\alpha = 1, \quad \text{for } F^D = 0 \quad \text{and} \quad \frac{\partial F^D}{\partial \mathbf{Y}} : \dot{\mathbf{Y}} > 0, \quad (9.28b)$$

$$\alpha = 0, \quad \text{for } F^D < 0 \quad \text{or} \quad \frac{\partial F^D}{\partial \mathbf{Y}} : \dot{\mathbf{Y}} \leq 0. \quad (9.28c)$$

9.3.3 Elastic-Brittle Damage Analysis of Concrete

As an application of the elastic constitutive equation (9.23) and the damage evolution equations (9.27) and (9.28), a uniaxial compression and a uniaxial tension process of cylindrical specimens of concrete will be analyzed.

(1) Uniaxial Compression

We introduce an orthogonal coordinate (x_1, x_2, x_3) , and select x_1 -axis in the axial direction of the specimen, whereas x_2 - and x_3 -axis are taken perpendicular to x_1 -axis. Then the components of stress and strain are expressed by

$$[\sigma] = \begin{bmatrix} \sigma_{11} & 0 & 0 \\ 0 & 0 & 0 \\ 0 & 0 & 0 \end{bmatrix}, \quad (\sigma_{11} < 0); \quad [\varepsilon] = \begin{bmatrix} \varepsilon_{11} & 0 & 0 \\ 0 & \varepsilon_{22} & 0 \\ 0 & 0 & \varepsilon_{33} \end{bmatrix}, \quad (\varepsilon_{11} < 0). \quad (9.29)$$

Hence the constitutive equation (9.23) and the damage-associated variable (9.24) are derived as follows:

$$\sigma_{11} = (\lambda + 2\mu) \varepsilon_{11} + \lambda \varepsilon_{22} + \lambda \varepsilon_{33}, \quad (9.30a)$$

$$\sigma_{22} = 0 = \lambda \varepsilon_{11} + [\lambda + 2\mu + 2\eta_2(\text{tr}\mathbf{D}) + 2\eta_4 D_{22}] \varepsilon_{22} + \lambda \varepsilon_{33}, \quad (9.30b)$$

$$\sigma_{33} = 0 = \lambda \varepsilon_{11} + \lambda \varepsilon_{22} + [\lambda + 2\mu + 2\eta_2(\text{tr}\mathbf{D}) + 2D_{33}] \varepsilon_{33}, \quad (9.30c)$$

$$Y_{11} = -\eta_2 \text{tr}(\boldsymbol{\varepsilon}^2), \quad (9.31a)$$

$$Y_{22} = -\eta_2 \text{tr}(\boldsymbol{\varepsilon}^2) - \eta_4 \left[(\varepsilon_{22})^2 + (\varepsilon_{33})^2 \right], \quad (9.31b)$$

$$Y_{33} = -\eta_2 \text{tr}(\boldsymbol{\varepsilon}^2) - \eta_4 \left[(\varepsilon_{22})^2 + (\varepsilon_{33})^2 \right]. \quad (9.31c)$$

Finally, the evolution equation (9.27) is expressed in the form

$$\dot{D}_{11} = \alpha \frac{Y_{11} (Y_{11} \dot{Y}_{11} + Y_{22} \dot{Y}_{22} + Y_{33} \dot{Y}_{33})}{2K_d [(Y_{11})^2 + (Y_{22})^2 + (Y_{33})^2]}, \quad (9.32a)$$

$$\dot{D}_{22} = \alpha \frac{Y_{22} (Y_{11} \dot{Y}_{11} + Y_{22} \dot{Y}_{22} + Y_{33} \dot{Y}_{33})}{2K_d [(Y_{11})^2 + (Y_{22})^2 + (Y_{33})^2]}, \quad (9.32b)$$

$$\dot{D}_{33} = \alpha \frac{Y_{33} (Y_{11} \dot{Y}_{11} + Y_{22} \dot{Y}_{22} + Y_{33} \dot{Y}_{33})}{2K_d [(Y_{11})^2 + (Y_{22})^2 + (Y_{33})^2]}, \quad (9.32c)$$

where the coefficient α has been given by Eq. (9.28).

(2) Uniaxial Tension

The uniaxial tension in x_1 -direction induces compressive strain in x_2 - and x_3 -direction. Then the stress-strain relation and the damage-associated variable are derived:

$$\sigma_{11} = [\lambda + 2\mu + 2\eta_2(\text{tr}\mathbf{D}) + 2\eta_4 D_{11}] \varepsilon_{11} + \lambda \varepsilon_{22} + \lambda \varepsilon_{33}, \quad (9.33a)$$

$$\sigma_{22} = 0 = \lambda \varepsilon_{11} + (\lambda + 2\mu) \varepsilon_{22} + \lambda \varepsilon_{33}, \quad (9.33b)$$

$$\sigma_{33} = 0 = \lambda \varepsilon_{11} + \lambda \varepsilon_{22} + (\lambda + 2\mu) \varepsilon_{33}, \quad (9.33c)$$

$$Y_{11} = -\eta_2 \text{tr}(\boldsymbol{\epsilon}^2) - \eta_4 (\varepsilon_{11})^2, \quad (9.34a)$$

$$Y_{22} = -\eta_2 \text{tr}(\boldsymbol{\epsilon}^2), \quad (9.34b)$$

$$Y_{33} = -\eta_2 \text{tr}(\boldsymbol{\epsilon}^2). \quad (9.34c)$$

The evolution equation of the damage variable, on the other hand, is given by Eq. (9.32), similarly to the case of the uniaxial compression. In this case, however, since the damage-associated variable is given by Eq. (9.34) instead of Eq. (9.31), damage development is predicted differently from the case of uniaxial compression.

Figure 9.5a and b shows the elastic-brittle damage behavior of high-strength concrete under uniaxial compression and uniaxial tension calculated by the above equations (Murakami and Kamiya 1997).

In the elastic-brittle damage caused by the development of microcracks, besides the anisotropic damage and its unilateral effect, the effect of frictional slip among microcrack surfaces may also be significant. In order to elucidate this problem, Halm and Dragon (1998) extended the free energy function of Eq. (9.16) by introducing a new internal variable to represent the slipped state, and discussed this problem. For more detail, refer to the reference.

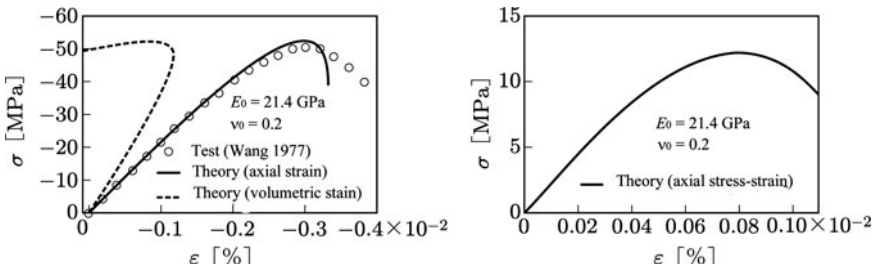


Fig. 9.5 Elastic-brittle damage in high-strength concrete under uniaxial compression and uniaxial tension

Source: Murakami and Kamiya (1997, p. 480, Fig. 1; p. 482, Fig. 4)

9.4 Anisotropic Brittle Damage Theory with Elastic Modulus Tensor as Damage Variable

Hereafter we consider some elaborated theories of brittle damage having more complex anisotropy than the orthotropy. We begin with the theory of Ju (1989) based on a fourth-order symmetric damage tensor, and apply it to the elastic-brittle damage processes of concrete and mortar.

9.4.1 Helmholtz Free Energy and Elastic Constitutive Equation

The elastic-plastic-brittle damage theory of Ju (1989) described in [Section 5.3.5](#) employs the fourth-order elastic modulus tensor \mathbb{C} as its damage variable, and incorporates the coupling between damage and plastic deformation. In the case of the elastic brittle damage, it needs only to remove the terms related to plastic deformation from [Eqs. \(5.112\)](#) through [\(5.115\)](#). Then, the Helmholtz free energy function ψ , stress tensor σ and the damage-associated variable \mathbb{Y} are readily given by

$$\rho\psi(\boldsymbol{\varepsilon}, \mathbb{C}) = \frac{1}{2}\boldsymbol{\varepsilon} : \mathbb{C} : \boldsymbol{\varepsilon}, \quad (9.35)$$

$$\sigma = \rho \frac{\partial \psi}{\partial \boldsymbol{\varepsilon}} = \mathbb{C} : \boldsymbol{\varepsilon}, \quad (9.36)$$

$$\mathbb{Y} = -\rho \frac{\partial \psi}{\partial \mathbb{C}} = -\frac{1}{2}\boldsymbol{\varepsilon} \otimes \boldsymbol{\varepsilon}, \quad (9.37)$$

where $\boldsymbol{\varepsilon}$ denotes elastic strain.

9.4.2 Evolution Equation of Brittle Damage

As regards the damage evolution, the following damage loading surface, similar to [Eq. \(5.118\)](#), will be considered:

$$F^D(\mathbb{Y}, B) = g(\mathbb{Y}) - B \leq 0, \quad (9.38)$$

where B is the threshold for the damage initiation. From this relation, the evolution equation of the damage variable \mathbb{C} is furnished as

$$\dot{\mathbb{C}} = \dot{A}^D \frac{\partial F^D}{\partial \mathbb{Y}}, \quad (9.39)$$

where \dot{A}^D is an indeterminate multiplier. The loading-unloading condition for the damage evolution is specified by Kuhn-Tucker relation (Ju 1989)

$$\dot{A}^D \geq 0, \quad F^D \leq 0, \quad \dot{A}^D F^D = 0. \quad (9.40)$$

In order to represent the unilateral effect on damage development, we introduce a new scalar variable in place of the damage associated variable \mathbb{Y} :

$$\xi \equiv \text{tr}(\mathbb{Y} : \mathcal{C}_{AC}), \quad (9.41a)$$

$$\mathcal{C}_{AC} = \mathbb{P}_\varepsilon^+ : \mathbb{C}_0 : \mathbb{P}_\varepsilon^+, \quad (9.41b)$$

where \mathcal{C}_{AC} denotes the *activated elastic modulus tensor* defined by Eq. (5.96). Since the elastic modulus tensor has been employed here as the damage variable, the quantity $\text{tr}(\mathbb{Y} : \mathcal{C}_{AC})$ represents the energy dissipation due to damage development. The variable ξ of Eq. (9.41a), therefore, can be interpreted as a scalar variable representing the magnitude of the dissipation brought about by the damage development in the tensile principal strain direction, i.e., by the magnitude of dissipation due to active damage. Moreover, Eq. (9.41) gives

$$\frac{\partial \xi}{\partial \mathbb{Y}} = \mathcal{C}_{AC} = \mathbb{P}_\varepsilon^+ : \mathbb{C}_0 : \mathbb{P}_\varepsilon^+. \quad (9.42)$$

By using the variable ξ of Eq. (9.41) in place of the damage-associated variable \mathbb{Y} , Eq. (9.38) can be expressed in the form

$$\bar{F}^D(\xi, B) = \bar{g}(\xi) - B \leq 0, \quad (9.43a)$$

$$\bar{g}(\xi) = g(\mathbb{Y}), \quad (9.43b)$$

where \bar{F}^D and \bar{g} are new functions given by rewriting F^D and g of Eq. (9.38).

As regards the damage hardening variable B of Eq. (9.43), we define an evolution equation

$$\dot{B} = \dot{\Lambda}^D H, \quad H \equiv \frac{\partial \bar{g}(\xi)}{\partial \xi}. \quad (9.44)$$

From these relations together with the consistency condition $\dot{\bar{F}}^D = 0$ for the damage loading surface (9.43), we have

$$\dot{\xi} = \dot{\Lambda}^D. \quad (9.45)$$

By the use of the above relations, the evolution equation (9.39) of anisotropic brittle damage finally leads to

$$\begin{aligned} \dot{\mathcal{C}} &= \dot{\Lambda}^D \frac{\partial F^D}{\partial \mathbb{Y}} = \dot{\Lambda}^D \frac{\partial \bar{F}^D}{\partial \xi} \frac{\partial \xi}{\partial \mathbb{Y}} \\ &= \dot{\xi} H \mathbb{P}_\varepsilon^+ : \mathbb{C}_0 : \mathbb{P}_\varepsilon^+. \end{aligned} \quad (9.46)$$

If a material undergoes, furthermore, the microcrack initiation not only by the tensile strain but also by the compressive strain, the above evolution equation can be extended as follows

$$\dot{\mathcal{C}} = \dot{\xi}^+ H^+ \mathbb{P}_\varepsilon^+ : \mathcal{C}_0 : \mathbb{P}_\varepsilon^+ - \dot{\xi}^- H^- \mathbb{P}_\varepsilon^- : \mathcal{C}_0 : \mathbb{P}_\varepsilon^-, \quad (9.47a)$$

$$\mathbb{P}_\varepsilon^- = \mathbb{I} - \mathbb{P}_\varepsilon^+, \quad (9.47b)$$

where \mathbb{I} is the fourth-order identity tensor.

9.4.3 Application to Elastic-Brittle Damage Analysis of Mortar

Ju (1989) incorporated the above evolution equation of brittle damage into a finite element program, and discussed the algorithm and its applicability.

Figure 9.6 shows the results of uniaxial unconfined compression tests of mortar cylindrical specimens together with the numerical results of the above theory. Figure 9.6a and b are the stress-strain curve in the axial direction and the resulting variation in Poisson's ratio.

In the tests of the specimens, microcracks first initiated in planes parallel to the axis, developed in the transverse and the axial direction, and finally lead to fracture in longitudinal splitting. As regards the analysis, on the other hand, the evolution equation of Eq. (9.47) was employed and the tensile strength was assumed to be 1/10 of the compressive strength.

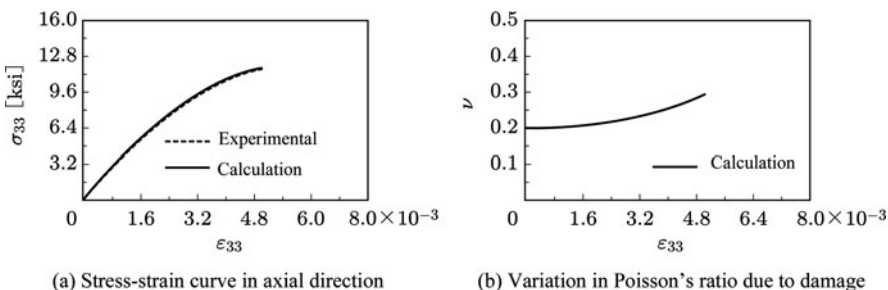


Fig. 9.6 Results of uniaxial unconfined compression tests of mortar cylindrical specimens
Source: Ju (1989, p. 829, Fig. 12; p. 830, Fig. 14)

9.5 Anisotropic Brittle Damage Theory with Compliance Tensor as Damage Variable

The problems of the anisotropic brittle damage can be discussed also by adopting the elastic compliance tensor as the damage variable. At the end of this chapter, we consider this subject by the use of the fourth-order elastic compliance tensor (Lubarda, Krajcinovic and Mastilovic 1994; Krajcinovic 1996).

9.5.1 Gibbs Potential, Evolution Equation of Damage

Let us first represent the elastic compliance tensor \mathbb{S} of an elastic-brittle damage material as the sum of \mathbb{S}_0 in its initial undamaged state and its variation \mathbb{S}^D due to the resulting damage

$$\mathbb{S} = \mathbb{S}_0 + \mathbb{S}^D. \quad (9.48)$$

Then, the damage state of the material can be specified by the fourth-order tensor \mathbb{S}^D .

The effect of damage history on its evolution can be described by the damage-strengthening internal variable β described in Sections 5.1 and 5.2. Then, Gibbs potential function per unit volume in the damaged state is expressed:

$$\begin{aligned} \rho\Gamma(\boldsymbol{\sigma}, \mathbb{S}^D, \beta) &= -\frac{1}{2}\boldsymbol{\sigma} : \mathbb{S} : \boldsymbol{\sigma} - U^D(\beta) \\ &= -\frac{1}{2}(\mathbb{S}_0 + \mathbb{S}^D) :: (\boldsymbol{\sigma} \otimes \boldsymbol{\sigma}) - U^D(\beta), \end{aligned} \quad (9.49)^4$$

where $\boldsymbol{\sigma}$ denotes a stress tensor, and function $U^D(\beta)$ represents the variation of the surface energy due to microcrack nucleation. The Helmholtz free energy function ψ is given by this relation together with Eq. (5.41)

$$\rho\psi(\boldsymbol{\epsilon}, \mathbb{S}^D, \beta) = \rho\Gamma(\boldsymbol{\sigma}, \mathbb{S}^D, \beta) + \boldsymbol{\sigma} : \boldsymbol{\epsilon}, \quad (9.50)$$

where $\boldsymbol{\epsilon}$ is the elastic strain tensor.

Let us assume that the damage process is isothermal and the thermal flux \mathbf{q} is vanishing. Then substitution of Eq. (9.50) into the Clausius-Duhem inequality (3.19) furnishes

$$\begin{aligned} \boldsymbol{\sigma} : \dot{\boldsymbol{\epsilon}} - \rho\dot{\Gamma} - \dot{\boldsymbol{\sigma}} : \boldsymbol{\epsilon} - \boldsymbol{\sigma} : \dot{\boldsymbol{\epsilon}} \\ = -\left(\boldsymbol{\epsilon} + \rho\frac{\partial\Gamma}{\partial\boldsymbol{\sigma}}\right) : \dot{\boldsymbol{\sigma}} - \rho\frac{\partial\Gamma}{\partial\mathbb{S}^D} :: \dot{\mathbb{S}}^D - \rho\frac{\partial\Gamma}{\partial\beta}\dot{\beta} \geq 0. \end{aligned} \quad (9.51)$$

The condition for this inequality to hold for arbitrary variation of stress $\dot{\boldsymbol{\sigma}}$ gives the elastic constitutive equation

$$\boldsymbol{\epsilon} = -\rho\frac{\partial\Gamma}{\partial\boldsymbol{\sigma}}. \quad (9.52)$$

Then, by introducing new variables

$$\mathbb{T} \equiv -\rho\frac{\partial\Gamma}{\partial\mathbb{S}^D}, \quad B \equiv \rho\frac{\partial\Gamma}{\partial\beta}, \quad (9.53)$$

⁴ According to the definition of Eq. (3.26), Gibbs potential Γ usually has a negative value.

the dissipation inequality (10.51) is expressed in terms of the generalized force and the generalized flux vectors \mathbf{X} and \mathbf{J} :

$$\begin{aligned}\Phi &= \mathbb{T} :: \dot{\mathbb{S}}^D + B\dot{\beta} \\ &= \mathbf{X} \cdot \mathbf{J} \geq 0,\end{aligned}\quad (9.54)$$

$$\mathbf{X} = \{\mathbb{T}, -B\}, \quad \mathbf{J} = \{\dot{\mathbb{S}}^D, \dot{\beta}\}. \quad (9.55)$$

Equation (9.54) implies that the variable \mathbb{T} is a generalized force associated with the generalized flux vector $\dot{\mathbb{S}}^D$. Furthermore, substitution of Eq. (9.49) into Eq. (9.53) furnishes the relation

$$\mathbb{T} = \frac{1}{2} \boldsymbol{\sigma} \otimes \boldsymbol{\sigma}. \quad (9.56)$$

As described in [Section 3.2](#), when the dissipation Φ can be expressed in the form of Eq. (9.54), we can postulate the existence of the dissipation potential function

$$F^D = F^D(\mathbb{T}, B; \mathbb{S}^D, \beta). \quad (9.57)$$

Then, the generalized flux vector \mathbf{J} of Eq. (9.55) can be derived as follows

$$\dot{\mathbb{S}}^D = \dot{\Lambda}^D \frac{\partial F^D}{\partial \mathbb{T}}, \quad \dot{\beta} = -\dot{\Lambda}^D \frac{\partial F^D}{\partial B}. \quad (9.58)$$

9.5.2 Unilateral Effect of Elastic Deformation

In view of the elastic compliance tensor \mathbb{S} of Eq. (9.48), the elastic constitutive equation (9.52) has an alternative form

$$\boldsymbol{\varepsilon} = \mathbb{S} : \boldsymbol{\sigma} = (\mathbb{S}_0 + \mathbb{S}^D) : \boldsymbol{\sigma}, \quad (9.59)$$

and the damage tensor \mathbb{S}^D represents the increase in the elastic compliance as a result of damage. However, due to the unilateral effect in crack behavior, the effect of \mathbb{S}^D on the elastic deformation of the material appears only in the state of activated microcracks. Then, the tensor \mathbb{S}^D can be expressed as the sum of its positive part \mathbb{S}^{D+} and the negative part \mathbb{S}^{D-} :

$$\mathbb{S}^D = \mathbb{S}^{D+} + \mathbb{S}^{D-}, \quad (9.60a)$$

$$\mathbb{S}^{D+} = \mathbb{P}_\sigma^+ : \mathbb{S}^D : \mathbb{P}_\sigma^+, \quad \mathbb{S}^{D-} = \mathbb{P}_\sigma^- : \mathbb{S}^D : \mathbb{P}_\sigma^-, \quad (9.60b)$$

where \mathbb{P}_σ^+ and \mathbb{P}_σ^- are the positive and the negative orthogonal projection tensors defined in [Section 5.3.2](#), respectively.

Therefore, the elastic constitutive equation incorporating the opening-closing effects of microcracks is furnished if we rewrite by Eqs. (9.59) and (9.60) as follows

$$\boldsymbol{\varepsilon} = \mathbb{S}_0 : \boldsymbol{\sigma} + \mathbb{S}^{D+} : \boldsymbol{\sigma}^+ + \mathbb{S}^{D-} : \boldsymbol{\sigma}^-, \quad (9.61a)^5$$

or

$$\dot{\boldsymbol{\varepsilon}} = (\mathbb{S}_0 + \mathbb{S}^{D+}) : \dot{\boldsymbol{\sigma}}^+ + (\mathbb{S}_0 + \mathbb{S}^{D-}) : \dot{\boldsymbol{\sigma}}^- + \dot{\mathbb{S}}^{D+} : \boldsymbol{\sigma}^+ + \dot{\mathbb{S}}^{D-} : \boldsymbol{\sigma}^-, \quad (9.61b)^5$$

where the positive and the negative stress $\boldsymbol{\sigma}^+$ and $\boldsymbol{\sigma}^-$ are given by Eqs. (5.89) and (5.91).

For the specific calculation of the damage variable \mathbb{S}^D , we assume the dissipation potential function of Eq. (9.57) in the form

$$F^D(\mathbb{T}, B; \mathbb{S}^D, \beta) = \mathbb{A} : \mathbb{T} - F^B(B), \quad (9.62a)$$

$$\mathbb{A} = \sum_{i=1}^3 \sum_{j=1}^3 a_{ij} \mathbf{N}_i \otimes \mathbf{N}_j, \quad \mathbf{N}_i = \mathbf{n}_i \otimes \mathbf{n}_i \quad (i, j = 1, 2, 3), \quad (9.62b)$$

where \mathbb{A} signifies a directional tensor of the fourth-order, and \mathbf{n}_i and a_{ij} ($= a_{ji}$) are the eigenvector of stress $\boldsymbol{\sigma}$ and a tensor of material constants.

Finally, the evolution equation of the damage tensor \mathbb{S}^D are derived by Eqs. (9.58) and (9.62) as

$$\dot{\mathbb{S}}^D = \dot{\mathbb{A}}^D \frac{\partial F^D}{\partial \mathbb{T}} = \dot{\mathbb{A}}^D \mathbb{A}. \quad (9.63)^6$$

In order that \mathbb{S}^D may represent the unilateral effect expressed in Eq. (9.60), the fourth-order tensor \mathbb{A} in this relation will be further decomposed as follows

$$\mathbb{A} = \mathbb{A}^+ + \mathbb{A}^-, \quad (9.64a)^6$$

$$\mathbb{A}^+ = c \left[\mathbf{N}_1 \otimes \mathbf{N}_1 + p (\mathbf{N}_1 \otimes \mathbf{N}_3)^S \right], \quad (9.64b)$$

$$\mathbb{A}^- = \mathbf{N}_3 \otimes \mathbf{N}_3 + q (\mathbf{N}_1 \otimes \mathbf{N}_3)^S, \quad (9.64c)$$

⁵ Though \mathbb{S}^{D+} and \mathbb{S}^{D-} of Eq. (9.61) are furnished by Eq. (9.63), the integration is not simple and straightforward. Moreover, for the change in stress sign, or the change of crack state between active and passive state, the constitutive equation of Eq. (9.61) may be discontinuous in some cases (Krajcinovic 1996).

⁶ The evolution equations of Eqs. (9.63) and (9.64) have been derived on the basis of the experimentally observed features of the microcrack patterns under simple loading histories for $\sigma_1 > \sigma_2 > \sigma_3$. As will be seen in Section 9.5.4, they describe well the damage development and its effect on the mechanical behavior of material under a uniaxial or a simple proportional loading. However, their applicability to the case of more general non-proportional loading is not obvious.

where subscripts 1 and 3 represent the directions of the maximum and the minimum principal stress \mathbf{n}_1 and \mathbf{n}_3 .

The evolution equation of the damage-strengthening variable β , on the other hand, is derived from Eqs. (9.58) and (9.62):

$$\dot{\beta} = -\dot{A}^D \frac{\partial F^D}{\partial B} = \dot{A}^D \frac{\partial F^B}{\partial B}. \quad (9.65)$$

9.5.3 Damage Surface and Loading Criterion

Calculation of damage rate \dot{S}^D by means of Eq. (9.63) necessitates the loading criterion for the damage development. Then we suppose a damage surface in the stress space

$$G(\sigma, \beta) = g(\sigma^+, \sigma^-) - h(\beta) = 0, \quad (9.66)$$

and postulate that the damage development is not induced by the stress state inside this surface.

Concerning the stress state on the damage surface, the consistency condition for Eq. (9.66) gives a relation

$$\frac{\partial g}{\partial \sigma^+} : \dot{\sigma}^+ + \frac{\partial g}{\partial \sigma^-} : \dot{\sigma}^- - \frac{\partial h}{\partial \beta} \dot{\beta} = 0. \quad (9.67)$$

Substitution of Eq. (9.58) into this relation furnishes the indeterminate multiplier \dot{A}^D of Eq. (9.63):

$$\dot{A}^D = \frac{\left(\frac{\partial g}{\partial \sigma^+} : \dot{\sigma}^+ + \frac{\partial g}{\partial \sigma^-} : \dot{\sigma}^- \right)}{\frac{\partial h}{\partial \beta} \frac{\partial F^B}{\partial B}}. \quad (9.68)$$

Since the progress of damage requires $\dot{A}^D > 0$, the loading conditions for the evolution equation of damage (9.58) are expressed as follow:

Hardening region:

$$\left(\frac{\partial h}{\partial \beta} \frac{\partial F^B}{\partial B} \right)^{-1} \left(\frac{\partial g}{\partial \sigma^+} : \dot{\sigma}^+ + \frac{\partial g}{\partial \sigma^-} : \dot{\sigma}^- \right) > 0, \quad (9.69a)$$

Softening Region:

$$\frac{\partial g}{\partial \sigma^+} : \dot{\sigma}^+ + \frac{\partial g}{\partial \sigma^-} : \dot{\sigma}^- < 0. \quad (9.69b)$$

It should be noted that the loading condition for the softening region (9.69b) is only the necessary condition for the damage progress, and is not the sufficient condition.

As a specific form of the damage surface of Eq. (9.66), we may consider (Lubarda et al. 1994; Kraječinović 1996):

$$\begin{aligned} g(\sigma^+, \sigma^-) &= \frac{1}{2}k \left[(\sigma^D)^+ : (\sigma^D)^+ + a(\sigma_H^+)^2 \right] \\ &\quad + \frac{1}{2} \left[(\sigma^D)^- : (\sigma^D)^- + b(\sigma_H^-)^2 \right], \end{aligned} \quad (9.70a)$$

$$(\sigma^D)^\pm = \sigma^\pm - \sigma_H^\pm \mathbf{I}, \quad \sigma_H^\pm = \frac{1}{3} \text{tr} \sigma^\pm. \quad (9.70b)$$

9.5.4 Application to Elastic-Brittle Damage of Salem Limestone

Let us now compare the above theory with the experimental results (Green 1992) on Salem limestone. Figure 9.7 shows the stress-strain curve of this material under uniaxial compression. The small circles in the figure indicate the experimental results of the Salem limestone, while the solid line shows the results of the fitting to the experiment by the following expression of Smith and Young (1955):

$$\sigma^- = E_*^- \varepsilon^- \exp\left(1 - \frac{\varepsilon^-}{\varepsilon_*^-}\right), \quad \text{for } \varepsilon^- \geq \varepsilon_0^-, \quad (9.71a)$$

$$\sigma^- = E_0 \varepsilon^-, \quad \text{for } \varepsilon^- \leq \varepsilon_0^-. \quad (9.71b)$$

The symbols σ_0^- , ε_0^- and E_0 in Fig. 9.7 and Eq. (9.71) denote the threshold of stress and strain for damage initiation at the point A, and Young's modulus of the undamaged state, while σ_*^- , ε_* and E_*^- are the stress and strain at the maximum stress point B and the corresponding secant modulus; the values of these material constants have been given as

$$\sigma_0^- = 60 \text{ MPa}, \quad \varepsilon_0^- = 1.6 \times 10^{-3}, \quad E_0 = 37.2 \text{ GPa}, \quad (9.72a)$$

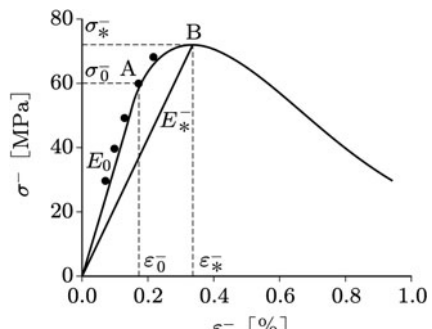


Fig. 9.7 Stress-strain curve of Salem limestone under uniaxial compression

Source: Lubarda et al. (1994, p. 690, Fig. 2)

$$\sigma_*^- = 72.8 \text{ MPa}, \quad \varepsilon_*^- = 3.2 \times 10^{-3}, \quad E_*^- = 22.8 \text{ GPa}. \quad (9.72\text{b})$$

In the case of uniaxial tension, on the other hand, the threshold stress and the strain for damage initiation and the Young's modulus in the undamaged state were identified as

$$\sigma_0^+ = 4.8 \text{ MPa}, \quad \varepsilon_0^+ = 1.3 \times 10^{-4}, \quad E_0 = 37.2 \text{ GPa}. \quad (9.73)$$

The material constants of Eq. (9.70a), furthermore, were given as

$$a = 3, \quad b = 1/150, \quad k = 104. \quad (9.74)$$

Finally, Fig. 9.8 shows the damage criterion in biaxial state of stress calculated by the above results, while Fig. 9.9 is the numerical prediction of the axial strain ε^- , lateral strain ε_l^- and the volumetric strain ε_v^- under a uniaxial compression tests.

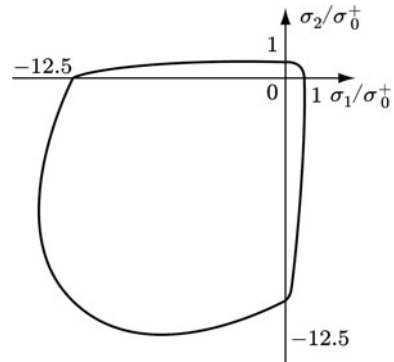


Fig. 9.8 Damage criterion of Salem limestone in biaxial state of stress

Source: Lubarda et al. (1994, p. 689, Fig. 1)

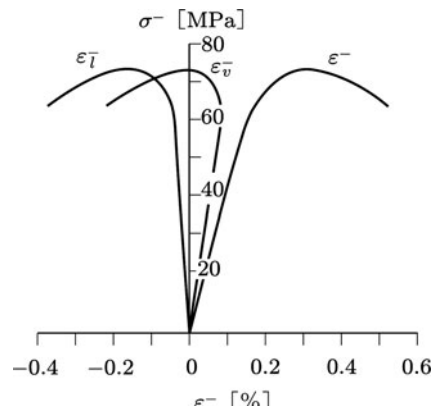


Fig. 9.9 Axial strain ε^- , lateral strain ε_l^- and volumetric strain ε_v^- of Salem limestone under uniaxial compression

Source: Lubarda et al. (1994, p. 694, Fig. 6)

Chapter 10

Continuum Damage Mechanics of Composite Materials

Damage and fracture of *composite materials* occur in various level of scale, and are much more complicated than those of uniform materials (Sadowski 2005, 2006). Continuum damage mechanics, however, furnishes effective means of damage and fracture analysis also for composite materials. The present chapter is concerned with the application of continuum damage mechanics theory to the damage analysis of composites mainly of polymer-, metal-, and ceramic-matrix.

In Section 10.1, to begin with, we discuss the elastic-plastic damage analysis of *fiber-reinforced plastic (FRP)* laminates by using two or three scalar damage variables. In Section 10.2, on the other hand, the elastic brittle damage theory of ceramics matrix composites is developed by the use of a fourth-order damage variable and by taking account of unilateral effects of cracks. Finally, a local damage theory of metal matrix composite will be described in Section 10.3.

10.1 Damage of Laminate Composites

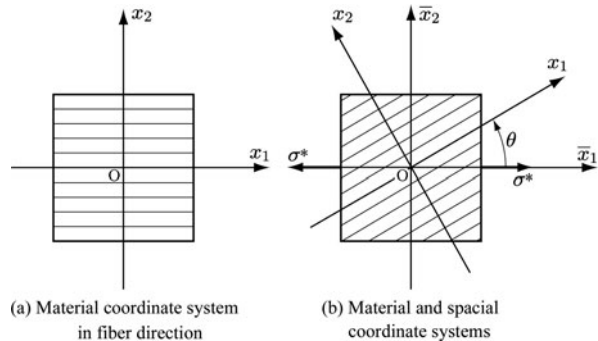
Fiber-reinforced composites, particularly the laminate composites composed of several plies of *fiber-reinforced laminae* (elementary plies) in different directions, are widely employed in engineering practice. We begin with the continuum damage mechanics theory of laminate composites by referring to the work of Ladevèze and others.

10.1.1 Damage Variables and Thermodynamic Potential

We first consider the damage of an elementary ply. The macroscopic mechanical property of a fiber-reinforced ply can be determined by homogenizing the local properties of fiber and matrix.

In the fiber direction, a ply generally shows elastic-brittle fracture, and hence the damage in this direction can be disregarded. However, in the direction perpendicular to the fiber, damage develops by the initiation and growth of microcracks in the matrix and/or in the *interface* between matrix and fiber. This damage in a lamina can be assumed to be uniform in its thickness, and induces the reduction in its rigidity.

Fig. 10.1 Coordinate systems for a unidirectional elementary ply



Let us suppose an orthogonal coordinate system $O-x_1x_2$ in the fiber direction and in the direction perpendicular to the fiber as shown in Fig. 10.1a. Then, the ply is orthotropic with respect to this *material coordinate system*. We denote Young's modulus of the ply in the fiber and in the perpendicular direction in the undamaged state by E_1^0 and E_2^0 , and the shear modulus in the direction parallel to the fiber by G_{12}^0 . Furthermore, Poisson's ratios for stresses in the fiber and in its perpendicular directions are denoted by ν_{12}^0 and ν_{21}^0 , respectively. Then, the elastic constitutive equation of this orthotropic material in the undamaged state is given by Eqs. (12.277) and (12.286) as follow:

$$\begin{aligned}\varepsilon_{11} &= \frac{\sigma_{11}}{E_1^0} - \nu_{21}^0 \frac{\sigma_{22}}{E_2^0}, & \varepsilon_{22} &= \frac{\sigma_{22}}{E_2^0} - \nu_{12}^0 \frac{\sigma_{11}}{E_1^0}, \\ \varepsilon_{12} &= \frac{\sigma_{12}}{2G_{12}^0}.\end{aligned}\tag{10.1a}$$

Among the material constants in these relations, Eq. (12.287) furnishes the following relations

$$\frac{\nu_{12}^0}{E_1^0} = \frac{\nu_{21}^0}{E_2^0}.\tag{10.1b}$$

Let us now consider Gibbs potential $\Gamma(\boldsymbol{\sigma})$ for the ply. By the use of matrix representation of Eq. (12.271) for the double contraction, together with that of the elastic constitutive equations (12.270b) and (12.286), the Gibbs potential of this material is expressed:

$$\begin{aligned}\rho\Gamma(\boldsymbol{\sigma}) &= -\frac{1}{2}\boldsymbol{\sigma} : (\mathbb{S} : \boldsymbol{\sigma}) \\ &= -\frac{1}{2} [\sigma_p] [W_{pq}] ([S_{rs}] [W_{sp}] [\sigma_q])\end{aligned}$$

$$\begin{aligned}
&= -\frac{1}{2} [\sigma_p] [W_{pr}] [S_{rp}] [\sigma_p] \\
&= -\frac{1}{2} \left\{ \frac{1}{E_1^0} (\sigma_{11})^2 + \frac{1}{E_2^0} (\sigma_{22})^{22} - \left(\frac{\nu_{12}^0}{E_1^0} + \frac{\nu_{21}^0}{E_2^0} \right) \sigma_{11} \sigma_{22} \right. \\
&\quad \left. + \frac{1}{2G_{12}^0} [(\sigma_{12})^2 + (\sigma_{21})^2] \right\}. \tag{10.2}^1
\end{aligned}$$

When a fiber-reinforced composite is subject to a compressive stress in the fiber direction, its elastic modulus decreases with the increase in the stress. Then, we now postulate that Young's modulus E_1^C in the fiber direction under compressive stress may be expressed by a relation

$$E_1^C = E_1^0 \left[1 - \frac{\varsigma}{E_1^0} < -\sigma_{11} > \right], \tag{10.3}$$

where ς and $< >$ signify a material constant and the Macauley bracket.

By dividing the normal stress into the cases of tensile and compressive stress, the Gibbs potential (10.2) for elastic deformation in undamaged state can be expressed in the form (Ladevèze 1992)

$$\begin{aligned}
\rho \Gamma(\sigma) = & -\frac{1}{2} \left\{ \frac{< \sigma_{11} >^2}{E_1^0} + \frac{\varphi < -\sigma_{11} >}{E_1^0} - \left(\frac{\nu_{12}^0}{E_1^0} + \frac{\nu_{21}^0}{E_2^0} \right) \sigma_{11} \sigma_{22} \right. \\
& \left. + \frac{< \sigma_{22} >^2}{E_2^0} + \frac{< -\sigma_{22} >^2}{E_2^0} + \frac{1}{2G_{12}^0} [(\sigma_{12})^2 + (\sigma_{21})^2] \right\}, \tag{10.4a}
\end{aligned}$$

where $\varphi < -\sigma_{11} >$ denotes a function which satisfies the relation

$$\begin{aligned}
\frac{\partial^2}{\partial \sigma_{11} \partial \sigma_{11}} \left[\frac{\varphi < -\sigma_{11} >}{E_1^0} \right] &= \frac{1}{E_1^C} \\
&= \frac{1}{E_1^0 \left[1 - \frac{\varsigma}{E_1^0} < -\sigma_{11} > \right]}. \tag{10.4b}
\end{aligned}$$

In the damaged state of the ply, on the other hand, the damage may be characterized by the decrease in the elastic modulus E_2 in the direction perpendicular to the fiber and in the shear modulus G_{12} in the direction parallel to the fiber. Thus, if we represent the damage state of this material by the reduction ratios D_T and D_S of

¹ The sign of the Gibbs potential conforms here to the definition of Eq. (3.26).

E_2 and G_{12} , they, respectively, imply the matrix-microcracking and the fiber-matrix debonding in the ply. Then, the Gibbs potential of the damaged material is derived by rewriting Eq. (10.4) in the form

$$\begin{aligned} \rho\Gamma(\sigma, D_S, D_T) = & -\frac{1}{2} \left\{ \frac{<\sigma_{11}>^2}{E_1^0} + \frac{\varphi <-\sigma_{11}>}{E_1^0} \right. \\ & - \left(\frac{v_{12}^0}{E_1^0} + \frac{v_{21}^0}{E_2^0} \right) \sigma_{11}\sigma_{22} + \frac{<\sigma_{22}>^2}{(1-D_T)E_2^0} \\ & \left. + \frac{<-\sigma_{22}>^2}{E_2^0} + \frac{1}{2(1-D_S)G_{12}^0} [(\sigma_{12})^2 + (\sigma_{21})^2] \right\}. \end{aligned} \quad (10.5)$$

By performing differential calculus in a similar procedure to [Section 4.3.4](#), the elastic constitutive equation and the generalized forces Y_T , Y_S associated with the damage variables D_T , D_S are derived:

$$\begin{aligned} \varepsilon_{11} = & -\rho \frac{\partial \Gamma}{\partial \sigma_{11}} \\ = & \frac{<\sigma_{11}>}{E_1^0} - \frac{<-\sigma_{11}>}{E_1^0 \left[1 - \frac{\varsigma}{E_1^0} <-\sigma_{11}> \right]} - \frac{1}{2} \left(\frac{v_{12}^0}{E_1^0} + \frac{v_{21}^0}{E_2^0} \right) \sigma_{22}, \end{aligned} \quad (10.6a)$$

$$\varepsilon_{12} = -\rho \frac{\partial \Gamma}{\partial \sigma_{12}} = \frac{\sigma_{12}}{2(1-D_S)G_{12}^0}, \quad (10.6b)$$

$$\begin{aligned} \varepsilon_{22} = & -\rho \frac{\partial \Gamma}{\partial \sigma_{22}} \\ = & -\frac{1}{2} \left(\frac{v_{12}^0}{E_1^0} + \frac{v_{21}^0}{E_2^0} \right) \sigma_{11} + \frac{<\sigma_{22}>}{(1-D_T)E_2^0} - \frac{<-\sigma_{22}>}{E_2^0}, \end{aligned} \quad (10.6c)$$

$$Y_S = -\rho \frac{\partial \Gamma}{\partial D_S} = \frac{(\sigma_{12})^2}{2(1-D_S)^2 G_{12}^0}, \quad (10.7a)$$

$$Y_T = -\rho \frac{\partial \Gamma}{\partial D_T} = \frac{<\sigma_{22}>^2}{2(1-D_T)^2 E_2^0}. \quad (10.7b)$$

10.1.2 Evolution Equation of Damage Variables

The damage of a ply is brought about by the *microcracks* in matrix parallel to the fiber and by the *debonding* of matrix/fiber interface. This damage state is represented here by the damage variables D_S and D_T .

According to Ladevèze (1992), we express the equivalent damage-associated variable Y (Y_S, Y_T) and the damage criterion:

$$Y = Y_S + bY_T, \quad (10.8a)$$

$$F^D = Y^{1/2} - Y_0^{1/2} \geq 0, \quad (10.8b)$$

where b is a material constant characterizing the effects of the damage-associated variables Y_S and Y_T , and will be given later. Then, by assuming that the damage state is described by the equivalent damage-associated variable Y and by noting the experimental results of Fig. 10.2 shown later, the evolution equations of D_S and D_T may be expressed as follow:

$$D_S = \frac{1}{(Y_C^S)^{1/2}} \left\langle Y^{1/2} - (Y_0)^{1/2} \right\rangle, \quad (10.9a)$$

$$D_T = \frac{1}{(Y_C^T)^{1/2}} \left\langle Y^{1/2} - (Y_0)^{1/2} \right\rangle, \quad (10.9b)$$

where $Y_C^S, Y_C^T, b = (Y_C^S)^{1/2}/(Y_C^T)^{1/2}$ are material constants, and Y_0 denotes the threshold for damage development.

The damage-associated variable, in general, specifies the rate of the damage variable, and not the damage variable itself. Thus, besides Eq. (10.9), the following evolution equation of damage also has been proposed (Ladevèze 1992):

$$\dot{D}_S = k \left\langle \frac{Y^{1/2} - [(Y_0)^{1/2} + (Y_C^S)^{1/2} D_S]}{(Y_C^S)^{1/2}} \right\rangle^n, \quad (10.10a)$$

$$\dot{D}_T = b\dot{D}_S + k' \left\langle \frac{(Y_T)^{1/2} - (Y_C^T)^{1/2} D_T}{(Y_C^T)^{1/2}} \right\rangle^{n'}, \quad (10.10b)$$

where k, k', n and n' are material constants.

10.1.3 Plastic Constitutive Equation of Damaged Material

As for the ply of Fig. 10.1a, it was assumed that the fiber is always elastic. Therefore, the plastic deformation (or the inelastic deformation) in the ply is caused by the development of microcracks in the matrix and by the debonding of the matrix/fiber interface. By the use of damage variables D_S and D_T together with the hypothesis of the inelastic energy equivalence of Eq. (2.73):

$$\boldsymbol{\sigma} : \dot{\boldsymbol{\epsilon}}^P = \tilde{\boldsymbol{\sigma}} : \dot{\tilde{\boldsymbol{\epsilon}}}^P, \quad (10.11)$$

the effective stress and the effective strain rate in the ply are given by

$$\tilde{\sigma}_{11} = \sigma_{11}, \quad \tilde{\sigma}_{12} = \frac{\sigma_{12}}{1 - D_S}, \quad \tilde{\sigma}_{22} = \frac{\sigma_{22}}{1 - D_T}, \quad (10.12a)$$

$$\dot{\tilde{\varepsilon}}_{11}^p = 0, \quad \dot{\tilde{\varepsilon}}_{12}^p = \dot{\varepsilon}_{12}^p(1 - D_S), \quad \dot{\tilde{\varepsilon}}_{22}^p = \dot{\varepsilon}_{22}^p(1 - D_T). \quad (10.12b)$$

By postulating the isotropic hardening of the material, the yield function can be expressed in the form

$$F^P = \tilde{\sigma}_{EQ} - R(p) - \sigma_Y \leq 0, \quad (10.13a)$$

$$\tilde{\sigma}_{EQ} = \left[(\tilde{\sigma}_{12})^2 + a^2(\tilde{\sigma}_{22})^2 \right]^{1/2}, \quad (10.13b)$$

$$R(p) = \beta p^\gamma, \quad (10.13c)$$

where a , β , γ are material constants.

By defining the rate of accumulated plastic strain

$$\dot{p} = \left[\left(\dot{\tilde{\varepsilon}}_{12}^p \right)^2 + (1/a)^2 \left(\dot{\tilde{\varepsilon}}_{22}^p \right)^2 \right]^{1/2}, \quad (10.14)$$

and by employing F^P of Eq. (10.13) as the plastic potential, the plastic constitutive equation can be derived as follow:

$$\dot{\tilde{\varepsilon}}_{12}^p = \dot{\Lambda}^P \frac{\partial F^P}{\partial \tilde{\sigma}_{12}} = \dot{\Lambda}^P \frac{\tilde{\sigma}_{12}}{\tilde{\sigma}_{EQ}} = \dot{p} \frac{\tilde{\sigma}_{12}}{R + \sigma_Y}, \quad (10.15a)$$

$$\dot{\tilde{\varepsilon}}_{22}^p = \dot{\Lambda}^P \frac{\partial F^P}{\partial \tilde{\sigma}_{22}} = a^2 \dot{\Lambda}^P \frac{\tilde{\sigma}_{22}}{\tilde{\sigma}_{EQ}} = a^2 \dot{p} \frac{\tilde{\sigma}_{22}}{R + \sigma_Y}. \quad (10.15b)$$

10.1.4 Application to Laminate Composites

The above theory of an elementary ply is applicable also to the damage of a laminate material, if the constituent plies are bonded perfectly and hence the delamination can be disregarded. We now apply the above results to a laminate of simple stacking-sequence $[+45^\circ, -45^\circ]_{2S}$, and consider the identification of the related material constants. The modeling of the interlaminar damage and the delamination will be discussed in Section 10.1.6 later.

(1) Uniaxial Tension of 45° Unidirectional Ply

We first employ a spacial coordinate system $O-\bar{x}_1\bar{x}_2$ of Fig. 10.1b. Then we consider a uniaxial tension of a $\theta = 45^\circ$ unidirectional ply subject to $\tilde{\sigma}_{11} = \sigma^*$.

The stress components in the ply with respect to the material coordinate system O-x₁x₂ are given by

$$\sigma_{11} = \sigma_{22} = \sigma_{12} = \frac{1}{2}\sigma^*. \quad (10.16)$$

The normal strain in the fiber direction is sufficiently small in comparison with that perpendicular to the fiber. The normal strain perpendicular to the fiber and the shear strain in the fiber direction, on the other hand, are of the same order to each other, and their components as to the O-x₁x₂ coordinate system are given as follows:

$$\varepsilon_{11} = 0, \quad \varepsilon_{12} = \frac{1}{2}(\varepsilon_{nn}^* - \varepsilon_{tt}^*), \quad \varepsilon_{22} = \frac{1}{2}(\varepsilon_{nn}^* + \varepsilon_{tt}^*), \quad (10.17)$$

where ε_{nn}^* and ε_{tt}^* are the normal strain component in the \bar{x}_1 -direction and that perpendicular to it.

Then, the strain-hardening variable, accumulated plastic strain rate, damage-associated variable and the damage variable are derived from Eqs. (10.13), (10.14) and (10.7) through (10.9) as follow:

$$\sigma^* = 2\left[\frac{1}{(1-D_S)^2} + \frac{a^2}{(1-D_T)^2}\right]^{-1/2} (\beta p^\gamma + \sigma_Y), \quad (10.18)$$

$$\dot{p} = \frac{1}{2}\left[\left(\dot{\varepsilon}_{nn}^{p*} - \dot{\varepsilon}_{tt}^{p*}\right)^2(1-D_S)^2 + \frac{1}{a^2}(\dot{\varepsilon}_{nn}^{p*} + \dot{\varepsilon}_{tt}^{p*})^2(1-D_T)^2\right]^{1/2}, \quad (10.19)$$

$$Y_S = \frac{1}{8}\frac{(\sigma^*)^2}{(1-D_S)^2 G_{12}^0}, \quad Y_T = \frac{1}{8}\frac{(\sigma^*)^2}{(1-D_T)^2 E_2^0}, \quad (10.20)$$

$$Y = \frac{1}{8}\left[\frac{1}{(1-D_S)^2 G_{12}^0} + \frac{b}{(1-D_T)^2 E_2^0}\right](\sigma^*)^2, \quad (10.21)$$

$$D_S = \frac{\sigma^*}{2(2Y_C^S)^{1/2}} \left[\frac{1}{(1-D_S)^2 G_{12}^0} + \frac{b}{(1-D_T)^2 E_2^0} \right]^{1/2} - \left(\frac{Y_0}{Y_C^S}\right)^{1/2}, \quad (10.22a)$$

$$D_T = \left(\frac{Y_C^S}{Y_C^T}\right)^{1/2} D_S. \quad (10.22b)$$

(2) Uniaxial Tension of a $[+45^\circ, -45^\circ]_{2S}$ Laminate

Then, we apply this theory to a laminate of $[+45^\circ, -45^\circ]_{2S}$. The laminate is supposed to be subject to a tensile stress σ^* in \bar{x}_1 direction in Fig. 10.1b.

The laminate material $[+45^\circ, -45^\circ]_{2S}$ is composed of an elementary ply of $\theta = 45^\circ$ described above and another ply with the symmetric fiber array as to \bar{x}_1 -axis laid on it. Then, the stress components of each ply with respect to the material coordinate system O- x_1x_2 are given, similarly to Eq. (10.16):

$$\sigma_{11} = \sigma_{22} = \sigma_{12} = (1/2)\sigma^*. \quad (10.23)$$

The normal strain in the fiber direction in a ply is sufficiently small in comparison with the shear strain. Hence the strain components in the laminate with respect to the material coordinate system are given by

$$\varepsilon_{11} = \varepsilon_{22} = 0, \quad \varepsilon_{12} = (1/2)(\varepsilon_{nn}^* - \varepsilon_{tt}^*). \quad (10.24)$$

We now apply Eqs. (10.6) through (10.15) to this loading state. Then, Eqs. (10.13) and (10.14) furnish the relations

$$\tilde{\sigma}_{EQ} = R + \sigma_Y = \tilde{\sigma}_{12} = \frac{1}{2} \frac{\sigma^*}{1 - D_S}, \quad (10.25a)$$

or

$$\sigma^* = 2(1 - D_S)(\beta p^\gamma + \sigma_Y), \quad (10.25b)$$

$$\dot{p} = \frac{1 - D_S}{2}(\dot{\varepsilon}_{nn}^{p*} - \dot{\varepsilon}_{tt}^{p*}). \quad (10.26)$$

We have assumed that the damage in the fiber direction does not occur in this material. Thus the damage-associated variable and the damage variable are derived from Eqs. (10.7) through (10.9) as follow

$$Y_S = \frac{1}{8} \frac{(\sigma^*)^2}{(1 - D_S)^2 G_{12}^0}, \quad Y_T = \frac{1}{8} \frac{(\sigma^*)^2}{E_2^0}, \quad (10.27)$$

$$Y = \frac{1}{8} \left[\frac{1}{(1 - D_S)^2 G_{12}^0} + \frac{b}{E_2^0} \right] (\sigma^*)^2, \quad (10.28)$$

$$D_S = \frac{\sigma^*}{2(2Y_C^S)^{1/2}} \left[\frac{1}{(1 - D_S)^2 G_{12}^0} + \frac{b}{E_2^0} \right]^{1/2} - \left(\frac{Y_0}{Y_C^S} \right)^{1/2}, \quad (10.29a)$$

$$D_T = 0. \quad (10.29b)$$

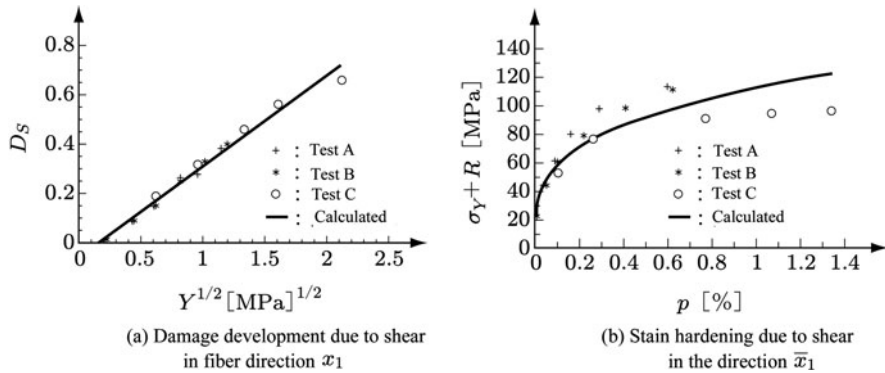


Fig. 10.2 Damage of IM 6/914 [±45]₂S laminate specimens under uniaxial tension
Source: Ladevèze and Le Dantec (1992, p. 261, Fig. 8; p. 261, Fig. 9)

By solving Eq. (10.29a), D_S can be obtained as a function of σ^* . Then, the material constants Y_0 , Y_C^S , b , β and γ are determined by comparing this relation with the results of experiments.

Ladevèze and others (Allix et al. 1990; Ladevèze and Le Dantec 1992) performed a series of elastic-plastic damage tests on carbon fiber-reinforced composite laminates, and identified the material constants of Y_0 , Y_C^S , Y_C^T , a , b and the strain-hardening function $R(p)$ by comparing the results with the above theory.

Figure 10.2a and b shows the damage development and the strain-hardening of this material calculated by the use of Eqs. (10.25) through (10.29). The above formulation has been extended also to the temperature range of -120°C through +120°C, and has been applied to damage analyses of composite materials with different ply stacking (Allix et al. 1994).

10.1.5 Brittle Damage in Fiber Direction

In the discussion hitherto, the effect of brittle fracture in the fiber direction of laminas has been disregarded. This effect, however, can be described if we rewrite the Gibbs potential (10.15) by introducing a new damage variable D_F for this purpose (Ladevèze et al. 1998):

$$\begin{aligned} \rho \Gamma(\sigma, D_\alpha) = & -\frac{1}{2(1-D_F)} \left[\frac{<\sigma_{11}>^2}{E_1^0} + \frac{\varphi <-\sigma_{11}>}{E_1^0} - \left(\frac{v_{12}^0}{E_1^0} + \frac{v_{21}^0}{E_2^0} \right) \sigma_{11} \sigma_{22} \right] \\ & - \frac{1}{2} \left\{ \frac{<\sigma_{22}>^2}{(1-D_T)E_2^0} + \frac{<-\sigma_{22}>^2}{E_2^0} + \frac{1}{2(1-D_S)G_{12}^0} [(\sigma_{12})^2 + (\sigma_{21})^2] \right\}, \end{aligned} \quad (10.30)$$

where D_α represents $\{D_S, D_T, D_F\}$ and D_F signifies the damage in the fiber direction. The function $\varphi < -\sigma_{11} >$ has been defined by Eq. (10.4b).

Then the elastic constitutive equation taking account of the brittle damage in fiber direction, and the damage-associated variables Y_S , Y_T , Y_F can be derived as follow

$$\varepsilon_{11} = \frac{1}{(1-D_F)} \left[\frac{\frac{<\sigma_{11}>}{E_1^0}}{E_1^0 \left(1 - \frac{\varsigma}{E_1^0} < -\sigma_{11} >\right)} - \frac{1}{2} \left(\frac{v_{12}^0}{E_1^0} + \frac{v_{21}^0}{E_2^0} \right) \sigma_{22} \right], \quad (10.31a)$$

$$\varepsilon_{12} = \frac{\sigma_{12}}{2(1-D_S)G_{12}^0}, \quad (10.31b)$$

$$\varepsilon_{22} = -\frac{1}{2(1-D_F)} \left(\frac{v_{12}^0}{E_1^0} + \frac{v_{21}^0}{E_2^0} \right) \sigma_{11} + \frac{<\sigma_{22}>}{(1-D_T)E_2^0} - \frac{<-\sigma_{22}>}{E_2^0}, \quad (10.31c)$$

$$Y_S = \frac{(\sigma_{12})^2}{2(1-D_S)^2 G_{12}^0}, \quad (10.32a)$$

$$Y_T = \frac{<\sigma_{22}>^2}{2(1-D_T)^2 E_2^0}, \quad (10.32b)$$

$$Y_F = \frac{1}{2(1-D_F)^2} \left[\frac{<\sigma_{11}>^2}{E_1^0} + \frac{\varphi < -\sigma_{11} >}{E_1^0} - \left(\frac{v_{12}^0}{E_1^0} + \frac{v_{21}^0}{E_2^0} \right) \sigma_{11} \sigma_{22} \right]. \quad (10.32c)$$

10.1.6 Interlaminar Damage and Delamination of Laminate Composites

An interlaminar interface can be modeled as a two-dimensional layer of infinitesimal thickness which transfers displacement and stress from a ply to another. We consider an orthogonal coordinate system O-x₁x₂x₃ as shown in Fig. 10.3, where x₁-axis is taken in the direction of the bisector of two fiber directions of the neighboring plies, and x₂- and x₃-axis are perpendicular to it.

We represent Young's modulus of the interface layer in the thickness direction in undamaged state and the shear modulus of in-plane shear in the x₁- and x₂-direction by k_0 , k_1^0 and k_2^0 , respectively. Furthermore, the damage state of the interface layer is represented by the reduction ratios D , D_1 and D_2 in the elastic moduli k_0 , k_1^0 and k_2^0 , respectively. Then the Gibbs potential of the interface layer in elastic-brittle damage state is expressed as follows (Allix and Ladevèze 1992; Ladevèze 1992).

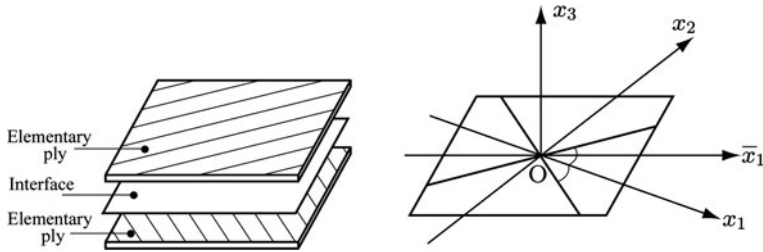


Fig. 10.3 Interface and orthogonal coordinate system $O-x_1x_2x_3$

$$\rho\Gamma = -\frac{1}{2} \left[\frac{<\sigma_{33}>^2}{k_0(1-D)} + \frac{<-\sigma_{33}>^2}{k_0} + \frac{(\sigma_{31})^2}{k_1^0(1-D_1)} + \frac{(\sigma_{32})^2}{k_2^0(1-D_2)} \right]. \quad (10.33)$$

Substitution of this relation into Eq. (3.65) furnishes the damage-associated variables Y_D , Y_{D1} and Y_{D2} of the damaged variables D , D_1 and D_2 :

$$Y_D = \frac{1}{2} \frac{<\sigma_{33}>^2}{k_0(1-D)^2}, \quad Y_{D1} = \frac{1}{2} \frac{(\sigma_{31})^2}{k_1^0(1-D_1)^2}, \quad Y_{D2} = \frac{1}{2} \frac{(\sigma_{32})^2}{k_2^0(1-D_2)^2}. \quad (10.34)$$

The equivalent damage-associated variable Y and the damage criterion can be defined similarly to Section 10.1.2:

$$Y = [Y_D + \gamma_1 Y_{D1} + \gamma_2 Y_{D2}], \quad (10.35)$$

$$F^D = Y^{1/2} - Y_0^{1/2} \geq 0, \quad (10.36)$$

where Y_0 is the threshold for damage initiation.

By postulating that the damage development is governed by the equivalent damage-associated variable, the evolution equations of damage can be expressed as

$$D = \frac{<Y^{1/2} - Y_0^{1/2}>}{Y_C^{1/2} - Y_0^{1/2}}, \quad D_1 = \gamma_1 D, \quad D_2 = \gamma_2 D, \quad (10.37)$$

where Y_C is the critical value for the occurrence of brittle fracture.

10.1.7 Damage Mesomodel of Laminates

Damage mechanics of laminates aims at the macroscopic modeling of their damage and deformation. As observed in Sections 10.1.4 through 10.1.6, the laminated composites are characterized by the stacking of two kinds of constituent layers: i.e., the *elementary ply* which is reinforced by long fibers in one direction and the

two-dimensional *interface* which transfers displacement and forces between two adjacent plies.

Though these elementary plies are subject to damage mainly by the matrix micro-cracking, fiber-matrix debonding, fiber breakage, and the delamination between adjacent plies.

Namely the essential hypothesis of this laminate model is that the damage and deformation of a laminate are identified by the mechanical states of the constituent elementary layers of the mesoscale, and does not depend on their stacking sequence. Thus this approach to laminates is called *damage mesomodel of laminates* (Allix and Ladevèze 1992; Ladevèze 2005; Ladevèze and Lubineau 2001). This damage model of laminates has been applied not only to static, but also to dynamic problems, e.g., the processes of damage, fracture and the energy dissipation under dynamic loading (Allix et al. 2003).

10.2 Elastic-Brittle Damage of Ceramic Matrix Composites

Fiber-reinforced ceramic matrix composites are often employed as structural components at elevated temperatures. As described in Chapter 9, brittle damage materials undergo the reduction in their rigidity and strength as a result of microcrack development. These effects, moreover, differ largely depending on whether the cracks are opening or closing, and thus a salient unilateral effect is observed in the behavior of these cracks.

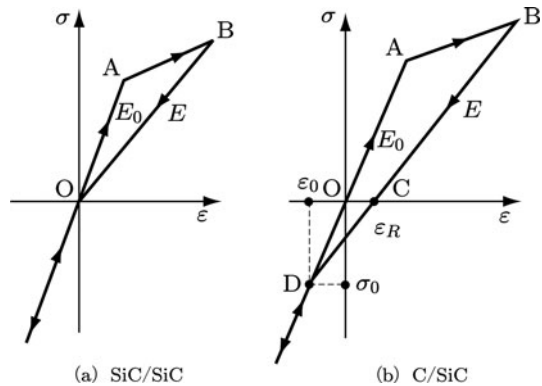
We now consider the modeling of elastic-brittle damage of ceramic matrix composites (Chaboche, Lesne, and Maire 1994, 1995) by taking account of the initial and the damage-induced anisotropy and the unilateral effect of damage. This model can be extended also to incorporate the effects of the viscoelasticity and the viscoplasticity (Chaboche, Lesn  , and Pottier 1998).

10.2.1 Elastic-Brittle Damage Behavior of Ceramic Matrix Composites and Its Unilateral Effect

Let us suppose an isothermal elastic deformation and a time independent damage process of a ceramic matrix composite. Then, the elastic-brittle damage behavior of the composite can be simplified as shown in Fig. 10.4, where the figures (a), (b) show the tension-compression behavior of SiC/SiC and C/SiC composites.

The bilinear branches OAB of the tensile processes of Fig. 10.4a and b represent the reduction in rigidity caused by the damage. The unloading- and inverse-loading branches BO and BD, on the other hand, show the closing behavior of *microcracks* which have been brought about in their loading process. In the case of the C/SiC composite of Fig. 10.4b, in particular, a residual stress has been induced due to the thermal expansion caused in the fabrication. The crack-closure and the *deactivation of damage* start at the *knee point* D(ε_0 , σ_0). The ε_R in the figure denotes the residual strain.

Fig. 10.4 Elastic-brittle damage behavior of ceramic matrix composites
Source: Chaboche et al. (1995, p. 14, Fig. 2)



10.2.2 Damage Variable and Thermodynamic Potential

Damage state of a fiber-reinforced composite of brittle matrix has initial anisotropy resulting from its fiber arrangement. The micocracks in the matrix due to damage develop generally in the direction parallel and perpendicular to the fibers, and hence its symmetry property (i.e., principal directions of the anisotropy) does not vary in the damage process. The damage state of the composite, therefore, can be represented by three scalar damage variables $d_i(i = 1, 2, 3)$ specifying the crack densities in the principal directions of the anisotropy of the material.

According to the matrix representation of tensors in [Section 12.7](#), the components of the fourth-order damage tensor \mathbb{D} can be expressed in terms of d_i as follow

$$\mathbb{D} = \begin{bmatrix} D_{11} & D_{12} & D_{13} & 0 & 0 & 0 \\ D_{12} & D_{22} & D_{23} & 0 & 0 & 0 \\ D_{13} & D_{32} & D_{33} & 0 & 0 & 0 \\ 0 & 0 & 0 & D_{44} & 0 & 0 \\ 0 & 0 & 0 & 0 & D_{55} & 0 \\ 0 & 0 & 0 & 0 & 0 & D_{66} \end{bmatrix}, \quad (10.38a)$$

$$\begin{aligned} D_{11} &= d_1, & D_{22} &= d_2, & D_{33} &= d_3, \\ D_{12} &= a_{12}(d_1 + d_2), & D_{13} &= a_{13}(d_1 + d_3), & D_{23} &= a_{23}(d_2 + d_3), \\ D_{44} &= a_{44}(d_2 + d_3), & D_{55} &= a_{55}(d_1 + d_3), & D_{66} &= a_{66}(d_1 + d_2), \end{aligned} \quad (10.38b)$$

where a_{12}, \dots, a_{66} are material constants.

Let the elastic modulus tensor of the material at the initial undamaged state be C_0 , and that at the damaged state with totally opening microcracks be $C(d_\alpha)$. Then,

the effective elastic modulus tensor \mathcal{C}_{EF} with microcracks in partial opening is given by Eq. (5.102):

$$\mathcal{C}_{EF}(d_\alpha) = \mathcal{C}(d_\alpha) + \eta \sum_{i=1}^3 H(-\bar{\varepsilon}_i) \mathbb{P}_i : [\mathcal{C}_0 - \mathcal{C}(d_\alpha)] : \mathbb{P}_i, \quad (10.39)$$

where η ($0 \leq \eta \leq 1$) and $H()$ denote a material constant representing the magnitude of the unilateral effect and the Heaviside function. The symbols \mathbb{P}_i and $\bar{\varepsilon}_i$, furthermore, are the fourth-order projection tensors with respect to the principal directions \mathbf{n}_i of the damage, and the component of the strain tensor $\bar{\boldsymbol{\varepsilon}}$ relative to the knee point, respectively, i.e.,

$$\mathbb{P}_i = \mathbf{n}_i \otimes \mathbf{n}_i \otimes \mathbf{n}_i \otimes \mathbf{n}_i, \quad (10.40a)$$

$$\bar{\varepsilon}_i = \mathbf{n}_i \cdot \bar{\boldsymbol{\varepsilon}} \cdot \mathbf{n}_i = \text{tr}(\mathbb{P}_i : \bar{\boldsymbol{\varepsilon}}), \quad (10.40b)$$

$$\bar{\boldsymbol{\varepsilon}} = \boldsymbol{\varepsilon} - \boldsymbol{\varepsilon}_0. \quad (10.40c)$$

In the particular case when all the microcracks are closed and are deactivated, the effective elastic modulus tensor \mathcal{C}_{EF} of Eq. (10.39) leads to the following form by substituting $H(-\bar{\varepsilon}_i) = 1$ in it:

$$\mathcal{C}_R(d_\alpha) = \mathcal{C}(d_\alpha) + \eta \sum_{i=1}^3 \mathbb{P}_i : [\mathcal{C}_0 - \mathcal{C}(d_\alpha)] : \mathbb{P}_i. \quad (10.41)$$

Let us now consider an elastic-brittle damage material having the mechanical response of Fig. 10.4b. Then the Helmholtz free energy function ψ is given by

$$\rho\psi(\boldsymbol{\varepsilon}, d_\alpha) = \frac{1}{2} \bar{\boldsymbol{\varepsilon}} : \mathcal{C}_{EF}(d_\alpha) : \bar{\boldsymbol{\varepsilon}} + \bar{\boldsymbol{\varepsilon}} : \mathcal{C}_R(d_\alpha) : \boldsymbol{\varepsilon}_0. \quad (10.42)$$

This relation together with Eq. (5.4) furnishes the elastic constitutive equation of this damaged material:

$$\begin{aligned} \boldsymbol{\sigma} &= \rho \frac{\partial \psi}{\partial \boldsymbol{\varepsilon}} \\ &= \mathcal{C}_{EF} : (\boldsymbol{\varepsilon} - \boldsymbol{\varepsilon}_0) + \mathcal{C}_R : \boldsymbol{\varepsilon}_0, \end{aligned} \quad (10.43a)$$

$$\mathcal{C}_R : \boldsymbol{\varepsilon}_0 = \sigma_0. \quad (10.43b)$$

As observed in this relation, the damaged material deforms according to the reduced elastic modulus tensor \mathcal{C}_{EF} in the unloading range of $\varepsilon_i \geq (\varepsilon_0)_i$. In the reversed loading range $\varepsilon_i \leq (\varepsilon_0)_i$, the unilateral crack-closure occurs at the strain $(\varepsilon_0)_i$. However, it should be noted that the elastic modulus in the strain range $\varepsilon_i < (\varepsilon_0)_i$ is not necessarily equal to the initial modulus \mathcal{C}_0 (Chaboche, Lesne and Maire 1995).

The residual strain $\boldsymbol{\varepsilon}_R$ in Fig. 10.4b, on the other hand, is given by Eq. (10.43a) with $\boldsymbol{\sigma} = \mathbf{0}$ and $\boldsymbol{\varepsilon} = \boldsymbol{\varepsilon}_0$

$$\boldsymbol{\varepsilon}_R = \left[\mathbb{I} - \mathcal{C}_{EF}^{-1} : \mathcal{C}_R \right] : \boldsymbol{\varepsilon}_0. \quad (10.44)$$

10.2.3 Damage Potential and Evolution Equation of Damage

The damage-associated variable Y_α of the damage d_α ($\alpha = 1, 2, 3$) can be derived from Eqs. (5.5) and (10.42):

$$\begin{aligned} Y_\alpha &= -\rho \frac{\partial \psi}{\partial d_\alpha}; \\ &= -\frac{1}{2} \bar{\boldsymbol{\varepsilon}} : \left[\frac{\partial \mathcal{C}}{\partial d_\alpha} - \eta \sum_{i=1}^3 H(-\bar{\varepsilon}_i) \mathbb{P}_i : \frac{\partial \mathcal{C}}{\partial d_\alpha} : \mathbb{P}_i \right] : \bar{\boldsymbol{\varepsilon}} - \bar{\boldsymbol{\varepsilon}} : \frac{\partial \mathcal{C}_R}{\partial d_\alpha} : \boldsymbol{\varepsilon}_0. \end{aligned} \quad (10.45)$$

As regards the damage development, we postulate the damage potential in the space of associated variable $\{Y_\alpha\}$:

$$F^D(Y_\alpha ; d_\alpha) = G(Y_\alpha) - B(d_\alpha) \leq 0, \quad (10.46)$$

where B is the threshold for damage development. This relation together with the consistency condition $\dot{F}^D = 0$ furnishes the evolution equation of the damage variables

$$\dot{d}_i = H(F^D) \frac{\left\langle \frac{\partial G}{\partial Y_\alpha} \dot{Y}_\alpha \right\rangle}{\frac{\partial B}{\partial d_\beta} \frac{\partial G}{\partial Y_\beta}} \frac{\partial G}{\partial Y_i}. \quad (10.47)$$

10.2.4 Application to Ceramic Matrix Composites

We now apply the above theory to the analysis of elastic-brittle damage of a SiC/SiC composite. Since the initial residual strain is insignificant in this composite, its damage behavior can be modeled as shown in Fig. 10.4a. Thus, by taking $\boldsymbol{\varepsilon}_0 = \mathbf{0}$, Eqs. (10.42), (10.43) and (10.39) lead, respectively, to

$$\rho\psi(\boldsymbol{\varepsilon}, d_\alpha) = \frac{1}{2} \boldsymbol{\varepsilon} : \mathcal{C}_{EF} : \boldsymbol{\varepsilon}, \quad (10.48)$$

$$\boldsymbol{\sigma} = \mathcal{C}_{EF} : \boldsymbol{\varepsilon}, \quad (10.49)$$

$$\mathcal{C}_{EF}(d_\alpha) = \mathcal{C}(d_\alpha) + \eta \sum_{i=1}^3 H(-\varepsilon_i) \mathbb{P}_i : [\mathcal{C}_0 - \mathcal{C}(d_\alpha)] : \mathbb{P}_i. \quad (10.50)$$

Then, let us consider the particular case of a SiC/SiC composite reinforced by symmetric plain weave cloth in the state of plane stress. By taking account of Eqs. (2.33) and (10.38) for the elastic modulus tensor of a damaged material, the tensor $\mathcal{C}(d_\alpha)$ is expressed as follow (Chaboche et al. 1994):

$$\begin{aligned} \mathcal{C}(d_\alpha) &= \begin{bmatrix} C_{11}^0(1 - D_{11}) & C_{12}^0(1 - D_{12}) & 0 \\ C_{12}^0(1 - D_{12}) & C_{22}^0(1 - D_{22}) & 0 \\ 0 & 0 & C_{66}^0(1 - D_{66}) \end{bmatrix} \\ &= \begin{bmatrix} C_{11}^0(1 - d_1) & C_{12}^0[1 - a_{12}(d_1 + d_2)] & 0 \\ C_{12}^0[1 - a_{12}(d_1 + d_2)] & C_{22}^0(1 - d_2) & 0 \\ 0 & 0 & C_{66}^0[1 - a_{66}(d_1 + d_2)] \end{bmatrix}, \end{aligned} \quad (10.51)$$

where C_{ij}^0 is the component of the matrix of elastic modulus tensor of the undamaged material.

By substituting Eqs. (10.50) and (10.51) into Eq. (10.48) of the free energy function $\psi(\boldsymbol{\varepsilon}, d_\alpha)$, and by applying the resulting relation to Eq. (5.5), we have the damage-associated variables Y_1 and Y_2 :

$$Y_1 = \frac{1}{2} \{ C_{11}^0 [1 - H(-\varepsilon_1)] (\varepsilon_1)^2 + 2a_{12} C_{12}^0 \varepsilon_1 \varepsilon_2 + a_{66} C_{66}^0 [1 - H(-\varepsilon_3)] (\varepsilon_3)^2 \}, \quad (10.52a)$$

$$Y_2 = \frac{1}{2} \{ 2a_{12} C_{12}^0 \varepsilon_1 \varepsilon_2 + C_{22}^0 [1 - H(-\varepsilon_2)] (\varepsilon_2)^2 + a_{66} C_{66}^0 [1 - H(-\varepsilon_3)] (\varepsilon_3)^2 \}, \quad (10.52b)$$

where the material constant η in Eq. (10.50) has been taken as $\eta = 1$.

In the derivation of Eq. (10.52), a second-order tensor basis for the Voigt representation

$$\begin{aligned} [\mathbf{N}_p] &= [N_1, N_2, N_3, \dots, N_6] \\ &= [\mathbf{n}_1 \otimes \mathbf{n}_1, \mathbf{n}_2 \otimes \mathbf{n}_2, \mathbf{n}_3 \otimes \mathbf{n}_3, \dots, \mathbf{n}_1 \otimes \mathbf{n}_2] \end{aligned} \quad (10.53a)$$

has been introduced first, and then the second term of the right-hand side of Eq. (10.50) has been rewritten in the following form in order to facilitate the differentiation of Eq. (5.5):

$$\begin{aligned}
& -\eta \sum_{i=1}^3 H(-\varepsilon_i) \mathbb{P}_i : \mathbb{C}(d_\alpha) : \mathbb{P}_i + O(\mathcal{C}_0) \\
& = -\eta \sum_{i=1}^3 H(-\varepsilon_i) \mathbf{n}_i \otimes \mathbf{n}_i \otimes \mathbf{n}_i \otimes \mathbf{n}_i : \\
& \quad C_{klmn}(d_\alpha) \mathbf{n}_k \otimes \mathbf{n}_l \otimes \mathbf{n}_m \otimes \mathbf{n}_n : \mathbf{n}_i \otimes \mathbf{n}_i \otimes \mathbf{n}_i \otimes \mathbf{n}_i + O(\mathcal{C}_0) \\
& = -\eta [H(-\varepsilon_1)C_{11}(d_\alpha)N_1 \otimes N_1 + H(-\varepsilon_2)C_{22}(d_\alpha)N_2 \otimes N_2 \\
& \quad + H(-\varepsilon_3)C_{33}(d_\alpha)N_3 \otimes N_3] + O(\mathcal{C}_0).
\end{aligned} \tag{10.53b}$$

It will be observed from Eq. (10.52) that Y_1 and Y_2 do not depend on d_1 and d_2 .

Finally, the damage potential of Eq. (10.46) must be specified. For this purpose, by taking account of the symmetry of the material, we introduce new damage-associated variables

$$\bar{Y}_1 = Y_1 + bY_2, \quad \bar{Y}_2 = Y_2 + bY_1, \tag{10.54}$$

where b is a material constant. By the use of these variables, we can derive the damage potential:

$$F_i^D = \left\{ 1 - \exp[k(\bar{Y}_i - Y_0)^p] \right\} - B \left(\frac{d_i}{d_c} \right), \quad (i = 1, 2), \tag{10.55}$$

where k , p , d_c , Y_0 and B are material constants. Figure 10.5 shows the results of experiments and the numerical simulation due to the above modeling for the 45° tension of the SiC/SiC composite.

Chaboche and others (1994) also derived another damage potential for a C/SiC composite of Fig. 10.4b, i.e.,

$$F = G(|Y|) - B(|d|) \leq 0, \tag{10.56a}$$

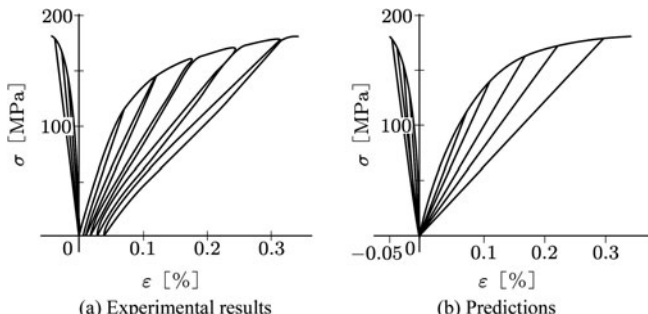


Fig. 10.5 45° tension of plain weave SiC/SiC composite

Source: Chaboche et al. (1994, p. 85, Fig. 3)

$$|Y| = [< Y_1 >^m + < Y_2 >^m + a < Y_2 >^m]^{1/m}, \quad (10.56b)$$

$$|d| = [(d_1)^2 + (d_2)^2 + (d_3)^2]^{1/2}, \quad (10.56c)$$

where a and m are material constants. They performed also analyses similar to the case of the SiC/SiC composite.

10.3 Local Theory of Metal Matrix Composites

In the above sections, the damage of a composite material has been modeled as if the material is a homogeneous anisotropic continuum. In the damage process of the actual composites, however, damage of each phase and their interface develop separately.

At the end of this chapter, we consider the *local theory* (Voyadjis and Kattan 1993) for the elastic-plastic damage of fiber-reinforced metal matrix composites. In the theory, damage in the matrix and that of the fiber are specified separately at the beginning, and then the overall mechanical state is homogenized by the use of micromechanics.

10.3.1 Local and Overall Configurations of Composites

Let us consider a representative volume element (RVE) of Fig. 10.6 for the composite material. The *overall current damaged configuration* is denoted by B_t , while the *local current damaged configurations* of the matrix and the fiber are signified by B_t^M and B_t^F , respectively. Furthermore, the corresponding fictitious undamaged configurations are represented by B_f , B_f^M and B_f^F . Here the word “local” implies that the mechanical states of the matrix and the fiber are treated separately. The superscripts

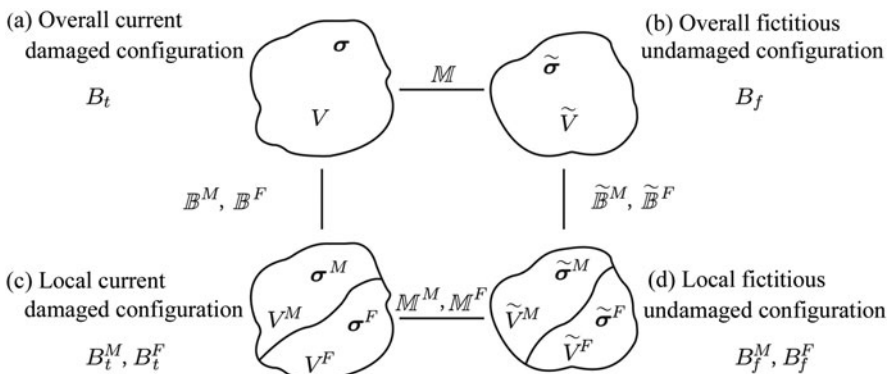


Fig. 10.6 Local damage theory of composite material

M and F signify the matrix and the fiber. The symbols \mathbb{M} , \mathbb{M}^M and \mathbb{M}^F of Fig. 10.6 denote the damage effect tensors of the respective configurations, and are related to the damaged states of the material.

According to the notion of effective stress and effective strain, the deformation and the damage behavior of a damaged material B_t can be described by the mechanical variables in the corresponding fictitious undamaged configuration B_f . Therefore, the damage analysis reflecting the local damage of the constituent phases of a composite can be performed by expressing the mechanical variables of the current damaged configurations B_t , B_t^M and B_t^F of Fig. 10.6a and c in terms of the corresponding variables of the fictitious undamaged configurations B_f , B_f^M and B_f^F of Fig. 10.6b and d.

In the following, referring to Voyatzis and Kattan (1993, 1999), we derive the relation between the mechanical variables in the local and the overall configurations of Fig. 10.6.

10.3.2 Local-Overall Relations of Stress and Strain

Let the volume of the matrix and the fiber in the local fictitious undamaged configurations B_f^M and B_f^F of Fig. 10.6d be \tilde{V}^M and \tilde{V}^F . Then, the volume fraction \tilde{c}^M and \tilde{c}^F of these elements are expressed, respectively by

$$\tilde{c}^M = \frac{\tilde{V}^M}{\tilde{V}}, \quad \tilde{c}^F = \frac{\tilde{V}^F}{\tilde{V}}, \quad (10.57a)$$

$$\tilde{c}^M + \tilde{c}^F = 1, \quad (10.57b)$$

$$\tilde{V} = \tilde{V}^M + \tilde{V}^F, \quad (10.57c)$$

where \tilde{V} denotes the volume of the overall representative volume element.

By integrating the overall and the local stresses in the respective fictitious undamaged configurations of Fig. 10.6b and d, the relation between the overall effective stress $\tilde{\sigma}$ in B_f and local effective stresses $\tilde{\sigma}^M$, $\tilde{\sigma}^F$ in B_f^M, B_f^F is derived as follow (Dvorak and Bahei-El-Din 1982, 1987):

$$\dot{\tilde{\sigma}} = \tilde{c}^M \dot{\tilde{\sigma}}^M + \tilde{c}^F \dot{\tilde{\sigma}}^F. \quad (10.58a)$$

A similar relation is obtained also for the current damaged configurations B_t , B_t^M and B_t^F :

$$\dot{\sigma} = c^M \dot{\sigma}^M + c^F \dot{\sigma}^F. \quad (10.58b)$$

As regards the effective strain rates $\dot{\tilde{\epsilon}}$, $\dot{\tilde{\epsilon}}^M$ and $\dot{\tilde{\epsilon}}^F$ in the fictitious undamaged configurations B_f , B_f^M , B_f^F , the local-overall relation is obtained similarly as above

$$\dot{\tilde{\epsilon}} = \tilde{c}^M \dot{\tilde{\epsilon}}^M + \tilde{c}^F \dot{\tilde{\epsilon}}^F. \quad (10.59)$$

If the effective strain in the configurations B_f and B_f^M can be divided into the sum of the elastic and the plastic strain, we have

$$\dot{\tilde{\boldsymbol{\epsilon}}} = \dot{\tilde{\boldsymbol{\epsilon}}}^e + \dot{\tilde{\boldsymbol{\epsilon}}}^p, \quad (10.60a)$$

$$\dot{\tilde{\boldsymbol{\epsilon}}}^M = \dot{\tilde{\boldsymbol{\epsilon}}}^{Me} + \dot{\tilde{\boldsymbol{\epsilon}}}^{Mp}, \quad (10.60b)$$

$$\dot{\tilde{\boldsymbol{\epsilon}}}^F = \dot{\tilde{\boldsymbol{\epsilon}}}^{Fe}, \quad (10.60c)$$

where the superscript e and p signify the elastic and the plastic part of strain, and the fiber was assumed to be elastic.

10.3.3 Strain- and Stress-Concentration Factors in Matrix and Fiber

In the composite material element in the fictitious undamaged configuration B_f of Fig. 10.6b, the undamaged elastic-plastic material is reinforced by the undamaged fiber. Thus, if the fourth-order tensors of stress-concentration factor of the matrix and the fiber are denoted by $\tilde{\mathbb{B}}^M$ and $\tilde{\mathbb{B}}^{Fe}$, the effective stress rates $\dot{\tilde{\sigma}}^M$, $\dot{\tilde{\sigma}}^F$ of the matrix and the fiber are expressed in terms of the effective stress rate $\dot{\tilde{\sigma}}$ in the overall configuration B_f :

$$\dot{\tilde{\sigma}}^M = \tilde{\mathbb{B}}^M : \dot{\tilde{\sigma}}, \quad \dot{\tilde{\sigma}}^F = \tilde{\mathbb{B}}^{Fe} : \dot{\tilde{\sigma}}. \quad (10.61)$$

The specific values of the tensor $\tilde{\mathbb{B}}^M$ and $\tilde{\mathbb{B}}^{Fe}$ in these relations can be obtained by Voigt model, VFD (Vanishing Fiber Diameter) model, or Mori-Tanaka model of micromechanics (Voyiadjis and Park 1994).

Substitution of Eq. (10.61) into Eq. (10.58) furnishes the relation between the tensors of the stress concentration factor $\tilde{\mathbb{B}}^M$ and $\tilde{\mathbb{B}}^{Fe}$:

$$\tilde{c}^M \tilde{\mathbb{B}}^M + \tilde{c}^F \tilde{\mathbb{B}}^{Fe} = \mathbb{I}, \quad (10.62a)$$

$$\mathbb{I} = (1/2)(\delta_{ik}\delta_{jl} + \delta_{ij}\delta_{jk}). \quad (10.62b)$$

This relation represents a condition which must be satisfied by the tensors of the stress concentration factor $\tilde{\mathbb{B}}^M$ and $\tilde{\mathbb{B}}^{Fe}$. In other words, if one of these tensors of the stress concentration factor has been known, the other tensor can be given by Eq. (10.62).

Relations similar to Eq. (10.61) must be derived also for the current damaged configurations B_t , B_t^M and B_t^F of Fig. 10.6a and c. If the stress concentration tensors in these configurations are denoted by \mathbb{B}^M and \mathbb{B}^{Fe} , the local-overall relations for stress rates are expressed by

$$\dot{\sigma}^M = \mathbb{B}^M : \dot{\sigma}, \quad \dot{\sigma}^F = \mathbb{B}^{Fe} : \dot{\sigma}. \quad (10.63)$$

As observed in Fig. 10.6, if the damaged states of the matrix and the fiber are known, the tensors of the stress concentration factors \mathbb{B}^M and \mathbb{B}^{Fe} can be derived by the use of the tensors $\tilde{\mathbb{B}}^M$ and $\tilde{\mathbb{B}}^{Fe}$ in the configurations B_f^M and B_f^F . The details of the procedure will be described in Section 10.3.5 later.

By substituting Eq. (10.63) into Eq. (10.58b), we have a similar relation as Eq. (10.62)

$$c^M \mathbb{B}^M + c^F \mathbb{B}^{Fe} = \mathbb{I}, \quad (10.64a)$$

$$c^M + c^F = 1, \quad (10.64b)$$

where c^M and c^F are the volume fractions of the matrix and the fiber in the configurations B_f^M and B_f^F .

Finally, similar relations can be derived also for the strain concentration factors for matrix and fiber. Let the tensors of strain concentration factors for the matrix and the fiber in the fictitious undamaged configuration B_f be denoted by \mathbb{A}^M and \mathbb{A}^{Fe} . Then the local-overall relations for effective strain rate tensors are given as follow

$$\dot{\tilde{\boldsymbol{\varepsilon}}}^M = \tilde{\mathbb{A}}^M : \dot{\tilde{\boldsymbol{\varepsilon}}}, \quad \dot{\tilde{\boldsymbol{\varepsilon}}}^F = \tilde{\mathbb{A}}^{Fe} : \dot{\tilde{\boldsymbol{\varepsilon}}}, \quad (10.65)$$

$$\tilde{c}^M \tilde{\mathbb{A}}^M + \tilde{c}^F \tilde{\mathbb{A}}^{Fe} = \mathbb{I}. \quad (10.66)$$

Furthermore, if the tensors of the strain concentration factors for the matrix and the fiber in the current damaged configuration B_t are denoted by \mathbb{A}^M and \mathbb{A}^{Fe} , the local-overall relations for strain rate tensor are expressed as

$$\dot{\boldsymbol{\varepsilon}}^M = \mathbb{A}^M : \dot{\boldsymbol{\varepsilon}}, \quad \dot{\boldsymbol{\varepsilon}}^F = \mathbb{A}^{Fe} : \dot{\boldsymbol{\varepsilon}}, \quad (10.67)$$

$$c^M \mathbb{A}^M + c^F \mathbb{A}^{Fe} = \mathbb{I}. \quad (10.68)$$

As will be shown in Section 10.3.5, once the damage state of matrix and fiber are known, the strain concentration factors \mathbb{A}^M and \mathbb{A}^{Fe} in the current damaged configuration B_t can be related to those $\tilde{\mathbb{A}}^M$ and $\tilde{\mathbb{A}}^{Fe}$ in the fictitious undamaged configuration B_f .

10.3.4 Local-Overall Relations for Damage State

Hitherto, the damage state of the matrix and that of the fiber have been specified separately. Thus, it is now necessary to derive a proper correlation between the damage state of the constituent phases to that of the overall composite. The damage state of the overall configuration and that of the local configurations of Fig. 10.6 can be expressed by the use of the respective damage effect tensors \mathbb{M} , \mathbb{M}^M and \mathbb{M}^F discussed in Section 2.3.2.

In view of Eq. (2.43), the effective stress tensors $\tilde{\sigma}^M$ and $\tilde{\sigma}^F$ in the fictitious undamaged configurations B_f^M and B_f^F can be given by the Cauchy stress tensors σ^M and σ^F in the current damaged configurations B_f^M and B_f^F as follow:

$$\tilde{\sigma}^M = \mathbb{M}^M : \sigma^M, \quad \tilde{\sigma}^F = \mathbb{M}^F : \sigma^F. \quad (10.69)$$

The effective stress tensor $\tilde{\sigma}$ of the overall undamaged configuration B_f , on the other hand, is related to the Cauchy stress tensor σ in the overall damaged configuration B_f :

$$\tilde{\sigma} = \mathbb{M} : \sigma. \quad (10.70)$$

Then, let us derive the relation between the overall damage effect tensor \mathbb{M} of Eq. (10.70) and the local damage effect tensors \mathbb{M}^M and \mathbb{M}^F of Eq. (10.69).

Firstly, the time derivative of Eq. (10.69) gives

$$\dot{\tilde{\sigma}}^M = \dot{\mathbb{M}}^M : \sigma^M + \mathbb{M}^M : \dot{\sigma}^M, \quad (10.71a)$$

$$\dot{\tilde{\sigma}}^F = \dot{\mathbb{M}}^F : \sigma^F + \mathbb{M}^F : \dot{\sigma}^F. \quad (10.71b)$$

By substituting these relations into Eq. (10.58) and by the use of Eq. (10.63), we have a relation

$$\begin{aligned} \dot{\tilde{\sigma}} &= (\tilde{c}^M \dot{\mathbb{M}}^M : \mathbb{B}^M + \tilde{c}^F \dot{\mathbb{M}}^F : \mathbb{B}^F) : \sigma \\ &\quad + (\tilde{c}^M \mathbb{M}^M : \mathbb{B}^M + \tilde{c}^F \mathbb{M}^F : \mathbb{B}^F) : \dot{\sigma}. \end{aligned} \quad (10.72)$$

The time derivatives of Eq. (10.70), on the other hand, gives

$$\dot{\tilde{\sigma}} = \dot{\mathbb{M}} : \sigma + \mathbb{M} : \dot{\sigma}. \quad (10.73)$$

The comparison between Eqs. (10.71) and (10.73) finally gives the local-overall relations of the damage effect tensors:

$$\dot{\mathbb{M}} = \tilde{c}^M \dot{\mathbb{M}}^M : \mathbb{B}^M + \tilde{c}^F \dot{\mathbb{M}}^F : \mathbb{B}^F, \quad (10.74a)$$

$$\mathbb{M} = \tilde{c}^M \mathbb{M}^M : \mathbb{B}^M + \tilde{c}^F \mathbb{M}^F : \mathbb{B}^F. \quad (10.74b)$$

10.3.5 Stress- and Strain-Concentration Factors in Fictitious Undamaged and Current Damaged Configurations

In the above section, the overall damage effect tensor \mathbb{M} in the current damaged state B_f was derived by taking account of the local fictitious undamaged states B_f^M

and B_t^F . We now derive the stress and strain concentration factors in the overall current damaged configuration B_t in terms of those at the fictitious undamaged configuration B_f .

For the local stress rate tensors in the current damaged configurations B_t^M , B_t^F and the fictitious undamaged configurations B_f^M , B_f^F , we have the following relations similar to Eq. (10.69):

$$\dot{\tilde{\sigma}}^M = \mathbb{M}^M : \dot{\sigma}^M, \quad \dot{\tilde{\sigma}}^F = \mathbb{M}^F : \dot{\sigma}^F. \quad (10.75)$$

Then, by substituting Eqs. (10.70) and (10.75) into Eq. (10.61) and by comparing the resulting relation with Eq. (10.63), we have

$$\mathbb{B}^M = (\mathbb{M}^M)^{-1} : \tilde{\mathbb{B}}^M : \mathbb{M}, \quad (10.76a)$$

$$\mathbb{B}^{Fe} = (\mathbb{M}^F)^{-1} : \tilde{\mathbb{B}}^{Fe} : \mathbb{M}. \quad (10.76b)$$

This relation implies that, when the damage effect tensors \mathbb{M} , \mathbb{M}^M , \mathbb{M}^F are known, the tensors of stress concentration factors \mathbb{B}^M , \mathbb{B}^{Fe} in these current damaged configurations can be determined by the tensors of the stress concentration factors $\tilde{\mathbb{B}}^M$, $\tilde{\mathbb{B}}^{Fe}$ in the fictitious undamaged configurations.

As regards the relations between the strain concentration factor in B_t and that in B_f , the relation between the overall strains in these configurations should be obtained first.

According to the hypothesis of *strain energy equivalence* described in Section 2.3, the effective strain tensor $\tilde{\boldsymbol{\epsilon}}^e$ in the undamaged configuration B_f corresponding to the elastic strain tensor $\boldsymbol{\epsilon}^e$ in the damaged configuration B_t is defined as

$$\tilde{\boldsymbol{\epsilon}}^e = \mathbb{M}^{-T} : \boldsymbol{\epsilon}^e. \quad (10.77)$$

Application of this hypothesis also to the local strains of the matrix and the fiber gives

$$\tilde{\boldsymbol{\epsilon}}^{Me} = (\mathbb{M}^M)^{-T} : \boldsymbol{\epsilon}^{Me}, \quad \tilde{\boldsymbol{\epsilon}}^{Fe} = (\mathbb{M}^F)^{-T} : \boldsymbol{\epsilon}^{Fe}. \quad (10.78)$$

By substituting Eqs. (10.77) and (10.78) into Eq. (10.65) and by comparing the resulting relations with Eq. (10.67), we have the relations between the tensors of strain concentration factors in the configurations B_t and B_f :

$$\mathbb{A}^{Me} = \mathbb{M}^M : \tilde{\mathbb{A}}^{Me} : \mathbb{M}^{-1}, \quad (10.79a)$$

$$\mathbb{A}^{Fe} = \mathbb{M}^F : \tilde{\mathbb{A}}^{Fe} : \mathbb{M}^{-1}. \quad (10.79b)$$

These relations facilitate the calculation of the strain concentration factors \mathbb{A}^{Me} and \mathbb{A}^{Fe} in the current damaged configuration B_t by the use of the strain concentration

factors $\tilde{\mathcal{A}}^{Me}$, $\tilde{\mathcal{A}}^{Fe}$ in the fictitious undamaged configuration B_f together with the damage effect tensors M , M^M and M^F .

Voyiadjis and Park (1994) extended the local damage theory described above to include also the damage in matrix/fiber interface.

10.3.6 Local Stress in Uniaxial Tension of Composites

As an application of the local damage theory discussed in the preceding sections, we consider a fiber-reinforced composite under uniaxial tension shown in Fig. 10.7, and calculate the local stresses.

Let us assume that both the matrix and the fiber are in elastic state. Then, Eq. (10.61) for uniaxial tension in the fiber direction has the expression

$$\tilde{\sigma}_{11}^M = \tilde{\mathcal{B}}^{Me} \tilde{\sigma}, \quad \tilde{\sigma}_{11}^F = \tilde{\mathcal{B}}^{Fe} \tilde{\sigma}, \quad (10.80)$$

where $\tilde{\mathcal{B}}^{Me}$ and $\tilde{\mathcal{B}}^{Fe}$ denote the elastic stress concentration factors at the matrix and the fiber in the fictitious undamaged configuration B_f of Fig. 10.7. They can be calculated if the properties of the composite elements are specified.

Equation (10.76), on the other hand, is expressed for the elastic uniaxial tension in the fiber direction

$$\mathcal{B}^{Me} = (M^M)^{-1} M \tilde{\mathcal{B}}^{Me}, \quad (10.81a)$$

$$\mathcal{B}^{Fe} = (M^F)^{-1} M \tilde{\mathcal{B}}^{Fe}, \quad (10.81b)$$

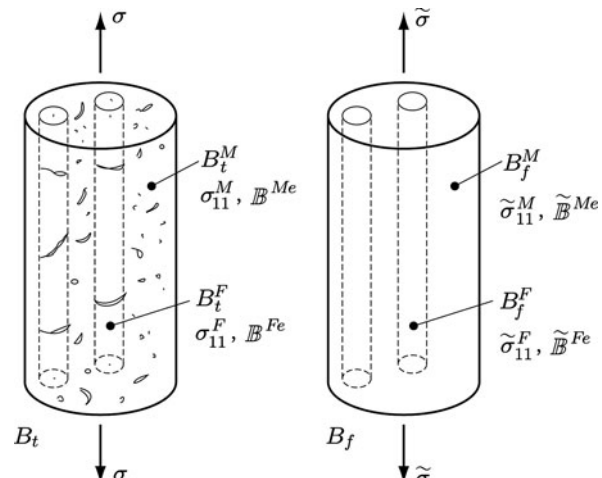


Fig. 10.7 Local stresses and stress concentration factors of a fiber-reinforced composite under uniaxial tension

where \mathcal{B}^{Me} and \mathcal{B}^{Fe} are the local elastic stress concentration factors in the current damaged configuration B_t . Furthermore, M , M^M and M^F denote the components of the overall and the local damage effect tensors in the tensile direction.

As an application of these relations, let us consider the following two cases of damage:

(1) Damaged Fiber and Undamaged Matrix ($0 \leq D_{11}^F \leq 1$, $D_{11}^M \equiv 0$)

To begin with, stress concentration factors in the current damaged configuration B_t in this case are given as

$$\mathcal{B}^{Me} = \frac{\sigma_{11}^M}{\sigma}, \quad \mathcal{B}^{Fe} = \frac{\sigma_{11}^F}{\sigma}. \quad (10.82)$$

Furthermore, the components M , M^M and M^F of the overall and the local damage effect tensors in the tensile direction are specified by

$$M = \frac{\tilde{\sigma}}{\sigma}, \quad M^M = \frac{\tilde{\sigma}_{11}^M}{\sigma_{11}^M} = 1, \quad M^F = \frac{\tilde{\sigma}_{11}^F}{\sigma_{11}^F} = \frac{1}{1 - D_{11}^F}. \quad (10.83)$$

Substitution of Eqs. (10.81) and (10.83) into Eq. (10.82) furnishes

$$\frac{\sigma_{11}^M}{\sigma} = \mathcal{B}^{Me} = (M^M)^{-1} M \tilde{\mathcal{B}}^{Me} = \frac{\tilde{\sigma}}{\sigma} \tilde{\mathcal{B}}^{Me}, \quad (10.84a)$$

$$\frac{\sigma_{11}^F}{\sigma} = \mathcal{B}^{Fe} = (M^F)^{-1} M \tilde{\mathcal{B}}^{Fe} = (1 - D_{11}^F) \frac{\tilde{\sigma}}{\sigma} \tilde{\mathcal{B}}^{Fe}. \quad (10.84b)$$

Thus, we finally have the ratio between the stresses in the fiber and the matrix:

$$\frac{\sigma_{11}^F}{\sigma_{11}^M} = \frac{\tilde{\mathcal{B}}^{Fe}}{\tilde{\mathcal{B}}^{Me}} (1 - D_{11}^F). \quad (10.85)$$

(2) Damaged Matrix and Undamaged Fiber ($0 \leq D_{11}^M \leq 1$, $D_{11}^F \equiv 0$)

In this case, the components of the overall and the local damage effect tensor are expressed as

$$M = \frac{\tilde{\sigma}}{\sigma}, \quad M^M = \frac{\tilde{\sigma}_{11}^M}{\sigma_{11}^M} = \frac{1}{1 - D_{11}^M}, \quad M^F = \frac{\tilde{\sigma}_{11}^F}{\sigma_{11}^F} = 1. \quad (10.86)$$

Thus, we have the stress concentration factors in the current damaged configuration B_t

$$\frac{\sigma_{11}^M}{\sigma} = \mathcal{B}^{Me} = (M^M)^{-1} M \tilde{\mathcal{B}}^{Me} = (1 - D_{11}^M) \frac{\tilde{\sigma}}{\sigma} \tilde{\mathcal{B}}^{Me}, \quad (10.87a)$$

$$\frac{\sigma_{11}^F}{\sigma} = \tilde{\mathcal{B}}^{Fe} = (M^F)^{-1} M \tilde{\mathcal{B}}^{Fe} = \frac{\tilde{\sigma}}{\sigma} \tilde{\mathcal{B}}^{Fe}. \quad (10.87b)$$

From these relations, the ratio between the stresses in the matrix and the fiber is derived as

$$\frac{\sigma_{11}^M}{\sigma_{11}^F} = \frac{\tilde{\mathcal{B}}^{Me}}{\tilde{\mathcal{B}}^{Fe}} (1 - D_{11}^M). \quad (10.88)$$

Figure 10.8 shows the prediction of Eqs. (10.85) and (10.88) calculated for a fiber-reinforced metal matrix lamina with the material property of Table 10.1. The value of the stress concentration factors $\tilde{\mathcal{B}}^{Me}$ and $\tilde{\mathcal{B}}^{Fe}$ have been calculated by the use of Mori-Tanaka method.

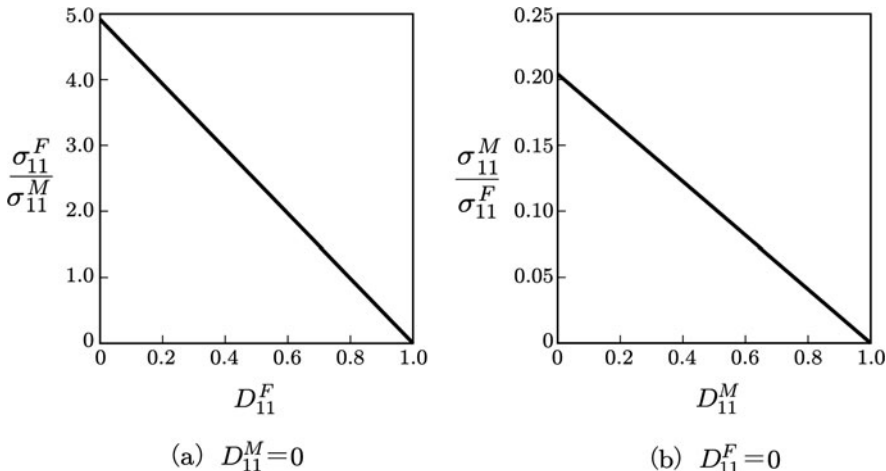


Fig. 10.8 Variation in the stress ratios in a fiber-reinforced lamina under uniaxial tension due to damage development

Source: Voyiadjis and Kattan (1999, p. 226, Fig. 10.3; p. 226, Fig. 10.4)

Table 10.1 Material properties of metal matrix fiber-reinforced composites

Material property	Matrix (Ti-14Al-21Nb)	Fiber (SiC)
Elastic modulus	8×10^4 MPa	41×10^4 MPa
Poisson's ratio	0.3	0.22
Initial volume fraction	0.65	0.35

Source: Voyiadjis and Kattan (1999, p. 228, Table 10.1)

For the application of the local theory of composites described in this section, we need the calculation of the states of the inelastic deformation and the damage of matrix and fiber. As regards the detail of the derivation of these constitutive and the evolution equations, together with the application of the local damage theory presented in this section to the specific problems of fiber-reinforced metal matrix composites, readers are referred to Voyiadjis and others (Voyiadjis and Kattan 1993, 1999; Kattan and Voyiadjis 2002).

Chapter 11

Local Approach to Damage and Fracture Analysis

Continuum damage mechanics facilitates not only the modeling of crack initiation due to damage development but also the analysis of the damage and fracture process up to the final fracture. The *local approach to fracture* by means of continuum damage mechanics and finite element method has developed as a systematic engineering method to analyze the whole process of damage and fracture.

At the end of this book, we consider the notion, applicability and the fundamental issues of this approach. Section 11.1 is concerned with its procedure, applicability and the related numerical problems. In Section 11.2, the material instability and the resulting loss of uniqueness will be discussed as the major causes of the mesh-sensitivity in time-independent (rate-independent) strain-softening materials. The method to obviate the difficulties in numerical calculation related to these causes will be discussed in Section 11.3. Finally, in Sections 11.4 and 11.5, the problems of the mesh-sensitivity in the case of time-dependent deformation, and the method of its regularization will be discussed briefly.

11.1 Local Approach to Fracture Based on Continuum Damage Mechanics and Finite Element Method

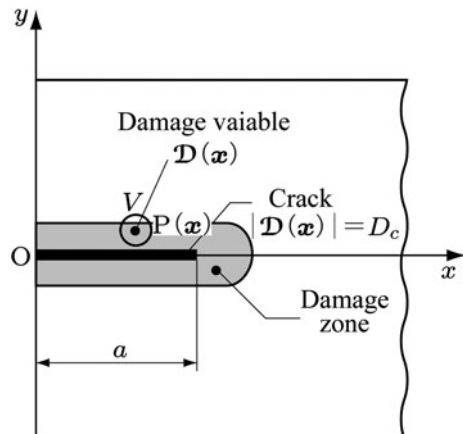
11.1.1 Local Approach to Fracture, Modeling of Fracture

In continuum damage mechanics, the damage state at an arbitrary point $P(x)$ in the material is represented by a properly defined *damage variable* $\mathcal{D}(x)$ ($0 \leq |\mathcal{D}| \leq D_C$), where D_C is the critical value of the damage variable at fracture.

According to this notion, a crack in a fracture process can be modeled as shown in Fig. 11.1. Namely a crack can be represented by a region where the damage state has attained to its critical state $|\mathcal{D}| = D_C$, i.e., by the *completely damaged zone* (CDZ). Then the development of the crack and its preceding damage can be elucidated by analyzing the local states of stress, strain and damage.

This method of fracture analysis is not based on the global fracture mechanics parameters defined by the stress and the strain fields in the global region around the

Fig. 11.1 Crack and damage field in local approach to fracture



crack, but on the local damage parameter at the tip of a relevant crack. Hence, this method is called a *local approach to fracture*.¹

Among local approaches of fracture, the method employing the damage mechanics and finite element method was proposed first by Hayhurst et al. (1975) for the creep-crack analyses of copper and aluminum plates. This method of analysis has

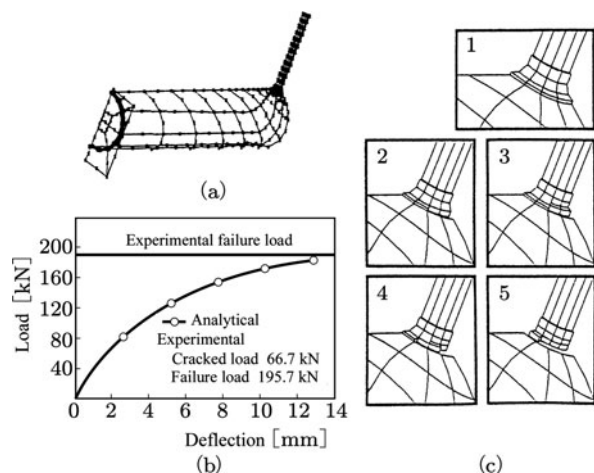


Fig. 11.2 Elastic-plastic fracture of a welded tubular T-joint

Source: Jubran and Cofer (1991, p. 749, Fig. 9; p. 750, Fig. 11; p. 750, Fig. 12)

¹ This term was first proposed by Pineau (1980). In order to supplement the limitations of the linear- or nonlinear-fracture mechanics essentially based on the global fracture mechanics parameters, a new method of fracture analysis developed around the end of 1970s by modeling the fracture toughness at the crack tip by the use of the local fracture criterion. Pineau named this methodology “*local approach to fracture*”.

the excellent possibility as a systematic engineering procedure for wide range of fracture problems, and has been applied to a number of fracture problems.

In this method of the local approach, in particular, the extension of a crack can be modeled by the development of finite elements of completely damaged state $|\mathcal{D}| = D_C$. Then the fracture of the finite elements is defined by the loss of the load carrying capacity or the loss of their rigidity.

Figures 11.2 and 11.3 are the examples of the fracture analyses by means of the local approach, and show the elastic-plastic fracture of a welded tubular T-joint in a space frame and the failure of a concrete gravity dam suffered from an earthquake of magnitude 6.5.

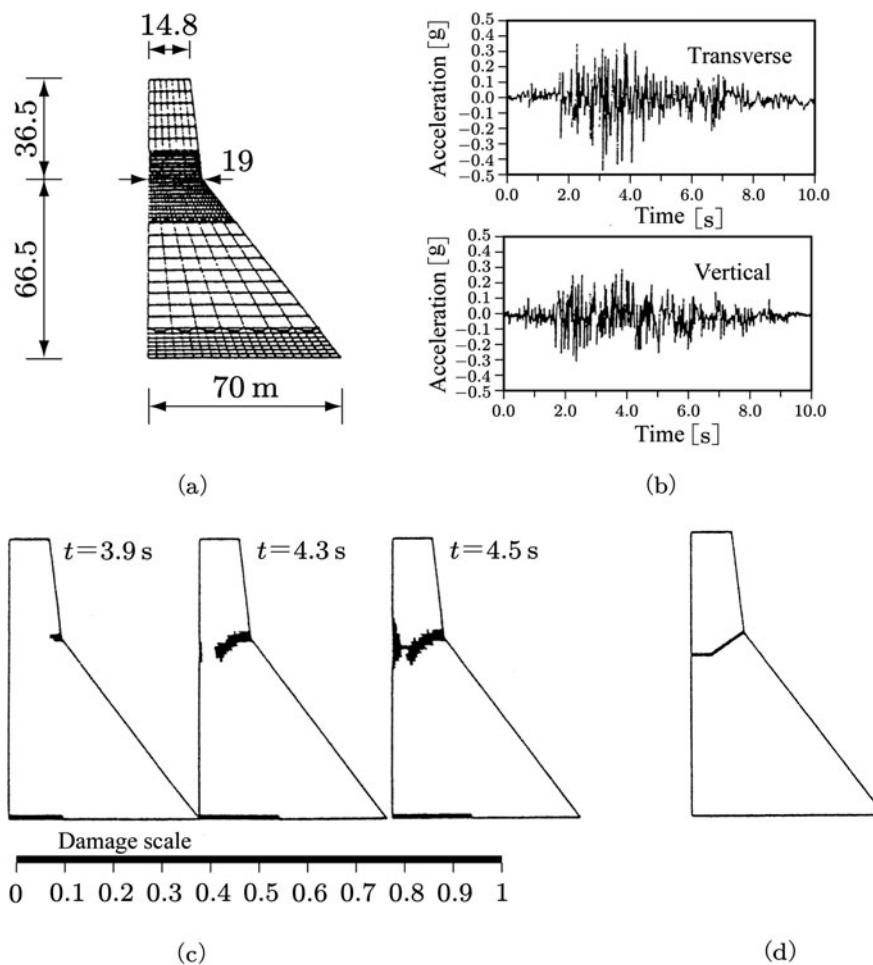


Fig. 11.3 Damage of a concrete gravity dam suffered from an earthquake of magnitude 6.5
Source: Ghrib and Tinawi (1995a, p. 165, Fig. 3; p. 166, Fig. 5; See also Ghrib and Tinawi 1995b)

11.1.2 Mesh-Sensitivity in Local Approach to Fracture

In the local approach of fracture by means of continuum damage mechanics and finite element method, the size and the configuration of a crack is governed by the division of the finite elements. In a damaged material, furthermore, material softening caused by damage may bring about the loss of uniqueness and the numerical stability.

Instability and mesh-dependence of numerical results in the local approach are crucial problems in its application, and have been extensively discussed as will be described below. According to these investigations, the causes of this *mesh-sensitivity* may be classified mainly into the followings:

- (1) Loss of uniqueness and *strain localization* due to strain softening
- (2) Damage localization
- (3) Stress singularity at crack tip

In the following, these issues will be discussed by dividing them into the cases of the time-independent and the time-dependent deformation.

11.2 Mesh-Sensitivity in Time-Independent Deformation

11.2.1 Stain-Softening and Mesh-Sensitivity

Increase in strain in the stress-strain relation of time-independent material often leads to the *strain-softening*, i.e., the *instability of material*. This onset of the material instability induces the loss of the positive-definiteness of the tangent rigidity matrix of the material, and hence the loss of the ellipticity of the equilibrium rate equation. This eventually leads to the loss of the *well-posedness*² of the rate boundary value problem.

In the case of the finite element analysis of time-independent material, the loss of well-posedness of the problem brings about a number of undesirable numerical results. Thus, the problems of numerical instability, mesh-sensitivity of their results as well as the procedure to avoid these difficulties in the finite element analysis of time-independent materials have been elucidated extensively (Pietruszczak and Mróz 1981; Bažant and Pijaudier-Cabot 1988; Simo 1989; de Borst et al. 1993; Besson 2010).

Figure 11.4 shows the softening of a quasi-brittle material (e.g., concrete, rock, etc.) caused by damage under uniaxial tension. Application of the local approach to the damage analysis of such a material is accompanied by salient mesh-sensitivity.

² A rate boundary value problem is said to be *well-posed*, if it admits a finite number of linearly independent solutions which depend continuously on the data (especially, on boundary conditions) and which constitute diffuse modes of deformation (de Borst et al. 1993; Besson et al. 2010).

Fig. 11.4 Damage development and strain-softening in a brittle material

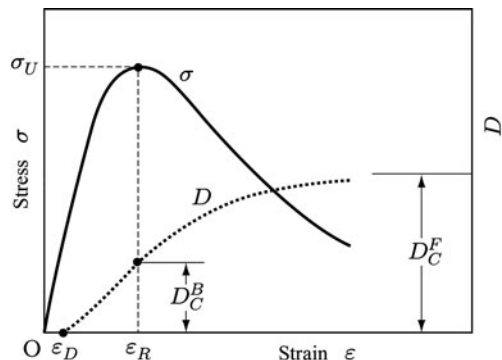
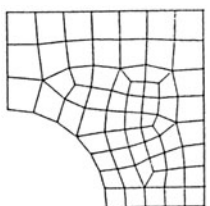
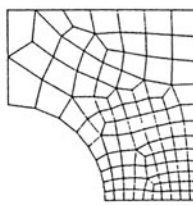


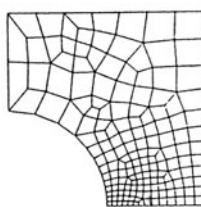
Figure 11.5 provides an example, and shows the load-displacement relation of an elastic-brittle plate with a central circular hole made of bilinear stress-strain material subjected to uniform tensile displacement at its upper end. Apparent mesh-dependence is observed in the numerical results of the plate with five different meshes.



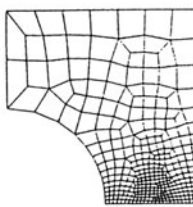
Mesh 1: 63 elements



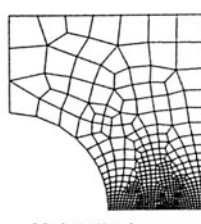
Mesh 2: 107 elements



Mesh 3: 163 elements

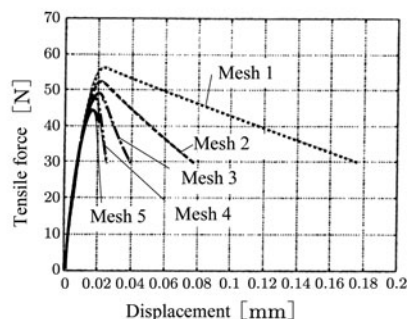
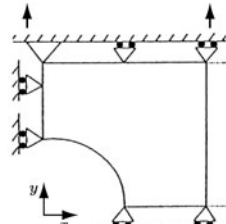


Mesh 4: 328 elements



Mesh 5: 504 elements

(a) Meshes for the quarter plate



(b) Force-displacement relation

Fig. 11.5 Mesh-dependence in damage analysis of an elastic-brittle plate with a circular hole
Source: de Vree et al. (1995, p. 585, Fig. 5; p. 585, Fig. 6)

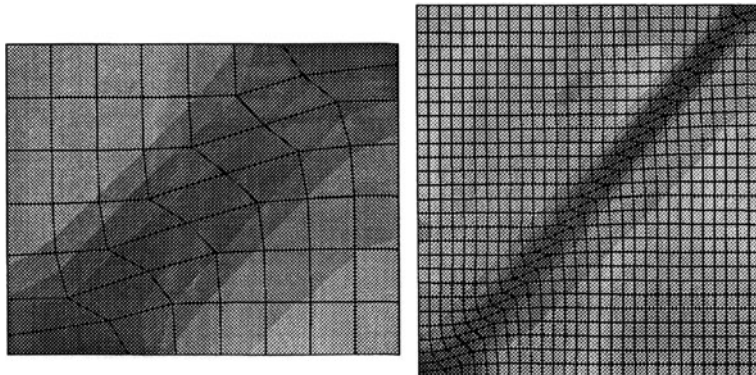


Fig. 11.6 Mesh-dependence of a localized shear band in a porous material

Source: Tvergaard and Needleman (1995, p. 1070, Fig. 4 (a, c))

One of the most characteristic aspects observed in the mesh-dependence of strain-softening materials is the occurrence of localized bands of deformation with the width nearly equal to the mesh size. The energy dissipation caused by the fracture is related mainly to its deformation band, and hence is governed by the size of the element. This fact implies a physically inconsistent fact that the mesh-refinement may lead to unlimitedly small dissipation for the fracture of material. This is an account for Fig. 11.5.

Figure 11.6 shows another example of damage analysis, i.e., the case of a porous plastic damage material. The salient mesh-dependent localized shear band is again observed.

11.2.2 Bifurcation of Deformation and Strain Localization

Material instability due to strain-softening causes the *bifurcation* of deformation, and gives rise to intense localization band of almost equal width to that of the mesh size.

Let us first consider the material instability due to damage. We suppose a time-independent material with the stress rate-strain rate relation of

$$\dot{\sigma} = \mathcal{C}(D) : \dot{\epsilon}, \quad (11.1)$$

where D and $\mathcal{C}(D)$ denote the isotropic damage variable and the tangent modulus tensor of the damaged material. The magnitude of the tensor $|\mathcal{C}(D)|$ decreases with the development of damage.

The condition of material stability due to Hill (1958) is expressed by

$$\text{tr} \dot{\epsilon}^T \dot{\sigma} > 0, \quad (11.2a)$$

or

$$\text{tr} \dot{\epsilon}^T \mathcal{C}(D) \dot{\epsilon} > 0. \quad (11.2b)$$

This leads to the condition of positive-definiteness of the tangent modulus tensor $\mathcal{C}(D)$

$$\det(\mathcal{C} + \mathcal{C}^T) > 0. \quad (11.3)$$

In a material described by Eq. (11.1), as far as the condition of Eq. (11.2) or (11.3) is satisfied, *uniqueness of deformation* is guaranteed and hence bifurcation of the deformation will not occur.

The onset of material instability, on the other hand, is given by the condition

$$\det(\mathcal{C} + \mathcal{C}^T) = 0. \quad (11.4)$$

This condition means the loss of positive-definiteness of the tensor $\mathcal{C}(D)$, and may result in the loss of ellipticity of the rate equation of equilibrium. This condition, furthermore, implies the loss of a necessary condition for well-posedness of the rate boundary value problem (Billardon and Doghri 1989; de Borst et al. 1993).

We next consider the relation between the bifurcation and the mesh-dependence of numerical results. For this purpose, we suppose a band of orientation \mathbf{n} in a material element B as shown in Fig. 11.7, and derive a condition under which the *discontinuity* of velocity gradient (or strain rate) between the regions inside and outside the band may be permitted.

Let us denote the field of quantities inside and outside the band by superscript (b) and (o) , and suppose that the discontinuity of velocity $\dot{\mathbf{q}}$ exists between these regions. We take arbitrary two points P and Q small distance $d\mathbf{x}$ apart across the interface as shown in Fig. 11.7b. Then, the difference in velocities $[\![d\mathbf{v}]\!]$ between the points P and Q is given by

$$\begin{aligned} [\![d\mathbf{v}]\!] &= \mathbf{v}^b - \mathbf{v}^o \\ &= \dot{\mathbf{q}}(\mathbf{n} \cdot d\mathbf{x}) = (\dot{\mathbf{q}} \otimes \mathbf{n})d\mathbf{x}, \end{aligned} \quad (11.5a)$$

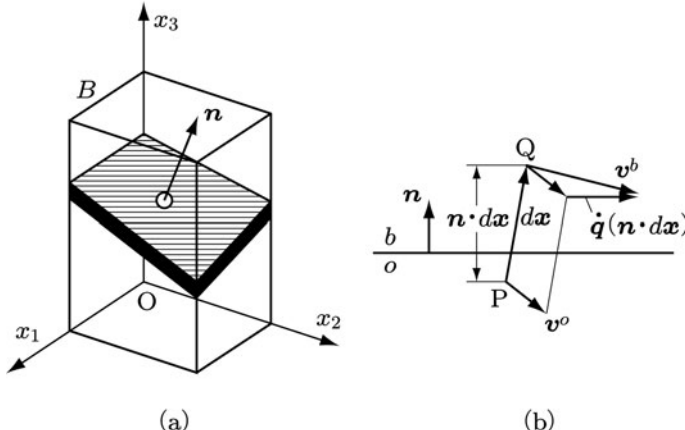


Fig. 11.7 Material element including a discontinuous deformation band

or

$$[\![dv]\!]_i = \dot{q}_i n_j dx_j. \quad (11.5b)$$

Thus, the jump of the strain rate $\dot{\epsilon}$ across the interface of the band is given by

$$\begin{aligned} \dot{\epsilon}_{ij}^{(b)} - \dot{\epsilon}_{ij}^{(o)} &= \frac{1}{2} \left[\frac{\partial [\![v]\!]_i}{\partial x_j} + \frac{\partial [\![v]\!]_j}{\partial x_i} \right] \\ &= \frac{1}{2} (\dot{q}_i n_j + \dot{q}_j n_i). \end{aligned} \quad (11.6)$$

The equilibrium of the forces on the element B , on the other hand, imposes the continuity of the traction rate across the interfaces

$$n_i (\dot{\sigma}_{ij}^{(b)} - \dot{\sigma}_{ij}^{(o)}) = 0. \quad (11.7)$$

Substitution of Eq. (11.1) into this relation gives

$$n_i C_{ijkl}(D) (\dot{\epsilon}_{kl}^{(b)} - \dot{\epsilon}_{kl}^{(o)}) = 0. \quad (11.8)$$

By the use of Eq. (11.6) and the symmetry of the tensor $C_{ijkl}(D)$, Eq. (11.8) finally leads to

$$[n_i C_{ijkl}(D) n_k] \dot{q}_l = 0. \quad (11.9)$$

In order that the bifurcation of strain rate may occur in the body B of Fig. 11.7, the discontinuous velocity \dot{q}_i different from 0 must be determined. This condition is derived from Eq. (11.9) in the form

$$\det[n_i C_{ijkl}(D) n_k] = 0. \quad (11.10)$$

Under this condition, the discontinuity in the velocity \dot{q}_i can be derived from Eq. (11.9).

In the particular case of a time-independent elastic material of isotropic damage, the tangent modulus tensor $C_{ijkl}(D)$ is given by Eqs. (12.278) and (12.279):

$$C_{ijkl}(D) = E(D) \left[\frac{\nu}{(1+\nu)(1-2\nu)} \delta_{ij} \delta_{kl} + \frac{1}{2(1+\nu)} (\delta_{ik} \delta_{jl} + \delta_{il} \delta_{jk}) \right]. \quad (11.11a)$$

Substitution of this relation into Eq. (11.10) yields

$$\begin{aligned} \det[n_i C_{ijkl}(D) n_k] &= \frac{E(D)}{2(1+\nu)(1-2\nu)} \det[n_j n_l + (1-2\nu) \delta_{jl}] \\ &= 0. \end{aligned} \quad (11.11b)$$

Since the matrix $[n_j n_l + (1 - 2\nu)\delta_{jl}]$ is positive-definite, the necessary condition for Eq. (11.11b) to hold for arbitrary direction \mathbf{n} results in

$$E(D) = 0. \quad (11.11c)$$

In the cases of uniaxial tension or uniaxial compression, the condition (11.11c) implies the maximum stress point of the stress-strain curve of Fig. 11.4. In a brittle material as shown in Fig. 11.4, the value of damage variable D_C^B at the onset of bifurcation is far smaller than the critical value D_C^F for fracture; i.e., $D_C^B \ll D_C^F$.

When the condition of Eq. (11.10) is satisfied, bifurcation starts to occur and the intense localization band is observed in the numerical results. Then, since the damage tends to be localized to a region as narrow as possible, the width and the direction of the damage band (i.e., the width and direction of the crack) is governed by the mesh division.

The instability of numerical calculation and the mesh-dependence of the numerical results may be induced not only by the material-softening and the resulting bifurcation discussed above, but also by other causes. The mesh-sensitivity in the local approach of time-dependent material will be described in Sections 11.4 and 11.5 later³.

11.3 Regularization of Strain and Damage Localization in Time-Independent Materials

The schemes to preserve the well-posedness of the boundary-value problems in order to avoid the instability and mesh-dependence in numerical calculation are called the *regularization* of the procedure.

In this section, some typical procedures of the regularization will be described with special emphasis on the applicability to the local approach in time-independent material.

11.3.1 Limitation of Mesh Size

The simplest method to prevent the localization is to impose a lower bound on the size of the finite element meshes (Bažant and Oh 1983; Bažant 1990; Bilby et al. 1994). This method is called a *crack band model* or a *cell model*. The method is often employed in practical engineering calculation because of its simplicity. Besides its simplicity, mesh size limitation method can also describe the mechanical effects of the internal structural size in concrete.

³ Bifurcation and the resulting localization in the general elastic-plastic and elastic-viscoplastic materials are referred to in Besson et al. (2010), where the problems of mesh dependence and its regularization in finite element analysis to be discussed in the subsequent Sections of 11.3 and 11.4 are also described.

The disadvantage of this procedure is its difficulty to secure the accuracy of calculation. Selection of appropriate mesh size for specific materials is another difficulty.

11.3.2 Mesh-Dependent Softening Modulus – Modification of Material Property by Mesh-Size

The most crucial difficulty of the strain and damage localization is the mesh-size dependence of the total dissipation up to fracture. Thus the second technique to obviate the localization is to impose a limit on damage dissipation, rather than on the size of the localization band.

As a scheme to avoid the localization, Pietruszczak and Mróz (1981) assumed the existence of a shear band of a specific width in a finite element, and derived a stiffness matrix of the element in plastic state by incorporating the effect of localized deformation in the band. On the basis of this matrix, they derived a modified overall strain softening modulus of the plastic deformation in terms of the shear-band width and the assumed mesh-size. Simo (1989), on the other hand, incorporated the energy release due to microcrack initiation into the internal dissipation of a finite element, and defined a modified strain-softening modulus expressed as a function of the energy-release rate and the mesh size. These modified stain-softening moduli can be easily implemented into a standard finite element code, and lead to very simple application.

In these methods, the change in the mesh-size (i.e., the change in the width of the localization band) is accompanied by the corresponding change in the strain softening modulus, and hence the mesh-dependence of the load-displacement relation and the global deformation can be averted. This scheme is called the *method of mesh-dependent softening modulus*, and its applicability has been demonstrated in different analyses. The damage analysis for the concrete gravity dam shown in Fig. 11.3 is an example of this application.

The disadvantage of this regularization is obvious. From a physical point of view, the consistency of using a mesh-dependent material property should be questionable. Moreover, though this method can describe reasonable global response, the prediction of local states is still mesh-dependent and may even furnish unrealistic results.

11.3.3 Nonlocal Damage Theory

One of the most rational schemes to suppress the strain and the damage localization is the *nonlocal damage theory* (Bažant and Pijaudier-Cabot 1988; Bažant 1990; Bažant and Jirasek 2002). In this method, it is supposed that the evolution of inelastic strain and/or damage at a point is governed not only by the state variables at the relevant point but also by their neighboring fields. Bažant and others (1984),

therefore, applied the concept of the nonlocal continuum to a strain-softening material, and defined the *nonlocal variable* for a local quantity $A(\mathbf{x})$

$$\bar{A}(\mathbf{x}) = \frac{1}{V_r(\mathbf{x})} \int_V h(\mathbf{s} - \mathbf{x}) A(\mathbf{s}) dV(\mathbf{s}), \quad (11.12a)$$

$$V_r(\mathbf{x}) = \int_V h(\mathbf{s} - \mathbf{x}) dV(\mathbf{s}), \quad (11.12b)$$

where V is the region of the body and $h(\mathbf{s} - \mathbf{x})$ denotes a *nonlocal weighting function* which decays with the distance $|\mathbf{s} - \mathbf{x}|$ monotonously.

In the beginning of this concept, all the state variables were expressed in the non-local forms (Bažant et al. 1984). However, the presence of spatial integrals and/or of the higher-order derivatives in the equations of equilibrium and in the boundary conditions results in difficulties of the finite-element formulation. In the later analyses, therefore, by noting that only the strain-softening variables suffice to be nonlocal, Bažant and others (Pijaudier-Cabot and Bažant 1987; Bažant and Pijaudier-Cabot 1988) defined a *nonlocal damage variable*

$$\bar{D}(\mathbf{x}) = \frac{1}{V_r(\mathbf{x})} \int_V h(\mathbf{s} - \mathbf{x}) D(\mathbf{s}) dV(\mathbf{s}), \quad (11.13a)$$

$$V_r(\mathbf{x}) = \int_V h(\mathbf{s} - \mathbf{x}) dV(\mathbf{s}). \quad (11.13b)$$

Besides the damage variable D , the nonlocal variables may be defined also for its associated variable Y (Bažant and Pijaudier-Cabot 1988) and the damage rate \dot{D} (Saanouni, Chaboche, and Lesne 1989):

$$\bar{Y}(\mathbf{x}) = \frac{1}{V_r(\mathbf{x})} \int_V h(\mathbf{s} - \mathbf{x}) Y(\mathbf{s}) dV(\mathbf{s}), \quad (11.14)$$

$$\bar{\dot{D}}(\mathbf{x}) = \frac{1}{V_r(\mathbf{x})} \int_V h(\mathbf{s} - \mathbf{x}) \dot{D}(\mathbf{s}) dV(\mathbf{s}). \quad (11.15)$$

As regards the weighting function $h(\mathbf{x})$ of Eqs. (11.12) through (11.15), the following Gaussian distribution function is frequently employed:

$$h(\mathbf{x}) = \exp \left\{ -\frac{|\mathbf{x}|^2}{2\ell^2} \right\}, \quad (11.16)$$

where ℓ denotes a material parameter called the *characteristic length*, and represents the maximum size of material inhomogeneity.

Though isotropic damage has been postulated in Eqs. (11.13) through (11.15), these nonlocal damage variables may be extended also to the case of anisotropic damage without any difficulty.

Integration of Eqs. (11.13) through (11.15) may be simplified if we superpose a lattice of an appropriate size related to the characteristic length ℓ on the finite element meshes, and then assume that the nonlocal strain and the nonlocal damage in a cell of the lattice are uniform. This method is called *cell model* (Hall and Hayhurst 1991; Bilby et al. 1994), or a *grid method* (de Vree et al. 1995).

The nonlocal damage theory described above is an effective method to regularize the strain localization in softening materials, and is one of the most important numerical procedures in the local method of fracture analysis. However, when applied to the problems of time-independent elastic-plastic damage, besides the complexity of the boundary conditions, the consistency condition of plastic deformation results in an integro-differential equation (de Borst et al. 1993). Furthermore, asymmetry of the tangent modulus matrix necessitates the increase in calculation time.

11.3.4 Gradient-Dependent Theory

The regularization of the strain-localization can be achieved also by replacing a local variable $A(x)$ in the constitutive and the evolution equation with the gradient-dependent nonlocal variable (Triantafyllidis and Aifantis 1986; de Borst et al. 1993)

$$\bar{A}(x) = A(x) + c_1 \nabla A(x) + c_2 \nabla^2 A(x) + \dots \quad (11.17)$$

where ∇ , ∇^2 , ... denote the gradients of the first-, second-, ..., order.

This *gradient-dependent theory* can be derived from the above nonlocal damage theory, and hence may be viewed as an alternative formulation of the nonlocal theory. Namely, expansion of the local variable $A(x + s)$ into Taylor series about $s = 0$ furnishes

$$\begin{aligned} A(x + s) &= A(x) + \nabla A(x)s + \frac{1}{2!} \nabla^2 A(x)ss Z \\ &\quad + \frac{1}{3!} \nabla \nabla^2 A(x)sss + \dots \end{aligned} \quad (11.18)$$

Then, by substituting this relation into Eq. (11.12a), integrating the resulting relation, and noting that the integration of the odd-order terms vanish, we have the nonlocal variable $\bar{A}(x)$ in the form

$$\begin{aligned} \bar{A}(x) &= \frac{1}{V_r(x)} \int_V h(s) A(x) dV(s) \\ &\quad + \frac{1}{2V_r(x)} \int_V h(s) \nabla^2 A(x) ss dV(s), \end{aligned} \quad (11.19)$$

where the terms of the order equal to and higher than fourth have been disregarded. By performing the integration and rewriting the resulting relation by the use of Eq. (11.12b), we have

$$\bar{\mathbf{A}}(\mathbf{x}) = \mathbf{A}(\mathbf{x}) + \frac{1}{2}\ell^2 \nabla^2 \mathbf{A}(\mathbf{x}), \quad (11.20)$$

i.e., the nonlocal variable of Eq. (12.17). Although inclusion of gradients entails additional numerical complexity, the gradient-dependent theory has a distinct advantage, in comparison with the nonlocal theory of Section 11.3.3, because the consistency condition of plasticity avoids the form of the integro-differential equation.

11.3.5 Cosserat Continuum

Mechanical behavior of a Cosserat continuum is characterized by couple stress tensor and microspin-gradient tensor in addition to stress and strain tensors. This implies that assumption of a Cosserat continuum introduces a characteristic length scale and provides the effect of regularization of the localization. Thus, by means of the Cosserat continuum approach, the rate boundary value problem may remain elliptic after the onset of material instability. Another advantage of this approach is the symmetry of the tangent modulus matrix in the finite element analysis (Mühlhaus and Vardoulakis 1987; de Borst et al. 1993).

11.3.6 Artificial Viscosity

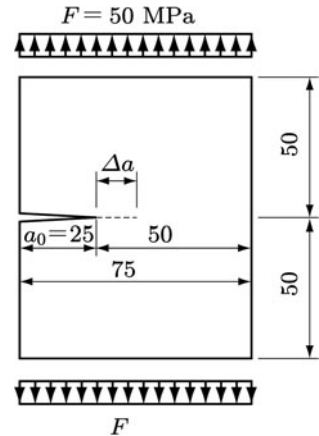
The addition of rate-dependent terms into the constitutive equation may avoid the loss of ellipticity in boundary-value problem, and hence may stabilize the numerical calculation (Simo 1989; de Borst et al. 1993). This added rate-dependence term is called *artificial viscosity*. The applicability of this procedure, however, is restricted to the problems of transient loading in some limited range of strain rate. The effect of the regularization decreases for very slow rate of loading, or for sufficiently high rates that the material approaches rate-independency. Brittle material is a typical example of the vanishing effect of artificial viscosity.

11.4 Mesh-Sensitivity in Time-Dependent Deformation

11.4.1 Mesh-Sensitivity in Creep Crack Analysis

As an example of mesh-sensitivity in time-dependent deformation, we shall consider creep crack extension in a cracked plate of Fig. 11.8.

Fig. 11.8 A cracked plate subject to uniaxial tension



The total strain rate $\dot{\varepsilon}_{ij}$ is assumed to be the sum of the elastic $\dot{\varepsilon}_{ij}^e$ and the creep strain rate $\dot{\varepsilon}_{ij}^c$

$$\dot{\varepsilon}_{ij} = \dot{\varepsilon}_{ij}^e + \dot{\varepsilon}_{ij}^c. \quad (11.21)$$

According to Kachanov-Rabotnov theory of creep damage, the evolution and the constitutive equation are given by Eqs. (8.12) and (8.13), i.e.,

$$\dot{D} = A \frac{\chi^m}{(1 - D)^p}, \quad \chi = \alpha \sigma_I + (1 - \alpha) \sigma_{EQ}, \quad (11.22)$$

$$\dot{\varepsilon}_{ij}^c = \frac{3}{2} B \left(\frac{\sigma_{EQ}}{1 - D} \right)^n \frac{\sigma_{ij}^D}{\sigma_{EQ}}. \quad (11.23)$$

The elastic constitutive equation, on the other hand, is given by

$$\sigma_{ij} = C_{ijkl}(D)(\varepsilon_{kl} - \varepsilon_{kl}^c), \quad (11.24a)$$

$$\dot{\sigma}_{ij} = C_{ijkl}(D)(\dot{\varepsilon}_{kl} - \dot{\varepsilon}_{kl}^c) + \dot{C}_{ijkl}(D)(\varepsilon_{kl} - \varepsilon_{kl}^c), \quad (11.24b)$$

$$C_{ijkl}(D) = E(D) \left[\frac{\nu}{(1 - 2\nu)(1 + \nu)} \delta_{ij} \delta_{kl} + \frac{1}{2(1 + \nu)} (\delta_{ik} \delta_{jl} + \delta_{il} \delta_{jk}) \right]. \quad (11.25)$$

Young's modulus of the damaged material $E(D)$ in this relation can be expressed as

$$\begin{aligned} E(D) &= E_0, & D < D_C, \\ &= 0, & D = D_C, \end{aligned} \quad (11.26a)$$

or

$$E(D) = E_0(1 - D), \quad (11.26b)$$

where E_0 is the Young's modulus of the undamaged material. A fully coupled elastic-damage analysis by the use of Eq. (11.26b) necessitates a large amount of computation.

In the calculation, the partly coupled analysis by Eq. (11.26a) was performed by employing four different sizes of the crack tip element $\Delta e = 1.00, 0.50, 0.10$ and 0.01 mm for the eight nodes iso-parametric element. The cracked plate of Fig. 11.8 was a 316 stainless steel specimen subject to uniform tensile stress $F = 50 \text{ MPa}$ at 650°C . The material constants in Eqs. (11.22) through (11.26) are given as follow:

$$\begin{aligned} A &= 9.0 \times 10^{-20}, & m = p = 2.8, & \alpha = 1.0, & B &= 2.13 \times 10^{-13}, \\ n &= 3.5, & D_C &= 0.99, & E_0 &= 1.44 \times 10^5, & \nu &= 0.314, \end{aligned} \quad (11.27)$$

where the units of stress and time are MPa and hour [h], respectively.

The extension of the crack was modeled by the development of finite elements of completely damaged state $D = D_C$, and the fracture of the element was represented by reducing its rigidity to that of sufficiently small magnitude (Liu et al. 1994; Lemaitre et al. 2009; Besson 2010). This method of crack extension is simplified largely in comparison with remeshing the elements to remove the fractured elements.

Figure 11.9 shows the relation between the crack extension rate da/dt and the crack extension length Δa . Although the crack extension rate depends largely on the mesh size Δe at first, the difference among them decreases with the growth of the crack. Namely the effect of mesh size is significant particularly in the early stage of the crack extension; i.e., in the time of the start of the crack extension and its incipient rate. This is confirmed also by the later discussion of Section 11.5.1.

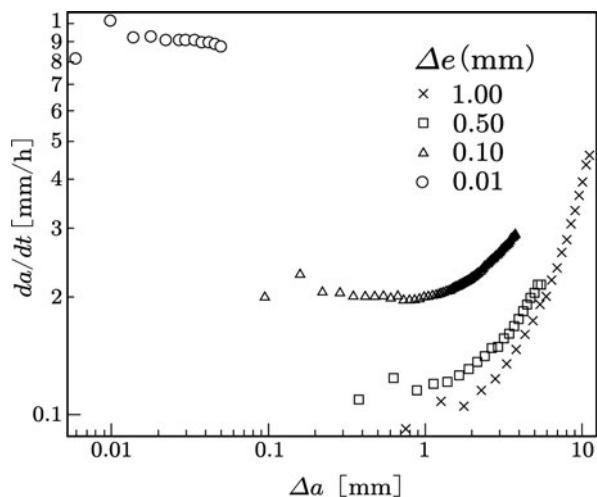


Fig. 11.9 Mesh-size dependence of crack extension rate
Source: Liu et al. (1994, p. 403, Fig. 5)

11.4.2 Bifurcation and Localization in Time-Dependent Deformation

In the case of time-dependent materials, one can show that the bifurcation can be eliminated from the causes of mesh-sensitivity. Let us suppose an elastic-creep damage material of Eqs. (11.21) through (11.27), and perform a bifurcation analysis similar to that of Section 11.2.2.

By substituting Eq. (11.24b) into Eq. (11.7), we have

$$\begin{aligned} n_i C_{ijkl}(D) \left(\dot{\varepsilon}_{kl}^{(b)} - \dot{\varepsilon}_{kl}^{(o)} \right) - n_i C_{ijkl}(D) \left(\dot{\varepsilon}_{kl}^{c(b)} - \dot{\varepsilon}_{kl}^{c(o)} \right) \\ - n_i C_{ijkl}(0) \left(\dot{D}^{(b)} \varepsilon_{kl}^{e(b)} - \dot{D}^{(o)} \varepsilon_{kl}^{e(o)} \right) = 0. \end{aligned} \quad (11.28)$$

Since the variables ε_{kl}^e , σ_{ij} and D have the identical values in the regions inside and outside of the band of Fig. 11.7, the creep rate $\dot{\varepsilon}_{kl}^c$ and the damage rate \dot{D} must be continuous across the interface. Hence, the second and the third terms in the left-hand side of Eq. (11.28) will vanish. Substitution of Eq. (11.6) into the resulting relation furnishes the following relation, similar to Eq. (11.9):

$$[n_i C_{ijkl}(D) n_k] \dot{q}_l = 0. \quad (11.29)$$

Namely, we have the bifurcation condition for elastic-creep damage materials identical to that of time-independent materials

$$\det[n_i C_{ijkl}(D) n_k] = 0. \quad (11.30)$$

By means of the similar procedure as in Section 11.2.2, Eq. (11.30) leads to the condition

$$E(D) = 0, \quad (11.31a)$$

or

$$D = D_C. \quad (11.31b)$$

This result means that the bifurcation in time-dependent material of Eq. (11.24) occurs at the final damage state of Eq. (11.31), and no bifurcation is induced preceding it.

11.5 Causes of Mesh-Sensitivity in Time-Dependent Deformation

Bifurcation in time-dependent materials does not occur preceding their final damage state. Hence mesh-sensitivity in these materials may be induced by causes other than the strain-softening, e.g., by the causes (2) and (3) discussed in Section 11.1.2. These problems will now be considered briefly.

11.5.1 Stress Singularity at Crack Tip

As a cause of the mesh-sensitivity of the creep-crack extension rate of Fig. 11.9, let us first consider the stress singularity at the crack-tip.

In the elastic-creep crack analysis of Fig. 11.8, the initial stress in the crack-tip element, or at its Gaussian point is given by the HRR stress field of Eq. (8.101)

$$\sigma \propto (\Delta e)^\lambda, \quad (11.32)$$

$$\lambda = -1/2, \quad (\text{linear elasticity}), \quad (11.33a)$$

$$= -1/(n+1), \quad (\text{power law creep}). \quad (11.33b)$$

Then the time t_{ig} of the start of crack extension at the crack-tip can be calculated by the evolution equation (11.22) of creep damage as follows (Liu et al. 1994)

$$t_{ig} \propto (\Delta e)^{-m\lambda}. \quad (11.34)$$

We suppose that stress field at the tip of pre-crack is elastic at the beginning. By the use of the stress singularity exponent $\lambda = -1/2$ and the creep damage exponent $m = 2.8$ of Eq. (11.27), Eq. (11.34) leads to

$$t_{ig} \propto (\Delta e)^{1.40}. \quad (11.35)$$

The creep crack analysis of Section 11.4.1, on the other hand, gave the results of Fig. 11.10. Small symbols and a straight line in the figure show the results of finite element analysis and their regression line.

$$t_{ig} \propto (\Delta e)^{1.57}, \quad (11.36)$$

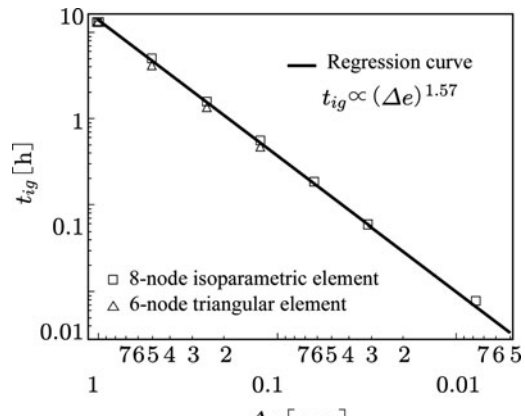


Fig. 11.10

Mesh-dependence of the time of the start of crack extension

Source: Liu et al. (1994, p. 401, Fig. 3)

which coincides fairly well with Eq. (11.35). This implies that the incipient creep crack extension is governed largely by the stress singularity at the crack tip. This feature applies also to the case of non-linear stress field caused by the damage development (Liu et al. 1994; Murakami and Liu 1996).

The mesh-dependence resulting from stress singularity is observed also for time-independent elastic brittle material (Bažant 1990).

11.5.2 Stress-Sensitivity of Damage Evolution Equation and Damage Localization

Damage localization is one of the apparent causes of mesh-dependence also in time-dependent materials, and this localization is largely related with the stress-sensitivity of the damage constitutive equation.

Kachanov-Rabotnov damage evolution equation (8.1) or (8.12) is quite sensitive to small variation of stress when the damage variable D approaches unity. Such difficulty can be excluded by the use of damage evolution with appropriate stress-dependence (Murakami, Liu, and Mizuno 2000).

11.5.3 Regularization of Mesh-Sensitivity in Time-Dependent Deformation

The mesh-sensitivity in time-dependent deformation due to the causes described in this section can be regularized by the following schemes:

- (1) Nonlocal damage theory (Pijaudier-Cabot and Bažant 1987; Saanouni et al. 1989; Murakami and Liu 1995)
- (2) Cell model or grid method of nonlocal damage theory (Hall and Hayhurst 1991; Murakami and Liu 1995; de Vree et al. 1995)
- (3) Stress-limitation method (Murakami and Liu 1995; Liu and Murakami 1996)
- (4) Regularization of damage evolution equation (Murakami and Liu 1995; Murakami, Liu, and Mizuno 2000)

Specific procedures of these methods can be found in the relevant references.

11.5.4 Analysis of Creep-Crack Extension by Means of Nonlocal Damage Theory

At the end of this section, the applicability of the nonlocal damage theory will be shown as one of the most successful method of regularization in time dependent deformation.

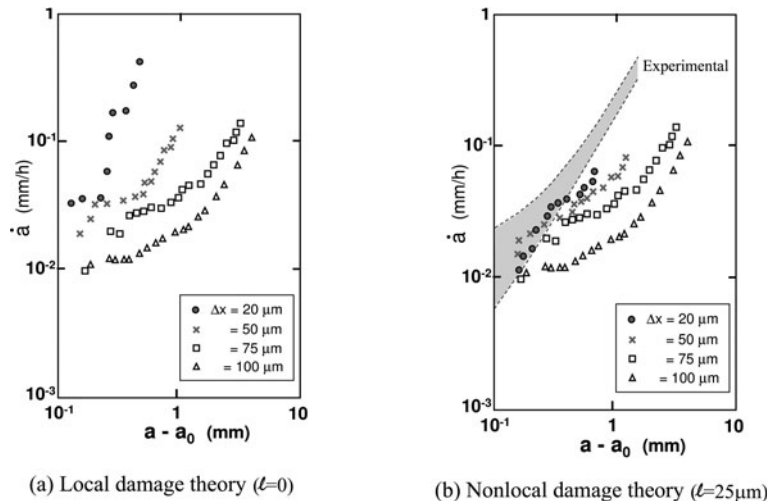


Fig. 11.11 Creep crack growth rates of Inconel 718 CT specimen at 500°C

Source: Saanouni et al. (1989), Lemaitre et al. (2009) (by courtesy of J. L. Chaboche)

Saanouni and others (1989) analyzed the creep-crack growth in a pre-cracked CT specimen by the use of nonlocal damage theory of Eq. (11.15), and elucidated its effectiveness. The analysis was performed for Inconel 718 specimens at 650°C in the state of plane strain, and Kachanov-Rabotnov creep constitutive equation (11.22) was employed. Four different values of the crack-tip mesh size $\Delta x = 100, 75, 50, 20 \mu\text{m}$ were selected. As the *characteristic length* ℓ of the non-localization in Eq. (11.16), the size $\ell = 25 \mu\text{m}$ of the order of the grain size of the material was postulated.

Figure 11.11a and b show the predicted creep crack growth rates by means of the local and the nonlocal analyses, while the dark region bounded by thin dotted lines in (b) represent the results observed in the tests performed in the corresponding conditions. While the results of local analysis of (a) depend largely on the mesh size Δx , those of nonlocal analysis of (b) show obvious convergence for mesh sizes smaller than $\Delta x = 50 \mu\text{m}$: i.e., twice the characteristic length $\ell = 25 \mu\text{m}$. In view of the fact that the material parameters employed here had been identified by the uniaxial and the multiaxial creep tests, the predictions of (b) coincide well with the experiments.

For the regularization by means of the nonlocal theory, the appropriate selection of the characteristic length ℓ is particularly important. The value ℓ should be an intrinsic material constant related to its microstructure, and is often determined in relation to its average grain size (Bažant and Pijaudier-Cabot 1988; Saanouni et al. 1989).

Appendix

Foundations of Tensor Analysis

Chapter 12

Foundations of Tensor Analysis – Tensor Algebra and Tensor Calculus

Continuum mechanics has been formulated mainly in the mathematical framework of tensor algebra and tensor calculus. The accurate understanding and the proper application of *continuum damage mechanics*, therefore, necessitate sound foundation of this mathematical subject.

The present chapter is the presentation of the foundation of tensor analysis in some detail for the convenience of readers not familiar enough with this important subject.

In Sections 12.1 through 12.4, the fundamentals of the tensor analysis in three-dimensional Euclidean space will be outlined. In Sections 12.5 through 12.7, furthermore, we will discuss differentiation of tensor functions with respect to their arguments, representation theorem of tensor functions, and the matrix representation of tensors and tensor relations. For more detailed references for these subjects, a number of excellent books listed at the end of this book will be helpful.

Though a variety of symbols are employed in this book, they stand for quantities, variables, suffixes or mathematical operations explained in the list at the beginning of this book, unless otherwise described.

12.1 Vectors and Tensors

12.1.1 Euclidean Vector Spaces and Tensors

In the vector space of elementary geometry, for each pair of vectors \mathbf{u} and \mathbf{v} , the *scalar product* (or *inner product*, or *dot product*)

$$\mathbf{u} \cdot \mathbf{v} = |\mathbf{u}| |\mathbf{v}| \cos \theta \quad (12.1)$$

is defined. The symbols $|\mathbf{u}|$ and $|\mathbf{v}|$ in this relation denote the *norm* (or *magnitude*) of the vectors \mathbf{u} and \mathbf{v} , and are given

$$|\mathbf{u}| = \sqrt{\mathbf{u} \cdot \mathbf{u}}, \quad |\mathbf{v}| = \sqrt{\mathbf{v} \cdot \mathbf{v}}. \quad (12.2)$$

The symbol θ , furthermore, is the angle between \mathbf{u} and \mathbf{v} .

For vectors \mathbf{u} , \mathbf{v} , \mathbf{w} and real numbers a , b , this scalar product has the following properties:

- (1) $\mathbf{u} \cdot \mathbf{v} = \mathbf{v} \cdot \mathbf{u}$,
- (2) $\mathbf{u} \cdot (av + bw) = a(\mathbf{u} \cdot \mathbf{v}) + b(\mathbf{u} \cdot \mathbf{w})$,
- (3) If $\mathbf{u} \cdot \mathbf{v} = \mathbf{0}$ for arbitrary \mathbf{u} , then $\mathbf{v} = \mathbf{0}$,
- (4) $\mathbf{u} \cdot \mathbf{u} > 0$ for $\mathbf{u} \neq \mathbf{0}$.

Suppose that a finite-dimensional vector space \mathcal{E}^n is defined over the field of real numbers. Then, if there exists a rule of composition which gives, for every pair of vectors \mathbf{u} and \mathbf{v} , a real number $\mathbf{u} \cdot \mathbf{v}$ having the properties (1)–(4) above, the vector space \mathcal{E}^n is referred to as a *Euclidean vector space*.

In the three-dimensional Euclidean vector space \mathcal{E}^3 , we can define a system of *orthonormal basis*

$$\{\mathbf{e}_i\} = \{\mathbf{e}_1, \mathbf{e}_2, \mathbf{e}_3\}, \quad \mathbf{e}_i \cdot \mathbf{e}_j = \delta_{ij}, \quad (i, j = 1, 2, 3), \quad (12.3)$$

where \mathbf{e}_i and \mathbf{e}_j , respectively, stand for one of the three *basis vectors* $\mathbf{e}_1, \mathbf{e}_2, \mathbf{e}_3$. The symbols i and j denote *indices*, while the symbol δ_{ij} is called the *Kronecker delta* defined by a relation

$$\delta_{ij} = \begin{cases} 1, & i = j \\ 0, & i \neq j \end{cases}. \quad (12.4)$$

By the use of the orthonormal basis \mathbf{e}_i , any vector \mathbf{u} in \mathcal{E}^3 can be represented uniquely by a linear combination of \mathbf{e}_i

$$\mathbf{u} = \sum_{i=1}^3 u_i \mathbf{e}_i = u_i \mathbf{e}_i, \quad (12.5)$$

where real number u_i is called the *Cartesian component* (or simply the *component*) of the vector \mathbf{u} with respect to the orthonormal basis $\{\mathbf{e}_i\}$ (see Fig. 12.1).

On the right-hand side of Eq. (12.5), we have adopted the *summation convention* (due to Einstein): i.e., the repetition of an index (only once) in the same term implies

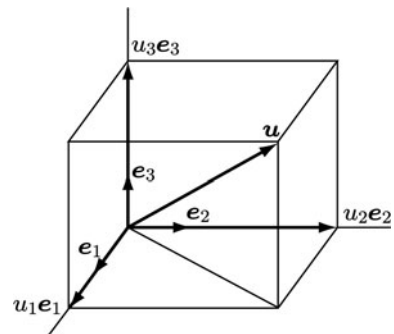


Fig. 12.1 Vector \mathbf{u} and its components

a summation over the range of this index unless otherwise indicated. The index that is summed over (e.g., i in Eq. (12.5)) is called a *dummy index*, whereas an index that is not summed over in a given term (e.g., i in Eq. (12.6) below) is said to be a *free index*. As observed from Eq. (12.5), it is immaterial which symbol is used for a dummy index because it just indicates summation.

The scalar product of the left hand side of Eq. (12.5) with a vector \mathbf{e}_i leads to

$$\mathbf{u} \cdot \mathbf{e}_i = (u_j \mathbf{e}_j) \cdot \mathbf{e}_i = u_j \delta_{ji} = u_i. \quad (12.6a)$$

Thus the component u_i of a vector \mathbf{u} is given by (Fig. 12.2)

$$u_i = \mathbf{u} \cdot \mathbf{e}_i. \quad (12.6b)$$

By the use of Eqs. (12.1) through (12.5), the scalar product and the norms of \mathbf{u} and \mathbf{v} can be written as

$$\begin{aligned} \mathbf{u} \cdot \mathbf{v} &= \left[\sum_{i=1}^3 u_i \mathbf{e}_i \right] \cdot \left[\sum_{j=1}^3 v_j \mathbf{e}_j \right] = u_i \mathbf{e}_i \cdot v_j \mathbf{e}_j \\ &= u_i v_j \mathbf{e}_i \cdot \mathbf{e}_j = u_i v_j \delta_{ij} = u_i v_i, \end{aligned} \quad (12.7a)^1$$

$$|\mathbf{u}| = \sqrt{u_i u_i}, \quad |\mathbf{v}| = \sqrt{v_i v_i}. \quad (12.7b)$$

A *linear transformation* which acts on a vector to generate another vector is referred to as a *tensor*. If a linear transformation, or a tensor \mathbf{S} assigns a vector \mathbf{v} to each vector \mathbf{u} , we may write

$$\mathbf{v} = \mathbf{S}\mathbf{u}. \quad (12.8)^2$$

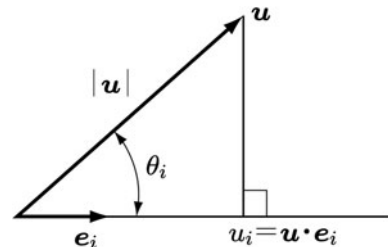


Fig. 12.2 Scalar product of vectors \mathbf{u} and \mathbf{e}_i

¹ In tensor analysis, designation of a vector or a tensor by the use of a bold-face letter, just as in the left-hand side of Eq. (12.7a), is called *direct notation* (or *absolute notation*). On the other hand, the designation of a vector or a tensor in terms of their components, as in the right-hand side of the second line of Eq. (12.7a) is said to be *index notation*.

² In the case of a scalar product between a tensor and a vector, or between two tensors, the dot (·) representing the scalar product is usually omitted by convention. Namely we do not write $\mathbf{S} \cdot \mathbf{u}$ nor $\mathbf{S} \cdot \mathbf{T}$.

Fig. 12.3 Linear transformation of a vector \mathbf{u} to another vector \mathbf{v} by a tensor S

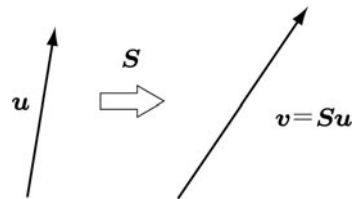


Figure 12.3 is a schematic representation of this relation. The specific operation of this relation implies a scalar product between a tensor S and a vector \mathbf{u} to give a new vector \mathbf{v} . This will be clarified after the definition of tensor components in Section 12.2.2.

Since the transformation S is linear, we have

$$S(a\mathbf{u} + \mathbf{v}) = aS\mathbf{u} + S\mathbf{v} \quad (12.9)^2$$

for all vectors \mathbf{u}, \mathbf{v} and all scalars a .

For two tensors S and T , we can define the sum $S + T$, the scalar multiplication aS by a scalar a , and the scalar product between S and T by the following rules

$$(S + T)\mathbf{u} = S\mathbf{u} + T\mathbf{u}, \quad (12.10)$$

$$(aS)\mathbf{u} = a(S\mathbf{u}), \quad (12.11)$$

$$(ST)\mathbf{u} = S(T\mathbf{u}), \quad (12.12)^2$$

where \mathbf{u} and a denote an arbitrary vector and an arbitrary scalar.

12.1.2 Product and Transpose of Tensors

A linear transformation or a tensor which assigns the zero vector $\mathbf{0}$ to all vector \mathbf{u} is called a *zero tensor* O , whereas a tensor which maps all vector \mathbf{u} to itself is called the *unit tensor* (or *identity tensor*) I , and can be written

$$O\mathbf{u} = \mathbf{0}, \quad (12.13)$$

$$I\mathbf{u} = \mathbf{u}. \quad (12.14)$$

The tensors O and I are called also a *zero linear transformation* and a *unit linear transformation*, respectively.

As for the linear transformation of Eq. (12.8), if another linear transformation S^{-1} can be defined so that

$$S^{-1}\mathbf{v} = \mathbf{u}, \quad (12.15)$$

the tensor \mathbf{S} is said to be *invertible*, and the tensor \mathbf{S}^{-1} is called an *inverse tensor* (or an *inverse transformation*) of \mathbf{S} . Eqs. (12.12) and (12.15) provide a reciprocal relation

$$\mathbf{S}\mathbf{S}^{-1} = \mathbf{S}^{-1}\mathbf{S} = \mathbf{I}. \quad (12.16)$$

By the use of this relation, we can show the following relations:

$$(\mathbf{ST})(\mathbf{T}^{-1}\mathbf{S}^{-1}) = \mathbf{I} = (\mathbf{ST})(\mathbf{ST})^{-1}, \quad (12.17)$$

$$(\mathbf{ST})^{-1} = \mathbf{T}^{-1}\mathbf{S}^{-1}. \quad (12.18)$$

If a new tensor \mathbf{S}^T can be defined such that

$$\mathbf{S}\mathbf{u} \cdot \mathbf{v} = \mathbf{u} \cdot \mathbf{S}^T\mathbf{v} \quad (12.19)$$

for all vectors \mathbf{u} and \mathbf{v} , the tensor \mathbf{S}^T is said to be the *transpose* of the tensor \mathbf{S} . By using Eq. (12.10) together with Eqs. (12.12), (12.14) and (12.19), we have the following relations:

$$(\mathbf{S} + \mathbf{T})^T = \mathbf{S}^T + \mathbf{T}^T, \quad (12.20)$$

$$(\mathbf{ST})^T = \mathbf{T}^T\mathbf{S}^T, \quad (12.21)$$

$$(\mathbf{S}^T)^T = \mathbf{S}, \quad (12.22)$$

$$\mathbf{I}^T = \mathbf{I}, \quad (12.23)$$

$$(\mathbf{S}^{-1})^T = (\mathbf{S}^T)^{-1} = \mathbf{S}^{-T}. \quad (12.24)$$

Equation (12.24) implies that the operations of the inverse and the transpose are commutative.

Tensors which satisfy the relation

$$\mathbf{S}^T = \mathbf{S} \quad (12.25)$$

or

$$\mathbf{S}^T = -\mathbf{S} \quad (12.26)$$

is called a *symmetric tensor* and an *antisymmetric tensor* (or *skew-symmetric tensor*), respectively. Any tensor \mathbf{S} can always be decomposed into a symmetric tensor \mathbf{S}^S and an antisymmetric tensor \mathbf{S}^A as follow:

$$\mathbf{S} = \mathbf{S}^S + \mathbf{S}^A, \quad (12.27a)$$

$$\mathbf{S}^S = (1/2)(\mathbf{S} + \mathbf{S}^T), \quad \mathbf{S}^A = (1/2)(\mathbf{S} - \mathbf{S}^T). \quad (12.27b)$$

This decomposition is unique, and is called *Cartesian decomposition* of a tensor \mathbf{S} .

If a symmetric tensor \mathbf{S} satisfies the relation

$$\mathbf{S}\mathbf{u} \cdot \mathbf{u} > 0 \quad (12.28)$$

for all vector $\mathbf{u} \neq \mathbf{0}$, the tensor \mathbf{S} is said to be a *positive tensor* (or a *positive definite tensor*).

12.2 Vector Product, Tensor Product and the Components of Tensors

12.2.1 Vector Product and Tensor Product

In the three-dimensional Euclidean vector space \mathcal{E}^3 , the *vector product* (or *outer product*, or *cross product*) of two vectors \mathbf{u} and \mathbf{v} is defined as

$$\mathbf{u} \times \mathbf{v} = (|\mathbf{u}| |\mathbf{v}| \sin \theta) \mathbf{n}, \quad (12.29)$$

where θ is the smallest angle between the vectors \mathbf{u} and \mathbf{v} (Fig. 12.4). The vector \mathbf{n} , on the other hand, is a unit vector perpendicular to the plane spanned by \mathbf{u} and \mathbf{v} , and its sense is determined such that $(\mathbf{u}, \mathbf{v}, \mathbf{n})$ gives a right-handed system. Thus the magnitude $|\mathbf{u} \times \mathbf{v}|$ characterizes the area of a parallelogram spanned by vectors \mathbf{u} and \mathbf{v} .

If the vectors \mathbf{u} and \mathbf{v} are represented by an orthonormal basis $\{\mathbf{e}_i\}$, the vector product of Eq. (12.29) can be expressed

$$\begin{aligned} \mathbf{u} \times \mathbf{v} &= e_{ijk} u_j v_k \mathbf{e}_i \\ &= \begin{vmatrix} \mathbf{e}_1 & \mathbf{e}_2 & \mathbf{e}_3 \\ u_1 & u_2 & u_3 \\ v_1 & v_2 & v_3 \end{vmatrix}, \end{aligned} \quad (12.30)$$

where the symbol e_{ijk} signifies the values

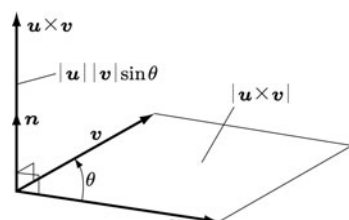


Fig. 12.4 Vector product of vectors \mathbf{u} and \mathbf{v}

$$e_{ijk} = \begin{cases} 1, & \text{for even permutation of } (i, j, k) \\ -1, & \text{for odd permutation of } (i, j, k) \\ 0, & \text{if there is a repeated index,} \end{cases} \quad (12.31)$$

and is called the *permutation symbol* (or *Eddington epsilon*, or *Levi-Civita symbol*). Between the permutation symbol and the Kronecker delta, we have the following relations:

$$e_{ijk}e_{lmk} = \delta_{il}\delta_{jm} - \delta_{im}\delta_{jl}, \quad (12.32a)$$

$$e_{ijk}e_{ljk} = 2\delta_{il}, \quad (12.32b)$$

$$e_{ijk}e_{ijk} = 3! = 6. \quad (12.32c)$$

For the right-handed orthonormal basis, Eq. (12.30) furnishes a relation

$$\mathbf{e}_1 \times \mathbf{e}_2 = \mathbf{e}_3. \quad (12.33a)$$

This can be written also in a more general form

$$\mathbf{e}_k \times \mathbf{e}_l = e_{klm}\mathbf{e}_m. \quad (12.33b)$$

The *tensor product* $\mathbf{a} \otimes \mathbf{b}$ of two vectors \mathbf{a}, \mathbf{b} is defined as a tensor which linearly transforms any vector \mathbf{u} into another vector with the direction of \mathbf{a}

$$(\mathbf{a} \otimes \mathbf{b})\mathbf{u} = (\mathbf{b} \cdot \mathbf{u})\mathbf{a}. \quad (12.34)$$

The tensor product is called also a *dyad*. Since the tensor product $\mathbf{a} \otimes \mathbf{b}$ transforms any vector into a vector parallel to the vector \mathbf{a} , Eq. (12.34) enables one to write

$$\mathbf{a} \otimes \mathbf{b} = \mathbf{a}(\mathbf{b} \cdot \mathbf{\cdot}). \quad (12.35)$$

Namely the tensor product $\mathbf{a} \otimes \mathbf{b}$ has a similar property to a tensor S of Eq. (12.8). Substitution of Eq. (12.5) into Eq. (12.34) gives

$$(\mathbf{e}_i \otimes \mathbf{e}_i)\mathbf{u} = (\mathbf{e}_i \cdot \mathbf{u})\mathbf{e}_i = u_i\mathbf{e}_i = \mathbf{u}. \quad (12.36)$$

In view of Eq. (12.14), we have a relation

$$\mathbf{e}_i \otimes \mathbf{e}_i = \mathbf{I} \quad (12.37a)$$

or

$$\mathbf{I} = \mathbf{e}_i \otimes \mathbf{e}_i = \mathbf{e}_1 \otimes \mathbf{e}_1 + \mathbf{e}_2 \otimes \mathbf{e}_2 + \mathbf{e}_3 \otimes \mathbf{e}_3, \quad (12.37b)$$

where \mathbf{I} is the unit tensor.

12.2.2 Tensor Components and Their Matrix Representation

As observed above, a tensor can be written in the form of the dyad of the basis vectors \mathbf{e}_i and \mathbf{e}_j . Namely a tensor S can be represented by the use of nine coefficients S_{ij}

$$\mathbf{S} = S_{ij}\mathbf{e}_i \otimes \mathbf{e}_j, \quad (12.38)$$

where the coefficients S_{ij} are called the *Cartesian components*, or simply the *components* of the tensor \mathbf{S} with respect to the orthonormal basis $\{\mathbf{e}_i\}$. The linear combination of the dyads is named a *dyadic*. By the use of Eq. (12.5), the tensor product $\mathbf{a} \otimes \mathbf{b}$ is expressed in the form

$$\mathbf{a} \otimes \mathbf{b} = a_i \mathbf{e}_i \otimes b_j \mathbf{e}_j = a_i b_j \mathbf{e}_i \otimes \mathbf{e}_j. \quad (12.39)$$

The tensor product $\mathbf{a} \otimes \mathbf{b}$, therefore, is a tensor which has the components $a_i b_j$.

Since a tensor S has nine components S_{ij} as observed in Eq. (12.38), it can be represented also in the form

$$[\mathbf{S}] = \begin{bmatrix} S_{11} & S_{12} & S_{13} \\ S_{21} & S_{22} & S_{23} \\ S_{31} & S_{32} & S_{33} \end{bmatrix}. \quad (12.40)$$

This is referred to as the *matrix representation* of a tensor S .

Equation (12.6) expresses the component u_i of a vector \mathbf{u} in terms of \mathbf{u} and its basis vector \mathbf{e}_i . Then how can the components S_{ij} of a tensor S be expressed by S and \mathbf{e}_i ?

By taking the product of S and \mathbf{e}_j , and then by using Eqs. (12.38), (12.34) and (12.3), we have

$$\begin{aligned} \mathbf{Se}_j &= S_{lk}(\mathbf{e}_l \otimes \mathbf{e}_k)\mathbf{e}_j = S_{lk}(\mathbf{e}_k \cdot \mathbf{e}_j)\mathbf{e}_l \\ &= S_{lj}\mathbf{e}_l. \end{aligned} \quad (12.41)$$

The scalar product of this equation with \mathbf{e}_i leads to

$$\begin{aligned} \mathbf{e}_i \cdot (\mathbf{Se}_j) &= \mathbf{e}_i \cdot (S_{lj}\mathbf{e}_l) = S_{lj}(\mathbf{e}_i \cdot \mathbf{e}_l) \\ &= S_{lj}\delta_{il} = S_{ij}. \end{aligned} \quad (12.42)$$

Hence, the components of the tensor S is given as

$$S_{ij} = \mathbf{e}_i \cdot \mathbf{Se}_j. \quad (12.43)$$

12.2.3 Axial Vector of Antisymmetric Tensor

The antisymmetric tensor defined by Eq. (12.26) has three independent non-zero components. Hence an antisymmetric tensor

$$\mathbf{W} = W_{ij}\mathbf{e}_i \otimes \mathbf{e}_j \quad (12.44)$$

can be specified by a vector \mathbf{w} in terms of a relation

$$w_k = -\frac{1}{2}e_{klm}W_{lm}. \quad (12.45)$$

By multiplying e_{kij} to the both sides of this relation and by using Eq. (12.32a), we have

$$e_{kij}w_k = -\frac{1}{2}(\delta_{il}\delta_{jm} - \delta_{im}\delta_{jl})W_{lm} = -W_{ij}$$

or

$$W_{ij} = -e_{kij}w_k. \quad (12.46)$$

Application of this tensor \mathbf{W} to an arbitrary vector \mathbf{u} and the use of Eq. (12.30) provide the relation

$$(\mathbf{W}\mathbf{u})_i = W_{ij}u_j = -e_{kij}w_ku_j = e_{ikj}w_ku_j = (\mathbf{w} \times \mathbf{u})_i. \quad (12.47)$$

From this relation, we finally have a general relation

$$\mathbf{W}\mathbf{u} = \mathbf{w} \times \mathbf{u}. \quad (12.48)$$

Figure 12.5 shows the schematic relation of Eq. (12.48). The vector \mathbf{w} defined by Eq. (12.45) is called an *axial vector* of the antisymmetric tensor \mathbf{W} .

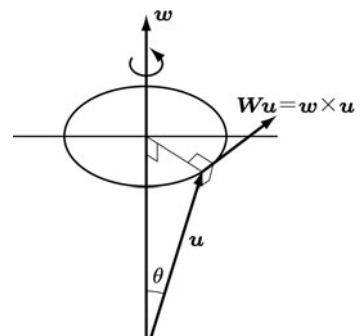


Fig. 12.5 Axial vector \mathbf{w} of an antisymmetric tensor \mathbf{W}

12.2.4 Trace and Contraction of Tensors

A scalar given by summing up the diagonal terms of the matrix representation Eq. (12.40) of a tensor S is called the *trace* of the tensor S , and is denoted by $\text{tr}S$:

$$\text{tr}S = S_{ii}. \quad (12.49)$$

Thus the trace of the dyad $\mathbf{a} \otimes \mathbf{b}$ of two vectors \mathbf{a}, \mathbf{b} is given by

$$\text{tr}(\mathbf{a} \otimes \mathbf{b}) = \text{tr}[(a_i \mathbf{e}_i) \otimes (b_j \mathbf{e}_j)] = a_i b_i = \mathbf{a} \cdot \mathbf{b}. \quad (12.50)$$

By the use of this relation, we have the trace of the dyad of basis vectors $\mathbf{e}_i, \mathbf{e}_j$

$$\text{tr}(\mathbf{e}_i \otimes \mathbf{e}_j) = \mathbf{e}_i \cdot \mathbf{e}_j = \delta_{ij}. \quad (12.51)$$

An operation in the index notation to equate two indices in a term, and to sum over these indices as dummy indices is called the *contraction*. In the direct notation, on the other hand, a contraction is implied by a dot (\cdot), by the scalar product or by the trace. The contractions between vectors \mathbf{a}, \mathbf{b} and tensors \mathbf{A}, \mathbf{B} , therefore, are expressed as follows:

$$\mathbf{a} \cdot \mathbf{b} = (a_i \mathbf{e}_i) \cdot (b_j \mathbf{e}_j) = a_i b_j (\mathbf{e}_i \cdot \mathbf{e}_j) = a_i b_j \delta_{ij} = a_i b_i, \quad (12.52)$$

$$\text{tr}\mathbf{A} = A_{ii}, \quad (12.53)$$

$$\begin{aligned} \mathbf{A} : \mathbf{B} &= (A_{ij} \mathbf{e}_i \otimes \mathbf{e}_j) : (B_{kl} \mathbf{e}_k \otimes \mathbf{e}_l) \\ &= A_{ij} B_{kl} (\mathbf{e}_i \otimes \mathbf{e}_j) : (\mathbf{e}_k \otimes \mathbf{e}_l) = A_{ij} B_{kl} (\mathbf{e}_i \cdot \mathbf{e}_k) (\mathbf{e}_j \cdot \mathbf{e}_l) = A_{ij} B_{kl} \delta_{ik} \delta_{jl} \\ &= A_{ij} B_{ij} = B_{ij} A_{ij}, \end{aligned} \quad (12.54a)$$

or

$$\begin{aligned} \mathbf{A} : \mathbf{B} &= \mathbf{B} : \mathbf{A} = \text{tr}(AB^T) \\ &= \text{tr}(A^T B) = \text{tr}(B^T A) = \text{tr}(BA^T). \end{aligned} \quad (12.54b)$$

The results of these contractions are all scalars.

The operation of summing over two set of indices, as observed in Eq. (12.54), is called the *double contraction*, in particular. A vector is characterized as a first-order tensor, as will be described in Section 12.2.5. Thus Eqs. (12.52) through (12.54) imply that a contraction reduces the order of tensors by two.

12.2.5 Higher-Order Tensors and Their Tensor Operations

In Section 12.1.1, a tensor was defined as a linear transformation which maps a vector to another vector. As observed in Eq. (12.38), since a tensor S is expressed

by a tensor product of two basis vectors \mathbf{e}_i and \mathbf{e}_j , the tensor S is strictly speaking a *second-order tensor*. A linear transformation of an arbitrary order, i.e., a linear transformation expressed by a tensor product of an arbitrary number of basis vectors, is also a tensor. By extending Eq. (12.38) into a tensor with larger number of basis vectors than two, we have a tensor

$$\mathcal{T} = T_{i_1 i_2 \dots i_n} \mathbf{e}_{i_1} \otimes \mathbf{e}_{i_2} \otimes \dots \mathbf{e}_{i_n}, \quad (12.55)$$

which is called a *nth-order tensor*, or a *tensor of order n*. The symbol $T_{i_1 i_2 \dots i_n}$ denotes the 3^n components of the tensor \mathcal{T} . In view of Eq. (12.55), a scalar and a vector are the *zeroth-order tensor* and the *first-order tensor*, respectively. However, the word “tensor” will imply hereafter the second-order tensor, unless otherwise mentioned.

Hitherto the scalar product and the tensor product of vectors were defined by Eqs. (12.7) and (12.39). The trace and the contraction of vectors and second-order tensors, furthermore, were discussed in Section 12.2.4. Then, the tensor operations among the tensors higher than the second-order will be performed as follows:

(1) Third-Order Tensor

According to the definition of Eq. (12.55), the third-order tensor \mathcal{A} is expressed by

$$\mathcal{A} = A_{ijk} \mathbf{e}_i \otimes \mathbf{e}_j \otimes \mathbf{e}_k. \quad (12.56)$$

As an example of the third-order tensor, we first take a tensor product of vectors \mathbf{a} , \mathbf{b} , \mathbf{c}

$$\mathbf{a} \otimes \mathbf{b} \otimes \mathbf{c}.$$

This product, in particular, is named a *triad* (or *triadic product*), and has the following important properties:

$$(\mathbf{a} \otimes \mathbf{b} \otimes \mathbf{c})\mathbf{u} = (\mathbf{c} \cdot \mathbf{u})\mathbf{a} \otimes \mathbf{b}, \quad (12.57)$$

$$(\mathbf{a} \otimes \mathbf{b} \otimes \mathbf{c}) : (\mathbf{u} \otimes \mathbf{v}) = (\mathbf{b} \cdot \mathbf{u})(\mathbf{c} \cdot \mathbf{v})\mathbf{a}, \quad (12.58)$$

$$\begin{aligned} (\mathbf{a} \otimes \mathbf{b} \otimes \mathbf{c}) : \mathbf{I} &= \mathbf{a} \otimes (\mathbf{b} \otimes \mathbf{c}) : (\mathbf{e}_i \otimes \mathbf{e}_i) \\ &= (\mathbf{b} \cdot \mathbf{e}_i)(\mathbf{c} \cdot \mathbf{e}_i)\mathbf{a} = (\mathbf{b} \cdot \mathbf{c})\mathbf{a}. \end{aligned} \quad (12.59)$$

The tensor products of plural vectors are called *polyad* in general.

Another example of the third-order tensor is a tensor composed of the permutation symbol of Eq. (12.31)

$$\mathcal{E} = e_{ijk} \mathbf{e}_i \otimes \mathbf{e}_j \otimes \mathbf{e}_k, \quad (12.60)$$

which is call the *permutation tensor*.

In Eqs. (12.6) and (12.43), the components u_i and S_{ij} of a vector \mathbf{u} and a tensor \mathbf{S} are expressed in terms of \mathbf{u} , \mathbf{S} and the basis vector \mathbf{e}_i . In the case of the third-order tensor, the components of \mathbf{A} is expressed in a similar form to these relations

$$A_{ijk} = (\mathbf{e}_i \otimes \mathbf{e}_j) : \mathbf{A} \mathbf{e}_k. \quad (12.61)$$

As an example of the application of Eqs. (12.57) through (12.59), the contraction between a third-order tensor \mathbf{A} and a second-order tensor \mathbf{B} is derived:

$$\begin{aligned} \mathbf{A} : \mathbf{B} &= A_{ijk} B_{lm} (\mathbf{e}_i \otimes \mathbf{e}_j \otimes \mathbf{e}_k) : (\mathbf{e}_l \otimes \mathbf{e}_m) \\ &= A_{ijk} B_{lm} (\mathbf{e}_j \cdot \mathbf{e}_l) (\mathbf{e}_k \cdot \mathbf{e}_m) \mathbf{e}_i \\ &= A_{ijk} B_{lm} \delta_{jl} \delta_{km} \mathbf{e}_i = A_{ijk} B_{jk} \mathbf{e}_i. \end{aligned} \quad (12.62)$$

(2) Forth-Order Tensor

According to Eq. (12.55), a fourth-order tensor \mathbf{A} is expressed by

$$\mathbf{A} = A_{ijkl} \mathbf{e}_i \otimes \mathbf{e}_j \otimes \mathbf{e}_k \otimes \mathbf{e}_l, \quad (12.63)$$

and has $3^4 = 81$ components A_{ijkl} .

An example of a fourth-order tensor is given by a tensor product of four vectors \mathbf{a} , \mathbf{b} , \mathbf{c} , \mathbf{d} , called a *tetrad*

$$\mathbf{a} \otimes \mathbf{b} \otimes \mathbf{c} \otimes \mathbf{d}.$$

As regards this tensor, there exist important relations similar to Eqs. (12.57) through (12.59):

$$(\mathbf{a} \otimes \mathbf{b} \otimes \mathbf{c} \otimes \mathbf{d}) \mathbf{u} = (\mathbf{d} \cdot \mathbf{u}) \mathbf{a} \otimes \mathbf{b} \otimes \mathbf{c}, \quad (12.64)$$

$$(\mathbf{a} \otimes \mathbf{b} \otimes \mathbf{c} \otimes \mathbf{d}) : (\mathbf{u} \otimes \mathbf{v}) = (\mathbf{c} \cdot \mathbf{u})(\mathbf{d} \cdot \mathbf{v}) \mathbf{a} \otimes \mathbf{b}, \quad (12.65)$$

$$\begin{aligned} (\mathbf{a} \otimes \mathbf{b} \otimes \mathbf{c} \otimes \mathbf{d}) : \mathbf{I} &= (\mathbf{a} \otimes \mathbf{b}) \otimes (\mathbf{c} \otimes \mathbf{d}) : (\mathbf{e}_i \otimes \mathbf{e}_i) \\ &= (\mathbf{c} \cdot \mathbf{e}_i)(\mathbf{d} \cdot \mathbf{e}_i) \mathbf{a} \otimes \mathbf{b} = (\mathbf{c} \cdot \mathbf{d}) \mathbf{a} \otimes \mathbf{b}. \end{aligned} \quad (12.66)$$

The components A_{ijkl} of the tensor \mathbf{A} are given by the following relation similar to Eqs. (12.43) and (12.61):

$$A_{ijkl} = (\mathbf{e}_i \otimes \mathbf{e}_j) : \mathbf{A} : (\mathbf{e}_k \otimes \mathbf{e}_l). \quad (12.67)$$

As observed in the preceding chapters, the products between a fourth-order tensor and a second-order tensor occur frequently in continuum mechanics. For example the scalar product of a fourth-order tensor \mathbf{A} and a second-order tensor \mathbf{B} is given:

$$\begin{aligned}\mathbb{A} : \mathbf{B} &= A_{ijkl} B_{mn} (\mathbf{e}_i \otimes \mathbf{e}_j \otimes \mathbf{e}_k \otimes \mathbf{e}_l) : (\mathbf{e}_m \otimes \mathbf{e}_n) \\ &= A_{ijkl} B_{mn} (\mathbf{e}_k \cdot \mathbf{e}_m) (\mathbf{e}_l \cdot \mathbf{e}_n) \mathbf{e}_i \otimes \mathbf{e}_j \\ &= A_{ijkl} B_{kl} \mathbf{e}_i \otimes \mathbf{e}_j.\end{aligned}\quad (12.68)$$

(3) Contractions and Tensor Products of Higher-Order

Besides the double contraction $\mathbf{A} : \mathbf{B} = A_{ij} B_{ij}$ of second-order tensors \mathbf{A}, \mathbf{B} defined by Eq. (12.54a), other operations of the double contraction are often employed. For example, by taking firstly the contraction $(\mathbf{e}_i \cdot \mathbf{e}_l)$ between the first basis of the tensor \mathbf{A} and the second one of the tensor \mathbf{B} , and then by taking the contraction $(\mathbf{e}_j \cdot \mathbf{e}_k)$ between the second basis of \mathbf{A} and the first one of \mathbf{B} , we have another operation of the double contraction $\mathbf{A} \cdot \cdot \mathbf{B} = A_{ij} B_{ji}$ designated by the symbol “..”.

By denoting the vectors by \mathbf{a}, \mathbf{b} , and the tensors of order two, three and four by $\mathbf{A}, \mathbf{B}, \mathcal{A}, \mathcal{B}$ and \mathbb{A}, \mathbb{B} , respectively, different operations of the contraction are summarized as follow:

$$\mathbf{a} \cdot \mathbf{b} = a_i b_i, \quad (12.69)$$

$$\mathbf{A} : \mathbf{B} = A_{ij} B_{ij} = \text{tr}(\mathbf{AB}^T) = \text{tr}(\mathbf{A}^T \mathbf{B}), \quad (12.70)$$

$$\mathbf{A} \cdot \cdot \mathbf{B} = A_{ij} B_{ji} = \text{tr}(\mathbf{AB}) = \text{tr}(\mathbf{BA}), \quad (12.71)$$

$$\mathcal{A} : \mathbf{B} = A_{ijk} B_{jk} \mathbf{e}_i, \quad (12.72)$$

$$\mathcal{A} \cdot \cdot \mathbf{B} = A_{ijk} B_{kj} \mathbf{e}_i, \quad (12.73)$$

$$\mathbb{A} : \mathbf{B} = A_{ijkl} B_{kl} \mathbf{e}_i \otimes \mathbf{e}_j, \quad (12.74)$$

$$\mathbb{A} \cdot \cdot \mathbf{B} = A_{ijkl} B_{lk} \mathbf{e}_i \otimes \mathbf{e}_j, \quad (12.75)$$

$$\mathbb{A} : \mathbb{B} = A_{ijkl} B_{klmn} \mathbf{e}_i \otimes \mathbf{e}_j \otimes \mathbf{e}_m \otimes \mathbf{e}_n, \quad (12.76)$$

$$\mathbb{A} \cdot \cdot \mathbb{B} = A_{ijkl} B_{lkmn} \mathbf{e}_i \otimes \mathbf{e}_j \otimes \mathbf{e}_m \otimes \mathbf{e}_n. \quad (12.77)$$

If the operations of Eqs. (12.70) and (12.71) are applied to the scalar products between dyads of orthonormal bases, or to the scalar products between tensors and dyads, we have the relations:

$$(\mathbf{e}_i \otimes \mathbf{e}_j) : (\mathbf{e}_k \otimes \mathbf{e}_l) = (\mathbf{e}_i \cdot \mathbf{e}_k)(\mathbf{e}_j \cdot \mathbf{e}_l) = \delta_{ik} \delta_{jl}, \quad (12.78a)$$

$$(\mathbf{e}_i \otimes \mathbf{e}_j) \cdot \cdot (\mathbf{e}_k \otimes \mathbf{e}_l) = (\mathbf{e}_j \cdot \mathbf{e}_k)(\mathbf{e}_i \cdot \mathbf{e}_l) = \delta_{il} \delta_{jk}, \quad (12.78b)$$

$$\mathbf{A} : (\mathbf{e}_i \otimes \mathbf{e}_j) = A_{ij}, \quad (12.79a)$$

$$\mathbf{A} \cdot \cdot (\mathbf{e}_i \otimes \mathbf{e}_j) = A_{ji}. \quad (12.79b)$$

Equation (12.79a), in particular, is a counterpart of Eq. (12.6) concerning the vector components. Moreover this equation is another expression of Eq. (12.43).

The tensor product “ \otimes ” of the two vectors \mathbf{a}, \mathbf{b} defined by Eq. (12.39) implies the multiplication of the basis vectors \mathbf{e}_i of the first vector \mathbf{a} to the basis \mathbf{e}_j of the second vector \mathbf{b} . As regards the higher order tensors, on the other hand, the operations of other tensor products “ $\underline{\otimes}$ ”, “ $\overline{\otimes}$ ”, etc. can be defined in addition to the product “ \otimes ” (He and Curnier 1995; Besson et al. 2010). The operations of these products are shown collectively as follow:

$$\mathbf{a} \otimes \mathbf{b} = a_i b_j \mathbf{e}_i \otimes \mathbf{e}_j, \quad (12.80)$$

$$\mathbf{A} \otimes \mathbf{B} = A_{ij} B_{kl} \mathbf{e}_i \otimes \mathbf{e}_j \otimes \mathbf{e}_k \otimes \mathbf{e}_l, \quad (12.81)$$

$$\mathbf{A} \underline{\otimes} \mathbf{B} = A_{ik} B_{jl} \mathbf{e}_i \otimes \mathbf{e}_j \otimes \mathbf{e}_k \otimes \mathbf{e}_l, \quad (12.82a)$$

$$\mathbf{A} \overline{\otimes} \mathbf{B} = A_{il} B_{jk} \mathbf{e}_i \otimes \mathbf{e}_j \otimes \mathbf{e}_k \otimes \mathbf{e}_l, \quad (12.82b)$$

$$\mathbf{A} \overline{\underline{\otimes}} \mathbf{B} = \frac{1}{2} (A_{ik} B_{jl} + A_{il} B_{jk}) \mathbf{e}_i \otimes \mathbf{e}_j \otimes \mathbf{e}_k \otimes \mathbf{e}_l. \quad (12.83)$$

At the end of this section, the transpose of the fourth-order tensors and the unit tensor of the fourth-order will be mentioned. The transpose \mathcal{C}^T of a fourth-order tensor \mathcal{C} is defined, similarly to the form of Eq. (12.19), as follows for any second order tensors \mathbf{A} and \mathbf{B} :

$$(\mathcal{C} : \mathbf{A}) : \mathbf{B} = (\mathbf{A} : \mathcal{C}^T) : \mathbf{B} = \mathbf{B} : (\mathcal{C} : \mathbf{A}). \quad (12.84)$$

As a result of this definition, we have the following relations:

$$(\mathcal{C}^T)^T = \mathcal{C}, \quad (12.85a)$$

$$(\mathcal{C}^T)_{ijkl} = (\mathcal{C})_{klji}, \quad (12.85b)$$

$$(\mathbf{A} \otimes \mathbf{B})^T = \mathbf{B} \otimes \mathbf{A}. \quad (12.86)$$

As regards the *fourth-order unit tensor*, the definition of two tensors \mathbb{I} and $\bar{\mathbb{I}}$

$$\mathbf{A} = \mathbb{I} : \mathbf{A}, \quad \mathbf{A}^T = \bar{\mathbb{I}} : \mathbf{A} \quad (12.87)$$

are available for any second-order tensor A . The tensors \mathbb{I} and $\bar{\mathbb{I}}$ of Eq. (12.87) are expressed:

$$\begin{aligned}\mathbb{I} &= \delta_{ik}\delta_{jl}\mathbf{e}_i \otimes \mathbf{e}_j \otimes \mathbf{e}_k \otimes \mathbf{e}_l \\ &= \mathbf{e}_i \otimes \mathbf{e}_j \otimes \mathbf{e}_i \otimes \mathbf{e}_j = \underline{\mathbf{I}} \otimes \mathbf{I},\end{aligned}\quad (12.88a)$$

$$\begin{aligned}\bar{\mathbb{I}} &= \delta_{il}\delta_{jk}\mathbf{e}_i \otimes \mathbf{e}_j \otimes \mathbf{e}_k \otimes \mathbf{e}_l \\ &= \mathbf{e}_i \otimes \mathbf{e}_j \otimes \mathbf{e}_j \otimes \mathbf{e}_i = \bar{\mathbf{I}} \otimes \underline{\mathbf{I}}.\end{aligned}\quad (12.88b)$$

These tensors enable us to define a *fourth-order symmetric identity tensor*:

$$\mathbb{I}^S = \frac{1}{2}(\mathbb{I} + \bar{\mathbb{I}}) = \frac{1}{2}(\delta_{ik}\delta_{jl} + \delta_{il}\delta_{jk})\mathbf{e}_i \otimes \mathbf{e}_j \otimes \mathbf{e}_k \otimes \mathbf{e}_l = \underline{\mathbb{I}} \otimes \bar{\mathbb{I}} \quad (12.88c)$$

12.3 Orthogonal Transformation, Invariants and Eigenvalues of Tensors

12.3.1 Orthogonal Transformation and Similar Tensors

A tensor \mathbf{Q} with a property

$$\mathbf{Q}^T = \mathbf{Q}^{-1} \quad (12.89a)$$

is called an *orthogonal tensor*, or an *orthogonal transformation*. Equation (12.89a) leads to a relation

$$\mathbf{Q}^T \mathbf{Q} = \mathbf{Q} \mathbf{Q}^T = \mathbf{I}. \quad (12.89b)$$

Applying \mathbf{Q} to arbitrary vectors \mathbf{u} and \mathbf{v} , we have the new vectors

$$\bar{\mathbf{u}} = \mathbf{Q}\mathbf{u}, \quad \bar{\mathbf{v}} = \mathbf{Q}\mathbf{v}. \quad (12.90)$$

By the use of Eq. (12.89b), a scalar product of $\bar{\mathbf{u}}$ and $\bar{\mathbf{v}}$ is

$$\bar{\mathbf{u}} \cdot \bar{\mathbf{v}} = \mathbf{Q}\mathbf{u} \cdot \mathbf{Q}\mathbf{v} = \mathbf{u} \cdot \mathbf{Q}^T \mathbf{Q}\mathbf{v} = \mathbf{u} \cdot \mathbf{v}. \quad (12.91)$$

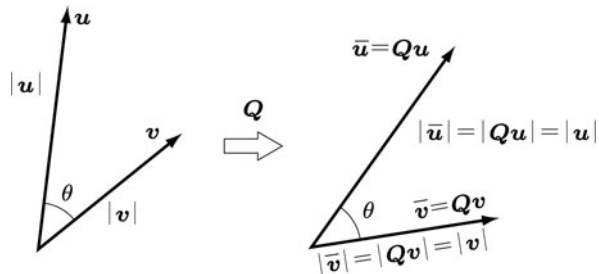
Namely, the scalar product of arbitrary two vectors does not change its value if the vectors are subject to the same orthogonal transformation.

In the particular case of $\mathbf{u} = \mathbf{v}$, we have

$$|\bar{\mathbf{u}}| = |\mathbf{Q}\mathbf{u}| = |\mathbf{u}|, \quad (12.92)$$

and the magnitude of a vector is also unchanged by the orthogonal transformation \mathbf{Q} . Moreover in view of Eq. (12.1), the angle between \mathbf{u} and \mathbf{v} is also unchanged. Thus

Fig. 12.6 Transformation of vectors by an orthogonal tensor \mathbf{Q}



an orthogonal transformation \mathbf{Q} provides a rotation of vectors. Figure 12.6 shows the property of the orthogonal tensor \mathbf{Q} .

Then, what is the effect of \mathbf{Q} on a second-order tensor? Since a tensor is specified by two bases, an arbitrary tensor \mathbf{S} is transformed by \mathbf{Q} into a new tensor

$$\bar{\mathbf{S}} = \mathbf{Q}\mathbf{S}\mathbf{Q}^T. \quad (12.93)$$

The tensor $\bar{\mathbf{S}}$ is said to be a *similar tensor* to \mathbf{S} .

By taking the determinant of the both-hand sides of Eq. (12.89b) and applying Eqs. (12.113) through (12.116) described later in Section 12.3.3, we have

$$\det \mathbf{Q} = \pm 1. \quad (12.94)$$

The cases of the positive and the negative sign of this relation are referred to as the *proper orthogonal tensor* and *improper orthogonal tensor*, respectively.

12.3.2 Transformation of Bases and that of Tensor Components

We will now consider the transformation of the bases, and discuss the associated transformation of the components of vectors and tensors.

Let $\{e_i\}$ and $\{e_{i'}\}$ be two orthonormal bases in an identical Euclidean vector space, and let $e_{i'}$ be given from e_i by the orthogonal transformation \mathbf{Q}

$$e_{i'} = \mathbf{Q}e_i = (Q_{jk}e_j \otimes e_k)e_i = Q_{ji}e_j, \quad (12.95)$$

where Q_{ij} is the components of \mathbf{Q} with respect to the basis e_i . As described in Section 12.3.1, each of three basis vectors $e_{i'} (i' = 1, 2, 3)$ is the vector rotated from the corresponding basis vectors $e_i (i = 1, 2, 3)$ by an identical angle.

An arbitrary vector \mathbf{u} in this case can be expressed in terms of either basis:

$$\mathbf{u} = u_i e_i = u_{j'} e_{j'}. \quad (12.96)$$

Substituting Eq. (12.95) into Eq. (12.96), we have

$$u_i = u_{j'} Q_{ij} = Q_{ij} u_{j'}. \quad (12.97)$$

The inverse transformations of Eqs. (2.95) and (2.97) are

$$\mathbf{e}_i = \mathbf{Q}^{-1} \mathbf{e}'_i = \left(\mathbf{Q}^{-1} \right)_{j'i'} \mathbf{e}'_j, \quad (12.98a)$$

$$u_{i'} = u_j \left(\mathbf{Q}^{-1} \right)_{i'j} = \left(\mathbf{Q}^{-1} \right)_{i'j} u_j, \quad (12.98b)$$

where $\left(\mathbf{Q}^{-1} \right)_{j'i'}$ is the components of \mathbf{Q}^{-1} with respect to the basis \mathbf{e}'_i .

Now we consider the vector $\bar{\mathbf{u}}$ defined by Eq. (12.90)

$$\bar{\mathbf{u}} = \mathbf{Qu}, \quad (12.99)$$

which is shown in Fig. 12.7. By denoting the components of $\bar{\mathbf{u}}$ with respect to \mathbf{e}'_i by \bar{u}'_i , we have a relation

$$\begin{aligned} \bar{\mathbf{u}} &= \bar{u}'_i \mathbf{e}'_i = \mathbf{Qu} = \mathbf{Qu}_i \mathbf{e}_i \\ &= u_i \mathbf{Q} \mathbf{e}_i = u_i \mathbf{e}'_i, \end{aligned} \quad (12.100)$$

and thus

$$\bar{u}'_i = u_i. \quad (12.101)$$

Namely, when a vector \mathbf{u} is transformed by \mathbf{Q} into a new vector $\bar{\mathbf{u}}$, the components \bar{u}'_i of $\bar{\mathbf{u}}$ with respect to the basis \mathbf{e}'_i has the same value as the components u_i of \mathbf{u} as regards the original basis \mathbf{e}_i . We should note the difference between Eqs. (12.101) and (12.98b).

Now in the case of a tensor S , it can be expressed as

$$S = S_{ij} \mathbf{e}_i \otimes \mathbf{e}_j = S'_{i'j'} \mathbf{e}'_i \otimes \mathbf{e}'_j. \quad (12.102)$$

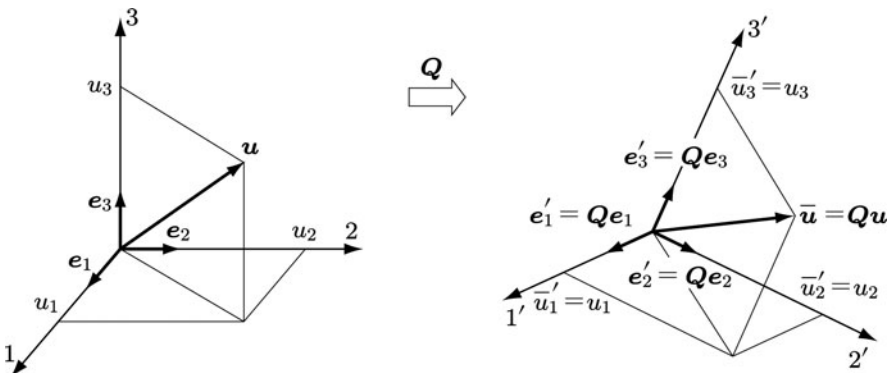


Fig. 12.7 Transformation of an orthonormal basis \mathbf{e}_i and a vector \mathbf{u} by an orthogonal tensor \mathbf{Q}

By substituting Eqs. (12.95) and (12.98a) into this relation, we have

$$S_{ij} = Q_{ik} S_{k'l'} (Q^T)_{lj}, \quad (12.103a)$$

$$S_{i'j'} = (Q^{-1})_{i'k'} S_{kl} (Q^{-T})_{j'l'}. \quad (12.103b)$$

We suppose further the similar tensor \bar{S} obtained by applying the transformation Q to S

$$\bar{S} = QSQ^{-1} = \bar{S}_{i'j'} e_{i'} \otimes e_{j'}. \quad (12.104)$$

By applying \bar{S} of this relation to the basis $e_{i'}$, and by using Eqs. (12.95) and (12.102), we have

$$\begin{aligned} \bar{S}e_{i'} &= (\bar{S}_{k'l'} e_{k'} \otimes e_{l'}) e_{i'} = \bar{S}_{k'i'} e_{k'} \\ &= (QSQ^{-1}) e_{i'} = QSe_i = Q(S_{kl} e_k \otimes e_l) e_i \\ &= QS_{ki} e_k = S_{ki} (Qe_k) = S_{ki} e_{k'}. \end{aligned} \quad (12.105a)$$

Comparison between the first and the third line of this relation gives

$$\bar{S}_{i'j'} = S_{ij}. \quad (12.105b)$$

Thus, it will be observed that the components of the similar tensor $\bar{S} = QSQ^{-1}$ with respect to the basis $e_{i'} = Qe_i$ have the same values to the components of a tensor S as regards the basis e_i . Note again the difference between Eqs. (12.105b) and (12.103b).

Finally, we show the concept of an isotropic tensor. If the components of a tensor S is unchanged by an arbitrary orthogonal transformation of its orthonormal basis e_i , or if we have the relation

$$S = QSQ^T \quad (12.106)$$

for an arbitrary orthogonal transformation Q , the tensor S is called an *isotropic tensor* or an *isotropic linear transformation*.

12.3.3 Trace and Determinant of Tensors

In Section 12.2.4, the trace of a tensor S was defined as the sum of the diagonal terms of the matrix representation (12.40):

$$\text{tr}S = S_{kk}. \quad (12.107)$$

From this definition, we can easily prove the following important properties

$$\text{tr}I = 3, \quad (12.108)$$

$$\text{tr}(S + T) = \text{tr}S + \text{tr}T, \quad \text{tr}(aS) = a\text{tr}S, \quad (12.109)$$

$$\text{tr}(S^T) = \text{tr}S, \quad \text{tr}(S^A) = 0, \quad \text{tr}(S^S) = \text{tr}S, \quad (12.110)$$

$$\text{tr}(S_1 S_2 \dots S_n) = \text{tr}(S_{i+1} S_{i+2} \dots S_n S_1 S_2 \dots S_i), \quad (i = 1, 2, \dots, n-1), \quad (12.111)$$

where a is a scalar different from zero.

We further consider the matrix representation of a tensor S of Eq. (12.40), and define the *determinant* of a tensor S as the determinant of the matrix of S :

$$\det S = \det[S]. \quad (12.112)$$

Then the determinants of the tensors can be proved to have the following properties:

$$\det I = 1, \quad (12.113)$$

$$\det(aS) = a^3 \det S, \quad (12.114)$$

$$\det(S^T) = \det S, \quad (12.115)$$

$$\det(S_1 S_2 \dots S_n) = \det S_1 \det S_2 \dots \det S_n. \quad (12.116)$$

The trace and the determinant of tensors shown in Eqs. (12.107) through (12.116) are all scalar-valued, and have been defined in terms of the components with respect to an orthonormal basis $\{e_i\}$. The values and expressions of the trace and the determinant are valid not only for the basis $\{e_i\}$ of Eq. (12.3), but also for any bases derived by any transformation including the orthogonal transformation. Thus $\text{tr}S$ and $\det S$ defined in this section are referred to as the *scalar invariants* or simply the *invariants*.

12.3.4 Eigenvalues, Eigenvectors and Principal Invariants of Tensors

We take an arbitrary tensor S in the three-dimensional Euclidean vector space \mathcal{E}^3 . Then suppose a problem to find a vector u and a scalar λ which satisfy the relation

$$Su = \lambda u. \quad (12.117)$$

This equation leads to

$$(S - \lambda I)u = 0, \quad (12.118a)$$

or

$$(S_{ij} - \lambda \delta_{ij}) u_j = 0 \quad (12.118b)$$

by the use of the Cartesian components of \mathbf{S} and \mathbf{u} . In order that this equation may have a solution other than $u_j = 0$, we have the condition

$$\det[S_{ij} - \lambda \delta_{ij}] = 0, \quad (12.119)$$

which is a cubic equation in λ .

If we expand the determinant of Eq. (12.119), we have

$$\det[S_{ij} - \lambda \delta_{ij}] = -\lambda^3 + I_1 \lambda^2 - I_2 \lambda + I_3 = 0, \quad (12.120a)$$

or

$$\det(\mathbf{S} - \lambda \mathbf{I}) = -\lambda^3 + I_1 \lambda^2 - I_2 \lambda + I_3 = 0, \quad (12.120b)$$

$$I_1 = \text{tr}\mathbf{S}, \quad I_2 = \frac{1}{2}[(\text{tr}\mathbf{S})^2 - \text{tr}(\mathbf{S}^2)], \quad I_3 = \det\mathbf{S}, \quad (12.121)$$

where I_1 , I_2 , I_3 are expressed in terms of the invariants mentioned in Section 12.3.3, and are called the *principal invariants* of the tensor \mathbf{S} . Equation (12.119) is named the *characteristic equation* of the tensor \mathbf{S} , and its solutions λ_1 , λ_2 , λ_3 are called *eigenvalues* (or *principal values*, or *proper values*) of the tensor \mathbf{S} .

Substitution of the eigenvalues λ_i ($i = 1, 2, 3$) into Eq. (12.118) gives a set of homogeneous algebraic equations for the vectors $u_j^{(i)}$, and the resulting solution $\mathbf{u}^{(i)}$ ($i = 1, 2, 3$) are called the *eigenvectors*, *proper vectors*, or the *principal directions* corresponding to the eigenvalues λ_i ($i = 1, 2, 3$). For a symmetric tensor \mathbf{S} , in particular, it can be shown that the eigenvalues λ_1 , λ_2 , λ_3 are all real, and that the three eigenvectors $\mathbf{u}^{(1)}, \mathbf{u}^{(2)}, \mathbf{u}^{(3)}$ are mutually orthogonal.

As the eigenvalues λ_i are the solution of the characteristic equation (12.119), we have

$$(\lambda - \lambda_1)(\lambda - \lambda_2)(\lambda - \lambda_3) = 0. \quad (12.122)$$

By expanding this equation and comparing it with Eq. (2.120), the principal invariants of \mathbf{S} can be expressed also in alternative forms:

$$I_1 = \lambda_1 + \lambda_2 + \lambda_3, \quad (12.123a)$$

$$I_2 = \lambda_1 \lambda_2 + \lambda_2 \lambda_3 + \lambda_3 \lambda_1, \quad (12.123b)$$

$$I_3 = \lambda_1 \lambda_2 \lambda_3. \quad (12.123c)$$

Now we will examine the properties of the eigenvalues and the eigenvectors of a similar tensor defined by Eq. (12.93). By denoting the eigenvalues and the eigenvectors of the similar tensor $\bar{\mathbf{S}}$ to \mathbf{S} by $\bar{\lambda}$, $\bar{\mathbf{u}}$, Eq. (12.118) has the form

$$(\bar{S} - \bar{\lambda}\mathbf{I})\bar{\mathbf{u}} = \mathbf{0}. \quad (12.124)$$

Substituting Eq. (12.93) into this equation and applying \mathbf{Q}^T from the left, and making use of Eq. (12.96), we have

$$(S - \bar{\lambda}\mathbf{I})\mathbf{Q}^T\bar{\mathbf{u}} = \mathbf{0}. \quad (12.125)$$

In view of the relation of Eq. (12.99), Eq. (12.125) leads to

$$(S - \bar{\lambda}\mathbf{I})\mathbf{u} = \mathbf{0}, \quad (12.126)$$

which is identical to Eq. (12.118). Hence the eigenvalues and the eigenvectors of the tensor \bar{S} are related to those of the tensor S :

$$\bar{\lambda} = \lambda, \quad \bar{\mathbf{u}} = \mathbf{Q}\mathbf{u}. \quad (12.127)$$

This implies that the tensor \bar{S} similar to S has the identical eigenvalues to S , and the eigenvectors are rotated by \mathbf{Q} from those of S .

Let us now discuss the properties of the eigenvalues and the eigenvectors in more detail. A set of eigenvectors of a symmetric tensor S is employed as an orthonormal basis $\{\mathbf{u}^{(i)}\}$ ($i = 1, 2, 3$), and the components of S are denoted by S_{ij} . Applying $\mathbf{u}^{(i)}$ and $\mathbf{u}^{(j)}$ from left and from right to S and using Eq. (12.117), we have

$$\begin{aligned} \mathbf{u}^{(i)} \cdot S \mathbf{u}^{(j)} &= \mathbf{u}^{(i)} \cdot (S_{kl} \mathbf{u}^{(k)} \otimes \mathbf{u}^{(l)}) \mathbf{u}^{(j)} \\ &= \mathbf{u}^{(i)} \cdot \mathbf{u}^{(k)} S_{kj} = S_{ij} \\ &= \mathbf{u}^{(i)} \cdot \lambda_j \mathbf{u}^{(j)} = \lambda_j \delta_{ij}, \quad (i, j = 1, 2, 3; \text{ no sum for } j). \end{aligned} \quad (12.128)$$

Namely, the components of the tensor S with respect to the bases of its eigenvectors are

$$S_{ij} = \lambda_j \delta_{ij}, \quad (i, j = 1, 2, 3; \text{ no sum for } j), \quad (12.129a)$$

or

$$[S] = \begin{bmatrix} \lambda_1 & 0 & 0 \\ 0 & \lambda_2 & 0 \\ 0 & 0 & \lambda_3 \end{bmatrix}. \quad (12.129b)$$

The set of the eigenvalues $(\lambda_1, \lambda_2, \lambda_3)$ is called the *spectrum* of the tensor S , and the expression of a tensor with the bases of its eigenvectors

$$S = \sum_{i=1}^3 \lambda_i \mathbf{u}^{(i)} \otimes \mathbf{u}^{(i)} \quad (12.130)$$

is called the *spectral decomposition* of S .

Substituting $\lambda = \lambda_1, \lambda_2, \lambda_3$ into Eq. (12.120) and expressing the resulting equations in a matrix form, we have

$$\begin{bmatrix} \lambda_1^3 & 0 & 0 \\ 0 & \lambda_2^3 & 0 \\ 0 & 0 & \lambda_3^3 \end{bmatrix} - I_1 \begin{bmatrix} \lambda_1^2 & 0 & 0 \\ 0 & \lambda_2^2 & 0 \\ 0 & 0 & \lambda_3^2 \end{bmatrix} + I_2 \begin{bmatrix} \lambda_1 & 0 & 0 \\ 0 & \lambda_2 & 0 \\ 0 & 0 & \lambda_3 \end{bmatrix} - I_3 \begin{bmatrix} 1 & 0 & 0 \\ 0 & 1 & 0 \\ 0 & 0 & 1 \end{bmatrix} = 0, \quad (12.131a)$$

or a more general relation for a tensor S in the three-dimensional Euclidean vector space \mathcal{E}^3

$$S^3 - I_1 S^2 + I_2 S - I_3 I = 0. \quad (12.131b)$$

This relation is known as the *Cayley-Hamilton theorem*.

Finally, by the use of Eq. (12.131), we will express $I_3 = \det S$ in terms of the traces of S . Taking the trace of Eq. (12.131b), and then applying Eq. (12.121), we have

$$\det S = \frac{1}{6}(\text{tr}S)^3 - \frac{1}{2}(\text{tr}S)(\text{tr}S^2) + \frac{1}{3}(\text{tr}S^3). \quad (12.132)$$

12.3.5 Isotropic Tensor Functions and Orthogonal Invariants

Let us now consider the isotropy of tensor functions. The *isotropy* of a tensor function with respect to a subgroup of the full orthogonal group means that the functional form remains unchanged if every quantity occurring as an argument or as the value is replaced by their rotated values obtained by any orthogonal transformation Q in the subgroup (Truesdell and Noll 1965; Leigh 1968).

For the sake of the subsequent discussion, we consider two orthogonal bases $\{\mathbf{e}_i\}$ and $\{\mathbf{e}'_i\}$ related by an orthogonal transformation Q

$$\mathbf{e}'_i = Q\mathbf{e}_i = Q_{ji}\mathbf{e}_j, \quad \mathbf{e}_i = Q^T\mathbf{e}'_i = (Q^T)_{j'i'}\mathbf{e}'_{j'}. \quad (12.133)$$

Denoting the components of a tensor S with respect to \mathbf{e}_i and \mathbf{e}'_i by S_{ij} and $S'_{i'j'}$, we have

$$S = S_{ij}\mathbf{e}_i \otimes \mathbf{e}_j = S'_{i'j'}\mathbf{e}'_{i'} \otimes \mathbf{e}'_{j'}, \quad (12.134a)$$

$$S'_{i'j'} = (Q^T)_{i'k'}S_{kl}Q_{l'j'}. \quad (12.134b)$$

Then the similar tensor \bar{S} is written as

$$\begin{aligned} \bar{S} &= QSQ^T = \bar{S}_{ij}\mathbf{e}_i \otimes \mathbf{e}_j \\ &= \bar{S}'_{i'j'}\mathbf{e}'_{i'} \otimes \mathbf{e}'_{j'} = S'_{i'j'}\mathbf{e}'_{i'} \otimes \mathbf{e}'_{j'}, \end{aligned} \quad (12.135)$$

where $\bar{S}_{ij}, \bar{S}'_{i'j'}$ are the components of \bar{S} with respect to the bases $\mathbf{e}_i, \mathbf{e}'_i$, and the last relation was derived by the use of Eq. (12.105b).

We suppose first a scalar valued tensor function

$$\varphi = f(\mathbf{S}). \quad (12.136)$$

According to the above definition, if the function $f(\mathbf{S})$ satisfies the relation

$$f(\mathbf{S}) = f(Q\mathbf{S}Q^T) \quad (12.137)$$

for every orthogonal transformation \mathbf{Q} , then we say that $f(\mathbf{S})$ is an *isotropic scalar-valued tensor function*.

Furthermore, a scalar-valued tensor function $f(\mathbf{S})$ is said to be an *orthogonal scalar invariant*, if the functional form of the function $f(\mathbf{S})$ expressed as a function of the components S_{ij} of the argument \mathbf{S} is the same for all orthogonal transformation of the basis:

$$f(S_{ij}, \mathbf{e}_i) = f(S_{ij}, Q\mathbf{e}_i). \quad (12.138)$$

This relation, together with Eqs. (12.133), (12.135), provides

$$\begin{aligned} f(\mathbf{S}) &= f(S_{ij}, \mathbf{e}_i) = f(S_{ij}, Q\mathbf{e}_i) \\ &= f(S_{ij}, \mathbf{e}_{i'}) = f(\bar{S}_{i'j'}, \mathbf{e}_{i'}) = f(Q\mathbf{S}Q^T), \end{aligned} \quad (12.139)$$

which is the same as Eq. (12.137). Hence, for a scalar-valued tensor function, the orthogonal invariance and the isotropy are equivalent.

In the case of a scalar-valued tensor function of several tensors $\mathbf{S}_1, \mathbf{S}_2, \dots, \mathbf{S}_k$

$$f = f(\mathbf{S}_1, \mathbf{S}_2, \dots, \mathbf{S}_k), \quad (12.140)$$

if we have the relation

$$f(\mathbf{S}_1, \mathbf{S}_2, \dots, \mathbf{S}_k) = f(Q\mathbf{S}_1Q^T, Q\mathbf{S}_2Q^T, \dots, Q\mathbf{S}_kQ^T) \quad (12.141)$$

for all \mathbf{S}_i and \mathbf{Q} , the function f is said to be *isotropic* and a *simultaneous orthogonal invariant*.

In the case of scalar-valued vector functions, if we have for all \mathbf{u}, \mathbf{u}_i and \mathbf{Q}

$$f(\mathbf{u}) = f(Q\mathbf{u}) \quad (12.142)$$

and

$$f(\mathbf{u}_1, \mathbf{u}_2, \dots, \mathbf{u}_k) = f(Q\mathbf{u}_1, Q\mathbf{u}_2, \dots, Q\mathbf{u}_k), \quad (12.143)$$

the functions $f(\mathbf{u})$ and $f(\mathbf{u}_1, \mathbf{u}_2, \dots, \mathbf{u}_k)$ are orthogonal invariant and simultaneous orthogonal invariant, respectively. Both of these functions are called *isotropic scalar-valued vector functions*.

We will now discuss the isotropy of a tensor-valued tensor function

$$\mathbf{T} = \mathbf{F}(\mathbf{S}). \quad (12.144)$$

Due to the definition of the isotropy, the tensor function \mathbf{F} is said to be an *isotropic tensor-valued tensor function*, if we have the relation

$$\mathbf{Q}\mathbf{T}\mathbf{Q}^T = \mathbf{F}(\mathbf{Q}\mathbf{S}\mathbf{Q}^T), \quad (12.145)$$

where \mathbf{Q} is an arbitrary orthogonal transformation.

As regards a function \mathbf{F} of several tensors $\mathbf{S}_1, \mathbf{S}_2, \dots$, and \mathbf{S}_k , \mathbf{F} is isotropic if a relation

$$\mathbf{Q}\mathbf{F}(\mathbf{S}_1, \mathbf{S}_2, \dots, \mathbf{S}_k)\mathbf{Q}^T = \mathbf{F}(\mathbf{Q}\mathbf{S}_1\mathbf{Q}^T, \mathbf{Q}\mathbf{S}_2\mathbf{Q}^T, \dots, \mathbf{Q}\mathbf{S}_k\mathbf{Q}^T) \quad (12.146)$$

holds for all \mathbf{S}_i and \mathbf{Q} .

By a similar argument, a vector-valued function $\mathbf{w}(\mathbf{S}, \mathbf{u})$ of a tensor \mathbf{S} and a vector \mathbf{u} is isotropic, if we have the relation

$$\mathbf{Q}\mathbf{w}(\mathbf{S}, \mathbf{u}) = \mathbf{w}(\mathbf{Q}\mathbf{S}\mathbf{Q}^T, \mathbf{Q}\mathbf{u}). \quad (12.147)$$

The notion of isotropy discussed in this section can be extended to the functions in which the values of the arguments and the function are arbitrary combination of scalar, vector and tensor of arbitrary order. If, in particular, the isotropy of a function is valid for a specific subgroup of the full orthogonal group, the function is said to be isotropic with respect to the subgroup.

12.4 Differentiation and Integral of Tensor Fields

When a scalar a , a vector \mathbf{u} and a tensor \mathbf{T} are defined as functions of the position \mathbf{x} of a material point P in some domain of a space, these functions $a(\mathbf{x})$, $\mathbf{u}(\mathbf{x})$ and $\mathbf{T}(\mathbf{x})$ are called a *scalar field*, a *vector field* and a *tensor field*, respectively.

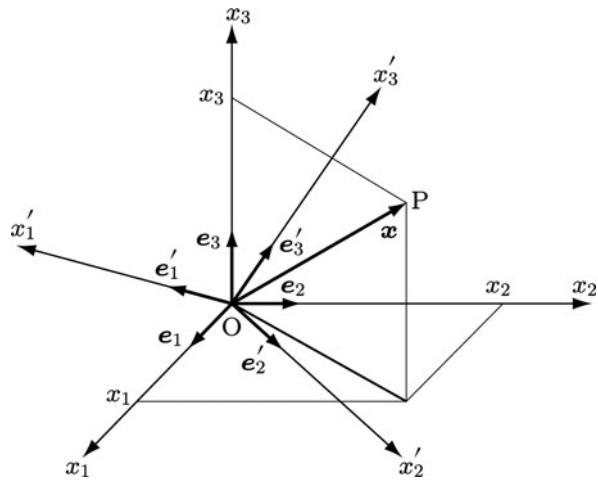
We will now discuss the differentiation and integral of tensor fields with respect to the position \mathbf{x} and the time t .

12.4.1 Euclidean Point Space and the Coordinate System

A space composed of a Euclidean vector space with an origin O, i.e., a reference point chosen arbitrarily in the space, is called an *Euclidean point space*. Then, any point P in a three-dimensional Euclidean point space \mathcal{P}^3 can be specified by a vector \overrightarrow{OP} as shown in Fig. 12.8. This vector is called a *position vector*.

Denoting the position vector of a point P by \mathbf{x} , we take two orthogonal coordinate systems O-x₁x₂x₃ and O-x'₁'x'₂'x'₃' sharing a common origin O as shown in Fig. 12.8.

Fig. 12.8 Orthogonal coordinate systems, basis vectors and a position vector



By the use of the orthonormal bases $\{\mathbf{e}_i\}$, $\{\mathbf{e}'_{i'}\}$ ($i, i' = 1, 2, 3$), the vector \mathbf{x} can be expressed in the form

$$\mathbf{x} = x_i \mathbf{e}_i = x'_{i'} \mathbf{e}'_{i'}, \quad (12.148)^3$$

where x_i , $x'_{i'}$ are the *coordinates* of the point P. If the orthogonal transformation from \mathbf{e}_i to $\mathbf{e}'_{i'}$ is denoted by \mathbf{Q} , Eq. (12.133) gives

$$\mathbf{e}'_{i'} = \mathbf{Q} \mathbf{e}_i = Q_{ji} \mathbf{e}_j, \quad (12.149a)$$

$$\mathbf{e}_i = \mathbf{Q}^T \mathbf{e}'_{i'} = (Q^T)_{j'i'} \mathbf{e}'_{j'} = Q_{j'i'} \mathbf{e}'_{j'}. \quad (12.149b)$$

Then, by applying Eq. (12.149) to \mathbf{e}_i and $\mathbf{e}'_{i'}$ of Eq. (12.148), the transformations between the coordinates x_i and $x'_{i'}$ are given:

$$x_i = Q_{ij} x'_{j'} = (\mathbf{e}_i \cdot \mathbf{e}'_{j'}) x'_{j'}, \quad (12.150a)$$

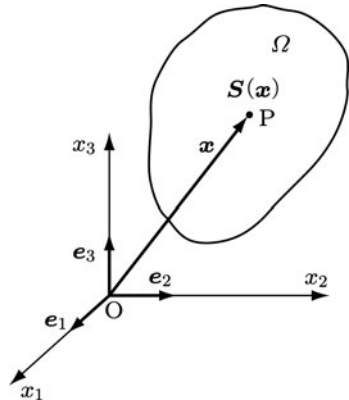
$$x'_{i'} = Q_{j'i'} x_j = (\mathbf{e}'_{i'} \cdot \mathbf{e}_j) x_j. \quad (12.150b)$$

12.4.2 Differentiation of Tensor Fields

Let us take a finite region Ω in a three-dimensional Euclidean point space \mathcal{P}^3 , and denote the position vector of a point in Ω by \mathbf{x} (Fig. 12.9). If we take a tensor function $\mathbf{S}(\mathbf{x})$ at a point \mathbf{x} , $\mathbf{S}(\mathbf{x})$ is expressed in terms of its components $S_{ij}(\mathbf{x})$ and the orthonormal basis $\{\mathbf{e}_i\}$, i.e.,

³A coordinate system based on an orthonormal basis is said to be an *orthonormal coordinate system*, or a *Cartesian coordinate system*.

Fig. 12.9 A finite region Ω and a tensor field in Euclidean point space



$$\mathbf{S}(\mathbf{x}) = S_{ij}(\mathbf{x}) \mathbf{e}_i \otimes \mathbf{e}_j. \quad (12.151)$$

When all the components $S_{ij}(\mathbf{x})$ of $\mathbf{S}(\mathbf{x})$ are continuous in the region Ω , the tensor field $\mathbf{S}(\mathbf{x})$ is said continuous in Ω . The function $\mathbf{S}(\mathbf{x})$ is differentiable in Ω if all the components are differentiable in Ω .

We define the *vector operator* (or *Nabla operator*, or *del operator*) ∇ by

$$\nabla \equiv \partial_i \mathbf{e}_i \equiv \frac{\partial}{\partial x_i} \mathbf{e}_i. \quad (12.152)$$

Equation (12.152) implies that the vector operator ∇ is a vector with the component $\partial_i \equiv \partial/\partial x_i$. Due to the *chain rule* and Eq. (12.150), we have

$$\partial_i = \frac{\partial}{\partial x_i} = \frac{\partial}{\partial x'_j} \frac{\partial x'_j}{\partial x_i} = Q_{i'j'} \partial_{j'}. \quad (12.153)$$

Thus the component of the vector operator is subject to the same coordinate transformation to Eq. (12.149). In view of Eqs. (12.153) and (12.149), it is expressed by

$$\nabla = \partial_i \mathbf{e}_i = (Q_{i'j'} \partial_{j'}) (Q_{i'k'} \mathbf{e}_{k'}) = \partial_{i'} \mathbf{e}_{i'}. \quad (12.154)$$

It will be observed from this equation that the operations of ∇ does not depend on the choice of the system of the orthonormal basis.

When the vector operator ∇ is applied to the fields of a scalar, vector and a tensor, different operations can be defined according to the way it is operated on them.

For a continuous and differentiable scalar field $f = f(\mathbf{x})$ in the region Ω , the *gradient* of $f(\mathbf{x})$ is defined as

$$\text{grad } f = \nabla f = \frac{\partial f}{\partial x_i} \mathbf{e}_i. \quad (12.155)$$

As to the gradient of a continuous and differentiable vector field $\mathbf{f}(\mathbf{x})$, we have several operations between ∇ and $\mathbf{f}(\mathbf{x})$, i.e., the tensor product, scalar product and the vector product. Moreover, each of these operators has two ways of operation; we have the case where the operator acts on the following quantity (acts to the right), and the case where it acts on the preceding quantity (acts to the left). Usual differentiation is the operation to the left.

Hence, for a vector field $\mathbf{f} = f(\mathbf{x})$, two types of gradient can be defined by

$$\text{grad } \mathbf{f} = \begin{cases} \mathbf{f} \otimes \nabla = (f_i \mathbf{e}_i) \otimes \frac{\partial}{\partial x_j} \mathbf{e}_j = \frac{\partial f_i}{\partial x_j} \mathbf{e}_i \otimes \mathbf{e}_j \\ \nabla \otimes \mathbf{f} = \frac{\partial}{\partial x_i} \mathbf{e}_i \otimes (f_j \mathbf{e}_j) = \frac{\partial f_j}{\partial x_i} \mathbf{e}_i \otimes \mathbf{e}_j \end{cases}. \quad (12.156a,b)$$

The *divergence* and the *curl* (or *rotation*) of a vector field, furthermore, are defined as follow:

$$\begin{aligned} \text{div } \mathbf{f} &= \mathbf{f} \cdot \nabla = \nabla \cdot \mathbf{f} \\ &= (f_i \mathbf{e}_i) \cdot \frac{\partial}{\partial x_j} \mathbf{e}_j = \frac{\partial}{\partial x_j} \mathbf{e}_i \cdot (f_i \mathbf{e}_j) = \frac{\partial f_i}{\partial x_i}, \end{aligned} \quad (12.157)$$

$$\text{curl } \mathbf{f} = \begin{cases} \mathbf{f} \times \nabla = (f_i \mathbf{e}_i) \times \frac{\partial}{\partial x_j} \mathbf{e}_j = \epsilon_{ijk} \frac{\partial f_i}{\partial x_j} \mathbf{e}_k \\ \nabla \times \mathbf{f} = \frac{\partial}{\partial x_i} \mathbf{e}_i \times (f_j \mathbf{e}_j) = \epsilon_{ijk} \frac{\partial f_j}{\partial x_i} \mathbf{e}_k \end{cases}. \quad (12.158a,b)$$

Finally, we have similar operations also for a tensor field of a n th-order tensor $\mathcal{T}(\mathbf{x})$:

$$\text{grad } \mathcal{T} = \begin{cases} \mathcal{T} \otimes \nabla \\ \nabla \otimes \mathcal{T} \end{cases}, \quad (12.159a,b)$$

$$\text{div } \mathcal{T} = \begin{cases} \mathcal{T} \cdot \nabla \\ \nabla \cdot \mathcal{T} \end{cases}, \quad (12.160a,b)$$

$$\text{curl } \mathcal{T} = \begin{cases} \mathcal{T} \times \nabla \\ \nabla \times \mathcal{T} \end{cases}, \quad (12.161a,b)$$

which are called the gradient, divergence and the curl of the tensor field $\mathcal{T}(\mathbf{x})$. It is easily seen from these equations that the gradient, divergence and the curl of a n th-order tensor, including a vector, give another tensor of order $n + 1$, $n - 1$ and n , respectively.

12.4.3 Integral of Tensor Fields and Gauss' Theorem

Suppose a convex region V bounded by a smooth surface S in \mathcal{P}^3 as shown in Fig. 12.10. The volume integral and the surface integral of a differentiable tensor field $\mathcal{T}(x)$ in this region can be written respectively

$$\int_V \mathcal{T} dV = \left(\int_V T_{i_1 i_2 \dots i_n} dV \right) \mathbf{e}_{i_1} \otimes \mathbf{e}_{i_2} \otimes \dots \otimes \mathbf{e}_{i_n}, \quad (12.162a)$$

$$\int_S \mathcal{T} dS = \left(\int_S T_{i_1 i_2 \dots i_n} dS \right) \mathbf{e}_{i_1} \otimes \mathbf{e}_{i_2} \otimes \dots \otimes \mathbf{e}_{i_n}. \quad (12.162b)$$

Hence, if a tensor is expressed in terms of its components with respect to a orthonormal basis $\{\mathbf{e}_i\}$, the integral of the tensor field is given by the integral of its components.

For a scalar field $f(x)$ differentiable in the region V , we have the following relation between the volume and the surface integral

$$\int_V \operatorname{grad} f dV = \int_V \nabla f dV = \int_S f \mathbf{n} dS, \quad (12.163a)$$

or

$$\int_V \frac{\partial f}{\partial x_i} dV = \int_S f n_i dS, \quad (12.163b)$$

where \mathbf{n} and n_i are the outward unit normal vector and its component. The relation of Eq. (12.163) is known as *Gauss' theorem*.

For the proof of Eq. (12.163), by taking the integral of the left hand-side of this relation along a segment L of Fig. 12.10, we have

$$\iiint_V \frac{\partial f}{\partial x_1} dx_1 dx_2 dx_3 = \iint_S (f^* - f^{**}) dx_2 dx_3, \quad (12.164)$$

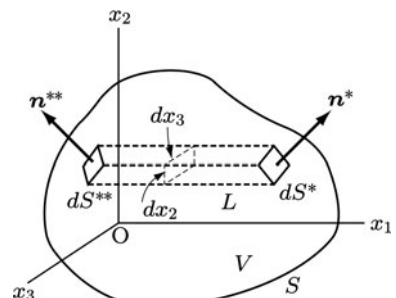


Fig. 12.10 Derivation of Gauss' theorem

where f^* and f^{**} are the values of f at the right and the left end of a line parallel to the x_1 -axis, respectively. Let dS^* and dS^{**} be the surface elements at the ends of the segment L . If the components of the outward unit normal vectors \mathbf{n}^* , \mathbf{n}^{**} at both ends are denoted by n_i^* , n_i^{**} , we have a relation

$$dx_2 dx_3 = n_1^* dS^* = -n_1^{**} dS^{**}. \quad (12.165)$$

Substitution of this equation into the right hand-side of Eq. (12.164) gives

$$\begin{aligned} \iint_S (f^* - f^{**}) dx_2 dx_3 &= \iint_S (f^* n_1^* dS^* + f^{**} n_1^{**} dS^{**}) \\ &= \int_S f n_1 dS. \end{aligned} \quad (12.166)$$

Then Eq. (12.164) leads to

$$\int_V \frac{\partial f}{\partial x_1} dV = \int_S f n_1 dS, \quad (12.167)$$

and thus Eq. (12.163) has been proved.

We have similar relations for a differentiable vector fields $\mathbf{f}(x)$ and a tensor field of n th-order $\mathcal{T}(x)$ as follow:

$$\int_V \operatorname{div} \mathbf{f} dV = \int_V \mathbf{f} \cdot \nabla dV = \int_S \mathbf{n} \cdot \mathbf{f} dS, \quad (12.168a)$$

$$\int_V \frac{\partial f_i}{\partial x_i} dV = \int_S f_i dS, \quad (12.168b)$$

$$\int_V \operatorname{div} \mathcal{T} dV = \begin{cases} \int_V \mathcal{T} \cdot \nabla dV = \int_S \mathcal{T} \cdot \mathbf{n} dS \\ \int_V \nabla \cdot \mathcal{T} dV = \int_S \mathbf{n} \cdot \mathcal{T} dS \end{cases}, \quad (12.169a,b)$$

$$\int_V \frac{\partial T_{i_1 i_2 \dots i_{n-1} j}}{\partial x_j} dV = \int_S n_j T_{i_1 i_2 \dots i_{n-1} j} dS, \quad (12.169c)$$

$$\int_V \frac{\partial T_{j i_2 i_3 \dots i_n}}{\partial x_j} dV = \int_S n_j T_{j i_2 i_3 \dots i_n} dS. \quad (12.169d)$$

Equation (12.168), in particular, represents the transformation of the volume integral of the divergence $\mathbf{f} \cdot \nabla$, and thus is called *Gauss' divergence theorem*.

Gauss' theorem holds also for other differential operations, and can be expressed in a unified form

$$\int_V \nabla * \mathcal{A} dV = \int_S \mathbf{n} * \mathcal{A} dS, \quad (12.170)$$

where “**” denotes either of the scalar product (\cdot) , tensor product (\otimes) or vector product (\times) , while \mathcal{A} signifies either of a scalar field, vector field or a tensor field. Gauss'

theorem discussed above is applicable not only to a convex regular region, but also to arbitrary regions which can be divided into finite number of the convex regular regions.

12.4.4 Material Time Derivative and Reynolds' Transport Theorem

In continuum mechanics, we often need to discuss the change in different field variables with the laps of time, in addition to the change in its position \mathbf{x} . Let $\mathcal{A}(\mathbf{x}, t)$ represent any of a scalar, vector and a tensor field. The rate of change of \mathcal{A} with respect to the time t at a fixed point \mathbf{x} is given by its partial derivative $\partial\mathcal{A}(\mathbf{x}, t)/\partial t$.

Then let us suppose another rate of change of \mathcal{A} which is measured on a *given* particle moving at a velocity \mathbf{v} . We represent it by $\dot{\mathcal{A}} = D\mathcal{A}/Dt$. Since the position of the particle moves from x_k to $x_k + v_k dt$ in an interval of time dt , we have

$$\begin{aligned}\dot{\mathcal{A}}(x_k, t)dt &= \mathcal{A}(x_k + v_k dt, t + dt) - \mathcal{A}(x_k, t) \\ &= \mathcal{A}(x_k, t) + \frac{\partial\mathcal{A}}{\partial x_k} v_k dt + \frac{\partial\mathcal{A}}{\partial t} dt - \mathcal{A}(x_k, t) + O(dt^2) \\ &= \frac{\partial\mathcal{A}}{\partial t} dt + \frac{\partial\mathcal{A}}{\partial x_k} v_k dt + O(dt^2).\end{aligned}\quad (12.171)$$

Hence $\dot{\mathcal{A}}$ is given as follows

$$\begin{aligned}\dot{\mathcal{A}} &\equiv \frac{D\mathcal{A}}{Dt} = \lim_{dt \rightarrow 0} \frac{1}{dt} [\mathcal{A}(x_k + v_k dt, t + dt) - \mathcal{A}(x_k, t)] \\ &= \frac{\partial\mathcal{A}}{\partial t} + \frac{\partial\mathcal{A}}{\partial x_k} v_k.\end{aligned}\quad (12.172)$$

The rate of change of \mathcal{A} given by this relation is called *material time derivative*, or simply *material derivative* of \mathcal{A} .

In the cases of a scalar f , vector \mathbf{f} and a tensor \mathbf{F} , the specific forms of Eq. (12.172) are expressed as follows:

$$\dot{f} = \frac{Df}{Dt} = \frac{\partial f}{\partial t} + \frac{\partial f}{\partial x_k} v_k = \frac{\partial f}{\partial t} + \frac{\partial f}{\partial x_k} \mathbf{v} \cdot \text{grad } f, \quad (12.173)$$

$$\dot{\mathbf{f}} = \frac{D\mathbf{f}}{Dt} = \frac{\partial \mathbf{f}}{\partial t} + \mathbf{v} \cdot \text{grad } \mathbf{f}, \quad (12.174a)$$

$$\dot{\mathbf{f}}_i = \frac{Df_i}{Dt} = \frac{\partial f_i}{\partial t} + v_k \frac{\partial f_i}{\partial x_k}, \quad (12.174b)$$

$$\dot{\mathbf{F}} = \frac{D\mathbf{F}}{Dt} = \frac{\partial \mathbf{F}}{\partial t} + \mathbf{v} \cdot \text{grad } \mathbf{F}, \quad (12.175a)$$

$$\dot{F}_{ij} = \frac{DF_{ij}}{Dt} = \frac{\partial F_{ij}}{\partial t} + v_k \frac{\partial F_{ij}}{\partial x_k}. \quad (12.175b)$$

In continuum mechanics, we often need to compute the material time derivative of the volume integral of physical quantities. In this case, the variation of the volume integral consists not only of the change of the integrand but also of the change in the region of integration.

Suppose again a continuously differentiable field $\mathcal{A}(x, t)$ defined in a region V , and write the volume integral of \mathcal{A} as

$$\mathcal{J}(t) = \iiint_V \mathcal{A}(x, t) dx_1 dx_2 dx_3, \quad (12.176)$$

where the symbol \mathcal{A} stands for any of a scalar, vector and a tensor field.

Let V and V' be the regions at times t and $t + dt$ occupied by the same set of particles as shown in Fig. 12.11. Then, the material time derivative of $\mathcal{J}(t)$ in Eq. (12.176) can be calculated by noting the change of the region V at time t into the corresponding region V' at time $t + dt$. Thus the material time derivative of $\mathcal{J}(t)$ can be written

$$\frac{D\mathcal{J}}{Dt} = \lim_{dt \rightarrow 0} \frac{1}{dt} \left[\int_{V'} \mathcal{A}(x, t + dt) dV - \int_V \mathcal{A}(x, t) dV \right]. \quad (12.177)$$

If we denote the region $V' - V$ by ΔV , ΔV is the volume which the boundary S has swept during the time interval dt . Since $V' = V + \Delta V$, Eq. (12.177) leads to

$$\begin{aligned} \frac{D\mathcal{J}}{Dt} &= \lim_{dt \rightarrow 0} \frac{1}{dt} \left[\int_V \mathcal{A}(x, t + dt) dV + \int_{\Delta V} \mathcal{A}(x, t + dt) dV - \int_V \mathcal{A}(x, t) dV \right] \\ &= \lim_{dt \rightarrow 0} \left\{ \frac{1}{dt} \int_V [\mathcal{A}(x, t + dt) - \mathcal{A}(x, t)] dV + \frac{1}{dt} \int_{\Delta V} \mathcal{A}(x, t + dt) dV \right\}, \end{aligned} \quad (12.178)$$

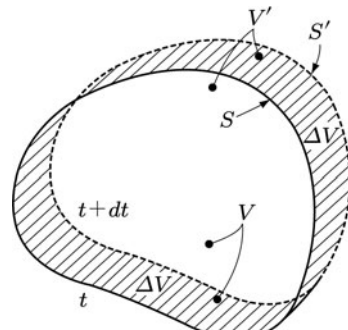


Fig. 12.11 Continuously changing region of integration

where the integral of the second term in the braces { } on the right hand-side represents the rate of change in the product of ΔV and $\mathcal{A}(\mathbf{x}, t)$. If n_i and v_i are the outward unit normal vector of S and the velocity of a particle at a point on S , the volume swept by a surface element dS in dt is $dV = v_i n_i dS dt$. Therefore Eq. (12.178) can be written in the form

$$\begin{aligned}\frac{D\mathcal{J}}{Dt} &= \frac{D}{Dt} \int_V \mathcal{A} dV \\ &= \int_V \frac{\partial \mathcal{A}}{\partial t} dV + \int_S \mathcal{A} v_i n_i dS.\end{aligned}\quad (12.179)$$

This important relation is known as *Reynolds' transport theorem*, and is applicable to any of a scalar, vector and a tensor field.

By rewriting the last integral by the use of Gauss' theorem (12.168) and the material time derivative of Eq. (12.172), Eq. (12.179) can be expressed also in the form

$$\begin{aligned}\frac{D}{Dt} \int_V \mathcal{A} dV &= \int_V \left[\frac{\partial \mathcal{A}}{\partial t} dV + \frac{\partial}{\partial x_i} (\mathcal{A} v_i) \right] dV \\ &= \int_V \left(\frac{D\mathcal{A}}{Dt} + \mathcal{A} \frac{\partial v_i}{\partial x_i} \right) dV.\end{aligned}\quad (12.180)$$

12.5 Differential Calculus of Tensor Functions

Differential calculus of a vector or a tensor function in the direct notation appears often in continuum damage mechanics. The ordinary operation of scalar functions, however, may not be applicable to this calculus. In this section, we first define the derivative of a vector-valued function of a vector. Then we extend it to more general tensor functions.

12.5.1 Total Differential and Derivative

Let \mathbf{f} , \mathbf{u} and \mathbf{v} be vectors in Euclidean vector space, and h be a scalar of real value. We suppose a vector-valued vector function $\mathbf{f}(\mathbf{u})$, and consider the variation of \mathbf{f} with respect to a small increment in the argument \mathbf{u} . Then, the *total differential* $\mathbf{f}'(\mathbf{u}; \mathbf{v})$ of \mathbf{f} at \mathbf{u} with increment \mathbf{v} is defined to be

$$\begin{aligned}\mathbf{f}'(\mathbf{u}; \mathbf{v}) &= \lim_{h \rightarrow 0} \frac{1}{h} [\mathbf{f}(\mathbf{u} + h\mathbf{v}) - \mathbf{f}(\mathbf{u})] \\ &= \frac{d}{dh} \mathbf{f}(\mathbf{u} + h\mathbf{v}) |_{h=0}.\end{aligned}\quad (12.181)$$

If $f'(\mathbf{u}; \mathbf{v})$ exists and is continuous in \mathbf{u} for every \mathbf{u} and \mathbf{v} in the domain of definition, f is said to be continuously differentiable. Since Eq. (12.181) can be extended to more general tensor functions, it may be called the *basic definition* of the total differential.

For an arbitrary scalar a , Eq. (12.181) gives

$$f'(\mathbf{u}; a\mathbf{v}) = af'(\mathbf{u}; \mathbf{v}). \quad (12.182)$$

Furthermore, for any vector \mathbf{t} in the same space as \mathbf{v} , Eq. (12.181) leads to

$$\begin{aligned} f'(\mathbf{u}; \mathbf{v} + \mathbf{t}) &= \lim_{h \rightarrow 0} \frac{1}{h} [f(\mathbf{u} + h\mathbf{v} + ht) - f(\mathbf{u} + ht)] \\ &\quad + \lim_{h \rightarrow 0} \frac{1}{h} [f(\mathbf{u} + ht) - f(\mathbf{u})] = f'(\mathbf{u}; \mathbf{v}) + f'(\mathbf{u}; \mathbf{t}). \end{aligned} \quad (12.183)$$

Equations (12.182) and (12.183) imply that $f'(\mathbf{u}; \mathbf{v})$ is a linear transformation of \mathbf{v} , and thus we can write

$$f'(\mathbf{u}; \mathbf{v}) = f'(\mathbf{u})\mathbf{v}, \quad (12.184)$$

where $f'(\mathbf{u})$ is a linear transformation, or a tensor which transforms the vector \mathbf{v} to the total differential $f'(\mathbf{u}; \mathbf{v})$. The tensor $f'(\mathbf{u})$ is called the *derivative* of f at \mathbf{u} , and is written also as $\partial f / \partial \mathbf{u}$ or $\partial_i f$.

The chain rule can be used also for the derivatives of a vector-valued vector function $\mathbf{f}(\mathbf{u})$ and a tensor-valued vector function $\mathbf{F}(\mathbf{u})$. For instance, for the derivative of a composed function $\mathbf{G}(\mathbf{u}) = \mathbf{G}(\mathbf{F}(\mathbf{u}))$, we have the chain rule

$$\mathbf{G}'(\mathbf{u}) = \mathbf{G}'(\mathbf{F})\mathbf{F}'(\mathbf{u}). \quad (12.185)$$

When \mathbf{u} of the function $\mathbf{F}(\mathbf{u})$ is a function of a scalar variable t , Eq. (12.185) gives

$$\dot{\mathbf{F}}(t) = \frac{d}{dt} \mathbf{F}(\mathbf{u}(t)) = \mathbf{F}'(\mathbf{u})\dot{\mathbf{u}}. \quad (12.186)$$

12.5.2 Derivative of Tensor Functions

As the application of the basic definition (12.181) of the total derivative, we now calculate the derivative of four representative examples of tensor functions.

(1) Scalar-Valued Vector Function $f(\mathbf{u})$

According to Eqs. (12.181) and (12.184), the total differential of a scalar-valued vector function $f(\mathbf{u})$ is derived as follows:

$$\begin{aligned} f'(\mathbf{u}; \mathbf{v}) &= \lim_{h \rightarrow 0} \frac{1}{h} [f(\mathbf{u} + h\mathbf{v}) - f(\mathbf{u})] \\ &= f'(\mathbf{u})\mathbf{v}. \end{aligned} \quad (12.187)$$

By using the orthonormal basis $\{\mathbf{e}_i\}$ ($i = 1, 2, 3$), we have

$$\mathbf{u} = u_k \mathbf{e}_k, \quad \mathbf{v} = v_k \mathbf{e}_k. \quad (12.188)$$

In a particular case of $\mathbf{v} = \mathbf{e}_k$, Eq. (12.187) leads to

$$\begin{aligned} f'(\mathbf{u}; \mathbf{e}_k) &= \lim_{h \rightarrow 0} \frac{1}{h} [f(\mathbf{u} + h\mathbf{e}_k) - f(\mathbf{u})] \\ &= \lim_{h \rightarrow 0} \frac{1}{h} [f((u_l + h\delta_{lk}) \mathbf{e}_l) - f(u_l \mathbf{e}_l)]. \end{aligned} \quad (12.189)$$

Since the basis \mathbf{e}_l is not affected by the operation of the right-hand side, Eq. (12.189) is written as

$$\begin{aligned} f'(\mathbf{u}; \mathbf{e}_k) &= \lim_{h \rightarrow 0} \frac{1}{h} [f(u_l + h\delta_{lk}) - f(u_l)] \\ &= \frac{\partial f(u_l)}{\partial u_k}, \end{aligned} \quad (12.190)$$

which is identical to the classical partial derivative of a scalar-valued scalar function. Thus we have

$$f'(\mathbf{u}; \mathbf{v}) = f'(\mathbf{u}; v_k \mathbf{e}_k) = f'(\mathbf{u}; \mathbf{e}_k)v_k = \frac{\partial f}{\partial u_k} v_k. \quad (12.191)$$

Comparison of this equation with Eq. (12.187) gives the derivative $f'(\mathbf{u})$ of this function $f(\mathbf{u})$:

$$f'(\mathbf{u}) = \frac{\partial f}{\partial \mathbf{u}} = \frac{\partial f}{\partial u_k} \mathbf{e}_k. \quad (12.192)$$

(2) Scalar-Valued Tensor Function $f(\mathbf{S})$

Equation (12.181) can be applied also to a scalar-valued tensor function. Let \mathbf{C} be an arbitrary tensor in the same vector space as a tensor \mathbf{S} . Then the total differential of $f(\mathbf{S})$ with increment \mathbf{C} is given as

$$f'(\mathbf{S}; \mathbf{C}) = f'(\mathbf{S})\mathbf{C}, \quad (12.193)$$

where the derivative $f'(\mathbf{S})$ stands for a linear transformation which transforms a tensor \mathbf{C} into the total differential $f'(\mathbf{S}; \mathbf{C})$.

By the same procedure as for $f(\mathbf{u})$ above, we obtain

$$f'(\mathbf{S}; \mathbf{C}) = f'(\mathbf{S}; C_{ij} \mathbf{e}_i \otimes \mathbf{e}_j) = f'(\mathbf{S}; \mathbf{e}_i \otimes \mathbf{e}_j) C_{ij} = \frac{\partial f}{\partial S_{ij}} C_{ij}. \quad (12.194)$$

This relation can be written also in the form

$$f'(\mathbf{S}; \mathbf{C}) = \text{tr} \left[\left(\frac{\partial f}{\partial \mathbf{S}} \right)^T \mathbf{C} \right]. \quad (12.195)$$

Comparing this with Eq. (12.193), we see that $f'(\mathbf{S})$ is given by

$$f'(\mathbf{S}) = \text{tr} \left[\left(\frac{\partial f}{\partial \mathbf{S}} \right)^T \right]. \quad (12.196)$$

This relation is useful when we calculate the derivative in direct notation; e.g., when we calculate the derivative of a thermodynamic potential expressed as a function of a tensor or its invariants. The example will be found in the following Section 12.5.3.

(3) Tensor-Valued Vector Function $\mathbf{F}(\mathbf{u})$

If \mathbf{v} is an arbitrary vector in the same vector space as \mathbf{u} , the total differential and the derivative of a tensor-valued vector function is given by

$$\mathbf{F}'(\mathbf{u}; \mathbf{v}) = \mathbf{F}'(\mathbf{u})\mathbf{v}. \quad (12.197)$$

Expressing \mathbf{F} and \mathbf{u} in an orthonormal basis $\{\mathbf{e}_i\}$, we have

$$\mathbf{F}(\mathbf{u}) = F(u_i, \mathbf{e}_i)_{jk} \mathbf{e}_j \otimes \mathbf{e}_k. \quad (12.198)$$

Since the basis is not affected by the operation of total differential, Eq. (12.198) gives

$$\mathbf{F}'(\mathbf{u}) = \frac{\partial F_{jk}}{\partial u_i} \mathbf{e}_j \otimes \mathbf{e}_k \otimes \mathbf{e}_i. \quad (12.199)$$

(4) Tensor-Valued Tensor Function $\mathbf{F}(\mathbf{S})$

Lastly we consider the derivative of a tensor-valued tensor function $\mathbf{F}(\mathbf{S})$:

$$\mathbf{F}'(\mathbf{S}; \mathbf{C}) = \mathbf{F}'(\mathbf{S})\mathbf{C}. \quad (12.200)$$

A similar procedure to the above gives

$$\mathbf{F}'(\mathbf{S}) = \frac{\partial F_{ij}}{\partial S_{kl}} \mathbf{e}_i \otimes \mathbf{e}_j \otimes \mathbf{e}_k \otimes \mathbf{e}_l. \quad (12.201)$$

12.5.3 Derivatives of Invariants

Derivatives of the principal invariants defined by Eq. (12.121) often appear in continuum mechanics. We will derive now the derivative of a scalar-valued tensor function $f(\mathbf{S}) = \text{tr}\mathbf{S}^k$ by applying the basic definition (12.181) of the total differential.

Suppose a scalar-valued tensor function $\text{tr}(\mathbf{S} + h\mathbf{C})^k$ with an arbitrary tensor \mathbf{C} in the space same to \mathbf{S} and an arbitrary scalar h of real value. By expanding $(\mathbf{S} + h\mathbf{C})^k$ into a polynomial and taking terms up to the first-order of h , we have

$$\begin{aligned} (\mathbf{S} + h\mathbf{C})^k &= \mathbf{S}^k + h(\mathbf{S}^{k-1}\mathbf{C} + \mathbf{S}^{k-2}\mathbf{CS} + \dots \\ &\quad + \mathbf{SCS}^{k-2} + \mathbf{CS}^{k-1}) + O(h^2). \end{aligned} \quad (12.202a)$$

The trace of this relation gives

$$\text{tr}(\mathbf{S} + h\mathbf{C})^k = \text{tr}\mathbf{S}^k + hk\text{tr}(\mathbf{S}^{k-1}\mathbf{C}) + O(h^2), \quad (12.202b)$$

where the order of the terms within a trace has been altered by the use of Eq. (12.111). Then application of Eqs. (12.181) and (12.195) to Eq. (12.202) leads to

$$\begin{aligned} f'(\mathbf{S}; \mathbf{C}) &= \text{tr} \left[\left(\frac{\partial \text{tr}\mathbf{S}^k}{\partial \mathbf{S}} \right)^T \mathbf{C} \right] = \lim_{h \rightarrow 0} \frac{1}{h} [\text{tr}(\mathbf{S} + h\mathbf{C})^k - \text{tr}\mathbf{S}^k] \\ &= k\text{tr}(\mathbf{S}^{k-1}\mathbf{C}). \end{aligned} \quad (12.203)$$

Since this relation must hold for an arbitrary \mathbf{C} , we finally have the derivative of $\text{tr}\mathbf{S}^k$

$$\frac{\partial \text{tr}\mathbf{S}^k}{\partial \mathbf{S}} = k(\mathbf{S}^{k-1})^T. \quad (12.204)$$

By means of this relation, the derivatives of the first and the second invariants I_1 , I_2 of Eq. (12.121) can be readily derived

$$\frac{\partial I_1}{\partial \mathbf{S}} = \mathbf{I}, \quad \frac{\partial I_2}{\partial \mathbf{S}} = (\text{tr}\mathbf{S})\mathbf{I} - \mathbf{S}^T. \quad (12.205)$$

The derivative of the third invariant $I_3 = \det\mathbf{S}$ of Eq. (12.121), however, necessitates the derivative of the determinant. We write first

$$\begin{aligned} \det(\mathbf{S} + h\mathbf{C}) &= \det \left[h\mathbf{S} \left(\frac{1}{h}\mathbf{I} + \mathbf{S}^{-1}\mathbf{C} \right) \right] \\ &= h^3(\det\mathbf{S}) \det \left(\frac{1}{h}\mathbf{I} + \mathbf{S}^{-1}\mathbf{C} \right). \end{aligned} \quad (12.206)$$

Then by rewriting $S^{-1}C = \bar{S}$, $-(1/h) = \bar{\lambda}$ and applying Eq. (12.120) to the last factor of Eq. (12.206), we have

$$\begin{aligned}\det\left(\frac{1}{h}\mathbf{I} + S^{-1}C\right) &= -\bar{\lambda}^3 + I_1(\bar{S})\bar{\lambda}^2 - I_2(\bar{S})\bar{\lambda} + I_3(\bar{S}) \\ &= h^{-3} + I_1(S^{-1}C)h^{-2} + I_2(S^{-1}C)h^{-1} + I_3(S^{-1}C).\end{aligned}\quad (12.207)$$

Substitution of this relation into the right-hand side of Eq. (12.206) furnishes

$$\begin{aligned}\det(S + hC) &= (\det S)[1 + hI_1(S^{-1}C) + h^2I_2(S^{-1}C) \\ &\quad + h^3I_3(S^{-1}C)].\end{aligned}\quad (12.208)$$

Applying further the basic definition (12.181) of the total differential to this relation, we obtain

$$I'_3(S; C) = (\det S)I_1(S^{-1}C) = \text{tr}[(\det S)S^{-1}C].\quad (12.209)$$

If we compare Eq. (12.209) with Eq. (12.195) and note that C is an arbitrary tensor, we finally arrive at the derivative of $I_3 = \det S$

$$\begin{aligned}\frac{\partial I_3}{\partial S} &= \frac{\partial(\det S)}{\partial S} \\ &= (\det S)S^{-T} = I_3S^{-T}.\end{aligned}\quad (12.210)$$

The derivative of I_3 can be derived simply also by differentiating Eq. (12.132) by the use of Eq. (12.204)

$$\frac{\partial I_3}{\partial S} = I_2\mathbf{I} - I_1S^T + (S^2)^T.\quad (12.211)$$

In view of the Cayley-Hamilton theorem (12.131b), Eq. (12.211) leads exactly to Eq. (12.210).

12.6 Representation Theorem for Tensor Functions

The orthogonal invariance and the isotropy of tensor functions were discussed in Section 12.3.5. Here we will elucidate the general representations of the orthogonal scalar invariants (i.e., the isotropic scalar-valued tensor functions) and the isotropic tensor-valued tensor functions.

12.6.1 Scalar Invariants of Tensors and Vectors

Let us discuss first a general form of function which the scalar invariant $f(\mathbf{S})$ of a symmetric tensor \mathbf{S} has.

When eigenvectors $\mathbf{u}^{(i)}$ ($i = 1, 2, 3$) are taken as the orthonormal basis $\{\mathbf{u}^{(i)}\}$, a tensor \mathbf{S} is expressed in the form of the spectral decomposition of (12.130). The eigenvalues λ_i are independent of all the orthogonal transformation of the basis. Therefore an invariant $f(\mathbf{S})$ of a symmetric tensor \mathbf{S} can be given by a symmetric function of λ_i ; i.e.,

$$f(\mathbf{S}) = f(\lambda_1, \lambda_2, \lambda_3). \quad (12.212)$$

Since λ_i are the roots of Eq. (12.120), λ_i can be specified by the coefficients of the equation, or by the principal invariants I_i ($i = 1, 2, 3$):

$$\lambda_i = \lambda_i(I_1, I_2, I_3). \quad (12.213)$$

Then substitution of Eq. (12.213) into Eq. (12.212) implies that the most general expression of the *orthogonal scalar invariants* of a symmetric tensor is given by

$$\begin{aligned} f(\mathbf{S}) &= f(I_1, I_2, I_3) \\ &= f(\text{tr}\mathbf{S}, \text{tr}\mathbf{S}^2, \text{tr}\mathbf{S}^3). \end{aligned} \quad (12.214)$$

The derivation of an invariant function of plural symmetric tensors or that of symmetric tensors and vectors is much more complicated. Thus, without detailed explanation, the general expression of the *simultaneous orthogonal invariants* $f(\mathbf{S}, \mathbf{T})$ of two symmetric tensors \mathbf{S}, \mathbf{T} and those of $f(\mathbf{S}, \mathbf{u})$ of a symmetric tensor \mathbf{S} and a vector \mathbf{u} are given as follow (Truesdell and Noll 1965; Leigh 1968; Spencer 1971):

$$\begin{aligned} f(\mathbf{S}, \mathbf{T}) &= f\{\text{tr}\mathbf{S}, \text{tr}\mathbf{S}^2, \text{tr}\mathbf{S}^3, \text{tr}\mathbf{T}, \text{tr}\mathbf{T}^2, \text{tr}\mathbf{T}^3, \\ &\quad \text{tr}(\mathbf{ST}), \text{tr}(\mathbf{ST}^2), \text{tr}(\mathbf{S}^2\mathbf{T}), \text{tr}(\mathbf{S}^2\mathbf{T}^2)\}, \end{aligned} \quad (12.215)$$

$$f(\mathbf{S}, \mathbf{u}) = f\{\text{tr}\mathbf{S}, \text{tr}\mathbf{S}^2, \mathbf{u}^2, \mathbf{u} \cdot \mathbf{S}\mathbf{u}, \mathbf{u} \cdot \mathbf{S}^2\mathbf{u}, \mathbf{u} \cdot \mathbf{S}^3\mathbf{u}\} \quad (12.216)$$

In Eq. (12.215), it has been assumed that the eigenvalues of one of the two tensors \mathbf{S}, \mathbf{T} are distinct.

12.6.2 Isotropic Tensor Functions of Tensors and Vectors

Suppose an isotropic tensor-valued tensor function

$$\mathbf{T} = \mathbf{F}(\mathbf{S}). \quad (12.217)$$

According to the argument of Section 12.3.5, a relation

$$\mathbf{Q}\mathbf{F}(\mathbf{S})\mathbf{Q}^T = \mathbf{F}(\mathbf{Q}\mathbf{S}\mathbf{Q}^T) \quad (12.218)$$

should hold for every orthogonal transformation \mathbf{Q} .

Then, let us now derive a general representation of such a function when \mathbf{S} and \mathbf{T} are symmetric. It can be proved that, when Eq. (12.218) holds, all the principal directions of \mathbf{S} are also the principal directions of $\mathbf{T} = \mathbf{F}(\mathbf{S})$. Let such principal directions be $\mathbf{u}^{(i)}$ ($i = 1, 2, 3$), and the corresponding principal values of \mathbf{S} and \mathbf{T} be λ_i and μ_i , respectively. Then the most general representation of the function (12.217) is

$$\mu_i = \mu_i(\lambda_i) = \varphi_0 + \varphi_1\lambda_i + \varphi_2\lambda_i^2 \quad (i = 1, 2, 3), \quad (12.219)$$

where φ_0 , φ_1 and φ_2 are the functions of λ_i ($i = 1, 2, 3$).

By noting that the principal directions of \mathbf{S} and \mathbf{T} are the same, it will be observed that Eq. (12.219) is the relation between the diagonal components of the matrix representation of a tensor relation

$$\mathbf{T} = \mathbf{F}(\mathbf{S}) = \varphi_0(\lambda_i)\mathbf{I} + \varphi_1(\lambda_i)\mathbf{S} + \varphi_2(\lambda_i)\mathbf{S}^2. \quad (12.220a)$$

Namely, Eq. (12.220a) is the most general representation of an *isotropic tensor-valued tensor function*. Since λ_i are functions of the principal invariants I_i ($i = 1, 2, 3$), Eq. (12.220a) can be expressed also in a form

$$\mathbf{T} = \mathbf{F}(\mathbf{S}) = \psi_0(I_i)\mathbf{I} + \psi_1(I_i)\mathbf{S} + \psi_2(I_i)\mathbf{S}^2. \quad (12.220b)$$

As a special case where $\mathbf{F}(\mathbf{S})$ is a linear isotropic tensor function $\mathbf{L}[\mathbf{S}]$, Eq. (12.220) is reduced to

$$\mathbf{T} = \mathbf{L}[\mathbf{S}] = a_0(\text{tr}\mathbf{S})\mathbf{I} + a_1\mathbf{S}, \quad (12.221)$$

where a_0 and a_1 denote constants.

General representations for isotropic tensor functions of plural symmetric tensors and those for symmetric tensors and vectors have been elucidated also. By leaving the details of the results to the references (Truesdell and Noll 1965; Spencer 1971), we show here two important results.

The general representation of the *isotropic tensor-valued function* $\mathbf{F}(\mathbf{S}, \mathbf{T})$ of two tensors \mathbf{S} and \mathbf{T} is given as

$$\begin{aligned} \mathbf{F}(\mathbf{S}, \mathbf{T}) &= \psi_0\mathbf{I} + \psi_1\mathbf{S} + \psi_2\mathbf{T} + \psi_3\mathbf{S}^2 + \psi_4\mathbf{T}^2 \\ &\quad + \psi_5(\mathbf{S}\mathbf{T} + \mathbf{T}\mathbf{S}) + \psi_6(\mathbf{S}^2\mathbf{T} + \mathbf{T}\mathbf{S}^2) \\ &\quad + \psi_7(\mathbf{S}\mathbf{T}^2 + \mathbf{T}^2\mathbf{S}) + \psi_8(\mathbf{S}^2\mathbf{T}^2 + \mathbf{T}^2\mathbf{S}^2), \end{aligned} \quad (12.222)$$

where $\psi_0, \psi_1 \dots, \psi_8$ are the functions of ten basic invariants shown in Eq. (12.215).

The general representation of *isotropic vector-valued function* $f(S, u)$ of a symmetric tensor S and a vector u are

$$f(S, u) = (\varphi_0 I + \varphi_1 S + \varphi_2 S^2) u, \quad (12.223)$$

where φ_0 , φ_1 and φ_2 are the functions of the invariants given in Eq. (12.216).

12.6.3 Representation of Tensor Functions of Higher-Order

Tensor-valued functions of the order higher than fourth, or tensor functions with the tensor arguments higher than fourth-order are often employed in continuum damage mechanics. Hence the representations of the scalar- or tensor-valued functions with tensor arguments of the second- and the fourth-order have been obtained. Because of their complexity, the details of the argument are referred to the references (e.g., Zheng 1994; Zheng and Betten 1995).

12.7 Matrix Representation of Tensors and Tensor Relations

For the calculation of tensor relations described hitherto, it is convenient to employ the matrix calculus by writing the tensor variables and the tensor relations in their matrix forms. At the end of this section, we discuss this problem.

12.7.1 Voigt Notation of Hooke's Law

Stress and strain are represented by second-order symmetric tensors σ and ϵ in the three-dimensional Euclidean vector space \mathcal{E}^3 , and have six independent components. Then the constitutive equation of linear elasticity, i.e., the *generalized Hooke's law*, is expressed by means of a fourth-order elastic modulus tensor C as

$$\sigma = C : \epsilon, \quad \text{or} \quad \sigma_{ij} = C_{ijkl} \epsilon_{kl}, \quad (12.224)$$

where we assume an arbitrary orthonormal basis.

Due to the symmetry of the stress and the strain tensor, the tensor C has the symmetry

$$C_{ijkl} = C_{jikl} = C_{ijlk} = C_{jilk}. \quad (12.225)$$

Hence among 81 components of C , the number of the independent components is reduced to 36. The symmetry of Eq. (12.225) is sometimes called *minor symmetry*.

When the material has the strain energy function W such that

$$\sigma = \frac{\partial W}{\partial \epsilon}, \quad \text{or} \quad \sigma_{ij} = \frac{\partial W}{\partial \epsilon_{ij}}, \quad (12.226)$$

the function W is expressed as

$$W = \frac{1}{2}\boldsymbol{\sigma} : \boldsymbol{\epsilon} = \frac{1}{2}\boldsymbol{\epsilon} : \mathbb{C} : \boldsymbol{\epsilon} = \frac{1}{2}C_{ijkl}\boldsymbol{\epsilon}_{ij}\boldsymbol{\epsilon}_{kl}. \quad (12.227)$$

Namely, the elastic modulus tensor \mathbb{C} has further symmetry between first two indices ij and those of the later two kl

$$C_{ijkl} = C_{klji}. \quad (12.228)$$

The elastic modulus tensor \mathbb{C} of a linear elastic material, therefore, has 21 independent components eventually. The symmetry of Eq. (12.228) is sometimes called *major symmetry*.

The calculation of Hooke's law (12.224) is often convenient if it is performed as the matrix calculus of six-dimensional matrices. For this purpose, symmetric tensors $\boldsymbol{\sigma}$ and $\boldsymbol{\epsilon}$ are expressed in the form of column vectors of six-dimension

$$\begin{aligned} [\sigma_p] &\equiv [\sigma_{11} \ \sigma_{22} \ \sigma_{33} \ \sigma_{23} \ \sigma_{31} \ \sigma_{12}]^T \\ &\equiv [\sigma_1 \ \sigma_2 \ \sigma_3 \ \sigma_4 \ \sigma_5 \ \sigma_6]^T, \end{aligned} \quad (12.229)$$

$$\begin{aligned} [\gamma_p] &\equiv [\varepsilon_{11} \ \varepsilon_{22} \ \varepsilon_{33} \ 2\varepsilon_{23} \ 2\varepsilon_{31} \ 2\varepsilon_{12}]^T \\ &\equiv [\gamma_1 \ \gamma_2 \ \gamma_3 \ \gamma_4 \ \gamma_5 \ \gamma_6]^T. \end{aligned} \quad (12.230)$$

The order of the array of the components in Eqs. (12.229), (12.230) should be noted.

It should be emphasized also that the strain components in Eq. (12.230) are the engineering strain rather than the tensor components.

As regards the components C_{ijkl} , by representing the first two indices ij and those of the later two kl by p and q ($p, q = 1, 2, \dots, 6$), respectively, they will be represented in the form of a six by six matrix

$$\begin{aligned} [C_{pq}] &\equiv \begin{bmatrix} C_{1111} & C_{1122} & C_{1133} & C_{1123} & C_{1131} & C_{1112} \\ C_{2211} & C_{2222} & C_{2233} & C_{2223} & C_{2231} & C_{2212} \\ C_{3311} & C_{3322} & C_{3333} & C_{3323} & C_{3331} & C_{3312} \\ C_{2311} & C_{2322} & C_{2333} & C_{2323} & C_{2331} & C_{2312} \\ C_{3111} & C_{3122} & C_{3133} & C_{3123} & C_{3131} & C_{3112} \\ C_{1211} & C_{1222} & C_{1233} & C_{1223} & C_{1231} & C_{1212} \end{bmatrix} \\ &\equiv \begin{bmatrix} C_{11} & C_{12} & C_{13} & C_{14} & C_{15} & C_{16} \\ C_{21} & C_{22} & C_{23} & C_{24} & C_{25} & C_{26} \\ C_{31} & C_{32} & C_{33} & C_{34} & C_{35} & C_{36} \\ C_{41} & C_{42} & C_{43} & C_{44} & C_{45} & C_{46} \\ C_{51} & C_{52} & C_{53} & C_{54} & C_{55} & C_{56} \\ C_{61} & C_{62} & C_{63} & C_{64} & C_{65} & C_{66} \end{bmatrix}. \end{aligned} \quad (12.231)$$

Then Eqs. (12.224), (12.227) and (12.226) lead to

$$[\sigma_p] = [C_{pq}][\gamma_q], \quad \text{or} \quad \sigma_p = C_{pq}\gamma_q, \quad (12.232)$$

$$W = \frac{1}{2}[\gamma_p]^T[C_{pq}][\gamma_q] = \frac{1}{2}C_{pq}\gamma_p\gamma_q, \quad (12.233)$$

$$[\sigma_p] = \frac{\partial W}{\partial [\gamma_p]}, \quad \text{or} \quad \sigma_p = \frac{\partial W}{\partial \gamma_p}. \quad (12.234)$$

The expressions of Eqs. (12.229) through (12.232) for stress, strain and the stress-strain relation are referred to as the *Voigt notation*.

12.7.2 Matrix Representation of Tensors of Second- and Fourth-Order

In the Voigt notation described above, while the stress vector of Eq. (12.229) is defined by the components of stress tensor, the strain vector of Eq. (12.230) is specified by the components of engineering strain, rather than those of strain tensor. This implies that Eqs. (12.229) through (12.232) are not the ordinary matrix representations in terms of tensor components. In order to avoid this inconvenience, we now discuss the general matrix representation of tensors of second- and fourth-order (Nemat-Nasser and Hori 1993).

By the use of the orthonormal basis $\{\mathbf{e}_i\}$ ($i = 1, 2, 3$) in the three-dimensional Euclidean vector space \mathcal{E}^3 , we can define the *second-order basis tensor*

$$\mathbf{e}_{ij} \equiv \mathbf{e}_i \otimes \mathbf{e}_j. \quad (12.235)$$

Then the nine basis tensors of second-order are expressed in the form of a row vector of nine-dimension

$$[\mathbf{e}_{ij}] \equiv [\mathbf{e}_{11} \ \mathbf{e}_{12} \ \mathbf{e}_{13} \ \mathbf{e}_{21} \ \mathbf{e}_{22} \ \mathbf{e}_{23} \ \mathbf{e}_{31} \ \mathbf{e}_{32} \ \mathbf{e}_{33}]. \quad (12.236)$$

Hence, the identity tensors of the second- and fourth-order of Eqs. (12.37) and (12.88a) are expressed in alternative forms

$$\mathbf{I} \equiv \delta_{ij}\mathbf{e}_{ij} = \mathbf{e}_{ii}, \quad \text{or} \quad I_{ij} \equiv \delta_{ij}, \quad (12.237)$$

$$\mathbb{I} \equiv \delta_{ik}\delta_{jl}\mathbf{e}_{ij} \otimes \mathbf{e}_{kl} = \mathbf{e}_{ij} \otimes \mathbf{e}_{ij}, \quad (12.238a)$$

or

$$I_{ijkl} \equiv \delta_{ik}\delta_{jl}. \quad (12.238b)$$

By the use of Eq. (12.236), an arbitrary second- and fourth-order tensor S and T are expressed in the forms

$$\mathbf{S} = S_{ij}\mathbf{e}_i \otimes \mathbf{e}_j = S_{ij}\mathbf{e}_{ij}, \quad (12.239)$$

$$\mathbb{T} = T_{ijkl}\mathbf{e}_i \otimes \mathbf{e}_j \otimes \mathbf{e}_k \otimes \mathbf{e}_l = T_{ijkl}\mathbf{e}_{ij} \otimes \mathbf{e}_{kl}. \quad (12.240)$$

Namely tensors \mathbf{S} and \mathbb{T} can be expressed, respectively, by a nine-dimensional column vector and a nine-dimensional matrix:

$$[\mathbf{S}] = [S_{\{ij\}}], \quad (12.241)$$

$$[\mathbb{T}] = [T_{\{ij\}\{kl\}}]. \quad (12.242)$$

In view of these relations, the tensor calculus with the tensors \mathbf{S} and \mathbb{T} can be written by the matrix calculus as follows;

$$\mathbb{T} : \mathbf{S} \Leftrightarrow [T_{\{ij\}\{kl\}}] [S_{\{kl\}}], \quad (12.243)$$

$$\mathbb{T}^T \Leftrightarrow [T_{\{kl\}\{ij\}}], \quad (12.244)$$

$$\mathbb{T}^{-1} \Leftrightarrow [T_{\{ij\}\{kl\}}]^{-1}, \quad (12.245)$$

$$\mathbb{T}^{-T} \Leftrightarrow [T_{\{ij\}\{kl\}}]^{-T}, \quad (12.246)$$

$$\mathbb{I} : \mathbf{S} = \mathbf{S} \Leftrightarrow [I_{\{ij\}\{kl\}}] [S_{\{kl\}}] = [S_{\{ij\}}], \quad (12.247)$$

$$\mathbb{T}^{-1} : \mathbb{T} = \mathbb{I} \Leftrightarrow [T_{\{ij\}\{mn\}}]^{-1} [T_{\{mn\}\{kl\}}] = [I_{\{ij\}\{kl\}}]. \quad (12.248)$$

12.7.3 Matrix Representation of Symmetric Tensors of Second- and Fourth-Order

In the cases of the symmetric tensors of second- and fourth-order, the number of independent components of the second-order basis tensor $\{\mathbf{e}_i \otimes \mathbf{e}_j\} = \{\mathbf{e}_{ij}\}$ in \mathcal{E}^3 is reduced from nine to six. Hence the results of Section 12.7.2 are no more applicable to symmetric tensors.

We first define the *second-order symmetric basis tensors*

$$\mathbf{e}_{ij}^S \equiv \frac{1}{2}(\mathbf{e}_{ij} + \mathbf{e}_{ji}^T) = \frac{1}{2}(\mathbf{e}_i \otimes \mathbf{e}_j + \mathbf{e}_j \otimes \mathbf{e}_i), (i, j = 1, 2, 3). \quad (12.249)$$

The basis tensor $\{\mathbf{e}_{ij}\}$ defined in Section 12.7.2 is orthonormal. However, in the case of $\{\mathbf{e}_{ij}^S\}$ derived above, we have

$$\begin{aligned} \mathbf{e}_{ij}^S : \mathbf{e}_{kl}^S &= \frac{1}{4} (\mathbf{e}_i \otimes \mathbf{e}_j + \mathbf{e}_j \otimes \mathbf{e}_i) : (\mathbf{e}_k \otimes \mathbf{e}_l + \mathbf{e}_l \otimes \mathbf{e}_k) \\ &= \frac{1}{2} (\delta_{ik}\delta_{jl} + \delta_{il}\delta_{jk}), \end{aligned} \quad (12.250)$$

where the magnitude of the components are not always 1. For instance, while $\mathbf{e}_{11}^S : \mathbf{e}_{11}^S = 1$, we have $\mathbf{e}_{12}^S : \mathbf{e}_{12}^S = 1/2$.

By the use of \mathbf{e}_{ij}^S , the second- and the fourth-order symmetric tensor S and T can be expressed as

$$S = S_{ij} \mathbf{e}_{ij}^S, \quad (12.251)$$

$$T = T_{ijkl} \mathbf{e}_{ij}^S \otimes \mathbf{e}_{kl}^S. \quad (12.252)$$

Thus, we always have $S = S^T$. However, it should be noted that, in view of the definition of transpose T^T of Eq. (12.85), the relation $T = T^T$ does not always hold.

The second-order symmetric basis tensor of Eq. (12.249) can be written by a row vector of six-dimension

$$\begin{aligned} [\mathbf{e}_{ij}^S] &\equiv [\mathbf{e}_{11}^S \ \mathbf{e}_{22}^S \ \mathbf{e}_{33}^S \ \mathbf{e}_{23}^S \ \mathbf{e}_{31}^S \ \mathbf{e}_{12}^S] \\ &\equiv [\mathbf{a}_1 \ \mathbf{a}_2 \ \mathbf{a}_3 \ \mathbf{a}_4 \ \mathbf{a}_5 \ \mathbf{a}_6], \end{aligned} \quad (12.253)$$

where new vectors, $\{\mathbf{e}_{ij}^S\} \equiv \{\mathbf{a}_p\}$ ($p = 1, 2, \dots, 6$), have been introduced for the sake of brevity. The double contraction between the components $\{\mathbf{e}_{ij}^S\}$ is reduced to a single contraction between the components $\{\mathbf{a}_p\}$. Moreover, as observed from Eq. (12.250), the basis $\{\mathbf{a}_p\}$ is orthogonal.

By using the basis vector $\{\mathbf{a}_p\}$, arbitrary symmetric tensors S and T are expressed in terms of their six and thirty six components S_{ij} and T_{ijkl} :

$$S = S_{11}\mathbf{a}_1 + S_{22}\mathbf{a}_2 + S_{33}\mathbf{a}_3 + 2S_{23}\mathbf{a}_4 + 2S_{31}\mathbf{a}_5 + 2S_{12}\mathbf{a}_6, \quad (12.254)$$

$$\begin{aligned} T = & T_{1111}\mathbf{a}_1 \otimes \mathbf{a}_1 + T_{1122}\mathbf{a}_1 \otimes \mathbf{a}_2 + T_{1133}\mathbf{a}_1 \otimes \mathbf{a}_3 \\ & + 2T_{1123}\mathbf{a}_1 \otimes \mathbf{a}_4 + 2T_{1131}\mathbf{a}_1 \otimes \mathbf{a}_5 + 2T_{1112}\mathbf{a}_1 \otimes \mathbf{a}_6 \\ & + \dots \\ & + 2T_{1211}\mathbf{a}_6 \otimes \mathbf{a}_1 + 2T_{1222}\mathbf{a}_6 \otimes \mathbf{a}_2 + 2T_{1233}\mathbf{a}_6 \otimes \mathbf{a}_3 \\ & + 4T_{1223}\mathbf{a}_6 \otimes \mathbf{a}_4 + 4T_{1231}\mathbf{a}_6 \otimes \mathbf{a}_5 + 4T_{1212}\mathbf{a}_6 \otimes \mathbf{a}_6. \end{aligned} \quad (12.255)$$

It should be noted that the coefficients of the bases \mathbf{a}_4 through \mathbf{a}_6 in the right-hand side of Eqs. (12.254) and (12.255) are twice as large as those of the bases \mathbf{a}_1 through \mathbf{a}_3 . To avoid this complexity, we now introduce a six by six *weighting matrix* (Nemat-Nasser and Hori 1993).

$$[W_{pq}] = \begin{bmatrix} 1 & 0 & 0 & 0 & 0 & 0 \\ 0 & 1 & 0 & 0 & 0 & 0 \\ 0 & 0 & 1 & 0 & 0 & 0 \\ 0 & 0 & 0 & 2 & 0 & 0 \\ 0 & 0 & 0 & 0 & 2 & 0 \\ 0 & 0 & 0 & 0 & 0 & 2 \end{bmatrix}. \quad (12.256)$$

Then in view of Eqs. (12.249) and (12.78a), the scalar product of the basis $\{\mathbf{a}_p\}$ leads to

$$\mathbf{a}_p \cdot \mathbf{a}_q = \mathbf{e}_{ij}^S : \mathbf{e}_{kl}^S = \begin{cases} \frac{1}{W_{pq}}, & p = q \\ 0, & p \neq q, \end{cases} \quad (12.257)$$

or

$$W_{pq} \mathbf{a}_p \cdot \mathbf{a}_q = \delta_{pq}, \quad (12.258)$$

(no sum for p and q , $p, q = 1, 2, \dots, 6$).

As observed from this relation, the weighting matrix can reduce the basis $\{\mathbf{a}_p\}$ to an orthonormal basis.

In order to derive the matrix representations of S and T expressed by Eqs. (12.254) and (12.255), we write first S and T in the forms of a six by one column vector and six by six matrix:

$$[S_p] \equiv [S_{11} \ S_{22} \ S_{33} \ S_{23} \ S_{31} \ S_{12}]^T \quad (12.259)$$

$$\equiv [S_1 \ S_2 \ S_3 \ S_4 \ S_5 \ S_6]^T,$$

$$[T_{pq}] \equiv \begin{bmatrix} T_{1111} & T_{1122} & T_{1133} & T_{1123} & T_{1131} & T_{1112} \\ T_{2211} & T_{2222} & T_{2233} & T_{2223} & T_{2231} & T_{2212} \\ T_{3311} & T_{3322} & T_{3333} & T_{3323} & T_{3331} & T_{3312} \\ T_{2311} & T_{2322} & T_{2333} & T_{2323} & T_{2331} & T_{2312} \\ T_{3111} & T_{3122} & T_{3133} & T_{3123} & T_{3131} & T_{3112} \\ T_{1211} & T_{1222} & T_{1233} & T_{1223} & T_{1231} & T_{1212} \end{bmatrix} \quad (12.260)$$

$$\equiv \begin{bmatrix} T_{11} & T_{12} & T_{13} & T_{14} & T_{15} & T_{16} \\ T_{21} & T_{22} & T_{23} & T_{24} & T_{25} & T_{26} \\ T_{31} & T_{32} & T_{33} & T_{34} & T_{35} & T_{36} \\ T_{41} & T_{42} & T_{43} & T_{44} & T_{45} & T_{46} \\ T_{51} & T_{52} & T_{53} & T_{54} & T_{55} & T_{56} \\ T_{61} & T_{62} & T_{63} & T_{64} & T_{65} & T_{66} \end{bmatrix}.$$

In view of Eq. (12.257), the double contraction of T and S can be given as

$$\begin{aligned}
T : S &= \left(T_{ijkl} e_{ij}^S \otimes e_{kl}^S \right) : \left(S_{pq} e_{pq}^S \right) \\
&= (T_{pq} \mathbf{a}_p \otimes \mathbf{a}_q) \cdot (S_r \mathbf{a}_r) = T_{pq} S_r (\mathbf{a}_q \cdot \mathbf{a}_r) \mathbf{a}_p \\
&= \mathbf{a}_p \left\{ (T_{p1} S_1 + T_{p2} S_2 + T_{p3} S_3) \right. \\
&\quad \left. + \frac{1}{2} [(2T_{p4})(2S_4) + (2T_{p5})(2S_5) + (2T_{p6})(2S_6)] \right\} \\
&= [\mathbf{a}_1 \ \mathbf{a}_2 \ \mathbf{a}_3 \ \mathbf{a}_4 \ \mathbf{a}_5 \ \mathbf{a}_6] \times \begin{bmatrix} T_{11} & T_{12} & T_{13} & T_{14} & T_{15} & T_{16} \\ T_{21} & T_{22} & T_{23} & T_{24} & T_{25} & T_{26} \\ T_{31} & T_{32} & T_{33} & T_{34} & T_{35} & T_{36} \\ T_{41} & T_{42} & T_{43} & T_{44} & T_{45} & T_{46} \\ T_{51} & T_{52} & T_{53} & T_{54} & T_{55} & T_{56} \\ T_{61} & T_{62} & T_{63} & T_{64} & T_{65} & T_{66} \end{bmatrix} \begin{bmatrix} S_1 \\ S_2 \\ S_3 \\ 2S_4 \\ 2S_5 \\ 2S_6 \end{bmatrix}. \tag{12.261}
\end{aligned}$$

Therefore the matrix representation of $T : S$ can be expressed as

$$T : S \Leftrightarrow [T_{pq}] [W_{qr}] [S_r]. \tag{12.262}$$

By means of a similar procedure, the matrix representation of the double contraction of two second-order symmetric tensors \mathbf{A} and \mathbf{B} can be expressed:

$$\mathbf{A} : \mathbf{B} \Leftrightarrow [A_p]^T [W_{pq}] [B_q] \tag{12.263}$$

The fourth-order identity tensor was defined by Eq. (12.238). The *fourth-order symmetric identity tensor* \mathbb{I}^S , on the other hand, is defined as a tensor which transforms a second-order symmetric tensor in \mathcal{E}^3 into itself, i.e.,

$$\begin{aligned}
\mathbb{I}^S &\equiv \delta_{ik} \delta_{jl} e_{ij}^S \otimes e_{kl}^S = e_{ij}^S \otimes e_{ij}^S \\
&= \frac{1}{2} (e_{ij} \otimes e_{ij} + e_{ij} \otimes e_{ji}) \\
&= \frac{1}{2} (\delta_{ik} \delta_{jl} + \delta_{il} \delta_{jk}) e_{ij} \otimes e_{kl}, \tag{12.264a}
\end{aligned}$$

or

$$I_{ijkl}^S = \frac{1}{2} (\delta_{ik} \delta_{jl} + \delta_{il} \delta_{jk}). \tag{12.264b}$$

By the use of the basis $\{\mathbf{a}_k\}$ of Eq. (12.253), \mathbb{I}^S of Eq. (12.264) leads to the form

$$\begin{aligned}
\mathbb{I}^S &= (\mathbf{a}_1 \otimes \mathbf{a}_1 + \mathbf{a}_2 \otimes \mathbf{a}_2 + \mathbf{a}_3 \otimes \mathbf{a}_3) \\
&\quad + \frac{1}{2} (\mathbf{a}_4 \otimes \mathbf{a}_4 + \mathbf{a}_5 \otimes \mathbf{a}_5 + \mathbf{a}_6 \otimes \mathbf{a}_6), \tag{12.264c}
\end{aligned}$$

and its matrix is expressed as

$$[I_{pq}^S] = [W_{pq}]^{-1} = \begin{bmatrix} 1 & 0 & 0 & 0 & 0 & 0 \\ 0 & 1 & 0 & 0 & 0 & 0 \\ 0 & 0 & 1 & 0 & 0 & 0 \\ 0 & 0 & 0 & 1/2 & 0 & 0 \\ 0 & 0 & 0 & 0 & 1/2 & 0 \\ 0 & 0 & 0 & 0 & 0 & 1/2 \end{bmatrix}. \quad (12.265)$$

It should be noted that, though the identity tensor \mathbb{I}^S defines an identity transformation in the sense that it transforms any second-order symmetric tensor into itself, its matrix is not a unit matrix.

As regards a fourth-order symmetric tensor \mathbb{T} in \mathcal{E}^3 , another fourth-order symmetric tensor \mathbb{T}^{-1} satisfying the relation

$$\mathbb{T}^{-1} : \mathbb{T} = \mathbb{T} : \mathbb{T}^{-1} = \mathbb{I}^S, \quad (12.266)$$

is said to be the *inverse tensor* of \mathbb{T} . The matrix representation of this relation is given as

$$[T_{pr}]^{-1} [W_{rs}] [T_{sq}] = [T_{pr}] [W_{rs}] [T_{sq}]^{-1} = [W_{pq}]^{-1}. \quad (12.267)$$

Applying $[W_{pq}]$ to this equation from the left or from the right and using Eq. (12.265), we obtain

$$([W_{ps}] [T_{st}]^{-1} [W_{iq}]) [T_{qr}] = [I_{pq}], \quad (12.268a)$$

or

$$[T_{pq}] ([W_{qs}] [T_{st}]^{-1} [W_{tr}]) = [I_{pr}], \quad (12.268b)$$

where $[I_{pr}]$ is a six by six unit matrix. Hence this equation together with Eq. (12.265) gives an important relation

$$[I_{pq}] = [W_{pr}] [I_{rq}^S] = [I_{pr}^S] [W_{rq}]. \quad (12.269)$$

According to the results of the above discussion, the matrix representations of the tensor relations among the stress σ , strain ϵ , elastic modulus tensor \mathbb{C} , the elastic compliance tensor $\mathbb{S}(= \mathbb{C}^{-1})$ and the strain energy function W are given:

$$\sigma = \mathbb{C} : \epsilon \Leftrightarrow [\sigma_p] = [C_{pr}] [W_{rq}] [\epsilon_q], \quad (12.270a)$$

$$\epsilon = \mathbb{S} : \sigma \Leftrightarrow [\epsilon_p] = [S_{pr}] [W_{rq}] [\sigma_q], \quad (12.270b)$$

$$W = \frac{1}{2} \boldsymbol{\sigma} : \boldsymbol{\varepsilon} \Leftrightarrow W = \frac{1}{2} [\sigma_p]^T [W_{pq}] [\varepsilon_q] \quad (12.271)$$

$$\mathcal{C} : \mathcal{S} = \mathbb{I}^S \Leftrightarrow [C_{pr}] [W_{rs}] [S_{sq}] = [I_{pq}^S], \quad (12.272a)$$

$$\mathcal{S} : \mathcal{C} = \mathbb{I}^S \Leftrightarrow [S_{pr}] [W_{rs}] [C_{sq}] = [I_{pq}^S]. \quad (12.272b)$$

In these relations, $[\sigma_p]$ and $[\varepsilon_p]$ are the six-dimensional column vectors of the stress $\boldsymbol{\sigma}$ and strain $\boldsymbol{\varepsilon}$, while $[C_{pr}]$ and $[S_{pr}]$ are the six by six matrices of the elastic modulus tensor \mathcal{C} and the elastic compliance tensor \mathcal{S} , respectively, and are given:

$$\begin{aligned} [\sigma_p] &\equiv [\sigma_1 \ \sigma_2 \ \sigma_3 \ \sigma_4 \ \sigma_5 \ \sigma_6]^T \\ &\equiv [\sigma_{11} \ \sigma_{22} \ \sigma_{33} \ \sigma_{23} \ \sigma_{31} \ \sigma_{12}]^T, \end{aligned} \quad (12.273a)$$

$$\begin{aligned} [\varepsilon_p] &\equiv [\varepsilon_1 \ \varepsilon_2 \ \varepsilon_3 \ \varepsilon_4 \ \varepsilon_5 \ \varepsilon_6]^T \\ &\equiv [\varepsilon_{11} \ \varepsilon_{22} \ \varepsilon_{33} \ \varepsilon_{23} \ \varepsilon_{31} \ \varepsilon_{12}]^T, \end{aligned} \quad (12.273b)$$

$$[C_{pq}] \equiv \begin{bmatrix} C_{11} & C_{12} & C_{13} & C_{14} & C_{15} & C_{16} \\ C_{21} & C_{22} & C_{23} & C_{24} & C_{25} & C_{26} \\ C_{31} & C_{32} & C_{33} & C_{34} & C_{35} & C_{36} \\ C_{41} & C_{42} & C_{43} & C_{44} & C_{45} & C_{46} \\ C_{51} & C_{52} & C_{53} & C_{54} & C_{55} & C_{56} \\ C_{61} & C_{62} & C_{63} & C_{64} & C_{65} & C_{66} \end{bmatrix} \quad (12.273c)$$

$$\equiv \begin{bmatrix} C_{1111} & C_{1122} & C_{1133} & C_{1123} & C_{1131} & C_{1112} \\ C_{2211} & C_{2222} & C_{2233} & C_{2223} & C_{2231} & C_{2212} \\ C_{3311} & C_{3322} & C_{3333} & C_{3323} & C_{3331} & C_{3312} \\ C_{2311} & C_{2322} & C_{2333} & C_{2323} & C_{2331} & C_{2312} \\ C_{3111} & C_{3122} & C_{3133} & C_{3123} & C_{3131} & C_{3112} \\ C_{1211} & C_{1222} & C_{1233} & C_{1223} & C_{1231} & C_{1212} \end{bmatrix},$$

$$[S_{pq}] \equiv \begin{bmatrix} S_{11} & S_{12} & S_{13} & S_{14} & S_{15} & S_{16} \\ S_{21} & S_{22} & S_{23} & S_{24} & S_{25} & S_{26} \\ S_{31} & S_{32} & S_{33} & S_{34} & S_{35} & S_{36} \\ S_{41} & S_{42} & S_{43} & S_{44} & S_{45} & S_{46} \\ S_{51} & S_{52} & S_{53} & S_{54} & S_{55} & S_{56} \\ S_{61} & S_{62} & S_{63} & S_{64} & S_{65} & S_{66} \end{bmatrix} \quad (12.273d)$$

$$\equiv \begin{bmatrix} S_{1111} & S_{1122} & S_{1133} & S_{1123} & S_{1131} & S_{1112} \\ S_{2211} & S_{2222} & S_{2233} & S_{2223} & S_{2231} & S_{2212} \\ S_{3311} & S_{3322} & S_{3333} & S_{3323} & S_{3331} & S_{3312} \\ S_{2311} & S_{2322} & S_{2333} & S_{2323} & S_{2331} & S_{2312} \\ S_{3111} & S_{3122} & S_{3133} & S_{3123} & S_{3131} & S_{3112} \\ S_{1211} & S_{1222} & S_{1233} & S_{1223} & S_{1231} & S_{1212} \end{bmatrix}.$$

In Section 12.7.1, the matrix representation (12.232) of generalized Hooke's law

$$[\sigma_p] = [C_{pq}] [\gamma_q] \quad (12.274)$$

was expressed in terms of the components of the engineering strain γ_p . Comparison of this equation with Eq. (12.270a) gives a relation

$$[\gamma_p] = [W_{pq}] [\varepsilon_q]. \quad (12.275)$$

That is to say, in the Voigt notation, the effect of the weighting matrix $[W_{pq}]$ arising from the transformation from the nine- to six-dimensional vector spaces has been included in the matrix $[\gamma_p]$ of the engineering strain.

As seen in Eqs. (12.270a) and (12.270b), the coefficient matrices $[C_{pr}] [W_{rq}]$ and $[S_{pr}] [W_{rq}]$ in the elastic constitutive equations are specified by matrices different from $[C_{pr}]$ and $[S_{pr}]$ of the elastic modulus and elastic compliance tensors of \mathbb{C} and \mathbb{S} .

To avoid this inconvenience in the discussion hereafter, we will introduce a new notation $[C_{pq}]$, $[S_{pr}]$ in roman type, and write the matrix representation of elastic constitutive equations Eqs. (12.270a) and (12.270b) as follows;

$$[\sigma_p] = [C_{pq}] [\varepsilon_q], \quad [C_{pq}] = [C_{pr}] [W_{rq}], \quad (12.276)$$

$$[\varepsilon_p] = [S_{pq}] [\sigma_q], \quad [S_{pq}] = [S_{pr}] [W_{rq}]. \quad (12.277)$$

12.7.4 Elastic Symmetry, Matrices of Elastic Modulus and Elastic Compliance

As described in Section 12.7.1, the elastic modulus tensor \mathbb{C} of linear elasticity has 21 independent components at the largest. The number reduces when the elastic property has specific symmetries in the material.

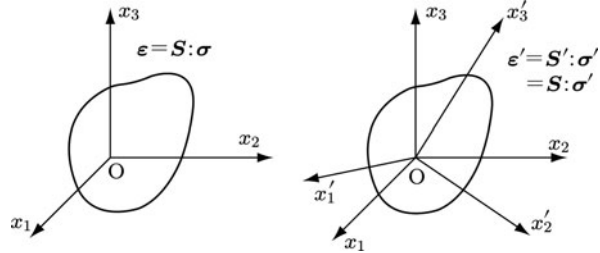
In the following, we derive the coefficient matrices $[C_{pq}]$, $[S_{pr}]$ of Eqs. (12.276) and (12.277) for some elastic symmetries important in engineering (Malvern 1969; Nemat-Nasser and Hori 1993).

(1) Isotropic Elastic Material

When a physical property does not depend on the direction in the material, the property is said to be *isotropic*. Therefore, if the functional form of the elastic constitutive equations (12.270) remains unchanged by an arbitrary orthogonal transformation of its coordinate systems (Fig. 12.12), the elastic property is isotropic.

In this case, the elastic modulus tensor should be a *fourth-order isotropic tensor*, and its general expression is given:

Fig. 12.12 An isotropic elastic material



$$\mathbb{C} = \lambda \mathbf{I} \otimes \mathbf{I} + 2\mu \mathbf{I}^S, \quad (12.278a)$$

or

$$C_{ijkl} = \lambda \delta_{ij} \delta_{kl} + \mu (\delta_{ik} \delta_{jl} + \delta_{il} \delta_{jk}). \quad (12.278b)$$

As observed from Eq. (12.278), the elastic property of an isotropic elastic material is specified by two independent elastic constants λ and μ . These λ and μ are called *Lamé constants*, and are related to *Young's modulus E*, *shear modulus G*, *bulk modulus K* and *Poisson's ratio v*:

$$\lambda = \frac{2Gv}{1-2v} = \frac{G(E-2G)v}{3G-E} = K - \frac{2}{3}G = \frac{Ev}{(1+v)(1-2v)}, \quad (12.279a)$$

$$\mu = G = \frac{\lambda(1-2v)}{2v} = \frac{2}{3}(K-\lambda) = \frac{E}{2(1+v)}. \quad (12.279b)$$

By the use of these results, the matrix of elastic modulus tensor $[\mathbb{C}_{pq}]$ of Eq. (12.276) for the isotropic elastic material is derived:

$$[\mathbb{C}_{pq}] = [C_{pr}] [W_{rq}] = \begin{bmatrix} C_{11} & C_{12} & C_{13} & 0 & 0 & 0 \\ C_{12} & C_{22} & C_{23} & 0 & 0 & 0 \\ C_{13} & C_{23} & C_{33} & 0 & 0 & 0 \\ 0 & 0 & 0 & 2C_{44} & 0 & 0 \\ 0 & 0 & 0 & 0 & 2C_{55} & 0 \\ 0 & 0 & 0 & 0 & 0 & 2C_{66} \end{bmatrix}, \quad (12.280a)$$

$$C_{11} = C_{22} = C_{33} = \lambda + 2\mu = \frac{E}{1+v} \frac{1-v}{1-2v}, \quad (12.280b)$$

$$C_{12} = C_{13} = C_{23} = \lambda = \frac{E}{1+v} \frac{v}{1-2v}, \quad (12.280c)$$

$$C_{44} = C_{55} = C_{66} = \mu = G = \frac{E}{2(1+v)} = \frac{C_{11} - C_{12}}{2}. \quad (12.280d)$$

By means of a similar procedure, the compliance matrix $[S_{pq}]$ of Eq. (12.277) is obtained:

$$[S_{pq}] = [S_{pr}] [W_{rq}]$$

$$= \begin{bmatrix} S_{11} & S_{12} & S_{13} & 0 & 0 & 0 \\ S_{12} & S_{22} & S_{23} & 0 & 0 & 0 \\ S_{13} & S_{23} & S_{33} & 0 & 0 & 0 \\ 0 & 0 & 0 & S_{44}/2 & 0 & 0 \\ 0 & 0 & 0 & 0 & S_{55}/2 & 0 \\ 0 & 0 & 0 & 0 & 0 & S_{66}/2 \end{bmatrix}, \quad (12.281a)$$

$$S_{11} = S_{22} = S_{33} = \frac{1}{E}, \quad S_{12} = S_{13} = S_{23} = -\frac{\nu}{E}, \quad (12.281b)$$

$$S_{44} = S_{55} = S_{66} = \frac{1}{G} = \frac{2(1+\nu)}{E}. \quad (12.281c)$$

(2) Transversely Isotropic Elastic Material

When a physical property is isotropic in a plane, the property is said to be *transverse isotropy*.

Suppose the x_1x_2 -plane in a material to be the plane of isotropy (Fig. 12.13). In this case, by the rotation of the coordinate system by 45° with respect to the material, the elastic constitutive equations (12.270a), (12.270b) or Eqs. (12.276), (12.277) should remain unchanged. Due to this condition, the elastic compliance matrix of the transversely isotropic elastic material is derived as follows:

$$[S_{pq}] = [S_{pr}] [W_{rq}]$$

$$= \begin{bmatrix} S_{11} & S_{12} & S_{13} & 0 & 0 & 0 \\ S_{12} & S_{22} & S_{23} & 0 & 0 & 0 \\ S_{13} & S_{23} & S_{33} & 0 & 0 & 0 \\ 0 & 0 & 0 & S_{44}/2 & 0 & 0 \\ 0 & 0 & 0 & 0 & S_{55}/2 & 0 \\ 0 & 0 & 0 & 0 & 0 & S_{66}/2 \end{bmatrix}, \quad (12.282a)$$

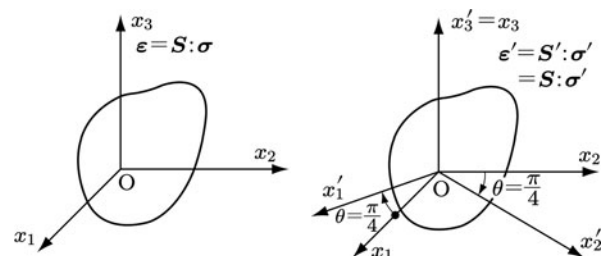


Fig. 12.13 A transversely isotropic elastic material

$$S_{11} = S_{22} = \frac{1}{E}, \quad S_{12} = -\frac{\nu}{E}, \quad S_{13} = S_{23} = -\frac{\nu_3}{E_3}, \quad (12.282b)^4$$

$$S_{33} = \frac{1}{E_3}, \quad S_{44} = S_{55} = \frac{1}{G_3}, \quad S_{66} = 2(S_{11} - S_{12}) = \frac{1}{G}. \quad (12.282c)^4$$

In these relations, E_3 signifies Young's modulus in the x_3 -direction, while E , G , ν , G_3 and ν_3 are given respectively as follows:

$$E = E_1 = E_2, \quad G = G_{12} = G_{21}, \quad \nu = \nu_{12} = \nu_{21}, \quad (12.283a)^4$$

$$G_3 = G_{31} = G_{32}, \quad \nu_3 = \nu_{31} = \nu_{32}. \quad (12.283b)^4$$

In addition, among the elastic constants related to the deformation in x_1x_2 -plane, there exists a relation

$$G = G_{12} = G_{21} = \frac{E}{2(1+\nu)}. \quad (12.284)$$

As can be seen in Eqs. (12.282) and (12.283), the elastic constants of the transverse isotropy consist of five independent constants of E , ν , E_3 , G_3 and ν_3 .

As regards the elastic modulus tensors of transverse isotropy, on the other hand, we have the matrix

$$\begin{aligned} [\mathbf{C}_{pq}] &= [C_{pr}] [W_{rq}] \\ &= \begin{bmatrix} C_{11} & C_{12} & C_{13} & 0 & 0 & 0 \\ C_{12} & C_{22} & C_{23} & 0 & 0 & 0 \\ C_{13} & C_{23} & C_{33} & 0 & 0 & 0 \\ 0 & 0 & 0 & 2C_{44} & 0 & 0 \\ 0 & 0 & 0 & 0 & 2C_{55} & 0 \\ 0 & 0 & 0 & 0 & 0 & 2C_{66} \end{bmatrix}, \end{aligned} \quad (12.285a)$$

$$C_{11} = C_{22} = A \left(\frac{1}{E} - \frac{\nu_3^2}{E_3} \right), \quad C_{12} = C_{21} = A \left(\frac{\nu}{E} + \frac{\nu_3^2}{E_3} \right), \quad (12.285b)$$

$$C_{13} = C_{23} = A \frac{(1+\nu)\nu_3}{E}, \quad C_{33} = A \frac{(1-\nu^2)E_3}{E^2}, \quad (12.285c)$$

$$C_{44} = C_{55} = G_3, \quad C_{66} = \frac{C_{11} - C_{12}}{2} = A \left(\frac{1-\nu}{2E} - \frac{\nu_3^2}{E_3} \right), \quad (12.285d)$$

⁴ E_i and G_{ij} ($i, j = 1, 2, 3$) denote Young's modulus in x_i -direction and the shear modulus in $x_i x_j$ -plane. The symbol $\nu_{ij} = -(\varepsilon_j/\varepsilon_i)$ is Poisson's ratio of the strain in x_j -direction to that of x_i -direction.

$$A = \frac{E^2 E_3}{(1 + \nu) [(1 - \nu) E_3 - 2\nu_3^2 E]}, \quad (12.285e)$$

where the values of E , ν , G_3 , ν_3 were specified by Eqs. (12.283a) and (12.283b).

(3) Orthotropic Elastic Material

When a physical property has symmetry with respect to two orthogonal planes, e.g., x_1x_3 - and x_2x_3 -planes, the property is said to be *orthotropic*. In this case, the property is symmetric also as to the x_1x_2 -plane.

Let us suppose a coordinate system O- $x_1x_2x_3$ as shown in Fig. 12.14. For an orthotropic material, the constitutive equation (12.270b) or (12.277) is unchanged by the rotation of the coordinate system by 180° about x_3 - and x_1 -axis with respect to the material. By this condition, the independent material constants of an orthotropic elastic material are reduced to nine, and its elastic compliance matrix is derived as follows:

$$\begin{aligned} [S_{pq}] &= [S_{pr}] [W_{rq}] \\ &= \begin{bmatrix} S_{11} & S_{12} & S_{13} & 0 & 0 & 0 \\ S_{12} & S_{22} & S_{23} & 0 & 0 & 0 \\ S_{13} & S_{23} & S_{33} & 0 & 0 & 0 \\ 0 & 0 & 0 & S_{44}/2 & 0 & 0 \\ 0 & 0 & 0 & 0 & S_{55}/2 & 0 \\ 0 & 0 & 0 & 0 & 0 & S_{66}/2 \end{bmatrix}, \quad (12.286a) \end{aligned}$$

$$S_{11} = \frac{1}{E_1}, \quad S_{22} = \frac{1}{E_2}, \quad S_{33} = \frac{1}{E_3}, \quad (12.286b)$$

$$S_{12} = -\frac{\nu_{12}}{E_1}, \quad S_{23} = -\frac{\nu_{23}}{E_2}, \quad S_{13} = -\frac{\nu_{13}}{E_3}, \quad (12.286c)$$

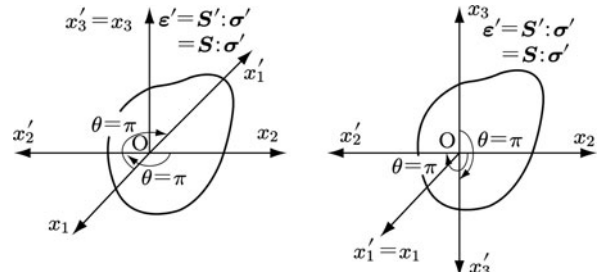


Fig. 12.14 An orthotropic elastic material

$$S_{44} = \frac{1}{G_{23}}, \quad S_{55} = \frac{1}{G_{31}}, \quad S_{66} = \frac{1}{G_{12}}. \quad (12.286d)$$

Due to the condition of the symmetry of the matrix $[S_{pq}]$, we further have the relations

$$\frac{\nu_{21}}{E_2} = \frac{\nu_{12}}{E_1}, \quad \frac{\nu_{31}}{E_3} = \frac{\nu_{13}}{E_1}, \quad \frac{\nu_{32}}{E_3} = \frac{\nu_{23}}{E_2}. \quad (12.287)$$

This may be viewed as a result of Betti's reciprocal theorem.

Although the matrix representation can be derived also for the elastic modulus tensor \mathcal{C} , the detailed expression is referred to relevant references because of its complexity.

References

Continuum Damage Mechanics

- Kachanov LM (1986) Introduction to continuum damage mechanics. Martinus Nijhoff Publishers, Dordrecht
- Kattan PI, Voyatzis GZ (2002) Damage mechanics with finite elements. Springer, Berlin
- Krajcinovic D (1996) Damage mechanics. North-Holland, Amsterdam
- Lemaitre J (1992) A course on damage mechanics. Springer, Berlin; 2nd Edition (1996)
- Lemaitre J, Desmorat R (2005) Engineering damage mechanics. Springer, Berlin
- Skrzypek J, Ganczarski A (1999) Modeling of material damage and failure of structures. Springer, Berlin
- Voyatzis GZ, Kattan PI (1999) Advances in damage mechanics: metals and metal matrix composites. Elsevier, Amsterdam

Tensor Analysis, Continuum Mechanics and Thermodynamics

- Becker E, Bürger W (1975) Kontinuumsmechanik: Eine Einführung in die Grundlagen und einfache Anwendungen. B. G. Teubner, Stuttgart
- Besson J, Cailletaud G, Chaboche J-L, Forest S, Blétry M (2010) Non-linear mechanics of materials. Springer, Dordrecht
- Chadwick P (1999) Continuum mechanics: concise theory and problems. George Allen and Unwin, London; 2nd Edition, Dover, New York (1976)
- De Groot SR, Mazur P (1962) Non-equilibrium thermodynamics. North-Holland, Amsterdam
- Eringen AC (1967) Mechanics of continua. Wiley, New York; 2nd Edition, Krieger, New York (1980)
- Fung YC (1965) Foundations of solid mechanics. Prentice-Hall, Englewood Cliffs, NJ
- Fung YC, Tong P (2001) Classical and computational solid mechanics. World Scientific Publishing, Singapore
- Germain P (1973) Cours de Mécanique des Milieux Continus. Masson et Cie, Paris
- Glansdorff P, Prigogine I (1971) Thermodynamic theory of structure, stability and fluctuations. Wiley, London
- Holzapfel GA (2000) Nonlinear solid mechanics: a continuum approach for engineering. Wiley, Chichester
- Itsukov M (2007) Tensor algebra and tensor analysis for engineers, with application to continuum mechanics. Springer, Berlin
- Jauzemis W (1967) Continuum mechanics. Macmillan, New York
- Leigh DC (1968) Nonlinear continuum mechanics. McGraw-Hill, New York

- Lemaître J, Chaboche JL (1985) Mécanique des Matériaux Soides. Dunod, Paris; Mechanics of solid materials. Cambridge University Press, Cambridge (1990)
- Lemaître J, Chaboche J-L, Benallal A, Desmorat R (2009) Mécanique des Matériaux Solides, 3rd edn. Dunod, Paris
- Malvern LE (1969) Introduction to the mechanics of a continuous medium. Prentice-Hall, Englewood Cliffs, NJ
- Maugin GA (1992) The thermomechanics of plasticity and fracture. Cambridge University Press, Cambridge
- Nemat-Nasser S, Hori M (1993) Micromechanics: overall properties of heterogeneous materials. North-Holland, Amsterdam; 2nd Revised Edition, Elsevier, Amsterdam (1999)
- Ogden RW (1984) Non-linear elastic deformations. Ellis-Horwood, Chichester; Dover, New York (1997)
- Truesdell C (1969) Rational thermodynamics. McGraw-Hill, New York; Enlarged Edition, Springer, Berlin (1984)
- Truesdell C, Noll W (1965) The non-linear field theories of mechanics. In: Flügge S (ed) Encyclopedia of physics, vol III/3. Springer, Berlin; 3rd Edition (2004)
- Truesdell C, Toupin RA (1960) The classical field theories. In: Flügge S (ed) Encyclopedia of physics, vol III/1. Springer, Berlin

Bibliography

- Allix O, Bahlouli N, Ladevèze P, Perret L (1994) Damage modeling of composite laminates at various temperatures. In: Allen DH, Ju JW (eds) *Damage mechanics in composites*. The American Society of Mechanical Engineers, New York, pp 21–35
- Allix O, Feissel P, Thévenet P (2003) A delay damage mesomodel of laminates under dynamic loading: basic aspects and identification issues. *Comput Struct* 81:1171–1191
- Allix O, Ladevèze P (1992) Interlaminar interface modelling for the prediction of delamination. *Compos Struct* 22:235–242
- Allix O, Ladevèze P, Le Dantec E, Vittecoq E (1990) Damage mechanics for composite laminates under complex loading. In: Boehler JP (ed) *Yielding, damage, and failure of anisotropic solids*. Mechanical Engineering Publications, London, pp 551–569
- Bao Y, Wierzbicki T (2004) On fracture locus in the equivalent strain and stress triaxiality space. *Int J Mech Sci* 46:81–98
- Bao Y, Wierzbicki T (2005) On the cut-off value of negative triaxiality for fracture. *Eng Fract Mech* 72:1049–1069
- Bathias C, Paris PC (2005) Gigacycle fatigue in mechanical practice. Marcel Dekker, New York
- Bažant ZP (1990) Recent advances in failure localization and nonlocal models. In: Shah SP, Swartz SE, Wang ML (eds) *Micromechanics of failure of quasi-ductile materials*. Elsevier Applied Science, London, pp 12–32
- Bažant ZP, Belytschko TB, Chang TP (1984) Continuum theory for strain- softening. *J Eng Mech Trans ASCE* 110:1666–1692
- Bažant ZP, Cedolin L (1983) Finite element modeling of crack band propagation. *J Struct Eng Trans ASCE* 109:69–82
- Bažant ZP, Jirasek M (2002) Nonlocal integral formulations of plasticity and damage: survey of progress. *J Eng Mech Trans ASCE* 128:1119–1149
- Bažant ZP, Oh BH (1983) Crack band theory for fracture of concrete. *Mater Struct* 16:155–177
- Bažant ZP, Pijaudier-Cabot G (1988) Nonlocal continuum damage, localization instability and convergence. *J Appl Mech Trans ASME* 55:287–293
- Becker E, Bürger W (1975) *Kontinuumsmechanik: Eine Einführung in die Grundlagen und einfache Anwendungen*. B. G. Teubner, Stuttgart
- Benallal A, Siad L (1997) Stress and strain fields in cracked damaged solids. *Technische Mechanik* 17:295–304
- Benallal A, Siad L (2001) Strain, stress and damage fields in damaged and cracked solids. In: Murakami S, Ohno N (eds) *IUTAM symposium on creep in structures*. Kluwer, Dordrecht, pp 151–163
- Benzerga AA (2002) Micromechanics of coalescence in ductile fracture. *J Mech Phys Solids* 50:1331–1362
- Benzerga AA, Besson J, Pineau A (2004a) Anisotropic ductile fracture, part I: experiments. *Acta Mater* 52:4623–4638

- Benzerga AA, Besson J, Pineau A (2004b) Anisotropic ductile fracture, part II: theory. *Acta Mater* 52:4639–4650
- Berg CA (1970) Plastic dilatation and void interaction. In: Kanninen MF et al (eds) *Inelastic behavior of solids*. McGraw-Hill, New York, pp 171–210
- Besson J, Guillemer-Neel C (2003) An extension of the Green and Gurson models to kinematic hardening. *Mech Mater* 35:1–18
- Besson J (2010) Continuum models of ductile fracture: a review. *Int J Damage Mech* 19:3–52
- Besson J, Steglich D, Brocks W (2003) Modeling of plane strain ductile rupture. *Int J Plast* 19:1517–1541
- Betten J (1986) Applications of tensor functions to the formulation of constitutive equations involving damage and initial anisotropy. *Eng Fract Mech* 25:573–584
- Bilby BA, Howard IC, Li ZH (1994) Mesh independent cell models for continuum damage theory. *Fatigue Fract Eng Mater Struct* 17:1221–1233
- Billardon R, Doghri I (1989) Localization bifurcation analysis for damage softening elasto-plastic materials. In: Mazars J, Bažant ZP (eds) *Cracking and damage – strain localization and size effect*. Elsevier Applied Science, London, pp 295–307
- Bluhm JI, Morrissey RJ (1966) Fracture in a tensile specimen. In: Yokobori T, Kawasaki T, Swedlow JL (eds) *Proceedings of the first international conference on fracture*, vol 3. The Japan Society for Strength and Fracture of Materials, Sendai, pp 1739–1780
- Bonora N (1997) A nonlinear CDM model for ductile failure. *Eng Fract Mech* 58:11–28
- Bonora N, Gentile D, Pirondi A, Newaz G (2005) Ductile damage evolution under triaxial state of stress: theory and experiments. *Int J Plast* 21:981–1007
- Boyle JT, Spence J (1983) Stress analysis for creep. Butterworths, London
- Brownrigg A, Spitzig WA, Richmond O, Teirlinck D, Embury JD (1983) The influence of hydrostatic pressure on the flow stress and ductility of spherodized 1045 steel. *Acta Metall* 31:1141–1150
- Brüning M, Chyra O, Albrecht D, Driemeier L, Alves M (2008) A ductile damage criterion at various stress triaxialities. *Int J Plast* 24:1731–1755
- Cadek J (1988) Creep in metallic materials. Elsevier, Amsterdam
- Cailletaud G, Levaillant C (1984) Creep-fatigue life prediction: What about initiation? *Nucl Eng Des* 83:279–292
- Cauvin A, Testa RB (1999) Damage mechanics: basic variables in continuum theories. *Int J Solids Struct* 36:747–761
- Chaboche JL (1977) Sur l'utilisation des variables d'état interne pour la description du comportement viscoplastique et de la rupture par endommagement. In: Nowacki WK (ed) *Problèmes Non-Linéaires de Mécanique (Proceedings of French-Polish symposium, Cracow 1977)*. PWN (State Publishing House of Science), Warsaw, 1980, pp 137–159
- Chaboche JL (1982) The concept of effective stress applied to elasticity and to viscoplasticity in the presence of anisotropic damage. In: Boehler JP (ed) *Mechanical behavior of anisotropic solids (Proceedings of Euromech Colloquium 115, Grenoble 1979)*. Martinus Nijhoff, The Hague, pp 737–760
- Chaboche JL (1984) Anisotropic creep damage in the framework of continuum damage mechanics. *Nucl Eng Technol* 79:309–319
- Chaboche JL (1986) Time independent constitutive theories for cyclic plasticity. *Int J Plast* 2:149–188
- Chaboche JL (1988) Continuum damage mechanics, part I general concepts; part II damage growth, crack initiation, and crack growth. *J Appl Mech Trans ASME* 55:59–72
- Chaboche JL (1989) Constitutive equations for cyclic plasticity and cyclic viscoplasticity. *Int J Plast* 5:247–302
- Chaboche JL (1992) Damage induced anisotropy: on the difficulties associated with the active/passive unilateral condition. *Int J Damage Mech* 1:148–171
- Chaboche JL (1993) Development of continuum damage mechanics for elastic solids sustaining anisotropic and unilateral damage. *Int J Damage Mech* 2:311–329

- Chaboche JL (1997) Thermodynamic formulation of constitutive equations and application to the viscoplasticity and viscoelasticity of metals and polymers. *Int J Solids Struct* 34:2239–2254
- Chaboche JL, Boudifa M, Saanouni K (2006) A CDM approach of ductile damage with plastic compressibility. *Int J Fract* 137:51–75
- Chaboche JL, Lesne PM, Maire JF (1994) Macroscopic modelling of inelastic and damage processes with unilateral effects in thermostructural composite materials. In: Allen DH, Ju JW (eds) *Damage mechanics in composites*. The American Society of Mechanical Engineers, New York, pp 75–86
- Chaboche JL, Lesne PM, Maire JF (1995) Continuum damage mechanics, anisotropy and damage deactivation for brittle materials like concrete and ceramic composites. *Int J Damage Mech* 4:5–22
- Chaboche JL, Lesn   O, Pottier T (1998) Continuum damage mechanics of composites; towards a unified approach. In: Voyatzis GZ, Ju JW, Chaboche JL (eds) *Damage mechanics in engineering materials*. Elsevier, Amsterdam, pp 3–26
- Chaboche JL, Rousset G (1983) On the plastic and viscoplastic constitutive equations, part I: rules developed with internal variable concept; part II: application of internal variable concepts to the 316 stainless steel. *J Press Vessel Technol Trans ASME* 105:153–164
- Chadwick P (1976) *Continuum mechanics, concise theory and problems*. George Allen and Unwin, London; 2nd Edition, Dover, New York (1999)
- Chandrakanth S, Pandey PC (1993) A new ductile damage evolution model. *Int J Fract* 60:73–76
- Chen XF, Chow CL (1995) On damage strain energy release rate. *Int J Damage Mech* 4:251–263
- Chow CL, Jie M (2004) Forming limits of AL6022 sheets with material damage consideration –theory and experimental validation. *Int J Mech Sci* 46:99–122
- Chow CL, Jie M, Wu X (2007) Localized necking criterion for strain- softening materials with anisotropic damage. *Int J Damage Mech* 16:265–281
- Chow CL, Lu TJ (1989a) A normative presentation of stress and strain for continuum damage mechanics. *Theor Appl Fract Mech* 12:161–187
- Chow CL, Lu TJ (1989b) On evolution laws of anisotropic damage. *Eng Fract Mech* 34:679–701
- Chow CL, Wang J (1987) An anisotropic theory of continuum damage mechanics for ductile fracture. *Eng Fract Mech* 27:547–558
- Chow CL, Wang J (1988) A finite element analysis of continuum damage mechanics for ductile fracture. *Int J Fract* 38:83–102
- Chow CL, Yang XJ (2004) A generalized mixed isotropic-kinematic hardening plastic model coupled with anisotropic damage for sheet metal forming. *Int J Damage Mech* 13:81–101
- Chow CL, Yu LG, Demerit MY (1997) A unified damage approach for predicting forming limit diagrams. *J Eng Mater Technol Trans ASME* 119:346–353
- Chow CL, Yu IG, Tai WH, Demerit MY (2001) Prediction of forming limit diagrams for AL6111-T4 under non-proportional loading. *Int J Mech Sci* 43:471–486
- Chu CC, Needleman A (1980) Void nucleation effects in biaxially stretched sheets. *J Eng Mater Technol Trans ASME* 102:249–256
- Cocks ACF, Leckie FA (1987) Creep constitutive equations for damaged materials. In: Wu TY, Hutchinson JW (eds) *Advances in applied mechanics*, vol 25. Academic, New York, pp 239–294
- Coleman BD, Gurtin ME (1967) Thermodynamics with internal state variables. *J Chem Phys* 47:597–613
- Coleman BD, Mizel VJ (1964) Existence of caloric equations of state in thermodynamics. *J Chem Phys* 40:1116–1125
- Cordebois JP, Sidoroff F (1982a) Damage induced elastic anisotropy. In: Boehler JP (ed) *Mechanical behavior of anisotropic solids*. Martinus Nijhoff Publishers, The Hague, pp 761–774
- Cordebois JP, Sidoroff F (1982b) Endommagement anisotrope en ´elasticit   et plasticit  . *Journal de M  canique Th  orique et Appliqu  e Num  ro Sp  cial*, 45–60

- Davison L, Stevens AL (1973) Thermodynamical constitution of spalling elastic bodies. *J Appl Phys* 44:668–674
- de Borst R, Sluys LJ, Mühlhaus HB, Pamin J (1993) Fundamental issues in finite element analyses of localization of deformation. *Eng Comput* 10:99–121
- De Groot SR, Mazur P (1962) Non-equilibrium thermodynamics. North-Holland, Amsterdam
- de Vree JHP, Brekelmans WAM, van Gils MAJ (1995) Comparison of nonlocal approaches in continuum mechanics. *Comput Struct* 55:581–588
- Desmorat R, Cantournet S (2008) Modeling microdefects closure effect with isotropic/anisotropic damage. *Int J Damage Mech* 17:65–96
- Desmorat R, Kane A, Seyed M, Sermage JP (2007) Two scale damage model and related numerical issues for thermo-mechanical high cycle fatigue. *Eur J Mech A/Solids* 26:909–935
- Dufailly J, Lemaitre J (1995) Modeling very low cycle fatigue. *Int J Damage Mech* 4:153–170
- Dunne FPE, Hayhurst DR (1992a) Continuum damage based constitutive equations for copper under high temperature creep and cyclic plasticity. *Proc R Soc London A* 437:545–566
- Dunne FPE, Hayhurst DR (1992b) Modelling of combined high-temperature creep and cyclic plasticity in components using continuum damage mechanics. *Proc R Soc London A* 437:567–589
- Dvorak GJ, Bahei-El-Din YA (1982) Plasticity analysis of fibrous composites. *J Appl Mech Trans ASME* 49:327–335
- Dvorak GJ, Bahei-El-Din YA (1987) A bimodal plasticity theory of fibrous composite materials. *Acta Mech* 69:219–241
- Dyson BF, Hayhurst DR, Lin J (1996) The ridged uniaxial testpiece: creep and fracture predictions using large-displacement finite-element analyses. *Proc R Soc London A* 452:655–676
- Evans HE (1984) Mechanisms of creep fracture. Elsevier, London
- François D, Pineau A, Zaoui A (1998) Mechanical behaviour of materials, vol II. Kluwer, Dordrecht
- Fung YC (1965) Foundations of solid mechanics. Prentice-Hall, Englewood Cliffs, NJ
- Fung YC (1977) A first course in continuum mechanics, 2nd edn. Prentice-Hall, Englewood Cliffs, NJ
- Germain P (1973) Cours de Mécanique des Milieux Continus. Masson et Cie, Paris
- Germain P, Nguyen QS, Suquet P (1983) Continuum thermodynamics. *J Appl Mech Trans ASME* 50:1010–1020
- Ghrib F, Tinawi R (1995a) An application of damage mechanics for seismic analysis of concrete gravity dams. *Earthquake Eng Struct Dyn* 24:157–173
- Ghrib F, Tinawi R (1995b) Nonlinear behaviour of concrete dams using damage mechanics. *J Eng Mech ASCE* 121:513–527
- Glansdorff P, Prigogine I (1971) Thermodynamic theory of structure, stability and fluctuations. Wiley, London
- Gologanu M, Leblond JB, Devaux J (1993) Approximate models for ductile metals containing non-spherical voids – case of symmetric prolate ellipsoidal cavities. *J Mech Phys Solids* 41:1723–1754
- Gologanu M, Leblond JB, Devaux J (1994) Approximate models for ductile metals containing non-spherical voids – case of axisymmetric oblate ellipsoidal cavities. *J Eng Mater Technol Trans ASME* 116:290–294
- Goodall IW, Hales R, Walters DJ (1981) On constitutive relations and failure criteria of an austenitic steel under cyclic loading at elevated temperature, In: Ponter ARS, Hayhurst DR (eds) Creep in structures. Springer, Berlin, pp 103–127
- Goods SH, Brown LM (1979) The nucleation of cavities by plastic deformation. *Acta Metall* 27:1–15
- Graf A, Hosford W (1994) The influence of strain-path changes on forming limit diagrams of A 6111-T4. *Int J Mech Sci* 36:897–910
- Green ML (1992) Laboratory tests on Salem limestone. Geomechanics Division, Structures Laboratory, Department of the Army, Vicksburg, Mississippi

- Gurson AL (1977) Continuum theory of ductile rupture by void nucleation and growth: part I Yield criteria and flow rules for porous ductile media. *J Eng Mater Technol Trans ASME* 99:2–15
- Hall FR, Hayhurst DR (1991) Modelling of grain size effects in creep crack growth using a non-local continuum damage approach. *Proc R Soc London A* 433:405–421
- Halm D, Dragon A (1998) An anisotropic model of damage and frictional sliding for brittle materials. *Eur J Mech A/Solids* 17:439–460
- Halm D, Dragon A, Charles Y (2002) A modular damage model for quasi-brittle solids – interaction between initial and induced anisotropy. *Arch Appl Mech* 72:498–510
- Halphen B, Nguyen QS (1975) Sur les matériaux standards généralisés. *J Mécanique* 14:39–63
- Hancock JW, Mackenzie AC (1976) On the mechanisms of ductile failure in high-strength steels subjected to multi-axial stress-states. *J Mech Phys Solids* 24:147–169
- Hansen NR, Schreyer HL (1994) A thermodynamically consistent framework for theories of elastoplasticity coupled with damage. *Int J Solids Struct* 31:359–389
- Hashin Z (1983) Analysis of composite materials – a survey. *J Appl Mech Trans ASME* 50:481–505
- Hashin Z (1988) The differential scheme and its application to cracked materials. *J Mech Phys Solids* 36:719–734
- Hayakawa K, Murakami S (1997) Thermodynamical modeling of elastic-plastic damage and experimental validation of damage potential. *Int J Damage Mech* 6:333–363
- Hayakawa K, Murakami S, Liu Y (1998) An irreversible thermodynamic theory for elastic-plastic-damage materials. *Eur J Mech A/Solids* 17:13–32
- Hayhurst DR (1972) Creep rupture under multi-axial states of stress. *J Mech Phys Solids* 20:381–390
- Hayhurst DR (2001) Computational continuum damage mechanics: its use in the prediction of creep in structures- past, present and future. In: Murakami S, Ohno N (eds) IUTAM symposium on creep in structures. Kluwer, Dordrecht, pp 175–188
- Hayhurst DR, Brown PR, Morrison CJ (1984) The role of continuum damage in creep crack growth. *Philos Trans R Soc London A* 311:131–158
- Hayhurst DR, Dimmer PR, Chernuka MW (1975) Estimates of the creep rupture lifetime of structures using the finite element method. *J Mech Phys Solids* 23:335–355
- He QC, Curnier A (1995) A more fundamental approach to damaged elastic stress-strain relations. *Int J Solids Struct* 32:1433–1457
- Hill R (1958) A general theory of uniqueness and stability in elastic-plastic solids. *J Mech Phys Solids* 16:236–249
- Hill R (1963) Elastic properties of reinforced solids: some theoretical principles. *J Mech Phys Solids* 11:357–372
- Holzapfel GA (2000) Nonlinear solid mechanics: a continuum approach for engineering. Wiley, Chichester
- Horii H, Nemat-Nasser S (1985) Compression-induced microcrack growth in brittle solids: axial splitting and shear failure. *J Geophys Res B4* 90:3105–3125
- Hutchinson JW (1968) Singular behaviour at the end of a tensile crack in a hardening materials. *J Mech Phys Solids* 16:13–31
- Itsukov M (2007) Tensor algebra and tensor analysis for engineers, with application to continuum mechanics. Springer, Berlin
- Janson J, Hult J (1977) Fracture mechanics and damage mechanics, a combined approach. *Journal de Mécanique Appliquée* 1:69–84
- Ju JW (1989) On energy-based coupled elastoplastic damage theories: constitutive modeling and computational aspects. *Int J Solids Struct* 25:803–833
- Jubran JS, Cofer WF (1991) Ultimate strength analysis of structural components using the continuum damage mechanics approach. *Comput Struct* 39:741–752
- Kachanov LM (1958) On rupture time under condition of creep, *Izvestia Akademi Nauk SSSR, Otd. Tekhn. Nauk*, No.8, 1958, 26–31 (in Russian)

- Kachanov LM (1974) Foundations of fracture mechanics (in Russian). Izdatelstvo Nauka, Moscow
- Kachanov LM (1986) Introduction to continuum damage mechanics. Martinus Nijhoff, Dordrecht
- Kachanov M (1980) Continuum model of medium with cracks. J Eng Mech Div Trans ASCE, EM5 106:039–1051
- Kachanov M (1987) Elastic solids with many cracks: A simple method of analysis. Int J Solids Struct 23:23–43
- Kanatani K (1984) Distribution of directional data and fabric tensors. Int J Eng Sci 22:149–164
- Kattan PI, Voyiadjis GZ (1990) A coupled theory of damage mechanics and finite strain elasto-plasticity, I. Damage and elastic deformations. Int J Eng Sci 28:421–435
- Kattan PI, Voyiadjis GZ (2002) Damage mechanics with finite elements. Springer, Berlin
- Kestin J, Rice JR (1970) Paradoxes in the application of thermodynamics to strained solids. In: Stuart EB, Gal-Or B, Brainard AJ (eds) A critical review of thermodynamics. Mono Book Corp, Baltimore, MD, pp 275–298
- Kobayashi H (1993) Fracture mechanics (in Japanese). Kyoritsu Shuppan, Tokyo
- Kowalewski ZL, Hayhurst DR, Dyson BF (1994) Mechanisms-based creep constitutive equations for an aluminum alloy. J Strain Anal 29:309–316
- Krajcinovic D (1983) Constitutive equations for damaging materials. J Appl Mech Trans ASME 50:355–360
- Krajcinovic D (1984) Continuum damage mechanics. Appl Mech Rev 37:1–6
- Krajcinovic D (1989) Damage mechanics. Mech Mater 8:117–197
- Krajcinovic D (1996) Damage mechanics. North-Holland, Amsterdam
- Krajcinovic D, Fonseka GU (1981) The continuous damage theory of brittle materials, part 1: general theory, part 2: uniaxial and plane response modes. J Appl Mech Trans ASME 48:809–824
- Krajcinovic D, Lemaître J (ed) (1987) Continuum damage mechanics – theory and applications, CISM Courses and Lectures No. 295. Springer, Wien
- Kraus H (1980) Creep analysis. Wiley, New York
- Kreuzer E (ed) (1994) Computerized symbolic manipulation in mechanics, CISM Courses and Lectures No. 343. Springer, Wien
- Lacy TE, McDowell DL, Willice PA, Talreja R (1997) On representation of damage evolution in continuum damage mechanics. Int J Damage Mech 6:62–95
- Ladevèze P (1992) A damage computational method for composite structures. Comput Struct 44:79–87
- Ladevèze P (2005) Multiscale computational damage modelling of laminate composites. In: Sadowski T (ed) Multiscale modelling of damage and fracture processes in composite materials. Springer, Wien, pp 171–212
- Ladevèze P, Allix O, L.Gornet, Lévéque D, Perret L (1998) A computational damage mechanics approach for laminates: identification and comparison with experimental results. In: Voyiadjis GZ, Ju J-W, Chaboche J-L (eds) Damage mechanics in engineering materials. Elsevier, Amsterdam, pp 481–500
- Ladevèze P, Le Dantec E (1992) Damage modelling of the elementary ply for laminated composites. Compos Sci Technol 43:257–267
- Ladevèze P, Lemaître J (1984) Damage effective stress in quasi-unilateral conditions. In: Proceeding of the 16th IUTAM congress, Lyngby, Denmark
- Ladevèze P, Lubineau G (2001) On a damage mesomodel for laminates: micro-meso relationships, possibilities and limits. Compos Sci Technol 61:2149–2158
- Leblond JB, Perrin G, Devaux J (1995) An improved Gurson-type model for hardenable ductile metals. Eur J Mech A/Solids 14:499–527
- Leigh DC (1968) Nonlinear continuum mechanics. McGraw-Hill, New York
- Lemaître J (1971) Evaluation of dissipation, damage in metals subjected to dynamic loading. In: Proceedings of international conference on the mechanical behavior of materials 1 (ICM 1), Kyoto

- Lemaitre J (1985) A continuous damage mechanics model for ductile fracture. *J Eng Mater Technol Trans ASME* 107:83–89
- Lemaitre J (1986) Local approach of fracture. *Eng Fract Mech* 25:523–537
- Lemaitre J (1987) Formulation and identification of damage kinetic constitutive equations. In: Krajcinovic D, Lemaitre J (eds) *Continuum damage mechanic: theory and applications*, CISM Courses and Lectures No. 295. Springer, Wien, pp 37–89
- Lemaitre J (1990) Micro-mechanics of crack initiation. *Int J Frac* 42:87–99
- Lemaitre J (1992) A course on damage mechanics. Springer, Berlin; 2nd Edition (1996)
- Lemaitre J, Chaboche JL (1978) Aspect phénoménologique de la rupture par endommagement. *Journal de Mécanique Appliquée* 2:317–365
- Lemaitre J, Chaboche JL (1985) *Mécanique des Matériaux Solides*, Dunod, Paris; Mechanics of solid materials, Cambridge University Press, Cambridge (1990)
- Lemaitre J, Chaboche J-L, Benallal A, Desmorat R (2009) *Mécanique des Matériaux Solides*, 3e edn. Dunod, Paris
- Lemaitre J, Desmorat R (2005) Engineering damage mechanics. Springer, Belrin
- Lemaitre J, Desmorat R, Sauzay M (2000) Anisotropic damage law of evolution. *Eur J Mech A/Solids* 19:187–208
- Lemaitre J, Doghri I (1994) Damage 90: a post-processor for crack initiation. *Comput Methods Appl Mech Eng* 115:197–232
- Lemaitre J, Dufailly J (1987) Damage measurements. *Eng Fract Mech* 28:643–661
- Lemaitre J, Sermage JP, Desmorat R (1999) A two scale damage concept applied to fatigue. *Int J Fract* 97:67–81
- Lin J, Liu Y, Dean TA (2005) A review on damage mechanisms, models and calibration methods under various deformation conditions. *Int J Damage Mech* 14:299–319
- Liu Y, Murakami S (1996) Creep crack growth analysis by use of a local approach incorporating perfect plasticity. In: Townley H, Asada Y, Tseng A (eds) *Proceedings of 6th international conference on creep and fatigue*. Mechanical Engineering Publications, London, pp 331–340
- Liu Y, Murakami S, Kanagawa Y (1994) Mesh-dependence and stress singularity in finite element analysis of creep crack growth by continuum damage mechanics approach. *Eur J Mech A/Solids* 13:395–418
- Lubarda VA, Krajcinovic D (1993) Damage tensors and the crack density distribution. *Int J Solids Struct* 30:2859–2877
- Lubarda VA, Krajcinovic D, Mastilovic S (1994) Damage model for brittle elastic solids with unequal tensile and compressive strengths. *Eng Fract Mech* 49:681–697
- Mahnken R (2002) Theoretical, numerical and identification aspects of a new model class for ductile damage. *Int J Plast* 18:801–831
- Malvern LE (1969) Introduction to the mechanics of a continuous medium. Prentice-Hall, Englewood Cliffs, NJ
- Matera R, Rustichelli F (1979) The evaluation of creep damage. In: Bernasconi G, Piatti G (eds) *Creep of engineering materials and structures*. Applied Science Publishers, London, pp 389–412
- Maugin GA (1992) The thermomechanics of plasticity and fracture. Cambridge University Press, Cambridge
- Mazars J (1986) A description of micro- and macro-scale damage of concrete structures. *Eng Fract Mech* 25:729–737
- Mazars J, Pijaudier-Cabot G (1989) Continuum damage theory – APPLICATION to concrete. *J Eng Mech* 115:345–365
- Mehta PK (1986) Concrete: structure, properties, and materials. Prentice-Hall, Englewood Cliffs, NJ
- Mori T, Tanaka K (1973) Average stress in matrix and average elastic energy of materials with misfitting inclusions. *Acta Metall* 21:571–574
- Mühlhaus HB, Vardoulakis I (1987) The thickness of shear bands in granular materials. *Geotechnique* 37:271–283

- Murakami S (1983) Notion of continuum damage mechanics and its application to anisotropic creep damage theory. *J Eng Mater Technol Trans ASME* 105:99–105
- Murakami S (1988) Mechanical modeling of material damage. *J Appl Mech Trans ASME* 55:280–286
- Murakami S (1993) Anisotropic damage in metals. In: Boehler JP (eds) *Failure criteria of structured media*. A.A. Balkema, Rotterdam, pp 99–119
- Murakami S, Hayakawa K, Liu Y (1998) Damage evolution and damage surface of elastic-plastic-damage materials under multiaxial loading. *Int J Damage Mech* 7:103–128
- Murakami S, Hirano T (2000) Effects of damage on the asymptotic fields of a mode III creep crack in steady-state growth. In: Benallal A (ed) *Continuous damage and fracture*. Elsevier, Paris, pp 65–70
- Murakami S, Hirano T, Liu Y (2000a) Asymptotic fields of stress and damage of a mode I creep crack in steady-state growth. *Int J Solids Struct* 37:6203–6220
- Murakami S, Hirano T, Liu Y (2001) Effects of damage on the asymptotic fields of a mode I creep crack in steady-stress growth. In: Murakami S, Ohno N (eds) *IUTAM symposium on creep in structures*. Kluwer, Dordrecht, pp 165–174
- Murakami S, Imaizumi T (1982) Mechanical description of creep damage state and its experimental verification. *Journal de Mécanique Théorique et Appliquée* 1:743–761
- Murakami S, Kamiya K (1997) Constitutive and damage evolution equations of elastic-brittle materials based on irreversible thermodynamics. *Int J Mech Sci* 39:473–486
- Murakami S, Kawai M, Rong H (1998) Finite element analysis of creep crack growth by a local approach. *Int J Mech Sci* 30:491–502
- Murakami S, Liu Y (1995) Mesh-dependence in local approach to creep fracture. *Int J Damage Mech* 4:230–250
- Murakami S, Liu Y (1996) Local approach of fracture based on continuum damage mechanics and the related problems. *Mater Sci Res Int* 2:131–142
- Murakami S, Liu Y, Mizuno M (2000b) Computational methods for creep fracture analysis by damage mechanics. *Comput Methods Appl Mech Eng* 183:15–33
- Murakami S, Ohno N (1981) A continuum theory of creep and creep damage. In: Ponter ARS, Hayhurst DR (eds) *Creep in structures, proceedings of 3rd IUTAM symposium*, Leicester, 1980. Springer, Berlin, pp 422–444
- Murakami S, Ohno N (1988) Continuum theory of material damage at high temperature. In: Ohtani R, Ohnami M, Inoue T (eds) *High temperature creep-fatigue*. Elsevier, London, pp 43–64
- Murakami S, Tominaga M, Rong H (1990) Formulation of elasticity-damage coupling and applicability of effective stress in damage mechanics. *Trans Japan Soc Mech Eng Series A Solid Mech Mater Eng* 56:2297–2304 (in Japanese)
- Nahshon K, Hutchinson JW (2008) Modification of the Gurson model for shear failure. *Eur J Mech A/Solids* 27:1–17
- Nahshon K, Xue Z (2009) A modified Gurson model and its application to puch-out experiments. *Eng Fract Mech* 76:997–1009
- Needham NG, Wheatley JE, Greenwood GW (1975) The creep fracture of copper and magnesium. *Acta Metall* 23:23–27
- Needleman A, Rice JR (1978) Limits to ductility set by plastic flow localization. In: Koistinen DP, Wang NM (eds) *Mechanics of sheet metal forming*. Plenum Press, New York, pp 237–265
- Needleman A, Triantafyllidis N (1978) Void growth and local necking in biaxially stretched sheets. *J Eng Mater Technol Trans ASME* 100:164–169
- Needleman A, Tvergaard V (1984) An analysis of ductile rupture in notched bars. *J Mech Phys Solids* 32:461–490
- Nemat-Nasser S, Hori M (1993) *Micromechanics: overall properties of heterogeneous materials*. North-Holland, Amsterdam; 2nd Revised Edition, Elsevier, Amsterdam (1999)
- Odqvist FKG und Hult J (1962) *Kriechfestigkeit Metallis c her Werkstoffe*. Springer, Berlin
- Ogden RW (1984) Non-linear elastic deformations. Ellis-Horwood, Chichester; Dover, New York (1997)

- Ohno N, Wang JD (1994) Kinematic hardening rules for simulation of ratchetting behavior. *Eur J Mech A/Solids* 13:519–531
- Onat ET, Leckie FA (1988) Representation of mechanical behavior in the presence of changing internal structure. *J Appl Mech Trans ASME* 55:1–10
- Oñate E, Kleiber M, Saracibar CA (1988) Plastic and viscoplastic flow of void-containing metals; applications to axisymmetric sheet forming problems. *Int J Numer Methods Eng* 25:227–251
- Onsager L (1931) Reciprocal relations in irreversible processes, I, II. *Phys Rev* 37:405–426; 1931; 38:2265–2279
- Ortiz M (1985) A constitutive theory for the inelastic behavior of concrete. *Mech Mater* 4:67–93
- Othman AM, Hayhurst DR, Dyson BF (1993) Skeletal point stresses in circumferentially notched tension bars undergoing tertiary creep modelled with physically based constitutive equations. *Proc R Soc London A* 441:343–358
- Pardoen T (2006) Numerical simulation of low stress triaxiality ductile fracture. *Comput Struct* 84:1641–1650
- Pardoen T, Hutchinson JW (2000) An extended model for void growth and coalescence. *J Mech Phys Solids* 48:2467–2512
- Pedersen TO (2000) Numerical modelling of cyclic plasticity and fatigue damage in cold-forging tools. *Int J Mech Sc* 42:799–818
- Penny RK, Marriott DL (1971) Design for creep. McGraw-Hill, New York
- Perrin IJ, Hayhurst DR (1999) Continuum damage mechanics analyses of type IV creep failure in ferritic steel crossweld specimens. *Int J Press Vessels Piping* 76:599–617
- Perzyna P (1966) Fundamental problems in viscoplasticity. In: Yih CS (ed) *Advances in applied mechanics*, vol 9. Academic, New York, pp 243–377
- Perzyna P (1971) Thermodynamic theory of viscoplasticity. In: Yih CS (ed) *Advances in applied mechanics*, vol 11. Academic, New York, pp 313–354
- Pietruszczak S, Mróz Z (1981) Finite element analysis of deformation of strain-softening materials. *Int J Numer Methods Eng* 17:327–334
- Pijaudier-Cabot G, Bažant ZP (1987) Nonlocal damage theory. *J Eng Mech Trans ASCE* 113:1512–1533
- Pineau A (1982) Review of fracture micromechanisms and a local approach to predicting crack resistance in low strength steels. In: François D (ed) *Advances in fracture research, proceedings of ICF 5* (1980). Pergamon Press, Oxford, pp 553–577
- Pineau A, Cailletaud G, Lindley TC (ed) (1996) Multiaxial fatigue and design. Mechanical Engineering Publications, London
- Pirondi A, Bonora N (2003) Modeling ductile damage under fully reversed cycling. *Comput Mater Sci* 26:129–141
- Rabier PJ (1989) Some remarks on damage theory. *Int J Eng Sci* 27:29–54
- Rabotnov Yu N (1968) Creep rupture. In: Hetenyi M, Vincenti M (eds) *Proceedings of applied mechanics conference*. Stanford University. Springer, Berlin, pp 342–349
- Rabotnov Yu N (1969) Creep problems in structural members. North-Holland, Amsterdam
- Raghavan P, Ghosh S (2005) A continuum damage mechanics model for unidirectional composites undergoing interfacial debonding. *Mech Mater* 37:955–979
- Rice JR (1971) Inelastic constitutive relations for solids: an internal-variable theory and its application to metal plasticity. *J Mech Phys Solids* 19:433–455
- Rice JR (1975) Continuum mechanics and thermodynamics of plasticity in relation to microscale deformation mechanics. In: Argon AS (ed) *Constitutive equations in plasticity*. MIT Press, Cambridge, pp 23–79
- Rice JR, Rosengren G (1968) Plane strain deformation near a crack tip in a power-law hardening material. *J Mech Phys Solids* 16:1–12
- Rice JR, Tracy DM (1969) On ductile enlargement of voids in triaxial stress fields. *J Mech Phys Solids* 17:210–217

- Rousselier G (1981) Finite deformation constitutive relations including ductile fracture damage. In: Nemat-Nasser S (ed) Three-dimensional constitutive relations and ductile fracture. North-Holland, Amsterdam, pp 331–355
- Rousselier G (1987) Ductile fracture models and their potential in local approach of fracture. *Nucl Eng Des* 105:97–111
- Saanouni K (ed) (2003) Numerical modelling in damage mechanics. Kogan Page Science, London
- Saanouni K (2006) Virtual metal forming including the ductile damage occurrence: actual state of the art and main perspectives. *J Mater Process Technol* 177:19–25
- Saanouni K, Chaboche JL (2003) Computational damage mechanics: application to metal forming. In: Milne I, Ritchie RO, Karihaloo B (eds) Comprehensive structural integrity, vol 3. Elsevier, Oxford, pp 321–376
- Saanouni K, Chaboche JL, Lesne PM (1989) On the creep crack-growth prediction by a nonlocal damage formulation. *Eur J Mech A/Solids* 8:437–459
- Saanouni K, Forster C, Ben Hatira F (1994) On the anelastic flow with damage. *Int J Damage Mech* 3:140–169
- Saanouni K, Lestriez P, Labergère C (2011) 2D adaptive FE simulations in finite thermo-elasto-viscoplasticity with ductile damage: application to orthogonal metal cutting by chip formation and breaking. *Int J Damage Mech* 20:23–61
- Saanouni K, Mariage JF, Cherouat A, Lestriez P (2004) Numerical prediction of discontinuous central bursting in axisymmetric forward extrusion by continuum damage mechanics. *Comput Struct* 82:2309–2332
- Saanouni K, Nesnas K, Hammi Y (2000) Damage modeling in metal forming processes. *Int J Damage Mech* 9:196–240
- Sadowski T (ed) (2005) Multiscale modelling of damage and fracture processes in composite materials. CISM Courses and Lectures No. 474. Springer, Wien
- Sadowski T (ed) (2006) IUTAM symposium on multiscale modelling of damage and fracture processes in composite materials. Springer, Dordrecht; Dolny, Poland (2005)
- Sermage JP, Lemaitre J, Desmorat R (2000) Multiaxial creep-fatigue under anisothermal conditions. *Fatigue Fract Eng Mater Struct* 23:241–252
- Simo JC (1989) Strain softening and dissipation: a unification of approaches. In: Mazars J, Bažant ZP (eds) Cracking and damage – strain localization and size effect. Elsevier, London, pp 440–461
- Simo JC, Ju JW (1987) Strain- and stress-based continuum damage models, I. Formulation; II. Computational aspects. *Int J Solids Struct* 23:821–869
- Skrzypek J, Ganczarski A (1999) Modeling of material damage and failure of structures. Springer, Berlin
- Smith GM, Young LE (1955) Ultimate theory in flexure by exponential function. *J Proc ACI* 52:349–359
- Spencer AJM (1971) Theory of invariants. In: Eringen AC (ed). Continuum physics, vol. I, Academic, New York
- Stören S, Rice JR (1975) Localized necking in thin sheets. *J Mech Phys Solids* 23:421–441
- Sun D, Siegele D, Voss B, Schmitt W (1988) Application of local damage models to the numerical analysis of ductile rupture. *Fatigue Fract Eng Mater Struct* 12:201–212
- Tai WH, Yang BX (1986) A new microvoid-damage model for ductile fracture. *Eng Fract Mech* 25:377–384
- Tanaka E (1994) A nonproportionality parameter and a cyclic viscoplastic constitutive model taking into account amplitude dependences and memory effects of isotropic hardening. *Eur J Mech A/Solids* 13:155–173
- Thomason PF (1990) Ductile fracture of metals. Pergamon Press, Oxford
- Thomson RD, Hancock JW (1984) Ductile failure by void nucleation, growth and coalescence. *Int J Fract* 26:99–112
- Triantafyllidis N, Aifantis EC (1986) A gradient approach to localization of deformation, I. Hyperelastic materials. *J Elasticity* 16:225–237

- Truesdell C (1969) Rational thermodynamics. MacGraw-Hill, New York; Enlarged Edition, Springer, Berlin (1984)
- Truesdell C, Noll W (1965) The non-linear field theories of mechanics. In: Flügge S (ed) Encyclopedia of physics, vol III/3. Springer, Berlin; 3rd Edition (2004)
- Truesdell C, Toupin RA (1960) The classical field theories. In: Flügge S (ed) Encyclopedia of physics, vol III/1. Springer, Berlin
- Tvergaard V (1981) Influence of void on shear band instabilities under plane strain conditions. *Int J Fract* 17:389–407
- Tvergaard V (1990) Material failure by void growth to coalescence. In: Hutchinson JW, Wu TY (eds) Advances in applied mechanics, vol 27. Academic, New York, pp 83–151
- Tvergaard V, Needleman A (1984) Analysis of the cup-cone fracture in a round tensile bar. *Acta Metall* 32:157–169
- Tvergaard V, Needleman A (1995) Effects of nonlocal damage in porous plastic solids. *Int J Solids Struct* 32:1063–1077
- Vakulenko AA, Kachanov M (1971) Continuum theory of cracked media, Izvestia AN SSSR, Mekhanika Tverdogo Tiela, No. 4, pp 159–166 (in Russian)
- Viswanathan R (1989) Damage mechanisms and life assessment of high-temperature components. ASM International, Metals Park, OH
- Voyiadjis GZ, Kattan PI (1990) A coupled theory of damage mechanic and finite strain elasto-plasticity, II. Damage and finite strain plasticity. *Int J Eng Sci* 28:505–524
- Voyiadjis GZ, Kattan PI (1993) Local approach to damage in elasto-plastic metal matrix composites. *Int J Damage Mech* 2:92–114
- Voyiadjis GZ, Kattan PI (1999) Advances in damage mechanics: metals and metal matrix composites. Elsevier, Amsterdam
- Voyiadjis GZ, Kattan PI (2009) A comparative study of damage variables in continuum damage mechanics. *Int J Damage Mech* 18:315–340
- Voyiadjis GZ, Park T (1994) Interfacial and local damage analysis of metal matrix composites. In: Allen DH, Ju JW (eds) Damage mechanic in composites. The American Society of Mechanical Engineers, New York, pp 87–108
- Wang PT (1977) Complete stress-strain curves of concrete and its effect on ductility of reinforced concrete members. Ph. D. Thesis, University of Illinois at Chicago Circle, Illinois
- Xia L, Shih C, Hutchinson J (1995) A computational approach to ductile crack growth under large scale yielding conditions. *J Mech Phys Solids* 43:389–413
- Yang Q, Chen X, Zhou WY (2005) On the structure of anisotropic damage yield criteria. *Mech Mater* 37:1049–1058
- Yazdani S, Schreyer HL (1988) An anisotropic damage model with dilatation for concrete. *Mech Mater* 7:231–244
- Yoshida E, Ichikawa Y (2007) Private communication (Nagoya University)
- Zheng Q-S (1994) Theory of representations for tensor functions: a unified invariant approach to constitutive equations. *Appl Mech Rev* 47:545–587
- Zheng Q-S, Betten J (1995) On the tensor-values function representations of 2nd-order and 4th-order tensors: part I. *Z Angew Mathematik Mechanik* 75:269–281
- Zheng Q-S, Betten J (1996) On damage effective stress and equivalence hypothesis. *Int J Damage Mech* 5:219–240
- Zhu X, Weinmann K, Chandra A (2001) A unified bifurcation analysis of sheet metal forming limits. *J Eng Mater Technol Trans ASME* 123:329–333

Index

A

- Absolute notation, 329
- Absolute temperature, 80
- Accelerating creep, 218
- Accumulated plastic strain, 89
- Activated elastic modulus tensor, 132, 137, 269
- Activation of crack, 256
- Active (state of crack), 127, 133, 255
- Anisotropic
 - brittle damage theory, 126, 262, 268, 270
 - creep damage theory, 217, 226
 - inelastic damage theory, 111, 119, 176
- Anisotropic damage, 23, 26, 28, 30
- Anisotropy parameter, 116, 182
- Antisymmetric tensor, 331
- Armstrong-Frederick evolution equation, 174
- Artificial viscosity, 317
- Associated variable, 68, 86, 96
- Asymptotic stress field (at crack tip), 249
- Atomic scale, 4
- Axial vector, 335

B

- Back stress, 78
- Bailey-Norton law, 222
- Basis
 - second-order, 292, 369
 - tensor, 292
 - transformation of, 342
 - vector, 328
- Bifurcation (of deformation), 310, 313, 320
- Bilateral effect, 104, 257
- Blanking, 169, 172
- Body force, 59
- Brittle damage, 7, 126, 253, 262, 268, 270
 - material, 127, 132, 253, 262
 - theory, 136, 262, 268
- Bulk modulus, 376

C

- Caloric equation of state, 63
- Cartesian
 - component, 328, 334
 - coordinate system, 351
 - decomposition, 332
- Cauchy's formula, 25, 60
- Cayley-Hamilton theorem, 348
- Cell model, 313, 316
- Ceramic matrix composite, 288–294
- Chain rule, 352, 359
- Characteristic equation, 346
- Characteristic length, 315, 323
- Chisel edge fracture, 6
- Clausius-Duhem inequality, 61, 82, 119
- Cleavage, 5
- Closed system (of thermodynamics), 57
- Coffin-Manson law, 210
- Complementary equation, 68
- Complementary strain energy, 38
 - equivalence of, 38, 52
- Completely damaged zone (CDZ), 305
- Compliance, *see* Elastic compliance
- Component
 - of tensor, 334
 - of vector, 328
- Composite material, 277
- Concrete, 254, 257, 266, 307
 - damage of, 254
 - elastic-brittle damage of, 266
 - mesoscopic behavior of, 257
- Conservation of mass, 60, 190
- Consistency condition, 90, 118, 186, 291
- Constitutive equation (model, theory), 65, 67, 68
 - creep, 219, 224, 227, 247
 - elastic, 44, 48, 67, 71, 366, 375
 - elastic-plastic, 88, 141, 176

- Constitutive equation (model, theory) (*cont.*)
- of Gurson, 184, 195
 - inelastic, 72, 81, 111
 - of isotropic elastic material, 48, 375
 - plastic, 88, 117, 124, 178
 - of Rousselier, 188, 193
 - thermodynamic, 65, 72, 81, 119
 - viscoplastic, 92, 231, 243
 - of void-containing material, 184
- Continuum damage mechanics (CDM), 3, 12, 54, 154
- Contraction, 336, 339
- double, 336
 - of higher-order, 339
- Coordinate, 351
- Coordinate system, 351
- Cartesian, 351
 - material, 278
 - orthogonal, 351
 - orthonormal, 351
 - spatial, 284
- Cosserat continuum, 317
- Crack band model, 313
- Crack-density tensor, 27
- Crack of mixed mode, 255
- Crack tip
- damage field, 247
 - stress field, 247
- Creep, 80, 217
- accelerating, 218
 - constitutive equation, 219, 223–224, 227, 229
 - curve, 217
 - steady state, 218
 - transient, 218
- Creep damage, 7, 16, 217, 221
- evolution equation, 219, 222, 224, 227–228
- Creep-fatigue
- damage, 10, 234, 236, 240, 242
 - interaction, 10, 234, 240
- Creep rupture, 8, 217, 222
- strain, 220–221
 - stress criterion of, 222
 - time, 219, 221, 233
- Critical value (of damage variable)
- (for creep-fatigue), 238
 - (for ductile fracture), 98, 153, 155, 158
 - (for fatigue), 203, 209
 - (for fracture, crack initiation), 77, 94, 149
- Cross product, 332
- Cup and cone fracture, 164
- Curl, 353
- Current damaged configuration, 23, 36, 42, 294
- Cycle number of damage start (fatigue), 203
- Cylindrical transverse isotropy, 135
- D**
- Damage, 3
- deactivation (of damage), 128, 288
 - effect tensor, 34, 37, 44
 - equivalent stress, 101, 105
 - localization, 251, 308, 313, 322
 - mechanical representation of, 15, 21
 - mechanics, 12
 - mechanism, 5, 106
 - modeling of, 15
 - scale of, 4
 - state, 16, 18, 21, 25
 - stress criterion, 99, 101, 105, 165, 222
- Damage-associated variable, 86, 96
- Damage dissipation potential (function, surface), 69, 88, 112, 115, 166, 170, 178
- Damage effect tensor, 34, 37, 44, 176
- matrix representation of, 44–48
- Damage evolution equation, 93, 117, 124, 176, 219, 224, 264
- Damage (loading) surface, 115, 125, 260, 274
- Damage mesomodel of laminate, 287
- Damage-strengthening variable, 82, 112, 114, 118, 126
- Damage tensor
- eighth-order, 30
 - fourth-order, 31, 126, 134, 289
 - second-order, 23, 26, 111, 262
- Damage variable, 12
- in terms of elastic compliance tensor, 270
 - in terms of elastic modulus tensor, 136, 268
 - scalar, 16, 22, 82, 258
 - tensor, 23, 31
 - vector, 22
- Deactivation (of crack, damage), 128, 288
- Debonding, 280
- Decohesion, 4–5, 154
- Deformation
- bifurcation of, 310, 319
 - uniqueness of, 311
- Delamination, 286
- Del operator, 352
- Dependent variable, 58
- Derivative
- of invariant, 362
 - of tensor function, 359
- Determinant
- of matrix, 345
 - of tensor, 344–345

- Deviatoric
strain tensor, 100
stress tensor, 87, 100
- Differentiation
of tensor field, 350
of tensor function, 358
- Diffused necking, 169
- Dilatancy, 257
- Dimple, 6
- Directional distribution of microvoid density, 28
- Direct notation, 329
- Discontinuity
of strain rate field, 311
of stress-strain relation, 138
- Dissipation, 68
of energy, 98–99
inequality, 68
maximum, 115, 137
- Dissipation potential (function, surface), 69, 84, 115, 123, 166
- Distribution function (of microvoid), 28
- Divergence, 353, 355
theorem (of Gauss), 355
- Dot product, 327
- Double contraction, 336
- Ductile damage, 7, 141, 143, 153, 184
model of, 155, 158
- Ductile fracture, 153, 192
- Dummy index, 329
- Dyad, 333
- Dyadic, 334
- E**
- Eddington epsilon, 333
- Effective area, 16, 17
reduction, 16
- Effective elastic modulus tensor, 132–133, 137, 290
- Effective strain tensor, 40, 299
- Effective stress, 15, 18, 31–32
tensor, 25, 31–32, 34
- Effective void volume fraction, 187
- Eigenvalue, 346
- Eigenvector, 346
- Eighth-order damage tensor, 30
- Elaborated two-scale damage model, 150, 204
- Elastic-brittle
damage, 126, 253, 266, 270, 275, 288
material, 126, 253, 262
- Elastic compliance
matrix of, 375
tensor, 37, 270, 373
- Elastic constitutive equation, 44, 48, 71, 84, 113, 176, 366
- Elastic damage, 10
- Elastic material
isotropic, 48, 375
orthotropic, 379
transversely isotropic, 377
- Elastic modulus
matrix of, 376
tensor, 43, 134, 137, 375
variation in, 19
- Elastic-plastic
constitutive equation, 88, 141, 148, 162, 176
damage, 10, 77, 96, 141
- Elastic-viscoplastic constitutive equation, 92, 243
- Elementary ply, 277, 287
- Energy
dissipation, 99
internal, 59
kinetic, 59
- Enthalpy, 64
- Entropy, 61, 63
balance, 63
flux, 62
source, 62
- Equation of continuity, 60
- Equation of motion, 61
- Equivalent
creep rate, 222, 227
effective stress, 142
plastic stain rate, 88, 142
stress, 87
- Euclidean point space, 350, 351
- Euclidean vector space, 328
- Evolution equation, 68, 70, 72
of anisotropic damage, 111
of elastic-brittle damage, 126, 264
of internal variable, 70, 72
of plastic damage, 93, 108, 117, 124
of viscoplastic damage, 93, 109, 231
of void volume fraction, 184
- External mechanical power, 59
- External variable, 57
- F**
- Fabric tensor, 30
- Fatigue, 8–10, 201
fracture, 9
high cycle, 9, 201–202, 204
life, 173, 203, 207–210
limit, 10

- Fatigue (*cont.*)
 low cycle, 8–9, 207
 very high cycle, 10, 201
 very low cycle, 9, 201, 212
- Fatigue damage, 8–9, 94, 173, 201
- Fiber-reinforced
 composite, 279, 289
 lamina (elementary ply), 277
 plastic (FRP), 277
- Fictitious undamaged
 configuration, 18, 23, 36, 42, 294, 298
 material, 18, 36
 state, 18–19, 23
- First law of thermodynamics, 59
- First-order tensor, 337
- Forging, 169, 172
- Forming limit, 167, 169, 176, 183
 diagram, 169, 176, 183
- Fourth-order
 damage tensor, 31, 111, 126, 134, 289
 identity (unit) tensor, 341, 368, 372
 isotropic tensor, 375
 symmetric identity tensor, 341, 372
 symmetric tensor, 369–370, 373
 tensor, 338
 unit (identity) tensor, 340
- Fracture
 critical value of damage for, 77, 98, 153
 cycle number, 203, 236
 limit (of sheet metal forming), 167
- Free index, 329
- G**
- Gauss' (divergence) theorem, 354–355
- Generalized flux (vector), 68–69, 72, 83, 112, 272
- Generalized force (vector), 68–69, 72, 83, 112, 272
- Generalized Hooke's law, 366, 375
 matrix representation of, 375
- Generalized normality law, 72, 74–75, 115
- Generalized standard material, 72–73, 75
- Geometrical configuration of microvoid, 26
- Gibbs
 free energy, 64
 function, 64
 potential, 64, 71, 103, 120, 258, 271, 278
 relation, 63
- Glide plane decohesion, 6, 9
- Gradient-dependent theory, 316
- Gradient (of scalar and tensor field), 316, 352–353
- Grain boundary cavity (void), 218, 227
- Grain boundary diffusion (microvoid diffusion), 6, 218
- Grain boundary sliding, 218
- Grid method, 316, 322
- GTN (Gurson-Tvergaard-Needleman) model, 187, 193, 196
 modification of, 195
- Gurson's constitutive model, 185
- Gurson's yield function, 184, 192
- H**
- HAZ (heat affected zone), 226
- Heat
 flux vector, 59
 generation, 59
 supply, 59
- Heaviside function, 102
- Helmholtz free energy (function), 64, 84, 107, 113, 136, 170, 262, 290
- Hidden variable, 57
- High cycle fatigue, 9, 201, 204
- Higher-order
 contraction, 339
 tensor, 336
 tensor product, 339
- Hooke's law (elastic constitutive equation), 48, 366, 375
- HRR (Hutchinson-Rice-Rosengren) stress field, 250
- Hydrostatic stress, 100
- Hypothesis of
 complementary strain energy equivalence, 38, 52
 local equilibrium, 58
 mechanical equivalence, 32
 strain energy equivalence, 40–41, 299
 strain equivalence, 36, 50, 85, 134, 223
 total energy equivalence, 43, 106–107, 171, 234
- I**
- Identity tensor, 330
 of fourth-order, 340–341, 368
 fourth-order symmetric, 341, 372
 of second-order, 368
- Improper orthogonal tensor, 342
- Independent variable, 58
- Index, 328
 dummy, 329
 free, 329
 notation, 329
- Inelastic constitutive equation, 72, 77, 81, 111
- Inner product, 327

- Integral of tensor field, 350, 354
Interface, 254, 277, 280–281, 286–288
Interlaminar damage, 286
Internal energy, 59
Internal variable, 57, 63, 65, 111
 evolution equation of, 68, 72
Invariant, 345–346
 derivative of, 362
 of deviatoric stress tensor, 196
 orthogonal, 349, 364
Inverse tensor, 331
 of fourth-order, 373
 of second order, 331
Inverse transformation, 331
Invertible (tensor), 331
Irreversible process, 58, 66, 70
Isochronous creep rupture curve, 221
Isotropic damage, 22, 77, 141, 257
 theory, 22, 257
Isotropic elastic material, 102, 375
 constitutive equation of, 375
Isotropic hardening, 78, 82, 87, 244
 variable, 78, 82, 111, 142, 244
Isotropic linear transformation, 344
Isotropic scalar-valued
 tensor function, 349, 363
 vector function, 349
Isotropic tensor, 344
 of fourth-order, 375
 function, 348, 350
Isotropic tensor-valued tensor function, 350, 364
Isotropic vector-valued function, 366
Isotropy
 of damage, 22, 77
 of physical property, 375
of tensor function, 348, 363
- K**
Kachanov-Rabotnov theory, 16, 218
Kachanov theory, 16, 219
Kinematic hardening, 78, 82, 87, 244
 variable, 78, 82, 111, 244
Kinetic energy, 59
Knee point, 288
Kronecker delta, 328, 333
Kuhn-Tucker relation, 109, 118
- L**
Lamé constants, 376
Lamina (elementary ply), 277
Laminate (composite), 277, 282, 286–287
Lankford value, 182
- Law
 of conservation of mass, 60, 190
 of energy conservation, 61
Levi-Civita symbol, 333
Ligament, 154, 184
Linear
 creep-fatigue damage law, 237
 cumulative damage law, 206
 ductile damage model, 155
 elasticity, 84, 366, 375
 transformation (tensor), 329–330
Load carrying effective area, 16, 24
Loading function, 79
Loading-unloading condition, 90, 92, 109, 118
Local
 approach to fracture, 305–306
 dependence, 70
 equilibrium (hypothesis of), 58
 state (principle of), 12, 58, 65
 theory (of composite), 294
Local current damaged configuration, 294
Local fictitious undamaged configuration, 294
Localization
of damage, 308, 313, 322
 of deformation, 184, 320
 of strain, 308, 310
Localized necking, 169, 176, 179
 criteria of, 179
Local-overall relation, 295
Lode (stress) parameter, 196
Logarithmic creep law, 81
Low cycle fatigue, 8, 201, 207
- M**
Macauley bracket, 102
Macroscopic scale (macroscale), 5
Magnitude (of vector), 327
Manson-Coffin law, 210
Mass
 conservation of, 60, 190
Material instability, 308, 310
Material coordinate system, 278
Material (time) derivative, 356
Matrix representation, 334, 366
 of damage effect tensor, 44
 of elastic compliance tensor, 375
 of elastic constitutive equation, 48, 375
 of elastic modulus tensor, 375
 of fourth-order symmetric tensor, 369
 of fourth-order tensor, 368
 of generalized Hooke's law, 375
 of second-order symmetric tensor, 369

- Matrix representation (*cont.*)
 - of second-order tensor, 334, 368
 - of tensor, 334, 366
 - of tensor relation, 366
- Maximum dissipation (principle of), 115, 137
- Mean strain, 100
- Mean stress, 100
- Mechanical power, 59
- Mesh-dependent softening modulus, 314
- Mesh-sensitivity (mesh-dependence), 308, 320
- Mesoscopic
 - behavior of concrete, 257
 - fracture, 208
 - scale (mesoscale), 5, 11, 145, 148
- Metal forming, 166–167, 172
- Metal matrix composite, 294
- Microcrack, 4, 254–255, 280, 288
 - initiation, 207, 238
- Microscopic scale (microscale), 4, 144, 147
- Microscopic void (microvoid, microcavity), 4, 20, 184
 - directional distribution of, 28
 - geometrical configuration of, 26
 - Miner-Palmgren law, 206
- Mixed mode crack, 255
- Momentum balance principle, 61
- Monkman-Grant relationship, 221
- N**
- Nabla operator, 352
- Necking, 6, 169, 176, 180, 183
- Negative orthogonal projection tensor, 130
- Negative-valued
 - strain tensor, 130
 - stress tensor, 131
- Net stress, 18
- Nonlinear creep-fatigue damage law, 237
- Nonlinear ductile damage model, 158
- Nonlocal
 - damage theory, 314, 322
 - damage variable, 315
 - variable, 315–316
 - weighting function, 315
- Non-steady state
 - creep, 222
 - creep damage theory, 222
- Norm, 327
- Normality law, 70
 - generalized, 72, 115
- Norton law, 80, 110, 219, 232
- n*th-order tensor, 337
- O**
- Observable variable, 57
- Onsager reciprocity relation, 70
- Opening-closing (of crack), 127, 132–133, 255
- Orthogonal
 - invariant, 348–349
 - scalar invariant, 349, 364
 - tensor, 341
 - transformation, 341
- Orthonormal
 - basis, 328, 332
 - coordinate system, 351
- Orthotropic elastic material, 379
- Orthotropy, 26, 115, 379
- Outer product, 332
- Overall current damaged configuration, 294
- Overall fictitious undamaged configuration, 294
- P**
- Passive (state of crack, damage), 127, 133, 255
- Permutation
 - symbol, 333, 337
 - tensor, 337
- Phenomenological relation (equation), 70
- Planar transverse isotropy, 135
- Plastic
 - compressibility, 197–200
 - deformation, 77, 80, 115, 123–124
 - dissipation potential (function, surface), 86, 115, 123, 178
 - potential surface, 86
- Plastic (inelastic) constitutive equation, 81, 88, 117, 124, 141, 176, 282
- Point fracture, 6
- Poisson's ratio, 376
- Polyad, 337
- Position vector, 350
- Positive
 - definite tensor, 332
 - orthogonal projection tensor, 130
 - tensor, 332
- Positive-valued
 - strain tensor, 129
 - stress tensor, 131
- Primary creep stage, 218
- Principal
 - direction, 346
 - invariant, 346
 - value, 346
- Principle
 - of local state, 12, 58
 - of maximum dissipation, 115
- Process (thermodynamic), 58

- Projection tensor
negative orthogonal, 130, 272
positive orthogonal, 130, 260
- Proper
orthogonal tensor, 342
value, 346
vector, 346
- Q**
- Quasi-brittle
damage, 144, 253
material, 253, 308
- Quasi-standard thermodynamic approach, 73, 75, 91, 124
- Quasi-unilateral effect, 104
- R**
- Ramberg-Osgood hardening law, 155, 162
- Rate of heat supply, 59
- Regularization, 313, 322
- Representation theorem (of tensor function), 363–366
- Representative volume element (RVE), 11–12
- Reversible (thermodynamic process), 58
- Reynolds' transport theorem, 358
- Rotation (of tensor and vector fields), 353
- Rousselier's constitutive model, 188, 193
- R-type void, 218
- S**
- Saint-Venant's condition, 51, 53–54
- Scalar
damaged variable, 22
field, 350
invariant, 345
product, 327
- Scale
atomic, 4
of damage, 4
macroscopic, 5
mesoscopic, 5
microscopic, 4
- Secondary creep stage, 218
- Second law of thermodynamics, 62
- Second-order
basis tensor, 368
damage tensor, 23–28
symmetric basis tensor, 369
tensor, 337
- Shear decohesion, 5
- Shear modulus, 376
- Sheet metal forming, 167, 176
limit, 167, 169
- Similar tensor, 342
- Simultaneous orthogonal invariant, 349, 364
- Skew-symmetric tensor, 331
- Slant fracture, 192, 195
- Spacial coordinate system, 282
- Spall damage, 10
- Spectral decomposition, 347
- Spectrum (of tensor), 347
- Standard thermodynamic approach, 73
- State
equation, 65, 67
function, 63, 65
potential, 65
variable, 12, 57
- Steady state creep, 218
rate, 219
- Strain
equivalence, 36, 50
localization, 308, 310, 313
softening, 308
- Strain energy
density release rate, 86, 97
equivalence, 41
function, 41
- Strain-hardening, 78
dissipation potential (function), 86–87
exponent, 156, 158
rate, 186
theory, 223
- Stress
criterion, 101, 110, 222
singularity, 249, 321
- Stress triaxiality, 101, 160, 164
function, 101, 143
- Subsequent yield stress, 78
- Substate variable (thermodynamic), 63
- Summation convention, 328
- Surface force, 25, 59
- Symmetric tensor, 331, 369–375
matrix representation of, 369–375
- Symmetrized effective stress tensor, 33–35
- Symmetry
elastic, 375–380
major, 367
minor, 366
- System (of thermodynamics), 57
- T**
- Tensile decohesion, 5
- Tensor, 329, 337
determinant of, 344–345
first-order, 337
fourth-order, 338, 340, 368

- Tensor (*cont.*)
 - higher-order, 336–341
 - matrix representation of, 366–380
 - n*th-order, 337
 - orthogonal, 341
 - second-order, 337, 369
 - third-order, 337–338
 - transpose of, 331, 340
 - zeroth-order, 337
- Tensor component, 334–341
 - transformation of, 342
- Tensor field, 350
 - differentiation of, 351–353
 - integral of, 354, 357
- Tensor function
 - derivative of, 358–361
 - integral of, 354–356
 - isotropy of, 348
 - representation theorem of, 363–366
- Tensor product, 333
 - of higher-order, 336–341
- Tertiary creep stage, 218
- Tetrad, 338
- Thermodynamic
 - characteristic function, 65
 - constitutive theory, 65–76, 81–88, 111–115, 119–120
 - equilibrium, 58
 - potential, 63–65, 66–70, 84–88,
 - process, 58
 - substrate variable, 63
- Thermodynamics
 - first law of, 59
 - second law of, 61–63
- Threshold value (of plastic strain), 77
 - (for creep-fatigue damage), 242
 - (for ductile damage, elastic-plastic damage), 156, 160
 - (for fatigue damage), 96, 147, 149
 - (for viscoplastic damage, creep damage), 233
- Time hardening theory, 223
- Total differential (of tensor function), 358
- Trace, 336, 344
- Traction, 59
- Transformation
 - of basis, 342–344
 - orthogonal, 341
 - tensor components, 342
- Transient creep, 218
- Transpose
 - of fourth-order tensor, 340
 - of second-order tensor, 331
- Transverse isotropy, 135, 377
- Transversely isotropic elastic material, 377
- Triad (triadic product), 337
- Two-damage variable model, 223
- Two-scale damage model, 144, 147, 204
- Type IV zone, 226
- U**
- Ultrahigh cycle fatigue, 10
- Unilateral effect, 104, 127, 257, 272, 288
- Unit linear transformation, 330
- Unit tensor, *see* identity tensor
- V**
- Vector
 - damage variable, 22
 - field, 350
 - operator, 352
 - product, 332
- Very high cycle fatigue, 10, 201
- Very low cycle fatigue, 9, 201, 212
- Viscoplastic
 - constitutive equation, 92, 241
 - deformation, 79
- Viscoplastic damage, 10, 93, 230
 - evolution equation of, 93, 231, 241
- Viscous deformation, 80
- Viscous stress, 80
- Void, 6, 20
 - growth, 6, 106, 185
 - volume fraction, 20, 184, 187, 191
- Void containing damaged material, 184
 - constitutive equation of, 184, 188, 195
- Voigt notation, 366–368, 375
- Von Mises yield condition, 87
- W**
- Weighting function, 315
- Weighting matrix, 370, 375
- Well-posedness (of rate boundary value problem), 308, 311
- W-type crack, 218
- Y**
- Yield
 - condition, 79, 87, 90, 123
 - function, 79, 80, 86, 115
 - surface, 78, 123
- Young's modulus, 376
- Z**
- Zero linear transformation (zero tensor), 330
- Zero tensor, 330
- Zeroth-order tensor, 337